MICROBIOTA IN AIRWAY DISEASES

EDITED BY: Emily K. Cope, Steven D. Pletcher and Kristi Biswas
PUBLISHED IN: Frontiers in Cellular and Infection Microbiology

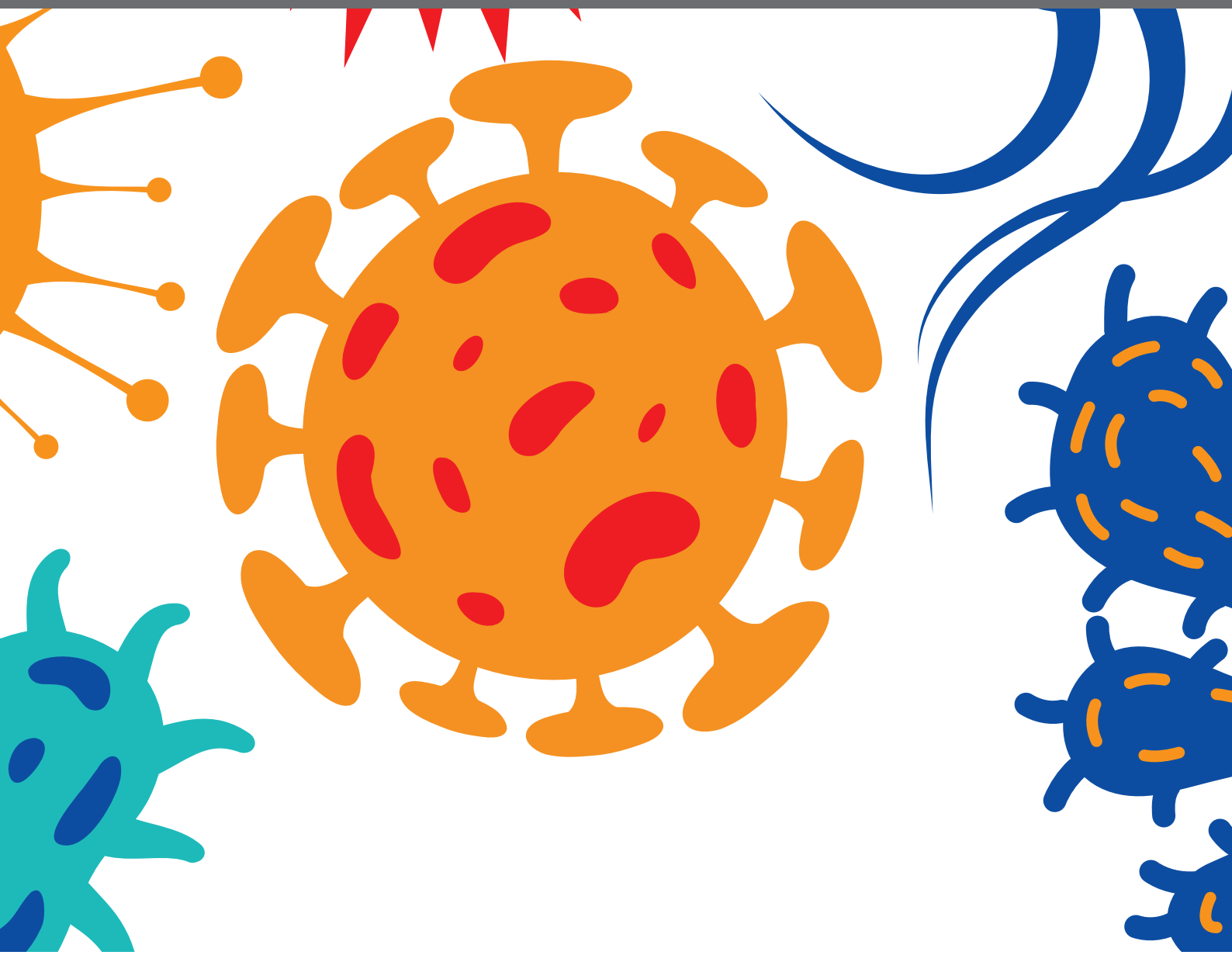

frontiers Research Topics

ISSN 1664-8714
ISBN 978-2-88971-659-3
DOI 10.3389/978-2-88971-659-3

About Frontiers

Frontiers is more than just an open-access publisher of scholarly articles: it is a pioneering approach to the world of academia, radically improving the way scholarly research is managed. The grand vision of Frontiers is a world where all people have an equal opportunity to seek, share and generate knowledge. Frontiers provides immediate and permanent online open access to all its publications, but this alone is not enough to realize our grand goals.

Frontiers Journal Series

The Frontiers Journal Series is a multi-tier and interdisciplinary set of open-access, online journals, promising a paradigm shift from the current review, selection and dissemination processes in academic publishing. All Frontiers journals are driven by researchers for researchers; therefore, they constitute a service to the scholarly community. At the same time, the Frontiers Journal Series operates on a revolutionary invention, the tiered publishing system, initially addressing specific communities of scholars, and gradually climbing up to broader public understanding, thus serving the interests of the lay society, too.

Dedication to Quality

Each Frontiers article is a landmark of the highest quality, thanks to genuinely collaborative interactions between authors and review editors, who include some of the world's best academicians. Research must be certified by peers before entering a stream of knowledge that may eventually reach the public - and shape society; therefore, Frontiers only applies the most rigorous and unbiased reviews.
Frontiers revolutionizes research publishing by freely delivering the most outstanding research, evaluated with no bias from both the academic and social point of view. By applying the most advanced information technologies, Frontiers is catapulting scholarly publishing into a new generation.

What are Frontiers Research Topics?

Frontiers Research Topics are very popular trademarks of the Frontiers Journals Series: they are collections of at least ten articles, all centered on a particular subject. With their unique mix of varied contributions from Original Research to Review Articles, Frontiers Research Topics unify the most influential researchers, the latest key findings and historical advances in a hot research area! Find out more on how to host your own Frontiers Research Topic or contribute to one as an author by contacting the Frontiers Editorial Office: frontiersin.org/about/contact

MICROBIOTA IN AIRWAY DISEASES

Topic Editors:
Emily K. Cope, Northern Arizona University, United States
Steven D. Pletcher, University of California, San Francisco, United States
Kristi Biswas, The University of Auckland, New Zealand

Citation: Cope, E. K., Pletcher, S. D., Biswas, K., eds. (2021). Microbiota in Airway Diseases. Lausanne: Frontiers Media SA. doi: 10.3389/978-2-88971-659-3

Table of Contents

04 ***Microbiotyping the Sinonasal Microbiome***
Ahmed Bassiouni, Sathish Paramasivan, Arron Shiffer, Matthew R. Dillon, Emily K. Cope, Clare Cooksley, Mahnaz Ramezanpour, Sophia Moraitis, Mohammad Javed Ali, Benjamin S. Bleier, Claudio Callejas, Marjolein E. Cornet, Richard G. Douglas, Daniel Dutra, Christos Georgalas, Richard J. Harvey, Peter H. Hwang, Amber U. Luong, Rodney J. Schlosser, Pongsakorn Tantilipikorn, Marc A. Tewfik, Sarah Vreugde, Peter-John Wormald, J. Gregory Caporaso and Alkis J. Psaltis

16 ***Longitudinal Associations of the Cystic Fibrosis Airway Microbiome and Volatile Metabolites: A Case Study***
Andrea Hahn, Katrine Whiteson, Trenton J. Davis, Joann Phan, Iman Sami, Anastassios C. Koumbourlis, Robert J. Freishtat, Keith A. Crandall and Heather D. Bean

32 ***A Novel Description of the Human Sinus Archaeome During Health and Chronic Rhinosinusitis***
Brett Wagner Mackenzie, Annie G. West, David W. Waite, Christian A. Lux, Richard G. Douglas, Michael W. Taylor and Kristi Biswas

44 ***Contribution of Short Chain Fatty Acids to the Growth of* Pseudomonas aeruginosa *in Rhinosinusitis***
Do-Yeon Cho, Daniel Skinner, Ryan C. Hunter, Christopher Weeks, Dong Jin Lim, Harrison Thompson, Christopher R. Walz, Shaoyan Zhang, Jessica W. Grayson, William E. Swords, Steven M. Rowe and Bradford A. Woodworth

56 ***Co-infection of* Malassezia sympodialis *With Bacterial Pathobionts* Pseudomonas aeruginosa *or* Staphylococcus aureus *Leads to Distinct Sinonasal Inflammatory Responses in a Murine Acute Sinusitis Model***
Keehoon Lee, Irene Zhang, Shari Kyman, Oliver Kask and Emily Kathryn Cope

71 ***Intranasal Application of* Lactococcus lactis W136 *Is Safe in Chronic Rhinosinusitis Patients With Previous Sinus Surgery***
Leandra Mfuna Endam, Saud Alromaih, Emmanuel Gonzalez, Joaquin Madrenas, Benoit Cousineau, Axel E. Renteria and Martin Desrosiers

86 ***The Fungal Microbiome and Asthma***
Erik van Tilburg Bernardes, Mackenzie W. Gutierrez and Marie-Claire Arrieta

102 ***SARS-CoV-2-Indigenous Microbiota Nexus: Does Gut Microbiota Contribute to Inflammation and Disease Severity in COVID-19?***
Indranil Chattopadhyay and Esaki M. Shankar

110 ***Identification of Microbiome Etiology Associated With Drug Resistance in Pleural Empyema***
Zhaoyan Chen, Hang Cheng, Zhao Cai, Qingjun Wei, Jinlong Li, Jinhua Liang, Wenshu Zhang, Zhijian Yu, Dongjing Liu, Lei Liu, Zhenqiang Zhang, Ke Wang and Liang Yang

120 ***The Airway Pathobiome in Complex Respiratory Diseases: A Perspective in Domestic Animals***
Núria Mach, Eric Baranowski, Laurent Xavier Nouvel and Christine Citti

frontiers in Cellular and Infection Microbiology

ORIGINAL RESEARCH
published: 08 April 2020
doi: 10.3389/fcimb.2020.00137

Microbiotyping the Sinonasal Microbiome

Ahmed Bassiouni[1], Sathish Paramasivan[1], Arron Shiffer[2], Matthew R. Dillon[2], Emily K. Cope[2], Clare Cooksley[1], Mahnaz Ramezanpour[1], Sophia Moraitis[1], Mohammad Javed Ali[3], Benjamin S. Bleier[4], Claudio Callejas[5], Marjolein E. Cornet[6], Richard G. Douglas[7], Daniel Dutra[8], Christos Georgalas[6†], Richard J. Harvey[9,10], Peter H. Hwang[11], Amber U. Luong[12], Rodney J. Schlosser[13], Pongsakorn Tantilipikorn[14], Marc A. Tewfik[15], Sarah Vreugde[1], Peter-John Wormald[1], J. Gregory Caporaso[2] and Alkis J. Psaltis[1]*

[1] Department of Otolaryngology, Head and Neck Surgery, University of Adelaide, Adelaide, SA, Australia, [2] Pathogen and Microbiome Institute, Northern Arizona University, Flagstaff, AZ, United States, [3] Dacryology Service, LV Prasad Institute, Hyderabad, India, [4] Department of Otolaryngology, Massachusetts Eye and Ear Infirmary, Harvard Medical School, Boston, MA, United States, [5] Department of Otolaryngology, Pontificia Universidad Catolica de Chile, Santiago, Chile, [6] Department of Otorhinolaryngology, Amsterdam UMC, Amsterdam, Netherlands, [7] Department of Surgery, The University of Auckland, Auckland, New Zealand, [8] Department of Otorhinolaryngology, University of São Paulo, São Paulo, Brazil, [9] Department of Otolaryngology, Rhinology and Skull Base, University of New South Wales, Sydney, NSW, Australia, [10] Faculty of Medicine and Health Sciences, Macquarie University, Sydney, NSW, Australia, [11] Department of Otolaryngology -Head and Neck Surgery, Stanford University, Stanford, CA, United States, [12] Department of Otolaryngology -Head and Neck Surgery, The University of Texas Health Science Center at Houston, Austin, TX, United States, [13] Department of Otolaryngology, Medical University of South Carolina, Charleston, SC, United States, [14] Department of Otorhinolaryngology, Faculty of Medicine, Siriraj Hospital, Mahidol University, Bangkok, Thailand, [15] Department of Otolaryngology - Head and Neck Surgery, McGill University, Montreal, QC, Canada

This study offers a novel description of the sinonasal microbiome, through an unsupervised machine learning approach combining dimensionality reduction and clustering. We apply our method to the International Sinonasal Microbiome Study (ISMS) dataset of 410 sinus swab samples. We propose three main sinonasal "microbiotypes" or "states": the first is *Corynebacterium*-dominated, the second is *Staphylococcus*-dominated, and the third dominated by the other core genera of the sinonasal microbiome (*Streptococcus*, *Haemophilus*, *Moraxella*, and *Pseudomonas*). The prevalence of the three microbiotypes studied did not differ between healthy and diseased sinuses, but differences in their distribution were evident based on geography. We also describe a potential reciprocal relationship between *Corynebacterium* species and *Staphylococcus aureus*, suggesting that a certain microbial equilibrium between various players is reached in the sinuses. We validate our approach by applying it to a separate 16S rRNA gene sequence dataset of 97 sinus swabs from a different patient cohort. Sinonasal microbiotyping may prove useful in reducing the complexity of describing sinonasal microbiota. It may drive future studies aimed at modeling microbial interactions in the sinuses and in doing so may facilitate the development of a tailored patient-specific approach to the treatment of sinus disease in the future.

Keywords: microbiome, sinus, next-generation sequencing, 16S rRNA gene, chronic rhinosinusitis, microbiotype, paranasal sinuses

OPEN ACCESS

Edited by:
D. Scott Merrell, Uniformed Services University, United States

Reviewed by:
Fabio S. Lima, University of Illinois at Urbana-Champaign, United States
Julio Villena, CONICET Centro de Referencia para Lactobacilos (CERELA), Argentina

***Correspondence:**
Alkis J. Psaltis
alkis.psaltis@adelaide.edu.au

†Present address:
Christos Georgalas, Medical School, University of Nicosia, Nicosia, Cyprus

Specialty section:
This article was submitted to Microbiome in Health and Disease, a section of the journal Frontiers in Cellular and Infection Microbiology

Received: *28 October 2019*
Accepted: *17 March 2020*
Published: *08 April 2020*

Citation:
Bassiouni A, Paramasivan S, Shiffer A, Dillon MR, Cope EK, Cooksley C, Ramezanpour M, Moraitis S, Ali MJ, Bleier BS, Callejas C, Cornet ME, Douglas RG, Dutra D, Georgalas C, Harvey RJ, Hwang PH, Luong AU, Schlosser RJ, Tantilipikorn P, Tewfik MA, Vreugde S, Wormald P-J, Caporaso JG and Psaltis AJ (2020) Microbiotyping the Sinonasal Microbiome. Front. Cell. Infect. Microbiol. 10:137. doi: 10.3389/fcimb.2020.00137

INTRODUCTION

Microbes present in any environment almost never live in isolation, but enter in various types of ecological relationships with one another (Lidicker, 1979; Faust and Raes, 2012). The end result of these interactions is either a domination of a certain organism, or coexistence through the establishment of metabolic or territorial niches (Coyte et al., 2015; Bauer et al., 2018). In each of these cases, a stable community configuration or state is reached (Lewontin, 1969; May, 1974; Beisner et al., 2003). The stable states of the human microbiota has been postulated based on the findings of high inter-individual variability coupled with relatively low temporal variability, taken as evidence of resilience against perturbations (Costello et al., 2009; Caporaso et al., 2011; Lozupone et al., 2012). Perturbations in an otherwise stable microbiome could be linked to the concept of "dysbiosis" (Olesen and Alm, 2016), which remains a vague term that attempts to explain the contribution of an unhealthy microbiome to disease (Olesen and Alm, 2016). Examining stable microbial states as "clusters," as opposed to the traditional analysis of the differential abundances of microbial taxa one at a time, could therefore provide another important ecological perspective in describing the microbiome and, through potential unraveling of common commensal-pathogen interactions (Brugger et al., 2016), exploring its relevance to health or disease.

High inter-individual variability represent one of the findings that has already been demonstrated in the microbiome inhabiting the paranasal sinuses (Biswas et al., 2015). This adds a significant challenge when we attempt to determine its role in Chronic Rhinosinusitis (CRS). CRS is a heterogenous, multi-factorial inflammatory disease of the sinuses, with a complex and incompletely understood aetiopathogenesis (Fokkens et al., 2012). Naturally, the potential role of the sinonasal microbiome and its "dysbiosis" in CRS pathophysiology has recently gained increased interest. The nature of the microbial dysbiosis and its role in disease causation and progression however remains unclear, with conflicting findings from the small sinonasal microbiome studies published thus far (Paramasivan et al., 2020). This provided the impetus for us to conduct the first multi-national, multicenter "International Sinonasal Microbiome Study (ISMS)" (Paramasivan et al., 2020). This study, the largest and most diverse of its kind to date, attempted to address many of the limitations of the smaller previous studies, by standardizing collection, processing and analysis of the samples. Furthermore, its large sample size and multinational recruitment, meant that it was more likely to capture geographical and center-based differences if present. A recent meta-analysis of published sinonasal 16S rRNA sequences revealed that the largest proportion of variance was attributed to differences between studies (Wagner Mackenzie et al., 2017), highlighting a role for performing a large multi-center study that employed a unified methodology.

Contrary to the findings of previous small single-center studies, our international cohort showed no significant differences in alpha or beta diversity between the three groups of patients analyzed: healthy control patients without CRS and the two phenotypes of CRS patients, those with polyps (CRSwNP) and those without (CRSsNP). The study however revealed a potential grouping of samples as demonstrated on beta diversity exploratory analysis (Paramasivan et al., 2020). Accordingly, we hypothesized that the bacteriology of the sinuses could be categorized into various clusters of similar compositions. We inquired whether these potential groups would aid in describing the sinonasal microbial composition of patients or associate with clinical features. Similar attempts performed on gut microbiota in healthy individuals were termed *enterotyping* (Arumugam et al., 2011). The clinical relevance of gut enterotypes remain the topic of research, and sometimes controversy. A previous exploration of clusters of sinus microbiota in patients was performed by Cope et al. (2017) in which the authors reported four compositionally distinct sinonasal microbial community states; the largest group of patients were dominated by a continuum of Staphylococcaceae and Corynebacteriaceae (Cope et al., 2017).

In this manuscript, we attempt "microbiotyping" to explain interpatient heterogeneity of the bacterial communities in the paranasal sinuses, and we describe "sinonasal microbiotypes" across the first large, multi-center cohort of individuals with and without CRS. We then describe the composition of these microbiotypes, explore potential clinical associations, and validate microbiotyping on a separate sinus microbiome dataset.

Abbreviations: AERD, aspirin-exacerbated respiratory disease; ANCOM, "Analysis of Compositions of Microbiomes" method; BLAST, "Basic Local Alignment Search Tool"; CRS, chronic rhinosinusitis; CRSsNP, chronic rhinosinusitis *sine* nasal polyps; CRSwNP, chronic rhinosinusitis with nasal polyps; ISMS, the International Sinonasal Microbiome Study; PCoA, principal coordinate analysis; PCs, principal components; QIIME 2, "Quantitative Insights Into Microbial Ecology 2" software; SparCC, "Sparse Correlations for Compositional data" algorithm.

MATERIALS AND METHODS

The "International Sinonasal Microbiome Study (ISMS)" Dataset

We perform the primary analysis on the dataset obtained from the "International Sinonasal Microbiome Study (ISMS)" project (Paramasivan et al., 2020). In summary, this dataset is a multi-center 16S-amplicon dataset which includes endoscopically-guided, guarded swabs collected from the sinuses (in particular the middle meatus/anterior ethmoid region) of 532 participants in 13 centers representing 5 continents. Details of sample collection, DNA extraction and sequencing methodologies are described in the original report (Paramasivan et al., 2020). The 16S gene region sequenced was the V3–V4 hypervariable region, utilizing primers (CCTAYGGGRBGCASCAG forward primer) and (GGACTACNNGGGTATCTAAT reverse primer) according to protocols at the sequencing facility (the Australian Genome Research Facility). Sequencing was done on the Illumina MiSeq platform (Illumina Inc., San Diego, CA) with 300-base-pairs paired-end Illumina chemistry.

Bioinformatics Pipeline

Details of the bioinformatic pipeline is detailed in the original report (Paramasivan et al., 2020). In summary, we utilized a QIIME 2-based pipeline (Quantitative Insights Into Microbial Ecology 2) (Bolyen et al., 2018). Forward and reverse fastq reads

were joined (Zhang et al., 2014), quality-filtered (Bokulich et al., 2013), abundance-filtered (Wang et al., 2018), then denoised using deblur (Amir et al., 2017) through QIIME 2-based plugins. This yielded a final feature table of high-quality, high-resolution Amplicon Sequence Variants (ASVs). Taxonomy assignment and phylogenetic tree generation (Janssen et al., 2018) was done against the Greengenes (DeSantis et al., 2006) database; and taxonomy was assigned using the QIIME 2 BLAST assigner (Bokulich et al., 2018). A rarefaction minimum depth cut-off was chosen at 400 and this yielded 410 samples out of the original 532 for downstream analysis. The same pipeline was then applied on DataSet Two for purposes of validation of microbiotyping. We chose to reproduce exactly all the original pipeline steps on DataSet Two, despite being a completely separate dataset, to reduce bias.

Delineating the Microbiotypes of the Sinonasal Microbiome

Our approach was guided by the "enterotyping" method described by Arumugam et al. (2011) with adaptations. We constructed a sample distance matrix using the Jensen-Shannon distance (JSD) metric, as used in the original "enterotypes" paper (Arumugam et al., 2011). The Jensen-Shannon distances were calculated between samples in the genus-level-assigned table in a pairwise fashion using the JSD function in the R package "philentropy" with a log ($\log_{10}$) base. Following this, Principal Coordinate analysis (PCoA) was done on the distance matrix for dimensionality reduction and visualization. Clustering was then performed using a standard K-means clustering algorithm, as implemented in the machine learning Python package scikit-learn (version 0.20.1) (Pedregosa et al., 2011) on the first two principal components (PCs) obtained from the PCoA, with the number of clusters (k) chosen at 3 based on visual inspection of the beta diversity PCoA plots. Average silhouette scores, as implemented in scikit-learn, for the range ($k = 2$–8) were calculated to assess clustering quality, and this revealed the highest silhouette scores: 0.61 and 0.6 for [$k = 4$] and [$k = 3$], respectively. The three resulting clusters were defined as the three sinonasal microbiotypes. For further exploration of the subgroups that constitute microbiotype 3, we used the hierarchical density-based clustering algorithm "hdbscan" (McInnes et al., 2017) on the full-dimensional feature table. Genera were projected onto the PCoA matrix using a biplot approach (Legendre and Legendre, 2012), as implemented in scikit-bio's function *"pcoa_biplot."* Genera were represented in the biplot figure as arrows, originating from the center of the plot pointing to the direction of the projected feature coordinates, and the lengths normalized as a percentage of the longest arrow. We utilized "Analysis of Compositions of Microbiomes (ANCOM)" (Mandal et al., 2015) for identifying differentially-abundant taxa. Taxa genus level and Staphylococcus species level co-occurrence/correlation analysis were done after taxonomy assignment using SparCC (Sparse Correlations for Compositional data) algorithm (Friedman and Alm, 2012), in the fast implementation in FastSpar (Watts et al., 2018).

Validating Microbiotypes on a Second Sinonasal Microbiome Dataset

To infer whether our classification could be generalizable to other sinonasal microbiome samples not included in this study, we sought to validate our microbiotyping approach on a separate, previously-unpublished, 16S dataset. This dataset includes sinonasal microbiome swabs collected from private and public patients attending the Otolaryngology Department (University of Adelaide) to have surgery done by the authors P-JW, AP or the Otorhinolaryngology Service at the Queen Elizabeth Hospital in Adelaide, South Australia. Similar to the main dataset, these included CRS patients who underwent endoscopic sinus surgery for this sinus disease, and non-CRS control patients who underwent other otolaryngological procedures, such as tonsillectomy, septoplasty, or skullbase tumor resection. Sample collection, and processing were done in a standardized fashion similar to that has been described in the ISMS main dataset, except that DNA extraction was carried out using the PowerLyzer Power-Soil DNA kit (MoBio Laboratories, Salona Beach, CA) as previously described (Chan et al., 2016), rather than the Qiagen DNeasy kit (Qiagen, Hilden, Germany). Similar to the ISMS samples, library preparation and 16S sequencing were done at the Australian Genome Research Facility, on the Illumina MiSeq platform (Illumina Inc., San Diego, CA, USA) with the 300-base-pairs paired-end chemistry. Libraries were generated by amplifying (341F−806R) primers against the V3–V4 hypervariable region of the 16S gene (CCTAYGGGRBGCASCAG forward primer; GGACTACNNGGGTATCTAAT reverse primer) (Yu et al., 2005). PCR was done using AmpliTaq Gold 360 master mix (Life Technologies, Mulgrave, Australia) following a two-stage PCR protocol (29 cycles for the first stage; and 8 cycles for the second, indexing stage). Sequencing was done over two MiSeq runs in January 2015. We termed this dataset in this manuscript "Dataset Two." This dataset comprises samples collected from 129 participants. Rarefaction at a cutoff of 400 reads was performed, to match what was performed for the main dataset, and samples with read number <400 were excluded; this yielded a final feature table containing 97 samples, representing 33 CRSsNP patients, 35 CRSwNP patients, and 29 controls.

We took two separate approaches to validation. The first approach is to replicate the previously-described unsupervised K-means microbiotyping methodology independently on samples in Dataset Two. We call this first approach the "unsupervised approach." The second approach is to use the K-means model that was fitted on the samples from the Main Dataset to predict labels (i.e., microbiotypes) of the samples in Dataset Two. As such, the Main Dataset is used as a "training dataset" in the language of machine learning. We called the second approach the "semi-supervised approach."

Statistical Analysis

All frontend analyses were done using the Jupyter notebook frontend (Kluyver et al., 2016) and utilizing the assistance of packages from the Scientific Python (Oliphant, 2007) stack (numpy, scipy, pandas, statsmodels), scikit-learn (Pedregosa

et al., 2011), scikit-bio (https://github.com/biocore/scikit-bio), and omicexperiment (https://www.github.com/bassio/omicexperiment). *P*-values were corrected for multiple comparisons using Benjamini-Hochberg's False Discovery Rate (FDR) method when applicable.

RESULTS

Basic Characteristics of the Study Cohort and Beta Diversity Plots

The main ISMS study cohort was described in our previous publication (Paramasivan et al., 2020). In brief, 410 samples were included in the analysis collected from 13 centers representing 5 continents. These samples are distributed along three diagnosis groups as follows: 99 CRSsNP patients, 172 CRSwNP patients, and 139 (non-CRS) controls. Beta diversity ordination plots (of weighted UniFrac and Jensen-Shannon distances) are shown in **Figure 1**. The plots do not reveal any distinct grouping by disease state or by center, but on visual inspection show a triangular arrangement suggesting that samples lie on a continuum between three distinct clusters, providing motivation for further analysis.

Composition of the Three Sinonasal Microbiotypes

We applied our microbiotyping approach through the unsupervised dimensionality reduction and clustering method described in the Methods. The principal components

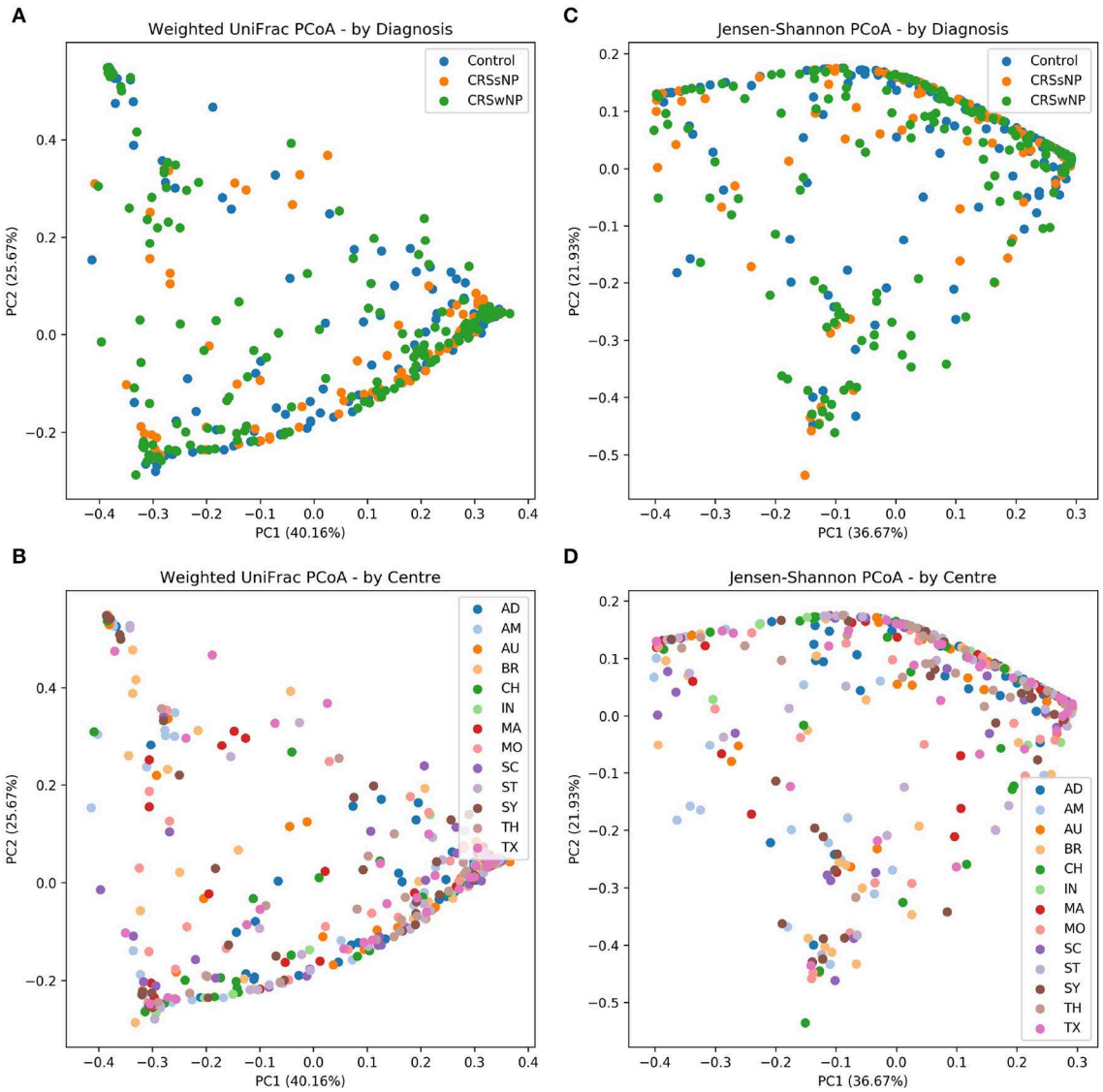

FIGURE 1 | Beta diversity ordination plots. **(A)** Weighted UniFrac PCoA - by Diagnosis. **(B)** Weighted UniFrac PCoA - by Centre. **(C)** Jensen-Shannon PCoA - by Diagnosis; **(D)** Jensen-Shannon PCoA - by Centre.

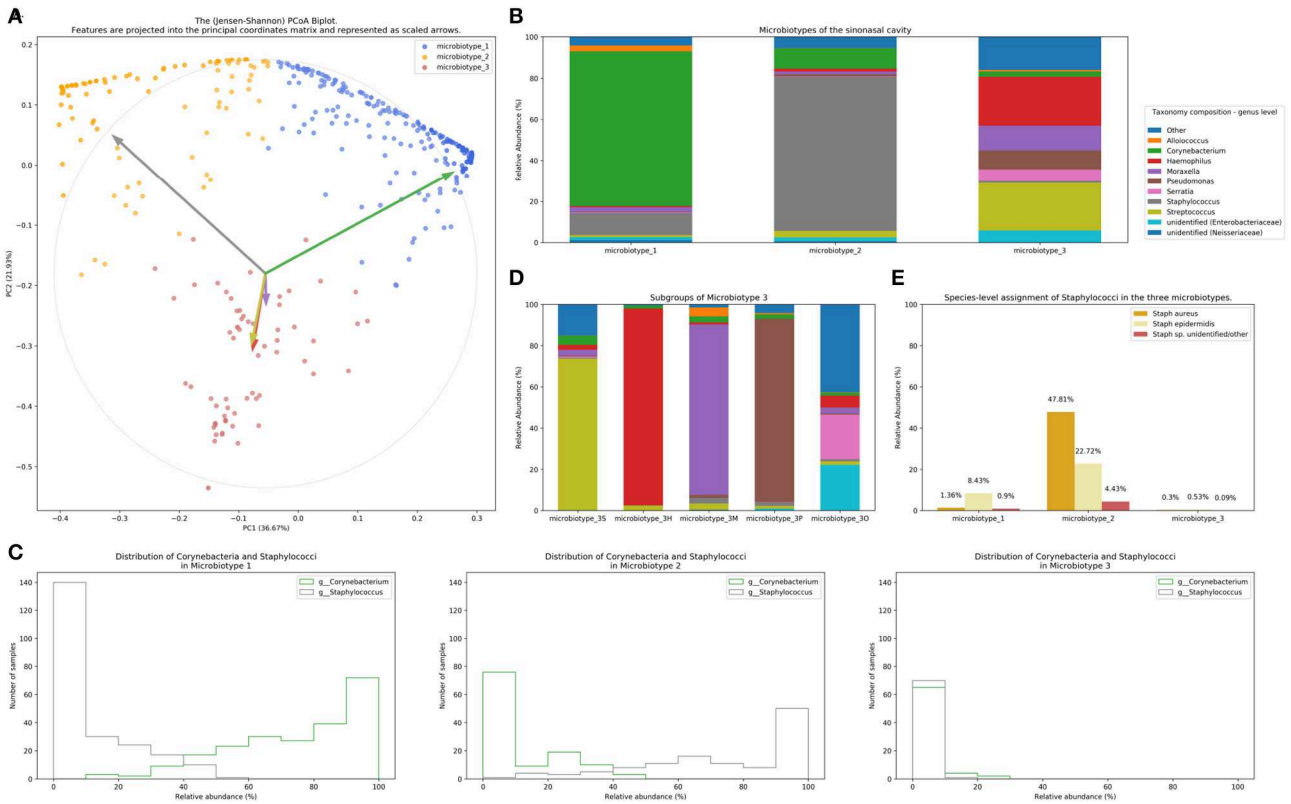

FIGURE 2 | Microbiotyping the sinonasal microbiome. **(A)** Illustration of the assigned microbiotypes on the Jensen-Shannon PCoA biplot. Arrows were used to depict the projection of the genera onto the PCoA matrix. Each arrow is indicated by the color of the genus according to the Legend. **(B)** Taxonomic composition of the three microbiotypes at the genus level. **(C)** Histograms demonstrating the relative abundance of Corynebacterium and Staphylococcus. **(D)** Subgroups of microbiotype 3 (hierarchical density-based clustering). **(E)** Distribution of staphylococcal species (mean relative abundance).

and the taxonomic composition of the resulting "sinonasal microbiotypes" is found in **Figures 2A,B**, respectively.

Microbiotype 1 is dominated by *Corynebacterium* (mean relative abundance of 75.29%). Microbiotype 2 is dominated by *Staphylococcus* (mean relative abundance of 74.96%). Microbiotype 3 contained samples that were mostly constituted of *Streptococcus*, *Haemophilus*, *Moraxella*, *Pseudomonas,* and other genera.

The Abundance/Prevalence tables for the microbiotypes is demonstrated in **Tables S1A–C**.

We used a PCoA biplot to project features (genera) onto the PCoA matrix (Legendre and Legendre, 2012). The 5 topmost abundant genera were overlaid on the PCoA plot as arrows, originating from the center of the plot and pointing to the direction of the projected feature coordinates (**Figure 2B**). Each arrow is indicated by the color of the genus according to the Legend in **Figure 2B**, and the length of each was normalized as a percentage of the longest arrow. The coloring of the samples in the PCoA scatter plot according to the microbiotype assignment is provided for additional illustration (**Figure 2A**). We note that the biplot arrows show a quasi-orthogonal arrangement between the key genera that constitute the microbiome.

The distributions of the relative adundances of *Corynebacterium* and *Staphylococcus* in all three microbiotypes were plotted in histograms (**Figure 2C**). It was noted that in microbiotype 1, most samples have a high abundance of Corynebacteria (i.e., Corynebacteria dominate), while Staphylococci appeared to dominate in microbiotype 2 in most samples.

Dissection of "Sinonasal Microbiotype 3"

We observed that Microbiotype 3 included various genera that did not cluster into the major two microbiotypes. It was also evident that this microbiotype is more heterogeneous. Applying the K-Means algorithm we showed poor clustering on only the first two and three Principal Components, since this group included multiple signatures with various dominant organisms. Accordingly, we employed the hierarchical density-based clustering algorithm "hdbscan" (McInnes et al., 2017) on the full-dimensional OTU table. One advantage of this algorithm is that it can estimate the number of clusters, without *a priori* specification by the user. This algorithm also has the ability to detect "outliers" that fail to cluster with the rest of the groups and detaches them into a separate "Miscellaneous/Other" group. We ran this algorithm on samples in Microbiotype 3 and this revealed four clusters, each dominated by one of the genera of *Streptococcus* (21 samples), *Haemophilus* (16 samples), *Moraxella* (9 samples), and *Pseudomonas* (7 samples), with a mean relative

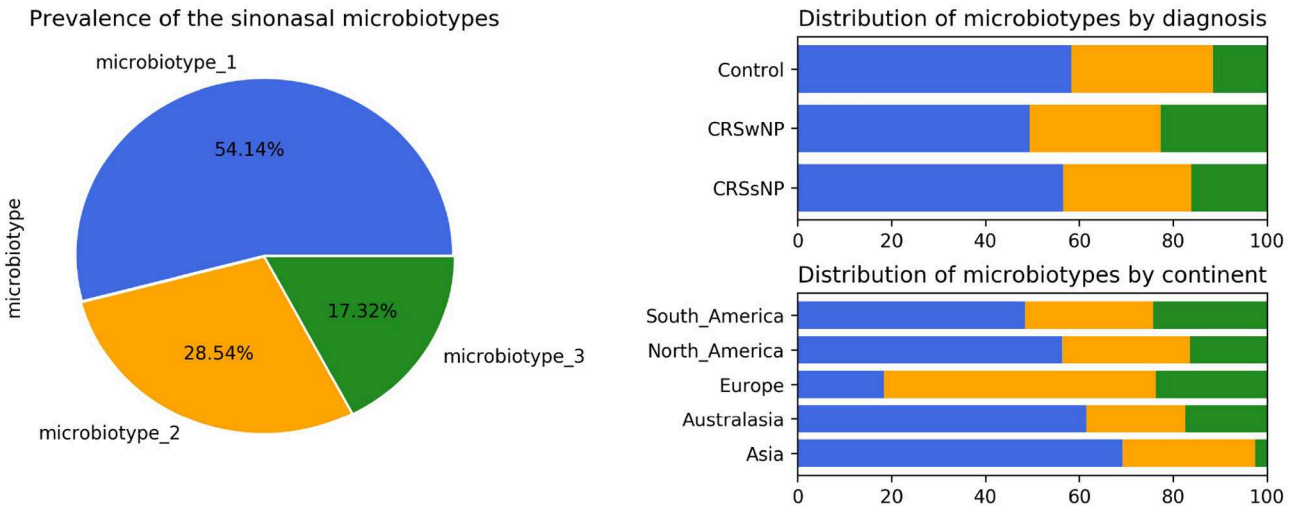

FIGURE 3 | Prevalence and distribution of the microbiotypes.

abundance ranging from 73.49 to 95.5%. The fifth cluster was the assigned "Miscellaneous/Other" group (18 samples). We term these "sub-microbiotypes": microbiotype 3S, 3H, 3M, 3P, and 3O, respectively (**Figure 2D**).

Exploring Microbiotypes at the Species-Level Reveals Potential Antagonism Between *Corynebacterium* Species and *Staphylococcus aureus*

At present, species level assignment is limited by the current technology of 16S-surveys, the current state of microbial databases in general, and by our chosen short-read sequencing methodology. However, species level associations hold clinical significance for sinus health, since *Staphylococcus aureus* has been traditionally associated with biofilm formation and superantigen elaboration, both of which are associated with more severe sinus disease and poorer response to treatment. Furthermore, nasal carriage of methicillin-resistant *Staphylococcus aureus* (MRSA) is a global health concern with implications that extend far beyond the sinuses. Moreover, our new QIIME 2-based pipeline (Bolyen et al., 2018) allows a higher "sub-OTU" resolution compared to older pipelines, offering an opportunity to resolve some taxa at species level when possible (Amir et al., 2017; Thompson et al., 2017).

We explored taxonomy assignment at the species level, with a focus on Staphylococcal species. Staphylococci were assigned to either *Staphylococcus aureus*, *Staphylococcus epidermidis,* or unclassified *Staphylococcus*. We found that almost all of the assigned *Staphylococcus aureus* species were clustered in Microbiotype 2, forming 47.81% mean relative abundance of this Microbiotype, compared to 1.36 and 0.3% in Microbiotype 1 and Microbiotype 3, respectively (**Figure 2E**). Differential abundance of both *Staphylococcus aureus* and *epidermidis* between the disease groups was confirmed as statistically significant using the ANCOM method.

In light of this finding, we hypothesized a reciprocal or antagonistic relationship between *Corynebacterium* sp. and *Staphylococcus aureus* and investigated this using the SparCC algorithm. This confirmed a significant negative correlation between Corynebacterium genus and the species *Staphylococcus aureus* (correlation coefficient $= -0.339$, $p = 0.001$). Interestingly, *Staphylococcus epidermidis* positively correlated with *Corynebacterium* (correlation coefficient $= 0.271$, $p = 0.001$). These results suggest that a benign or probiotic role is played by both *Corynebacterium* spp. and *Staphylococcus epidermidis* when interacting with *Staphylococcus aureus*. This should be viewed in the context of previous literature and in the context of the current limitations of 16S-sequencing, and is elaborated on in the discussion.

Prevalence and Distribution of the Microbiotypes in Different Diagnoses and Centers

Microbiotype 1 was assigned to 222 samples (54.1%), microbiotype 2 to 117 samples (28.5%), and microbiotype 3 to 71 samples (17.3%). The prevalence distribution of the sinonasal microbiotypes did not appear to significantly differ by the disease state of the sinuses (**Figure 3**). However, a Chi-Squared test on the contingency table by center showed significantly different distributions by center (FDR-corrected $p < 0.001$): there was a higher prevalence of microbiotype 2 in our European center (Amsterdam), and a higher prevalence of microbiotype 1 in Asian and Australasian centers, with a much lower prevalence of microbiotype 3 in Asia (**Figure 3** and **Table 1**).

Associations of Microbiotypes With Clinical Variables

We then explored the distribution of the three microbiotypes among multiple clinical variables in **Table 2**. This shows no

TABLE 1 | Distribution of microbiotypes by diagnosis and continent.

Variable	Value	Microbiotype_1	Microbiotype_2	Microbiotype_3	*p*-value
Diagnosis	CRSsNP	56 (56.6%)	27 (27.3%)	16 (16.2%)	0.507
	CRSwNP	85 (49.4%)	48 (27.9%)	39 (22.7%)	
	Control	81 (58.3%)	42 (30.2%)	16 (11.5%)	
Continent	Asia	27 (69.2%)	11 (28.2%)	1 (2.6%)	<0.001
	Australasia	67 (61.5%)	23 (21.1%)	19 (17.4%)	
	Europe	7 (18.4%)	22 (57.9%)	9 (23.7%)	
	North America	89 (56.3%)	43 (27.2%)	26 (16.5%)	
	South America	32 (48.5%)	18 (27.3%)	16 (24.2%)	

TABLE 2 | Distribution of microbiotypes by various clinical variables.

Variable	Value	Microbiotype_1	Microbiotype_2	Microbiotype_3	*P*-value
Asthma	No	162 (56.4%)	81 (28.2%)	44 (15.3%)	0.906
	Yes	55 (51.4%)	31 (29.0%)	21 (19.6%)	
Aspirin sensitivity	No	202 (55.3%)	106 (29.0%)	57 (15.6%)	0.077
	Yes	12 (48.0%)	5 (20.0%)	8 (32.0%)	
Diabetes	No	189 (54.9%)	98 (28.5%)	57 (16.6%)	0.979
	Yes	22 (55.0%)	11 (27.5%)	7 (17.5%)	
GORD	No	177 (55.3%)	93 (29.1%)	50 (15.6%)	0.979
	Yes	35 (55.6%)	17 (27.0%)	11 (17.5%)	
Current smoker	No	204 (54.4%)	110 (29.3%)	61 (16.3%)	0.077
	Yes	15 (57.7%)	4 (15.4%)	7 (26.9%)	
Primary surgery	No	92 (47.2%)	57 (29.2%)	46 (23.6%)	0.114
	Yes	130 (60.5%)	60 (27.9%)	25 (11.6%)	

significant difference for some variables including asthma, aspirin sensitivity, GORD, diabetes mellitus, and current smoking status (FDR-corrected $p > 0.05$; Chi-squared test). The cross tabulation however revealed a statistically significant association with "aspirin sensitivity" or aspirin-exacerbated respiratory disease (AERD) ($p = 0.02$), although this did not persist after correction for multiple comparisons (corrected $p = 0.077$). Patients who were aspirin-sensitive (or suffering from AERD) showed less prevalence of microbiotypes 1, 2, and a higher prevalence of microbiotype 3, compared to those who were not aspirin-sensitive.

Validation of Sinonasal Microbiotyping on a Separate Dataset

We validated our approach on a separate 16S dataset we called Dataset Two. As described in the Methods section, we validated this using an independent unsupervised approach and a semi-supervised approach guided by the Main Dataset.

The first unsupervised approach yielded three clusters similar to the microbiotypes described on the Main Dataset, with one cluster exhibiting high mean relative abundance of Corynebacteria, a second cluster exhibiting high mean relative abundance of Staphylococcus, and a third cluster with other dominant genera. Plotting the first two Principal Components (**Figure 4A**) resulting from PCoA on the Jensen-Shannon distance matrix revealed the same triangular distribution of samples observed in **Figure 1**.

Prevalence of the microbiotypes in this dataset (using the unsupervised approach) was as follows: microbiotype 1 assigned 39.2% of samples, microbiotype 2 with 26.8% of samples, and microbiotype 3 with 34.0%.

The second semi-supervised approach yielded similar results (**Figure 4**; Supplementary Jupyter notebook), differing in the classification of only 3 samples (out of 97 samples; i.e., 3.09%; see **Supplementary Jupyter Notebook**). Two of these samples show *Staphylococcus* dominating the samples in combination with *Haemophilus*, with no overt dominance of one taxon over the other, making them more-or-less transitional samples between the signatures of microbiotypes 2 and 3. The third sample was dominated by *Staphylococcus* and *Corynebacterium*, making it a transitional sample between microbiotype 1 and microbiotype 2, with Staphylococcal species assigned to *epidermidis*, making this more appropriately assigned to microbiotype 1 (see **Supplementary Jupyter Notebook**).

These results validate the microbiotyping approach and suggest that our approach and dataset could be used to guide classification of sinonasal samples sequenced in future separate studies (**Figure 4**). Moreover, it points toward a potential clinical relevance of performing sinonasal microbiotyping.

DISCUSSION

We demonstrate that the microbiota of most sinus swab samples could be classified into distinct signatures or archetypes, which we have termed "sinonasal microbiotypes." We observed three main microbiotypes: the most prevalent being a *Corynebacterium*-dominated microbiotype (microbiotype 1), then a *Staphylococcus*-dominated microbiotype (microbiotype 2), and microbiotype 3 which includes samples dominated by *Streptococcus*, *Haemophilus*, *Moraxella*, *Pseudomonas*, and other genera.

As we have previously reported (Paramasivan et al., 2020), the sinus microbiota are dominated by the genera *Corynebacterium* and *Staphylococcus* (microbiotypes 1 and 2). A similar clustering approach to the sinus microbiome was applied by Cope et al., who utilized Dirichlet multinomial mixture models, and reported that most samples in their study were occupied by a continuum of Staphylococcaceae and Corynebacteriaceae (Cope et al., 2017). It appears that, regardless the statistical or clustering methodology utilized, it is most likely that the sinonasal microbiome consists of core organisms (Paramasivan et al., 2020) that potentially have distinct co-occurrence patterns.

Staphylococcus aureus has been perceived to be an important pathogen in sinus inflammatory disease. *Staphylococcus aureus* biofilms may act as a nidus for recurrent infections (Jervis-Bardy et al., 2011; Drilling et al., 2014) and as a "nemesis" of otherwise-successful sinus surgery (Psaltis et al., 2008; Foreman and Wormald, 2010; Singhal et al., 2011). *Staphylococcus aureus* is also a producer of exotoxins, which in some cases can serve as superantigens, and these have been previously described as playing an important role in the pathogenesis of CRSwNP (Bachert et al., 2008). *Pseudomonas aeruginosa* biofilms are also virulent organisms that are difficult to eradicate from the

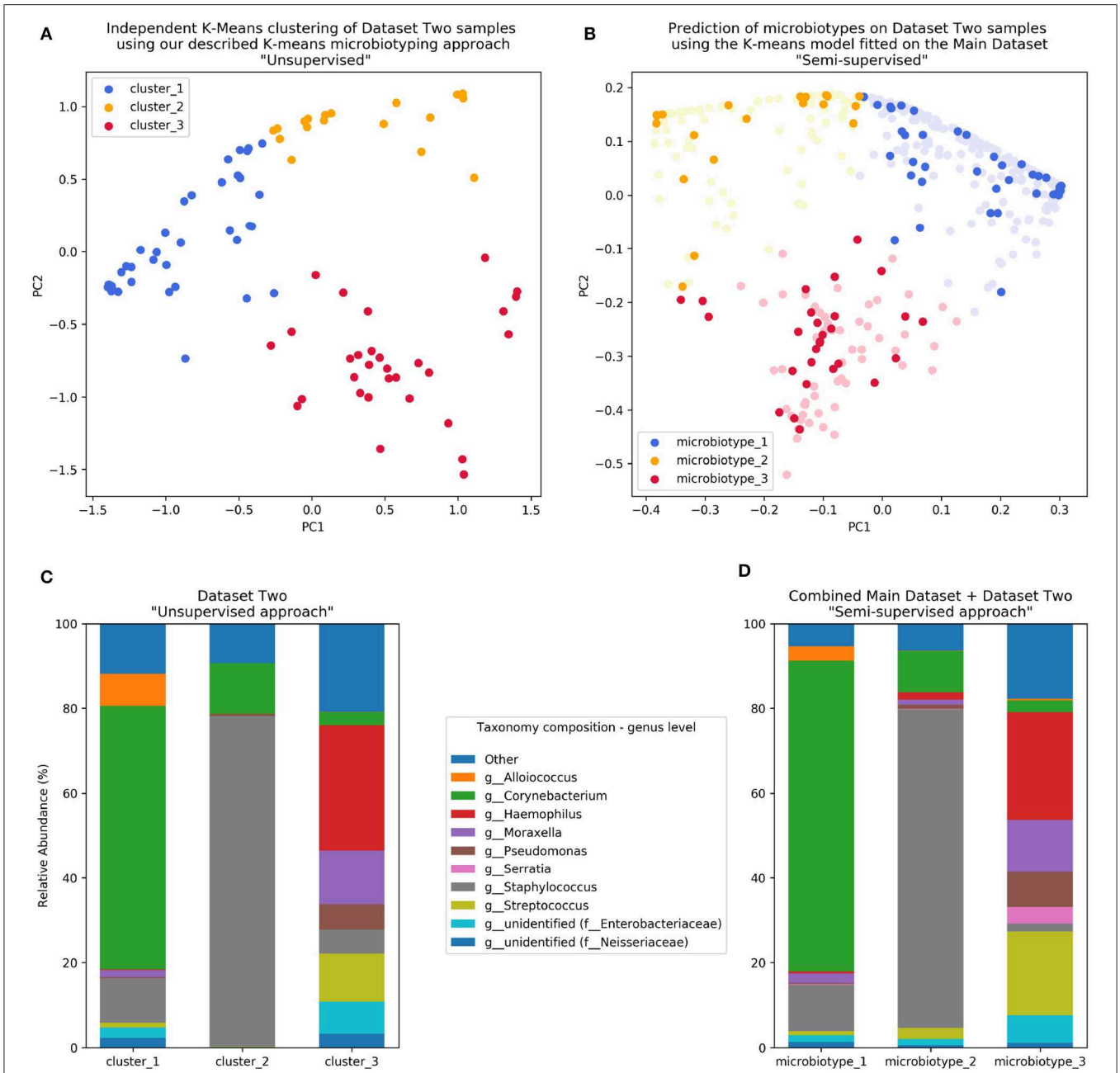

FIGURE 4 | Validation of microbiotyping approach on Dataset Two. **(A)** Independent K-Means clustering of Dataset Two samples using our described K-means microbiotyping approach "Unsupervised." **(B)** Prediction of microbiotypes on Dataset Two samples using the K-means model fitted on the Main Dataset "Semi-supervised." **(C)** Taxa composition of Dataset Two samples as per the "Unsupervised approach." **(D)** Taxa Composition of the combined Main Dataset and Dataset Two samples as per the "Semi-supervised approach."

sinuses, and have been associated with worse clinical outcomes (Bendouah et al., 2006). Both these organisms are important pathogens in the chronic mucociliary dysfunction exhibited in cystic fibrosis. However, methicillin-resistant *Staphylococcus aureus* (MRSA) is an important nasal colonizer that could asymptomatically colonize the nose. What determines the clinical course, between asymptomatic colonization vs. symptomatic pathogenicity, remains an interesting topic of research. In this study, we identified a potential reciprocal relationship between *Staphylococcus aureus* and *Corynebacterium*. Being aware of the challenges of compositional data analysis, we utilized for this purpose the specialized SparCC algorithm which infers correlations from compositional data (Friedman and Alm, 2012). This finding needs to be supported by future co-culture experiments, but suggests that *Corynebacterium* sp. may be a "cornerstone" of sinus microbial health. It is important to note that our bioinformatic methodology has been intentionally designed to utilize state-of-the-art software

methods at every step of the analysis pipeline, in order to maximize the resolution of taxonomy assignment (Amir et al., 2017; Bokulich et al., 2018; Bolyen et al., 2018). Nevertheless, our approach is still confined within the limitations of current 16S sequencing methodologies, and the confidence of assignment is reduced beyond the genus level. Our analysis pipeline could not delineate between different Corynebacteria at the species level and *Staphylococcus aureus* at the strain level. Hence functional difference between samples with same species remain to be determined using a functional metagenomics approach. A recent study suggest that by incorporating location information or "sample-level metadata" into species-level assignment accuracy could be improved (Kaehler et al., 2019). In our study, the differential relationships of both *Staphylococcus aureus* and *epidermidis* toward *Corynebacteria* (negative and positive associations, respectively) could be of clinical significance and is worthy of future investigation. We performed a *post-hoc* inspection of species-level assignment in Dataset Two, to investigate whether this finding will be reproducible in a separate dataset. This confirmed clustering of almost all *Staphylococcus aureus* species in microbiotype 2 (**Supplementary Results in Jupyter Notebook**).

The finding of a potential reciprocal relationship between *Staphylococcus aureus* and *Corynebacterium spp.* has to be placed in the context of similar previous findings from the literature. The competitive inhibition between *Staphylococcus aureus* and *Corynbacteria* were demonstrated in early studies *in vitro* (Parker and Simmons, 1959; Barrow, 1963). More recently, it has been shown that even these *S. aureus* strains that survive killing by Corynebacteria *in vitro* exhibit a decreased virulence profile (Ramsey et al., 2016; Hardy et al., 2019). *In vivo*, a negative correlation has been demonstrated between *Staphylococcus aureus* and various Corynbacterial species (including *C. accolens* and *C. pseudodiphthericum*) in the anterior nares in several studies (Uehara et al., 2000; Lina et al., 2003; Wos-Oxley et al., 2010; Johnson et al., 2015; Liu et al., 2015). Some interventional studies suggest a probiotic potential as *Corynebacteria* successfully reduced rates of Staphylococcal colonization when inoculated into the anterior nares (Uehara et al., 2000; Kiryukhina et al., 2013). Moreover, Johnson et al. (2015) showed that colonization of the anterior nares by *Corynebacteria* was associated with a lower prevalence of *S. aureus* related skin and soft tissue infections. In the paranasal sinuses, the previously-referenced study by Cope et al. (2017) is the first to demonstrate a reciprocal relationship between *Staphylococcaceae* and *Corynebacteriaceae*. In addition to competitive antagonism with *S. aureus*, the probiotic role of Corynebacteria includes its resistance to Respiratory Syncytial Virus and the pathologenic *Streptococcus pneumoniae*, demonstrated in an animal model (Kanmani et al., 2017). It also includes its contribution to the stability of the microbiome and the reduced incidence of Respiratory Tract Infections, where this has been demonstrated in children (Biesbroek et al., 2014; Bosch et al., 2017). On the other hand, the probiotic role of *Staphylococcus epidermidis* has been demonstrated in a murine nasal bacterial interaction model (Cleland et al., 2014).

The distribution of the sinonasal microbiotypes was found to be not significantly dis-similar amongst healthy controls and CRS patients. This result mirrored the findings of the traditional differential abundance approach undertaken in our first report (Paramasivan et al., 2020). There appeared to be no significant associations with other clinical variables such as asthma and aspirin-sensitivity after controlling for multiple comparisons (**Table 2**). The distribution of the microbiotypes however differed according to center/location of collection (**Figure 3**). As such, we cannot conclude based on our study that microbiotypes could function independently as a disease biomarker. It could be the case that chronicity of inflammation -on its own- is not a determinant of a dysbiotic microbiome, but whether there is a clinically-evident "sinus infection" current at the time of sample collection. In this theory, stable chronic sinuses with no overt signs of acute or chronic infection, may remain similar to a "healthy sinus microbiome." Only when the sinuses are clinically infected (as evident on clinical symptoms and endoscopic findings), the microbiota become disrupted and the dysbiosis exaggerated. It is important to note that *Streptococcus*, *Haemophilus,* and *Moraxella* (represented here in microbiotype 3) have been traditionally implicated in acute infections of the upper respiratory tract including acute rhinosinusitis and acute otitis media. Patients with clinically obvious acute exacerbations were not included in the original dataset (Paramasivan et al., 2020). An alternative possibility is that with advancing sequencing technology, and with complementary methods such as shotgun metagenomics or metatranscriptomics, we could unravel the constitution and function of sinonasal microbiotypes at a higher resolution in the future, which might uncover some difference between healthy and diseased states.

Asia and Australasia showed an over-representation of microbiotype 1. Europe had a higher prevalence of microbiotype 2. Unfortunately, the study only included one European center (Amsterdam) so it is difficult to be certain whether this finding generalizes to other locations in Europe. The driving factors for these geographical differences could be multiple, including but not limited to clinical practices such as local antibiotic prescriptions for CRS and timing of recruitment of patients for sinus surgery, as discussed previously (Paramasivan et al., 2020). And as mentioned in our previous analysis, it is difficult to conclude a "causative role" for geography given only our data (Paramasivan et al., 2020).

We have adapted our methodology from the enterotyping approach taken by Arumugam et al. (2011) for classifying bacterial signatures of the gut microbiome. In their original manuscript, they described three different enterotypes in the gut dominated by *Prevotella*, *Bacteroidetes*, and *Ruminococcus,* respectively (Arumugam et al., 2011). Several papers have correlated gut enterotypes with various clinical variables (Wu et al., 2011; Vandeputte et al., 2016). Despite this, enterotyping as an approach to population stratification has not been without its controversies. Several authors have criticized the definition of distinct clusters, since it neglects intra-cluster variation and gradients between clusters (Jeffery et al., 2012; Koren et al., 2013; Knights et al., 2014; Costea et al., 2018). We provide answers to previous critique (Knights et al., 2014) to enterotyping as it applies to our study in **Table S2**. It is important to note these valid criticisms to any community typing approach. In our

experiment, the clusters or types lie on a continuum, with some samples falling in the gradients between two, or perhaps even all three microbiotypes (see ordination plots). The histograms in **Figure 2** also suggest this, but they do show most samples in each microbiotype feature a high relative abundance of a dominating genus in many samples. We investigated a simple dominance measure, the Berger-Parker alpha diversity index (Berger and Parker, 1970), in the combined datasets' 507 samples. The Berger-Parker index simply reports the relative abundance of the most dominant taxon in a sample. This found that only 24.9% of samples had a dominating taxon that only had a relative abundance of 50% or less. On the other hand, 51.9% of samples had the dominant taxon exhibiting a relative abundance of >70% of the sample (**Supplementary Results in Jupyter Notebook**; **Figure S1**). This shows that in most samples, there is one dominating organism. Based on these results, the microbiotyping approach is therefore proposed to reduce complexity about modeling bacterial interactions in the sinuses, and not to suggest that each type is a walled-off discrete cluster. Further investigations into the local substructures of each type will be required to further explore the roles and interactions of its constituent taxa. Another limitation of our description of microbiotypes is that they may as well-describe different community "states" rather than community "types," since we do not have longitudinal data to describe how these clusters behave with the passage of time and treatments. Hence, we could not confirm whether these are stable, consistent communities across time. It may well be that intermediate samples lying between two or more microbiotypes are representing a transitional state. An important future avenue of research is to conduct a longitudinal study to investigate the temporal stability of these clusters.

We predict that ongoing sinonasal microbiome research and consequent large meta-analyses of microbiota studies, with novel meta-analytic tools and platforms (Gonzalez et al., 2018) enabling such large-scale studies, will allow the refinement of these types and further clarify their clinical/microbiological utility. Our methodological approach to describe the microbiotypes is not exclusive, as alternative statistical or machine-learning approaches could be employed to investigate them. In light of this, we expect that international multi-center standardization and rationalization of the sinonasal microbiotypes would be possible in the future, similar to the recent proposed effort to standardize enterotyping of the gut microbiota by Costea et al. (2018).

CONCLUSION

We examined our International Sinonasal Microbiome Study 16S dataset through an approach modeled on human gut microbiome enterotyping and we found three major microbial community types or "microbiotypes" as clusters that lie on a continuum, based on an unsupervised machine learning approach that involved dimensionality reduction and clustering. Microbiotypes did not show an association with disease state or clinical variable, suggesting that they could not function as independent disease biomarkers. The description of these microbiotypes has also unveiled a potential reciprocal relationship between *Staphylococcus aureus* and *Corynebacterium* spp. in the sinuses that requires further investigation in future studies. The findings were validated on a separate previously unpublished sinus bacterial 16S gene dataset. Microbiotypes are therefore proposed to reduce the complexity of modeling bacterial interactions in the sinuses, and in this sense hold microbiological and clinical relevance.

DATA AVAILABILITY STATEMENT

Sequencing data for this article has been uploaded to the figshare repository. The international sinonasal microbiome study (ISMS) Dataset could be found at this https://doi.org/10.6084/m9.figshare.11871420. Sequencing data for the Sinonasal Microbiotypes Dataset Two could be found at this https://doi.org/10.6084/m9.figshare.8015198.

ETHICS STATEMENT

The studies involving human participants were reviewed and approved by the Queen Elizabeth Hospital Human Research Ethics Committee (approval HREC/14/TQEHLMH/222). The patients/participants provided their written informed consent to participate in this study. The project was approved by the respective institutional human research ethics boards of all sample-collection centres. The details of all ethics applications are provided in **Table S1** in the original ISMS publication (Paramasivan et al., 2020).

AUTHOR'S NOTE

This manuscript has been released as a Pre-Print at https://www.biorxiv.org/content/10.1101/549311v3 (Bassiouni et al., 2019).

AUTHOR CONTRIBUTIONS

AB wrote primary and revised versions of manuscript and main data analysis. SP, AS, MD, and JC shared in analyzing the data. JC provided bioinformatics QIIME 2 pipeline design, data analysis supervision and critique. EC provided data analysis consultation. JC, EC, AP, SV, and P-JW provided critical review and edits of manuscript drafts. MA, BB, CCa, MC, RD, DD, CG, RH, PH, AL, RS, PT, MT, P-JW, and AP sample collection. CCo, MR, and SM processed samples for sequencing. AP conceived project idea, collaborations, and design. All authors read and approved the final manuscript.

SUPPLEMENTARY MATERIAL

The Supplementary Material for this article can be found online at: https://www.frontiersin.org/articles/10.3389/fcimb.2020.00137/full#supplementary-material

REFERENCES

Amir, A., McDonald, D., Navas-Molina, J. A., Kopylova, E., Morton, J. T., Zech Xu, Z., et al. (2017). Deblur rapidly resolves single-nucleotide community sequence patterns. *mSystems*. 2:e00191-16. doi: 10.1128/mSystems.00191-16

Arumugam, M., Raes, J., Pelletier, E., Le Paslier, D., Yamada, T., Mende, D. R., et al. (2011). Enterotypes of the human gut microbiome. *Nature* 473, 174–180. doi: 10.1038/nature09944

Bachert, C., Zhang, N., Patou, J., van Zele, T., and Gevaert, P. (2008). Role of Staphylococcal superantigens in upper airway disease. *Curr. Opin. Allergy Clin. Immunol.* 8, 34–38. doi: 10.1097/ACI.0b013e3282f4178f

Barrow, G. I. (1963). Microbial antagonism by *Staphylococcus aureus*. *Microbiology* 31, 471–481. doi: 10.1099/00221287-31-3-471

Bassiouni, A., Paramasivan, S., Shiffer, A., Dillon, M. R., Cope, E. K., Cooksley, C., et al. (2019). Microbiotyping the sinonasal microbiome. *bioRxiv* 549311. doi: 10.1101/549311

Bauer, M. A., Kainz, K., Carmona-Gutierrez, D., and Madeo, F. (2018). Microbial wars: competition in ecological niches and within the microbiome. *Microb. Cell* 5, 215–219. doi: 10.15698/mic2018.05.628

Beisner, B. E., Haydon, D. T., and Cuddington, K. (2003). Alternative stable states in ecology. *Front. Ecol. Environ.* 1, 376–382. doi: 10.1890/1540-9295(2003)001<0376:ASSIE>2.0.CO;2

Bendouah, Z., Barbeau, J., Hamad, W. A., and Desrosiers, M. (2006). Biofilm formation by *Staphylococcus aureus* and *Pseudomonas aeruginosa* is associated with an unfavorable evolution after surgery for chronic sinusitis and nasal polyposis. *Otolaryngol. Head Neck Surg.* 134, 991–996. doi: 10.1016/j.otohns.2006.03.001

Berger, W. H., and Parker, F. L. (1970). Diversity of planktonic foraminifera in deep-sea sediments. *Science* 168, 1345–1347. doi: 10.1126/science.168.3937.1345

Biesbroek, G., Tsivtsivadze, E., Sanders, E. A. M., Montijn, R., Veenhoven, R. H., Keijser, B. J. F., et al. (2014). Early respiratory microbiota composition determines bacterial succession patterns and respiratory health in children. *Am. J. Respir. Crit. Care Med.* 190, 1283–1292. doi: 10.1164/rccm.201407-1240OC

Biswas, K., Hoggard, M., Jain, R., Taylor, M. W., and Douglas, R. G. (2015). The nasal microbiota in health and disease: variation within and between subjects. *Front. Microbiol.* 9:134. doi: 10.3389/fmicb.2015.00134

Bokulich, N. A., Kaehler, B. D., Rideout, J. R., Dillon, M., Bolyen, E., Knight, R., et al. (2018). Optimizing taxonomic classification of marker-gene amplicon sequences with QIIME 2's q2-feature-classifier plugin. *Microbiome* 6:90. doi: 10.1186/s40168-018-0470-z

Bokulich, N. A., Subramanian, S., Faith, J. J., Gevers, D., Gordon, J. I., Knight, R., et al. (2013). Quality-filtering vastly improves diversity estimates from Illumina amplicon sequencing. *Nat. Methods* 10, 57–59. doi: 10.1038/nmeth.2276

Bolyen, E., Rideout, J. R., Dillon, M. R., Bokulich, N. A., Abnet, C., Al-Ghalith, G. A., et al. (2018). QIIME 2: reproducible, interactive, scalable, and extensible microbiome data science. *PeerJ. Preprints* 6: e27295v1. doi: 10.7287/peerj.preprints.27295v2

Bosch, A. A. T. M., de Steenhuijsen Piters, W. A. A., van Houten, M. A., Chu, M. L. J. N., Biesbroek, G., Kool, J., et al. (2017). Maturation of the infant respiratory microbiota, environmental drivers, and health consequences. a prospective cohort study. *Am. J. Respir. Critic. Care Med.* 196, 1582–1590. doi: 10.1164/rccm.201703-0554OC

Brugger, S. D., Bomar, L., and Lemon, K. P. (2016). Commensal-pathogen interactions along the human nasal passages. *PLoS Pathog.* 12:e1005633. doi: 10.1371/journal.ppat.1005633

Caporaso, J. G., Lauber, C. L., Costello, E. K., Berg-Lyons, D., Gonzalez, A., Stombaugh, J., et al. (2011). Moving pictures of the human microbiome. *Genome Biol.* 12:R50. doi: 10.1186/gb-2011-12-5-r50

Chan, C. L., Wabnitz, D., Bardy, J. J., Bassiouni, A., Wormald, P.-J., Vreugde, S., et al. (2016). The microbiome of otitis media with effusion. *Laryngoscope* 126, 2844–2851. doi: 10.1002/lary.26128

Cleland, E. J., Drilling, A., Bassiouni, A., James, C., Vreugde, S., and Wormald, P.-J. (2014). Probiotic manipulation of the chronic rhinosinusitis microbiome. *Int. Forum Allergy Rhinol.* 4, 309–314. doi: 10.1002/alr.21279

Cope, E. K., Goldberg, A. N., Pletcher, S. D., and Lynch, S. V. (2017). Compositionally and functionally distinct sinus microbiota in chronic rhinosinusitis patients have immunological and clinically divergent consequences. *Microbiome* 5:53. doi: 10.1186/s40168-017-0266-6

Costea, P. I., Hildebrand, F., Arumugam, M., Bäckhed, F., Blaser, M. J., Bushman, F. D., et al. (2018). Enterotypes in the landscape of gut microbial community composition. *Nat. Microbiol.* 3, 8–16. doi: 10.1038/s41564-017-0072-8

Costello, E. K., Lauber, C. L., Hamady, M., Fierer, N., Gordon, J. I., and Knight, R. (2009). Bacterial community variation in human body habitats across space and time. *Science* 326, 1694–1697. doi: 10.1126/science.1177486

Coyte, K. Z., Schluter, J., and Foster, K. R. (2015). The ecology of the microbiome: networks, competition, and stability. *Science* 350, 663–666. doi: 10.1126/science.aad2602

DeSantis, T. Z., Hugenholtz, P., Larsen, N., Rojas, M., Brodie, E. L., Keller, K., et al. (2006). Greengenes, a chimera-checked 16S rRNA gene database and workbench compatible with ARB. *Appl. Environ. Microbiol.* 72, 5069–5072. doi: 10.1128/AEM.03006-05

Drilling, A., Coombs, G. W., Tan, H.-L., Pearson, J. C., Boase, S., Psaltis, A., et al. (2014). Cousins, siblings, or copies: The genomics of recurrent Staphylococcus aureus infections in chronic rhinosinusitis. *Int. Forum Allergy Rhinol.* 4, 953–960. doi: 10.1002/alr.21423

Faust, K., and Raes, J. (2012). Microbial interactions: from networks to models. *Nat. Rev. Microbiol.* 10, 538–550. doi: 10.1038/nrmicro2832

Fokkens, W. J., Lund, V. J., Mullol, J., Bachert, C., Alobid, I., Baroody, F., et al. (2012). EPOS 2012: European position paper on rhinosinusitis and nasal polyps A summary for otorhinolaryngologists. *Rhinology* (2012) 50, 1–12. doi: 10.4193/Rhino50E2

Foreman, A., and Wormald, P.-J. (2010). Different biofilms, different disease? A clinical outcomes study. *Laryngoscope* 120, 1701–1706. doi: 10.1002/lary.21024

Friedman, J., and Alm, E. J. (2012). Inferring correlation networks from genomic survey data. *PLoS Comput. Biol.* 8:e1002687. doi: 10.1371/journal.pcbi.1002687

Gonzalez, A., Navas-Molina, J. A., Kosciolek, T., McDonald, D., Vázquez-Baeza, Y., Ackermann, G., et al. (2018). Qiita: rapid, web-enabled microbiome meta-analysis. *Nat. Methods* 15, 796–798. doi: 10.1038/s41592-018-0141-9

Hardy, B. L., Dickey, S. W., Plaut, R. D., Riggins, D. P., Stibitz, S., Otto, M., et al. (2019). *Corynebacterium pseudodiphtheriticum* exploits *Staphylococcus aureus* virulence components in a novel polymicrobial defense strategy. *Mbio* 10:e02491-18. doi: 10.1128/mBio.02491-18

Janssen, S., McDonald, D., Gonzalez, A., Navas-Molina, J. A., Jiang, L., Xu, Z. Z., et al. (2018). Phylogenetic placement of exact amplicon sequences improves associations with clinical information. *mSystems*. 3:e00021-18. doi: 10.1128/mSystems.00021-18

Jeffery, I. B., Claesson, M. J., O'Toole, P. W., and Shanahan, F. (2012). Categorization of the gut microbiota: enterotypes or gradients? *Nat. Rev. Microbiol.* 10, 591–592. doi: 10.1038/nrmicro2859

Jervis-Bardy, J., Foreman, A., Boase, S., Valentine, R., and Wormald, P.-J. (2011). What is the origin of *Staphylococcus aureus* in the early postoperative sinonasal cavity? *Int. Forum Allergy Rhinol.* 1, 308–312. doi: 10.1002/alr.20050

Johnson, R. C., Ellis, M. W., Lanier, J. B., Schlett, C. D., Cui, T., and Merrell, D. S. (2015). Correlation between nasal microbiome composition and remote purulent skin and soft tissue infections. *Infect. Immun.* 83, 802–811. doi: 10.1128/IAI.02664-14

Kaehler, B. D., Bokulich, N. A., McDonald, D., Knight, R., Caporaso, J. G., Huttley, G. A. (2019). Species abundance information improves sequence taxonomy classification accuracy. *Nat Commun.* 10:4643. Available online at: https://www.nature.com/articles/s41467-019-12669-6

Kanmani, P., Clua, P., Vizoso-Pinto, M. G., Rodriguez, C., Alvarez, S., Melnikov, V., et al. (2017). Respiratory commensal bacteria *Corynebacterium pseudodiphtheriticum* improves resistance of infant mice to respiratory syncytial virus and *Streptococcus pneumoniae* superinfection. *Front. Microbiol.* 8:1613. doi: 10.3389/fmicb.2017.01613

Kiryukhina, N. V., Melnikov, V. G., Suvorov, A. V., Morozova, Y. A., and Ilyin, V. K. (2013). Use of *Corynebacterium pseudodiphtheriticum* for elimination of *Staphylococcus aureus* from the nasal cavity in volunteers exposed to abnormal microclimate and altered gaseous environment. *Probiotics Antimicrob. Proteins* 5, 233–238. doi: 10.1007/s12602-013-9147-x

Kluyver, T., Ragan-Kelley, B., Pérez, F., Granger, B., Bussonnier, M., Frederic, J., et al. (2016). "Jupyter notebooks a publishing format for reproducible computational workflows," in *Positioning and Power in Academic Publishing: Players, Agents and Agendas*, eds F. Loizides and B. Scmidt (Göttingen: IOS Press), 87–90.

Knights, D., Ward, T. L., McKinlay, C. E., Miller, H., Gonzalez, A., McDonald, D., et al. (2014). Rethinking "enterotypes". *Cell Host Microbe* 16, 433–437. doi: 10.1016/j.chom.2014.09.013

Koren, O., Knights, D., Gonzalez, A., Waldron, L., Segata, N., Knight, R., et al. (2013). A guide to enterotypes across the human body: meta-analysis of microbial community structures in human microbiome datasets. *PLoS Comput. Biol.* 9:e1002863. doi: 10.1371/journal.pcbi.1002863

Legendre, P., and Legendre, L. (2012). *Numerical Ecology*. Amsterdam; Boston, MA: Elsevier.

Lewontin, R. C. (1969). The meaning of stability. *Brookhaven Symp. Biol.* 22, 13–24.

Lidicker, W. Z. (1979). A clarification of interactions in ecological systems. *Bioscience* 29, 475–477. doi: 10.2307/1307540

Lina, G., Boutite, F., Tristan, A., Bes, M., Etienne, J., and Vandenesch, F. (2003). Bacterial competition for human nasal cavity colonization: role of Staphylococcal agr alleles. *Appl. Environ. Microbiol.* 69, 18–23. doi: 10.1128/AEM.69.1.18-23.2003

Liu, C. M., Price, L. B., Hungate, B. A., Abraham, A. G., Larsen, L. A., Christensen, K., et al. (2015). *Staphylococcus aureus* and the ecology of the nasal microbiome. *Sci. Adv.* 1:e1400216. doi: 10.1126/sciadv.1400216

Lozupone, C. A., Stombaugh, J. I., Gordon, J. I., Jansson, J. K., and Knight, R. (2012). Diversity, stability and resilience of the human gut microbiota. *Nature* 489, 220–230. doi: 10.1038/nature11550

Mandal, S., Van Treuren, W., White, R. A., Eggesb,ø, M., Knight, R., and Peddada, S. D. (2015). Analysis of composition of microbiomes: a novel method for studying microbial composition. *Microb. Ecol. Health Dis.* 26:27663. doi: 10.3402/mehd.v26.27663

May, R. M. (1974). *Stability and Complexity in Model Ecosystems*. 2nd Edn. Princeton, NJ: Princeton University Press.

McInnes, L., Healy, J., and Astels, S. (2017). Hdbscan: hierarchical density based clustering. *J. Open Sour. Sof.* 2:205. doi: 10.21105/joss.00205

Olesen, S. W., and Alm, E. J. (2016). Dysbiosis is not an answer. *Nat. Microbiol.* 1:16228. doi: 10.1038/nmicrobiol.2016.228

Oliphant, T. E. (2007). Python for scientific computing. *Comput. Sci. Eng.* 9, 10–20. doi: 10.1109/MCSE.2007.58

Paramasivan, S., Bassiouni, A., Shiffer, A., Dillon, M. R., Cope E. K., Cooksley, C., et al. (2020). The international sinonasal microbiome study (ISMS): a multi-centre, multi-national characterization of sinonasal bacterial ecology. *Allergy*. doi: 10.1111/all.14276

Parker, M. T., and Simmons, L. E. (1959). The inhibition of *Corynebacterium diphtheriae* and other gram-positive organisms by *Staphylococcus aureus*. *J. Gen. Microbiol.* 21, 457–476. doi: 10.1099/00221287-21-2-457

Pedregosa, F., Varoquaux, G., Gramfort, A., Michel, V., Thirion, B., Grisel, O., et al. (2011). Scikit-learn: machine learning in python. *J. Mach. Learn. Res.* 12, 2825–2830. doi: 10.5555/1953048.2078195

Psaltis, A. J., Weitzel, E. K., Ha, K. R., and Wormald, P.-J. (2008). The effect of bacterial biofilms on post-sinus surgical outcomes. *Am. J. Rhinol.* 22, 1–6. doi: 10.2500/ajr.2008.22.3119

Ramsey, M. M., Freire, M. O., Gabrilska, R. A., Rumbaugh, K. P., and Lemon, K. P. (2016). *Staphylococcus aureus* shifts toward commensalism in response to *Corynebacterium* species. *Front. Microbiol.* 7:1230. doi: 10.3389/fmicb.2016.01230

Singhal, D., Foreman, A., Bardy, J.-J., and Wormald, P.-J. (2011). Staphylococcus aureus biofilms: nemesis of endoscopic sinus surgery. *Laryngoscope* 121, 1578–1583. doi: 10.1002/lary.21805

Thompson, L. R., Sanders, J. G., McDonald, D., Amir, A., Ladau, J., Locey, K. J., et al. (2017). A communal catalogue reveals Earth's multiscale microbial diversity. *Nature* 551, 457–463. doi: 10.1038/nature24621

Uehara, Y., Nakama, H., Agematsu, K., Uchida, M., Kawakami, Y., Abdul Fattah, A. S., et al. (2000). Bacterial interference among nasal inhabitants: eradication of *Staphylococcus aureus* from nasal cavities by artificial implantation of *Corynebacterium* sp. *J. Hosp. Infect.* 44, 127–133. doi: 10.1053/jhin.1999.0680

Vandeputte, D., Falony, G., Vieira-Silva, S., Tito, R. Y., Joossens, M., and Raes, J. (2016). Stool consistency is strongly associated with gut microbiota richness and composition, enterotypes and bacterial growth rates. *Gut* 65, 57–62. doi: 10.1136/gutjnl-2015-309618

Wagner Mackenzie, B., Waite, D. W., Hoggard, M., Douglas, R. G., Taylor, M. W., and Biswas, K. (2017). Bacterial community collapse: a meta-analysis of the sinonasal microbiota in chronic rhinosinusitis. *Environ. Microbiol.* 19, 381–392. doi: 10.1111/1462-2920.13632

Wang, J., Zhang, Q., Wu, G., Zhang, C., Zhang, M., and Zhao, L. (2018). Minimizing spurious features in 16S rRNA gene amplicon sequencing. *PeerJ Preprints* 6:e26872v1. doi: 10.7287/peerj.preprints.26872v1

Watts, S. C., Ritchie, S. C., Inouye, M., and Holt, K. E. (2018). FastSpar: rapid and scalable correlation estimation for compositional data. *bioRxiv* 272583. doi: 10.1101/272583

Wos-Oxley, M. L., Plumeier, I., von Eiff, C., Taudien, S., Platzer, M., Vilchez-Vargas, R., et al. (2010). A poke into the diversity and associations within human anterior nare microbial communities. *ISME J.* 4, 839–851. doi: 10.1038/ismej.2010.15

Wu, G. D., Chen, J., Hoffmann, C., Bittinger, K., Chen, Y.-Y., Keilbaugh, S. A., et al. (2011). Linking long-term dietary patterns with gut microbial enterotypes. *Science* 334, 105–108. doi: 10.1126/science.1208344

Yu, Y., Lee, C., Kim, J., and Hwang, S. (2005). Group-specific primer and probe sets to detect methanogenic communities using quantitative real-time polymerase chain reaction. *Biotechnol. Bioeng.* 89, 670–679. doi: 10.1002/bit.20347

Zhang, J., Kobert, K., Flouri, T., and Stamatakis, A. (2014). PEAR: a fast and accurate illumina paired-end reAd mergeR. *Bioinformatics* 30, 614–620. doi: 10.1093/bioinformatics/btt593

Conflict of Interest: MA receives royalties from Springer for his treatise Principles and Practice of Lacrimal Surgery and Atlas of Lacrimal Drainage Disorders. BB received grant funding R01 NS108968-01 NIH/NINDS; and is a consultant for: Gyrus ACMI Olympus, Canon, Karl Storz, Medtronic, and Sinopsys; and has equity in: Cerebent, Inc., Arrinex. The work of JC, MD, and AS was funded in part by National Science Foundation Award 1565100 to JC. The work of EC was partially funded under the State of Arizona Technology and Research Initiative Fund (TRIF), administered by the Arizona Board of Regents, through Northern Arizona University. RD received consultancy fees from Lyra Therapeutics and is a consultant for Medtronic. RH is a consultant with Medtronic, Olympus and NeilMed pharmaceuticals, and has been on the speakers' bureau for Glaxo-Smith-Kline, Seqirus and Astra-Zeneca. PH has consultancies with Arrinex, Bioinspire, Canon, Lyra Therapeutics, Medtronic, Tivic. AL serves as a consultant for Aerin Medical (Sunnyvale, CA), Arrinex (Redwood City, CA), Lyra Therapeutics (Watertown, MA), and Stryker (Kalamazoo, MI) and is on the advisory board for ENTvantage (Austin, TX). AL's department receives funding from Genetech/Roche (San Francisco, CA) and AstraZeneca (Cambridge, England). SP is supported by a Garnett Passe and Rodney Williams Memorial Foundation Academic Surgeon Scientist Research Scholarship. AP is a consultant for Aerin Devices and ENT technologies and is on the speakers' bureau for Smith and Nephew, and received consultancy fees from Lyra Therapeutics. RS received grant support from OptiNose, Entellus, and Intersect ENT and is a consultant for Olympus, Meda, and Arrinex. MT is a principal Investigator for Sanofi, Roche/Genentech, AstraZeneca; and speaker/consultant for Stryker, Ondine Biomedical, Novartis, MEDA, Mylan; and receives royalties for book sales from Thieme. P-JW receives royalties from Medtronic, Integra, and Scopis, and is a consultant for NeilMed.

The remaining authors declare that the research was conducted in the absence of any commercial or financial relationships that could be construed as a potential conflict of interest.

frontiers in Cellular and Infection Microbiology

ORIGINAL RESEARCH
published: 28 April 2020
doi: 10.3389/fcimb.2020.00174

Longitudinal Associations of the Cystic Fibrosis Airway Microbiome and Volatile Metabolites: A Case Study

Andrea Hahn[1,2,3], Katrine Whiteson[4], Trenton J. Davis[5,6], Joann Phan[4], Iman Sami[2,7], Anastassios C. Koumbourlis[2,7], Robert J. Freishtat[2,8], Keith A. Crandall[9] and Heather D. Bean[5,6]**

[1] Division of Infectious Diseases, Children's National Health System, Washington, DC, United States, [2] Department of Pediatrics, George Washington University School of Medicine and Health Sciences, Washington, DC, United States, [3] Center for Genetic Medicine Research, The Children's Research Institute, Washington, DC, United States, [4] Department of Molecular Biology and Biochemistry, University of California at Irvine, Irvine, CA, United States, [5] School of Life Sciences, Arizona State University, Tempe, AZ, United States, [6] Center for Fundamental and Applied Microbiomics, The Biodesign Institute, Arizona State University, Tempe, AZ, United States, [7] Division of Pulmonary and Sleep Medicine, Children's National Health System, Washington, DC, United States, [8] Division of Emergency Medicine, Children's National Health System, Washington, DC, United States, [9] Computational Biology Institute and Department of Biostatistics & Bioinformatics, Milken Institute School of Public Health, George Washington University, Washington, DC, United States

OPEN ACCESS

Edited by:
Steven D. Pletcher, University of California, San Francisco, United States

Reviewed by:
Patrick J. Pirrotte, Translational Genomics Research Institute, United States
Sarah Maddocks, Cardiff Metropolitan University, United Kingdom

***Correspondence:**
Andrea Hahn
alhahn@childrensnational.org
Heather D. Bean
Heather.D.Bean@asu.edu

Specialty section:
This article was submitted to Microbiome in Health and Disease, a section of the journal Frontiers in Cellular and Infection Microbiology

Received: 04 September 2019
Accepted: 01 April 2020
Published: 28 April 2020

Citation:
Hahn A, Whiteson K, Davis TJ, Phan J, Sami I, Koumbourlis AC, Freishtat RJ, Crandall KA and Bean HD (2020) Longitudinal Associations of the Cystic Fibrosis Airway Microbiome and Volatile Metabolites: A Case Study. Front. Cell. Infect. Microbiol. 10:174. doi: 10.3389/fcimb.2020.00174

The identification of 16S rDNA biomarkers from respiratory samples to describe the continuum of clinical disease states within persons having cystic fibrosis (CF) has remained elusive. We sought to combine 16S, metagenomics, and metabolomics data to describe multiple transitions between clinical disease states in 14 samples collected over a 12-month period in a single person with CF. We hypothesized that each clinical disease state would have a unique combination of bacterial genera and volatile metabolites as a potential signature that could be utilized as a biomarker of clinical disease state. Taxonomy identified by 16S sequencing corroborated clinical culture results, with the majority of the 109 PCR amplicons belonging to the bacteria grown in clinical cultures (*Escherichia coli* and *Staphylococcus aureus*). While alpha diversity measures fluctuated across disease states, no significant trends were present. Principle coordinates analysis showed that treatment samples trended toward a different community composition than baseline and exacerbation samples. This was driven by the phylum Bacteroidetes (less abundant in treatment, $\log_2$ fold difference -3.29, $p = 0.015$) and the genus *Stenotrophomonas* (more abundant in treatment, $\log_2$ fold difference 6.26, $p = 0.003$). Across all sputum samples, 466 distinct volatile metabolites were identified with total intensity varying across clinical disease state. Baseline and exacerbation samples were rather uniform in chemical composition and similar to one another, while treatment samples were highly variable and differed from the other two disease states. When utilizing a combination of the microbiome and metabolome data, we observed associations between samples dominated *Staphylococcus* and *Escherichia* and higher relative abundances of alcohols, while samples dominated by *Achromobacter* correlated with a metabolomics shift toward more oxidized volatiles. However, the microbiome and metabolome data were not tightly correlated; examining both the metagenomics and

metabolomics allows for more context to examine changes across clinical disease states. In our study, combining the sputum microbiome and metabolome data revealed stability in the sputum composition through the first exacerbation and treatment episode, and into the second exacerbation. However, the second treatment ushered in a prolonged period of instability, which after three additional exacerbations and treatments culminated in a new lung microbiome and metabolome.

Keywords: cystic fibrosis, microbiome, metabolome, pulmonary medicine, pediatrics

INTRODUCTION

Cystic fibrosis (CF) is a genetic disease affecting more than 30,000 people in the United States, associated with both intermittent and chronic suppurative lung infections (Wagener et al., 2013; MacKenzie et al., 2014). For the past 15 years, 16S rDNA amplicon sequencing has been a commonly used research methodology to describe the microbiota within the CF airway (Rogers et al., 2004; Harris et al., 2007; Guss et al., 2011). While most studies are cross-sectional, a small number of longitudinal studies have been performed to determine if unique microbial signatures correspond with clinical state before and after the onset of a pulmonary exacerbation, a clinical disease state associated with increased respiratory symptoms, increased airway inflammation, and decreased pulmonary function (Zhao et al., 2012; Carmody et al., 2013; Zemanick et al., 2013). These longitudinal studies have revealed that each CF subject harbors a distinct microbial community, making broad interpretations across persons with CF that could be used in clinical practice elusive (Caverly and LiPuma, 2018). More recent studies have employed unbiased whole genome shotgun sequencing techniques, which can provide more granular information, including species, and strain specificity (Moran Losada et al., 2014; Bacci et al., 2017; Feigelman et al., 2017; Hahn et al., 2018a).

Current clinical practice relies on culturing pathogens from sputum samples, however, culture-independent approaches such as the 16S rDNA amplicon sequencing described above have revealed that CF airways are dominated by bacteria from two main populations: slow-growing opportunistic pathogens (e.g., *Pseudomonas aeruginosa*, *Stenotrophomonas maltophilia*, *Burkholderia cepacia* and others), and anaerobes common to the oral cavity that migrate to the airways in the context of poor mucociliary clearance (e.g., *Streptococcus* spp., *Rothia mucilaginosa* and others). Metabolomics offers another culture independent approach to profile clinical samples. A few studies investigating different classes of metabolites from CF breath and sputum have emerged, although it is difficult to determine whether the molecules have human or microbial origin. One study using parallel breath metabolomics and shotgun sequencing found that a microbial fermentation product, 2,3-butanedione, was associated with *Streptococcus* spp. and *Rothia mucilaginosa*, and became less abundant after treatment for pulmonary exacerbation (Whiteson et al., 2014). These data, in combination with studies that are identifying volatile metabolite signatures associated with common CF pathogens in culture (Bean et al., 2016; Bos et al., 2016; Phan et al., 2017; Nasir et al., 2018) and the host's immune response to infection (Bean et al., 2015), suggest that there may be changes in the volatile metabolome of an exacerbation that correspond to microbiome changes. The volatile metabolome may be able to complement genomics as an additional culture-independent method for identifying exacerbation onset and recovery, and/or understanding the root causes of these events.

These factors influenced our initial motivation to identify associations between bacterial genera and volatile metabolites within CF sputum that tracked with variations in clinical state (baseline, exacerbation, and treatment). The objective of this study was to identify the level of intra-person variability between clinical states by deeply examining a single person with CF as a case study that could inform study design in a larger cohort of study participants. We hypothesized that specific associations between bacterial genera and volatile metabolites would be reflective of changes between clinical states.

MATERIALS AND METHODS

Setting and Study Population

This is a study of a single young child with cystic fibrosis (homozygous F508del) with respiratory samples and clinical data collected across five acute pulmonary exacerbations over a 12 month period. The samples used in this study were from a larger prospective, longitudinal study conducted at Children's National Health System (CNHS) (Hahn et al., 2019). The study was approved 02/20/15 by the Institutional Review Board (Pro5655) at CNHS. Parental consent was obtained for the study participant prior to respiratory sample collection and extraction of data from electronic medical records.

Subject Encounters

Respiratory samples and clinical data were collected at three research encounter types. The first encounter occurred when the study participant was being seen for a regular clinic visit and had not received intravenous (IV) antibiotics for at least 30 days prior (Baseline, B) (Zhao et al., 2012). The next encounter occurred when the study participant presented for a sick visit with at least 4 of 12 Fuchs criteria present and hospital admission for administration of IV antibiotics was required (Exacerbation, E) (Fuchs et al., 1994). The third encounter type occurred while the study participant was on antibiotic therapy (Treatment, T). A new baseline sample was obtained at the study participant's next follow up visit, at least 30 days after completion of antibiotic therapy. However, if the study participant's next exacerbation

occurred prior to the 30 day window, the time point was treated as an exacerbation. During each encounter, a sputum respiratory sample was obtained and corresponding clinical data were collected. Lung function testing was collected clinically following ATS spirometry guidelines and were reported using NHANES III reference values (National Center for Health Statistics, 2001; Miller et al., 2005).

Respiratory Sample Collection, Storage, and Processing

Sputum samples were obtained from the study participant using sterile collection cups and were stored at 4°C for up to 24 h prior to processing. Sputum samples were homogenized in the following manner: washed 1:1 v/v with sterile normal saline, mixed 1:1 v/v with dithiothreitol (DTT; Sputasol, Fisher Healthcare, Houston TX), vortexed, and heated in a 37°C heated water bath for 10 min. Samples were then pelleted through centrifugation (12,000 g × 10 min). Supernatants were removed and stored at −80°C until they were analyzed for volatile metabolites. Cell pellets were frozen at −80°C until they underwent DNA extraction.

DNA Extraction

Sample pellets were thawed and a 500 μL combination of lysozyme (20 mg/mL, Sigma-Aldrich, St. Louis MO) and lysostaphin (200 μg/mL, Sigma-Aldrich, St. Louis MO) was applied to chemically lyse the bacterial cell walls. DNA extraction was then performed using the DSP Virus/Pathogen Midi Kit and the Complex800_V6_DSP protocol on the QIAsymphony SP (Qiagen, Valencia CA).

Next Generation Sequencing and Bioinformatics

Sequencing of all samples was performed by the University of Michigan Host Microbiome Initiative (Ann Arbor MI) according to published protocols (Kozich et al., 2013; Seekatz et al., 2015). Briefly, extracted DNA was amplified for the V4 region of the 16S rRNA gene (16S rDNA) using PCR primers (forward primer GTGCCAGCMGCCGCGGTAA; reverse primer TAATCTWTGGGVHCATCAGG) (Kozich et al., 2013). The PCR cycle was as follows: 95°C × 2 min (1x); 95°C × 20 s, 55°C × 15 s, 72°C × 5 min (30x); 72°C × 10 min (1X); 4°C (until sequencing). Libraries were normalized using SequalPrep Normalization Plate Kit (Life Technologies, Carlsbad CA), and concentration measured using Kapa Biosystems Library Quantification Kit (Kapa Biosystems, Wilmington MA). A MiSeq sequencing platform was used to perform the dual-index sequencing strategy, resulting in paired-end reads of ∼250 basepairs (bp). Raw FASTQ files were processed in mothur (version 1.39.5), utilizing default settings outlined on the MiSeq SOP (https://www.mothur.org/wiki/MiSeq_SOP, accessed 8 FEB 2018) to generate operational taxonomic unit (OTU) tables (Schloss et al., 2009; Kozich et al., 2013). Specifically, this included the following steps: (1) combining paired reads (quality scores per base had to be > 25 minimum for paired gap sequence and 6 points better than paired mismatch; otherwise the consensus base was set to an N); (2) removing sequences > 275 bp; (3) combining duplicate sequences; (4) aligning sequences to the SILVA_v123 bacterial reference alignment (obtained from http://www.mothur.org); (5) removing sequences outside the expected alignment region of V4 (position 1968 to 11550); (6) pre-clustering sequences differing by 2 bp; (7) removing chimeras; (8) removing non-bacterial sequences, including those that align to Chloroplasts, Eukaryotes, or Archaea; and lastly (9) clustering into OTUs at the 0.03 threshold (97% sequence similarity).

The 16S rDNA sequence files were also analyzed using DADA2 to establish amplicon sequencing variants (ASVs) (Callahan et al., 2016). Prior to importing our sequences into R, FlexBar 3.4 was used to trim adapters and low quality sequences (Roehr et al., 2017). Imported sequences underwent further quality trimming using functions within DADA2 (fastqPairedFilter). Trimmed amplicon sequences were denoised (function dada) and chimeras were removed (function isBimeraDenovo). Taxonomic classification was performed by aligning denoised sequences to an RDP dataset (https://benjjneb.github.io/dada2/training.html), with the taxonomy assigned based on the least minBoot bootstrap confidence.

For 3 sputum samples, shotgun whole genome sequencing (WGS) was also performed at the New York Genome Center (New York NY) using the X10 (Illumina, San Diego CA). WGS libraries were prepared using the Illumina TruSeq Nano DNA Library Preparation Kit in accordance with manufacturer's instructions. Briefly, 100 ng of DNA was sheared using the Covaris LE220 sonicator (adaptive focused acoustics). DNA fragments underwent end-repair, bead-based size selection, adenylation, and Illumina sequencing adapter ligation. Ligated DNA libraries were enriched with PCR amplification (using 8 cycles). Final libraries were evaluated using fluorescent-based assays including PicoGreen (Life Technologies) or Qubit Fluorometer (invitrogen) and Fragment Analyzer (Advanced Analytics) or BioAnalyzer (Agilent 2100). Libraries were sequenced on an Illumina HiSeq X sequencer (v2.5 chemistry) using 2 × 150 bp cycles. FASTQ files were screened for quality using FastQC (bioinformatics.babraham.ac.uk/projects/fastqc/) and trimmed using FlexBar 3.4 (Roehr et al., 2017). OTU tables were created using Pathoscope 2.0, which includes a step for filtering human DNA contamination (Hong et al., 2014). The reference database was created using sequences identified in the National Center for Biotechnology Information (NCBI) Bacteria and Virus reference and representative genome database. This database contains at least one genome for each species in the Entrez genome collection that has assembly data. In addition, we also added complete genome assemblies for all *Pseudomonas aeruginosa*, *Burkholderia cepacia*, and *Burkholderia cenocepacia,* allowing for strain-specific identification of these species.

KneadData (http://huttenhower.sph.harvard.edu/kneaddata) was used to remove human DNA contamination prior to performing functional analyses. The presence of antibiotic resistance genes was detected using MEGAres and AMRPlusPlus using a Galaxy pipeline (Lakin et al., 2017).

Volatile Metabolite Analysis

For volatile metabolomics analysis, the sputum sample supernatants were thawed overnight at 4°C, vortexed for ∼2 s to homogenize, and 250 μl of the samples were transferred into 2 mL GC vials with PTFE silicone caps. The vials and caps had been heat treated for 24 h at 100°C to reduce the contribution of exogenous volatile organic compounds to the samples. Technical duplicates were prepared for all samples, and the samples were maintained at 4°C until analysis, which was completed within 48 h of removing the samples from the −80°C freezer.

For metabolomics analysis, the order of analysis for the samples and technical duplicates was randomized. Prior to sample analysis, the mass spectrometer was calibrated using perfluorotributylamine. Sputum samples were incubated at 50°C for 2 min with agitation, then the volatile metabolites were sampled with heating and agitation for 10 min via headspace solid phase microextraction (HS-SPME) using a 1 cm triphase fiber (divinylbenzene/carboxen/polydimethylsiloxane, 50/30 μm; Supelco/Millipore Sigma). The volatile molecules were desorbed for 180 s at 250°C, and injected splitlessly onto a comprehensive two-dimensional gas chromatograph with a time-of-flight mass spectrometer (GC×GC-TOFMS; Pegasus 4D, Leco Corp.), equipped with an autosampler (MPS Robotic, Gerstel, Inc.). The volatile metabolites were separated on a two-dimensional column set of an Rxi-624Sil (60 m × 250 μm × 1.4 μm; length × internal diameter × film thickness; Restek) first column and a Stabilwax (1 m × 250 μm × 0.55 μm; Restek) second column, joined by a press-fit connection. The primary oven was initialized at 35°C with a 0.5 min hold, then heated at 5°C/min to a final temperature of 230°C (5 min hold). The secondary oven and modulator temperatures were maintained with +5°C and +20°C offsets, respectively, relative to the primary oven. The quad-jet modulator was operated with a 3 s modulation period (0.75 s hot and cold pulses). The helium carrier gas flow rate was 2 ml/min. The transfer line and ionization source temperatures were 250°C. Compounds were ionized by electron impact at −70 eV and mass spectra were acquired with unit mass resolution at 100 Hz over a range of 29–400 *m/z*.

Retention indices (RI) for the sputum metabolites were calculated using external alkane standards (C_6-C_{15}), which were analyzed by HS-SPME GC×GC-TOFMS. The standards were heated to 50°C for 2 min with agitation, then sampled for 2 min using a 1 cm triphase SPME fiber. The alkanes were desorbed from the fiber for 180 s at 250°C and injected with a 50:1 split. All other chromatography and mass spectrometry parameters were the same as for the sputum samples. RIs for sputum volatile compounds eluting prior to hexane or after pentadecane were extrapolated.

Metabolomics data collection, processing, and alignment were performed using ChromaTOF with Statistical Compare, version 4.71 (Leco Corp.). The baseline was drawn through the middle of the noise and the signal-to-noise (S/N) cutoff for initial peak finding was 50 for a minimum of two apexing masses. Subpeaks were combined when the second dimension retention time decrease was ≤ 100 ms and the mass spectral match score was ≥ 500. Peaks were aligned across chromatograms when the first dimension retention time shift was ≤ 3 s (one modulation period) and the mass spectral match score was ≥ 600. A second round of peak discovery was performed on the aligned chromatograms, adding peaks with S/N ≥ 10 if the peak was present in at least one chromatogram with a S/N ≥ 50.

Suspected contaminants, chromatographic artifacts (e.g., atmospheric gasses, siloxanes, phthalates), and peaks eluting prior to acetone at 358 s, which were poorly modulated, were removed from peak tables prior to statistical post-processing. The arithmetic means of technical duplicates were calculated and used for subsequent analyses.

Compounds were assigned to the following chemical classes based upon their second-dimension retention times and matches to the mass spectrum and retention index data in the NIST 14 library: hydrocarbons, alcohols, ethers, aldehydes, ketones, carboxylic acids/esters, aromatics, or sulfur-containing. If more than one functional group was present on a molecule, then the compound was assigned to the chemical class of the highest oxidation state.

Statistical Analysis

Continuous variables were compared using *t*-test while categorical variables were compared using Chi-square or Fisher's exact test. Richness and alpha diversity was measured by the number of observed OTUs, the Shannon Index and the inverse Simpson's Index using Explicet v.2.10.5 (Robertson et al., 2013; Wagner et al., 2018). OTU and taxonomy tables were imported into Rstudio for subsequent analyses using the packages *randomForest* v.4.6-14, *DESeq2* v.1.24.0, and *phyloseq* v.1.28.0 to classify samples based on a forest of trees, determine differential abundance, and create principle coordinates analysis (PCoA) plots, respectively (Liaw and Wiener, 2002; McMurdie and Holmes, 2013; Love et al., 2014). Permutational multivariate analysis of variance (PERMANOVA) was also calculated to measure the significance of differences in overall bacterial distribution using the *adonis* function of the Rstudio package *vegan* v.2.5–5 (Oksanen et al., 2017).

The metabolomics data were normalized using probabilistic quotient normalization (Dieterle et al., 2006), and both the metabolomics and genomics data were $\log_{10}$ transformed. The reads for OTUs assigned to *Escherichia* and *Staphylococcus* were summed to create a single variable, referred to as "normal pathogens." Manhattan distances between samples were calculated using standardized variables (OTUs and/or chemical classes) using the Rstudio package *factoextra* v.1.0.5.

RESULTS

Clinical Course

A young school-age child experienced five exacerbations over 12 months. The child was considered to have an advanced disease stage (with a forced expiratory volume in 1 s, FEV1, < 40%) and severe disease aggressiveness (with an FEV1 < 80% at age < 10 years) (Konstan et al., 2009). Past history included multiple acute pulmonary exacerbations where respiratory

cultures had grown many antibiotic resistant organisms, including the following: methicillin resistant *Staphylococcus aureus* (MRSA), *Pseudomonas aeruginosa*, *Stenotrophomonas maltophilia*, *Achromobacter xylosoxidans*, and an extended beta-lactamase (ESBL) producing *Escherichia coli*, among others. At study enrollment, the child was receiving thrice weekly azithromycin, inhaled tobramycin (TOBI) every other month, and was alternating oral linezolid and trimethoprim-sulfamethoxazole (trim-sulfa) at two week intervals with a two week break in between. Sputum was collected from the subject at 14 time points over the 12 month study, encompassing baseline (B), exacerbation (E), and treatment (T) periods. Antibiotics during the study were selected by the clinical team, but were typically geared toward treatment of the ESBL *E. coli* using a carbapenem, specifically meropenem or imipenem (E1–E5) and amikacin (E1, E3–E5), and MRSA with linezolid (E1, E2, and E5). The clinical characteristics surrounding each sample collection during the study period are shown in **Table 1**.

Taxonomic Profile and Microbial Diversity

We performed Next Generation 16S rDNA sequencing on the 14 sputum samples. Across all samples there were 109 individual OTUs identified, with individual samples averaging 24 OTUs (standard deviation (SD) 8.3, range 12–48). Three genera dominated the samples, *Escherichia*, *Staphylococcus,* and *Achromobacter/Alcaligenes* (**Figure 1**), corresponding to the three most commonly and abundantly cultured pathogens during the study period (**Table 1**). Alpha diversities were calculated to evaluate the balance of the number of bacteria identified and their relative abundance to each other (**Figure 2**). The average Shannon diversity index was 0.967 (SD 0.479, range 0.083–2.017) and the average inverse Simpson's index was 2.102 (SD 0.899, range 1.022–4.345). Linear regression was performed to determine if the three dominant genera across samples explained the change in alpha diversity measures over time. No significant differences were found in the number of OTUs, Shannon diversity ($R^2 = 0.132$, $p = 0.687$), or Inverse Simpson diversity ($R^2 = 0.135$, $p = 0.678$).

TABLE 1 | Study participant clinical characteristics.

Sample ID, Day sample obtained	Clinical culture results	Suppressive antibiotics (inhaled or oral)	IV Antibiotics given for pulmonary exacerbation	Days of IV antibiotic therapy	FEV1 (percent predicted)
B-1 Day 0	MSSA, *E. coli*	Azithromycin, TOBI ON	NA	NA	31
E-1 Day 28	*E. coli*	Azithromycin, TOBI OFF	Meropenem, amikacin, linezolid	20	26
T-1 Day 37	NA	NA			41
B-2 Day 77	Normal respiratory flora	Azithromycin, linezolid, TOBI OFF	NA	NA	36
E-2 Day 84	MRSA, *E. coli*	Azithromycin, linezolid, TOBI OFF	Piperacillin-tazobactam, imipenem-cilastatin, linezolid	13	36
T-2 Day 93	NA	NA			43
E-3 Day 132	MRSA, *E. coli*	Azithromycin, trim-sulfa, TOBI ON	Meropenem, amikacin	29	Not obtained
T-3 Day 148	NA	NA			35
B-4 Day 189	MRSA, *E. coli*	Azithromycin, trim-sulfa, TOBI OFF	NA	NA	27
E-4 Day 210	Normal respiratory flora	Azithromycin, trim-sulfa, TOBI OFF	Meropenem, amikacin	29	28
T-4 Day 225	NA	NA			30
E-5 Day 273	MSSA, *E. coli, A. xylosoxidans*	Azithromycin, TOBI OFF	Meropenem, amikacin, linezolid	26	Not obtained
T-5 Day 284	NA	NA			47
B-6 Day 343	*A. xylosoxidans*	Azithromycin, trim-sulfa, TOBI OFF	NA	NA	35

FEV1, forced expiratory volume in one second, MSSA, methicillin-sensitive Staphylococcus aureus; MRSA, methicillin-resistant S. aureus; NA, not available; TOBI ON/OFF, inhaled tobramycin on or off; trim-sulfa, trimethoprim-sulfamethoxazole.

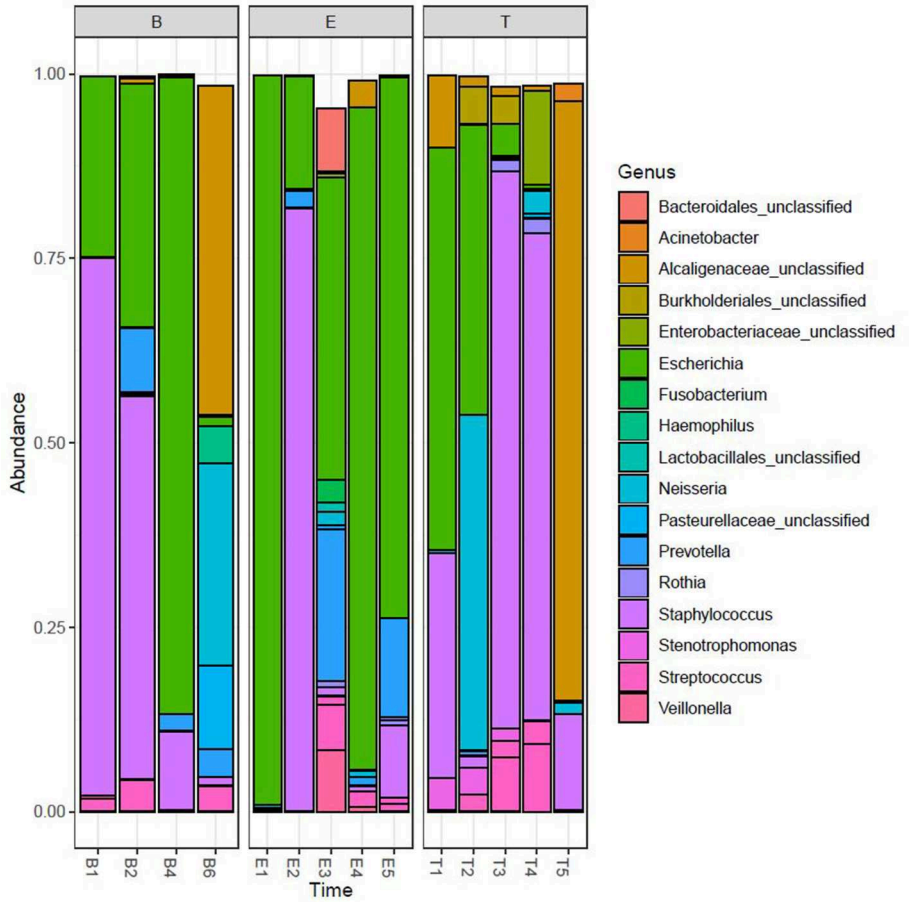

FIGURE 1 | Relative taxonomic abundance. Relative abundance as determined by operational taxonomic units (OTUs). The top 20 OTUs are included. B, Baseline; E, Exacerbation; T, Treatment.

To better understand differences in overall community composition between the samples, we evaluated Bray-Curtis distances. The PCoA plots for Axis 1 vs. Axis 2, as well as the variation between samples on Axis 1 alone, are shown in **Figure 3**. There was no significant difference based on encounter type (baseline, exacerbation, or treatment) when evaluating by phyla or OTU using PERMANOVA ($p = 0.760$ and $p = 0.433$, respectively). However, the treatment samples clustered together when evaluating by OTU (**Figure 3B**), and warranted further investigation.

Additional analysis of the bacterial phyla and genera present by encounter type was performed using Random Forest. Prior to analysis, the phyla and OTU were assessed to determine prevalence across samples, and those with a prevalence of $< 50\%$ were not included in subsequent analysis. This left 4 of 6 phyla and 15 of 109 OTUs as variables. In the analysis of phyla, 500 trees were added with 2 variables tried at each split. A proximity plot from one of the analyses showed significant overlap of encounter types when evaluating by phyla present (**Figure 4A**), and the out of bag (OOB) estimate of the error rate was 64.3%. The variable importance for phyla present within encounter type was evaluated. Bacteroidetes had a mean decrease accuracy of 8.46 and a mean decrease Gini of 3.34 and Actinobacteria had a mean decrease accuracy of 3.29 and a mean decrease Gini of 1.97, with an OOB estimate of the error rate of 57.1% (**Figure 4B**). For the analysis by OTU, 500 trees were added with 3 variables tried at each split. The proximity plot for this analysis showed the treatment samples were more distinct (**Figure 4C**); however, the OOB estimate of error rate remained high at 64.3%. The variable importance was also evaluated for the OTUs present per encounter type. *Stenotrophomonas* was associated with a mean decrease accuracy of 6.33 and a mean decrease Gini of 1.09, with an OOB estimate of the error rate of 64.3% (**Figure 4D**).

We next evaluated for a differential abundance of certain phyla or OTUs based on encounter type using *DESeq2*. Similar to what we found in the Random Forest analyses, Bacteroidetes were less abundant in treatment samples compared to baseline and exacerbations samples ($\log_2$-fold difference -3.29, adjusted $p = 0.015$). Also corroborating our Random Forest analyses, *Stenotrophomonas* was more abundant in treatment samples compared to baseline or exacerbation samples ($\log_2$-fold difference 6.26, adjusted $p = 0.003$).

We also evaluated our 16S rDNA sequencing data by determining amplicon sequencing variants (ASVs). We found a similar relative abundance of the most dominant genera using both methods (**Supplementary Figure 1** and **Supplementary Table 1**). Therefore, we felt confident in using our OTU generated results for subsequent comparisons to our volatile metabolomic data.

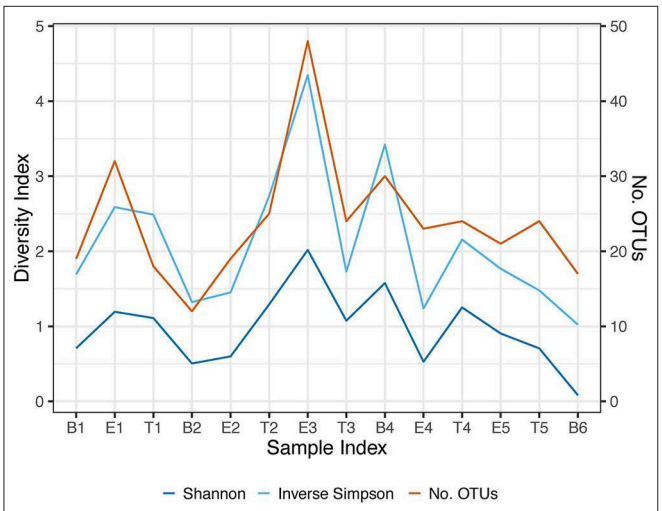

FIGURE 2 | Longitudinal representation of alpha diversity measures. Number of observed OTUs, Shannon Index, and the Inverse Simpson's Index are included. The right axis represents the values of the number of observed OTUs. The left axis represents the values of the Shannon and Inverse Simpson's index. B, Baseline; E, Exacerbation; T, Treatment.

Three samples (B1, E3, and E5) also underwent shotgun whole genome sequencing, allowing for additional analyses. These results are included in the **Supplementary Data**. Briefly, we found a significantly different abundance of the primary bacterial pathogens (*Escherichia coli, Staphylococcus aureus,* and *Achromobacter xylosoxidans*) in the shotgun sequencing data compared to the 16S sequencing data (**Supplementary Figure 2** and **Supplementary Table 1**). We also found 30 different types of bacteriophages within these samples, with the majority of the bacteriophages identified being associated with *Staphylococcus* (n = 15, 50%) and Enterobacteria/*Escherichia* (n = 12, 40%), which were the predominant bacteria within the microbiome community (**Supplementary Figure 3**). Lastly, we found a higher percentage of sequencing reads mapped to an antibiotic resistance gene in the exacerbation samples compared to the baseline sample (**Supplementary Figure 4**). The majority of antibiotic resistance genes identified were due to multi-drug resistance mechanisms (e.g., porins and efflux pumps), while the next most common were aminoglycosides, beta-lactams, and fluoroquinolones. These findings corroborated the antibiotic resistance recognized in the corresponding clinical cultures and suggest shotgun metagenomics provides deeper insights into the microbiome diversity as well as antibiotic resistance.

Volatile Metabolite Analysis

We analyzed the headspace volatiles of the sputum samples using comprehensive two-dimensional gas chromatography–time-of-flight mass spectrometry (GC×GC-TOFMS). After data alignment and artifact removal, we detected 460 non-redundant volatile metabolites from the fourteen sputum samples, all of

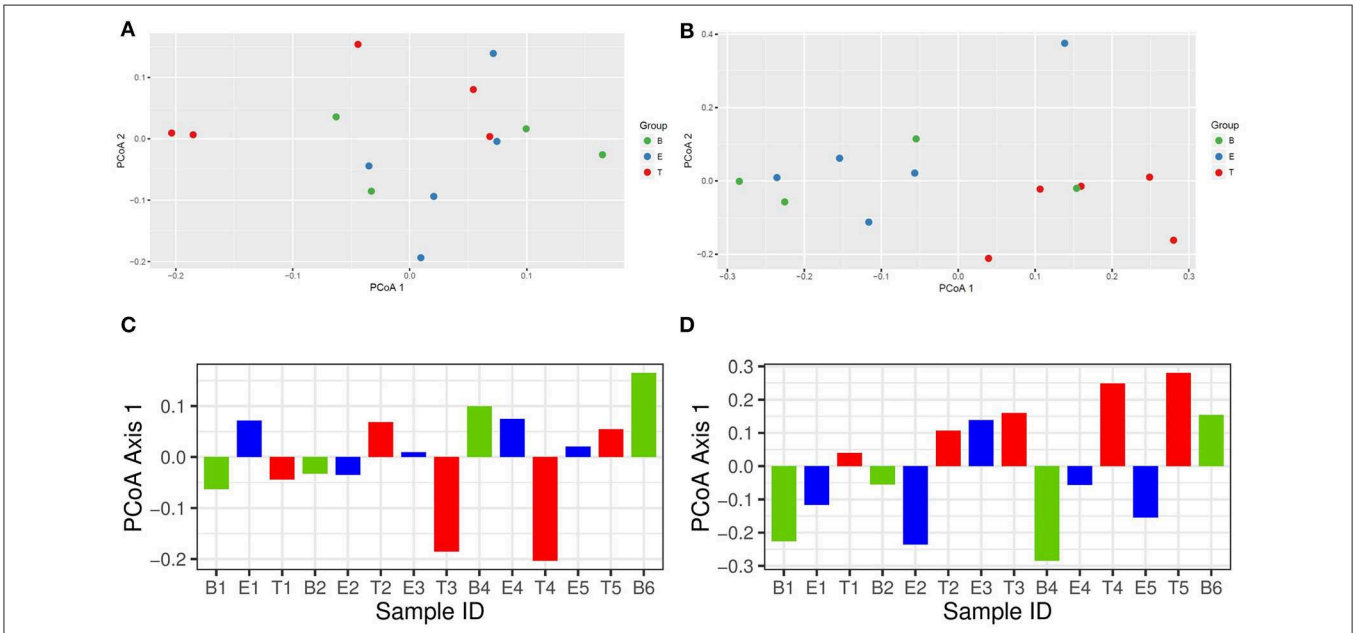

FIGURE 3 | Bray-Curtis distance PCoA with log transformed counts. **(A)** Phylum Axis 1 vs. Axis 2. **(B)** OTU Axis 1 vs. Axis 2. **(C)** Phylum Axis 1 by Sample ID. **(D)** OTU Axis 1 by Sample ID.

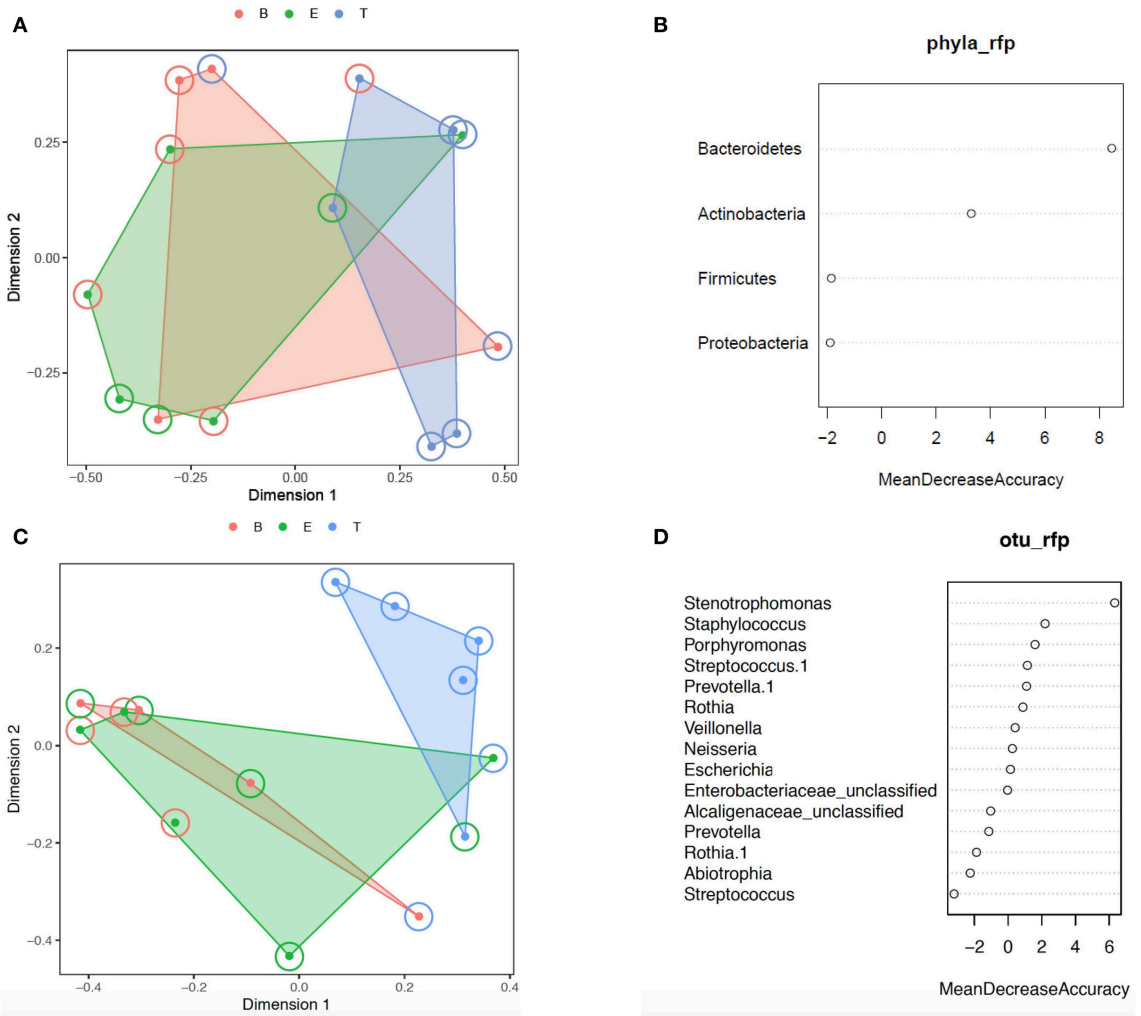

FIGURE 4 | Random forest analysis. **(A)** Phylum proximity plot by encounter type. **(B)** Variable importance plot for Phylum. **(C)** OTU proximity plot by encounter type. **(D)** Variable importance plot for OTU. B, Baseline (red); E, Exacerbation (green); T, Treatment (blue).

which were detected in at least two specimens, with a median frequency-of-observation (FOO) of 12 specimens. While we expect that the dithiothreitol treatment of the sputum altered the metabolome of the samples, e.g., affecting the relative abundances of sulfurous compounds, all sputum samples were similarly processed, and thus we assumed that comparative analyses between baseline, exacerbation, and treatment samples were not impacted. Since our hypothesis for this study was that the volatile metabolomes would change with clinical disease state, we reduced our list of variables to those in the top 50th percentile for variance across samples (calculated as the relative standard deviation, with missing values replaced with zeros), yielding 229 volatile metabolites for subsequent analyses with a median FOO of 8 specimens. We tested for associations of specific volatile metabolites to disease state using pair-wise comparisons of ET vs. B, EB vs. T, and E vs. TB. We did not identify any analytes that were significantly different using Wilcoxon signed rank with Benjamini-Hochberg correction ($\alpha = 0.05$). We also performed supervised Random Forest using the same categories, with 100 models each initialized with 499 trees. We built models using all observations, as well as using balanced class sizes created by down-sampling. Based on error estimates averaged over all trees, the resulting models were overfit, with out of bag class errors exceeding 60% in all models. The feature set of individual metabolites is sparse (i.e., many missing values), which we posited was contributing to the overfitting. Therefore, for subsequent analyses, we used chemical classes for correlation analyses, reducing the number of features by two orders of magnitude with no missing values.

We observed that the total intensity of the volatile metabolite signature (as determined via total peak area) varied from sample to sample (**Figure 5**), with treatment samples having the highest mean and median metabolite signal intensity (**Supplementary Figure 5**). The higher signal intensity in treatment samples was correlated with the detection of more

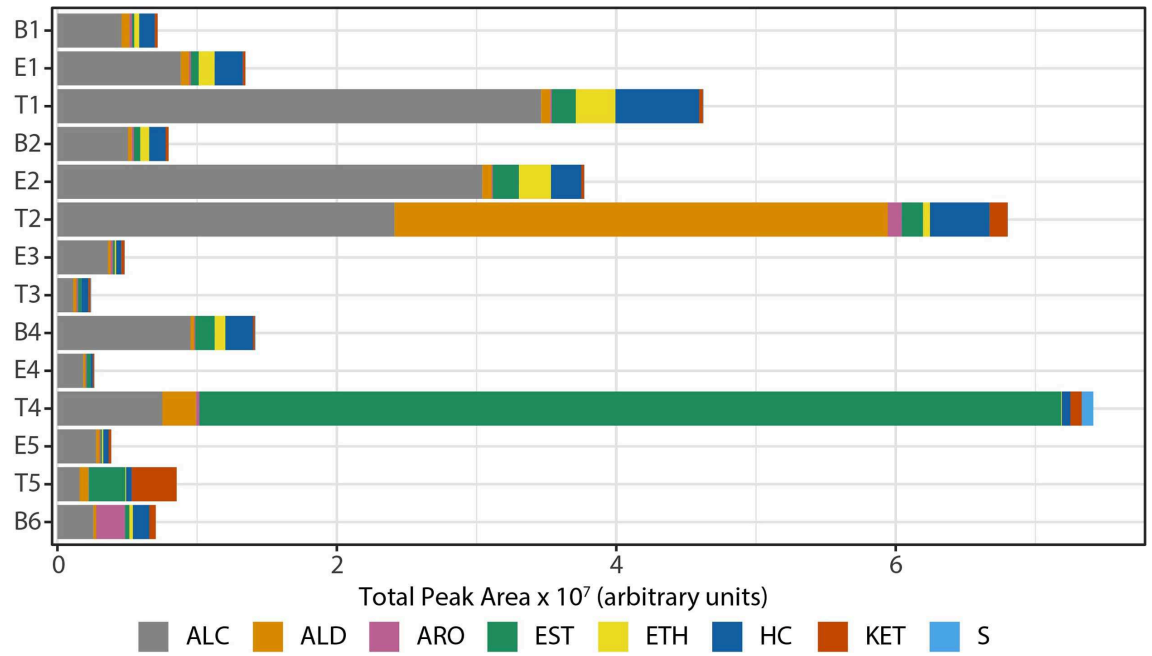

FIGURE 5 | Composition of sputum volatile metabolomes by chemical class, represented in absolute signal intensity. HC, hydrocarbons; ALC, alcohols; ETH, ethers; ALD, aldehydes; KET, ketones; CA/EST, carboxylic acids and esters; ARO, aromatics; S, sulfur-containing; B, baseline; E, exacerbation; T, treatment.

compounds in those samples, but the correlation between total peak area and the number of detected compounds was weak ($R^2 = 0.48$; **Supplementary Figure 5**). While there was no statistically significant difference in the mean signal intensity by disease state, baseline samples had the least amount of variation across all time points (**Supplementary Figure 5**). The intensity of the volatile metabolite signals differed across time from B1 to E2 (**Figure 5**), however the chemical composition of the volatiles varied little, and was dominated by alcohols (**Figures 5**, **6**). At T2 we observed a dramatic shift in the volatile metabolites, with the relative abundance of aldehyde molecules increasing by 100-fold, followed by a return to the same initial chemical composition for specimens collected from E3 to E4. Treatment 4 again had major metabolic shifts, this time due to an increase in two carboxylic acids, octanoic acid and decanoic acid. These two compounds were detected at eight other time points, but at concentrations that were 100-fold to 10,000-fold lower. T4 also had a 10-fold increase in the concentration of aldehydes compared to the preceding four samples. The last two time points, T5 and B6, had entirely unique chemical compositions with a high proportion of ketones in the former and aromatic compounds in the latter. We did not find that disease state correlated to a sputum metabolome chemical composition. Rather, we found that baseline and exacerbation samples were rather uniform in chemical composition and similar to one another, with a relatively high abundance of alcohols, while treatment samples differed from the other two disease states and were highly variable treatment to treatment (**Figure 6**).

Associations of Microbes and Metabolites

To explore correlations between the sputum microbiomes and metabolomes, we first evaluated the two data sets for concurrent changes across the samples (**Figures 6**). While there were significant fluctuations in the relative abundances in *Staphylococcus* and *Escherichia* reads from B1 to E5, for most time points these two genera constituted the majority of the taxa detected in the sputum. The exceptions to this rule were observed at T2 and E3, with the transient increases in *Neisseria* and *Prevotella*, respectively, and T4, with a relative increase in *Streptococcus* and unclassified *Enterobacteriaceae* with a near loss of *Escherichia*. These sputum microbiome fluctuations co-occurred with observable fluctuations in the volatile metabolome composition. Additionally, at T5 and B6 the microbiome composition shifted to dominance by *Alcaligenaceae*, with *Escherichia* and *Staphylococcus* becoming minor constituents. Again, this significant shift in microbiome was reflected in the metabolome, where the previous dominance by alcohols was lost.

To quantify the similarities and differences between sputum samples, we calculated Manhattan distances based on chemical classes of the metabolomes (**Figure 7A**) and the microbiome compositions (**Figure 7B**). Using the relative abundances of chemical classes from the metabolome data, we observe that the sample collected during T4 differs the most strikingly from all preceding samples (**Figure 7A**). The chemical composition of E5 returned to a state that was similar to early baseline and exacerbation samples, followed by another significant chemical shift in T5. To analyze the microbiome data, we reduced the influence of the stochastic shifts in the

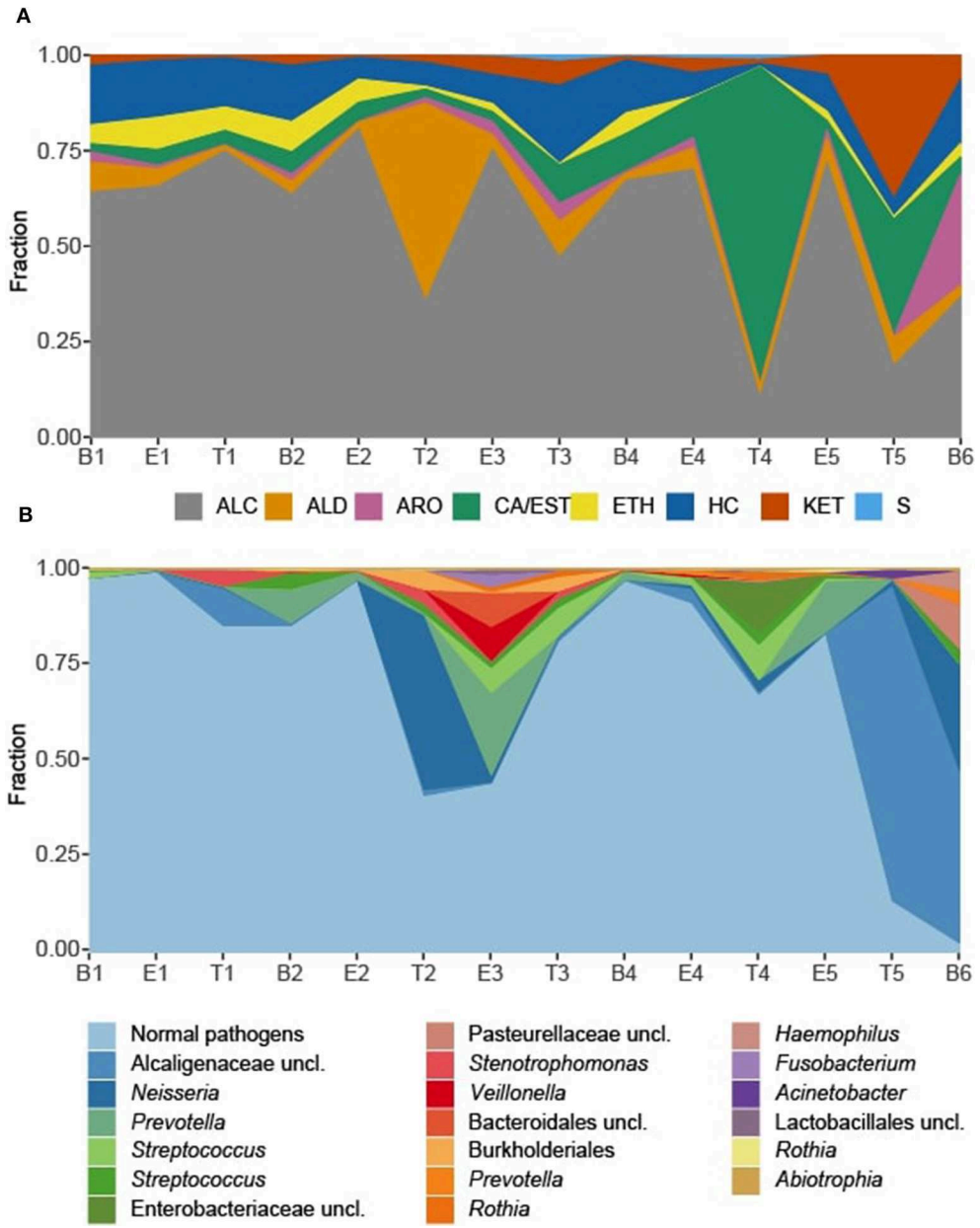

FIGURE 6 | Sputum metabolome and microbiome composition. **(A)** Sputum metabolome composition by chemical class, ordered by time of collection. **(B)** Sputum microbiome composition by OTU. *Escherichia* and *Staphylococcus* reads, representing the "normal pathogens" have been summed to highlight deviations in other taxa of the sputum microbiome. B, baseline; E, exacerbation; T, treatment; HC, hydrocarbons; ALC, alcohols; ETH, ethers; ALD, aldehydes; KET, ketones; CA/EST, carboxylic acids and esters; ARO, aromatics and heteroaromatics; S, sulfurous.

proportions of *Staphylococcus* vs. *Escherichia* reads—i.e., the study participant's "normal pathogens"—by summing those reads prior to calculating the distances. The result is that differences in the relative proportions of the other 21 most abundant OTUs are emphasized. We observed that the microbiome of sputum sample E3 showed the first major shift in composition, and was unlike any other samples collected. This correlated to our observation that the microbiome of E3 had the highest alpha diversity. The high microbiome diversity was temporary, however, with samples B4 and E4 resembling early samples due to the returning dominance of the normal pathogens.

While there were unifying features in the dissimilarity matrices constructed using microbiome and metabolome data (e.g., the uniqueness of T4), they were not fully synchronized. However, we posited that combining the data sets would present a more holistic picture of this study participant's lung disease, and therefore we calculated the dissimilarities between samples using a concatenated microbiome and metabolome data set

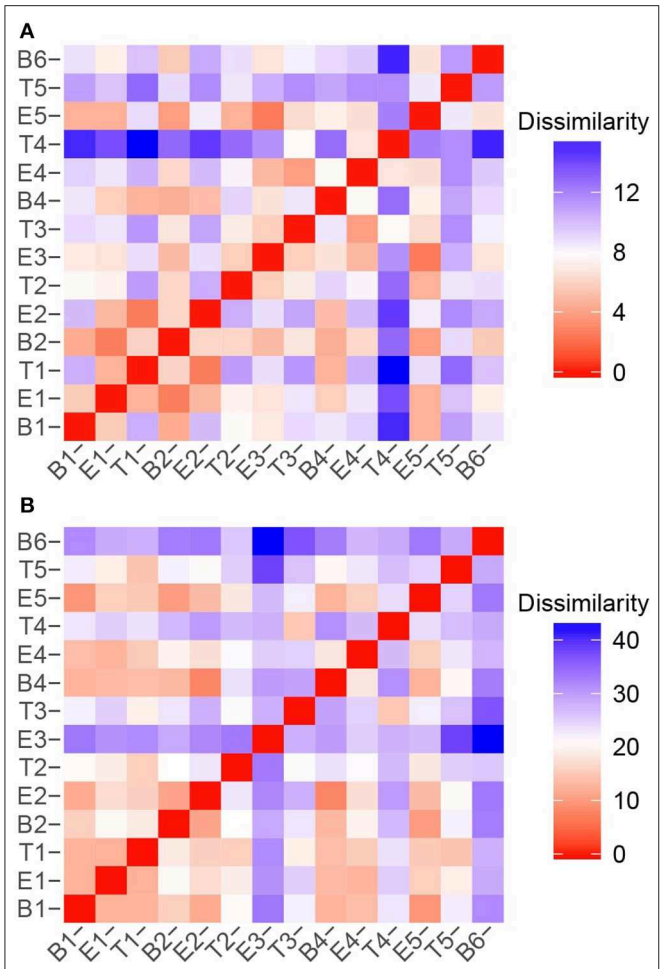

FIGURE 7 | Sample to sample variation represented as dissimilarity matrices using Manhattan distances calculated with unstandardized variables. **(A)** Chemical class relative abundances were used as variables. **(B)** OTU relative abundances were used as variables. The *Staphylococcus* and *Escherichia* reads, representing the study participant's "normal pathogens" were summed to reduce the influence of their stochastic changes, and enhance the influence of the other OTUs on the dissimilarity matrices.

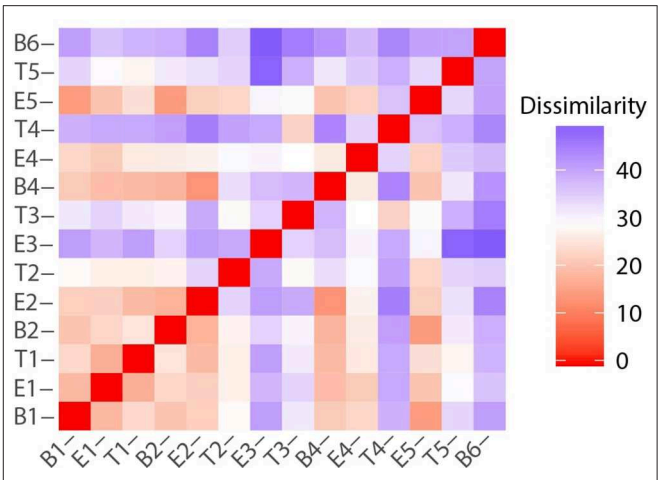

FIGURE 8 | Sample to sample variation represented as a dissimilarity matrix using Manhattan distances calculated with chemical class abundance and proportions of the top 23 most abundant OTUs as standardized variables.

(**Figure 8**). We again observe that sputum samples B1 through E2 were highly similar, which was followed by a sustained period of variance. With the exception of B4 and E4, when comparing any pair of proximate samples from T2 to B6, their dissimilarities were higher than the median, largely driven by the uniqueness of samples collected during treatment periods. While B1, B2, and B4 baseline samples all had similar microbiome-metabolome compositions (i.e., higher than median similarities), we observe that the last specimen, B6, is indeed distinctly different from every other sample previously collected, baseline or otherwise.

Next, we explored the potential associations of specific microbes to individual metabolites by performing Spearman and Pearson Rank analyses between 16S OTU abundances and metabolite signal intensities. We found no statistically-significant correlations, whether we binned all metabolites that are known to be associated with *E. coli* or *S. aureus*, the two best-studied bacterial volatile metabolomes represented in this sample set (Allardyce et al., 2006; Filipiak et al., 2012; Tait et al., 2014; Baptista et al., 2019; Jenkins and Bean, 2019), or treated metabolites independently, e.g., correlated *E. coli* relative abundance to indole absolute or relative abundance. Lastly, we returned to the chemical classification data, and examined the relationship between bacteria and metabolome composition with a distance-based linear model (**Figure 9**). The position of each point in **Figure 9** is dictated by the Bray-Curtis similarity of the airway microbiome composition in each sample, and the superimposed vectors showing which chemical classes are best correlated with the microbial communities. From this view, we observe that the highly similar microbiome compositions of samples B1—E2, B4, E4, and E5, characterized by dominance with the study participant's normal pathogens (i.e., *Staphylococcus* or *Escherichia*), are highly associated with a higher relative abundance of alcohols. Interestingly, T3 and T4 were also dominated by *Staphylococcus*, but did not cluster with the other Staph-dominated samples. The microbiome composition in these specimens does contain more *Streptococcus* spp., and is strongly associated with an increase in sulfur-containing compounds and carboxylic acids/esters in T3 and T4, respectively. We observed that sample T2, characterized by its high abundance of *Neisseria*, is correlated with increased detection of aldehydes. The distinctly clustering outlier samples T5 and B6, dominated by *Achromobacter*, correlated with a shift toward more oxidized compounds (aromatics, ketones) and away from hydrocarbons and alcohols.

DISCUSSION

Prior studies of both the microbiomes and metabolomes in the CF lung have suggested high inter-person variability, which can be greater than the variability identified between clinical states, thereby limiting broad extrapolation of research findings to the

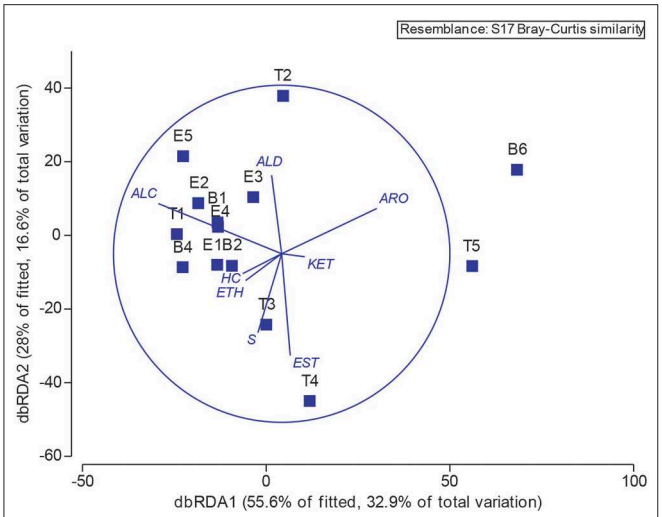

FIGURE 9 | Operational taxonomic unit and chemical class overlay. Distance-based linear model recapitulates the relationship between the airway microbiomes in each sample. Superimposed are vectors showing which chemical classes are best correlated with the microbial communities. Length and direction of vectors correspond to the strength of the association between the metabolite and the microbial communities. B, baseline; E, exacerbation; T, treatment. HC, hydrocarbons; ALC, alcohols; ETH, ethers; ALD, aldehydes; KET, ketones; EST, carboxylic acids and esters; ARO, aromatics and heteroaromatics; S, sulfurous.

general CF population (Carmody et al., 2013; Quinn et al., 2016). A cross-sectional study comparing paired baseline and exacerbation samples found some persons with CF exhibiting little change and other persons with dramatic changes in bacterial community structure (Carmody et al., 2013). A study of the LC-MS derived metabolome capturing larger and more polar molecules (e.g., immune lipids) in the sputum of 11 individuals with CF found that the individual source had a larger influence than clinical state, with only 12% of over 4,000 identified metabolites being unique to pulmonary exacerbation samples (Quinn et al., 2016). These findings support a personalized approach to identifying microbiome and metabolomic changes consistent with changes across clinical states.

With this study, we sought to investigate changes in both the airway microbiome and volatile metabolome of a single person with CF over a 12 month period of recurrent pulmonary exacerbations. We found that although the study participant retained a set of core bacteria that dominated the bacterial community during most baseline and exacerbation samples (specifically *Escherichia coli* and *Staphylococcus aureus*), a transition to a new dominant bacterium (*Achromobacter xylosoxidans*) occurred after the study participant's fifth antibiotic course. This new bacterium continued to grow in subsequent respiratory cultures for at least 6 months following the study. Interestingly, this change in dominant bacterium did not seem to correlate with a change in treatment antibiotics used, as similar IV and oral antibiotics were used throughout the 12 month time period. Alpha diversity measures were also not associated with the transition in dominant organism. When examining community bacterial structure using both PCoA and Random Forest, we found that treatment samples tended to cluster together, albeit not significantly. One bacterial phylum (Bacteroidetes) and one bacterial genus (*Stenotrophomonas*) were significantly more abundant in treatment samples compared to baseline and exacerbation samples using two different analysis measures (Random Forest and DESeq2). While our Random Forest analysis had a high OOB estimation of error, it is worth noting that with repeated assessments of the same data set, Bacteroidetes and *Stenotrophomonas* remained the most important variables and treatment samples were always differentiated from baseline and exacerbation samples in the proximity plots.

Similar to our results, prior longitudinal studies of the CF airway have not always found a significant change in the relative abundance of bacteria to be associated with exacerbation onset (Whelan et al., 2017; Sherrard et al., 2019). While we found rather consistent differences in both bacterial relative abundance and volatile metabolites when comparing treatment samples to baseline and exacerbation samples, this has not always been observed in other studies. One study found no consistent differences in Shannon diversity across stable, intermediate, or treatment samples over time, even though diversity was always fluctuating (Whelan et al., 2017). Some studies have found increases in fermentative anaerobes are associated with the onset of exacerbation (Tunney et al., 2011; Carmody et al., 2013, 2018). Another study obtaining enhanced cultures longitudinally found more constant communities in stable persons with CF, while those with frequent exacerbations had higher variability in their community structures (Sherrard et al., 2019). As our study participant experienced multiple exacerbations during the study, this may explain, in part, the changing relative abundance and alpha diversity we saw.

A deeper analysis of one baseline and two exacerbation samples confirmed that *E. coli* and *S. aureus* were the dominant bacteria within the airway, but the relative abundance was different when analyzed via 16S and shotgun sequencing. This difference is likely multifactorial, including PCR amplification bias associated with 16S rDNA sequencing, potential misclassification bias from human DNA contamination, and differences in reference databases used for sequence alignment (Hahn et al., 2018b). However, with shotgun sequencing we were also able to explore additional characteristics potentially important to clinical response, including the presence of bacteriophages and antibiotic resistance genes.

Prior metagenomic studies of the CF airway have found that the majority of DNA viruses identified were bacteriophages (Moran Losada et al., 2016). In our study, we had similar findings; more than 70% of the viral reads were attributed to bacteriophages, and most were associated with Enterobacteria, *Escherichia*, and *Staphylococcus*. These phages can have important clinical impacts. First, filamentous phages associated with *E. coli* have been shown to promote biofilm formation (Secor et al., 2015). Second, *S. aureus* bacteriophages in the CF airway were associated with genomic alterations of the bacterium, likely passing on virulence traits and perhaps enhancing its ability to survive despite antibiotic pressures (Goerke et al., 2004). Lastly, bacteriophages in general have been shown to transfer antibiotic

resistance, such as efflux pumps, beta-lactam resistance, and fluoroquinolone resistance, particularly within the CF lung (Fancello et al., 2011; Brown-Jaque et al., 2018).

In our evaluation of antibiotic resistance detected by shotgun sequencing, we found that the results were generally consistent with the clinical cultures, and more sequences aligned to antibiotic resistance genes in the two exacerbation samples. One caveat is that the potential for MRSA was detected by sequencing in 2 of 3 samples where the corresponding cultures grew MSSA; this signifies the limitations of making antibiotic decisions on clinical culture results alone. Furthermore, prior studies have shown that multidrug antibiotic resistance is associated with decreased alpha diversity, the presence of *Achromobacter* species, and lower pulmonary function (Bacci et al., 2017; Hahn et al., 2018c). Several studies utilizing shotgun sequencing to analyze the CF airway have also found a congruence of antibiotic resistance detected in clinical cultures, and an association of antibiotic resistance with *E. coli* and *A. xylosoxidans* (Lim et al., 2014; Bacci et al., 2017; Feigelman et al., 2017). Importantly, genes encoding resistance to antibiotics not recently used can be present, suggesting that the development of antibiotic resistance in the CF lung is partly related to direct antibiotic pressures, partly through the presence of multidrug efflux pumps, and partly through the presence of mobile elements encoding resistance that are carried in bacteriophages as mentioned earlier (Fancello et al., 2011; Lim et al., 2014; Brown-Jaque et al., 2018).

The primary goals of the study were to identify microbiome and metabolome characteristics indicative of clinical state (baseline, exacerbation, and treatment) and to evaluate intra-person variability between clinical disease states. We observed that the baseline and exacerbation specimens did not significantly differ in either their microbiome or metabolome, but that treatment specimens T2-T5 and the final baseline sample (B6) were dissimilar from the rest. However, because the sputum characteristics of these samples are all unique, we are unable to identify specific microbiome or metabolome signatures of treatment, nor determine definitive associations between the microbiome and metabolome compositions we observed. Additionally, the common trait of these specimens' microbiomes is a reduction in the study participant's normal pathogens and concomitant increase in other taxa, but published data on the volatile metabolomes of bacteria other than *P. aeruginosa*, *S. aureus*, *E. coli*, and *Mycobacteria* spp. are relatively scarce. The dominance of the T4 metabolome by octanoic and decanoic acids co-occurred with the highest relative abundance of *Streptococcus* and *Rothia* in any sample. Generally, though, mid-chain fatty acids are characterized as antibacterial against a broad range of Gram positive and Gram negative pathogens (Desbois and Smith, 2010), and free and derivatized forms of octanoic and decanoic acids have been shown to inhibit *Staphylococcus* spp., *Streptococcus* spp., *Neisseria gonorrhoeae*, and *E. coli* growth (Kabara et al., 1972; Bergsson et al., 1999; Skrivanová et al., 2008). It is also feasible that these two compounds are associated with treatment rather than infection, as decanoic acid is commonly used as a solubilizing agent in medications, and mid-chain fatty acid esters are common prodrugs used to improve lipophilicity.

In the baseline and exacerbation samples, we observed large variations in the relative abundances of *S. aureus* and *E. coli* 16S amplicon sequencing reads, however, we did not find correlated fluctuations in volatile metabolites that are produced by these bacteria. *In vitro* experiments have demonstrated that both *E. coli* and *S. aureus* produce volatile alcohols (Allardyce et al., 2006). Therefore, one possible explanation is that the production of alcohols by *S. aureus* and *E. coli* are similar in the environment of the CF lung, and aggregating the metabolome into chemical classes removes the species-specific correlations we would otherwise observe. However, we did attempt to find correlations between *S. aureus* or *E. coli* reads and the abundances of their known metabolites, and failed to do so. Interestingly, we did observe reductions in the relative abundance of alcohols when the relative abundance of the normal pathogens decreased, consistent with the reduced alcohol production observed when these organisms are dosed with antibiotics above minimum inhibitory concentrations *in vitro* (Allardyce et al., 2006). It is also possible that the VOCs observed were indicative of clinical state rather than correlating directly with the abundance of an individual species, perhaps due to variations in functional genetics and/or expression of bacterial genes. This would still provide a useful tool that could be translated into clinical practice, but requires further study.

By integrating both the metabolome and microbiome data, we observed an overall smoothing of the sputum characteristics that help to reveal time/treatment-dependent patterns. While changes in the sputum did not clearly correlate with clinical disease state (i.e., predict exacerbation onset), they did correlate with clinical culture data and revealed when the character of the lung environment was and was not changing. The microbiome and metabolome data also suggested that there was a fundamental shift in the study participant's lung disease during and after the 5th treatment, which correlated to culture results; beginning with B6, and for at least 6 months afterward, the subject consistently cultured *A. xylosoxidans*, and *E. coli* was not detected again.

Limitations to the study include the translational capacity of a longitudinal study design from a single person with CF. However, the inter-individual variability in the CF airway microbiome is often high, frequently influenced by the dominant organism which may be different between study participants, and can lead to limitations in interpreting results due to that variability (Boutin et al., 2015). Thus, understanding intra-person variability across clinical states can inform future study design in larger cohorts (Caverly et al., 2019; Hahn and Zemanick, 2019). Furthermore, n-of-1 studies can still provide important data to the literature, and may provide a way forward for using the CF microbiome and metabolome in individualized medicine (Lillie et al., 2011). Moving forward into larger cohorts, it may be necessary to look at changes between each study participant as a series of n-of-1 studies instead of averaging species relative abundance, diversity measures, etc., to truly begin to bring these findings into meaningful clinical practice. By itself, this study shows that antibiotic treatment has the largest impact on taxonomic relative abundance and the metabolome, and there may be little dissimilarity between baseline and exacerbation in a CF person experiencing

frequent pulmonary exacerbations. Another limitation was the lack of inclusion of WGS data for treatment samples, as these time points showed the most variability in our cohort. Unfortunately, we were limited in the amount of bacterial DNA available and were only able to perform WGS on baseline and exacerbation samples.

In summary, we found that using a combination of metabolome and microbiome data, we could corroborate changes in community structure and metabolism in the lung environment over the span of a year in a subject with unstable lung disease, and these data correlated with short-term and long-term clinical culture data. For this particular dataset, the greatest amount of change was associated with antibiotic treatment. Future directions include performing a similar analysis of the association between the bacterial microbiome and volatile metabolites in a larger cohort. The results from this study will allow us to incorporate the level of intra-person variability observed so that we may be able to detect a potential signature that could be utilized in identifying transitions between clinical states.

DATA AVAILABILITY STATEMENT

The sequence dataset supporting the conclusions of this article is available in the NCBI SRA repository under BioProject PRJNA437613 (16S sequencing data) and PRJNA515276 (trimmed and human filtered whole genome shotgun sequencing data). For PRJNA437613, the sample IDs are as follows: B1 AHCF01a, B2 AHCF01d, B4 AHCF01d3, B6 AHCF01d5, E1 AHCF01b, E2 AHCF01b2, E3 AHCF01b3, E4 AHCF01b4, E5 AHCF01b5, T1 AHCF01c, T2 AHCF01c2, T3 AHCF01c3, T4 AHCF01c4, and T5 AHCF01c5.

ETHICS STATEMENT

The studies involving human participants were reviewed and approved by Children's National Health System. Written informed consent to participate in this study was provided by the participants' legal guardian/next of kin.

AUTHOR CONTRIBUTIONS

AH designed the study and obtained and maintained IRB approval. IS and AK were responsible for identifying eligible study subjects and obtaining consent. AH, HB, KW, RF, and KC designed the study experiments and determined the appropriate bioinformatic and statistical approaches for analyzing the data. AH, HB, TD, JP, and KW were responsible for data collection and analysis. AH and HB wrote the text of the manuscript. AH, HB, KW, TD, and JP generated the manuscript figures. All authors provided critical review of the manuscript and approved of the final manuscript as written.

FUNDING

AH and the study experiments were funded in part by a K12 Career Development Program K12HL119994 through the National Heart, Lung and Blood Institute. AH was also funded by the Margaret Q. Landenberger Foundation, and by a Harry Shwachman Clinical Investigator Award from the Cystic Fibrosis Foundation. JP and KW were supported by NIH R01 HL 136647-01. The shotgun sequencing performed in this study was funded by a voucher from the Clinical and Translational Science Institute at Children's National. This project was also partially supported by Award Number UL1TR000075 from the NIH National Center for Advancing Translational Sciences. Its contents are solely the responsibility of the authors and do not necessarily represent the official views of the National Institutes of Health.

ACKNOWLEDGMENTS

The authors would like to acknowledge the GWU Colonial One High Performance Computing Cluster for computational time.

SUPPLEMENTARY MATERIAL

The Supplementary Material for this article can be found online at: https://www.frontiersin.org/articles/10.3389/fcimb.2020.00174/full#supplementary-material

REFERENCES

Allardyce, R. A., Hill, A. L., and Murdoch, D. R. (2006). The rapid evaluation of bacterial growth and antibiotic susceptibility in blood cultures by selected ion flow tube mass spectrometry. *Diagn. Microbiol. Infect. Dis.* 55, 255–261. doi: 10.1016/j.diagmicrobio.2006.01.031

Bacci, G., Mengoni, A., Fiscarelli, E., Segata, N., Taccetti, G., Dolce, D., et al. (2017). A different microbiome gene repertoire in the airways of cystic fibrosis patients with severe lung disease. *Int. J. Mol. Sci.* 18:1654. doi: 10.3390/ijms18081654

Baptista, I., Santos, M., Rudnitskaya, A., Saraiva, J. A., Almeida, A., and Rocha, S. M. (2019). A comprehensive look into the volatile exometabolome of enteroxic and non-enterotoxic *Staphylococcus aureus* strains. *Int. J. Biochem. Cell Biol.* 108, 40–50. doi: 10.1016/j.biocel.2019.01.007

Bean, H. D., Jiménez-Díaz, J., Zhu, J., and Hill, J. E. (2015). Breathprints of model murine bacterial lung infections are linked with immune response. *Eur. Respir. J.* 45, 181–190. doi: 10.1183/09031936.00015814

Bean, H. D., Rees, C. A., and Hill, J. E. (2016). Comparative analysis of the volatile metabolomes of *Pseudomonas aeruginosa* clinical isolates. *J. Breath Res.* 10:047102. doi: 10.1088/1752-7155/10/4/047102

Bergsson, G., Steingrímsson, Ó., and Thormar, H. (1999). *In vitro* susceptibilities of *Neisseria gonorrhoeae* to fatty acids and monoglycerides. *Antimicrob. Agents Chemother.* 43, 2790–2792. doi: 10.1128/AAC.43.11.2790

Bos, L. D. J., Meinardi, S., Blake, D., and Whiteson, K. (2016). Bacteria in the airways of patients with cystic fibrosis are genetically capable of producing VOCs in breath. *J. Breath Res.* 10:047103. doi: 10.1088/1752-7163/10/4/047103

Boutin, S., Graeber, S. Y., Weitnauer, M., Panitz, J., Stahl, M., Clausznitzer, D., et al. (2015). Comparison of microbiomes from different niches of upper and lower airways in children and adolescents with cystic fibrosis. *PLoS ONE* 10:e0116029. doi: 10.1371/journal.pone.0116029

Brown-Jaque, M., Oyarzun, L. R., Cornejo-Sánchez, T., Martín-Gómez, M. T., Gartner, S., de Gracia, J., et al. (2018). Detection of bacteriophage particles containing antibiotic resistance genes in the sputum of cystic fibrosis patients. *Front. Microbiol.* 9:856. doi: 10.3389/fmicb.2018.00856

Callahan, B. J., McMurdie, P. J., Rosen, M. J., Han, A. W., Johnson, A. J. A., and Holmes, S. P. (2016). DADA2: high-resolution sample inference from Illumina amplicon data. *Nat Methods*. 13, 581–583. doi: 10.1038/nmeth.3869

Carmody, L. A., Caverly, L. J., Foster, B. K., Rogers, M. A. M., Kalikin, L. M., Simon, R. H., et al. (2018). Fluctuations in airway bacterial communities associated with clinical states and disease stages in cystic fibrosis. *PLoS ONE* 13:e0194060. doi: 10.1371/journal.pone.0194060

Carmody, L. A., Zhao, J., Schloss, P. D., Petrosino, J. F., Murray, S., Young, V. B., et al. (2013). Changes in cystic fibrosis airway microbiota at pulmonary exacerbation. *Ann. Am. Thorac. Soc.* 10, 179–187. doi: 10.1513/AnnalsATS.201211-107OC

Caverly, L. J., and LiPuma, J. J. (2018). Cystic fibrosis respiratory microbiota: unraveling complexity to inform clinical practice. *Expert Rev. Respir. Med.* 12, 857–865. doi: 10.1080/17476348.2018.1513331

Caverly, L. J., Lu, J., Carmody, L. A., Kalikin, L. M., Shedden, K., Opron, K., et al. (2019). Measures of cystic fibrosis airway microbiota during periods of clinical stability. *Ann. Am. Thorac. Soc.* 16, 1534–1542. doi: 10.1513/AnnalsATS.201903-270OC

Desbois, A. P., and Smith, V. J. (2010). Antibacterial free fatty acids: activities, mechanisms of action and biotechnological potential. *Appl. Microbiol. Biotechnol.* 85, 1629–1642. doi: 10.1007/s00253-009-2355-3

Dieterle, F., Ross, A., Schlotterbeck, G., and Senn, H. (2006). Probabilistic quotient normalization as robust method to account for dilution of complex biological mixtures. Application in1H NMR metabonomics. *Anal. Chem.* 78, 4281–4290. doi: 10.1021/ac051632c

Fancello, L., Desnues, C., Raoult, D., and Rolain, J. M. (2011). Bacteriophages and diffusion of genes encoding antimicrobial resistance in cystic fibrosis sputum microbiota. *J. Antimicrob. Chemother.* 66, 2448–2454. doi: 10.1093/jac/dkr315

Feigelman, R., Kahlert, C. R., Baty, F., Rassouli, F., Kleiner, R. L., Kohler, P., et al. (2017). Sputum DNA sequencing in cystic fibrosis: non-invasive access to the lung microbiome and to pathogen details. *Microbiome* 5:20. doi: 10.1186/s40168-017-0234-1

Filipiak, W., Sponring, A., Baur, M. M., Filipiak, A., Ager, C., Wiesenhofer, H., et al. (2012). Molecular analysis of volatile metabolites released specifically by *Staphylococcus aureus* and *Pseudomonas aeruginosa*. *BMC Microbiol.* 12:113. doi: 10.1186/1471-2180-12-113

Fuchs, H. J., Borowitz, D. S., Christiansen, D. H., Morris, E. M., Nash, M. L., Ramsey, B. W., et al. (1994). Effect of aerosolized recombinant human DNase on exacerbations of respiratory symptoms and on pulmonary function in patients with cystic fibrosis. The pulmozyme study group. *N. Engl. J. Med.* 331, 637–642. doi: 10.1056/NEJM199409083311003

Goerke, C., Papenberg, S., Dasbach, S., Dietz, K., Ziebach, R., Kahl, B. C., et al. (2004). Increased frequency of genomic alterations in *Staphylococcus aureus* during chronic infection is in part due to phage mobilization. *J. Infect. Dis.* 189, 724–734. doi: 10.1086/381502

Guss, A. M., Roeselers, G., Newton, I. L. G., Young, C. R., Klepac-Ceraj, V., Lory, S., et al. (2011). Phylogenetic and metabolic diversity of bacteria associated with cystic fibrosis. *ISME J.* 5, 20–29. doi: 10.1038/ismej.2010.88

Hahn, A., Bendall, M. L., Gibson, K. M., Chaney, H., Sami, I., Perez, G. F., et al. (2018a). Benchmark evaluation of true single molecular sequencing to determine cystic fibrosis airway microbiome diversity. *Front. Microbiol.* 9:1069. doi: 10.3389/fmicb.2018.01069

Hahn, A., Burrell, A., Fanous, H., Chaney, H., Sami, I., Perez, G., et al. (2018c). Antibiotic multidrug resistance in the cystic fibrosis airway microbiome is associated with decreased diversity. *Heliyon* 4:e00795. doi: 10.1016/j.heliyon.2018.e00795

Hahn, A., Fanous, H., Jensen, C., Chaney, H., Sami, I., Perez, G. F., et al. (2019). Changes in microbiome diversity following beta-lactam antibiotic treatment are associated with therapeutic versus subtherapeutic antibiotic exposure in cystic fibrosis. *Sci. Rep.* 9:2534. doi: 10.1038/s41598-019-38984-y

Hahn, A., Warnken, S., Pérez-Losada, M., Freishtat, R. J., and Crandall, K. A. (2018b). Microbial diversity within the airway microbiome in chronic pediatric lung diseases. *Infect. Genet. Evol.* 63, 316–325. doi: 10.1016/j.meegid.2017.12.006

Hahn, A., and Zemanick, E. T. (2019). Bacterial community variability: outliers may be leading us astray. *Ann. Am. Thorac. Soc.* 16, 1499–1501. doi: 10.1513/AnnalsATS.201909-716ED

Harris, J. K., De Groote, M. A., Sagel, S. D., Zemanick, E. T., Kapsner, R., Penvari, C., et al. (2007). Molecular identification of bacteria in bronchoalveolar lavage fluid from children with cystic fibrosis. *Proc. Natl. Acad. Sci. U.S.A.* 104, 20529–20533. doi: 10.1073/pnas.0709804104

Hong, C., Manimaran, S., Shen, Y., Perez-Rogers, J. F., Byrd, A. L., Castro-Nallar, E., et al. (2014). PathoScope 2.0: a complete computational framework for strain identification in environmental or clinical sequencing samples. *Microbiome* 2:33. doi: 10.1186/2049-2618-2-33

Jenkins, C. L., and Bean, H. D. (2019). Influence of media on the differentiation of Staphylococcus spp. by volatile compounds. *J. Breath Res.* 14:016007. doi: 10.1088/1752-7163/ab3e9d

Kabara, J. J., Swieczkowski, D. M., Conley, A. J., and Truant, J. P. (1972). Fatty acids and derivatives as antimicrobial agents. *Antimicrob. Agents Chemother.* 2, 23–28. doi: 10.1128/AAC.2.1.23

Konstan, M. W., Wagener, J. S., and VanDevanter, D. R. (2009). Characterizing aggressiveness and predicting future progression of CF lung disease. *J. Cyst. Fibros.* 8, S15–S19. doi: 10.1016/S1569-1993(09)60006-0

Kozich, J. J., Westcott, S. L., Baxter, N. T., Highlander, S. K., and Schloss, P. D. (2013). Development of a dual-index sequencing strategy and curation pipeline for analyzing amplicon sequence data on the miseq illumina sequencing platform. *Appl. Environ. Microbiol.* 79, 5112–5120. doi: 10.1128/AEM.01043-13

Lakin, S. M., Dean, C., Noyes, N. R., Dettenwanger, A., Ross, A. S., Doster, E., et al. (2017). MEGARes: an antimicrobial resistance database for high throughput sequencing. *Nucleic Acids Res.* 45, D574–D580. doi: 10.1093/nar/gkw1009

Liaw, A., and Wiener, M. (2002). Classification and regression by randomForest. *R. News.* 2, 18–22. Available online at: https://www.r-project.org/doc/Rnews/Rnews_2002-3.pdf

Lillie, E. O., Patay, B., Diamant, J., Issell, B., Topol, E. J., and Schork, N. J. (2011). The n-of-1 clinical trial: the ultimate strategy for individualizing medicine? *Per. Med.* 8, 161–173. doi: 10.2217/pme.11.7

Lim, Y. W., Evangelista, J. S., Schmieder, R., Bailey, B., Haynes, M., Furlan, M., et al. (2014). Clinical insights from metagenomic analysis of sputum samples from patients with cystic fibrosis. *J. Clin. Microbiol.* 52, 425–437. doi: 10.1128/JCM.02204-13

Love, M. I., Huber, W., and Anders, S. (2014). Moderated estimation of fold change and dispersion for RNA-seq data with DESeq2. *Genome Biol.* 15:550. doi: 10.1186/s13059-014-0550-8

MacKenzie, T., Gifford, A. H., Sabadosa, K. A., Quinton, H. B., Knapp, E. A., Goss, C. H., et al. (2014). Longevity of patients with cystic fibrosis in 2000 to 2010 and beyond: survival analysis of the Cystic Fibrosis Foundation Patient Registry. *Ann. Intern. Med.* 161, 233–241. doi: 10.7326/M13-0636

McMurdie, P. J., and Holmes, S. (2013). Phyloseq: an R package for reproducible interactive analysis and graphics of microbiome census data. *PLoS ONE* 8:e61217. doi: 10.1371/journal.pone.0061217

Miller, M. R., Hankinson, J., Brusasco, V., Burgos, F., Casaburi, R., Coates, A., et al. (2005). Standardisation of spirometry. *Eur. Respir. J.* 26, 319–338. doi: 10.1183/09031936.05.00034805

Moran Losada, P., Chouvarine, P., Dorda, M., Hedtfeld, S., Mielke, S., Schulz, A., et al. (2016). The cystic fibrosis lower airways microbial metagenome. *ERJ Open Res.* 2, 00096–2015. doi: 10.1183/23120541.00096-2015

Moran Losada, P., Tummler, B., Wiehlmann, L., and Chouvarine, P. (2014). Whole metagenome shotgun sequencing analysis of microbiome of cystic fibrosis- and COPD patients. *Eur. Respir. J.* 44:P1212. Available online at: https://erj.ersjournals.com/content/44/Suppl_58/P1212

Nasir, M., Bean, H. D., Smolinska, A., Rees, C. A., Zemanick, E. T., and Hill, J. E. (2018). Volatile molecules from bronchoalveolar lavage fluid can "rule-in" *Pseudomonas aeruginosa* and "rule-out" *Staphylococcus aureus* infections in cystic fibrosis patients. *Sci Rep.* 8:826. doi: 10.1038/s41598-017-18491-8

National Center for Health Statistics (2001). *The Third National Health and Nutrition Examination Survey (NHANES III), 1988–94, Series 11, No. 9A Data Release*. Hyattsville, MD: Centers for Disease Control and Prevention. Available online at: https://wwwn.cdc.gov/nchs/data/nhanes3/9a/Readme.txt

Oksanen, J., Blanchet, F. G., Friendly, M., Kindt, R., Legendre, P., Mcglinn, D., et al. (2017). *vegan: Community Ecology Package*. R Packag version 2.4-4. Available online at: https://CRAN.R-project.org/package=vegan

Phan, J., Meinardi, S., Barletta, B., Blake, D. R., and Whiteson, K. (2017). Stable isotope profiles reveal active production of VOCs from human-associated microbes. *J. Breath Res.* 11:017101. doi: 10.1088/1752-7163/aa5833

Quinn, R. A., Lim, Y. W., Mak, T. D., Whiteson, K., Furlan, M., Conrad, D., et al. (2016). Metabolomics of pulmonary exacerbations reveals the personalized nature of cystic fibrosis disease. *PeerJ*. 4:e2174. doi: 10.7717/peerj.2174

Robertson, C. E., Harris, J. K., Wagner, B. D., Granger, D., Browne, K., Tatem, B., et al. (2013). Explicet: graphical user interface software for metadata-driven management, analysis and visualization of microbiome data. *Bioinformatics* 29, 3100–3101. doi: 10.1093/bioinformatics/btt526

Roehr, J. T., Dieterich, C., and Reinert, K. (2017). Flexbar 3.0 - SIMD and multicore parallelization. *Bioinformatics* 33, 2941–2942. doi: 10.1093/bioinformatics/btx330

Rogers, G. B., Carroll, M. P., Serisier, D. J., Hockey, P. M., Jones, G., and Bruce, K. D. (2004). Characterization of bacterial community diversity in cystic fibrosis lung infections by use of 16S ribosomal DNA terminal restriction fragment length polymorphism profiling. *J. Clin. Microbiol.* 42, 5176–5183. doi: 10.1128/JCM.42.11.5176-5183.2004

Schloss, P. D., Westcott, S. L., Ryabin, T., Hall, J. R., Hartmann, M., Hollister, E. B., et al. (2009). Introducing mothur: open-source, platform-independent, community-supported software for describing and comparing microbial communities. *Appl. Environ. Microbiol.* 75, 7537–7541. doi: 10.1128/AEM.01541-09

Secor, P. R., Sweere, J. M., Michaels, L. A., Malkovskiy, A. V., Lazzareschi, D., Katznelson, E., et al. (2015). Filamentous bacteriophage promote biofilm assembly and function. *Cell Host Microbe* 18, 549–559. doi: 10.1016/j.chom.2015.10.013

Seekatz, A. M., Theriot, C. M., Molloy, C. T., Wozniak, K. L., Bergin, I. L., and Young, V. B. (2015). Fecal microbiota transplantation eliminates *Clostridium difficile* in a murine model of relapsing disease. *Infect. Immun.* 83, 3838–3846. doi: 10.1128/IAI.00459-15

Sherrard, L. J., Einarsson, G. G., Johnston, E., O'Neill, K., McIlreavey, L., McGrath, S. J., et al. (2019). Assessment of stability and fluctuations of cultured lower airway bacterial communities in people with cystic fibrosis. *J. Cyst. Fibros.* 18, 808–816. doi: 10.1016/j.jcf.2019.02.012

Skrivanová E., Molatová Z., and Marounek, M. (2008). Effects of caprylic acid and triacylglycerols of both caprylic and capric acid in rabbits experimentally infected with enteropathogenic *Escherichia coli* O103. *Vet. Microbiol.* 126, 372–376. doi: 10.1016/j.vetmic.2007.07.010

Tait, E., Perry, J. D., Stanforth, S. P., and Dean, J. R. (2014). Identification of volatile organic compounds produced by bacteria using HS-SPME-GC-MS. *J. Chromatogr. Sci.* 52, 363–373. doi: 10.1093/chromsci/bmt042

Tunney, M. M., Klem, E. R., Fodor, A. A., Gilpin, D. F., Moriarty, T. F., McGrath, S. J., et al. (2011). Use of culture and molecular analysis to determine the effect of antibiotic treatment on microbial community diversity and abundance during exacerbation in patients with cystic fibrosis. *Thorax* 66, 579–584. doi: 10.1136/thx.2010.137281

Wagener, J. S., Rasouliyan, L., Vandevanter, D. R., Pasta, D. J., Regelmann, W. E., Morgan, W. J., et al. (2013). Oral, inhaled, and intravenous antibiotic choice for treating pulmonary exacerbations in cystic fibrosis. *Pediatr. Pulmonol.* 48, 666–673. doi: 10.1002/ppul.22652

Wagner, B. D., Grunwald, G. K., Zerbe, G. O., Mikulich-Gilbertson, S. K., Robertson, C. E., Zemanick, E. T., et al. (2018). On the use of diversity measures in longitudinal sequencing studies of microbial communities. *Front. Microbiol.* 9:1037. doi: 10.3389/fmicb.2018.01037

Whelan, F. J., Heirali, A. A., Rossi, L., Rabin, H. R., Parkins, M. D., and Surette, M. G. (2017). Longitudinal sampling of the lung microbiota in individuals with cystic fibrosis. *PLoS ONE* 12:e0172811. doi: 10.1371/journal.pone.0172811

Whiteson, K. L., Meinardi, S., Lim, Y. W., Schmieder, R., Maughan, H., Quinn, R., et al. (2014). Breath gas metabolites and bacterial metagenomes from cystic fibrosis airways indicate active pH neutral 2,3-butanedione fermentation. *ISME J.* 8, 1247–1258. doi: 10.1038/ismej.2013.229

Zemanick, E. T., Harris, J. K., Wagner, B. D., Robertson, C. E., Sagel, S. D., Stevens, M. J., et al. (2013). Inflammation and airway microbiota during cystic fibrosis pulmonary exacerbations. *PLoS ONE*. 8:e62917. doi: 10.1371/journal.pone.0062917

Zhao, J., Schloss, P. D., Kalikin, L. M., Carmody, L. A., Foster, B. K., Petrosino, J. F., et al. (2012). Decade-long bacterial community dynamics in cystic fibrosis airways. *Proc. Natl. Acad. Sci. U.S.A.* 109, 5809–5814. doi: 10.1073/pnas.1120577109

Conflict of Interest: The authors declare that the research was conducted in the absence of any commercial or financial relationships that could be construed as a potential conflict of interest.

frontiers in Cellular and Infection Microbiology

ORIGINAL RESEARCH
published: 06 August 2020
doi: 10.3389/fcimb.2020.00398

A Novel Description of the Human Sinus Archaeome During Health and Chronic Rhinosinusitis

Brett Wagner Mackenzie[1], Annie G. West[2], David W. Waite[2]*, Christian A. Lux[2], Richard G. Douglas[1], Michael W. Taylor[2] and Kristi Biswas[1]*

[1] Department of Surgery, The University of Auckland, Auckland, New Zealand, [2] School of Biological Sciences, The University of Auckland, Auckland, New Zealand

Human microbiome studies remain focused on bacteria, as they comprise the dominant component of the microbiota. Recent advances in sequencing technology and optimization of amplicon sequencing protocols have allowed the description of other members of the microbiome, including eukaryotes (fungi) and, most recently, archaea. There are no known human-associated archaeal pathogens. Their diversity and contribution to health and chronic respiratory diseases, such as chronic rhinosinusitis (CRS), are unknown. Patients with CRS suffer from long-term sinus infections, and while the microbiota is hypothesized to play a role in its pathogenesis, the exact mechanism is poorly understood. In this cross-sectional study, we applied a recently optimized protocol to describe the prevalence, diversity and abundance of archaea in swab samples from the middle meatus of 60 individuals with and without CRS. A nested PCR approach was used to amplify the archaeal 16S rRNA gene for sequencing, and bacterial and archaeal load (also based on 16S rRNA genes) were estimated using Droplet Digital™ PCR (ddPCR). A total of 16 archaeal amplicon sequence variants (ASVs) from the phyla *Euryarchaeota* and *Thaumarchaeota* were identified. Archaeal ASVs were detected in 7/60 individuals, independent of disease state, whereas bacterial ASVs were detected in 60/60. Bacteria were also significantly more abundant than archaea. The ddPCR method was more sensitive than amplicon sequencing at detecting archaeal DNA in samples. Phylogenetic trees were constructed to visualize the evolutionary relationships between archaeal ASVs, isolates and clones. ASVs were placed into phylogenetic clades containing an apparent paucity of human-associated reference sequences, revealing how little studied the human archaeome is. This is the largest study to date to examine the human respiratory-associated archaeome, and provides the first insights into the prevalence, diversity and abundance of archaea in the human sinuses.

Keywords: human microbiome, archaea, bacteria, 16S rRNA gene, chronic rhinosinusitis, Droplet Digital™ PCR

OPEN ACCESS

Edited by:
Marloes Dekker Nitert, The University of Queensland, Australia

Reviewed by:
Martin Desrosiers, University of Montreal Hospital Centre (CRCHUM), Canada
Renate Lux, University of California, Los Angeles, United States

****Correspondence:***
Brett Wagner Mackenzie
bc.wagner@auckland.ac.nz
David W. Waite
david.waite@auckland.ac.nz

Specialty section:
This article was submitted to Microbiome in Health and Disease, a section of the journal Frontiers in Cellular and Infection Microbiology

Received: *30 January 2020*
Accepted: *29 June 2020*
Published: *06 August 2020*

Citation:
Wagner Mackenzie B, West AG, Waite DW, Lux CA, Douglas RG, Taylor MW and Biswas K (2020) A Novel Description of the Human Sinus Archaeome During Health and Chronic Rhinosinusitis. Front. Cell. Infect. Microbiol. 10:398. doi: 10.3389/fcimb.2020.00398

INTRODUCTION

Human-associated microbial communities are diverse and occupy site-specific niches. These microbes are intrinsically linked to human health, by helping maintain homeostatic functions and contributing to both acute and chronic disease. To date, most human microbiome research has focused on bacteria, as they are the dominant members of the microbiome

(Sender et al., 2016) However, recent advances in sequencing technologies have expanded research to include fungi, other eukaryotes, archaea, and viruses (Hoffmann et al., 2013; Lim et al., 2015; Monaco et al., 2016; Hannigan et al., 2018; Hoggard et al., 2019). The composition and contribution of these lesser-known members to both health and disease states remains an exciting area for human microbiome research.

Species of the domain Archaea are characterized by a unique cell wall structure that assists survival in extreme conditions such as hydrothermal vents, salt lakes, anoxic and highly acidic or alkaline environments (Eichler, 2003). Recent research suggests that archaea may be as widely distributed as bacteria and colonize a diverse range of hosts (Lloyd et al., 2013; Moissl-Eichinger et al., 2018). Most of the human microbiome research investigating the archaeome (the archaeal portion of the human microbiome) focuses on the gut, where methanogens are the dominant archaea (Miller and Wolin, 1985; Dridi et al., 2009; Miragoli et al., 2017; Wampach et al., 2017). More recently, archaeal signatures have been detected in subgingival dental plaque, skin, lung, sinus and nares samples (Lepp et al., 2004; Dridi et al., 2011; Hulcr et al., 2012; Probst et al., 2013; Oh et al., 2014; Koskinen et al., 2017; Moissl-Eichinger et al., 2017; Pausan et al., 2018; Wagner Mackenzie et al., 2018).

The lack of any known archaeal pathogen presumably contributes to the paucity of studies investigating the prevalence, composition and role of the human archaeome, especially during health and disease. No studies to date have specifically examined the composition or diversity of the sinus archaeome. Of particular interest is the composition of the sinus microbiome during health and chronic rhinosinusitis (CRS). CRS is a disease affecting up to 6.4% of the population and characterized by long-term inflammation of the sinuses (Dietz de Loos et al., 2019). CRS is associated with both a substantial impact on the quality of life of patients that suffer from this disease and high health care costs (Rudmik, 2017; Bhattacharyya et al., 2019). Although the microbiome is hypothesized to play a role in the etiology of CRS and/or the exacerbation of symptoms, no microbial pathogen or disease-specific microbial community profile has been identified to date (Hoggard et al., 2017; Cho et al., 2020). The overwhelming proportion of human DNA from sinus samples has so far limited the insights gleaned from metagenomic studies, therefore many studies employ amplicon sequencing techniques to focus on bacterial associations with disease. The only study to date which applied metagenomic sequencing to CRS sinus samples reported the presence of archaea, but the absence of healthy subjects and technical controls limited the conclusions that could be drawn (Wagner Mackenzie et al., 2018).

Recent studies have evaluated primer-pairs and data processing pipelines for targeting the archaeal component of the human microbiome for amplicon sequencing (Koskinen et al., 2017; Pausan et al., 2018). Studies by Pausan et al. optimized the detection and quantification of archaea in a variety of samples from different sites, including swab samples from the upper nasal cavity. Although the total number of samples investigating the upper respiratory archaeome was small [Koskinen et al. ($n = 2$) and Pausan et al. ($n = 7$)] a diverse range of archaea were nonetheless detected.

In this cross-sectional study, we applied the optimized protocols by Pausan *et al.* to investigate the prevalence, diversity and abundance of archaea in the human sinuses and any associations with disease state. Specifically, we used 16S rRNA gene amplicon sequencing to assess microbiota composition, and Droplet Digital™ PCR to estimate total bacterial and archaeal loads.

MATERIALS AND METHODS

Sample Collection

For this study, 40 participants undergoing endoscopic sinus surgery and 20 healthy volunteers with no history of sinus disease, asthma, or recent antibiotic usage (≤6 months) were recruited. Of the 40 that underwent surgery, participants had CRS with nasal polyps (CRSwNP) ($n = 16$), CRS without polyps (CRSsNP) ($n = 15$), or were disease control participants ($n = 9$). Disease control participants were defined as patients undergoing endoscopic sinonasal surgery for reasons unrelated to CRS. The bacterial composition of the 40 participants undergoing surgery has been published previously as part of a different study (Wagner Mackenzie et al., 2019).

All participants were ≥18 years of age. CRS patients with immunodeficiencies or vasculitis were excluded. Pairs of sterile, endoscope-guided rayon swab samples (Copan Diagnostics, Inc., Murrieta, CA) were collected from the left middle meatus of all individuals. Swab samples were stored in RNA*later*™ (Thermo Fisher Scientific, New Zealand) at 4°C overnight, then transferred to −20°C until processed. This study was approved by the New Zealand Health and Disability Ethics Committee (NTX/08/12/126) and all patients provided informed consent.

Nucleic Acids Extraction and Target Gene Amplification

Samples from healthy volunteers were thawed on ice, and DNA was extracted from pairs of swabs using the Qiagen® AllPrep DNA/RNA Mini Kit (Bio-Strategy Ltd, Auckland, New Zealand) as previously described (Wagner Mackenzie et al., 2019). DNA from all samples, including those from the previous study, was extracted in a consistent manner. Briefly, after bead-beating to lyse cells and two wash steps to remove impurities, sterile PCR-grade water (32 μL) was added to the spin column filter and incubated for 5 min before DNA was eluted by centrifuging for 1 min at 11,200 × g. The eluate was centrifuged through the spin column filter a second time to increase DNA concentration. A negative extraction containing 200 μL of sterile water and PCR amplification of PCR-grade water was performed to assess for microbial contamination of the DNA extraction kit and PCR reagents.

A nested PCR approach using primers optimized by Pausan et al. was applied to amplify the bacterial and archaeal 16S rRNA gene (Pausan et al., 2018). Briefly, up to 100 ng of template DNA from each of the 60 participants was amplified in duplicate. For the first PCR, each reaction was performed in a final volume of 20 μL that included: 2.5 μL of 10X Buffer,

10 mM $MgCl_2$, 2.5 mM dNTPs, 0.1 μL HotStar DNA Polymerase (Qiagen), and 0.5 μL of 10 mM of each primer S-D-ARCH-0344-a-S-20 (ACG GGG YGC AGC AGG CGC GA) and S-D-ARCH-1041-a-A-18 (GGC CAT GCA CCW CCT CTC), 13.9 μL PCR-grade water, and 1 μL template DNA. Negative controls comprised PCR-grade water, and genomic DNA obtained from *Escherichia coli* (bacterial) and *Halorussus* (archaeal) were used as positive controls in all PCRs. Thermocycling conditions were as follows: 15 min initial denaturation at 95°C, followed by 12 cycles of 94°C for 30 s, 56°C for 45 s, and 72°C for 1 min, with a final extension step at 72°C for 10 min. Amplicons were not purified after the first PCR, to limit the risk of contamination.

Two microliters of the resulting PCR product were transferred into a second PCR containing 2.5 μL of 10X Buffer, 10 mM $MgCl_2$, 2.5 mM dNTPs, 0.1 μL HotStar DNA Polymerase (Qiagen), and 0.5 μL of 10 mM of each barcoded primer for Illumina sequencing S-D-Arch-0519-a-S-15 (TCG TCG GCA GCG TCA GAT GTG TAT AAG AGA CAG CAG CMG CCG CGG TAA) and S-D-Arch-0786-a-A-20 (GTC TCG TGG GCT CGG AGA TGT GTA TAA GAG ACA GGG ACT ACV SGG GTA TCT AAT), and 17.9 μL PCR-grade water for a final volume of 25 μL. Thermocycling conditions were as follows: 15 min initial denaturation at 95°C, followed by 35 cycles of 95°C for 30 s, 55°C for 30 s, and 70°C for 40 s, with a final extension step at 70°C for 3 min. Template of controls from the first PCR were included in the second PCR. Additional controls for the second PCR included PCR-grade water, and *E. coli* and archaeal *Halorussus* genomic DNA.

Amplicons from each PCR step were visualized by agarose gel electrophoresis. Replicate, nested PCR products from each sample were purified using Agencourt AMPure beads (Beckman Coulter Life Sciences Inc., USA) according to manufacturer instructions. PCR products were quantified using the High Sensitivity (HS) kit on the Qubit® Fluorometer 1.0 (Invitrogen Co., Carlsbad, USA). Negative DNA extraction and positive *Halorussus* controls were included in purification and sequencing. Purified amplicons were submitted to Auckland Genomics Ltd for library preparation using a dual-indexing approach with Nextera technology and sequencing (2 × 300 bp, paired-end) on Illumina MiSeq. All sequencing data have been deposited with NCBI under BioProject ID number PRJNA599016.

Bioinformatic Analyses

Amplicon sequence data were processed according to the pipeline recommended in previous human archaeome studies (Koskinen et al., 2017; Pausan et al., 2018) using the open source package DADA2 (Callahan et al., 2016) in R version 3.6.1 RStudio Team (2020) following a modified version of the DADA2 pipeline tutorial v1.12 (https://benjjneb.github.io/dada2/tutorial.html). Briefly, raw sequences were quality filtered using the parameters truncLen=c(240,280) and trimLeft=c(17,21) to remove primers, and maxN=0 and maxEE=c(3,5) to remove poor quality sequences. Quality filtered sequences were merged, denoised, and amplicon sequence variants (ASVs) were inferred. The resulting ASVs were assigned taxonomy using the SILVA v128 database to be consistent with other archaeal sequencing from respiratory-associated samples. Those ASVs that were detected in both the negative DNA extraction control and in samples were either subtracted or completely removed from the final ASV table. It is important to note that 13 sequence counts were detected in the DNA extraction control that were assigned to the same ASV as the positive control (archaeal ASV1, *Halorussus*). This ASV was also detected in the samples, and 13 counts were subtracted from each of the samples where it was detected. No other archaea were detected in the DNA extraction control. Samples were rarefied to an even depth of 11,644 quality-filtered, taxon-assigned ASV sequence counts per sample. The rarefied and contaminant-corrected ASV table was used for all downstream processing unless otherwise noted.

Alpha and beta diversity analyses and taxa plots were generated using "phyloseq" version 1.28.0 package in R version 3.6.1 (McMurdie and Holmes, 2013). Observed ASVs, Shannon, and Inverse Simpson diversity analyses were calculated using the "estimate_richness" command. Box plots were generated using the R package "ggplot2" to visualize alpha diversity results (Wickham, 2016). A Bray-Curtis distance matrix was generated using the "ordinate" function and visualized using the "plot_ordination" command. Permutational analysis of variance was implemented using the "Adonis" command in the vegan package in R version 3.6.1 to assess the contribution of diagnosis to variance in the model (Oksanen et al., 2019).

Differences in microbial communities within groups at ASV level were evaluated. First, ASVs with <0.01% relative abundance across the rarefied dataset were removed. This resulted in 460 taxon-assigned ASVs. Differences between groups were then evaluated using a Kruskal-Wallis rank sum test to generate overall *p*-values that indicated a significant difference existed at least once across the groups, then pairwise comparisons were made between treatment groups using Dunn's test with "BH" *p*-value correction for multiple pairwise comparisons. To visualize differences in abundance of specific ASVs, box plots were generated as previously described.

Phylogenetic Tree Inference

Phylogenetic trees were constructed to depict the relationship of all the archaeal ASVs identified in this study to known archaeal taxa. Sequences were aligned by using the online SINA alignment tool (version 1.2.11) (Pruesse et al., 2012) which was then imported into ARB version 6.0.6 (Ludwig et al., 2004). For each archaeal phylum (i.e., *Euryarchaeota* and *Thaumarchaeota*), a 50% conservation filter was constructed and used to filter the sequences of ASVs and a manually selected set of reference sequences. Alignments were then exported and maximum-likelihood phylogenetic inference performed with IQ-Tree version 1.6.9 (Nguyen et al., 2015) using the GTR model of nucleotide substitution with Gamma-distributed rate heterogeneity. For each tree, 1,000 bootstrap re-samplings were performed to assess node support. The resulting trees were visualized and color-coded according to the archaeal family level using the Interactive Tree of Life resource version 4 (Letunic and Bork, 2019).

Quantification of Archaeal and Bacterial 16S rRNA Gene Copies

Droplet Digital™ PCR (ddPCR) was used to measure absolute quantities of bacterial and archaeal DNA in each sample. Droplet generation, PCR amplification, and QX200 droplet readings were conducted using the QX200 Droplet Digital™ PCR System and QuantaSoft™ Software according to the manufacturer's instructions (Bio-Rad Laboratories, New Zealand). Briefly, the V1-V3 regions of the bacterial 16S rRNA gene were amplified using primers 8F and 341R (Biswas et al., 2015). Each ddPCR reaction contained 11 μL EvaGreen®, 0.5 μL 10 μM 8F forward primer, 0.5 μL 10 μM 341R reverse primer, 9 μL of sterile PCR-grade water, and 1 μL of sample DNA for a total volume of 22 μL. A positive control of *E. coli* DNA and a negative control of 1x ddPCR buffer with PCR-grade sterile water were included. Thermocycling conditions were as follows: enzyme activation at 95°C for 5 min, followed by 40 cycles of denaturation at 95°C for 30 s and annealing/extension at 60°C for 1 min. A single signal stabilization step at 4°C for 5 min then 90°C for 5 min was carried out. The same protocol was followed for archaea, substituting bacterial primers with archaeal primers S-D-Arch-0787-a-S-20 (ATT AGA TAC CCS BGT AGT CC) and S-D-Arch-0958-a-A-19 (YCC GGC GTT GAM TCC AAT T) (Pausan et al., 2018). Droplets were analyzed using the QuantaSoft™ Software according to the manufacturer's recommendations. Manual thresholds were set for droplet counts. Box plots were generated to visualize the data as previously described.

Statistical Analyses

All data were analyzed according to patient diagnosis: healthy, control, CRSsNP, or CRSwNP. All statistical analyses were conducted in R version 3.6.1. Data were checked for normality using the command "normcheck" in the package "s20x" version 3.1-28 followed by ANOVA for normally distributed data or Kruskal-Wallis test for non-normally distributed data. If a significant difference was detected, pairwise comparisons were conducted with Tukey's HSD *post-hoc* test or Mann-Whitney U-test for normal and non-normally distributed data, respectively. *P*-value levels <0.05 are considered significant unless otherwise stated.

RESULTS

Demographic statistical analyses revealed significant differences in the age of subjects at the time of sampling between the four cohorts, with healthy subjects being younger (average age ± standard deviation 26.1 ± 7.9 years) than disease control (45.8 ± 6.4), CRSsNP (46.3±13.8), and CRSwNP (52.8 ± 12.5) cohorts ($p < 0.001$). There were significantly fewer females in the CRSwNP cohort (2/16, $p < 0.05$), both CRSsNP and CRSwNP had significantly higher instances of asthma than healthy and disease controls, and CRSwNP patients had significantly higher Lund-Mackay scores than CRSsNP (**Table 1**).

Sequence data quality filtering, correction for contamination, and rarefaction to 11,644 sequences per sample resulted in a total of 2,127 ASVs across 60 samples. The majority of ASVs in the rarefied data table were bacterial (2,111 bacterial ASVs compared to 16 archaeal ASVs). The archaeal positive control was assigned correctly to the archaeal genus *Halorussus*, and no other archaeal ASVs detected in samples were also detected in the positive control. After corrections for contamination, 15 archaeal ASVs were unique to samples.

"Adonis" analyses suggested that diagnosis contributed significantly to differences observed between microbial communities ($R^2 = 0.083$, $p = 0.009$). The presence of archaea in a subject's microbiome did not contribute significantly to variance observed in the dataset ($p > 0.05$), and presence of archaea in the microbiome was not associated with disease status ($p > 0.05$).

Archaea Are Less Prevalent, Diverse, and Abundant Than Bacteria

Archaeal ASVs were detected in 7/60 subjects (healthy: $n = 2$, disease control: $n = 1$, CRSsNP: $n = 1$, CRSwNP: $n = 3$). Of the 16 ASVs detected across the dataset, 8 were assigned to the archaeal phylum *Euryarchaeota* and 8 to the *Thaumarchaeota* (**Table S1**). The average relative abundance of archaea in a subject's microbiota, when present (± standard deviation), was 14.7% ± 18.3% (range 0.03–45%). Interpersonal archaeal diversity was high, and no consistent archaeal profile was observed across samples where archaea were detected (**Figure 1**). Furthermore, in patients where archaeal ASVs were detected, only one or two dominant archaea-assigned ASVs were reported, and these ASVs were members of the same archaeal class. No skewing by disease state according to the archaeal portion of the microbiota was observed.

In contrast to the low prevalence of archaea, bacteria-assigned ASVs were detected in every sample in this study (60/60). The most abundant bacterial ASV, on average, across the entire dataset was assigned to the genus *Corynebacterium_1* (23.3% ± 25.9%). Other prevalent and abundant ASVs included *Staphylococcus*, *Dolosigranulum*, *Moraxella*, *Lawsonella*, and *Haemophilus* (**Figure 1**). Across the dataset, a total of 23 bacterial phyla were detected. However, the majority of these phyla were detected at very low relative abundances.

The absolute quantities of bacteria and archaea in each sample were measured using ddPCR. Bacterial DNA was detected in all samples, with an average number of 23,483 ± 68,862 bacterial 16S rRNA gene copies per sample (**Figure 2**). ddPCR was more sensitive than Illumina MiSeq amplicon sequencing for detecting archaeal DNA. Archaeal DNA was detected in 51/60 subjects, although at extremely low quantities on average (20 ± 23 archaeal 16S rRNA gene copies per sample). Overall, bacterial load was significantly greater than that for archaea ($p < 0.0001$).

Archaeal Amplicon Sequencing Reveals Broad Phylogenetic Diversity

Since many of the archaeal ASVs belonging to the phylum *Thaumarchaeota* could not be classified beyond the level of class, phylogenetic trees were inferred to provide greater insight into the archaeal sequences recovered in this dataset. For the phylogenetic tree construction, all archaea-assigned sequences

TABLE 1 | Patient demographics and results from statistical analyses.

Variables	Healthy controls ($n = 20$)	Disease controls ($n = 9$)	CRSsNP ($n = 15$)	CRSwNP ($n = 16$)	Unadjusted test p-value
Age	26.1±7.9	45.8±6.4	46.3±13.8	52.8±12.5	**$p < 0.001$**
European	13/20	6/9	13/15	12/16	$p > 0.05$
Female	9/20	6/9	6/15	2/16	**$p < 0.05$**
Lund-Mackay score	NA	NA	13.1±2.8	19.4±4.4	**$p < 0.001$**
Asthma	0	0	13/15	6/16	**$p < 0.001$**
Antibiotics*	1/20	0	0/15	3/16	$p > 0.05$
Never smoked	20/20	7/9	14/15	14/16	$p > 0.05$
Bacterial MiSeq prevalence (100%)	20/20	9/9	15/15	16/16	$p > 0.05$
Bacterial ddPCR prevalence (100%)	20/20	9/9	15/15	16/16	$p > 0.05$
Archaeal MiSeq prevalence (13%)	2/20	1/9	1/15	3/16	$p > 0.05$
Archaeal ddPCR prevalence (85%)	17/20	8/9	14/15	12/16	$p > 0.05$

*Continuous variables were tested for normality using Shapiro-Wilk normality test followed by analysis of variance then Tukey multiple comparisons of means for pairwise comparisons. Means ± standard deviations are shown. Categorical variables were tested using a Fisher's exact test. Significant results ($p < 0.05$) are shown in bold typeface. MiSeq prevalence refers to detection of ASVs with amplicon sequencing, and ddPCR prevalence refers to Droplet Digital™ PCR detection with Domain-specific primers. *Antibiotic prescription within 4 weeks of sample collection.*

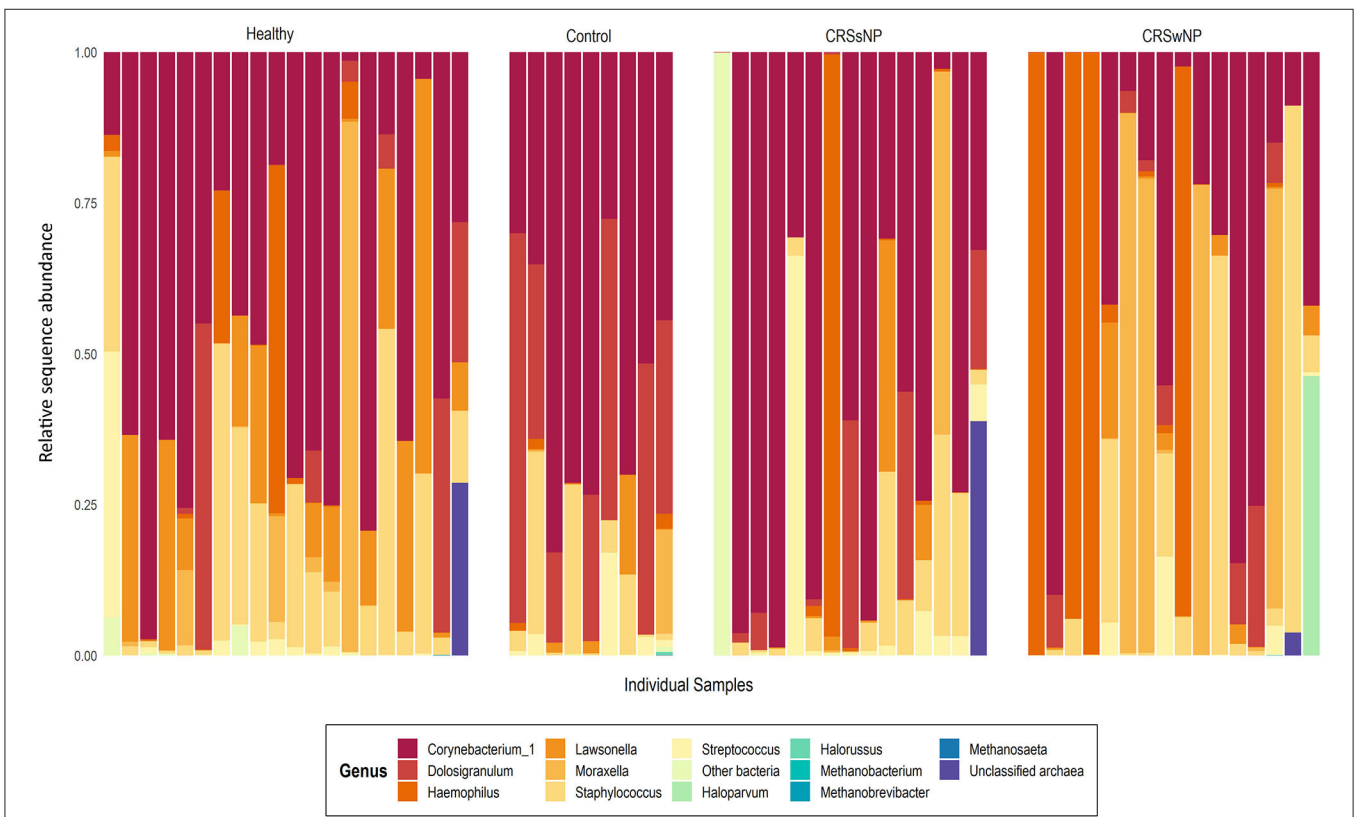

FIGURE 1 | Taxa bar-plot showing the microbial communities recovered from each middle meatus swab sample in this study. Subjects are grouped according to disease state. Relative sequence abundances (%) of the seven most abundant bacterial genera, with all other genera grouped in "Other bacteria," are shown, as well as all detected archaea classified to genus-level. Other archaeal amplicon sequence variants which could not be classified to genus-level are grouped as "Unclassified archaea".

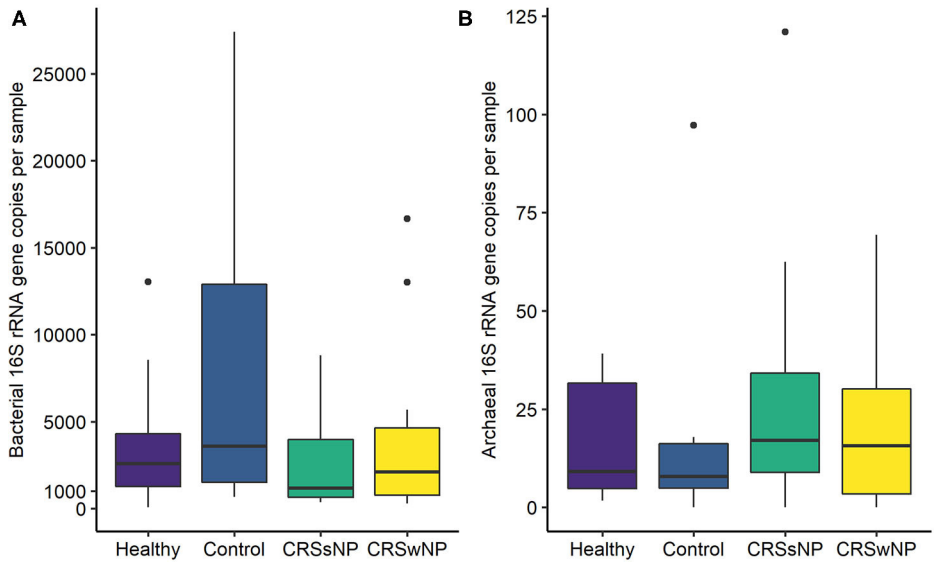

FIGURE 2 | Box plots depicting **(A)** bacterial and **(B)** archaeal 16S rRNA gene copy numbers measured using Droplet Digital™ PCR. Some outlier samples have been removed from graph **(A)** for visualization purposes; outlier datapoints were included in all statistical analyses. No significant differences in bacterial or archaeal loads were observed between groups. Note the differences in y-axes scales between **(A,B)**. Median values are indicated by the solid black line within each box, extending to the upper and lower quartile values.

recovered in the dataset before rarefaction were included. Details of the ASV nucleotide sequence, corresponding ASV number used in this study, and taxonomic identification can be found in **Table S1**. Three additional ASVs recovered from the archaea positive control (ASVs 17, 18, 19—all found at very low counts) were included in phylogenetic reconstructions; these ASVs were not found in any subject samples, but were included nonetheless.

The archaeal assigned sequences in this study clustered into six archaeal families. **Figure 3** depicts the position of archaeal ASVs 1,2,7,8,9,14,15,16,17, and 19 which clustered amongst other archaeal representatives in the *Haloferacaceae*, *Halomicrobiaceae*, *Methanosaetaceae*, and *Methanobacteriaceae* families. Archaeal ASVs 3,4,5,6,10,11,12, and 13, which were identified as *Thaumarchaeota*, clustered with isolates belonging to the family *Nitrososphaeraceae* (**Figure 4**). Archaeal ASV 18, with only 4 sequence counts recovered from the positive control, clustered with the candidate archaeal family *SCGC AB-179-E04*. The representatives of archaea in the inferred phylogenetic trees were isolated from a very diverse range of environments. Congruence of assignments between phylogenetic tree reconstruction and the SILVA v128 sequences was low, highlighting the critical need for advancing both archaeal phylogeny and taxonomy.

Microbial Characteristics Associated With Diagnosis

While no archaeal ASVs were associated with diagnosis, samples from healthy volunteers had significantly more ASVs on average than those from control, CRSsNP and CRSwNP cohorts (Observed species metric, $p < 0.001$) (**Figure S1**). Additionally, control participants had significantly higher richness of ASVs when compared with CRSwNP samples. Although healthy volunteers tended to have higher Shannon and Inverse Simpson diversity when compared to other groups this was not significant (Shannon and Inverse Simpson $p > 0.05$).

Pairwise comparisons of ASVs between groups revealed a number of bacteria-assigned ASVs that were significantly differentially abundant (**Table S2**). No archaeal ASVs were observed as significantly associated with any group. Comparisons between CRSsNP and CRSwNP ASV abundances revealed only one ASV, associated with the bacterial genus *Moraxella*, to be significantly different between the two groups. This ASV was more abundant in CRSwNP (**Figure S2**). Increased relative abundances of ASV4, associated with *Dolosigranulum*, characterized control subject sinus microbiota. The largest number of significant differences observed between groups was among healthy volunteers compared with controls, CRSsNP and CRSwNP. An increased relative abundance of ASVs from the bacterial genera *Burkholderia-Paraburkholderia*, *Flectobacillus*, *Dyella*, *Ralstonia*, *Actinomyces*, and *Lawsonella* were associated with healthy volunteers (**Figure S2**).

Comparisons of bacterial gene copy numbers between groups did not reveal any significant differences ($p > 0.05$). No significant differences were observed in the number of archaeal gene copy numbers between groups ($p > 0.05$).

DISCUSSION

In this study we applied recently optimized methodologies to evaluate the prevalence, diversity and abundance of archaea in human sinuses during health and chronic disease (Pausan et al., 2018). The diversity and composition of archaea in the

FIGURE 3 | Phylogenetic inference of archaeal amplicon sequences from the middle meatuses of the subjects in this study. Support of internal nodes was determined through 1,000 bootstrap resamplings, and is represented on nodes with >90% bootstrap support (black), 70–90% support (gray), 50–70% support (white). Scale bar represents 1% sequence divergence. The tree is colored according to archaeal families *Haloferacaceae*, *Halomicrobiaceae*, *Methanosaetaceae*, and *Methanobacteriaceae*. Corresponding archaeal ASV taxon assignments from this study are found in **Table S1**.

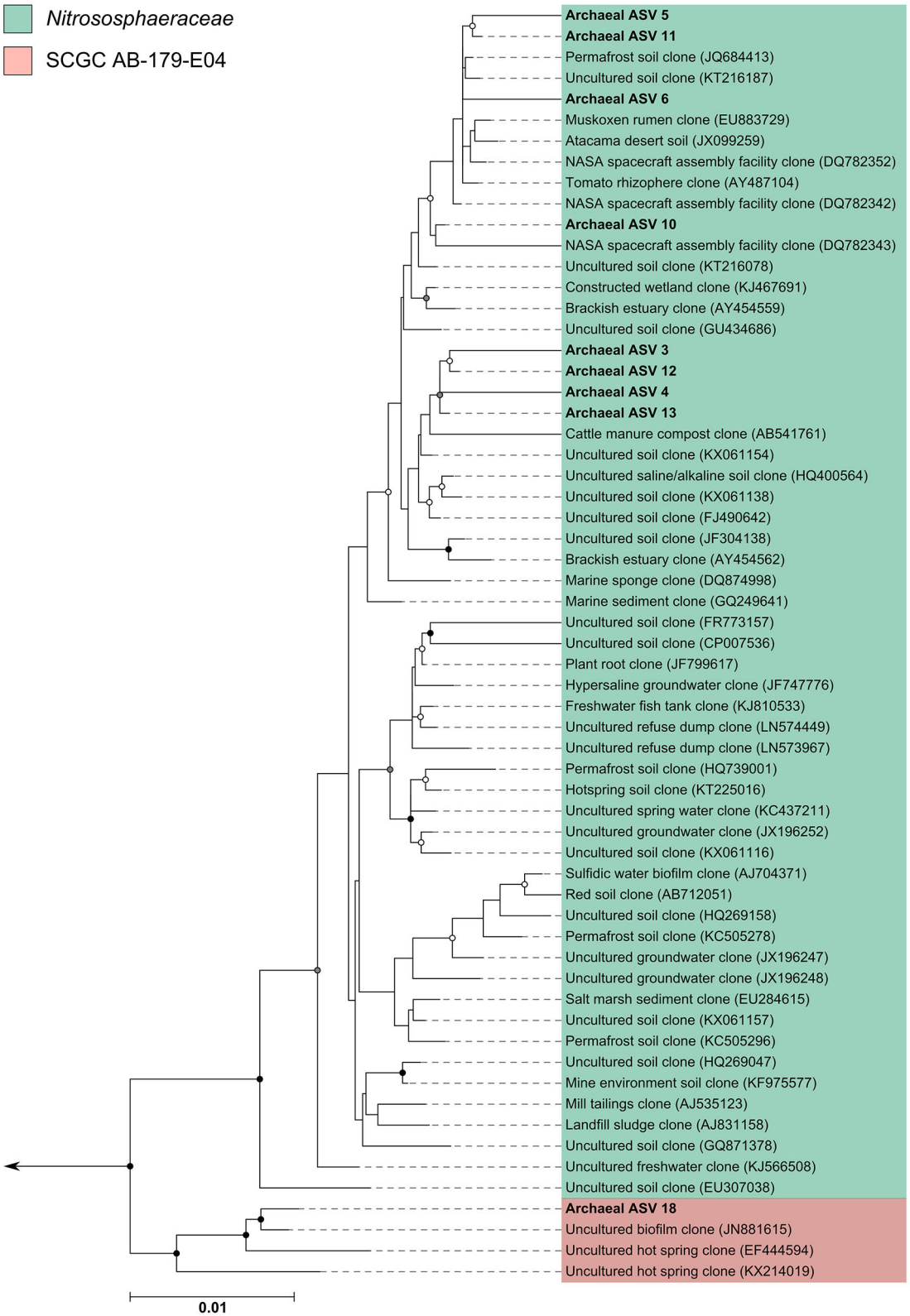

FIGURE 4 | Phylogenetic inference of archaeal amplicon sequences from the middle meatuses of the subjects in this study. Support of internal nodes was determined through 1,000 bootstrap resamplings, and is represented on nodes with >90% bootstrap support (black), 70–90% support (gray), 50–70% support (white). Scale bar represents 1% sequence divergence. The tree is colored according to archaeal families *Nitrososphaeraceae* and *SCGC AB-179-E04*. Corresponding archaeal ASV taxon assignments from this study are found in **Table S1**.

sinuses exhibited high interpersonal variation, and we observed no association of archaea with disease state. High interpersonal variation of both archaeal and bacterial communities is a common theme in human microbiome research (Caporaso et al., 2011; Biswas et al., 2015; Hoggard et al., 2016; Lloyd-Price et al., 2017; Pausan et al., 2018), and our results support this observation.

The prevalence and diversity of archaea across the 60 subjects in our study was lower than in other studies; however this may be partly attributed to a number of factors such as sampling method, sequencing depth, sequencing type (amplicon vs. metagenomic) and/or sampling site. In this study, members from both *Euryarchaeota* and *Thaumarchaeota* phyla were detected which have been previously reported. However, we did not recover any members from *Woesearchaeota* which were detected in nares swabs from other human archaeome studies (Koskinen et al., 2017; Pausan et al., 2018). Interestingly, the samples in our study had a very low prevalence and abundance of *Methanobrevibacteriaceae*, which was the main archaeal representative detected in a previous study in our group which applied metagenomic sequencing to sinus swabs (Wagner Mackenzie et al., 2018).

There may be differences in sampling site of the upper respiratory tract (upper nares vs. the sinuses) or geographic differences in the composition of the archaeome. The effect of sampling site within the sinonasal cavity is unclear, and a consensus has not been reached regarding the effect on bacterial community composition (Biswas et al., 2015; Lal et al., 2017; Copeland et al., 2018). Sampling site may play a larger role in the recovery of other less abundant members of the microbiota. Additionally, a recent world-wide study collected middle meatus swabs samples from CRS and control subjects from 13 centers across 5 continents (Paramasivan et al., 2019). Minor, but significant differences in bacterial community composition associated with geographic location were identified. These results suggest that other members of the microbiota, such as archaea and especially fungi, may respond to geographic-driven changes. Together, these effects may partly explain the differences observed between our results and those from other studies.

The human archaeome is drastically understudied when compared with environmental microbiomes. Although the human archaeome is an exciting new area for research, larger studies are required in order to contextualize the results from the few studies published to date. In addition to bacteria and archaea, other microbes such as fungi and viruses are present in the sinuses during health and CRS disease (Lloyd-Price et al., 2017; Zhao et al., 2017; Goggin et al., 2019; Hoggard et al., 2019). Cross-kingdom interactions and co-occurrence patterns in the human airway microbiome should be investigated further. In parallel to amplicon studies that can give insight into archaeal community composition, genome reconstruction of human-associated archaea, either from metagenomic data or directed culturing, should be undertaken in order to ascertain the ecological functions and roles of these organisms. Archaea, in general, are underrepresented in microbial databases, and it is therefore unsurprising that phylogenetic inference clustered the archaeal sequences recovered from the sinus samples in this study with taxa from a diverse array of seemingly unrelated environments. Although we did not observe or identify an association of the archaeal aspect of the sinus microbiota with disease, subsequent studies are necessary as human archaeome research is in its infancy and the archaeal representatives in taxonomic databases are continually updated.

Archaea are characterized by their unique cell wall membrane in addition to differences in DNA repair, genetic features, biochemical and metabolic capabilities (Bang and Schmitz, 2015). These phenotypic and genotypic differences likely result in functionally distinct roles in the human airway microbiome, however, so few studies only allow for speculation. Recent studies suggest that the human immune system recognizes and can be activated by archaea (Hirai et al., 2013; Bang et al., 2014). Furthermore, archaea are characterized by a lack of peptidoglycan in their cell wall, which makes these microbes resistant to a wide spectrum of antibiotics (Khelaifia and Drancourt, 2012). Determining how archaea interact with the host and respond to antimicrobials may help resolve the role of these microbes in both health and disease.

One advantage of employing the primers used in this study is that it allowed us to investigate the bacterial portion of the microbiota in parallel to archaea. The low prevalence of archaea in our study limited our ability to produce reliable correlations between bacteria and archaea. However, a well-established syntrophy exists between methanogenic archaea and bacteria in the gut and this relationship may help explain the presence of methanogens in the sinuses (Samuel et al., 2007). There is also some evidence to support the association of sulfate-reducing bacteria with *M. oralis* in subgingival dental plaque (Nguyen-Hieu et al., 2013). Other studies have hypothesized that low levels of ammonium found on the skin may foster the growth of members from the phylum *Thaumarchaeota* (Probst et al., 2013). The associations of archaea and bacteria in health and chronic diseases may become apparent in subsequent studies with larger sample sizes.

Our results confirmed previous associations of bacterial composition and diversity with CRS disease. Similar to previous studies, we observed significantly increased alpha diversity in the sinus microbiota of healthy subjects when compared with disease control, CRSsNP and CRSwNP subjects (Abreu et al., 2012; Hoggard et al., 2016; Wagner Mackenzie et al., 2016; Cope et al., 2017). It should be noted, however, that the significantly younger age of the healthy subjects compared with disease controls and both CRS cohorts may influence this observation (Aleman and Valenzano, 2019). Interestingly, and in support of a previously published meta-analysis by our group, we observed a significantly increased relative abundance of ASVs assigned as *Burkholderia-Paraburkholderia* and *Ralstonia* with healthy subjects (Wagner Mackenzie et al., 2016). The relative abundances of these ASVs were very low, $< 1\%$ of total relative abundance on average in healthy subjects for both *Burkholderia-Paraburkholderia* and all three *Ralstonia* ASVs, but were nonetheless significant after corrections for multiple pairwise comparisons. The meta-analysis included published sequences from previous studies, and the samples sequenced here were not included. Members of the

Burkholderiaceae family (and other skin-associated bacteria) have been associated with DNA extraction kit contamination (Glassing et al., 2016), however in our study we have corrected for contamination. The associations of these taxa with healthy sinuses are intriguing and should be investigated further to ascertain if they are an artifact of methodology or if they are indeed biologically meaningful.

CONCLUSION

The results from this study suggest it is unlikely that the archaeal portion of the sinus microbiota significantly influences or is influenced by disease state. However, it is likely that the sinus bacterial community is associated with CRS or is influenced by disease state. The exact nature of this association remains unclear. To our knowledge, this is the largest study to date examining the human associated respiratory archaeome. We observed a lower prevalence, diversity and abundance of archaea when compared with bacteria. We strongly recommend future studies include investigations of archaea in human microbiome samples in order to better understand the role of archaea in human health, but also to better characterize this domain in general.

DATA AVAILABILITY STATEMENT

The datasets generated for this study can be found in the NCBI under accession number PRJNA599016.

ETHICS STATEMENT

The studies involving human participants were reviewed and approved by the New Zealand Health and Disability Ethics Committee (NTX/08/12/126). The patients/participants provided their written informed consent to participate in this study.

AUTHOR CONTRIBUTIONS

BW designed the experiment, conducted lab work, processed sequencing data, interpreted results, and wrote the manuscript. AW and DW contributed to data analyses and manuscript review. CL assisted with sample collection and processing. RD collected samples from patients, provided laboratory space, and edited the manuscript. MT and KB designed the experiment and edited the manuscript. All authors contributed to the article and approved the submitted version.

FUNDING

This study was generously funded by the Garnett Passe and Rodney Williams Memorial Foundation Charitable Trust Project Grant No. 3716403.

ACKNOWLEDGMENTS

A special thanks to Karen M. Houghton and Jean Power from GNS Science, New Zealand for providing the archaeal DNA used as the positive control in this study. We thank all the subjects for their participation in this study.

SUPPLEMENTARY MATERIAL

The Supplementary Material for this article can be found online at: https://www.frontiersin.org/articles/10.3389/fcimb.2020.00398/full#supplementary-material

Figure S1 | Box plots depicting alpha diversity comparisons between the groups in this study (healthy, control, CRSsNP or CRSwNP) according to **(A)** number of observed ASVs, **(B)** Shannon, or **(C)** Inverse Simpson metrics. Median values are indicated by the solid black line within each box, extending to the upper and lower quartile values. Outlier data points are indicated as closed black circles. Significant differences between groups are shown above each box with an asterisk (*).

Figure S2 | Box plots depicting those ASVs which were identified as having significantly different relative sequence abundances between healthy ($n = 20$), control ($n = 9$), CRSsNP ($n = 15$), and CRSwNP ($n = 16$) groups. Kruskal-Wallis rank sum test generated overall p-values that indicated a significant difference existed at least once, and then pairwise comparisons were made between treatments using Dunn's test with "BH" p-value adjustment (precise p-values are in **Table S2**). Median values are indicated by the solid black line within each box, extending to the upper and lower quartile values. Outlier data points are indicated as closed black circles.

Table S1 | Amplicon sequence variants (ASVs) assigned to Archaea that were detected in this study. Archaeal ASV sequences were used for placement in archaeal phylogenetic trees. *Archaeal ASVs detected only in samples, +Archaeal ASVs detected only in PCR controls, "__" indicates an ASV could not be confidently assigned at this taxonomic resolution.

Table S2 | Evaluation of differences in microbial communities between groups at ASV level. Kruskal-Wallis rank sum test generated overall p-values that indicated a significant difference existed at least once across the groups, then pairwise comparisons were made between groups using Dunn's test with "BH" p-value correction for multiple pairwise comparisons. $p < 0.05$ were considered significant and are shown. __ = non-significant $p > 0.05$.

REFERENCES

Abreu, N. A., Nagalingam, N. A., Song, Y., Roediger, F. C., Pletcher, S. D., Goldberg, A. N., et al. (2012). Sinus microbiome diversity depletion and *Corynebacterium tuberculostearicum* enrichment mediates rhinosinusitis. *Sci. Transl. Med.* 4, 151ra24. doi: 10.1126/scitranslmed.3003783

Aleman, F. D. D., and Valenzano, D. R. (2019). Microbiome evolution during host aging. *PLoS Pathog.* 15:e1007727. doi: 10.1371/journal.ppat.1007727

Bang, C., and Schmitz, R. A. (2015). Archaea associated with human surfaces: not to be underestimated. *FEMS Microbiol. Rev.* 39, 631–648. doi: 10.1093/femsre/fuv010

Bang, C., Weidenbach, K., Gutsmann, T., Heine, H., and Schmitz, R. A. (2014). The intestinal archaea *Methanosphaera stadtmanae* and *Methanobrevibacter smithii* activate human dendritic cells. *PLoS ONE* 9:e99411. doi: 10.1371/journal.pone.0099411

Bhattacharyya, N., Villeneuve, S., Joish, V. N., Amand, C., Mannent, L., Amin, N., et al. (2019). Cost burden and resource utilization in patients with chronic rhinosinusitis and nasal polyps. *Laryngoscope* 129, 1969–1975. doi: 10.1002/lary.27852

Biswas, K., Hoggard, M., Jain, R., Taylor, M. W., and Douglas, R. G. (2015). The nasal microbiota in health and disease: variation within and between subjects. *Front. Microbiol.* 9:134. doi: 10.3389/fmicb.2015.00134

Callahan, B. J., McMurdie, P. J., Rosen, M. J., Han, A. M., Johnson, A. J. A., and Holmes, S. P. (2016). DADA2: high resolution sample inference from Illumina amplicon data. *Nat. Methods* 13, 581–583. doi: 10.1038/nmeth.3869.DADA2

Caporaso, J. G., Lauber, C. L., Costello, E. K., Berg-Lyons, D., Gonzalez, A., Stombaugh, J., et al. (2011). Moving pictures of the human microbiome. *Genome Biol.* 12:R50. doi: 10.1186/gb-2011-12-5-r50

Cho, D. Y., Hunter, R. C., and Ramakrishnan, V. R. (2020). The microbiome and chronic rhinosinusitis. *Immunol. Allergy Clin. North Am.* 40, 251–263. doi: 10.1016/j.iac.2019.12.009

Cope, E. K., Goldberg, A. N., Pletcher, S. D., and Lynch, S. V. (2017). Compositionally and functionally distinct sinus microbiota in chronic rhinosinusitis patients have immunological and clinically divergent consequences. *Microbiome* 5, 53. doi: 10.1186/s40168-017-0266-6

Copeland, E., Leonard, K., Carney, R., Kong, J., Forer, M., Naidoo, Y., et al. (2018). Chronic rhinosinusitis: potential role of microbial dysbiosis and recommendations for sampling sites. *Front. Cell. Infect. Microbiol.* 8, 1–14. doi: 10.3389/fcimb.2018.00057

Dietz de Loos, D., Lourijsen, E. S., Wildeman, M. A. M., Freling, N. J. M., Wolvers, M. D. J., Reitsma, S., et al. (2019). Prevalence of chronic rhinosinusitis in the general population based on sinus radiology and symptomatology. *J. Allergy Clin. Immunol.* 143, 1207–1214. doi: 10.1016/j.jaci.2018.12.986

Dridi, B., Henry, M., El Khéchine, A., Raoult, D., and Drancourt, M. (2009). High prevalence of *Methanobrevibacter smithii* and *Methanosphaera stadtmanae* detected in the human gut using an improved DNA detection protocol. *PLoS ONE* 4:e7063. doi: 10.1371/journal.pone.0007063

Dridi, B., Raoult, D., and Drancourt, M. (2011). Archaea as emerging organisms in complex human microbiomes. *Anaerobe* 17, 56–63. doi: 10.1016/j.anaerobe.2011.03.001

Eichler, J. (2003). Facing extremes: archaeal surface-layer (glyco)proteins. *Microbiology* 149, 3347–3351. doi: 10.1099/mic.0.26591-0

Glassing, A., Dowd, S. E., Galandiuk, S., Davis, B., and Chiodini, R. J. (2016). Inherent bacterial DNA contamination of extraction and sequencing reagents may affect interpretation of microbiota in low bacterial biomass samples. *Gut Pathog.* 8, 1–12. doi: 10.1186/s13099-016-0103-7

Goggin, R. K., Bennett, C. A., Bialasiewicz, S., Vediappan, R. S., Vreugde, S., Wormald, P. J., et al. (2019). The presence of virus significantly associates with chronic rhinosinusitis disease severity. *Allergy* 74, 1569–1572. doi: 10.1111/all.13772

Hannigan, G. D., Duhaime, M. B., Koutra, D., and Schloss, P. D. (2018). Biogeography and environmental conditions shape bacteriophage-bacteria networks across the human microbiome. *PLoS Comput. Biol.* 14, 1–24. doi: 10.1371/journal.pcbi.1006099

Hirai, K., Maeda, H., Omori, K., Yamamoto, T., Kokeguchi, S., and Takashiba, S. (2013). Serum antibody response to group II chaperonin from *Methanobrevibacter oralis* and human chaperonin CCT. *Pathog. Dis.* 68, 12–19. doi: 10.1111/2049-632X.12041

Hoffmann, C., Dollive, S., Grunberg, S., Chen, J., Li, H., Wu, G. D., et al. (2013). Archaea and fungi of the human gut microbiome: correlations with diet and bacterial residents. *PLoS ONE* 8:e66019. doi: 10.1371/journal.pone.0066019

Hoggard, M., Biswas, K., Zoing, M., Wagner Mackenzie, B., Taylor, M. W., and Douglas, R. G. (2016). Evidence of microbiota dysbiosis in chronic rhinosinusitis. *Int. Forum Allergy Rhinol.* 7, 7–11. doi: 10.1002/alr.21871

Hoggard, M., Mackenzie, B. W., Jain, R., Taylor, M. W., Biswas, K., and Douglas, R. G. (2017). Chronic rhinosinusitis and the evolving understanding of microbial ecology in chronic inflammatory mucosal disease. *Clin. Microbiol. Rev.* 30, 321–348. doi: 10.1128/CMR.00060-16

Hoggard, M., Zoing, M., Biswas, K., Taylor, M. W., and Douglas, R. G. (2019). The sinonasal mycobiota in chronic rhinosinusitis and control patients. *Rhinology* 57, 190–199. doi: 10.4193/Rhin18.256

Hulcr, J., Latimer, A. M., Henley, J. B., Rountree, N. R., Fierer, N., Lucky, A., et al. (2012). A jungle in there: bacteria in belly buttons are highly diverse, but predictable. *PLoS ONE* 7:e47712. doi: 10.1371/journal.pone.0047712

Khelaifia, S., and Drancourt, M. (2012). Susceptibility of archaea to antimicrobial agents: applications to clinical microbiology. *Clin. Microbiol. Infect.* 18, 841–848. doi: 10.1111/j.1469-0691.2012.03913.x

Koskinen, K., Pausan, M. R., Perras, A. K., Bang, M. B. C., Mora, M., Schilhabel, A., et al. (2017). First insights into the diverse human archaeome: specific detection of archaea in the gastrointestinal tract. *MBio* 8, 1–17. doi: 10.1128/mBio.00824-17

Lal, D., Keim, P., Delisle, J., Barker, B., Rank, M. A., Chia, N., et al. (2017). Mapping and comparing bacterial microbiota in the sinonasal cavity of healthy, allergic rhinitis, and chronic rhinosinusitis subjects. *Int. Forum Allergy Rhinol.* 7, 561–569. doi: 10.1002/alr.21934

Lepp, P. W., Brinig, M. M., Ouverney, C. C., Palm, K., Armitage, G. C., and Relman, D. A. (2004). Methanogenic Archaea and human periodontal disease. *Proc. Natl. Acad. Sci. U.S.A.* 101, 6176–6181. doi: 10.1073/pnas.0308766101

Letunic, I., and Bork, P. (2019). Interactive Tree Of Life (iTOL) v4: recent updates and new developments. *Nucleic Acids Res.* 47, W256–W259. doi: 10.1093/nar/gkz239

Lim, E. S., Zhou, Y., Zhao, G., Bauer, I. K., Droit, L., Ndao, I. M., et al. (2015). Early life dynamics of the human gut virome and bacterial microbiome in infants. *Nat. Med.* 21, 1228–1234. doi: 10.1038/nm.3950

Lloyd, K. G., May, M. K., Kevorkian, R. T., and Steen, A. D. (2013). Meta-analysis of quantification methods shows that archaea and bacteria have similar abundances in the subseafloor. *Appl. Environ. Microbiol.* 79, 7790–7799. doi: 10.1128/AEM.02090-13

Lloyd-Price, J., Mahurkar, A., Rahnavard, G., Crabtree, J., Orvis, J., Hall, A. B., et al. (2017). Strains, functions and dynamics in the expanded Human Microbiome Project. *Nature* 550, 61–66. doi: 10.1038/nature23889

Ludwig, W., Strunk, O., Westram, R., Richter, L., Meier, H., Yadhukumar, A., et al. (2004). ARB: a software environment for sequence data. *Nucleic Acids Res.* 32, 1363–1371. doi: 10.1093/nar/gkh293

McMurdie, P. J., and Holmes, S. (2013). Phyloseq: an R package for reproducible interactive analysis and graphics of microbiome census data. *PLoS ONE* 8:e61217. doi: 10.1371/journal.pone.0061217

Miller, T. L., and Wolin, M. J. (1985). *Methanosphaera stadtmaniae* gen. nov., sp. nov.: a species that forms methane by reducing methanol with hydrogen. *Arch. Microbiol.* 141, 116–122. doi: 10.1007/BF00423270

Miragoli, F., Federici, S., Ferrari, S., Minuti, A., Rebecchi, A., Bruzzese, E., et al. (2017). Impact of cystic fibrosis disease on archaea and bacteria composition of gut microbiota. *FEMS Microbiol. Ecol.* 93, 1–13. doi: 10.1093/femsec/fiw230

Moissl-Eichinger, C., Pausan, M., Taffner, J., Berg, G., Bang, C., and Schmitz, R. A. (2018). Archaea are interactive components of complex microbiomes. *Trends Microbiol.* 26, 70–85. doi: 10.1016/j.tim.2017.07.004

Moissl-Eichinger, C., Probst, A. J., Birarda, G., Auerbach, A., Koskinen, K., Wolf, P., et al. (2017). Human age and skin physiology shape diversity and abundance of Archaea on skin. *Sci. Rep.* 7, 1–10. doi: 10.1038/s41598-017-04197-4

Monaco, C. L., Gootenberg, D. B., Zhao, G., Handley, S. A., Ghebremichael, M. S., Lim, E. S., et al. (2016). Altered virome and bacterial microbiome in human immunodeficiency virus-associated acquired immunodeficiency syndrome. *Cell Host Microbe* 19, 311–322. doi: 10.1016/j.chom.2016.02.011

Nguyen, L. T., Schmidt, H. A., Von Haeseler, A., and Minh, B. Q. (2015). IQ-TREE: a fast and effective stochastic algorithm for estimating maximum-likelihood phylogenies. *Mol. Biol. Evol.* 32, 268–274. doi: 10.1093/molbev/msu300

Nguyen-Hieu, T., Khelaifia, S., Aboudharam, G., and Drancourt, M. (2013). Methanogenic archaea in subgingival sites: a review. *Apmis* 121, 467–477. doi: 10.1111/apm.12015

Oh, J., Byrd, A. L., Deming, C., Conlan, S., Barnabas, B., Blakesley, R., et al. (2014). Biogeography and individuality shape function in the human skin metagenome. *Nature* 514, 59–64. doi: 10.1038/nature13786

Oksanen, J., Blanchet, F. G., Friendly, M., Kindt, R., Legendre, P., McGlinn, D., et al. (2019). *vegan: Community Ecology Package*. R package version 2.5-5. Available online at: https://CRAN.R-project.org/package=vegan

Paramasivan, S., Bassiouni, A., Shiffer, A., Dillon, M. R., Cope, E. K., Cooksley, C., et al. (2019). The international sinonasal microbiome study (ISMS): a multi-centre, multi-national collaboration characterising the microbial ecology of the sinonasal cavity. *bioRxiv* 548743. doi: 10.1101/548743

Pausan, M. R., Csorba, C., Singer, G., Till, H., Schöpf, V., Santigli, E., et al. (2018). Measuring the archaeome: detection and quantification of archaea signatures in the human body. *bioRxiv*. doi: 10.1101/334748

Probst, A. J., Auerbach, A. K., and Moissl-Eichinger, C. (2013). Archaea on human skin. *PLoS ONE* 8:e65388. doi: 10.1371/journal.pone.0065388

Pruesse, E., Peplies, J., and Glöckner, F. O. (2012). SINA: accurate high-throughput multiple sequence alignment of ribosomal RNA genes. *Bioinformatics* 28, 1823–1829. doi: 10.1093/bioinformatics/bts252

RStudio Team (2020). *RStudio: Integrated Development for R.* Boston, MA: RStudio; PBC. Available online at: http://www.rstudio.com/

Rudmik, L. (2017). Economics of chronic rhinosinusitis. *Curr. Allergy Asthma Rep.* 17:20. doi: 10.1007/s11882-017-0690-5

Samuel, B. S., Hansen, E. E., Manchester, J. K., Coutinho, P. M., Henrissat, B., Fulton, R., et al. (2007). Genomic and metabolic adaptations of *Methanobrevibacter smithii* to the human gut. *Proc. Natl. Acad. Sci. U.S.A.* 104, 10643–10648. doi: 10.1073/pnas.0704189104

Sender, R., Fuchs, S., and Milo, R. (2016). Are we really vastly outnumbered? Revisiting the ratio of bacterial to host cells in humans. *Cell* 164, 337–340. doi: 10.1016/j.cell.2016.01.013

Wagner Mackenzie, B., Baker, J., Douglas, R. G., Taylor, M. W., and Biswas, K. (2019). Detection and quantification of *Staphylococcus* in chronic rhinosinusitis. *Int. Forum Allergy Rhinol.* 9, 1462–1469. doi: 10.1002/alr.22425

Wagner Mackenzie, B., Waite, D. W., Biswas, K., Douglas, R. G., and Taylor, M. W. (2018). Assessment of microbial DNA enrichment techniques from sino-nasal swab samples for metagenomics. *Rhinol. Online* 1, 160–193. doi: 10.4193/rhinol/18.052

Wagner Mackenzie, B., Waite, D. W., Hoggard, M., Douglas, R. G., Taylor, M. W., and Biswas, K. (2016). Bacterial community collapse: a meta-analysis of the sinonasal microbiota in chronic rhinosinusitis. *Environ. Microbiol.* 19, 381–392. doi: 10.1111/1462-2920.13632

Wampach, L., Heintz-Buschart, A., Hogan, A., Muller, E. E. L., Narayanasamy, S., Laczny, C. C., et al. (2017). Colonization and succession within the human gut microbiome by archaea, bacteria, and microeukaryotes during the first year of life. *Front. Microbiol.* 8:738. doi: 10.3389/fmicb.2017.00738

Wickham, H. (2016). *ggplot2: Elegant Graphics for Data Analysis.* New York, NY: Springer-Verlag.

Zhao, Y. C., Bassiouni, A., Tanjararak, K., Vreugde, S.,Wormald, P.-J., and Psaltis, A. J. (2017). Role of fungi in chronic rhinosinusitis through ITS sequencing. *Laryngoscope.* 128, 16–22. doi: 10.1002/lary.26702

Conflict of Interest: The authors declare that the research was conducted in the absence of any commercial or financial relationships that could be construed as a potential conflict of interest.

frontiers in Cellular and Infection Microbiology

ORIGINAL RESEARCH
published: 11 August 2020
doi: 10.3389/fcimb.2020.00412

Contribution of Short Chain Fatty Acids to the Growth of *Pseudomonas aeruginosa* in Rhinosinusitis

Do-Yeon Cho[1,2,3], Daniel Skinner[1], Ryan C. Hunter[4], Christopher Weeks[1], Dong Jin Lim[1], Harrison Thompson[1], Christopher R. Walz[1], Shaoyan Zhang[1], Jessica W. Grayson[1], William E. Swords[2,5], Steven M. Rowe[2,6] and Bradford A. Woodworth[1,2]*

[1] Department of Otolaryngology Head and Neck Surgery, University of Alabama at Birmingham, Birmingham, AL, United States, [2] Gregory Fleming James Cystic Fibrosis Research Center, University of Alabama at Birmingham, Birmingham, AL, United States, [3] Division of Otolaryngology, Department of Surgery, Veteran Affairs Medical Center, Birmingham, AL, United States, [4] Department of Microbiology and Immunology, University of Minnesota, Minneapolis, MN, United States, [5] Department of Medicine and Microbiology, University of Alabama at Birmingham, Birmingham, AL, United States, [6] Department of Medicine, Pediatrics, Cell Developmental and Integrative Biology, University of Alabama at Birmingham, Birmingham, AL, United States

OPEN ACCESS

Edited by:
Emily K. Cope, Northern Arizona University, United States

Reviewed by:
Daniel Champlin Propheter, University of Texas Southwestern Medical Center, United States
Janakiram Seshu, University of Texas at San Antonio, United States

***Correspondence:**
Do-Yeon Cho
dycho@uabmc.edu

Specialty section:
This article was submitted to Microbiome in Health and Disease, a section of the journal Frontiers in Cellular and Infection Microbiology

Received: *04 March 2020*
Accepted: *06 July 2020*
Published: *11 August 2020*

Citation:
Cho D-Y, Skinner D, Hunter RC, Weeks C, Lim DJ, Thompson H, Walz CR, Zhang S, Grayson JW, Swords WE, Rowe SM and Woodworth BA (2020) Contribution of Short Chain Fatty Acids to the Growth of Pseudomonas aeruginosa in Rhinosinusitis. Front. Cell. Infect. Microbiol. 10:412. doi: 10.3389/fcimb.2020.00412

Background: Chronic rhinosinusitis (CRS) is characterized by complex bacterial infections with persistent inflammation. Based on our rabbit model of sinusitis, blockage of sinus ostia generated a shift in microbiota to a predominance of mucin degrading microbes (MDM) with acute inflammation at 2 weeks. This was followed by conversion to chronic sinus inflammation at 3 months with a robust increase in pathogenic bacteria (e.g., *Pseudomonas*). MDMs are known to produce acid metabolites [short chain fatty acids (SCFA)] that have the potential to stimulate pathogen growth by offering a carbon source to non-fermenting sinus pathogens (e.g., *Pseudomonas*). The objective of this study is to evaluate the concentrations of SCFA within the mucus and its contribution to the growth of *P. aeruginosa*.

Methods: Healthy and sinusitis mucus from the rabbit model were collected and co-cultured with the PAO1 strain of *P. aeruginosa* for 72 h and colony forming units (CFUs) were determined with the targeted quantification of three SCFAs (acetate, propionate, butyrate). Quantification of SCFAs in healthy and sinusitis mucus from patients with *P. aeruginosa* was also performed via high performance liquid chromatography.

Results: To provide evidence of fermentative activity, SCFAs were quantified within the mucus samples from rabbits with and without sinusitis. Acetate concentrations were significantly greater in sinusitis mucus compared to controls (4.13 ± 0.53 vs. 1.94 ± 0.44 mM, $p < 0.01$). After 72 h of co-culturing mucus samples with PAO1 in the presence of mucin medium, the blue-green pigment characteristic of *Pseudomonas* was observed throughout tubes containing sinusitis mucus. CFUs were higher in cultures containing mucus samples from sinusitis ($8.4 \times 10^9 \pm 4.8 \times 10^7$) compared to control ($1.4 \times 10^9 \pm 2.0 \times 10^7$) or no mucus ($1.5 \times 10^9 \pm 2.1 \times 10^7$) ($p < 0.0001$). To provide evidence of fermentative activity in human CRS with *P. aeruginosa*, the presence of SCFAs in human

mucus was analyzed and all SCFAs were significantly higher in CRS with *P. aeruginosa* compared to controls ($p < 0.05$).

Conclusion: Given that SCFAs are solely derived from bacterial fermentation, our evidence suggests a critical role for mucin-degrading bacteria in generating carbon-source nutrients for pathogens. MDM may contribute to the development of recalcitrant CRS by degrading mucins, thus providing nutrients for potential pathogens like *P. aeruginosa*.

Keywords: anaerobes, short chain fatty acid, pseudomonas, mucin-fermenter, fermentation, rhinosinusitis, Chronic sinusitis, hypoxia

INTRODUCTION

Chronic rhinosinusitis (CRS), characterized by dysfunctional mucociliary clearance (MCC) with subsequent microbial colonization, is known as a multifactorial disease process where bacterial infection may play a role in the commencement or progression of the inflammatory response (Ramakrishnan et al., 2013). CRS patients have complex sinus microbial communities that incite persistent inflammation and airway damage (Lee and Lane, 2011). Despite the high density of bacteria that colonize the airway, nutrient sources that sustain bacterial growth *in vivo* and the derivation of those nutrients are not well-characterized. Recently, our laboratory successfully created a rabbit model of CRS by blocking the sinus drainage pathway (Cho et al., 2017a). Key data generated from this model indicate a clear sequence of events that augment our understanding of recalcitrant CRS pathophysiology: (1) blockage of sinus ostia generates a shift in microbiota to a predominance of anaerobes and (2) the shift from acute to chronic sinus inflammation is subsequently associated with a robust increase in pathogenic bacteria (e.g., *Pseudomonas*). How the two events are mechanistically related is unknown, but critical to understanding disease pathogenesis and the potential for intervention.

Abundant nutrient sources are provided by airway mucus to living organisms in the microenvironment and mucins are the major macromolecular constituents of mucus that provide a large carbon reservoir [e.g., short chain fatty acids (SCFA)] (Flynn et al., 2016). Mucins are the main nutrient source for niche-specific microbiota of the gut and oral cavity (Flynn et al., 2016). Therefore, mucin degrading microbes (MDM, primary mucin degrader) are thought to modify the nutritional landscape of the microenvironment and stimulate the growth of secondary colonizers (Kolenbrander, 2011). It is well-known that similar interactions exist between the commensal gut microbiota and the mucus layer of the human intestine (Cameron and Sperandio, 2015). Although the common sinus pathogen, *Pseudomonas aeruginosa*, cannot derive SCFAs endogenously (Flynn et al., 2016), little is known regarding the degradation of airway mucins as a source of SCFAs by these or other opportunistic pathogens in the upper airway.

Data from observational studies (Tunney et al., 2008) and the rabbit model (Cho et al., 2017a) indicate a shift in the microbiota to predominately anaerobic bacteria with impaired MCC. In rabbits, production of bioavailable nutrients (SCFA) for pathogenic bacteria follows and there was a subsequent shift from acute to chronic inflammation with robust generation of pathogenic microbes (e.g., *P. aeruginosa*). Since *P. aeruginosa* cannot derive SCFAs (e.g., acetate and propionate) from the host mucus through fermentation on their own, we hypothesized that anaerobic bacteria may ferment mucins into SCFA forms usable by *P aeruginosa*. This would provide a novel mechanistic basis for recalcitrant CRS pathogenesis following MCC disruption that occurs with acute respiratory infections/inflammation and subsequent compromise of the sinus ostia by edema (Crabbe et al., 2014). Therefore, the objective of this study is to evaluate the concentrations of SCFA within the sinonasal mucus (from rabbit and human) and its contribution to the growth of *P. aeruginosa*.

METHODS

PAO1 Stock Preparation

Pseudomonas aeruginosa (PAO1 strain) was expanded from glycerol frozen stock by inoculating 50 ml of lysogeny broth (LB) followed by overnight growth at 37°C on a shaker at 200 rpm. Cultures were streaked on LB agar plates according to the quadrant method and grown in a static incubator at 37°C overnight at least twice to confirm conformity of cultures. From the plate, an isolated colony was grown in 10 ml of LB-Miller broth at 37°C on a shaker at 200 rpm overnight. Cultures were diluted with fresh LB-Miller broth to an inoculation concentration of 1×10^4 to make a PAO1 stock for further experiments.

Animal Model

This study was approved by the Institutional Animal Care and Use Committee (IACUC Approval number 21687) at the University of Alabama at Birmingham (UAB). *Pasteurella*-free, female, New Zealand white rabbits (2–4 kg) were used for the study. Before initiation, rabbits were acclimatized to the animal facility for at least 1 week. For any procedure, rabbits were anesthetized with [ketamine (20 mg/kg) (MWI, Boise, ID), dextomitor (0.25 mg/kg) (Zoetis Inc., Kalamazoo, MI), buprenorphine (0.03 mg/kg) (Reckitt Benckiser Pharmaceuticals Inc., Richmond, VA), and carprofen (5 mg/kg) (Zoetis Inc.,

Kalamazoo, MI)] in a warm room for comfort. Rabbits did not receive any antibiotics before or during this study.

Mucus Collection From Rabbit Model of Sinusitis

Based on our previous experiments, MDMs dominated on week 2 after blocking the sinus drainage pathway in the rabbit and therefore mucus samples were collected at week 2 (Cho et al., 2017a). A total of four rabbits were used to create a rabbit model of acute sinusitis without providing exogenous bacteria or pathogens as described previously (Cho et al., 2017a). A sterile synthetic sponge (Merocel®, Medtronic, Minneapolis, MN) was inserted in the left (unilateral) middle meatus (natural outflow tract of maxillary sinus) of New Zealand white rabbits for 2 weeks and the sponge was removed on week 2. To confirm acute sinusitis, rabbits were examined with micro-computed tomography (microCT) scanning using SPECT/CT (X-SPECT system, Gamma Medica, Northridge, CA) and nasal endoscopy [1.7 mm 30-degree endoscope (Karl Storz, Tuttlingen, Germany)] on Week 0 and 2. Mucus samples were collected on Week 0 (control) and Week 2 (sinusitis) using a special suction catheter created by our laboratory. To evaluate whether targeting fermentative anaerobes halts the sinusitis progression from acute to chronic, metronidazole (50 mg/kg, twice a day for 5 days) was administered to the acute sinusitis rabbits (week 2). MicroCT scans were repeated at week 6 (between acute and chronic) to assess for CT evidence of sinusitis (opacification). Sinus opacification grading was performed using Kerschner's rabbit Sinus CT grading system [scoring each imaging study based on estimated percent (%) opacification of the maxillary sinus: 1 for $<$10%, 2 for 10–19%, 3 for 20–29%, 4 for 30–39%, 5 for 40–49%, 6 for 50–59%, 7 for 60–69%, 8 for 70–79%, 9 for 80–89%, and 10 for 90% $\leq$] (Kerschner et al., 2000). Opacification % was measured using the ImageJ version 1.50i (National Institutes of Health, Bethesda, MD) by two blinded judges.

In vitro Co-culturing

To test whether MDMs at week 2 are able to generate metabolites from mucin that could simultaneously stimulate *P. aeruginosa* growth, mucus samples collected at week 2 were co-cultured with PAO1. In a polystyrene culture tube (Fisher Scientific Company, Pittsburg PA), a bottom agar plug was made by adding 900 μL of 0.7% agar inoculated with 100 μL of mucus collected from rabbits (Day 0 or Week 2) or 0.7% agar (negative control) ($n = 4$). After allowing this to solidify, a top plug was made with 450 μL of 1.5% minimal media agar inoculated with the 1/1,000 dilution of an overnight culture of *P. aeruginosa* (PAO1). After solidification, co-cultures were placed at 37°C for 72 h. Agar plugs were then removed from the upper phase and homogenized by pipetting in 10 mL of phosphate buffered saline. Colony forming units (CFU) per tube were determined by serial dilution and plating on LB agar.

Mucus Collection and Culture From Human Chronic Sinusitis

To understand the concentration of SCFAs in human CRS with *P. aeruginosa*, mucus samples were collected from the middle meatus. This study was approved by the Institutional Review Board (IRB approval number 300003118) at the University of Alabama at Birmingham and all patients provided written informed consent. Subjects ($\geq$18 years of age) visiting the University of Alabama at Birmingham sinus clinic were recruited for the study. Patient eligibility criteria were designed to limit enrollment to healthy individuals and patients who clearly have CRS based on Sinus and Allergy health partnership criteria (Benninger et al., 2003; Orlandi et al., 2016). Control patients were enrolled based on endoscopic procedures for unilateral benign tumors (where the opposite side could be tested) and other disease entities where sinus inflammation was not present (e.g., CSF leaks, nasal septal deviation, benign nasal tumor, and turbinate hypertrophy). Demographic and clinical data were prospectively collected, de-identified, and stored in a securely encrypted electronic database. For cultures, specimens were obtained in the clinic or operating room (OR) with ESwabs (COPAN Diagnostics, Inc., Murrieta, CA) for hospital laboratory culture. Culture swabs were endoscopically guided to the area of interest with care taken to avoid contamination from the nares. The mucosal surface and overlying mucus of the middle meatus (from frontal, ethmoid, and/or maxillary sinuses) was aggressively swabbed for at least five full rotations until fully saturated. Culture swabs were sent to the hospital clinical microbiology laboratory for aerobic and anaerobic culture for bacterial growth and isolation. For metabolite quantification, mucus samples from the area of interest were collected in the clinic or OR using a modified catheter suction created by our laboratory (Cho et al., 2017a,b; Durmowicz et al., 2018).

Metabolite Quantification

Targeted quantification of SCFAs was performed via high performance liquid chromatography (HPLC). The system consisted of a Shimadzu SCL-10A system controller, LC-10AT liquid chromatograph, SIL-10AF autoinjector, SPD-10A UV-Vis detector, and CTO-10A column oven. Separation of compounds was performed with an Aminex HPX-87H guard column and an HPX-87H cation-exchange column (Bio-Rad, Hercules, CA). The mobile phase consisted of 0.05 N H_2SO_4, set at a flow rate of 0.5 mL min^{-1}. The column was maintained at 50°C and the injection volume was 50 μL. Amino acid and metabolite (acetate and propionate) quantification from enrichment supernatants were performed by Millis Scientific, Inc. (Baltimore, MD) using liquid chromatography–mass spectrometry and gas chromatography–mass spectrometry (GC–MS). Samples for amino acid quantification were spiked with 1 μL of uniformly labeled amino acids (Cambridge Isotope Labs) and derivatized using AccQ-Tag reagent (Waters Corp.) for 10 min at 50°C. A Waters Micromass Quatro LC–MS interfaced with a Waters Atlantis dC18 (3 μm 2.1 × 100 mm) column was used. Reverse-phase LC was used for separation (mobile phases A: 10 mM ammonium formate in 0.5% formic acid, B: methanol) with a constant flow rate (0.2 mL min^{-1}) and a column temperature of 40°C. Electrospray ionization was used to generate ions in the positive mode and multiple reaction monitoring was used to quantify amino acids. Samples (~100 μL) for acetate and propionate quantification were first diluted

(150 μL water), spiked with internal standards (10 μL of 1,000 ppm acetate [$^{13}C_2$] and 1,000 ppm propionate [$^{13}C_1$]) and acidified using 2 μL of 12N HCl. After equilibration at 60°C for 2 h, carboxen/polydimethylsiloxane solid phase microextraction (SPME) fiber was used to adsorb the headspace at 60°C for 30 min. Acids were then desorbed into the gas chromatograph inlet for 2 min. A 30 m × 0.32 mm ID DB-624 column attached to a Thermo Electron Trace gas chromatograph with helium carrier gas (2.0 mL min^{-1}) was used for separation of analytes. A Waters Micromass Quatro GC mass spectrometer was used for detection and quantification of target ions.

Effect of SCFA on PAO1 Growth

To test the effects of SCFA on *P. aeruginosa* growth, we incubated PAO1 strains with SCFA at varying concentrations. Each SCFA medium was prepared by adding individual SCFA to M9 minimal salts media at different concentrations, obtained from Sigma (St. Louis, MO). PAO1 seeding solution was prepared by adding 300 μl PAO-1 stock to 50 ml LB-Miller broth. 100 μl of PAO1 seeding solution was inoculated into 700 μl SCFAs media solutions on a 48-well plate and incubated at 37°C for 12 h. The final concentration of each SCFA was 0.01, 0.1, 1, or 10 mM based on *in vivo* HPLC data. Optical density (OD) of planktonic PAO1 growth was measured at 600 nm using a microplate reader. Additionally, to assess the growth of PAO1 strains in the presence of all 3 SCFAs, the colony counts of PAO1 were compared between the single (the most dominant SCFA) vs. 3 SCFAs after incubating 12 h in M9 minimal salts media (repeated × 10).

Statistical Analysis

Statistical analyses were conducted using Excel 2018 and GraphPad Prism 6.0 software (La Jolla, Ca) with significance set at $P < 0.05$. Statistical evaluation utilized unpaired Student *t*-tests or analysis of variance (ANOVA) based on the characteristics of analysis. Data is expressed ± standard error of the mean.

RESULTS

Mucus Samples From Acute Sinusitis Rabbits Support the Growth of PAO1 *in vitro*

To test whether the mucus samples from acute sinusitis in the rabbit model enriched with MDMs and SCFAs could simultaneously stimulate PAO1 growth, the mucus samples were co-cultured with PAO1 in a minimal mucin medium. Once the lower agar phase containing the mucus had solidified, PAO1 was suspended in buffered 0.7% agar medium without mucin (i.e., no carbon source) and was placed in the upper portion of the tube. This experimental setup establishes an oxygen gradient allowing anaerobes to grow, and restricts the movement of microbes but allows metabolites to freely diffuse (Flynn et al., 2016). Under these conditions, *P. aeruginosa* would be expected to achieve a higher cell density if provided with diffusible growth substrates from the mucus (lower phase). Co-culture growth was monitored over a 72-h period. After 72 h, a diffusible blue-green pigment (pyocyanin) characteristic of *P. aeruginosa* growth was observed throughout the co-culture tubes contained with sinusitis mucus (week 2) (**Figure 1A**). By contrast, no observable pigment was produced in the tubes contained with control mucus (Day 0) or without any mucus. Colony counts of the upper phase were significantly higher in those tubes containing mucus samples from week 2 (sinusitis: CFU/tube = $8.4 \times 10^9 \pm 4.8 \times 10^7$, $n = 4$) compared to tubes containing control mucus ($1.4 \times 10^9 \pm 2.0 \times 10^7$, $n = 4$) or no mucus ($1.5 \times 10^9 \pm 2.1 \times 10^7$, $n = 4$), with a magnitude 5-fold increase ($p < 0.0001$) (**Figure 1B**).

Mucus Samples From Acute Sinusitis Rabbits Contain Short Chain Fatty Acids (SCFA)

To provide evidence of fermentative activity *in vivo*, 3 SCFAs (acetate, propionate and butyrate) were quantified using GC-MS within the mucus samples from rabbits on day 0 (Control) and week 2 (Sinusitis). SCFAs were found at millimolar (or less) concentrations in all mucus samples and we were able to detect all three SCFAs (**Figure 2**). Acetate concentrations were significantly higher in the mucus samples collected on week 2 (Sinusitis), relative to day 0 (Control) (4.13 ± 0.53 vs. 1.94 ± 0.44 mM, $p < 0.01$, $n = 4$). Propionate and butyrate concentrations were not significantly elevated in the mucus samples from sinusitis compared to those from control [Propionate = 0.042 ± 0.023 vs. 0.019 ± 0.005 mM, $p = 0.38$ ($n = 4$); Butyrate = 0.028 ± 0.014 vs. 0.005 ± 0.002 mM, $p = 0.085$ ($n = 4$)] even though there was a trend.

Human Mucus Samples From CRS With *P. aeruginosa* Contain Significantly Higher SCFAs

To provide the evidence of fermentative activity in human CRS with *P. aeruginosa*, we analyzed the presence of SCFAs in human mucus samples from controls and CRS with *P. aeruginosa*. Of those human mucus samples collected in the clinic or OR, eight samples were collected from controls and six from CRS with *P. aeruginosa*. All CRS patients with *P. aeruginosa* presented with purulence in the sinus cavity (without any recent use of oral or intravenous antibiotics for at least 2 weeks). Of those 6 CRS with *P. aeruginosa* mucus samples, mucus-degrading microbes were present in five samples (83.3%) from our hospital clinical microbiology laboratory report (**Table 1**). Using GC-MS, 3 SCFAs (acetate, propionate, and butyrate) were quantified in human mucus samples collected from eight controls and 6 CRS patients with *P. aeruginosa* with active purulent drainage. SCFAs were found at mM concentrations in all mucus samples (**Figure 4**). SCFAs from CRS patients with *P. aeruginosa* were also significantly higher than those from controls: (1) acetate = 0.77 ± 0.13 vs. 0.19 ± 0.07 mM ($p < 0.001$), (2) propionate = 0.012 ± 0.004 vs. 0.002 ± 0.000 ($p = 0.019$), (3) butyrate = 0.004 ± 0.001 vs. 0.0005 ± 0.000 ($p < 0.01$) (**Figure 3**). Collectively, data presented here demonstrate the presence of significantly higher quantities of fermentation metabolites in CRS with *P. aeruginosa*.

SCFAs Increase PAO1 Growth *in vitro*

To understand the role of SCFAs in the growth of PAO1 *in vitro*, the growth of PAO1 with multiple concentrations of

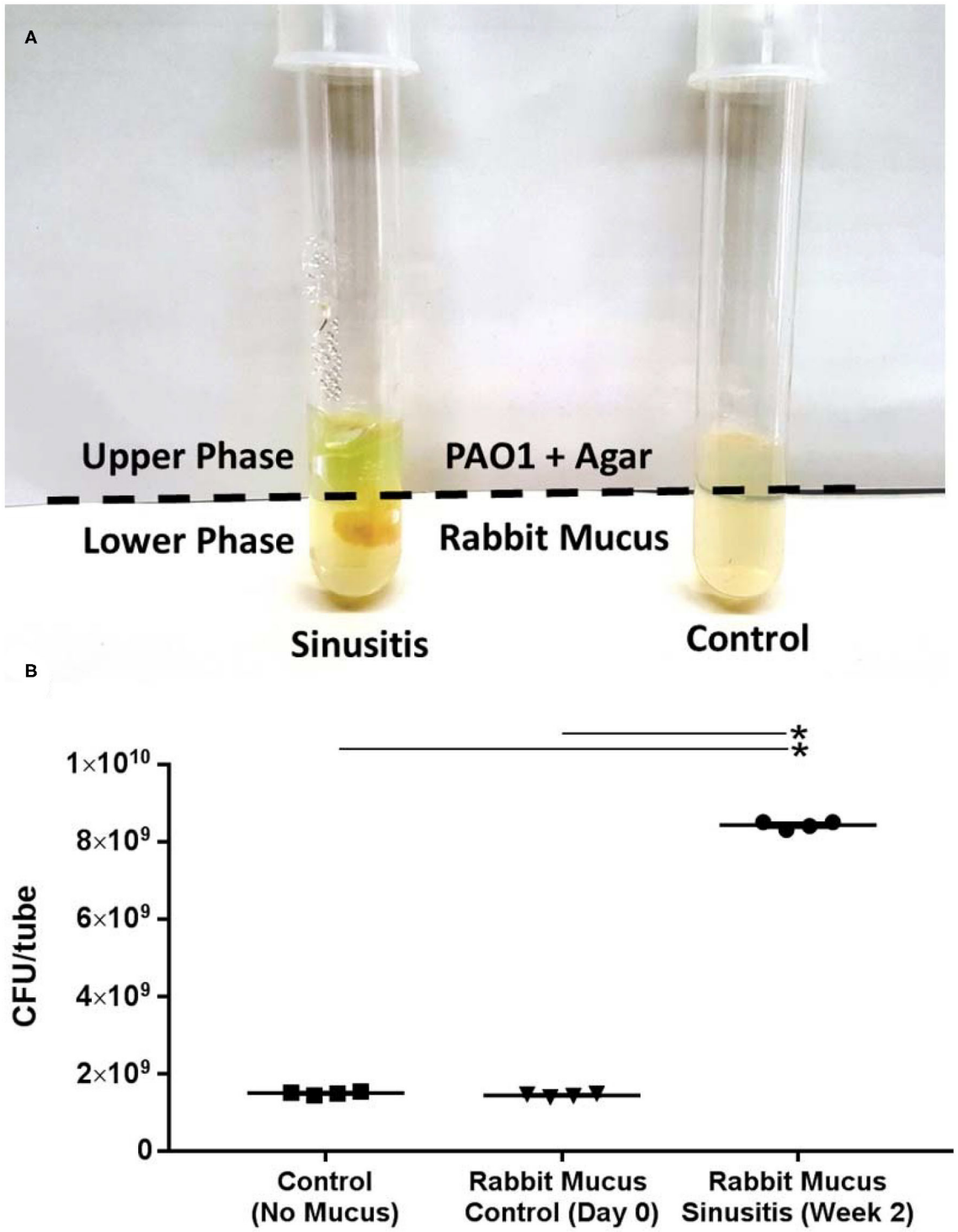

FIGURE 1 | Mucus samples from Rabbit Sinusitis support the growth of PAO1 *in vitro.* **(A)** The mucus samples were co-cultured with PAO1 in an anaerobic minimal mucin medium. After 72 h, a diffusible blue-green pigment (pyocyanin) characteristic of *P. aeruginosa* growth was observed throughout the co-culture tubes containing sinusitis mucus (week 2). **(B)** Colony counts were significantly higher in those tubes contained with the mucus samples from week 2 (sinusitis: CFU/tube = $8.4 \times 10^9 \pm 4.8 \times 10^7$) compared to tubes containing control mucus ($1.4 \times 10^9 \pm 2.0 \times 10^7$) or no mucus ($1.5 \times 10^9 \pm 2.1 \times 10^7$), with a magnitude (5×) increase ($p < 0.0001$). *Represents statistical significance ($p < 0.05$).

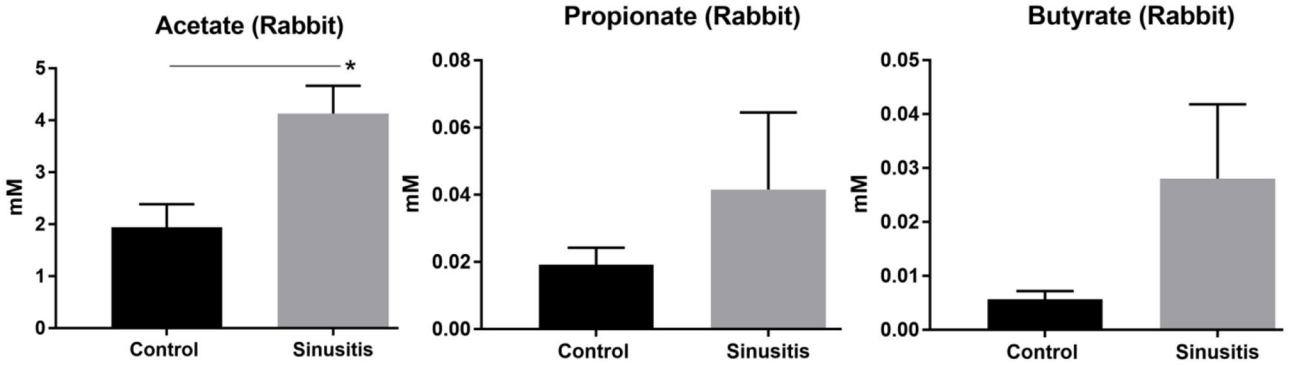

FIGURE 2 | Concentrations of short chain fatty acids (SCFA) in mucus samples from rabbits. Acetate concentrations were significantly higher in the mucus samples collected on week 2 (Sinusitis), relative to day 0 (Control) (4.13 ± 0.53 vs. 1.94 ± 0.44 mM, $p < 0.01$, $n = 4$). Propionate and butyrate concentrations were higher in the mucus samples from sinusitis compared to those from control (propionate $= 0.042 \pm 0.023$ vs. 0.019 ± 0.005 mM, $p = 0.38$; Butyrate $= 0.028 \pm 0.014$ vs. 0.005 ± 0.002 mM, $p = 0.085$) but statistical significance was lacking ($n = 4$). All groups consisted of at least four experiments. *Represents statistical significance ($p < 0.05$).

TABLE 1 | Presence of Mucin degrading microbes in *P. aeruginosa* culture positive patients.

No.	Age	Comorbidities	Location of culture	Mucin degrading microbes
#1	69	DM	Frontal sinus	*Streptococcus intermedius*
#2	39	Asthma, Mannose-binding lectin protein deficiency	Ethmoid sinus	*Enterobacter cloacae*
#3	32	CF (ΔF508/ΔF508)	Frontal sinus	*Cutibacterium acnes, Enterobacter cloacae*
#4	71	Immunocompromised (post-KT)	Maxillary sinus	None
#5	78	DM, Prostate cancer	Middle meatus	*Klebsiella oxytoca*
#6	52	DM, COPD	Ethmoid sinus	*Rothia mucilaginosa, Streptococcus salivarius*

DM, Diabetes mellitus; CF, Cystic fibrosis; KT, Kidney transplantation; COPD, Chronic obstructive pulmonary disease.

SCFAs was monitored. Concentrations of SCFAs were chosen based on the previous HPLC findings above (**Figure 2**). As acetate concentrations were above 1 mM in the rabbit mucus samples, we utilized four different concentrations of acetate (0.01, 0.1, 1, and 10 mM). Because propionate and butyrate were <1 mM, two different concentrations (0.01 and 0.1 mM) below 1 mM were used. Normalized OD values were compared to the average OD from control (without adding SCFAs) for acetate, propionate, and butyrate (**Figure 4A**). In the presence of acetate, PAO1 exhibited increased growth from 0.01 to 10 mM and statistical significance was noted between 0.1 and 10 mM compared to control [normalized OD values at 600 nm: 0.01 mM $= 7.3 \pm 0.02$ ($n = 4$), 0.1 mM $= 9.6 \pm 0.04$ ($n = 4$), 1 mM $= 11.04 \pm 0.02$ ($n = 4$), and 10 mM 13.8 ± 0.02 ($n = 4$), $p < 0.0001$ (ANOVA with *post-hoc* Tukey–Kramer)]. In the presence of propionate, statistical significance was noted in both concentrations [normalized OD values at 600 nm: 0.01 mM $= 12.3 \pm 0.02$ ($n = 4$), 0.1 mM $= 15 \pm 0.04$ ($n = 4$), $p < 0.01$ (ANOVA)]. However, the growth increases of PAO1 observed with butyrate were not statistically significant in the analysis of these two concentrations [0.01 mM $= 10 \pm 0.03$ ($n = 4$), 0.1 mM $= 11.5 \pm 0.05$ ($n = 4$), $p = 0.096$ (ANOVA)]. Additionally, as acetate is the major SCFA (at least 50 or 200-fold higher than propionate or butyrate) in **Figure 3**, the growth of PAO1 strains was compared in the presence of acetate alone (0.5 mM) vs. 3 SCFAs (acetate 0.5 mM, propionate 0.01 mM, Butyrate 0.005 mM). Colony counts were significantly higher when PAO1 strains were grown with acetate alone or 3 SCFAs compared to controls (Control $= 2.45 \times 10^6 \pm 1.7 \times 10^5$ CFU/ml ($n = 10$), Acetate $= 3.63 \times 10^6 \pm 1.58 \times 10^5$ CFU/ml ($n = 10$), Three SCFAs $= 4.33 \times 10^6 \pm 3.0 \times 10^5$ CFU/ml ($n = 10$), ANOVA, $p < 0.0001$) (**Figure 4B**). Even though there was a trend toward higher colony counts when PAO1s were treated with 3 SCFAs, statistical significance was lacking between the acetate alone and 3 SCFAs (Tukey's multiple comparison test, $p = 0.077$).

Targeting Anaerobes Halts the Radiographic Evidence of Sinusitis Progression

To evaluate whether targeting fermentative anaerobes halts sinusitis progression from acute to chronic stages, acute sinusitis rabbits (week 2) were treated with metronidazole for 5 days. At week 6 (midpoint between acute and chronic), the metronidazole treatment group ($n = 3$) had marked improvement of opacification compared to the control group without treatment ($n = 3$) (**Figure 5**). CT scores were significantly higher in rabbits without metronidazole treatment (Kerschner scale, $n = 3$, 4.13 ± 1.21) compared to those rabbits treated with metronidazole ($n = 3$, 1.67 ± 0.76) ($p = 0.040$) at week 6. Radiographically, the progression to sinusitis was halted by metronidazole treatment.

DISCUSSION

In this study, we investigated the role of SCFAs (produced by mucin fermenting anaerobes) in the growth of *P. aeruginosa*

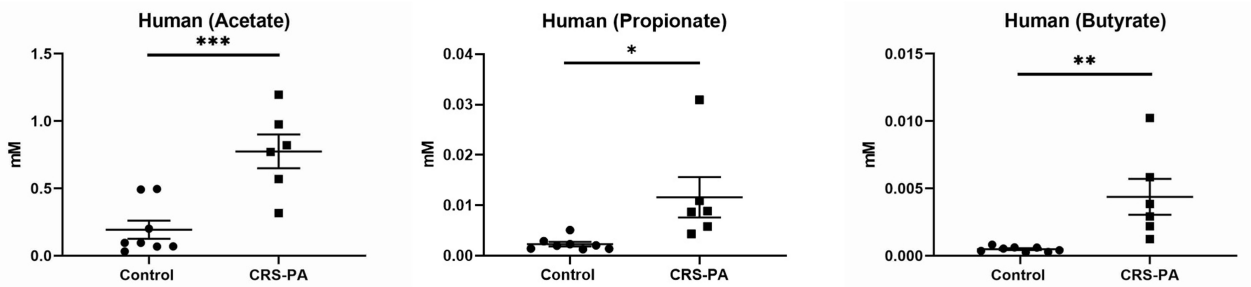

FIGURE 3 | Concentrations of short chain fatty acids (SCFA) in human mucus samples SCFAs from CRS patients with *P. aeruginosa* (PA) ($n = 6$) were compared to those from controls ($n = 8$): (1) acetate = 0.77 ± 0.13 vs. 0.19 ± 0.07 mM ($p < 0.001$; (2) propionate = 0.012 ± 0.004 vs. 0.002 ± 0.000 ($p = 0.019$; (3) butyrate = 0.004 ± 0.001 vs. 0.0005 ± 0.000 ($p < 0.01$) [*represents statistical significance $p < 0.05$, **$p < 0.01$, and ***$p < 0.001$].

in rhinosinusitis. To our knowledge, this is the first study to quantitatively assess the presence of SCFAs in the human mucus including patients with CRS. While *Pseudomonas* ineffectually utilizes mucins as a carbon source on its own (Flynn et al., 2016), we determined that mucin fermentation by MDMs can stimulate the growth of *P. aeruginosa*. Moreover, we revealed that SCFAs were also abundant and available in CRS patients with and without *P. aeruginosa*. Together, these results suggest that the high levels of utilizable metabolites present in sinus mucus may be derived from bacterial mucin degradation by anaerobes in the sinus cavity, which may contribute to the establishment and progression of recalcitrant CRS (Cho et al., 2020).

Under normal oxygen conditions, most bacteria preferentially oxidize glucose and other saccharides to pyruvate and shuttle pyruvate through the citric acid cycle. Both processes require oxygen as the final electron acceptor. In anaerobic conditions, bacteria must choose an alternative route by using the energy of another biochemical reaction, and thus bypassing oxidative respiration (Zumft, 1997; Ragsdale and Pierce, 2008). The process of fermentation involves the release of energy from compounds without utilizing exogenous oxygen (e.g., muscle cells during exercise through the formation of lactic acid; Ghorbani et al., 2015). Cystic fibrosis (CF) airway disease is one condition which gives rise to persistent bacterial colonization, coupled with an anaerobic microenvironment. The CF airway includes a thick mucus layer, rendered hypoxic through the metabolism of host immune cells and bacteria. Under these circumstances, bacteria can produce SCFAs through the fermentation process. Fermentation of carbohydrates within the mucus results in the formation of SCFAs (e.g., propionate, butyrate, and acetate), which can thus influence the progression and resolution of infection and inflammation in the airways (Ghorbani et al., 2015). SCFAs have been shown to downregulate immune cell inflammatory responses, promote neutrophil chemotaxis, induce inflammatory protein expression in epithelial cells, inhibit proliferation, and strengthen epithelial tight junctions in the gastrointestinal tract (Ferreira et al., 2012; Vieira et al., 2012). In the large intestine, SCFAs are found at concentrations ranging from 30 to 150 mM, which is significantly higher than the concentrations found in the airway (Mortensen and Clausen, 1996; Smith et al., 2013). While high mM concentrations impair growth, low mM concentrations (<10 mM) boost the growth of potential pathogens (e.g., *Pseudomonas*) and upregulate IL-8 in CF primary airway epithelium (Ghorbani et al., 2015). These molecules easily penetrate the airway tissue because of their low molecular weight and subsequently interrupt host cell activity and host defense systems by inducing apoptosis in fibroblasts and lymphocytes (Tonetti et al., 1987; Kurita-Ochiai et al., 1995; Sato et al., 2016). It is also possible that SCFAs may influence *P. aeruginosa* biofilm formation, which will be investigated in future experiments.

It is interesting to note that SCFA levels were higher in rabbits than human samples in both controls and non-controls. Every species appear to have different microbial fermentation patterns even if they have similar diets (Kroliczewska et al., 2018). This is the first report (to our knowledge) to evaluate SCFA levels in rabbit sinonasal mucus and we will require more numbers to strictly define normal SCFA levels in rabbit sinuses. However, the high fiber intake in the diet encourages the growth of species that ferment fiber into metabolites as SCFAs, and thus rabbits' baseline could be higher than humans as previously shown in the gut (Cummings et al., 1987; Tomova et al., 2019). Furthermore, for experimental conditions, we intentionally created an anaerobic environment in the sinus cavity and the SCFA levels were measured during the acute sinusitis phase in the rabbit model. By contrast, the human samples were collected from the (postoperative) sinuses or middle meatus in CRS patients. Therefore, the SCFAs from rabbits may have been generated at higher levels than observed in human samples.

Based on our experiments, all 3 SCFAs were significantly higher in CRS with *P. aeruginosa*. Our clinical results are also consistent with CF bronchoalveolar lavage fluid findings in other studies (Ghorbani et al., 2015; Mirkovic et al., 2015; Flynn et al., 2016). The ratio of propionate to acetate (1:50) in our human sinusitis samples was comparable to Flynn et al.'s experiments in human CF sputum/saliva samples (Flynn et al., 2016). As explained by Flynn et al., only a small amount of propionate is generated *in vivo* or it may be used by microorganisms in a cross-feeding relationship. When we compared the CFUs between

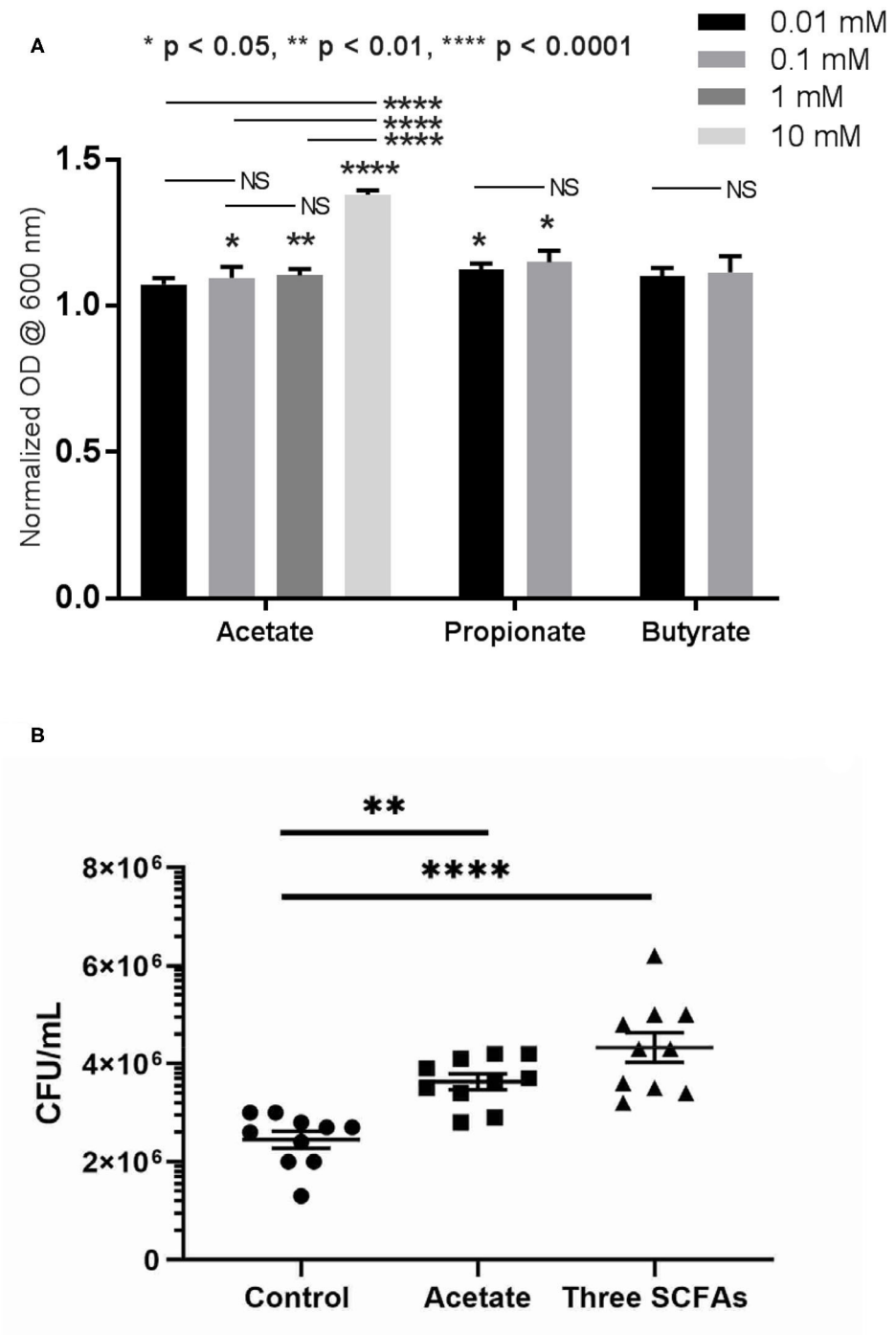

FIGURE 4 | Growth of PAO1 with SCFAs. **(A)** PAO1 growths were compared to controls in the presence of different concentrations of acetate (between 0.1 and 10 mM): normalizzed OD values at 600 nm: 0.01 mM = 7.3 ± 0.02 ($n = 4$), 0.1 mM = 9.6 ± 0.04 ($n = 4$), 1 mM = 11.04 ± 0.02 ($n = 4$), and 10 mM 13.8 ± 0.02 ($n = 4$). In the presence of propionate, statistical significance was noted in both concentrations compared to controls (Normalized OD values at 600 nm: 0.01 mM = 12.3 ± 0.02 ($n = 4$), 0.1 mM = 15 ± 0.04 ($n = 4$). However, no statistically significant growth of PAO1 was seen with butyrate at these two concentrations [0.01 mM = 10 ± 0.03 ($n = 4$), 0.1 mM = 11.5 ± 0.05 ($n = 4$), $p = 0.096$]. (one-way ANOVA, NS = no significance). **(B)** Colony counts were significantly higher when PAO1 strains were grown with acetate alone or three SCFAs compared to controls (Control = $2.45 \times 10^6 \pm 1.7 \times 10^5$ CFU/ml ($n = 10$), Acetate = $3.63 \times 10^6 \pm 1.58 \times 10^5$ CFU/ml ($n = 10$), 3 SCFAs = $4.33 \times 10^6 \pm 3.0 \times 10^5$ CFU/ml ($n = 10$), ANOVA, $p < 0.0001$, (*$p < 0.05$, **$p < 0.01$, and ****$p < 0.0001$).

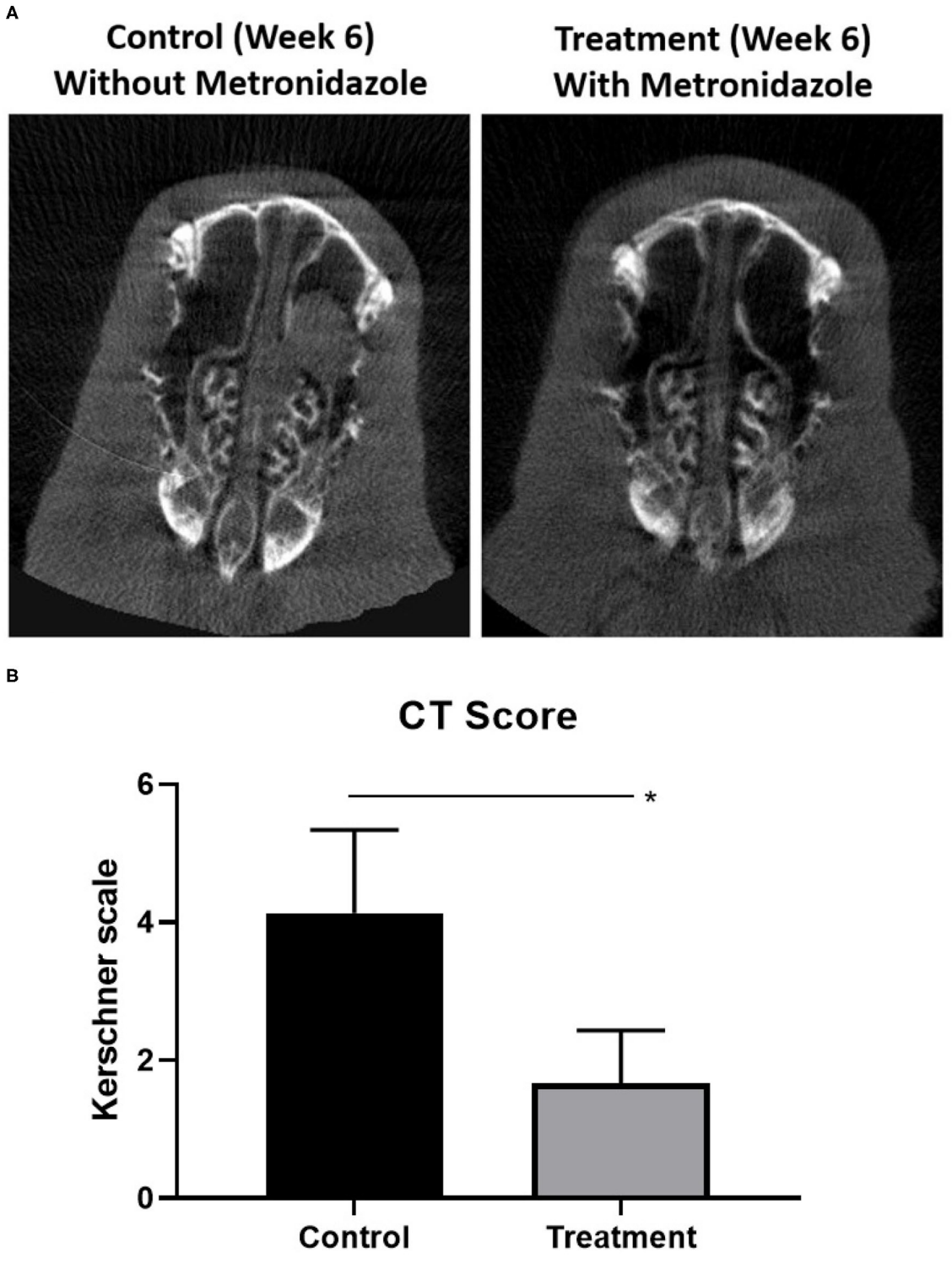

FIGURE 5 | Radiographic progression of sinusitis when targeting anaerobes. **(A)** At week 6 (midpoint between acute and chronic), the metronidazole treatment group ($n = 3$) had marked improvement of opacification compared to the control group without treatment ($n = 3$). **(B)** Scores were significantly higher in rabbits without metronidazole treatment (Kerschner scale, $n = 3$, 4.13 ± 1.21) compared to those rabbits treated with metronidazole ($n = 3$, 1.67 ± 0.76) ($p = 0.040$) at week 6 ($^*p < 0.05$).

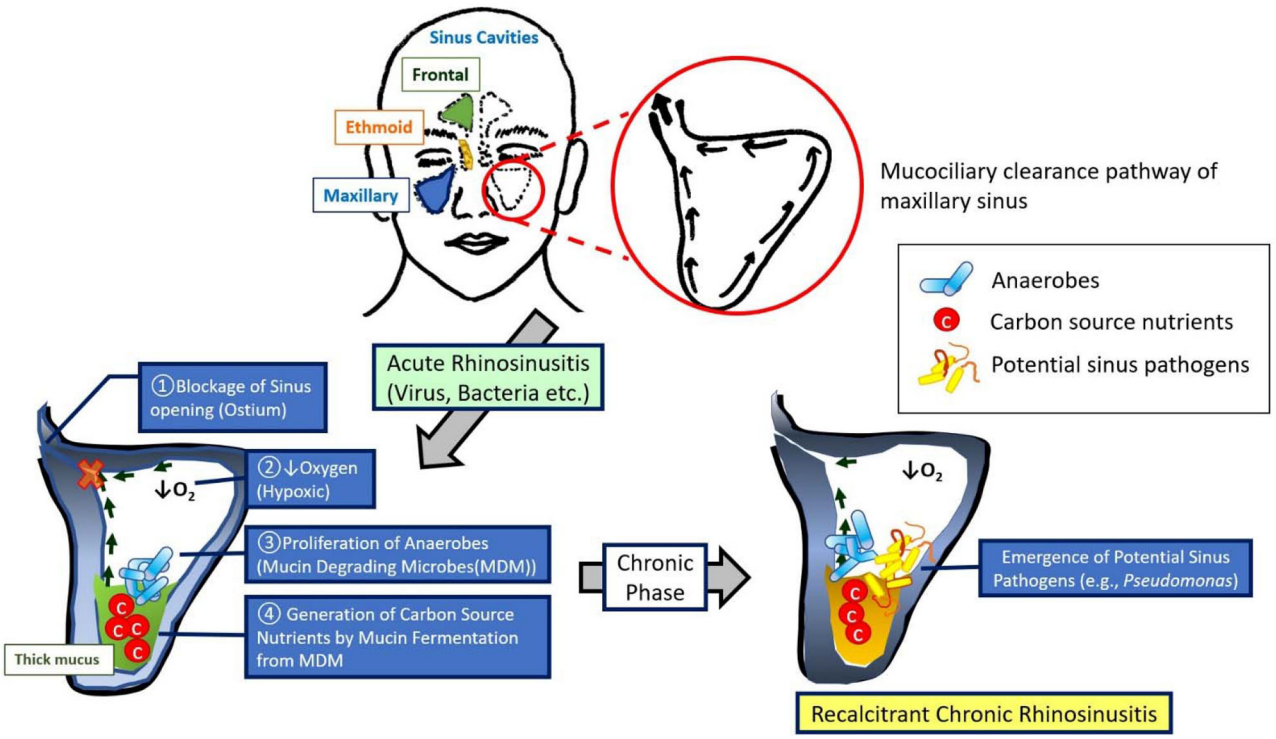

FIGURE 6 | Model for the development of recalcitrant chronic rhinosinusitis. This model demonstrates a sequence of events that augment our understanding of recalcitrant CRS pathophysiology: (1) blockage of sinus ostia generates a shift in microbiota to a predominance of anaerobes, mucin metabolites [short chain fatty acids (SCFAs)] produced by these anaerobes are abundant within the mucus during an acute anaerobic stage, and (3) the shift from acute to chronic sinus inflammation is associated with a robust increase in pathogenic bacteria (e.g., *P. aeruginosa*).

the acetate alone and three SCFAs, an additional growth of *P. aeruginosa* could be clinically presumable in the presence of multiple nutrients, even though statistical significance was lacking in this experiment. When comparing the total SCFA concentrations before and after antibiotic treatment in patients presenting with a CF pulmonary exacerbation, the mean SCFA concentrations were significantly lower after the treatment (Ghorbani et al., 2015).

Our results suggest the role of hypoxia in recalcitrant CRS pathophysiology (**Figure 6**). Hypoxia due to sinus closure at the ostiomeatal complex at the junction of the ethmoid and maxillary sinuses is widely considered a major pathogenic mechanism leading to the development of CRS and is strongly supported by proof that hypoxia is present at the surface epithelium in diseased sinuses of closed ostia (Aanaes et al., 2011). Targeting mucin-fermenting anaerobes and their metabolites could be a novel therapeutic strategy for the treatment of CRS by restoring the microbial community in diseased sinuses to the original non-infected pristine status.

There are several limitations to this study. Our hypothesis is from the animal model not human subjects, and this may not reflect the human *in vivo* environment. Even though some well-controlled microbiota studies using animal models have also shown inter-study variations due to confounding factors (e.g., origin, maternal effects, environmental conditions) (Nguyen et al., 2015), the advantages of the rabbit model are numerous in that it enables us to control for a number of variables that are inherent in human samples including genetics, medical history, environmental allergies/pollutants, and medication use (Cho et al., 2018). As this is a clinical pilot study to assess the concentrations of SCFAs in CRS patients, the size and homogeneity of the clinical samples limit the study's generalizability. In addition, we did not include any microbiome-related analyses or molecular based quantification of the microorganisms that colonize the mucus layers of human samples. A much larger group of patients will be recruited for future studies. Additionally, *Bacteroides* (one of the most common anaerobes in the rabbit model) is not one of the common anaerobes in human sinusitis and there could be other nutrients other than SCFAs, which are derived by fermentation that sustain bacterial growth in humans. Therefore, we are planning to test the capability of patient-derived, anaerobic microbiota (Taxa: *Streptococcus, Peptostreptococcus, Propionibacterium, Fusobacterium*, and *Prevotella*) to support the growth of *P. aeruginosa* isolates using an *in vitro* and *in vivo* cross-feeding co-culture model.

CONCLUSION

Given that SCFAs are solely derived from bacterial fermentation, our experiments propose a critical role for mucin-fermenting bacteria in generating carbon-source nutrients for pathogenic

bacteria in the airway. Mucin fermenting anaerobes may contribute to the development of recalcitrant CRS by degrading mucins, thus providing nutrients for potential pathogens like *P. aeruginosa*.

DATA AVAILABILITY STATEMENT

The datasets generated for this study are available on request to the corresponding author.

ETHICS STATEMENT

The studies involving human participants were reviewed and approved by Institutional Review Board (IRB approval number 300003118) at the University of Alabama at Birmingham. The patients/participants provided their written informed consent to participate in this study. The animal study was reviewed and approved by Institutional Animal Care and Use Committee (IACUC Approval number 21687) at the University of Alabama at Birmingham (UAB).

AUTHOR CONTRIBUTIONS

D-YC designed the study, carried out the experiments, and took the lead in writing the manuscript with support from RH, SR, WS, and BW (concept of experiments and editing). DS, DL, HT, CRW, and SZ carried out the rabbit and *in vitro* experiments and contributed to sample preparation. JG performed statistical analysis. All authors provided critical feedback, helped shape the research, analysis, and manuscript.

FUNDING

This work was supported by National Institutes of Health (NIH)/National Heart, Lung, and Blood Institute (1 R01 HL133006-05) to BW; National Institute of Diabetes and Digestive and Kidney Diseases (5P30DK072482-02) to SR; and NIH/National Institutes of Allergy and Infectious disease (K08AI146220), John W. Kirklin Research and Education Foundation Fellowship Award, UAB Faculty Development Research Award, American Rhinologic Society New Investigator Award, Triological Society Career Development Award, and Cystic Fibrosis Foundation K08 Boost Award (CHO20A0-KB) to D-YC.

ACKNOWLEDGMENTS

A part of this manuscript was presented at North American Cystic Fibrosis Conference 2018 in Denver, Colorado.

REFERENCES

Aanaes, K., Rickelt, L. F., Johansen, H. K., von Buchwald, C., Pressler, T., Hoiby, N., et al. (2011). Decreased mucosal oxygen tension in the maxillary sinuses in patients with cystic fibrosis. *J. Cyst. Fibros.* 10, 114–120. doi: 10.1016/j.jcf.2010.12.002

Benninger, M. S., Fergusonm, B. J., Hadley, J. A., Hamilos, D. L., Jacobs, M., Kennedy, D. W., et al. (2003). Adult chronic rhinosinusitis: definitions, diagnosis, epidemiology, and pathophysiology. *Otolaryngol. Head Neck Surg.* 129(Suppl.3), S1–32. doi: 10.1016/S0194-5998(03)01397-4

Cameron, E. A., and Sperandio, V. (2015). Frenemies: signaling and nutritional integration in pathogen-microbiota-host interactions. *Cell Host Microbe*. 18, 275–284. doi: 10.1016/j.chom.2015.08.007

Cho, D. Y., Hoffman, K., Skinner, D., Mackey, C., Lim, D. J., Alexander, G. C., et al. (2017a). Tolerance and pharmacokinetics of a ciprofloxacin-coated sinus stent in a preclinical model. *Int. Forum Allergy Rhinol.* 7, 352–358. doi: 10.1002/alr.21892

Cho, D. Y., Lim, D. J., Mackey, C., Skinner, D., Weeks, C., Gill, G. S., et al. (2018). Preclinical therapeutic efficacy of the ciprofloxacin-eluting sinus stent for Pseudomonas aeruginosa sinusitis. *Int. Forum Allergy Rhinol.* 8, 482–489. doi: 10.1002/alr.22081

Cho, D. Y., Mackey, C., Van Der Pol, W. J., Skinner, D., Morrow, C. D., Schoeb, T. R., et al. (2017b). Sinus microanatomy, and microbiota in a rabbit model of rhinosinusitis. *Front Cell Infect. Microbiol.* 7:540. doi: 10.3389/fcimb.2017.00540

Cho, D. Y., Skinner, D., Lim, D. J., McLemore, J. G., Koch, C. G., Zhang, S., et al. (2020). The impact of *Lactococcus lactis* (probiotic nasal rinse) co-culture on growth of patient-derived strains of Pseudomonas aeruginosa. *Int Forum Allergy Rhinol.* 10, 444–449. doi: 10.1002/alr.22521

Crabbe, A., Ledesma, M. A., and Nickerson, C. A. (2014). Mimicking the host and its microenvironment in vitro for studying mucosal infections by *Pseudomonas aeruginosa*. *Pathog. Dis.* 71, 1–19. doi: 10.1111/2049-632X.12180

Cummings, J. H., Pomarem, E. W., Branchm, W. J., Naylor, C. P., and Macfarlane, G. T. (1987). Short chain fatty acids in human large intestine, portal, hepatic and venous blood. *Gut* 28, 1221–127. doi: 10.1136/gut.28.10.1221

Durmowicz, A. G., Lim, R., Rogers, H., Rosebraugh, C. J., and Chowdhury, B. A. (2018). The U.S. Food and Drug Administration's Experience with Ivacaftor in *Cystic Fibrosis*. Establishing efficacy using *in vitro* data in lieu of a clinical trial. *Ann. Am. Thorac. Soc.* 15, 1–2. doi: 10.1513/AnnalsATS.201708-668PS

Ferreira, T. M., Leonel, A. J., Melo, M. A., Santos, R. R., Cara, D. C., Cardoso, V. N., et al. (2012). Oral supplementation of butyrate reduces mucositis and intestinal permeability associated with 5-Fluorouracil administration. *Lipids* 47, 669–678. doi: 10.1007/s11745-012-3680-3

Flynn, J. M., Niccum, D., Dunitz, J. M., and Hunter, R. C. (2016). Evidence and role for bacterial mucin degradation in cystic fibrosis airway disease. *PLoS Pathog.* 12:e1005846. doi: 10.1371/journal.ppat.1005846

Ghorbani, P., Santhakumar, P., Hu, Q., Djiadeu, P., Wolever, T. M., Palaniyar, N., et al. (2015). Short-chain fatty acids affect cystic fibrosis airway inflammation and bacterial growth. *Eur. Respir. J.* 46, 1033–1045. doi: 10.1183/09031936.00143614

Kerschner, J. E., Cruz, M. J., Beste, D. J., Donahue, K. M., and Kehl, K. S. (2000). Computed tomography vs. magnetic resonance imaging of acute bacterial sinusitis: a rabbit model. *Am. J. Otolaryngol.* 21, 298–305. doi: 10.1053/ajot.2000.9874

Kolenbrander, P. E. (2011). Multispecies communities: interspecies interactions influence growth on saliva as sole nutritional source. *Int. J. Oral Sci.* 3, 49–54. doi: 10.4248/IJOS11025

Kroliczewska, B., Mista, D., Korzeniowska, M., Pecka-Kielb, E., and Zachwieja, A. (2018). Comparative evaluation of the quality and fatty acid profile of meat from brown hares and domestic rabbits offered the same diet. *Meat Sci.* 145, 292–299. doi: 10.1016/j.meatsci.2018.07.002

Kurita-Ochiai, T., Fukushima, K., and Ochiai, K. (1995). Volatile fatty acids, metabolic by-products of periodontopathic bacteria, inhibit lymphocyte proliferation and cytokine production. *J. Dent. Res.* 74, 1367–1373. doi: 10.1177/00220345950740070801

Lee, S., and Lane, A. P. (2011). Chronic rhinosinusitis as a multifactorial inflammatory disorder. *Curr. Infect. Dis. Rep.* 13, 159–168. doi: 10.1007/s11908-011-0166-z

Mirkovic, B., Murray, M. A., Lavelle, G. M., Molloy, K., Azim, A. A., Gunaratnam, C., et al. (2015). The role of short-chain fatty acids, produced by anaerobic

bacteria, in the cystic fibrosis airway. *Am. J. Respir. Crit. Care Med*. 192, 1314–1324. doi: 10.1164/rccm.201505-0943OC

Mortensen, P. B., and Clausen, M. R. (1996). Short-chain fatty acids in the human colon: relation to gastrointestinal health and disease. *Scand. J. Gastroenterol*. 216, 132–148. doi: 10.3109/00365529609094568

Nguyen, T. L., Vieira-Silva, S., Liston, A., and Raes, J. (2015). How informative is the mouse for human gut microbiota research? *Dis. Model Mech*. 8, 1–16. doi: 10.1242/dmm.017400

Orlandi, R. R., Kingdom, T. T., Hwang, P. H., Smith, T. L., Alt, J. A., Baroody, F. M., et al. (2016). International consensus statement on allergy and rhinology: rhinosinusitis. *Int. Forum Allergy Rhinol*. 6(Suppl.1), S22–209.

Ragsdale, S. W., and Pierce, E. (2008). Acetogenesis and the Wood–Ljungdahl pathway of CO(2) fixation. *Biochim. Biophys. Acta*. 1784, 1873–1898. doi: 10.1016/j.bbapap.2008.08.012

Ramakrishnan, V. R., Feazel, L. M., Gitomer, S. A. Ir D., Robertson, C. E., and Frank, D. N. (2013). The microbiome of the middle meatus in healthy adults. *PLoS ONE* 8:e85507. doi: 10.1371/journal.pone.0085507

Sato, M., Yoshida, Y., Nagano, K., Hasegawa, Y., Takebe, J., and Yoshimura, F. (2016). Three CoA transferases involved in the production of short chain fatty acids in *Porphyromonas gingivalis*. *Front Microbiol.* 7:1146. doi: 10.3389/fmicb.2016.01146

Smith, P. M., Howitt, M. R., Panikov, N., Michaud, M., Gallini, C. A., Bohlooly, Y. M., et al. (2013). The microbial metabolites, short-chain fatty acids, regulate colonic Treg cell homeostasis. *Science* 341, 569–573. doi: 10.1126/science.1241165

Tomova, A., Bukovsky, I., Rembert, E., Yonas, W., Alwarith, J., Barnard, N. D., et al. (2019). The effects of vegetarian and vegan diets on gut microbiota. *Front Nutr*. 6:47. doi: 10.3389/fnut.2019.00047

Tonetti, M., Eftimiadi, C., Damiani, G., Buffa, P., Buffa, D., and Botta, G. A. (1987). Short chain fatty acids present in periodontal pockets may play a role in human periodontal diseases. *J. Periodontal. Res*. 22, 190–191. doi: 10.1111/j.1600-0765.1987.tb01565.x

Tunney, M. M., Field, T. R., Moriarty, T. F., Patrick, S., Doering, G., Muhlebach, M. S., et al. (2008). Detection of anaerobic bacteria in high numbers in sputum from patients with cystic fibrosis. *Am. J. Respir. Crit. Care Med*. 177, 995–1001. doi: 10.1164/rccm.200708-1151OC

Vieira, E. L., Leonel, A. J., Sad, A. P., Beltrao, N. R., Costa, T. F., Ferreira, T. M., et al. (2012). Oral administration of sodium butyrate attenuates inflammation and mucosal lesion in experimental acute ulcerative colitis. *J. Nutr. Biochem*. 23, 430–436. doi: 10.1016/j.jnutbio.2011.01.007

Zumft, W. G. (1997). Cell biology and molecular basis of denitrification. *Microbiol. Mol. Biol. Rev*. 61, 533–616. doi: 10.1128/.61.4.533-616.1997

Conflict of Interest: The authors declare that the research was conducted in the absence of any commercial or financial relationships that could be construed as a potential conflict of interest.

frontiers in Cellular and Infection Microbiology

ORIGINAL RESEARCH
published: 04 September 2020
doi: 10.3389/fcimb.2020.00472

Co-infection of *Malassezia sympodialis* With Bacterial Pathobionts *Pseudomonas aeruginosa* or *Staphylococcus aureus* Leads to Distinct Sinonasal Inflammatory Responses in a Murine Acute Sinusitis Model

*Keehoon Lee, Irene Zhang†, Shari Kyman†, Oliver Kask† and Emily Kathryn Cope**

Center for Applied Microbiome Sciences, The Pathogen and Microbiome Institute, Northern Arizona University, Flagstaff, AZ, United States

OPEN ACCESS

Edited by:
D. Scott Merrell, Uniformed Services University, United States

Reviewed by:
Joseph P. Zackular, University of Pennsylvania, United States
Richard George Douglas, The University of Auckland, New Zealand

***Correspondence:**
Emily Kathryn Cope
emily.cope@nau.edu

†Present address:
Irene Zhang, MIT, Department of Biology, Cambridge, MA, United States
Shari Kyman, Translational Genomics, Phoenix, AZ, United States
Oliver Kask, Stanford University, Department of Microbiology and Immunology, Stanford, CA, United States

Specialty section:
This article was submitted to Microbiome in Health and Disease, a section of the journal Frontiers in Cellular and Infection Microbiology

Received: *02 March 2020*
Accepted: *31 July 2020*
Published: *04 September 2020*

Citation:
Lee K, Zhang I, Kyman S, Kask O and Cope EK (2020) Co-infection of Malassezia sympodialis With Bacterial Pathobionts Pseudomonas aeruginosa or Staphylococcus aureus Leads to Distinct Sinonasal Inflammatory Responses in a Murine Acute Sinusitis Model. Front. Cell. Infect. Microbiol. 10:472. doi: 10.3389/fcimb.2020.00472

Host-associated bacteria and fungi, comprising the microbiota, are critical to host health. In the airways, the composition and diversity of the mucosal microbiota of patients are associated with airway health status. However, the relationship between airway microbiota and respiratory inflammation is not well-understood. Chronic rhinosinusitis (CRS) is a complex disease that affects up to 14% of the US population. Previous studies have shown decreased microbial diversity in CRS patients and enrichment of either *Staphylococcus aureus* or *Pseudomonas aeruginosa*. Although bacterial community composition is variable across CRS patients, *Malassezia* is a dominant fungal genus in the upper airways of the majority of healthy and CRS subjects. We hypothesize that distinct bacterial-fungal interactions differentially influence host mucosal immune response. Thus, we investigated *in vitro* and *in vivo* interactions between *Malassezia sympodialis, P. aeruginosa*, and *S. aureus*. The *in vitro* interactions were evaluated using the modified Kirby-Bauer Assay, Crystal Violet assay for biofilm, and FISH. A pilot murine model of acute sinusitis was used to investigate relationships with the host immune response. *S. aureus* and *P. aeruginosa* were intranasally instilled in the presence or absence of *M. sympodialis* ($n = 66$ total mice; 3–5/group). Changes in the microbiota were determined using 16S rRNA gene sequencing and host immune response was measured using quantitative real-time PCR (qRT-PCR). *In vitro*, only late stage planktonic *P. aeruginosa* and its biofilms inhibited *M. sympodialis*. Co-infection of mice with *M. sympodialis* and *P. aeruginosa* or *S. aureus* differently influenced the immune response. In co-infected mice, we demonstrate different expression of fungal sensing (Dectin-1), allergic responses (IL-5, and IL-13) and inflammation (IL-10, and IL-17) in murine sinus depending on the bacterial species that co-infected with *M. sympodialis* ($p < 0.05$). The pilot results suggest that species-specific interactions in airway-associated microbiota may be implicated

driving immune responses. The understanding of the role of bacterial-fungal interactions in CRS will contribute to development of novel therapies toward manipulation of the airway microbiota.

Keywords: malassezia, sinus microbiome, bacterial-fungal interactions, interkingdom interactions, *Staphylococcus aureus*, *Pseudomonas aeruginosa*

INTRODUCTION

Emerging studies of the microbiota, defined as bacteria, fungi, viruses, and archaea that inhabit a niche, have profoundly altered our understanding of the role of the human microbiota in health and disease. The range of effects that these complex microbial assemblages have on human physiology is unimaginably broad. For example, many studies suggest that gastrointestinal microbiota are related to not only intestinal diseases but also obesity (Moise, 2017), cancers (Gopalakrishnan et al., 2018), allergies (Fujimura et al., 2016), and neurological disorders (Elizabeth and Zabielski, 2013). In the gut, *Clostridium* produces the short-chain fatty acid (SCFA) butyrate, which contributes to the polarization of FOXP3+CD4+ regulatory T-cells. In addition to butyrate, gut microbes produce propionate and acetic acid, which can act as ligands for G protein-coupled receptors (GPCRs) and affect neutrophil chemotaxis, regulation of regulatory T cells (Treg), and dendritic cell (DC) maturation (Kau et al., 2011; Thaiss et al., 2016). However, our understanding of the respiratory tract microbiota remains nascent, even though it is one of the first body sites to make contact with microorganisms after birth and has a larger surface area than the skin or GI tract (Fröhlich et al., 2016). The development of culture-independent methods has shown that complex, site-specific microbial communities inhabit the upper and lower airways (Brill et al., 2016; Pletcher et al., 2018).

Chronic rhinosinusitis (CRS) is a common upper respiratory inflammatory disease affecting ∼14% of the Western population and costing about $65 billion each year in disease management (Caulley et al., 2015). CRS is diagnosed through a combination of patient history, nasal endoscopy, and radiography and is characterized by symptoms lasting at least 12 consecutive weeks (Sedaghat, 2017). The primary goal of CRS treatments is to manage the symptoms and improve patients' quality of life. Medical management for CRS includes nasal saline irrigation (Gupta and Singh, 2010), topical intranasal and oral corticosteroids (Epperson et al., 2019), and antibiotics if a pathogen is cultured (Mattila, 2012). If medicinal management is unsuccessful, endoscopic sinus surgery is performed. Even though these treatment methods can improve symptoms, the recurrence rate of CRS is as high as 78.9% (Sedaghat, 2017; Calus et al., 2019).

The sinuses harbor a complex bacterial and fungal microbiome. A recent study from our group demonstrated that the sinus bacterial microbiota exists in four different compositional states each dominated by one of four different bacterial families and low-abundance co-colonizers. Each bacterial community state was associated with a distinct host inflammatory response in CRS patients (Cope et al., 2017). In another study using targeted qPCR, we demonstrated that *Malassezia* was the predominant fungal taxa across all patient subgroups (Gelber et al., 2016). Recent sequence-based studies have confirmed that *Malassezia* species, including *M. restricta* and *M. sympodialis,* are dominant core members of the sinus fungal microbiome (Carter and Amedee, 2014; Cleland et al., 2014; Hoggard et al., 2019; Wagner Mackenzie et al., 2019). *Malassezia* is a dimorphic and lipophilic fungus that is commonly found on the skin as a commensal organism. An opportunistic pathogen, *Malassezia* produces virulence factors such as lipases, phospholipases, and allergens that can damage epithelial integrity and trigger predominantly T_H2 immune responses (Blanco and Garcia, 2008; Boekhout et al., 2010). In the GI tract, a study showed that *Malassezia* was associated with the colonic mucosa of Crohn's disease patients and exacerbated colitis in mouse models (Limon et al., 2019). However, the role of *Malassezia* in the respiratory tract has not been studied.

Interactions between bacteria and fungi are critical mediators of microbial community composition and function. Several studies investigating the interactions between bacteria and fungi have focused predominantly on another dimorphic yeast, *Candida albicans,* and bacterial co-colonizers. Distinct types of interactions not only affect the survival of the bacteria but also affect both fungal and bacterial virulence and host immune responses. For example, the interaction between *C. albicans* and *Staphylococcus aureus*, a bacterial pathogen, results in increased *C. albicans* hyphal formation and higher invasiveness of *S. aureus* into mucosal membranes by attaching to the hyphae of *C. albicans* (Schlecht et al., 2015). These studies of fungal and bacterial interactions suggest that we need to consider bacterial-fungal interactions to advance our understanding of chronic airway diseases such as cystic fibrosis (CF) and chronic rhinosinusitis (CRS) in the context of microbial interactions and relationships with the host immune response.

In this study, we hypothesized that bacterial co-colonizers, selected from our prior studies of the CRS bacterial microbiota, differentially interact with *Malassezia* and that this drives specific sinonasal immune responses dependent on innate immune sensing of fungi. Here, we investigated the *in vitro* and *in vivo* interactions between *Malassezia sympodialis* and bacterial pathogens, *Pseudomonas aeruginosa* and *Staphylococcus aureus*. *Malassezia* is the predominant fungal genus in the sinuses (Gelber et al., 2016; Hoggard et al., 2019), and *S. aureus* and *P. aeruginosa* are predominant members of two of the four described bacterial community states in CRS (Cope et al., 2017), and they are commonly isolated bacteria in CRS patients (Zhang et al., 2015). We evaluated *in vivo* influence of bacterial-*Malassezia* co-infection using a murine model of sinonasal

disease (Abreu et al., 2012). These pilot studies suggest that *in vitro* interactions between *S. aureus* or *P. aeruginosa* with *M. sympodialis* are highly dependent on the species of bacteria and co-infection of *M. sympodialis* with either *S. aureus* or *P. aeruginosa* yields distinct sinonasal immune responses.

MATERIALS AND METHODS

Bacterial and Fungal Species

We used two bacterial species, which were previously demonstrated to be related to CRS endotypes, and one fungal genus that belongs to the dominant fungal genus in the nasal passage, *Malassezia*. The bacterial species used were isolated from CRS patients: *Pseudomonas aeruginosa* EC1 (Cope et al., 2016) and *Staphylococcus aureus*. Species IDs were confirmed by sequencing the full length 16S rRNA gene. The fungal species, *Malassezia sympodialis*, was gifted by Paal Anderson (University of Copenhagen).

Bacterial and Fungal Growth Media

P. aeruginosa and *S. aureus* were incubated in Sabouraud Dextrose Agar (SDA, HIMEDIA®) and SD broth. The lawn of *M. sympodialis* was grown on an SDA plate overlaid with ∼300 µl sterile olive oil. Olive oil was not used in broth media for any organism as it inhibited some aspects of microbial growth. SDA with olive oil was not an optimal media because it inhibited aspects of microbial growth. The co-cultured biofilm experiment, the preparation for fluorescence *in-situ* hybridization (FISH) staining, and the *in vivo* mouse experiment were prepared using different media. The *P. aeruginosa* and *S. aureus* cultures were prepared in brain heart infusion broth (BHIB, BD Difco™). *M. sympodialis* were prepared in modified Dixon (mDixon) media. Briefly, the contents of the modified Dixon media are 36 g malt extract (MP Biomedicals), 10 g Bacto™ peptone (Life Technologies), 10 ml Tween 40 (Sigma-Aldrich), and 2 ml glycerol (Sigma-Aldrich) added to 1 L dH_2O before pH was adjusted to 6.0 (Guillot et al., 1998). The desiccated ox bile and antibiotics were omitted from the original Dixon media in order to facilitate use in co-culture experiments with other bacterial species.

In vitro Bacterial-Fungal Inhibitory Relationship Assay

We performed a modified Kirby-Bauer test to evaluate antagonistic relationships between *M. sympodialis* and *S. aureus* or *P. aeruginosa.* Each filter paper disc contained four different growth modes of *P. aeruginosa* or *S. aureus* culture (early phase planktonic: incubate for 3 h at 37°C with shaking; late phase planktonic: incubate for 24 h at 37°C with shaking). Growth discs containing biofilms were incubated for 24 h at 37°C in a 24-well plate. Biofilm discs were removed from the 24-well plate and immediately used in this assay. Finally, discs were inoculated with the cell-free supernatant fluid from late-phase planktonic bacterial growth media. The cell-free supernatant was prepared by filter-sterilizing the culture-supernatant after centrifugation at 8,000 × g for 1 min using a 0.22 µm syringe filter (MilliporeSigma™ Millex™). Discs were placed on the *M. sympodialis* lawn on Sabouraud Dextrose Agar (SDA) plates. The sterile Sabouraud Dextrose Broth (SDB) and 10% bleach solution on the discs were used for negative and positive growth inhibition controls, respectively. The plates were incubated at 30°C for 72 h, and the diameter of the inhibition zone around the discs was measured. This experiment was performed in triplicate.

Crystal Violet Biofilm Assay

Primary broth cultures of *P. aeruginosa* or *S. aureus* were grown in brain heart infusion broth (BHIB, BD Difco™) for 24 h at 37°C with shaking. 100 µl of the primary cultures were transferred into fresh 10 ml of modified Dixon (mDixon) and incubated for 4 h at 37°C with shaking to reach the exponential growth phase. The exponential growth phase cultures were diluted 1:100 in 150 µl of mDixon broth in a sterile 96-well plate (Cafarchia et al., 2012). To grow the *M. sympodialis* biofilm, the primary culture was grown in mDixon for 48 h at 30°C with shaking. 100 µl of the primary cultures were transferred into fresh 10 ml of mDixon and incubated for 6 h at 30°C with shaking to reach the exponential growth phase. The exponential growth phase cultures diluted 1:50 in 150 µl of mDixon in a sterile 96 well plates. For the polymicrobial biofilms, 1.5 ml of diluted the exponential growth phase culture of *M. sympodialis* and *P. aeruginosa* or *S. aureus* in mDixon were combined in a sterile 96 well plates. All the biofilm plates were grown at 30°C for 48 hrs without agitation. Biofilms were quantified using the crystal violet biofilm assay, as previously described (O'Toole, 2011). Briefly, the media from the 96 wells were discarded, and the wells were rinsed with distilled water and dried. 200 µl of 1% crystal violet staining solution was added to the wells to stain the biofilms for 10 min. The crystal violet staining solution was discarded and then the wells were rinsed with distilled water 3 times. The crystal violet stained biofilms were dried in the air for 3 h and 200 µl of 70% ethanol was added to extract the crystal violet stain from the biofilms. The amount of crystal violet stain in the 70% ethanol was measured by observing the optical density at 600 nm wavelength with (BioTek Synergy™ HT). Uninoculated wells were used as negative controls. This experiment was repeated in quadruplicate.

In vivo Murine Challenge Experiment

The *in vivo* model was modified from a previous study by Abreu et al. (2012). This experiment was performed once, and we used the same number of animals in this study per group ($n = 3$ mice/group for molecular analysis, $n = 2$ mice/group for Fluorescent *in situ* Hybridization as applicable) as previously published (Abreu et al., 2012). These studies were approved under NAU IACUC approval number 16-008. Mice were acclimatized for 5 days prior to the experiments. Two groups of balb/c mice ($n = 66$ total) were used: an antimicrobial-naive group ($n = 3$ mice/group for molecular analysis and $n = 2$ mice for fluorescent *in-situ* hybridization), and an antimicrobial-treated group ($n = 3$ mice/group for molecular analysis). The antimicrobial-treated mice were intranasally administered with augmentin (15 mg/kg) and fluconazole (100 mg/kg) for 5 days after a 5 day acclimatization period. Each group was intranasally

infected with one either (1) saline (control), (2–4) single species microorganisms (1.0×10^8 cells of *P. aeruginosa, S. aureus,* or *M. sympodialis*), or (5–6) dual-species microorganisms (1.0×10^8 cells of *P. aeruginosa* and *M. sympodialis,* or *S. aureus* and *M. sympodialis*). The antimicrobial-naive and -treated mice were infected with the six infection groups mentioned above for 3 days. One day after the third infection, the mice were euthanized using CO_2, and the sinonasal tissue was harvested and stored in 700 μl of RNAlater for microbiome and immunological analysis (**Figure S1**).

Sinonasal Microbiome Analysis

The harvested sinonasal tissue samples in RNA*later*® (Sigma-Aldrich) were stored at 4°C for 24 h before processing the samples. After 24 h in RNA*later*®, DNA and RNA were extracted from the sinonasal tissue samples using the Allprep DNA/RNA mini kit (Qiagen). The V4 region of the 16S rRNA gene was amplified from DNA by polymerase chain reaction (PCR) using a 515f forward primer with an adapter sequence, AATGATACGGCGACCACCGAGATC-TACACTATGGTAATTGTGTGCCAGCMGCCGCGGTAA, and the 806r indexed primers for reverse primers (Integrated DNA Technologies). The PCR reactions were carried out in 25 μL containing 1 μL of DNA template, 1x TaKaRa® Ex Taq PCR buffer (Mg2+ plus), 0.2 mM TaKaRa® dNTP mixture, 0.625 U TaKaRa® Ex Taq HS polymerase, 0.56 mg/μL BSA, 0.4 μM of each primer, and 16.375 μL of water. The PCRs were performed using a SimpliAmp® thermocycler (Applied Biosystems) under the following conditions: 98 °C for 2 min to release the polymerase antibody, followed by 30 cycles of 98°C for 20 s, 50°C for 30 s, and 72°C for 45 s. A final extension step of 72°C for 10 min was then conducted to ensure the completion of all fragments. All samples were triplicated and pooled in order to minimize the random amplification bias. The PCR amplicons were confirmed by agarose gel electrophoresis and quantified using Qubit 4 fluorometer (ThermoFisher Scientific). Amplicons were pooled at 50 ng/sample. The pooled amplicons were sequenced using Illumina MiSeq v3 (Illumina, inc.) at Translational Genomics North (TGen-North). The sequence data were analyzed using a bioinformatics platform, QIIME 2 (Bolyen et al., 2019).

Murine Immune Gene Expression Analysis

The immunological responses were analyzed by measuring gene expression of the key immune responses in CRS (Baba et al., 2015; Hamilos, 2015; Hulse, 2016), such as genes for *interleukin (IL)-2, IL-5, IL-10, IL-13, IL-17, MUC5AC, Dectin-1,* and *Tumor Necrosis Factor (TNF)-α*, by quantitative reverse transcription polymerase chain reaction (qRT-PCR) using the 1 ng/μl of cDNA, which was synthesized from the extracted mRNA. Gene expression was normalized to glyceraldehyde-3-phosphate dehydrogenase (GAPDH) gene (**Table 1**). qRT-PCR was done using QuantStudio™ 12k Flex Real-time PCR System (Applied Biosystems™) with *Power* SYBR™ Green PCR MasterMix (Applied Biosystems™). The qRT-PCR condition consists of hold (50°C for 2 min and 95°C for 10 min.), PCR (40 cycles of 95°C for 15 sec. and 60°C for 1 min.), and melt curve cycle (95°C for 15 sec. and decrease to 60°C by 1.6°C /s).

Fluorescence *in situ* Hybridization (FISH) of Polymicrobial Biofilms and Mouse Sinonasal Specimens

The bacterial pathogens, *P. aeruginosa* or *S. aureus*, and *M. sympodialis* co-developed biofilms were observed under the confocal laser scanning microscope (CLSM) using FISH. The biofilms were developed according to the protocol above. The biofilms were hybridized using the universal eubacterial probe, EUB 388, and *Malassezia* genus specific probe (**Table 2**). The biofilms were carefully transferred to glass slides and air-dried. The air-dried biofilms were fixed by dipping the slides in 50, 70, and 95% ETOH for 3 min each, and washed with DI water. The fixed biofilms were hybridized with 1 μl of the EUB 388 probe (10 nM) and 1 μl of the *Malassezia*_genus probe (10 nM) in 18 μl of the hybridization buffer for 90 min at 46°C in a hybridization chamber with damped paper with 5 ml of hybridization buffer for humidity. The hybridized biofilms were washed in a 48°C washing buffer for 30 min. The washed biofilms were rinsed briefly with DI water and mounted using VECTASHIELD® (VECTOR Laboratories). The hybridization buffer contained 0.9M NaCl, 20 mM Tris/HCl (pH 8.0), 0.01% SDS, and 35% formamide. The washing buffer contained 0.08M NaCl, 20 mM Tris/HCl (pH 8.0), 5 mM EDTA, and 0.01% SDS. Sinonasal specimens were prepared by fixing the skinned head of mice in methanol-Carnoy's fixative (60% methanol, 30% chloroform, 10% glacial acetic acid) for 24 h. Heads were decalcified in EDTA for 10 days, then embedded in a paraffin block. The micro-sectioned sinonasal tissue slide was prepared using the paraffin-embedded samples. The sinonasal tissue slides were deparaffinized by incubating the slide in xylene twice for 5 min each and washing it with 100% ethanol twice for 5 min each. The deparaffinized slides were hybridized using the same protocol with different probes. The probes used in the mouse sinonasal specimen FISH were 1 μl of 3 μM DAPI (4′,6-Diamidino-2-Phenylindole, Dihydrochloride), 1 μl of 10 nM *P. aeruginosa* specific probe (Paeru), 1 μl of 10 nM *S. aureus* specific probe (Saure), and 2 μl of 10 nM *Malassezia*_genus probe in 16 ul of the hybridization buffer (**Table 2**).

Bioinformatics and Statistical Analysis

For all comparisons, an α of 0.05 was considered significant. All *p*-values were corrected for false discovery using the Story method (Krzywinski and Altman, 2014). 16S rRNA gene sequences were analyzed using QIIME 2 version 2018.11 and 2019.1.0 (Bolyen et al., 2019); www.QIIME2.org). Sequences were demultiplexed and then truncated at 183 bases of the demultiplexed sequences to achieve a quality of >Q20 for all bases. Demultiplexed sequences were denoised and grouped into amplicon sequence variants (ASVs) using dada2 (Callahan et al., 2016). The feature table was rarified to a sampling depth of 1,134 sequences. A phylogenetic tree was built by aligning sequences with MAFFT and a phylogenetic tree was built using FastTree2 (Price et al., 2010; Katoh and

TABLE 1 | Primers used in this study.

Primer	Sequence	Reference
IL-2F	GTCACATTGACACTTGTGCTCC	Telander et al., 1999
IL-2R	AGTCAAATCCAGAACATGCCG	
IL-4F	TCGGCATTTTGAACGAGGTC	Kim et al., 2011
IL-4R	GAAAAGCCCGAAAGAGTCTC	
IL-5F	ATGGAGATTCCCATGAGCAC	
IL-5R	GTCTCTCCTCGCCACACTTC	
IL-10F	GCGTCGTGATTAGCGATGATG	Trandem et al., 2011
IL-10R	CTCGAGCAAGTCTTTCAGTCC	
IL-17F	GGACTCTCCACCGCAATGA	Atarashi et al., 2008
IL-17R	GGCACTGAGCTTCCCAGATC	
IFNg-F	CTACCTTCTTCAGCAACAGC	Oestreich et al., 2012
IFNg-R	GCTCATTGAATGCTTGGCGC	
GADPH-F	CCTCGTCCCGTAGACAAAATG	Ueda et al., 2010
GADPH-R	TCTCCACTTTGCCACTGCAA	
MUC5AC-F	AGCTACAGTGCAACTGGACC	Lin et al., 2014
MUC5AC-R	GGACACAGATGATGGTGACA	
IL13-F	AGGAGCTGAGCAACATCACAC	Kimura et al., 2014
IL13R	CCATAGCGGAAAAGTTGCTT	
TNF-α-F	GTAGCCCACGTCGTAGCAA	
TNF-α-R	AAATGGCAAATCGGCTGAC	
Dectin-1_F	ATCAGCATTCTTCCCCAACTCG	
Dectin-1_R	CAGTTCCTTCTCACAGATACTGTATGA	

Standley, 2013) which was subsequently rooted by midpoint rooting. Taxonomy was assigned to ASVs with a Naive Bayes classifier trained on the Greengenes 13_8 99% OTU database (DeSantis et al., 2006), using the q2-feature-classifier taxonomy classification plugin (Bokulich et al., 2018). Within-sample (α-diversity) was calculated using Pielou's Evenness index and a Kruskal Wallis test was used to compare across experimental groups. Between-sample (β-diversity) metrics were calculated using the UniFrac phylogenetic distance (Lozupone and Knight, 2005), Bray-Curtis, and Jaccard metrics (Goodrich et al., 2014). Permutational analysis of variance (PERMANOVA) between sinonasal communities of infection groups within antibiotic-treated and -naive groups was calculated on the Bray-Curtis dissimilarity matrix. The significance of the bacterial-fungal inhibitory relationship using the Kirby Bauer method was calculated using a paired *t*-test, and the Mann-Whitney *U*-test was used to compare the degree of biofilm development between the groups. For *in vivo* murine experiments, an unpaired *t*-test was used for comparisons of the murine immune gene expression.

RESULTS

In vitro Bacterial and Fungal Interactions

To assess whether differential interactions between *M. sympodialis* and *S. aureus* or *P. aeruginosa* exist *in vitro*, we used a modified Kirby-Bauer inhibition assay and a crystal violet biofilm quantification assay. *Malassezia sympodialis* lawn was plated and paper discs inoculated with early phase planktonic, late phase planktonic, 24 h biofilm, and cell-free supernatant of the late phase planktonic culture were placed on the *M. sympodialis* lawn. We observed significantly larger inhibition zones when *P. aeruginosa* late phase planktonic and biofilm were applied to the discs compared to the control discs (paired *t*-test $p = 0.0006$ and 0.0255, respectively). The late phase planktonic *P. aeruginosa* and 10% bleach solution were not significantly different (**Figure 1A**, paired *t*-test, $p = 0.4226$). *S. aureus* did not inhibit *M. sympodialis* in any treatment group (**Figure 1A**, paired *t*-test $p > 0.05$). Biofilm formation was measured using the crystal violet assay for biofilm development. Dual-species biofilms of *P. aeruginosa* and *M. sympodialis* were significantly reduced compared to the *M. sympodialis* single-species biofilm (**Figure 1B**, Mann-Whitney *U*-test $p = 0.0286$). Dual-species *S. aureus* and *M. sympodialis* dual-species biofilms were slightly increased compared to either single-species biofilms but this did not reach statistical significance (**Figure 1B**, Mann-Whitney *U*-test $p = 0.0571$). In order to determine spatial organization of bacteria and *Malassezia in vitro*, dual-species biofilms were grown for 48 h and viewed using Fluorescent *in situ* Hybridization (FISH) and CLSM. The co-cultured biofilms of *M. sympodialis* with *S. aureus* or *P. aeruginosa* were stained using FISH probes EUB 388 and *Malassezia*_genus. *In vitro* FISH of the *M. sympodialis* with *P. aeruginosa* showed inhibition of *M. sympodialis* as we were only able to observe *P. aeruginosa* (**Figure S2**). However, there was clear colocalization of *S. aureus* and *M. sympodialis in vitro* (**Figure S2**). These results are the first to demonstrate species-specific interactions with a clinically relevant species of *Malassezia (M. sympodialis)* and two common airway pathobionts, *P. aeruginosa* and *S. aureus*.

Sinonasal Microbiome Analysis

We next sought to understand whether nasal instillation of *M. sympodialis* or bacterial pathobionts altered the bacterial sinonasal microbiome composition or diversity ($n = 3$ mice per group were used for microbiome analysis). We were interested in whether the introduction of a potential fungal pathobiont would significantly change the surrounding bacterial community members. We anticipated that nasal administration of *S. aureus* or *P. aeruginosa* would result in dominance of the respective taxa in both antibiotic-treated and antibiotic-naïve mice. Indeed, we found that introduction of bacteria, but not fungi, significantly altered the composition of the murine sinonasal bacterial microbiome. Between-sample diversity (beta-diversity) was significantly different between antibiotic-naïve and antibiotic-treated mice (**Figure 2A**, PERMANOVA, $p = 0.001$, Bray-Curtis Dissimilarity). There was no distinct separation between the infection groups of the antibiotic-treated samples (**Figure 2B**, PERMANOVA, $p = 0.585$), whereas the antibiotic-naïve mice

TABLE 2 | FISH probes used in this study.

Probe	Target	Fluor	Sequence 5′-3′	Reference
EUB 388	Bacteria	Alexa 594	GCTGCCTCCCGTAGGAGT	Trebesius et al., 2000
Malassezia_genus	*Malassezia*	Alexa 532	CCGATATTTAGCTTTAGATGGAGTCTA	This study
Paeru	*P. aeruginosa*	Alexa 594	GGTAACCGTCCCCCTTGC	Hogardt et al., 2000
Saure	*S. aureus*	Alexa 660	GAAGCAAGCTTCTCGTCCG	Hogardt et al., 2000

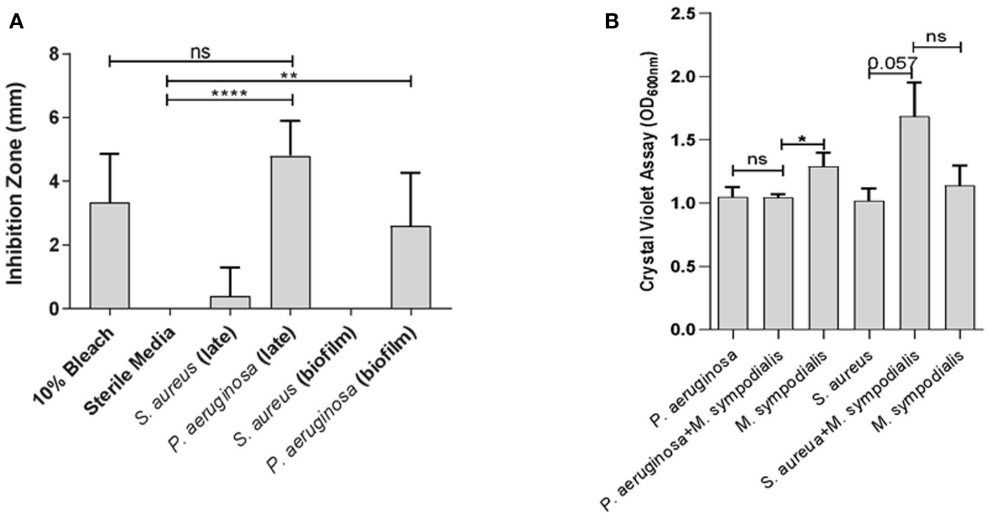

FIGURE 1 | *In vitro* interactions between *Malassezia sympodialis* and different growth stages of *Pseudomonas aeruginosa* or *Staphylococcus aureus*. Zones of inhibition indicating antagonistic interactions in the modified Kirby-Bauer assay **(A)**, and quantification of biofilm development with *P. aeruginosa* and/or *M. sympodialis* or with *S. aureus* and/or *M. sympodialis* **(B)**. (ns, not statistically significant; $^{*}P \leq 0.05$, $^{**}P \leq 0.005$, $^{****}P \leq 0.00005$).

samples clustered by the bacterial species inoculated (**Figure 2C**, PERMANOVA, $p = 0.001$). The *M. sympodialis* infected mice clustered with control mice and the co-infected mice clustered with the singly infected groups (**Figure 2C**), indicating that introduction of *M. sympodialis* does not significantly alter the murine sinonasal bacterial microbiome. We also classified taxonomy to examine relative abundances of taxa across groups. We have generated taxonomic barplots of relative abundance of 20 most abundant taxa overall which covers 90.494% of total taxa observed in our study (**Figure 3**). The taxonomic barpolts represent relative abundance of the top 20 taxa in sinonasal samples (**Figure 3A**) or the averaged relative abundances of each treatment group (**Figure 3B**). Taxonomic barplots show that the sinonasal microbiota was dominated by the bacterial species introduced intranasally only in the antibiotic-naïve mice (**Figure 3** and **Supplemental Information**). Surprisingly, the composition of the sinonasal bacterial microbiota in the antibiotic-treated mice did not show obvious changes by the infected bacterial species as shown in the antibiotic-naïve groups (**Figure 3**, PERMANOVA, $p = 0.001$). The antibiotic-treated groups possess high portions of *Staphylococcus sciuri, Cytophagaceae, Lactobacillus iners,* and *Dyella* species, which were not detected in the antibiotic-naïve samples, and *Bacteriodalis*: S24-7 (*Muribaculaceae*) was detected only in the antibiotic-naïve group (**Figure 3**, interactive visualization in the supplemental information and on https://github.com/e-cope/malassezia-ms and can be viewed on view.qiime2.org). These results suggest that presence of *P. aeruginosa* and *S. aureus* on the sinonasal mucosa in antibiotic-naïve mice 1 day after intranasal instillation, but also show that *M. sympodialis* has a negligible effect on the sinonasal bacterial microbiota in this experiment.

Analysis of the Sinonasal Immune Response

We next sought to determine whether co-infection with different combinations of *P. aeruginosa, S. aureus,* and *M. sympodialis* leads to distinct sinonasal immune responses. Gene expression of *IL-5, IL-13, IL-17, MUC5AC*, and *Dectin-1* were measured using reverse transcriptase quantitative PCR ($n = 3$ mice/group). *IL-5* gene expression significantly increased in *S. aureus* and *M. sympodialis* co-infected mice in antibiotic-naïve mice compared to control, *S. aureus* singly or *M. sympodialis* singly infected mice (**Figure 4A**, unpaired *t*-test, $p = 0.0111$, and $p = 0.0188$, respectively). However, *IL-5* gene expression was not elevated in antibiotic-treated mice co-infected with *S. aureus* and *M. sympodialis* (**Figure 4D**). *IL-5* expression significantly increased

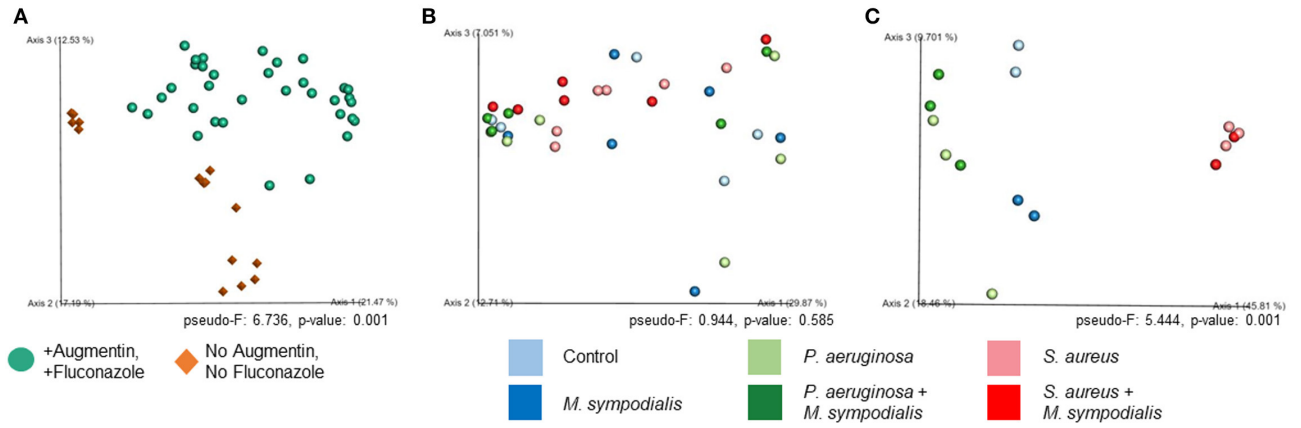

FIGURE 2 | Principal Coordinates Analysis of Bray-Curtis Dissimilarity of the Murine Sinonasal Microbiome. Two groups of mice, antibiotic-treated or -naive, were intranasally infected with either one species of bacteria, *P. aeruginosa* (light green), *S. aureus* (light red), or fungi, *M. sympodialis* (dark blue), or two species, *M. sympodialis* with *P. aeruginosa* (dark green) or *S. aureus* (dark red). **(A)** represents beta-diversity of antibiotic-treated (solid sphere) and antibiotic-naïve (diamond) mice groups. **(B)** represents beta-diversity of the infection groups in the antibiotic-treated mice, and **(C)** represents beta-diversity of the infection groups in the antibiotic-naïve mice.

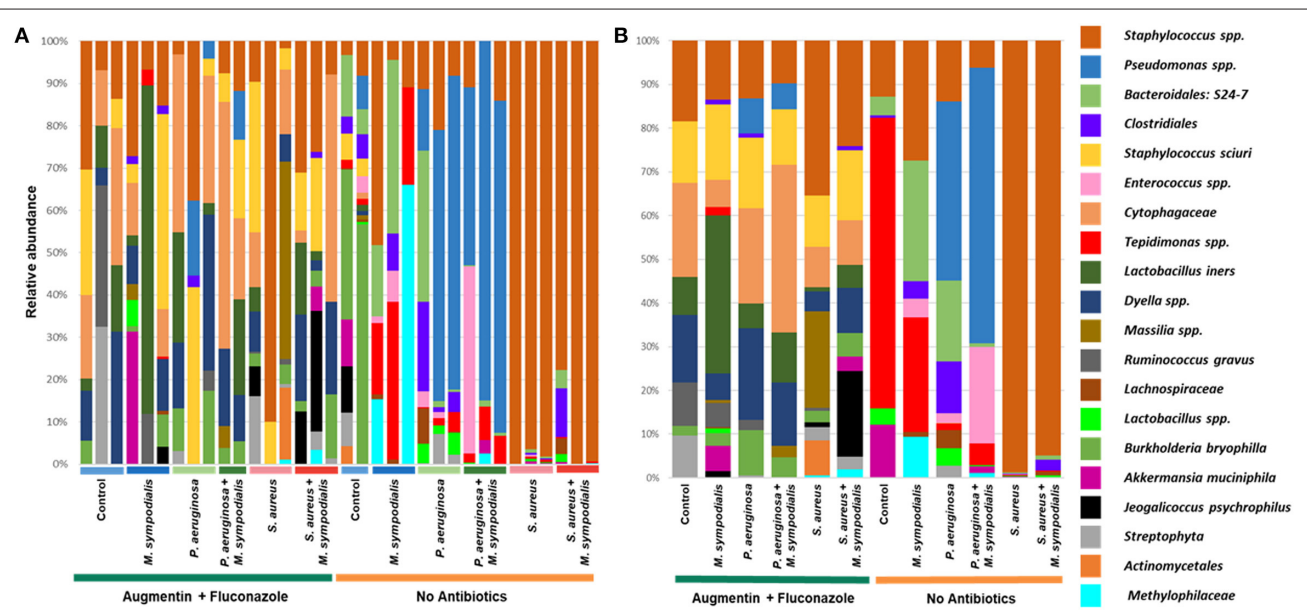

FIGURE 3 | Relative bacterial abundances in sinonasal microbiota of mice. Two groups of mice, antibiotic-treated or -naive, were intranasally infected with either one species of bacteria, *P. aeruginosa* or *S. aureus*, or fungi, *M. sympodialis*, or two species, *M. sympodialis* with *P. aeruginosa* or *S. aureus*. The 20 most abundant taxa covers 90.494% of total sequence hits. **(A)** represents relative abundance of each sinonasal samples, and **(B)** represents the averaged relative abundances of each treatment group samples. The legend is an orderly representation of 20 most abundant bacterial taxa, top taxa being the most abundant.

in the antibiotic-treated mice singly infected with *P. aeruginosa* (**Figure 4D**). *IL-13* gene expression had the same pattern as the *IL-5* gene expression. *IL-13* gene expression increased significantly in *S. aureus* and *M. sympodialis* co-infected, antibiotic-naïve mice compared to the *S. aureus* singly, or *M. sympodialis* singly infected mice (**Figure 4B**, unpaired *t*-test, $p = 0.035$, $p = 0.0017$, respectively). In antibiotic-treated mice, none of the infection groups had significant changes in *IL-13* gene expression (**Figure 4E**, unpaired *t*-test, $p > 0.05$).

IL-17 gene expression significantly increased in *S. aureus* singly infected mice compared to controls (unpaired *t*-test, $p = 0.0001$) and *M. sympodialis* singly infected mice (unpaired *t*-test, $p = 0.0001$) in the antibiotic-naïve group. We observed a slight increase in increased in both co-infected mice, *P. aeruginosa* + *M. sympodialis* and *S. aureus* + *M. sympodialis* compared to the *M. sympodialis* singly infected mice in the antibiotic-naïve group but this was not statistically significant (**Figure 4C**, unpaired *t*-test, $p = 0.061$, $p = 0.075$). *IL-17* gene expression did not

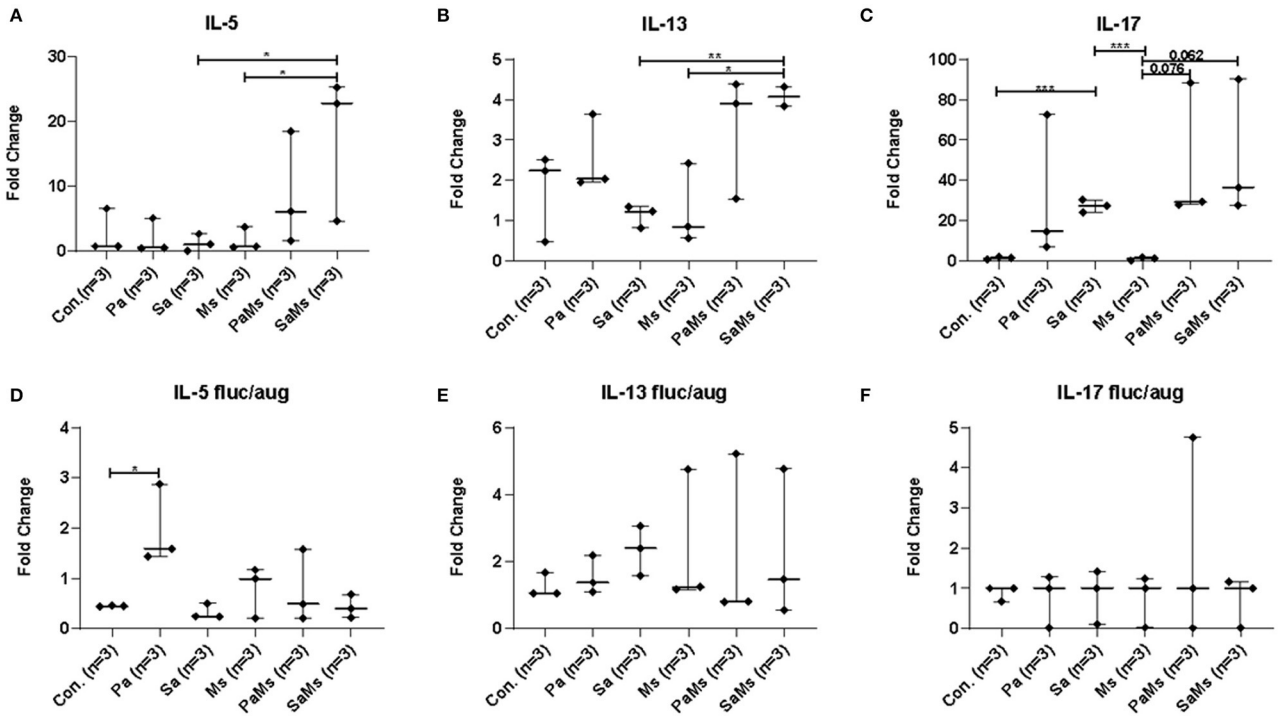

FIGURE 4 | Relative gene expression of interleukin-5, interleukin-13, and interleukin-17 in the murine sinonasal cavity. The relative gene expression of IL-5 **(A,D)**, IL-13 **(B,E)** and IL-17 **(C,F)** in antibiotic-naïve **(A–C)** and antibiotic-treated **(D–F)** mice in different infection groups, saline treated group **(Con.)** *P. aeruginosa* infected group **(Pa)**, *S. aureus* infected group **(Sa)**, *M. sympodialis* infected group **(Ms)**, *P. aeruginosa* and *M. sympodialis* co-infected group **(PaMs)**, and *S. aureus* and *M. sympodialis* co-infected group **(SaMs)**, were measured by qRT-PCR. Gene expression was normalized with GAPDH, a housekeeping gene. Between-group comparisons without *p*-values were not statistically significant. (*$P \leq 0.05$, **$P \leq 0.005$, ***$P \leq 0.0005$).

change in any of the infection groups when mice were treated with antibiotics prior to infection (**Figure 4F**, unpaired *t*-test, $p > 0.05$).

MUC5AC gene expression significantly increased in antibiotic-naïve mice co-infected with *P. aeruginosa* and *M. sympodialis* when compared to control mice, *M. sympodialis* singly, and *P. aeruginosa* singly infected mice. We observed a slight but non-significant increase in *MUC5AC* gene expression in mice co-infected with *S. aureus* and *M. sympodialis* compared to mice singly infected with *S. aureus* or *M. sympodialis* (**Figure 5A**, unpaired *t*-test > 0.05). Of interest, *MUC5AC* gene expression was significantly decreased in *M. sympodialis* singly infected mice compared to *S. aureus* infected antibiotic-naïve mice (**Figure 5A**, unpaired *t*-test, $p = 0.0059$). In antibiotic-treated mice, *MUC5AC* was significantly increased in *S. aureus* singly, *M. sympodialis* singly infected mice, and *S. aureus* and *M. sympodialis* co-infected mice compared to control mice (**Figure 5B**, unpaired *t*-test, $p < 0.05$). We also evaluated the expression of *dectin-1*, a c-type lectin receptor involved in the recognition of *Malassezia* (Kistowska et al., 2014). *Dectin-1* expression significantly increased in *P. aeruginosa* singly infected, *P. aeruginosa* and *M. sympodialis* co-infected, and *S. aureus* and *M. sympodialis* co-infected mice compared to controls in the antibiotic-naïve group (**Figure 5C**, unpaired *t*-test, $p < 0.05$). *M. sympodialis* infection did not induce *dectin-1* gene expression, and *dectin-1* expression was not different between either co-infection group compared to the corresponding single bacterial infected mice (**Figure 5C**). In antibiotic-treated mice, *dectin-1* gene expression was not significantly different between control, *P. aeruginosa* singly infected, *S. aureus* singly infected, and *S. aureus* and *M. sympodialis* co-infected mice but it significantly decreased in *M. sympodialis* singly infected and *P. aeruginosa* and *M. sympodialis* co-infected mice compared to all other groups (**Figure 5D**, unpaired *t*-test, $p < 0.05$). In this pilot experiment, antibiotic-treated mice appeared to have a suppressive immune phenotype compared to antibiotic-naïve mice when infected with *P. aeruginosa, S. aureus,* or *M. sympodialis*. Future studies will confirm these findings in replicate experiments with additional mice.

Ex vivo FISH on Murine Sinonasal Tissue

We used FISH to determine the spatial organization and confirm colonization of *M. sympodialis, P. aeruginosa*, and *S. aureus ex vivo* in the sinonasal cavity of mice that exhibited differential immune responses. *In vitro* FISH of the *M. sympodialis* with *P. aeruginosa* showed inhibition of *M. sympodialis* but there was clear colocalization of *S. aureus* and *M. sympodialis* (**Figure S2**). These results were confirmed in the sinonasal cavity of antibiotic-naïve mice after co-infection of each bacterial pathobiont with *M. sympodialis*. In control

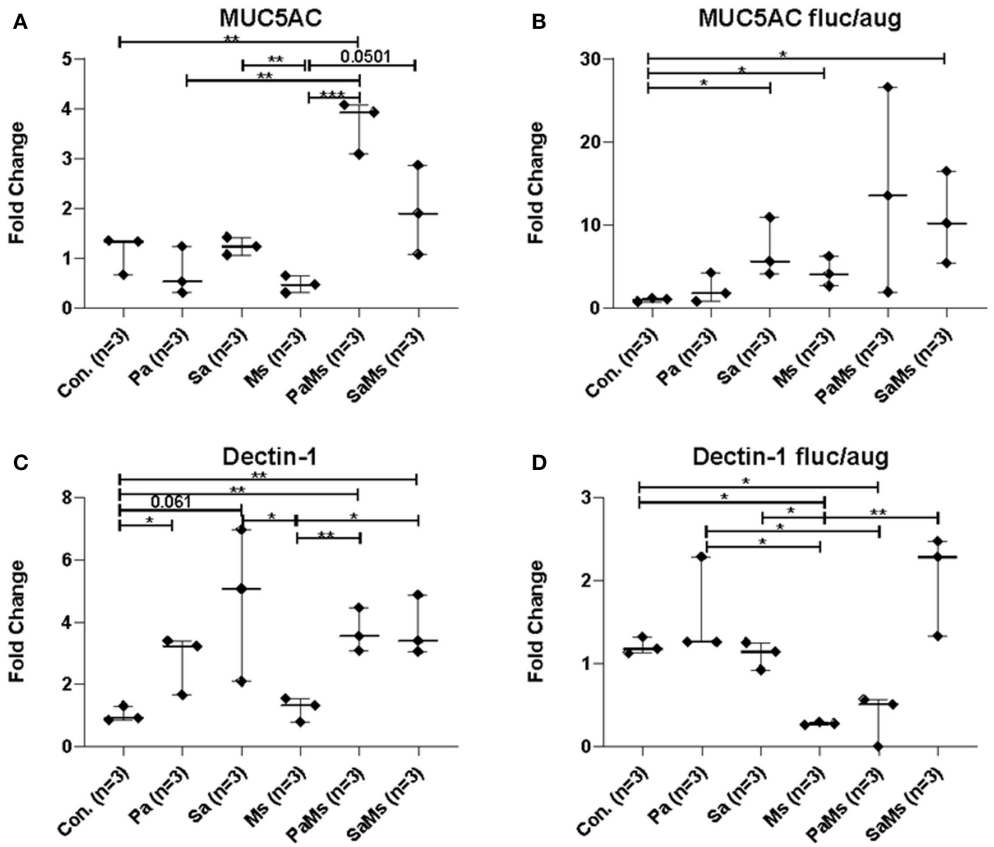

FIGURE 5 | Relative gene expression of MUC5AC and Dectin-1 in the murine sinonasal cavity. Relative gene expressions of MUC5AC **(A,B)** and Dectin-1 **(C,D)** in antibiotic-naïve **(A,C)** and antibiotic-treated **(B,D)** mice on different infection groups, saline treated group **(Con.)** *P. aeruginosa* infected group **(Pa)**, *S. aureus* infected group **(Sa)**, *M. sympodialis* infected group **(Ms)**, *P. aeruginosa* and *M. sympodialis* co-infected group **(PaMs)**, and *S. aureus* and *M. sympodialis* co-infected group **(SaMs)**, were measured by qRT-PCR. The gene expression was normalized with GAPDH, a housekeeping gene. Between group comparisons without *p*-value were not statistically significant. (* $P \leq 0.05$, ** $P \leq 0.005$, *** $P \leq 0.0005$).

antibiotic-naïve mice, we observed *Malassezia* colonization and *S. aureus* biofilms, supporting our microbiome results (**Figure 6A**), and demonstrating the presence of *Malassezia* in the sinonasal microbiota. As expected, we observed increased *Malassezia* staining in mice singly infected with *M. sympodialis*. Endogenous *S. aureus* biofilms were also present, but we didn't observe strong colocalization of these two taxa in mice singly infected with *M. sympodialis* (**Figure 6B**). Notably, in mice co-instilled with *M. sympodialis* and *S. aureus* we demonstrate strong co-colonization of both microorganisms (**Figure 6D**). We also demonstrate potential intramucosal colonization of *M. sympodialis* and *S. aureus*, which may contribute to the differential immune response we observed in these mice. Intramucosal colonies of bacteria, most often *Staphylococcus* spp., have been observed in CRS patients, but the implications are unclear (Wood et al., 2012; Kim et al., 2013). Mice co-infected with *M. sympodialis* and *P. aeruginosa* had notably increased *P. aeruginosa* and less endogenous *S. aureus* colonies. We did not observe strong colocalization of *P. aeruginosa* with *Malassezia*, nor did we show a decrease in *Malassezia* genus (**Figure 6C**). These results show, for the first time, the spatial organization of *Malassezia* with bacterial pathobionts both *in vitro* and *ex vivo*.

DISCUSSION

Physical and chemical interactions between fungi and bacteria play important roles in various ecosystems, such as in biofilm infections (Schlecht et al., 2015), in the oral cavity (Janus et al., 2016), in soil (Warmink and van Elsas, 2009), or in food products (Kastman et al., 2016). These cross-kingdom interactions result in changes to microbial fitness and virulence levels (Shirtliff et al., 2009; Schlecht et al., 2015). In this study, we investigated the interaction between predominant sinonasal bacterial pathogens, *P. aeruginosa* and *S. aureus*, and a dominant fungus present in the upper respiratory tract, *M. sympodialis* (Findley et al., 2013; Cope et al., 2017). Our goal was to assess the influence of microbial interactions in the upper airway on bacterial microbiome composition and immune response.

Here, we present two main conclusions. First, we show that there are species-specific interactions *in vitro* between a predominant member of sinonasal mycobiota, *Malassezia*, and

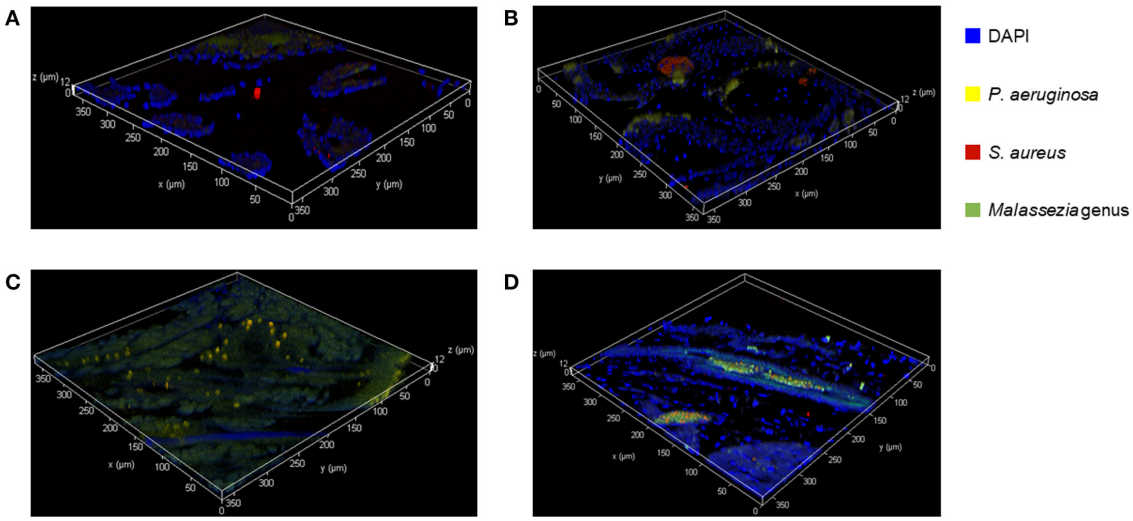

FIGURE 6 | Fluorescent *in-situ* Hybridization (FISH) of the mice sinonasal tissues. Murine sinonasal tissues are hybridized with DAPI (blue) for tissue cells, and with FISH probes for *P. aeruginosa* (Alexa 594, pseudo-colored in yellow), *S. aureus* (Alexa 660, pseudo-colored in red) or genus *Malassezia* (Alexa 488, pseudo-colored in green). Hybridized specimens were observed using a confocal laser scanning microscope (CLSM) for 3 dimensional analysis. **(A)** Control, **(B)** *M. sympodialis* infected mouse, **(C)**, *M. sympodialis* and *P. aeruginosa* infected mouse, and **(D)** *M. sympodialis* and *S. aureus* infected mouse.

major pathobionts associated with CRS (*P. aeruginosa* or *S. aureus*), and that co-infections with *M. sympodialis* and *P. aeruginosa* or *S. aureus* leads to distinct immune responses. This conclusion is supported by the *in vitro* studies and the increased immune response in co-infected mice. The second conclusion is that an intact sinonasal microbiota may be required for inducing distinct immune responses mediated by bacterial-fungal interactions. This is also inferred from the immune response analyses which shows that mice with depleted sinonasal microbiota by antimicrobial treatment had a suppressed immune response to intranasal pathobiont challenge. These pilot results are limited by a small sample size in mice and represent a single experiment. Taken together, these results seem to indicate that resident microbiota, and not just the single bacterial pathobionts, may be critical in inducing an immune response. Future studies using a larger sample size, longitudinal, and multiple-'omics analyses are necessary to identify the directionality and mechanism driving interactions.

In order to understand the interactions between *S. aureus, P. aeruginosa,* and *M. sympodialis*, we performed a modified Kirby-Bauer inhibition assay, a crystal violet biofilm quantification assay, and *in vitro* Fluorescent *in situ* Hybridization (FISH). The results from the Kirby-Bauer inhibition assay indicated that the late growth phase and biofilm-mode of *P. aeruginosa* inhibit *M. sympodialis* growth. The early growth phase and the cell-free supernatant of late growth phase *P. aeruginosa* did not inhibit *M. sympodialis* (data not shown), suggesting that inhibition of *M. sympodialis* by *P. aeruginosa* may require direct cell-cell contact and the inhibition mechanism may be dependent on the density of *P. aeruginosa*. In addition, quorum sensing (QS) molecules, which can trigger changes in biofilm physiology and gene expression and require high microbial density, may influence the observed negative interactions between *P. aeruginosa* and *M. sympodialis*. One possible inhibitory mechanism between *P. aeruginosa* and *M. sympodialis* is the type VI secretion system (T6SS). T6SS is a QS-regulated nanomachinery system in bacterial membranes that allow the bacteria to inject toxins into other cell membranes or cytoplasm (Gallique et al., 2017). *P. aeruginosa* possesses 3 genes for T6SS, H1-, H2-, and H3-T6SS, and H2- and H3-T6SS act not only against prokaryotes but also against eukaryotes (Hood et al., 2010; Trunk et al., 2018). A recently published study showed that programmed inhibitor cells can target bacterial species in a complex microbial community using T6SS (Ting et al., 2020), indicating a potential role for T6SS in altering microbiota composition.

We demonstrated a commensal or synergistic interaction between *S. aureus* and *M. sympodialis*. We observed a small positive effect on biofilm development when *S. aureus* was co-cultured with *M. sympodialis* in contrast to decreased biofilm growth when *P. aeruginosa* and *M. sympodialis* were cultured together. The *in vitro* FISH images also demonstrated colocalization of *M. sympodialis* and *S. aureus* in a biofilm but not with *P. aeruginosa*. This indicates that there may be a positive interaction between *M. sympodialis* and *S. aureus*. Other studies have shown positive interactions between the dimorphic yeast, *Candida albicans*, and *S. aureus* (Shirtliff et al., 2009; Schlecht et al., 2015). In these studies, co-existence of *S. aureus* and *C. albicans* induced fungal hyphae formation, and *S. aureus* formed biofilm specifically on fungal hyphae. As a result of this interaction, the hyphal form of *C. albicans* penetrated into the host tissue to obtain nutrients, and *S. aureus* secured a niche to invade host tissue, which increased the virulence of both microbes (Schlecht et al., 2015). There also are studies that reported a high incidence of co-existence of *S. aureus* and

Malassezia spp in dermatological diseases, such as seborrheic dermatitis, atopic dermatitis, and erythroceruminous otitis (Buda and Miedzobrodzki, 2016; Nuttall, 2016; Tamer et al., 2018). Thus, the interaction between *M. sympodialis* and *S. aureus* may also have an influence on the host immune response related to chronic rhinosinusitis and should be studied further. Furthermore, we performed FISH on sinonasal specimens in order to confirm how co-infection impacts the abundance and localization of *Malassezia* in mice. We demonstrated an increase in *Malassezia* genus abundance in sinonasal tissue of mice singly infected with *M. sympodialis*, but we did not observe colocalization of *Malassezia* with endogenous *Staphylococci*. Of interest, in mice co-infected with exogenous *Malassezia* and *S. aureus*, we observed colocalization of both taxa in the submucosa. Submucosal *S. aureus* has been observed in chronic rhinosinusitis, but the implications are unclear. In one study, epithelial invasion of *S. aureus* was associated with an elevated immune response (Sachse et al., 2010), and in other studies, submucosal *S. aureus* is associated with reduced eosinophilia (Wood et al., 2012). Overall, these pilot results support that the interactions we observed *in vitro* are maintained in an acute sinusitis model *in vivo*. Future studies will evaluate the spatial organization of the microbiota in murine sinus tissue using Combinatorial Labeling and Spectral (CLASI)-FISH in a larger sample size.

The sinonasal microbiome was altered by antibiotic use and infection. The bacterial composition of the antibiotic-naïve mice was driven by the infected bacterial species, though we did not observe the same effect in antibiotic-treated mice. For the microbiome analyses, we grouped sequences into Amplicon Sequence Variants (ASVs), or 100% OTUs using DADA2. This is a relatively new approach that allows higher resolution than clustering into 97% OTUs, as was the previous gold standard. This allows us to differentiate some native *Staphylococcus* taxa from those we instilled into the murine nasal cavity if they differ by a single nucleotide. However, There are still limitations to 16S rRNA amplicon sequencing, including an inability to distinguish between species (*Staphylococcus aureus* and *Staphylococcus epidermidis*), particularly using the V4 region of the 16S rRNA gene. We did not detect any endogenous *Pseudomonas* in any control sample, though other studies have detected *Pseudomonas* in the murine airways (Cope et al., 2016). This could be due to different strains and vivarium conditions across studies. Our microbiome results show that the sinonasal microbiota of mice infected with *P. aeruginosa* or *S. aureus* were dominated by the infected bacterial species regardless of the co-infection with *M. sympodialis*. Interestingly, *M. sympodialis* infection alone did not significantly alter the composition of the sinonasal bacterial communities. These results indicated that the murine sinonasal microbiota was altered by antibiotic treatments, and these changes impaired colonization by the newly infected bacteria. The pathobionts, *P. aeruginosa* and *S. aureus*, were introduced to the undisturbed sinonasal microbiota and successfully colonized, becoming the predominant bacterial genera present in the sinonasal microbiota. Future studies should include additional animals in replicate experiments to confirm these results.

Antibiotic treatment affected the sinonasal immune response after single- and co-infection. Augmentin and Fluconazole were used to examine the effect of single or co-infections without the bias of an intact sinonasal microbiota. In a prior study of acute sinusitis, Abreu et al. demonstrated that the depletion of native microbiota using Augmentin resulted in increased goblet cell hyperplasia after nasal instillation of the pathobiont *Corynebacterium tuberculostearicum* compared to antibiotic-naïve mice with an intact sinonasal microbiome (Abreu et al., 2012). For this reason, we decided to include an antibiotic-treated group and antibiotic-naïve group to compare immune responses when the sinonasal microbiota are intact or depleted. We observed no statistically significant changes between different infection groups in the antibiotic-treated mice with one exception of increased IL-5 gene expression in *P. aeruginosa*-infected mice. However, there were several statistically significant immune responses in the antibiotic-naïve mice, in which we also observed major changes to the sinonasal microbiome. The interaction between *S. aureus* and *M. sympodialis* may contribute to the induction of Th2 and Th17 immune responses. IL-5 and IL-13 were elevated in *S. aureus* and *M. sympodialis* co-infected mice. These cytokines are involved in Th2 immune response, leading to increased mucus production and allergic response (Pope et al., 2001). In CRS, IL-5 expression is a signature immune endotype, often associated with concurrent asthma or nasal polyps (Tomassen et al., 2016; Hoggard et al., 2018). MUC5AC expression was also elevated in co-infected mice, which is downstream of IL-13 gene expression. Interestingly, we observed the greatest increase in *M. sympodialis* and *P. aeruginosa*-infected mice in the presence of an intact sinonasal microbiome. IL-17 expression was elevated in *S. aureus* infected mice. Th17 is another signature of CRS inflammatory endotypes, and may contribute to polyp generation in human disease (Tomassen et al., 2016; Miljkovic et al., 2017). IL-17 is required for protection against *S. aureus* cutaneous infection, so the induction of IL-17 in the sinonasal cavity may be protective (Cho et al., 2010). Pulmonary infection with *S. aureus* also induces a prominent Th17 response in mice (Frank et al., 2012). Interestingly, IL-17 was repressed in antibiotic-treated mice, suggesting a role for the sinonasal microbiome in Th17 induction in the airways as has been demonstrated in the GI tract, dependent on colonization with Segmented Filamentous Bacteria (Ivanov et al., 2009). However, we did not observe a significant immune response in the antibiotic-naive mice singly infected with *M. sympodialis*, indicating that the endogenous *S. aureus* strain is either at a low abundance and thus insufficiently interacts with *M. sympodialis*, or that the endogenous *Staphylococci* have a different interaction with *Malassezia* compared to the pathobiont that we co-infected mice with. Importantly, we actually observed a suppressive effect when *M. sympodialis* was singly inoculated into the mice.

We were surprised that depletion of the sinonasal microbiota generally suppressed the immune response; this result was in contradiction to our hypothesis and to prior studies (Abreu et al., 2012; Cope et al., 2016). In the current study, we administered antibiotics intranasally, while prior studies have used oral antibiotics. Intranasal antibiotics may have had a

more robust effect on the sinonasal mucosal microbiome. In addition, we depleted both the bacterial and fungal microbiota using augmentin and fluconazole, while other studies have only used antibiotics targeting bacteria. It's possible that depleting the sinonasal fungal microbiota along with the bacterial microbiota, we have inhibited the potential for colonization, or that the remaining microbiota (e.g., *Lactobacilli*) are inhibitory toward exogenous *M. sympodialis*, *S. aureus*, or *P. aeruginosa*. We don't think that there are residual antibiotics after 24 h, prior studies have shown that when Augmentin and Fluconazole are cleared from the system ∼1 day after the oral or intravenous administration (Foulstone and Reading, 1982; Ripa et al., 1993). However, this is a possibility that we will address in future studies.

Malassezia has the ability to bind C-type lectin, a protein that recognizes fungal carbohydrates and can induce an immune response by binding to ligand (Graham and Brown, 2009). Studies of atopic eczema have shown that the cellular component of *Malassezia* affects the expression of a C-type lectin receptor gene, *dectin-1*, which results in aggravation of the disease, as measured by increased IL-6/IL-8 gene expression and β-hexosaminidase, histamine, and tryptase release (Ribbing et al., 2011). In both antibiotic-treated and antibiotic-naïve mice infected with *M. sympodialis* alone, we observed no increase in *dectin-1* gene expression. This was a surprising finding, but we also observed differential regulation of *dectin-1* in mice infected with *M. sympodialis* with bacterial co-colonizers. When mice were co-infected with *M. sympodialis* and *S. aureus, dectin-1* expression increased compared to *M. sympodialis* singly infected group, which may be due to increased *M. sympodialis* virulence mediated by the synergistic interaction with *S. aureus*. These results support our hypothesis that the interaction between *S. aureus* and *M. sympodialis* leads to a change in microbial community behavior, leading to increased fungal sensing. Future studies will seek to define the mechanisms underlying these findings. Dectin-1 activation can lead to increased Th2-type CD4+ T cell responses elicited by plasmacytoid dendritic cells, which could be one mechanism leading to elevated IL-5 and IL-13 gene expression in our study (Upchurch et al., 2016). Dectin-1 expression is also increased in CRS polyp tissue; future studies could evaluate whether this is correlated with co-colonization of *S. aureus* and *Malassezia* species (Gong et al., 2013). Interestingly, *dectin-1* expression also increased in antibiotic-naïve mice that were singly infected with bacteria (*S. aureus* or *P. aeruginosa*), but this was not observed in antibiotic-naïve mice singly infected with *M. sympodialis*. This could be due to bacterial interactions with endogenous *Malassezia* present in the murine sinonasal cavity or due to the sensing of bacterial ligands by Dectin-1, as has been demonstrated in the lungs with Dectin-1 sensing of non-typeable *Haemophilus influenzae* (Heyl et al., 2015).

This study has limitations. First, we are presenting findings based on a single pilot murine experiment of 3–5 animals per group. These numbers and replicates were based on published studies of acute sinusitis (Abreu et al., 2012; Cope et al., 2016) but we acknowledge that future studies should aim to replicate these findings in a larger sample size across different strains of mice. Thus, while exciting, these findings should be considered in the context of a small samples size in a single experiment. We plan to address these pitfalls in future studies that are based off these initial findings.

In conclusion, we demonstrate that interkingdom, species-specific interactions between a predominant member of sinonasal mycobiota, *Malassezia*, and major pathobionts associated with CRS (*P. aeruginosa* or *S. aureus*) leads to distinct immune responses at the sinonasal mucosa. *Malassezia* is an understudied fungal taxa with potential importance in a myriad of gut, skin, and respiratory disease (Hoggard et al., 2019; Limon et al., 2019; Ianiri et al., 2020). We also demonstrated that an endogenous sinonasal microbiota may be required for inducing distinct immune responses mediated by bacterial-fungal interactions. Further studies of the mechanisms contributing to these interactions, such as quorum sensing or dectin-1 mediated activation of CD4+ Th2 cells, is necessary for understanding the pathophysiology of CRS and developing microbiome-mediated therapeutics.

DATA AVAILABILITY STATEMENT

Sequence data for this study have been deposited in the NCBI. Short Read Archive (SRA) under BioProject ID PRJNA610287.

ETHICS STATEMENT

The animal study was reviewed and approved by Northern Arizona University Institutional Animal Care and Use Committee (IACUC).

AUTHOR CONTRIBUTIONS

KL was the main investigator of the project and wrote the most part of the manuscript. OK contributed in animal experiments, processing samples, and analyzing the bioinformatics data. IZ and SK contributed in *in-vitro* experiments, *in-vivo* experiments, and processing samples. EC was the corresponding author who contributed in designing the research project, funding, and writing the manuscript. All authors contributed to the article and approved the submitted version.

FUNDING

This work was partially supported by the Technology Research Initiative Fund (TRIF).

SUPPLEMENTARY MATERIAL

The Supplementary Material for this article can be found online at: https://www.frontiersin.org/articles/10.3389/fcimb.2020.00472/full#supplementary-material

Figure S1 | *In vivo* mouse co-infection experimental scheme. **(A)** acclimatized mice were intranasally infected with designated microbes for each group. Antibiotics were treated with Fluconazole (15 mg/kg) and Augmentin (100 mg/kg) for 5 days for the antibiotic-treated group. All mice were intranasally infected with designated microbes for each group. **(B)** The representation of infected microbes for each group.

Figure S2 | Fluorescent *in-situ* hybridization (FISH) observed using confocal laser scanning microscopy (CLSM) confirmed the inhibition of *P. aeruginosa* on *M. sympodialis* and shows the coexistence of *S. aureus* and *M. sympodialis*.

Figure S3 | Principal Coordinates Analysis of Unweighted UniFrac distances of the sinonasal microbiota. Two groups of mice, antibiotic-treated or -naive, were intranasally infected with either one species of bacteria, *P. aeruginosa* (light green), *S. aureus* (light red), or fungi, *M. sympodialis* (dark blue), or two species, *M. sympodialis* with *P. aeruginosa* (dark green) or *S. aureus* (dark red). **(A)** represents beta-diversity of antibiotic-treated (solid sphere) and antibiotic-naïve (diamond) mice groups. **(B)** represents beta-diversity of the infection groups in the antibiotic-treated mice, and **(C)** represents phylogenetically weighted beta-diversity of the infection groups in the antibiotic-naïve mice.

Figure S4 | Principal Coordinates Analysis of Weighted UniFrac distances of the sinonasal microbiota. Two groups of mice, antibiotic-treated or -naive, were intranasally infected with either one species of bacteria, *P. aeruginosa* (light green), *S. aureus* (light red), or fungi, *M. sympodialis* (dark blue), or two species, *M. sympodialis* with *P. aeruginosa* (dark green) or *S. aureus* (dark red). **(A)** represents beta-diversity of antibiotic-treated (solid sphere) and antibiotic-naïve (diamond) mice groups. **(B)** represents beta-diversity of the infection groups in the antibiotic-treated mice, and **(C)** represents beta-diversity of the infection groups in the antibiotic-naïve mice.

Figure S5 | Principal Coordinates Analysis of Jaccard distances of the sinonasal microbiota. Two groups of mice, antibiotic-treated or -naive, were intranasally infected with either one species of bacteria, *P. aeruginosa* (light green), *S. aureus* (light red), or fungi, *M. sympodialis* (dark blue), or two species, *M. sympodialis* with *P. aeruginosa* (dark green) or *S. aureus* (dark red). **(A)** represents beta-diversity of antibiotic-treated (solid sphere) and antibiotic-naïve (diamond) mice groups. **(B)** represents beta-diversity of the infection groups in the antibiotic-treated mice, and **(C)** represents beta-diversity of the infection groups in the antibiotic-naïve mice.

Supplemental Information | Relative bacterial abundances in sinonasal microbiota of intranasally infected mice with either bacteria or fungus or both. Available at this link (https://view.qiime2.org/visualization/?type=html&src=https%3A%2F%2Fdl.dropbox.com%2Fs%2F7r7k1c4ridwv8qv%2FDay1-sinus_taxa-barplot.qzv%3Fdl%3D1) or on github at https://github.com/e-cope/malassezia-ms. (Taxonomic level 7, Sort samples by Description and TreatmentGroup). The interactive QIIME 2 analysis file can be viewed at https://view.QIIME2.org/.

REFERENCES

Abreu, N. A., Nagalingam, N. A., Song, Y., Roediger, F. C., Pletcher, S. D., Goldberg, A. N., et al. (2012). Sinus microbiome diversity depletion and Corynebacterium tuberculostearicum enrichment mediates rhinosinusitis. *Sci. Transl. Med.* 4:151ra124. doi: 10.1126/scitranslmed.3003783

Atarashi, K., Nishimura, J., Shima, T., Umesaki, Y., Yamamoto, M., Onoue, M., et al. (2008). ATP drives lamina propria T(H)17 cell differentiation. *Nature* 455, 808–812. doi: 10.1038/nature07240

Baba, S., Kagoya, R., Kondo, K., Suzukawa, M., Ohta, K., and Yamasoba, T. (2015). T-cell phenotypes in chronic rhinosinusitis with nasal polyps in Japanese patients. *Allergy Asthma Clin. Immunol.* 11:33. doi: 10.1186/s13223-015-0100-2

Blanco, J. L., and Garcia, M. E. (2008). Immune response to fungal infections. *Vet. Immunol. Immunopathol.* 125, 47–70. doi: 10.1016/j.vetimm.2008.04.020

Boekhout, T., Guého-Kellermann, E., Mayser, P., and Velegraki, A. (2010). *Malassezia and the Skin: Science and Clinical Practice*. Berlin; Heidelberg: Springer Science & Business Media.

Bokulich, N. A., Kaehler, B. D., Rideout, J. R., Dillon, M., Bolyen, E., Knight, R., et al. (2018). Optimizing taxonomic classification of marker-gene amplicon sequences with QIIME 2's q2-feature-classifier plugin. *Microbiome* 6:90. doi: 10.1186/s40168-018-0470-z

Bolyen, E., Rideout, J. R., Dillon, M. R., Bokulich, N. A., Abnet, C. C., Al-Ghalith, G. A., et al. (2019). Reproducible, interactive, scalable and extensible microbiome data science using QIIME 2. *Nat. Biotechnol.* 37, 852–857. doi: 10.1038/s41587-019-0209-9

Brill, S., James, P., Cuthbertson, L., Cox, M., Cookson, W., Wedzicha, J., et al. (2016). Profiling the COPD airway microbiome using quantitative culture and 16S rRNA gene sequencing. *Eur. Respir. J.* 48(Suppl. 60):OA1787. doi: 10.1183/13993003.congress-2016.OA1787

Buda, A., and Miedzobrodzki, J. (2016). The role of *Staphylococcus aureus* in secondary infections in patients with atopic dermatitis (AD). *Pol. J. Microbiol.* 65, 253–259. doi: 10.5604/17331331.1215600

Cafarchia, C., Figueredo, L. A., Favuzzi, V., Surico, M. R., Colao, V., Iatta, R., et al. (2012). Assessment of the antifungal susceptibility of *Malassezia pachydermatis* in various media using a CLSI protocol. *Vet. Microbiol.* 159, 536–540. doi: 10.1016/j.vetmic.2012.04.034

Callahan, B. J., McMurdie, P. J., Rosen, M. J., Han, A. W., Johnson, A. J. A., and Holmes, S. P. (2016). DADA2: High-resolution sample inference from Illumina amplicon data. *Nat. Methods* 13, 581–583. doi: 10.1038/nmeth.3869

Calus, L., Van Bruaene, N., Bosteels, C., Dejonckheere, S., Van Zele, T., Holtappels, G., et al. (2019). Twelve-year follow-up study after endoscopic sinus surgery in patients with chronic rhinosinusitis with nasal polyposis. *Clin. Transl. Allergy* 9:30. doi: 10.1186/s13601-019-0269-4

Carter, J. M., and Amedee, R. G. (2014). Contrasting the microbiomes from healthy volunteers and patients with chronic rhinosinusitis. *Am. J. Rhinol. Allergy* 28:182. doi: 10.2500/194589214810960481

Caulley, L., Thavorn, K., Rudmik, L., Cameron, C., and Kilty, S. J. (2015). Direct costs of adult chronic rhinosinusitis by using 4 methods of estimation: results of the US medical expenditure panel survey. *J. Allergy Clin. Immunol.* 136, 1517–1522. doi: 10.1016/j.jaci.2015.08.037

Cho, J. S., Pietras, E. M., Garcia, N. C., Ramos, R. I., Farzam, D. M., Monroe, H. R., et al. (2010). IL-17 is essential for host defense against cutaneous *Staphylococcus aureus* infection in mice. *J. Clin. Investig.* 120, 1762–1773. doi: 10.1172/jci40891

Cleland, E. J., Bassiouni, A., Boase, S., Dowd, S., Vreugde, S., and Wormald, P.-J. (2014). The fungal microbiome in chronic rhinosinusitis: richness, diversity, postoperative changes and patient outcomes. *Int. Forum Allergy Rhinol.* 4, 259–265. doi: 10.1002/alr.21297

Cope, E. K., Goldberg, A. N., Pletcher, S. D., and Lynch, S. V. (2016). A chronic rhinosinusitis-derived isolate of *Pseudomonas aeruginosa* induces acute and pervasive effects on the murine upper airway microbiome and host immune response. *Int. Forum Allergy Rhinol.* 6, 1229–1237. doi: 10.1002/alr.21819

Cope, E. K., Goldberg, A. N., Pletcher, S. D., and Lynch, S. V. (2017). Compositionally and functionally distinct sinus microbiota in chronic rhinosinusitis patients have immunological and clinically divergent consequences. *Microbiome* 5:53. doi: 10.1186/s40168-017-0266-6

DeSantis, T. Z., Hugenholtz, P., Larsen, N., Rojas, M., Brodie, E. L., Keller, K., et al. (2006). Greengenes, a chimera-checked 16S rRNA gene database and workbench compatible with ARB. *Appl. Environ. Microbiol.* 72, 5069–5072. doi: 10.1128/AEM.03006-05

Elizabeth, M., and Zabielski, R. (2013). "Gut microbiome and brain-gut axis in autism — aberrant development of gut-brain communication and reward circuitry," in *Recent Advances in Autism Spectrum Disorders - Volume I*, ed M. Fitzgerald (InTech).

Epperson, M. V., Phillips, K. M., Caradonna, D. S., Gray, S. T., and Sedaghat, A. R. (2019). Predictors of efficacy for combination oral and topical corticosteroids to treat patients with chronic rhinosinusitis with nasal polyps. *Int. Forum Allergy Rhinol.* 9, 1436–1442. doi: 10.1002/alr.22431

Findley, K., Oh, J., Yang, J., Conlan, S., Deming, C., Meyer, J. A., et al. (2013). Topographic diversity of fungal and bacterial communities in human skin. *Nature* 498, 367–370. doi: 10.1038/nature12171

Foulstone, M., and Reading, C. (1982). Assay of amoxicillin and clavulanic acid, the components of Augmentin, in biological fluids with high-performance liquid chromatography. *Antimicrob. Agents Chemother.* 22, 753–762. doi: 10.1128/aac.22.5.753

Frank, K. M., Zhou, T., Moreno-Vinasco, L., Hollett, B., Garcia, J. G. N., and Bubeck Wardenburg, J. (2012). Host response signature to *Staphylococcus aureus* alpha-hemolysin implicates pulmonary Th17 response. *Infect. Immun.* 80, 3161–3169. doi: 10.1128/IAI.00191-12

Fröhlich, E., Mercuri, A., Wu, S., and Salar-Behzadi, S. (2016). Measurements of deposition, lung surface area and lung fluid for simulation of inhaled compounds. *Front. Pharmacol.* 7:181. doi: 10.3389/fphar.2016.00181

Fujimura, K. E., Sitarik, A. R., Havstad, S., Lin, D. L., Levan, S., Fadrosh, D., et al. (2016). Neonatal gut microbiota associates with childhood multisensitized atopy and T cell differentiation. *Nat. Med.* 22, 1187–1191. doi: 10.1038/nm.4176

Gallique, M., Bouteiller, M., and Merieau, A. (2017). The type VI secretion system: a dynamic system for bacterial communication? *Front. Microbiol.* 8:1454. doi: 10.3389/fmicb.2017.01454

Gelber, J. T., Cope, E. K., Goldberg, A. N., and Pletcher, S. D. (2016). Evaluation of malassezia and common fungal pathogens in subtypes of chronic rhinosinusitis. *Int. Forum Allergy Rhinol.* 6, 950–955. doi: 10.1002/alr.21777

Gong, J., Wang, P., Qiu, Z.-H., and Chen, Q.-J. (2013). Increased expression of dectin-1 in nasal polyps. *Am. J. Otolaryngol.* 34, 183–187. doi: 10.1016/j.amjoto.2012.10.003

Goodrich, J. K., Di Rienzi, S. C., Poole, A. C., Koren, O., Walters, W. A., Caporaso, J. G., et al. (2014). Conducting a microbiome study. *Cell* 158, 250–262. doi: 10.1016/j.cell.2014.06.037

Gopalakrishnan, V., Helmink, B. A., Spencer, C. N., Reuben, A., and Wargo, J. A. (2018). The influence of the gut microbiome on cancer, immunity, and cancer immunotherapy. *Cancer Cell* 33, 570–580. doi: 10.1016/j.ccell.2018.03.015

Graham, L. M., and Brown, G. D. (2009). The Dectin-2 family of C-type lectins in immunity and homeostasis. *Cytokine* 48, 148–155. doi: 10.1016/j.cyto.2009.07.010

Guillot, J., Breugnot, C., de Barros, M., and Chermette, R. (1998). Usefulness of modified Dixon's medium for quantitative culture of Malassezia species from canine skin. *J. Vet. Diagn. Invest.* 10, 384–386. doi: 10.1177/104063879801000418

Gupta, V., and Singh, S. (2010). Nasal saline irrigation for chronic rhinosinusitis. *Int. J. Clin. Rhinol.* 3, 145–147. doi: 10.5005/jp-journals-10013-1050

Hamilos, D. L. (2015). Drivers of chronic rhinosinusitis: Inflammation versus infection. *J. Allergy Clin. Immunol.* 136, 1454–1459. doi: 10.1016/j.jaci.2015.10.011

Heyl, K. A., Klassert, T. E., Heinrich, A., Müller, M. M., Klaile, E., Dienemann, H., et al. (2015). Dectin-1 is expressed in human lung and mediates the proinflammatory immune response to nontypeable haemophilus influenzae. *Pneumologie* 69:e01492–14. doi: 10.1055/s-0035-1544861

Hogardt, M., Trebesius, K., Geiger, A. M., Hornef, M., Rosenecker, J., and Heesemann, J. (2000). Specific and rapid detection by fluorescent *in situ* hybridization of bacteria in clinical samples obtained from cystic fibrosis patients. *J. Clin. Microbiol.* 38, 818–825. doi: 10.1128/JCM.38.2.818-825.2000

Hoggard, M., Waldvogel-Thurlow, S., Zoing, M., Chang, K., Radcliff, F. J., Mackenzie, B. W., et al. (2018). Inflammatory endotypes and microbial associations in chronic rhinosinusitis. *Front. Immunol.* 9:2065. doi: 10.3389/fimmu.2018.02065

Hoggard, M., Zoing, M., Biswas, K., Taylor, M. W., and Douglas, R. G. (2019). The sinonasal mycobiota in chronic rhinosinusitis and control patients. *Rhinology* 57, 190–199. doi: 10.4193/Rhin18.256

Hood, R. D., Singh, P., Hsu, F., Güvener, T., Carl, M. A., Trinidad, R. R. S., et al. (2010). A type VI secretion system of *Pseudomonas aeruginosa* targets a toxin to bacteria. *Cell Host Microbe* 7, 25–37. doi: 10.1016/j.chom.2009.12.007

Hulse, K. E. (2016). Immune mechanisms of chronic rhinosinusitis. *Curr. Allergy Asthma Rep.* 16:1. doi: 10.1007/s11882-015-0579-0

Ianiri, G., Coelho, M. A., Ruchti, F., Sparber, F., McMahon, T. J., Fu, C., et al. (2020). HGT in the human and skin commensal Malassezia: A bacterially derived flavohemoglobin is required for NO resistance and host interaction. *Proc. Natl. Acad. Sci. U.S.A.* 117:202003473. doi: 10.1073/pnas.2003473117

Ivanov, I. I., Atarashi, K., Manel, N., Brodie, E. L., Shima, T., Karaoz, U., et al. (2009). Induction of intestinal Th17 cells by segmented filamentous bacteria. *Cell* 139, 485–498. doi: 10.1016/j.cell.2009.09.033

Janus, M. M., Willems, H. M. E., and Krom, B. P. (2016). Candida albicans in multispecies oral communities; a keystone commensal? *Adv. Exp. Med. Biol.* 931, 13–20. doi: 10.1007/5584_2016_5

Kastman, E. K., Kamelamela, N., Norville, J. W., Cosetta, C. M., Dutton, R. J., and Wolfe, B. E. (2016). Biotic interactions shape the ecological distributions of *Staphylococcus species*. *MBio* 7:e01157-16. doi: 10.1128/mBio.01157-16

Katoh, K., and Standley, D. M. (2013). MAFFT multiple sequence alignment software version 7: improvements in performance and usability. *Mol. Biol. Evol.* 30, 772–780. doi: 10.1093/molbev/mst010

Kau, A. L., Ahern, P. P., Griffin, N. W., Goodman, A. L., and Gordon, J. I. (2011). Human nutrition, the gut microbiome and the immune system. *Nature* 474, 327–336. doi: 10.1038/nature10213

Kim, D. Y., Park, B. S., Hong, G. U., Lee, B. J., Park, J. W., Kim, S. Y., et al. (2011). Anti-inflammatory effects of the R2 peptide, an inhibitor of transglutaminase 2, in a mouse model of allergic asthma, induced by ovalbumin. *Br. J. Pharmacol.* 162, 210–225. doi: 10.1111/j.1476-5381.2010.01033.x

Kim, R., Freeman, J., Waldvogel-Thurlow, S., Roberts, S., and Douglas, R. (2013). The characteristics of intramucosal bacteria in chronic rhinosinusitis: a prospective cross-sectional analysis. *Int. Forum Allergy Rhinol.* 3, 349–354. doi: 10.1002/alr.21117

Kimura, Y., Chihara, K., Honjoh, C., Takeuchi, K., Yamauchi, S., Yoshiki, H., et al. (2014). Dectin-1-mediated signaling leads to characteristic gene expressions and cytokine secretion via spleen tyrosine kinase (Syk) in rat mast cells. *J. Biol. Chem.* 289, 31565–31575. doi: 10.1074/jbc.M114.581322

Kistowska, M., Fenini, G., Jankovic, D., Feldmeyer, L., Kerl, K., Bosshard, P., et al. (2014). Malassezia yeasts activate the NLRP 3 inflammasome in antigen-presenting cells via S yk-kinase signalling. *Exp. Dermatol.* 23, 884–889. doi: 10.1111/exd.12552

Krzywinski, M., and Altman, N. (2014). Comparing samples—part II. *Nat. Methods* 11, 355–356. doi: 10.1038/nmeth.2900

Limon, J. J., Tang, J., Li, D., Wolf, A. J., Michelsen, K. S., Funari, V., et al. (2019). Malassezia Is associated with crohn's disease and exacerbates colitis in mouse models. *Cell Host Microbe* 25, 377–388.e6. doi: 10.1016/j.chom.2019.01.007

Lin, C.-H., Shen, M.-L., Zhou, N., Lee, C.-C., Kao, S.-T., and Wu, D. C. (2014). Protective effects of the polyphenol sesamin on allergen-induced T(H)2 responses and airway inflammation in mice. *PLoS One* 9:e96091. doi: 10.1371/journal.pone.0096091

Lozupone, C., and Knight, R. (2005). UniFrac: a new phylogenetic method for comparing microbial communities. *Appl. Environ. Microbiol.* 71, 8228–8235. doi: 10.1128/AEM.71.12.8228-8235.2005

Mattila, P. S. (2012). Treatment of chronic rhinosinusitis with antibiotics. *Clin. Infect. Dis.* 54, 69–70. doi: 10.1093/cid/cir757

Miljkovic, D., Psaltis, A. J., Wormald, P. J., and Vreugde, S. (2017). Chronic rhinosinusitis with polyps is characterized by increased mucosal and blood Th17 effector cytokine producing cells. *Front. Physiol.* 8:898. doi: 10.3389/fphys.2017.00898

Moise, A. M. R. (2017). *The Gut Microbiome: Exploring the Connection between Microbes, Diet, and Health*. ABC-CLIO Available online at: https://market.android.com/details?id=book-0oE5DwAAQBAJ

Nuttall, T. (2016). Successful management of otitis externa. *In Pract.* 38, 17–21. doi: 10.1136/inp.i1951

Oestreich, K. J., Mohn, S. E., and Weinmann, A. S. (2012). Molecular mechanisms that control the expression and activity of Bcl-6 in TH1 cells to regulate flexibility with a TFH-like gene profile. *Nat. Immunol.* 13, 405–411. doi: 10.1038/ni.2242

O'Toole, G. A. (2011). Microtiter dish biofilm formation assay. *J. Vis. Exp.* 47:2437. doi: 10.3791/2437

Pletcher, S. D., Goldberg, A. N., and Cope, E. K. (2018). Loss of microbial niche specificity between the upper and lower airways in patients with cystic fibrosis. *Laryngoscope* 129, 544–550. doi: 10.1002/lary.27454

Pope, S. M., Brandt, E. B., Mishra, A., Hogan, S. P., Zimmermann, N., Matthaei, K. I., et al. (2001). IL-13 induces eosinophil recruitment into the lung by an IL-5- and eotaxin-dependent mechanism. *J. Allergy Clin. Immunol.* 108, 594–601. doi: 10.1067/mai.2001.118600

Price, M. N., Dehal, P. S., and Arkin, A. P. (2010). FastTree 2–approximately maximum-likelihood trees for large alignments. *PLoS ONE* 5:e9490. doi: 10.1371/journal.pone.0009490

Ribbing, C., Engblom, C., Lappalainen, J., Lindstedt, K., Kovanen, P. T., Karlsson, M. A., et al. (2011). Mast cells generated from patients with atopic eczema have enhanced levels of granule mediators and an impaired Dectin-1 expression. *Allergy* 66, 110–119. doi: 10.1111/j.1398-9995.2010.02437.x

Ripa, S., Ferrante, L., and Prenna, M. (1993). Pharmacokinetics of fluconazole in normal volunteers. *Chemotherapy* 39, 6–12. doi: 10.1159/000238967

Sachse, F., Becker, K., Von Eiff, C., Metze, D., and Rudack, C. (2010). *Staphylococcus aureus* invades the epithelium in nasal polyposis and

induces IL-6 in nasal epithelial cells *in vitro*. *Allergy* 65, 1430–1437. doi: 10.1111/j.1398-9995.2010.02381.x

Schlecht, L. M., Peters, B. M., Krom, B. P., Freiberg, J. A., Hänsch, G. M., Filler, S. G., et al. (2015). Systemic *Staphylococcus aureus* infection mediated by *Candida albicans* hyphal invasion of mucosal tissue. *Microbiology* 161, 168–181. doi: 10.1099/mic.0.083485-0

Sedaghat, A. R. (2017). Chronic rhinosinusitis. *Am. Fam. Phys.* 96, 500–506.

Shirtliff, M. E., Peters, B. M., and Jabra-Rizk, M. A. (2009). Cross-kingdom interactions: *Candida albicans* and bacteria. *FEMS Microbiol. Lett.* 299, 1–8. doi: 10.1111/j.1574-6968.2009.01668.x

Tamer, F., Yuksel, M. E., Sarifakioglu, E., and Karabag, Y. (2018). *Staphylococcus aureus* is the most common bacterial agent of the skin flora of patients with seborrheic dermatitis. *Dermatol Pract Concept* 8, 80–84. doi: 10.5826/dpc.0802a04

Telander, D. G., Malvey, E. N., and Mueller, D. L. (1999). Evidence for repression of IL-2 gene activation in anergic T cells. *J. Immunol.* 162, 1460–1465.

Thaiss, C. A., Zmora, N., Levy, M., and Elinav, E. (2016). The microbiome and innate immunity. *Nature* 535, 65–74. doi: 10.1038/nature18847

Ting, S.-Y., Martínez-García, E., Huang, S., Bertolli, S. K., Kelly, K. A., Cutler, K. J., et al. (2020). Targeted depletion of bacteria from mixed populations by programmable adhesion with antagonistic competitor cells. *Cell Host Microbe*. 28:313–321.e6. doi: 10.1016/j.chom.2020.05.006

Tomassen, P., Vandeplas, G., Van Zele, T., Cardell, L.-O., Arebro, J., Olze, H., et al. (2016). Inflammatory endotypes of chronic rhinosinusitis based on cluster analysis of biomarkers. *J. Allergy Clin. Immunol.* 137, 1449–1456.e4. doi: 10.1016/j.jaci.2015.12.1324

Trandem, K., Jin, Q., Weiss, K. A., James, B. R., Zhao, J., and Perlman, S. (2011). Virally expressed interleukin-10 ameliorates acute encephalomyelitis and chronic demyelination in coronavirus-infected mice. *J. Virol.* 85, 6822–6831. doi: 10.1128/JVI.00510-11

Trebesius, K., Leitritz, L., Adler, K., Schubert, S., Autenrieth, I. B., and Heesemann, J. (2000). Culture independent and rapid identification of bacterial pathogens in necrotising fasciitis and streptococcal toxic shock syndrome by fluorescence *in situ* hybridisation. *Med. Microbiol. Immunol.* 188, 169–175. doi: 10.1007/s004300000035

Trunk, K., Peltier, J., Liu, Y.-C., Dill, B. D., Walker, L., Gow, N. A. R., et al. (2018). The type VI secretion system deploys antifungal effectors against microbial competitors. *Nat Microbiol* 3, 920–931. doi: 10.1038/s41564-018-0191-x

Ueda, Y., Kayama, H., Jeon, S. G., Kusu, T., Isaka, Y., Rakugi, H., et al. (2010). Commensal microbiota induce LPS hyporesponsiveness in colonic macrophages via the production of IL-10. *Int. Immunol.* 22, 953–962. doi: 10.1093/intimm/dxq449

Upchurch, K., Oh, S., and Joo, H. (2016). Dectin-1 in the control of Th2-type T cell responses. *Recep. Clin. Investig.* 3:e1094. doi: 10.14800/rci.1094

Wagner Mackenzie, B., Chang, K., Zoing, M., Jain, R., Hoggard, M., Biswas, K., et al. (2019). Longitudinal study of the bacterial and fungal microbiota in the human sinuses reveals seasonal and annual changes in diversity. *Sci. Rep.* 9:17416. doi: 10.1038/s41598-019-53975-9

Warmink, J. A., and van Elsas, J. D. (2009). Migratory response of soil bacteria to *Lyophyllum* sp. strain karsten in soil microcosms. *Appl. Environ. Microbiol.* 75, 2820–2830. doi: 10.1128/aem.02110-08

Wood, A. J., Fraser, J. D., Swift, S., Patterson-Emanuelson, E. A. C., Amirapu, S., and Douglas, R. G. (2012). Intramucosal bacterial microcolonies exist in chronic rhinosinusitis without inducing a local immune response. *Am. J. Rhinol. Allergy* 26, 265–270. doi: 10.2500/ajra.2012.26.3779

Zhang, Z., Adappa, N. D., Doghramji, L. J., Chiu, A. G., Cohen, N. A., and Palmer, J. N. (2015). Different clinical factors associated with *Staphylococcus aureus* and *Pseudomonas aeruginosa* in chronic rhinosinusitis. *Int. Forum Allergy Rhinol.* 5, 724–733. doi: 10.1002/alr.21532

Conflict of Interest: The authors declare that the research was conducted in the absence of any commercial or financial relationships that could be construed as a potential conflict of interest.

frontiers in Cellular and Infection Microbiology

ORIGINAL RESEARCH
published: 12 October 2020
doi: 10.3389/fcimb.2020.00440

Intranasal Application of *Lactococcus lactis W136* Is Safe in Chronic Rhinosinusitis Patients With Previous Sinus Surgery

*Leandra Mfuna Endam[1], Saud Alromaih[2], Emmanuel Gonzalez[3], Joaquin Madrenas[4], Benoit Cousineau[3], Axel E. Renteria[1,5] and Martin Desrosiers[1,5,6]**

[1] Centre de Recherche du Centre Hospitalier de l'Université de Montréal (CRCHUM), Montreal, QC, Canada, [2] Faculty of Medicine, King Saud University, Riyadh, Saudi Arabia, [3] Department of Microbiology and Immunology, Microbiome and Disease Tolerance Centre (MDTC), McGill University, Montreal, QC, Canada, [4] The Lundquist Institute for Biomedical Innovation at Harbor-UCLA Medical Center, Torrance, CA, United States, [5] Division of Otolaryngology-Head and Neck Surgery, Centre Hospitalier de l'Université de Montréal (CHUM), Montreal, QC, Canada, [6] Los Angeles Biomedical Research Institute at Harbor-UCLA Medical Center, Torrance, CA, United States

OPEN ACCESS

Edited by:
Emily K. Cope,
Northern Arizona University,
United States

Reviewed by:
Sarah Vreugde,
University of Adelaide, Australia
Rayees Sheikh,
University of Illinois at Chicago,
United States

***Correspondence:**
Martin Desrosiers
desrosiers_martin@hotmail.com

Specialty section:
This article was submitted to Microbiome in Health and Disease, a section of the journal Frontiers in Cellular and Infection Microbiology

Received: 05 February 2020
Accepted: 16 July 2020
Published: 12 October 2020

Citation:
Endam LM, Alromaih S, Gonzalez E, Madrenas J, Cousineau B, Renteria AE and Desrosiers M (2020) Intranasal Application of Lactococcus lactis W136 Is Safe in Chronic Rhinosinusitis Patients With Previous Sinus Surgery. Front. Cell. Infect. Microbiol. 10:440. doi: 10.3389/fcimb.2020.00440

Objective: Modulation of the dysbiotic gut microbiome with "healthy" bacteria via a stool transplant or supplementation is increasingly practiced, however this approach has not been explored in the nasal passages. We wished to verify whether *Lactococcus lactis W136* (*L. lactis W136)* bacteria could be safely applied via irrigation to the nasal and sinus passages in individuals with chronic rhinosinusitis (CRS) with previous undergone endoscopic sinus surgery, and whether this was accompanied by bacterial community flora modification.

Study Design: Prospective open-label pilot trial of safety and feasibility.

Setting: Academic tertiary hospital center.

Subjects and Methods: Twenty-four patients with CRS refractory to previous medical and surgical therapy received a 14-day course of BID sinus irrigations containing 1.2×10^9 CFU live *L. lactis W136*. Patients were monitored for safety using questionnaire, sinus endoscopy, otoscopy, UPSIT-40 smell testing, and endoscopically-obtained conventional sinus culture and a swab for 16S microbiome profiling.

Results: All 24 patients receiving at least one treatment successfully completed treatment. *L. lactis W136* probiotic treatment was safe, with no major adverse events or new infections. Treatment was associated with improvement in sinus symptoms, QOL, and mucosal scores, which remained improved during the subsequent 14-day observation period. Microbiome changes associated with treatment were limited to an increase of the pathobiont *Dolosigranulum pigrum*, a bacteria identified as potentially beneficial in the upper airways. Subgroup analysis suggested differences in microbiomes and responses for CRSsNP and CRSwNP phenotypes, but these did not attain significance.

Conclusion: Intranasal irrigation of live *L. lactis W136* bacteria to patients with refractory chronic rhinosinusitis was safe, and was associated with effects on symptoms, mucosal aspect and microbiome composition. Intranasal bacteria may thus find a role as a treatment strategy for CRS.

Clinical Trials Registration: www.ClinicalTrials.gov. identifier: NCT04048174.

Keywords: chronic rhinosinusitis (CRS), probiotics, *Lactococcus lactis W136*, sinus irrigation, CRS treatment, sinus microbiome, refractory CRS

INTRODUCTION

Chronic rhinosinusitis (CRS) is considered a complex disease, where multiple factors, including inflammatory cell infiltrate, microbiome dysbiosis, and dysfunction of the sinus epithelium interact to initiate and maintain the clinical phenotypes of chronic rhinosinusitis with nasal polyposis (CRSwNP) and chronic rhinosinusitis without nasal polyps (CRSsNP) (Meltzer et al., 2004; Van Zele et al., 2006; Nader et al., 2010; Stephenson et al., 2010). Current treatment options center on the combinations of topical and oral corticosteroids and surgery (Desrosiers et al., 2011). However, even following surgery, endoscopic signs of recurrence are seen in over 50% of the patients by 4 months after surgery, and even post-operative therapy with topical corticosteroid drops or sprays does not prevent the recurrence of disease (Meltzer et al., 2004; Stjarne et al., 2009). These patients, with CRS refractory to medical and surgical therapy, undergo considerable suffering and discomfort and represent a considerable burden to the health care system. Novel alternate therapies are thus urgently required.

The microbiome dysbiosis present in CRS may represent a novel treatment opportunity via microbiome supplementation (Wagner Mackenzie et al., 2017; Chalermwatanachai et al., 2018). Microbiome-based therapies are increasingly common in the digestive tract. Stool "transplants," where healthy flora from normal donors are introduced into diseased colon, has been shown to control colonic inflammation of various etiologies (Snelling, 2005; Wolvers et al., 2010; Aroniadis and Brandt, 2013). Supplementation with orally administered probiotics for restoring gastrointestinal microbiome has shown varying results in the literature going from little improvement (Kristensen et al., 2016) to being beneficial (Oelschlaeger, 2010; Ferrario et al., 2014; Bjerg et al., 2015; Brahe et al., 2015).

In the sinuses, the microbiome is believed to play a beneficial role in health maintenance. Conventional culture techniques have shown healthy sinuses after ESS to be associated with *S. epidermidis* (Al-Shemari et al., 2007), a Gram-positive coccus. The mechanisms by which *S. epidermidis* promote health in the nose and sinuses remain incompletely described but can be extrapolated from other models. In mice, intranasally administered *S. epidermidis* interfered with *S. aureus* colonization via direct interference or modification of the ecological niche (Abreu et al., 2012; Cleland et al., 2014). Other mechanisms besides direct bacterial interference are believed to be responsible for the beneficial effects seen. In atopic dermatitis (AD), a disorder with pathophysiologic and microbiome features similar to CRS, immunomodulatory effects of the bacteria on epithelium of dendritic cells may also be playing important roles. In AD, *S. epidermidis* is required to dampen inflammation following injury, via interaction of lipoteichoic acid (LTA; a TLR2 ligand present in the capsule of *S. epidermidis*) with innate immune receptors (Lai et al., 2009).

However, the therapeutic potential *S. epidermidis* was tempered by safety concerns regarding the risks of disease production when applied directly to the delicate nasal and sinus passages. Despite its strong potential as a therapeutic commensal, *S. epidermidis* can represent a formidable pathogen in certain settings, notably the neonatal intensive care unit and infection of intrvascular foreign bodies (Moles et al., 2020) This was thus of particular concern in CRS patients, where anatomical barriers to the sinuses have been removed at surgery, and motivated us to search for a suitable candidate which might retain some of the desirable properties of *S. epidermidis*, but with lesser safety concerns.

We thus needed to identify a potentially suitable non-pathogenic Gram-positive coccus for intranasal application. *L. lactis* appears to be a reasonable candidate. It has an excellent safety profile in animal experiments and human use, and shares with *S. epidermidis* the following characteristics believed to be beneficial. A Gram-positive cocci, it possesses a surface capsule rich in LTA motifs, and is free of pathogenic genes. Its safety profile is incontrovertible. *L. lactis has* been used in the food industry for over 100 years (Song et al., 2017), conferring it "Generally Recognized as Safe (GRAS)" status in the US, EU, and Canada (Doty et al., 1984; Schwartz et al., 2016) for oral administration. *In vitro* studies have supported the safety and immunomodulatory capacities of *L. lactis* for intranasal use (Schwartz et al., 2016). Primary epithelial cell cultures raised from sinus mucosa showed no evidence of toxicity when exposed to a supernatant of this strain, while peripheral blood monocyte preparations (PBMC) showed IL-10 induction without evidence of toxicity or excessive Th1-type inflammation (Schwartz et al., 2016). Intranasal

Abbreviations: Eos, eosinophils; CFU, colony-forming units; CI, confidence interval; CRS, chronic rhinosinusitis; CRSsNP, chronic rhinosinusitis without nasal polyps; CRSwNP, chronic rhinosinusitis with nasal polyps; ESS, endoscopic sinus surgery; ET, Eustachian tube; IgE, immunoglobulin E; *L. lactis W136, Lactococcus lactis W136;* MCID, minimal clinically important difference; POSE, peri-operative sinus endoscopy; QOL, quality of life; *S aureus, Staphylococcus aureus;* SNSS, sino-nasal symptom score; SNOT-22, Sino-nasal Outcome Test 22 items; UPSIT-40, University of Pennsylvania Smell Identification Test 40-items; WBC, white blood cells.

administration in mice was also reported to be well-tolerated (Oelschlaeger, 2010).

We wished to verify if topical administration of *L. lactis W136* to the nasal and sinus cavities would be safe for patients with chronic rhinosinusitis refractory to medical and surgical treatment. To this end, we performed an unblinded prospective trial to assess the effects of intranasal administration of *L. lactis* in patients with chronic rhinosinusitis.

METHODS

Patient Selection

We included patients presenting persistent signs and symptoms of CRSsNP or CRSwNP despite previous technically adequate surgery and continued use of maximal medical therapy, including high-volume budesonide irrigations post-operatively ("refractory" CRS). Excluded were patients <18 years, cystic fibrosis, with technical reasons for ESS failure, active sinus infection with purulence, pain, and/or hyperthermia, or with immune suppression from disease or medication. Complete patient recruitment and enrolment flow chart is presented in **Figure 1** as per CONSORT standards.

Sample size needed to detect of side effects occurring at a frequency of 8% or greater with a 95% CI was calculated to be 24 (using ± 1 SD as an estimate of variability). As our primary concern was safety, a number was used which balanced resources available with capacity of identifying frequent side effects.

Study Design

The trial took place from November 18, 2013 to December 12, 2015 at the Centre Hospitalier de l'Université de Montréal (CHUM), an academic reference center, and was performed by a single ENT surgeon (MD) (Clinicaltrials.gov identifier: NCT04048174.) Patients with CRS refractory to medical and surgical therapy (Meltzer et al., 2004; Desrosiers et al., 2011) were enrolled in a prospective, single-arm, open-label trial. The single arm trial design was selected to ensure maximal patient exposure to *L. lactis W136* and minimize "carry-over" effect from bacterial treatment. While no placebo control was used in this study, all patients underwent a run-in period during which all medications were ceased, including corticosteroid sprays, high volume budesonide rinses. All antibiotics were ceased 30 days prior to recruitment. Only saline irrigations was allowed, both as a rescue medication and to control for the potentially beneficial effects of saline therapy used as vehicle for the bacteria.

Approval was obtained from Health Canada for intranasal administration of live *L. lactis W136* bacteria (Health Canada registration number: 191920) and the CHUM Institutional Review Board and Ethics committee (Registration No. 12.288) prior to trial performance. *L. lactis W136* was furnished free of charge by Agropur Dairy Cooperative (St Hubert, QC, Canada). Patients were drawn from ongoing clinical activities, and consent obtained by a member of the study team not involved in clinical care of the patients. No financial incentive was prided for participation, apart from reimbursement of hospital parking expenses. All measures were obtained and processed ensuring patient data protection and confidentiality.

The treatment protocol is outlined in **Figure 2**. Following recruitment, a 2-week washout period occurred during which all sinus medications were ceased, save for nasal and sinus irrigation with 120 mL of 0.9% saline solution administered twice-daily using the NeilMed Pediatric Sinus Rinse system (NeilMed Pharmaceuticals Inc., Santa Rosa, CA). Subjects were then treated with 14 days of BID irrigations containing 1.2×10^9 colony forming units (CFU) of live *L. lactis W136* suspended in 120 mL 0.9% buffered saline (10^7 CFU/mL concentration). This was followed by a second 14-day period during where only the irrigation with saline was continued. For each application, 120 ml (pediatric size) of clean water was mixed with the appropriate NeilMed SinusRinse pediatric packet, and the frozen *L. lactis* added. If the pellet was difficult to dislodge from the Eppendorf tube, a drop or two of saline form the NeilMed bottle was put in the Eppendorf to dissolve it. Patients shook the bottle, and then rinsed their nose over the sink. The head was held at a 45° angle and the irrigation fluid irrigated through one nostril and out the other. Treatment was done until no product was left. Technique was demonstrated to the patient and the first irrigation was performed under direct observation. A new bottle was supplied for every rinsing to avoid cleaning the bottle in between uses.

Lactococcus lactis W136 was provided to subjects in frozen format for reconstitution in single-dose containers. *L. lactis W136* was reconstituted immediately prior to administration in 120 mL of buffered saline 0.9% solution using a 120 mL nasal irrigation device. A new irrigation bottle was supplied for each application. The first application was administered in clinic under supervision.

Assessments were performed at the beginning and end of the washout period, at the initiation of *L. lactis W136* treatment (day 0), and at day 1, 7, 14, and 28 after initiation of the tested therapy. Symptomatology was assessed using total sinonasal symptom score (SNSS), validated disease-specific quality of life questionnaire; Sino-nasal Outcome Test 22 item (SNOT-22) (Hopkins et al., 2009) and aspect of the sinus mucosa as assessed by a validated endoscopy score (POSE score) (Wright and Agrawal, 2007). Additional monitoring for safety included monitoring: (i) sense of smell using the UPSIT-40 (Doty et al., 1984) (40-item University of Pennsylvania Smell Identification Test (Sensonics, Inc., Haddon Heights, NJ), (ii) Possible adverse effects on middle ear and Eustachian tube function by monitoring middle ear status using otomicroscopy to improve diagnostic accuracy, (iii) endoscopically-obtained swab cultures (COPAN, Becton & Dickinson Company, Sparks, MD, USA) to identify overgrowth by pathogenic or probiotic bacteria. Safety was further assessed by monitoring adverse events.

Samples were collected by standard culture swab for routine culture and a nasal brushing for 16S microbiome analysis obtained at Do, prior to first probiotic application, treatment, and at D14, the day following the last treatment. All probiotic irrigations were performed at least 12 h prior to the D14 visit.

Samples for 16S were processed at the Surette Laboratory (Hamilton, ON, Canada) where DNA extraction, 16S rRNA gene amplification and sequencing was performed. DNA was extracted from the whole swabs and its concentration

measured with a Nanodrop 2000c Spectrophotometers (Fisher Scientific, Hampton, NH, USA). The quality of the extracted DNA was evaluated on a 1% agarose gel. Libraries were prepared by amplifying the V3 hypervariable region of the 16S rRNA gene based on a modified version of the libraries described by Bartram et al. (2011). Primers used were GC-341F (5′-CCTACGGGAGGCAGCAG-3′) and 518R (5′-ATTACCGCGGCTGCTG-3′). Amplicons were amplified by PCR and normalized according to the obtained concentrations prior to sequencing. The MiSeq

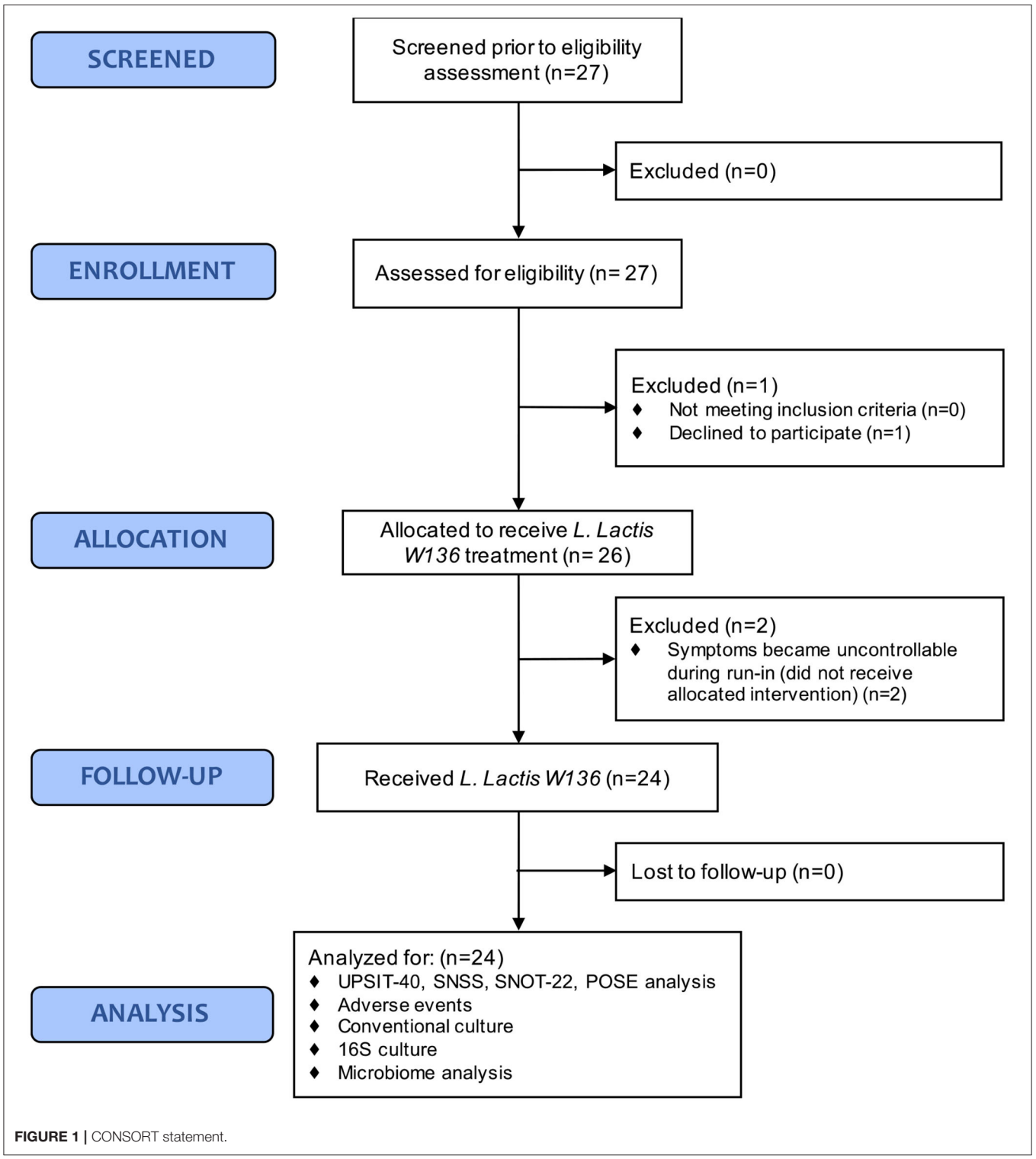

FIGURE 1 | CONSORT statement.

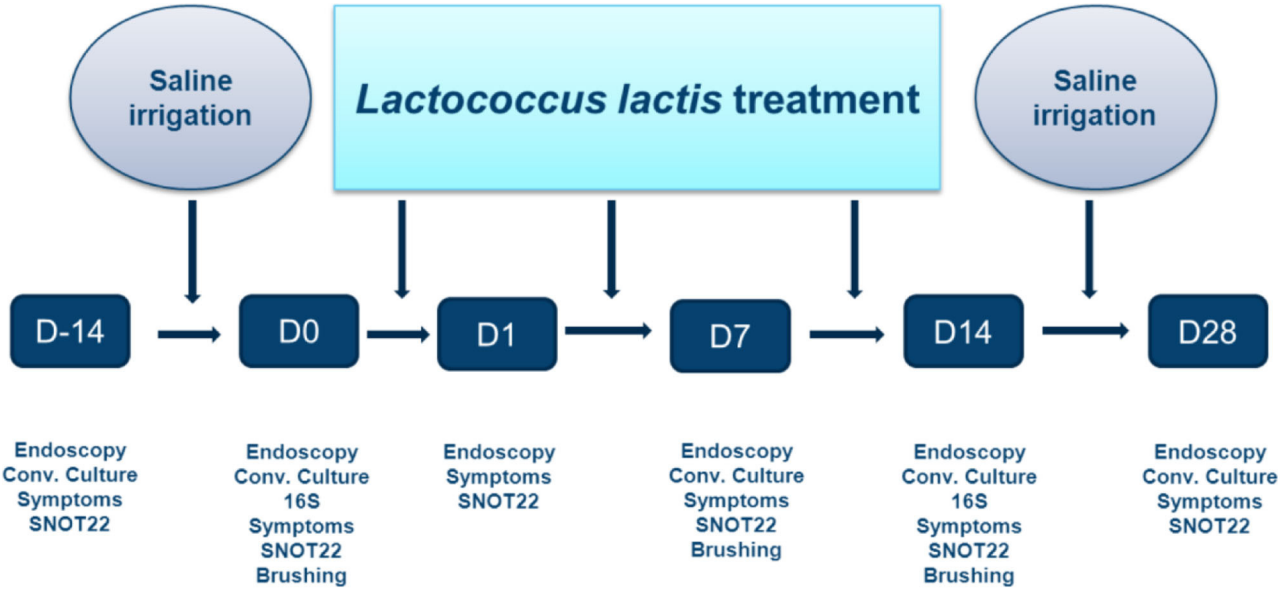

FIGURE 2 | Timeline of probiotic trial. Study protocol showing initial 14 days saline-only washout period; 14 days of *L. lactis W136* followed by 14 day saline-only observational period (D, Day).

TABLE 1 | Population baseline characteristics.

CRSwNP/CRSsNP (*n*)	**17/7**
Age (mean ± SD)	54.9 ± 11.9 years
Gender (*n*)	Female = 13 (54%)
Ethnicity (*n*)	22 (Caucasian); 2 (Arabic)
Asthma [*n* (%)]	18 (75%)
Number of previous ESS (mean ± SD)	2.08 ± 1.14
History of allergy (seasonal) [*n* (%)]	5 (21%)
Current smoker	0 (0%)
WBC (10^9/L) (mean ± SD)	6.83 ± 1.29
Eos (10^9/L) (mean ± SD)	0.39 ± 0.32
IgE kIU/L(mean ± SD)	275.8 ± 397.7

n, number; SD, standard deviation.

platform was used for 250 bp paired-end sequencing of PCR products.

Statistical Analysis

Response to treatment was determined by calculating time-weighted average scores over the study period from day 0 to day 28, using "time" as day 0 as the baseline value. Results were expressed in term of confidence intervals (CI).

Microbiome Analysis

Sequence reads were processed and annotated using the ANCHOR pipeline (Gonzalez et al., 2019). Briefly, sequences were aligned and dereplicated before selection of OTUs using a count threshold of 14 across all samples. Annotation queried four sequence repositories with strict BLASTn criteria (>99% identity and coverage): NCBI curated bacterial and Archaea RefSeq, NCBI nt, SILVA, and Ribosomal Database Project (RDP). When the highest identity/coverage was shared amongst multiple different (Gonzalez et al., 2018) putative annotation, all were retained and reported; borrowed from the idea of secondary annotation in metatranscriptomics. Amplicons with low-counts (<14) were binned to high-count sequences in a second BLASTn, using a lower threshold of >98% identity/coverage (secondary count capture). Alpha diversity was measured using Shannon and inverse Simpson indices within Phyloseq R package (McMurdie and Holmes, 2013). Beta diversity was estimated using Bray-Curtis dissimilarity and the Constrained Analysis of Principal Coordinates (CAP) ordination method. Dispersion ellipses were drawn using veganCovEllipse function from Vegan package in R (Oksanen et al., 2016). Significant distance was evaluated between the groups using non-parametric analysis of similarities (ANOSIM) on normalized counts based on Bray distances (R Vegan package). Differential abundance analysis on 16S rRNA gene amplicons was performed using DESeq2 (Love et al., 2014), which can perform well with uneven library sizes and sparsity common to 16S rRNA gene data (Weiss et al., 2017; Gonzalez et al., 2018; Minerbi et al., 2019). A differential abundance selection parameter of false discovery rate (FDR; Benjamini-Hochberg procedure) <0.05 was applied. Raw counts were transformed using regularized log transformation across samples (rlog function, R phyloseq package).

RESULTS

Twenty-seven patients who met inclusion/exclusion criteria were recruited. One patient was withdrawn before initiation of the trial because of scheduling issues, and two other patients withdrawn

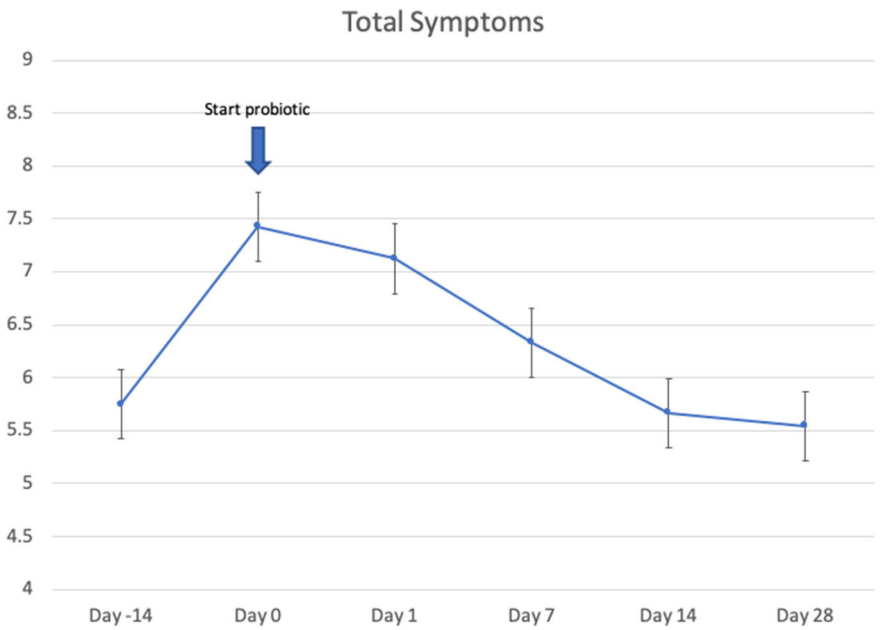

FIGURE 3 | Effect of *L. lactis W136* on total nasal symptom score ($n = 24$). Time-weighted average scores over the study period from day 0 (D0) to day 28 (D28).

during the saline treatment period as their symptoms became intolerable following withdrawal of usual sinus medication during run-in. None of these patients received *L. lactis W136* (**Figure 1**).

Twenty-four patients received *L. lactis W136,* and all 24 successfully completed the study. Their baseline characteristics are summarized in **Table 1**. Overall, 14 days of treatment with *L. lactis W136* was well-tolerated and all 24 patients were able to complete a full course. No acute infections occurred. The saline only washout period was associated with a deterioration in most parameters, with increased symptoms, decreased disease specific QOL, and deteriorated mucosal aspect. Following initiation of treatment, symptoms progressively improved over the subsequent 28-day treatment and observation period (Mean change = 6.0; 95% CI: 4.65–7.36) (**Figure 3**). Pattern of response showed progressive improvement during the 14 days of *L. lactis W136* administration, with improvements maintained over the 14-day post-treatment observation period. Individual symptoms of facial pain, headache, nasal congestion, need to blow nose and post-nasal drip all followed a similar pattern of improvement (**Figure 4**). Symptoms showing greatest magnitudes of improvement were for the symptoms of "Nasal congestion" (95% CI: 1.10–1.81), "Post-nasal drip" (95% CI: 1.04–1.67) and "Need to blow nose" (95% CI: 1.26–1.81). SNOT-22 scores followed a similar pattern as for symptomatology. SNOT-22 score significantly improved over the course of the trial (95% CI: 27.28–46.87). Again, improvement persisted following administration of probiotic, and was maintained at the 28-day point (**Figure 5**). Mucosal aspect as assessed by endoscopic score demonstrated a similar pattern of improvement as for sinus symptoms and QOL (95% CI: 10.32 to 16.28) (**Figure 6**). Sense of smell as assessed by UPSIT-40 scores remained stable during the trial, with no evidence of impairment from therapy (95% CI: −3.46 to 2.13) (**Figure 7**).

Bacteriology and Microbiome Assessment

Conventional culture identified no noticeable change in patterns of collection or in type of bacteria collected over the course of treatment (**Table 2**). This was further explored using culture-independent 16S microbiome assessment. Samples were able to be collected from all 24 patients. An average of 82,347 (range between 15,352 and 347,360) counts per sample ($N = 48$) were obtained grouped into 6,820 OTUs. Following *L. lactis W136* administration, there was no change in alpha diversity between both sample groups (**Figure 8A**). Phylum analysis (**Figure 8B**) suggested differences in microbiome composition, however CAP plots showed no major differences (**Figure 8C**). Differential abundance analysis using DESeq2 showed a significant decrease in the abundance of *Dolosigranulum pigrum* in post-therapy patients (**Figure 8D**).

CRSwNP vs. CRSsNP Sub-Group Analysis

Exploratory analysis of CRSwNP and CRSsNP phenotypes was performed to verify comparability of groups at baseline and response to *L. lactis W136* administration. There was no significant difference at baseline scores for symptoms, SNOT-22, and endoscopy, nor was there any difference in response. The sole exception to this was the greater presence of polyps, as expected, in the polyp group (CRSwNP). There was however a difference between bacteria suggested by

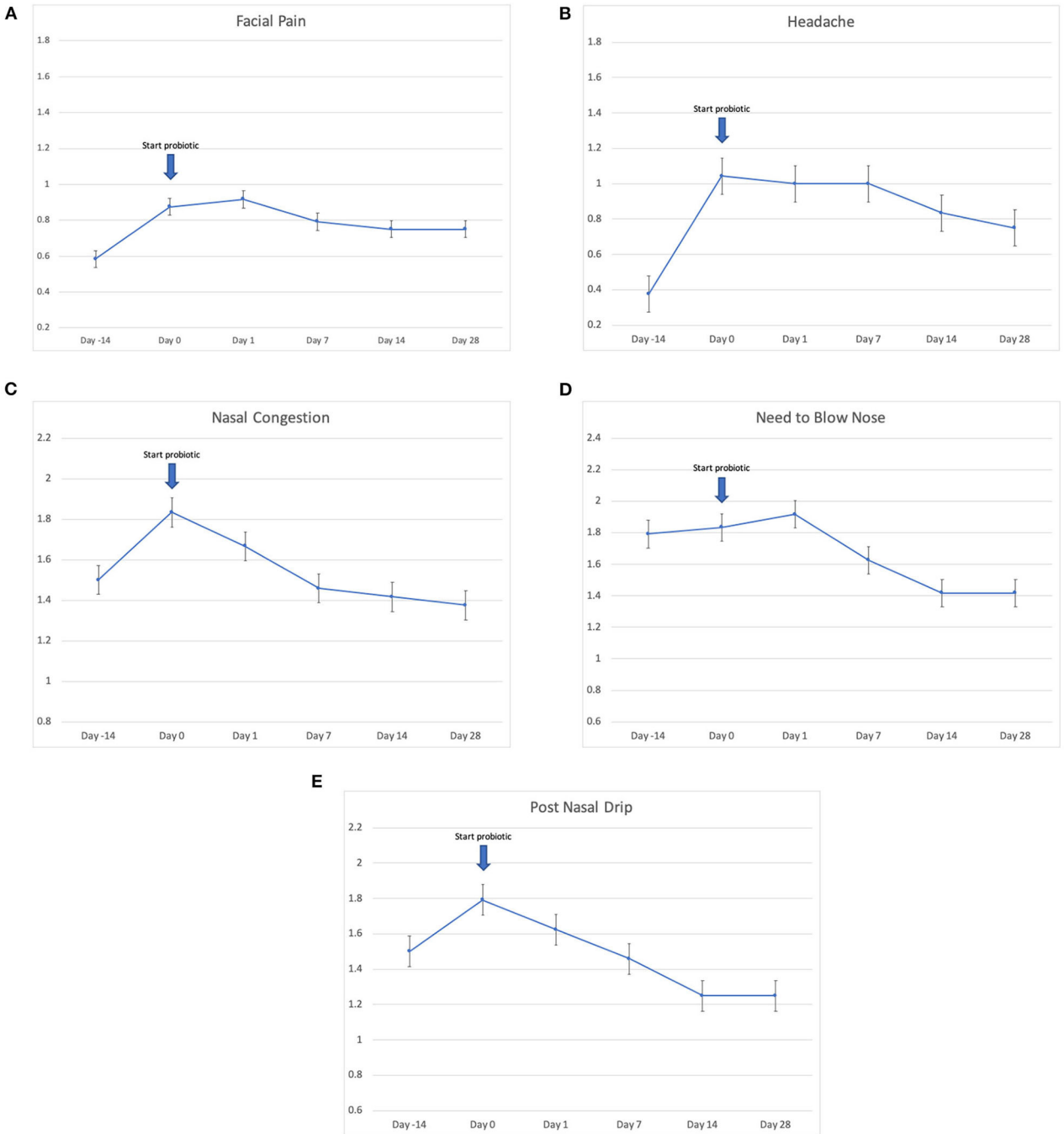

FIGURE 4 | Effect of *L. lactis W136* on individual nasal symptoms (0–3 scale). **(A)** Facial pain; **(B)** headache; **(C)** nasal congestion; **(D)** need to blow nose; and **(E)** post-nasal drip ($n = 24$). Time-weighted average scores over the study period from day 0 (D0) to day 28 (D28).

conventional culture results between the CRSwNP and CRSsNP groups (**Table 3**).

This was explored further by assessing the microbiome composition at baseline and response to treatment separately for polyp and non-polyp subgroups. At baseline, differences in composition were seen between CRSsNP and CRSwNP groups (**Figure 9**). Notably, the CRSsNP group was characterized by a decrease in alpha diversity. Furthermore, at phylum level, these samples showed an increased relative abundance of *Proteobacteria*. When assessing differences at species level, the CRSsNP group demonstrated an increased abundance of *Dolosigranulum pigrum*, *Rothia mucilaginosa*, *Lachnospiraceae* spp., and *Staphylococcus hominis*. Differential abundance differences

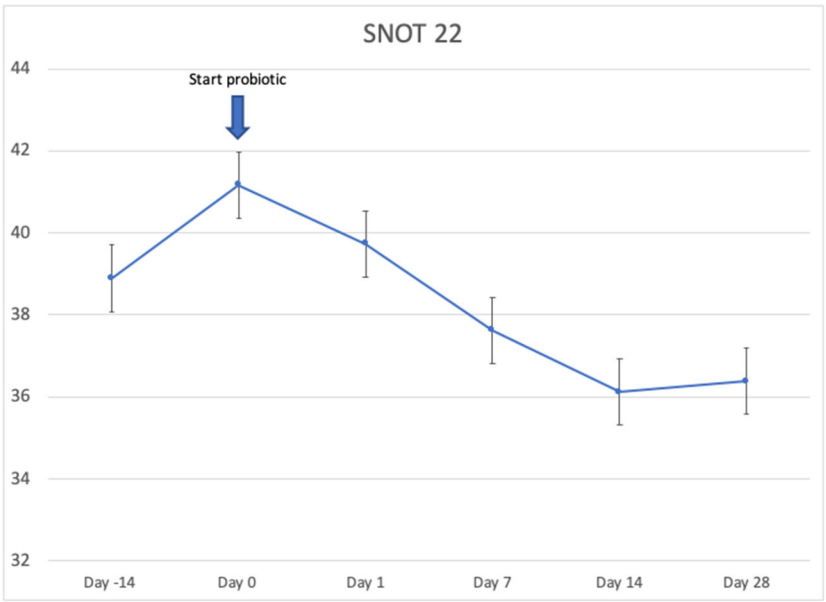

FIGURE 5 | Effect of *L. lactis W136* on SNOT-22. Mean of total score of the 22 items from quality of life questionnaire ($n = 24$). Time-weighted average scores over the study period from day 0 (D0) to day 28 (D28).

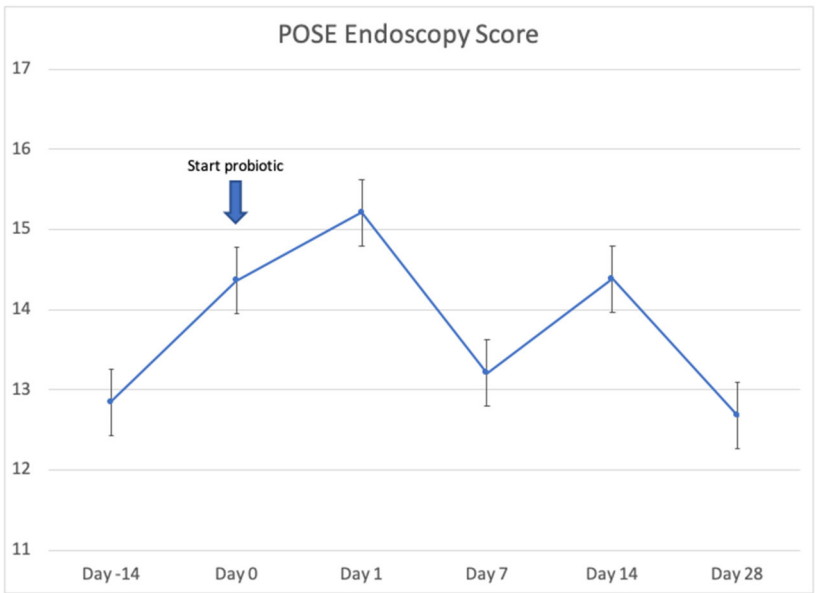

FIGURE 6 | Effect of *L Lactis W136* on sinus endoscopy: Total POSE score. ($n = 24$).

were also found. In fact, *Stenotrophomonas maltophilia*, multiple species of *Pseudomonas aeruginosa* and *Pseudomonas stutzeri* were found in higher proportion in CRSwNP patients. Changes associated with therapy were different for both groups (**Figure 10**). For CRSsNP, changes in microbiome was limited to the increase in *Turicibacter* spp., which was present only after treatment but at low levels. For CRSwNP, treatment was associated with reduced abundance of *Staphylococcus* MS (multiple species), *Peptostreptococcae* MS, *Enterobacialles* MS, and increased abundance of *Dolosigranulum pigrum.*

Adverse Events

No serious adverse events occurred during this clinical trial (**Table 4**). Two patients showed evidence of middle ear effusion during the trial period, without symptoms or signs if acute

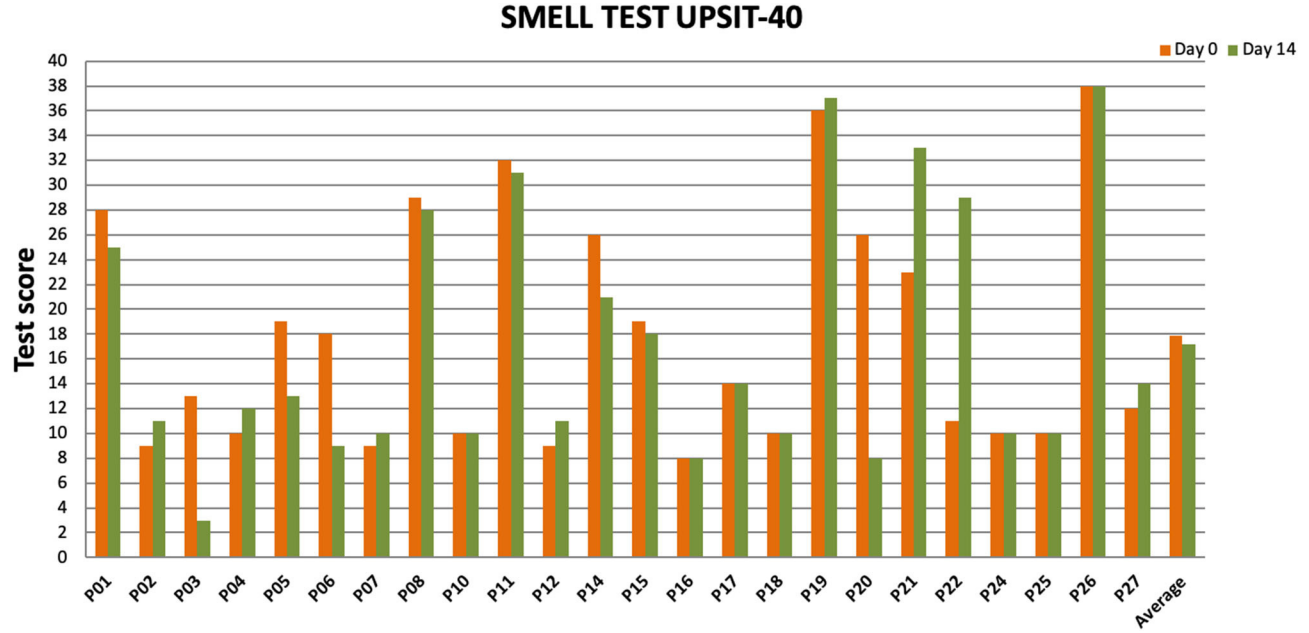

FIGURE 7 | Impact of *L. lactis W136* treatment on olfaction. UPSIT-40 scores prior to (Day 0) and immediately following treatment (Day 14) presented individually for all patients ($n = 24$) (D, Day).

TABLE 2 | Bacteriology by conventional culture over the trial period.

	D-14 (%)	D0 (16S) (%)	D7 (%)	D14 (16S) (%)	D28	*p*-value
Culture + rate	100.0	83.3	95.7	95.8	100.0	NS
Oropharyngeal flora	45.8	45.8	34.8	45.8	54.2	NS
Corynebacterium spp.	4.2	0.0	4.3	4.2	4.2	NS
Coagulase-negative staphylococci	25.0	8.3	21.7	20.8	8.3	NS
Staphylococcus aureus	37.5	20.8	39.1	37.5	37.5	NS
Streptococcus pneumoniae	4.2	4.2	0.0	0.0	12.5	NS
Haemophilus influenzae	4.2	0.0	4.3	4.2	0.0	NS
Pseudomonas aeruginosa	29.2	33.3	30.4	33.3	33.3	NS
Enterobacter cloacae	4.2	0.0	0.0	0.0	0.0	NS
Escherichia coli	4.2	4.2	8.7	8.3	8.3	NS
Pseudomonas putida	4.2	0.0	4.3	4.2	4.2	NS
Proteus mirabilis	4.2	4.2	4.3	4.2	0.0	NS
Serratia marcescens	4.2	4.2	0.0	0.0	0.0	NS
Alternaria spp.	4.2	0.0	0.0	0.0	0.0	NS

There was no overgrowth of new pathogenic species and no growth of L. lactis on conventional culture before or after administration of L. lactis W136.

infection. One patient had effusion and otorrhea already at time of inclusion. All patients reported ear fullness and ear pain in pre-treatment SNOT-22, suggesting pre-existing ET/middle ear disease. Effusion resolved completely in all patients without additional treatment at 1-month follow-up after end of study. Minor adverse events included: headache, migraines, nasal congestion, dental infection, throat pain, cold sore, gastroenteritis, nasal allergy, and shoulder pain; together all accounting for <4%. Some events were related to their condition of chronic rhinosinusitis and the other events pre-existed before the trial and medications were taken since before the trial.

DISCUSSION

This study offers further support that topical application of live bacteria directly to the nasal and sinus cavities via nasal

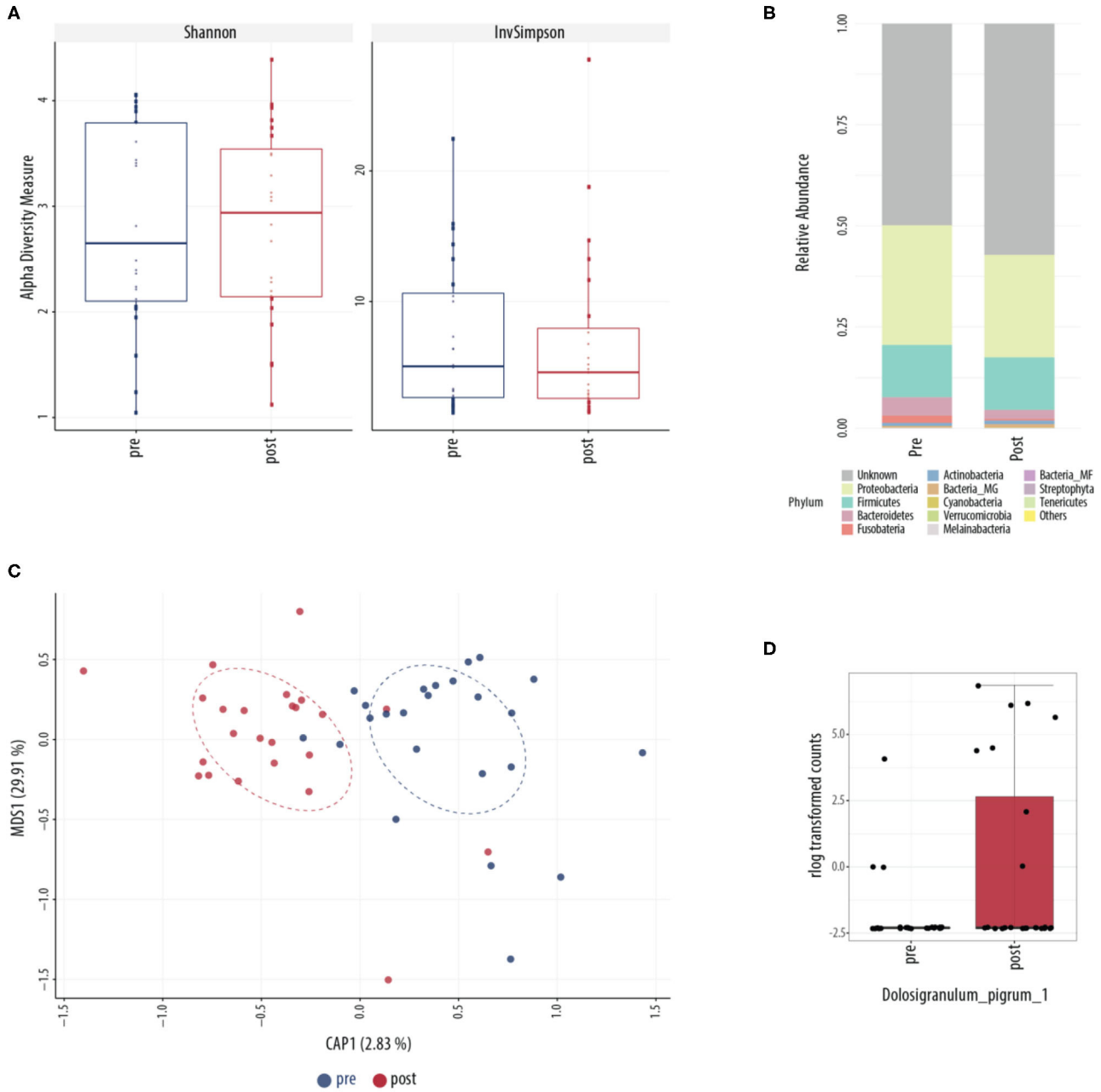

FIGURE 8 | Sinus microbial analysis of patients before and after ESS. **(A)** A comparison of alpha diversity indices (Shannon and inverse Simpson). **(B)** Compared relative abundance (from raw counts). **(C)** Canonical analysis of principal coordinates of taxa abundance from raw counts. No significant differences between the groups were observed in alpha and beta diversities. **(D)** Differentially abundant OTUs (FDR < 0.05) between the pre-surgery (pre, $n = 24$) and post-surgery (post, $n = 24$) groups. The main axis represents the fold change (log_2) in relative abundance of significantly different OTUs between the two groups and their normalized counts. Values represent mean score for all enrolled patients ($n = 24$). Change in microbiome is calculated from day 0 to day 14 period (D, Day, D0, introduction of probiotic; D14, end of treatment).

irrigation administration is safe and well-tolerated in CRS patients refractory to previous medical and surgical therapy.

While administration of live bacteria to the sinuses is a relatively novel concept, this adds to existing evidence in animal and human models supporting that topical intranasal bacterial therapy is safe (Desrosiers et al., 2011; Cope and Lynch, 2015; Marchisio et al., 2015). Additionally, despite that this was not a placebo-controlled trial, during the period of administration of *L. lactis W136*, participants demonstrated improvements in their global sinus condition, as assessed by sinus symptoms, disease-specific quality of life indices, and endoscopically-assessed mucosal aspect of the sinuses. This was in marked contrast to the

TABLE 3 | Conventional culture subgroup analysis according to CRSsNP and CRSwNP phenotypes.

Bacterial isolate	CRSsNP D-14 (%)	CRSwNP D-14 (%)	All D-14 (%)	*t*-test CRSwNP vs. CRSsNP
Oropharyngeal flora	29	53	46	0.30
Corynebacterium ssp.	14	0	4	0.36
Coagulase-negative staphylococci	14	29	25	0.42
Staphylococcus aureus	57	29	38	0.26
Streptococcus pneumoniae	14	0	4	0.36
Haemophilus influenzae	14	0	4	0.36
Pseudomonas aeruginosa	43	24	29	0.42
Enterobacter cloacae complex	0	6	4	0.33
Escherichia coli	0	6	4	0.33
Proteus mirabilis	14	0	4	0.36
Pseudomonas putida	0	6	4	0.33
Serratia marcescens	0	6	4	0.33
Alternaria ssp.	0	6	4	0.33

T-test compares CRSsNP and CRSwNP groups.

saline-only run-in period where symptoms and sinus endoscopy deteriorated rapidly.

The mechanisms by which the *L. lactis W136* could be exerting its effects in the study remains to be described, but mechanisms including modulation of immune responses and bacterial displacement of pathogenic species can be suspected from mechanisms previously identified in other disease models. *L. lactis* is a well-known probiotic bacterium, with immunomodulatory and antibacterial properties (Oelschlaeger, 2010). Immune modulation by lactic acid bacteria is well-described, the immunomodulatory effect exerted both via induction of IL-10 secretion (de Moreno de Leblanc et al., 2011) and silencing of TLR2 signaling (Fischer et al., 2011; Kaesler et al., 2016). For *L. lactis W136*, previous *in vitro* studies have confirmed that exposure to *L. lactis* increases IL-10 induction in a suspension of peripheral blood mononuclear cells (Moles et al., 2020).

Interference with other pathogens in the sinus cavities may also play a role. In this study, *Dolosigranulum pigrum* was seen in low abundance pre-treatment and was increased in abundance following *L. lactis W136* treatment. *D. pigrum* has only recently been identified in the microbiome of cystic fibrosis lungs (Lopes et al., 2017), where it is described as a pathogen with the capacity to form biofilms of large biomass which are resistant to conventional antibiotic therapy. Intriguingly, it may also have a role in regulation of other pathogens and is considered to play a key role in inflammatory disorders of the nose, nasopharynx, and paranasal sinuses (Brugger et al., 2016). Working alone, *in vitro* it is capable of inhibiting the growth of *S. aureus*, and, in combination with *Corynebacterium pseudodiphthericum*, it is capable of inhibiting the growth of *Streptococcus pneumoniae* and *Haemophilus influenzae* (Brugger et al., 2020). *D. pigrum* has been suggested as a novel "probiotic" bacteria (Lappan and Peacock, 2019). However, direct administration of live *D. pigrum* will require careful assessment because of its potential for producing human disease, thus it may find a role as a marker of microbiome status than a therapeutic agent.

CRSwNP and CRSsNP phenotypes appeared to have different microbiome patterns, both at baseline and in terms of response to treatment. At baseline, CRSsNP appears to have an over-abundance *Pseudomonas* spp. mainly including *Pseudomonas aeruginosa*, while in CRSwNP, other species predominate. Apart from the lower relative abundance of *D. pigrum* in the CRSsNP group, it is interesting to note the low relative abundance of *Akkermansia muciniphila* in the CRSsNP group. Reduced levels of *A. muciniphila* are associated with obesity, diabetes, cardiometabolic diseases, low-grade inflammation (Cani and de Vos, 2017), and lesser responses to PD-1 inhibitors for cancer (Routy et al., 2018). Supplementation with *A. mucinophilia* as a novel probiotic has recently been proposed (Zhou and Zhang, 2019).

Overall, these microbiome differences may reflect differing mechanisms of disease development which create unique microenvironments selecting for dysbiotic flora. Changes in the microbiome associated with *L. lactis 136* treatment differ between these two entities. CRSsNP microbiomes were not greatly impacted by administration of *L. lactis W136*. This is consistent with *in vitro* observations where co-culture of *L. lactis W136* with clinical isolates of *P. aeruginosa* did not have an effect (Cho et al., 2020). While *L. lactis* administration is associated with an increase in *Turicibacter*, a bacterium implicated in serotonin metabolism (Fung et al., 2019), its abundance here is so low it is difficult to believe it is playing a great role in disease causation or prevention. In CRSwNP, increased abundance of *D. pigrum* following *L. lactis W136* treatment suggests an unexpected protective role for this bacterium.

These observations emphasize that the effects of microbiome supplementation may thus be more complex than direct associations suggested by *in vitro* susceptibility testing methods. Instead of exerting their effects directly, bacteria may interact with the mucosal barrier or mucosal immunity to compete for the ecological niche that then effect the observed changes. In addition, apparently different patterns of changes in the microbiome for CRSwNP and CRSsNP suggest these might be best considered as distinct entities for future assessments. This may contribute to different responses during interaction with *L. lactis W136* and suggest that future trials consider these entities separately.

The occurrence of middle ear effusion in two subjects is worthy of further discussion. The mechanism of development of ear effusion is unknown but may be related to other factors than probiotic administration, such as (i) deterioration of pre-existing Eustachian tube dysfunction and/or upper respiratory tract disease following withdrawal of therapy or (ii) performance of nasal irrigation. ET dysfunction is frequent in CRS patients particularly in those with severe disease (Stoikes and Dutton, 2005; Maniakas et al., 2018) and may deteriorate following withdrawal of CRS medication. This concept is supported by a recent clinical trial of 60 patients treated with Dupilumab or placebo for CRSwNP where otitis media developed in a patient

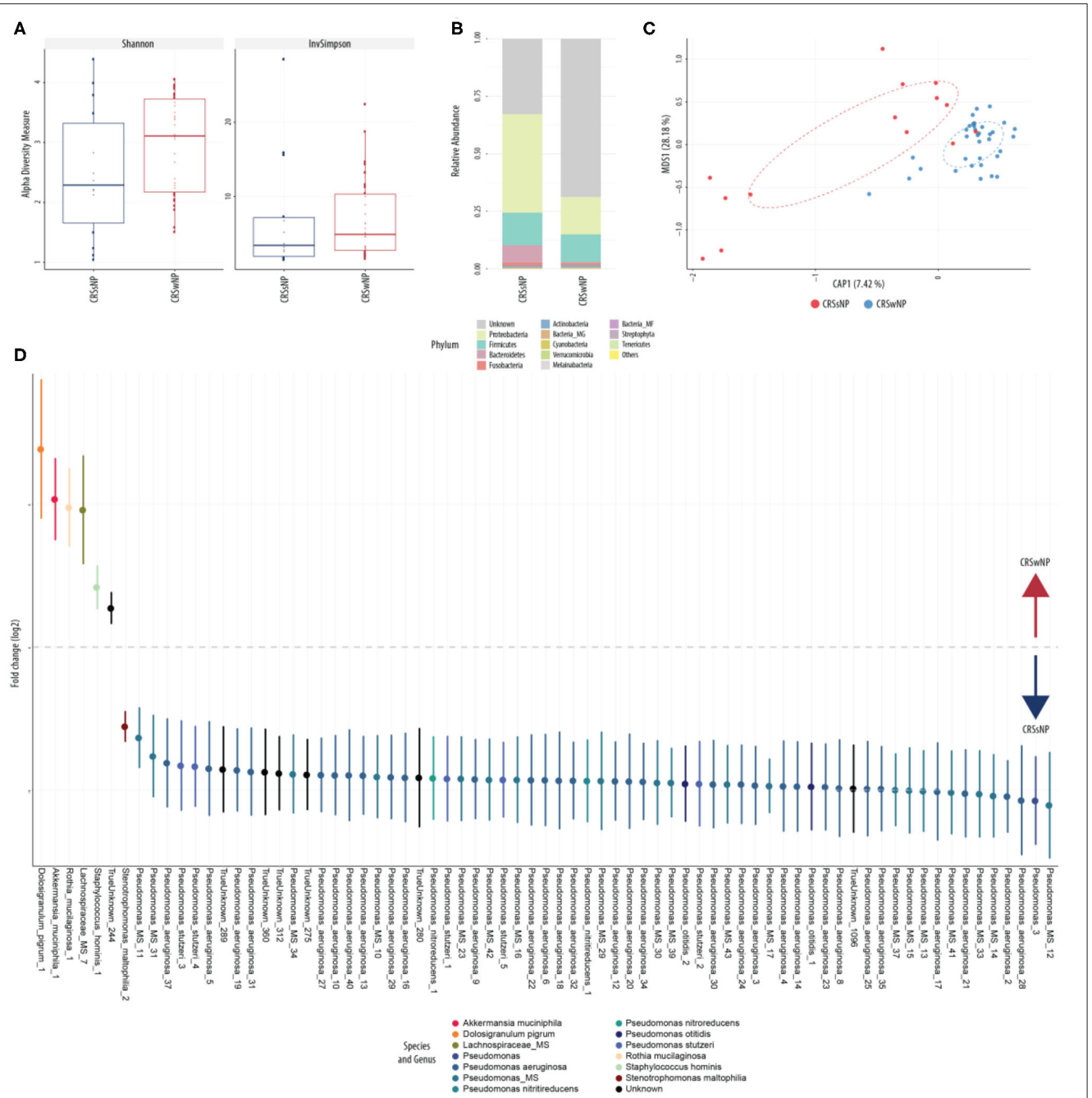

FIGURE 9 | Sinus microbial analysis of patients without and with nasal polyps (CRSsNP, $n = 7$; CRSwNP, $n = 17$). **(A)** Comparison of alpha diversity indices (Shannon and inverse Simpson). **(B)** Comparison of relative abundance (from raw counts). **(C)** Canonical analysis of principal coordinates of taxa abundance from raw counts. Significant differences between the groups was observed in beta diversities (PERMANOVA, $p < 0.01$). **(D)** Differentially abundant OTUs (FDR < 0.05) between patients with polyps and patients without. The main axis represents the fold change (log_2) in relative abundance of significantly different OTUs between the two groups and their normalized counts.

in the untreated placebo group treated only saline irrigation (Bachert et al., 2016).

Study Limitations

This pilot study is not a parallel group-controlled trial, but rather a feasibility and safety study to better understand the feasibility of this therapeutic approach. We understand this is a limitation but, the placebo or therapeutic effects of vehicle administration (saline) have been controlled for by using saline irrigations during the run-in period while all other sinus medications were ceased, thus we feel that effects observed following initiation of therapy are secondary to the latter and not the saline irrigation.

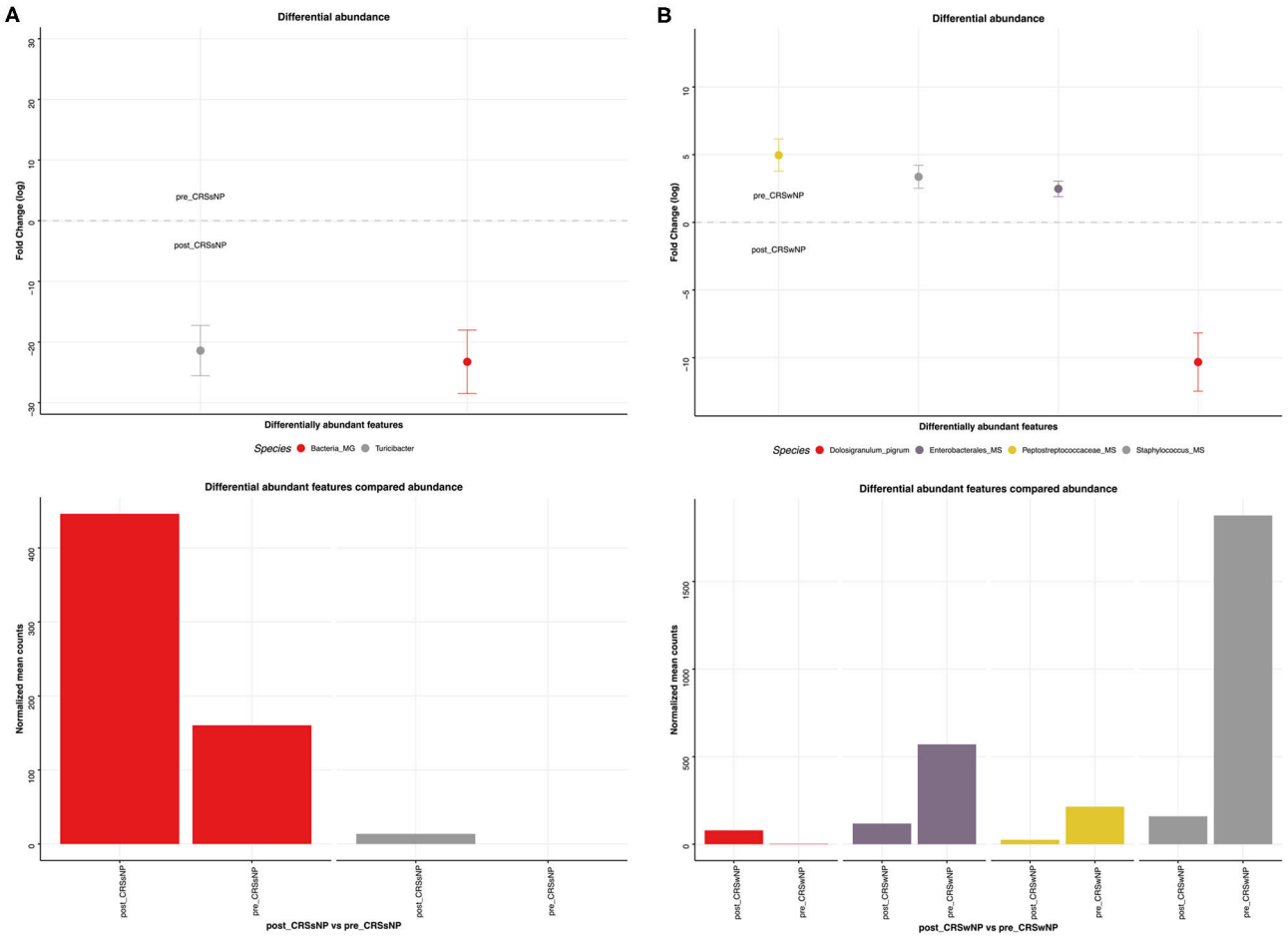

FIGURE 10 | Sinus microbial analysis of microbiome modifications before and after *L. lactis W136* administration. **(A)** For CRSsNP ($n = 7$) and **(B)** For CRSwNP ($n = 17$) subgroups. Differentially abundant OTUs (FDR < 0.05) between before and after *L. lactis W136* administration. The main axis represents the fold change (log_2) in relative abundance of significantly different OTUs between the two groups and their normalized counts.

TABLE 4 | Adverse events occurring during study period.

Adverse event	Frequency	Resolved at end of trial?
Middle ear effusion (non-infectious)	2/24 (8.2%)	Y
Headache	1/24 (4.1%)	Y
Migraines	1/24 (4.1%)	Y
Nasal congestion	1/24 (4.1%)	Y
Dental infection	1/24 (4.1%)	Y
Throat pain	1/24 (4.1%)	Y
Cold sore	1/24 (4.1%)	Y
Gastroenteritis	1/24 (4.1%)	Y
Nasal allergy	1/24 (4.1%)	Y
Shoulder pain	1/24 (4.1%)	Y

All events are recorded.

The effect of saline irrigation alone in severe CRS is expected to be limited. This is confirmed by the aggravation of symptoms and deterioration of QOL and mucosal aspect following withdrawal of medications during the run-in period. In addition, saline irrigations have been shown not to influence microbiome composition in CRS patients (Liu et al., 2015). That *L. lactis W136* was associated with a time-dependent improvement suggests it may be having an effect, possibly via one of the mechanisms postulated above.

CONCLUSION

Topical intranasal administration of live *L. lactis W136* for 14 days in patients with chronic rhinosinusitis refractory to medical and surgical therapy was well-tolerated, without serious adverse events or new infections. Improvements noted in symptoms, quality of life, and mucosal aspect suggest that topical administration of *Lactococcus lactis W136* may potentially represent novel alternative therapy for patients with sinus disease, making it worthy of further investigation.

DATA AVAILABILITY STATEMENT

The original contributions presented in the study are publicly available. This data can be found here: https://www.ncbi.nlm.nih.gov/sra/PRJNA638899.

ETHICS STATEMENT

The studies involving human participants were reviewed and approved by CHUM Institutional Review Board and Ethics committee (Registration No. 12.288). The patients/participants provided their written informed consent to participate in this study.

AUTHOR CONTRIBUTIONS

LE, SA, JM, BC, and MD contributed conception and design of the study. LE, SA, EG, and AR organized the database. EG performed the statistical analysis. MD wrote the first draft of the manuscript. LE, SA, EG, AR, and MD wrote sections of the manuscript. All authors contributed to the manuscript revision, read, and approved the submitted version.

FUNDING

This research work was supported by a McGill Faculty of Medicine Grant. *Lactococcus lactis W136* Probiotic: Donation, AgroPur Dairy Cooperative (St Hubert, QC, CAN); SinusRinse® nasal irrigation apparatus: Donation, NeilMed® Pharmaceuticals Inc. (Santa Rosa, CA, USA). None of the sponsors had influence on the research question, trial design or execution, data analysis, or the manuscript.

ACKNOWLEDGMENTS

We thank Dr. Michael Surette of the Farncombe Family Digestive Health Research Institute, McMaster University, Hamilton, Ontario, Canada, for invaluable advice on the microbiome of the respiratory tract.

REFERENCES

Abreu, N. A., Nagalingam, N. A., Song, Y., Roediger, F. C., Pletcher, S. D., Goldberg, A. N., et al. (2012). Sinus microbiome diversity depletion and Corynebacterium tuberculostearicum enrichment mediates rhinosinusitis. *Sci. Transl. Med.* 4:151ra124. doi: 10.1126/scitranslmed.3003783

Al-Shemari, H., Abou-Hamad, W., Libman, M., and Desrosiers, M. (2007). Bacteriology of the sinus cavities of asymptomatic individuals after endoscopic sinus surgery. *J. Otolaryngol.* 36, 43–48. doi: 10.2310/7070.2006.0019

Aroniadis, O. C., and Brandt, L. J. (2013). Fecal microbiota transplantation: past, present and future. *Curr. Opin. Gastroenterol.* 29, 79–84. doi: 10.1097/MOG.0b013e32835a4b3e

Bachert, C., Mannent, L., Naclerio, R. M., Mullol, J., Ferguson, B. J., Gevaert, P., et al. (2016). Effect of subcutaneous dupilumab on nasal polyp burden in patients with chronic sinusitis and nasal polyposis: a randomized clinical trial. *JAMA* 315, 469–479. doi: 10.1001/jama.2015.19330

Bartram, A. K., Lynch, M. D., Stearns, J. C., Moreno-Hagelsieb, G., and Neufeld, J. D. (2011). Generation of multimillion-sequence 16S rRNA gene libraries from complex microbial communities by assembling paired-end illumina reads. *Appl. Environ. Microbiol.* 77, 3846–3852. doi: 10.1128/AEM.02772-10

Bjerg, A. T., Sorensen, M. B., Krych, L., Hansen, L. H., Astrup, A., Kristensen, M., et al. (2015). The effect of *Lactobacillus paracasei* subsp. paracasei *L. casei* W8(R) on blood levels of triacylglycerol is independent of colonisation. *Benef. Microbes* 6, 263–269. doi: 10.3920/BM2014.0033

Brahe, L. K., Le Chatelier, E., Prifti, E., Pons, N., Kennedy, S., Blædel, T., et al. (2015). Dietary modulation of the gut microbiota–a randomised controlled trial in obese postmenopausal women. *Br. J. Nutr.* 114, 406–417. doi: 10.1017/S0007114515001786

Brugger, S. D., Bomar, L., and Lemon, K. P. (2016). Commensal–Pathogen Interactions along the Human Nasal Passages. *PLOS Pathogens* 12:e1005633. doi: 10.1371/journal.ppat.1005633

Brugger, S. D., Eslami, S. M., Pettigrew, M. M., Escapa, I. F., Henke, M. T., Kong, Y., et al. (2020). *Dolosigranulum pigrum cooperation and competition in human nasal microbiota*. *bioRxiv*. 678698. doi: 10.1101/678698

Cani, P. D., and de Vos, W. M. (2017). Next-generation beneficial microbes: the case of *Akkermansia muciniphila*. *Front. Microbiol.* 8:1765. doi: 10.3389/fmicb.2017.01765

Chalermwatanachai, T., Vilchez-Vargas, R., Holtappels, G., Lacoere, T., Jáuregui, R., Kerckhof, F. M., et al. (2018). Chronic rhinosinusitis with nasal polyps is characterized by dysbacteriosis of the nasal microbiota. *Sci. Rep.* 8:7926. doi: 10.1038/s41598-018-26327-2

Cho, S.-T., Kung, H.-J., Huang, W., Hogenhout, S. A., and Kuo, C.-H. (2020). Species boundaries and molecular markers for the classification of 16SrI phytoplasmas inferred by genome analysis. *Front. Microbiol.* 11:1531. doi: 10.3389/fmicb.2020.01531

Cleland, E. J., Drilling, A., Bassiouni, A., James, C., Vreugde, S., and Wormald, P. J. (2014). Probiotic manipulation of the chronic rhinosinusitis microbiome. *Int. Forum Allergy Rhinol.* 4, 309–314. doi: 10.1002/alr.21279

Cope, E. K., and Lynch, S. V. (2015). Novel microbiome-based therapeutics for chronic rhinosinusitis. *Curr. Allergy Asthma Rep.* 15:504. doi: 10.1007/s11882-014-0504-y

de Moreno de Leblanc, A., Del Carmen, S., Zurita-Turk, M., Rocha, C. S., van de Guchte, M., Azevedo, V., et al. (2011). Importance of IL-10 modulation by probiotic microorganisms in gastrointestinal inflammatory diseases. *ISRN Gastroenterol.* 2011:892971. doi: 10.5402/2011/892971

Desrosiers, M., Evans, G. A., Keith, P. K., Wright, E. D., Kaplan, A., Bouchard, J., et al. (2011). Canadian clinical practice guidelines for acute and chronic rhinosinusitis. *J. Otolaryngol. Head Neck Surg.* 40(Suppl. 2):S99–193. doi: 10.1186/1710-1492-7-2

Doty, R. L., Shaman, P., and Dann, M. (1984). Development of the University of Pennsylvania Smell Identification Test: a standardized microencapsulated test of olfactory function. *Physiol. Behav.* 32, 489–502. doi: 10.1016/0031-9384(84)90269-5

Ferrario, C., Taverniti, V., Milani, C., Fiore, W., Laureati, M., De Noni, I., et al. (2014). Modulation of fecal Clostridiales bacteria and butyrate by probiotic intervention with *Lactobacillus paracasei* DG varies among healthy adults. *J. Nutr.* 144, 1787–1796. doi: 10.3945/jn.114.197723

Fischer, K., Stein, K., Ulmer, A. J., Lindner, B., Heine, H., and Holst, O. (2011). Cytokine-inducing lipoteichoic acids of the allergy-protective bacterium *Lactococcus lactis* G121 do not activate via Toll-like receptor 2. *Glycobiology* 21, 1588–1595. doi: 10.1093/glycob/cwr071

Fung, T. C., Vuong, H. E., Luna, C. D. G., Pronovost, G. N., Aleksandrova, A. A., Riley, N. G., et al. (2019). Intestinal serotonin and fluoxetine exposure modulate bacterial colonization in the gut. *Nat. Microbiol.* 4, 2064–2073. doi: 10.1038/s41564-019-0540-4

Gonzalez, E., Pitre, F. E., and Brereton, N. J. B. (2019). ANCHOR: a 16S rRNA gene amplicon pipeline for microbial analysis of multiple environmental samples. *Environ. Microbiol.* 21, 2440–2468. doi: 10.1111/1462-2920.14632

Gonzalez, E., Pitre, F. E., Pag,é, A. P., Marleau, J., Guidi Nissim, W., St-Arnaud, M., et al. (2018). Trees, fungi and bacteria: tripartite metatranscriptomics of a root microbiome responding to soil contamination. *Microbiome* 6:53. doi: 10.1186/s40168-018-0432-5

Hopkins, C., Gillett, S., Slack, R., Lund, V. J., and Browne, J. P. (2009). Psychometric validity of the 22-item Sinonasal Outcome Test. *Clin. Otolaryngol.* 34, 447–454. doi: 10.1111/j.1749-4486.2009.01995.x

Kaesler, S., Skabytska, Y., Chen, K. M., Kempf, W. E., Volz, T., Köberle, M., et al. (2016). Staphylococcus aureus-derived lipoteichoic acid induces temporary T-cell paralysis independent of Toll-like receptor 2. *J. Allergy Clin. Immunol.* 138, 780.e6–790.e6. doi: 10.1016/j.jaci.2015.11.043

Kristensen, N. B., Bryrup, T., Allin, K. H., Nielsen, T., Hansen, T. H., and Pedersen, O. (2016). Alterations in fecal microbiota composition by probiotic supplementation in healthy adults: a systematic review of randomized controlled trials. *Genome Med.* 8:52. doi: 10.1186/s13073-016-0300-5

Lai, Y., Di Nardo, A., Nakatsuji, T., Leichtle, A., Yang, Y., Cogen, A. L., et al. (2009). Commensal bacteria regulate Toll-like receptor 3-dependent inflammation after skin injury. *Nat. Med.* 5, 1377–1382. doi: 10.1038/nm.2062

Lappan, R., and Peacock, C. S. (2019). Corynebacterium and Dolosigranulum: future probiotic candidates for upper respiratory tract infections. *Microbiol. Aust.* 40, 172–177. doi: 10.1071/MA19051

Liu, C. M., Kohanski, M. A., Mendiola, M., Soldanova, K., Dwan, M. G., Lester, R., et al. (2015). Impact of saline irrigation and topical corticosteroids on the postsurgical sinonasal microbiota. *Int. Forum Allergy Rhinol.* 5, 185–190. doi: 10.1002/alr.21467

Lopes, S. P., Azevedo, N. F., and Pereira, M. O. (2017). Developing a model for cystic fibrosis sociomicrobiology based on antibiotic and environmental stress. *Int. J. Med. Microbiol.* 307, 460–470. doi: 10.1016/j.ijmm.2017.09.018

Love, M. I., Huber, W., and Anders, S. (2014). Moderated estimation of fold change and dispersion for RNA-seq data with DESeq2. *Genome Biol.* 15:550. doi: 10.1186/s13059-014-0550-8

Maniakas, A., Desrosiers, M., Asmar, M. H., Al Falasi, M., Endam, L. M., Hopkins, C., et al. (2018). Eustachian tube symptoms are frequent in chronic rhinosinusitis and respond well to endoscopic sinus surgery. *Rhinology* 56, 118–121. doi: 10.4193/Rhin17.165

Marchisio, P., Santagati, M., Scillato, M., Baggi, E., Fattizzo, M., Rosazza, C., et al. (2015). *Streptococcus salivarius* 24SMB administered by nasal spray for the prevention of acute otitis media in otitis-prone children. *Eur. J. Clin. Microbiol. Infect. Dis.* 34, 2377–2383. doi: 10.1007/s10096-015-2491-x

McMurdie, P. J., and Holmes, S. (2013). phyloseq: an R package for reproducible interactive analysis and graphics of microbiome census data. *PLoS ONE.* 8:E61217. doi: 10.1371/journal.pone.0061217

Meltzer, E. O., Hamilos, D. L., Hadley, J. A., Lanza, D. C., Marple, B. F., Nicklas, R. A., et al. (2004). Rhinosinusitis: establishing definitions for clinical research and patient care. *Otolaryngol. Head Neck Surg.* 131(Suppl. 6), S1–S62. doi: 10.1016/j.otohns.2004.09.067

Minerbi, A., Gonzalez, E., Brereton, N. J. B., Anjarkouchian, A., Dewar, K., Fitzcharles, M. A., et al. (2019). Altered microbiome composition in individuals with fibromyalgia. *Pain* 160, 2589–2602. doi: 10.1097/j.pain.0000000000001640

Moles, L., Gómez, M., Moroder, E., Bustos, G., Melgar, A., Del Campo, R., et al.: (2020). *Staphylococcus epidermidis* in feedings and feces of preterm neonates. *PLoS ONE* 15:e0227823. doi: 10.1371/journal.pone.0227823

Nader, M. E., Abou-Jaoude, P., Cabaluna, M., and Desrosiers, M. (2010). Using response to a standardized treatment to identify phenotypes for genetic studies of chronic rhinosinusitis. *J. Otolaryngol. Head Neck Surg* 39, 69–75.

Oelschlaeger, T. A. (2010). Mechanisms of probiotic actions - a review. *Int. J. Med. Microbiol.* 300, 57–62. doi: 10.1016/j.ijmm.2009.08.005

Oksanen, J., Blanchet, F. G., Friendly, M., Kindt, R., Legendre, P., McGlinn, D., et al. (2016) *vegan: Community Ecology Package. R package version 2.4-3*. Vienna: R Foundation for Statistical Computing. [Google Scholar].

Routy, B., Le Chatelier, E., Derosa, L., Duong, C. P. M., Alou, M. T., Daillère, R., et al. (2018). Gut microbiome influenceefficacy of PD-1-based immunotherapy against epithelial tumors. *Science* 359, 91–97. doi: 10.1126/science.aan3706

Schwartz, J. S., Peres, A. G., Mfuna Endam, L., Cousineau, B., Madrenas, J., and Desrosiers, M. (2016). Topical probiotics as a therapeutic alternative for chronic rhinosinusitis: a preclinical proof of concept. *Am. J. Rhinol. Allergy* 30, 202–205. doi: 10.2500/ajra.2016.30.4372

Snelling, A. M. (2005). Effects of probiotics on the gastrointestinal tract. *Curr. Opin. Infect. Dis.* 18, 420–426. doi: 10.1097/01.qco.0000182103.32504.e3

Song, A. A., In, L. L. A., Lim, S. H. E., and Rahim, R. A. (2017). A review on *Lactococcus lactis*: from food to factory. *Microb. Cell Fact.* 16:55. doi: 10.1186/s12934-017-0754-1

Stephenson, M. F., Mfuna, L., Dowd, S. E., Wolcott, R. D., Barbeau, J., Poisson, M., et al. (2010). Molecular characterization of the polymicrobial flora in chronic rhinosinusitis. *J. Otolaryngol. Head Neck Surg.* 39, 182–187.

Stjarne, P., Olsson, P., and Alenius, M. (2009). Use of mometasone furoate to prevent polyp relapse after endoscopic sinus surgery. *Arch. Otolaryngol. Head Neck Surg.* 135, 296–302. doi: 10.1001/archoto.2009.2

Stoikes, N. F., and Dutton, J. M. (2005). The effect of endoscopic sinus surgery on symptoms of eustachian tube dysfunction. *Am. J. Rhinol.* 19, 199–202. doi: 10.1177/194589240501900214

Van Zele, T., Claeys, S., Gevaert, P., Van Maele, G., Holtappels, G., Van Cauwenberge, P., et al. (2006). Differentiation of chronic sinus diseases by measurement of inflammatory mediators. *Allergy* 61, 1280–1289. doi: 10.1111/j.1398-9995.2006.01225.x

Wagner Mackenzie, B., Waite, D. W., Hoggard, M., Douglas, R. G., Taylor, M. W., and Biswas, K. (2017). Bacterial community collapse: a meta-analysis of the sinonasal microbiota in chronic rhinosinusitis. *Environ. Microbiol.* 19, 381–392. doi: 10.1111/1462-2920.13632

Weiss, S., Xu, Z. Z., Peddada, S., Amir, A., Bittinger, K., Gonzalez, A., et al. (2017). Normalization and microbial differential abundance strategies depend upon data characteristics. *Microbiome* 5:27. doi: 10.1186/s40168-017-0237-y

Wolvers, D., Antoine, J. M., Myllyluoma, E., Schrezenmeir, J., Szajewska, H., and Rijkers, G. T. (2010). Guidance for substantiating the evidence for beneficial effects of probiotics: prevention and management of infections by probiotics. *J. Nutr.* 140, 698S—712S. doi: 10.3945/jn.109.113753

Wright, E. D., and Agrawal, S. (2007). Impact of perioperative systemic steroids on surgical outcomes in patients with chronic rhinosinusitis with polyposis: evaluation with the novel Perioperative Sinus Endoscopy (POSE) scoring system. *Laryngoscope* 117(11 Pt 2 Suppl. 115), 1–28. doi: 10.1097/MLG.0b013e31814842f8

Zhou, J. C., and Zhang, X. W. (2019). Akkermansia muciniphila: a promising target for the therapy of metabolic syndrome and related diseases. *Chin. J. Nat. Med.* 17, 835–841. doi: 10.1016/S1875-5364(19)30101-3

Conflict of Interest: MD is the founder of Probionase Therapies Inc., a start-up company founded following the conclusion of this trial to develop probiotic bacteria for therapeutic purposes.

The remaining authors declare that the research was conducted in the absence of any commercial or financial relationships that could be construed as a potential conflict of interest.

frontiers in Cellular and Infection Microbiology

REVIEW
published: 26 November 2020
doi: 10.3389/fcimb.2020.583418

The Fungal Microbiome and Asthma

Erik van Tilburg Bernardes[1,2†], *Mackenzie W. Gutierrez*[1,2†] *and Marie-Claire Arrieta*[1,2*]

[1] Department of Physiology and Pharmacology, Snyder Institute for Chronic Diseases, University of Calgary, Calgary, AB, Canada, [2] Department of Pediatrics, Alberta Children's Hospital Research Institute, University of Calgary, Calgary, AB, Canada

Asthma is a group of inflammatory conditions that compromises the airways of a continuously increasing number of people around the globe. Its complex etiology comprises both genetic and environmental aspects, with the intestinal and lung microbiomes emerging as newly implicated factors that can drive and aggravate asthma. Longitudinal infant cohort studies combined with mechanistic studies in animal models have identified microbial signatures causally associated with subsequent asthma risk. The recent inclusion of fungi in human microbiome surveys has revealed that microbiome signatures associated with asthma risk are not limited to bacteria, and that fungi are also implicated in asthma development in susceptible individuals. In this review, we examine the unique properties of human-associated and environmental fungi, which confer them the ability to influence immune development and allergic responses. The important contribution of fungi to asthma development and exacerbations prompts for their inclusion in current and future asthma studies in humans and animal models.

Keywords: asthma, allergic responses, immune development, microbiome, mycobiome, environmental fungi

OPEN ACCESS

Edited by:
Emily K. Cope, Northern Arizona University, United States

Reviewed by:
Lisa Stinson, University of Western Australia, Australia
Irina Leonardi, Cornell University, United States

****Correspondence:***
Marie-Claire Arrieta
marie.arrieta@ucalgary.ca

†These authors have contributed equally to this work

Specialty section:
This article was submitted to Microbiome in Health and Disease, a section of the journal Frontiers in Cellular and Infection Microbiology

Received: *14 July 2020*
Accepted: *29 October 2020*
Published: *26 November 2020*

Citation:
van Tilburg Bernardes E, Gutierrez MW and Arrieta M-C (2020) The Fungal Microbiome and Asthma. Front. Cell. Infect. Microbiol. 10:583418. doi: 10.3389/fcimb.2020.583418

INTRODUCTION

Asthma is one of the most common immune-mediated disorders affecting infants around the globe (Wong and Chow, 2008; Lai et al., 2009). Although a heterogeneous group of conditions, all asthma cases are characterized by chronic airway inflammation, bronchial hypersensitivity, and transient respiratory obstruction (Martinez and Vercelli, 2013). Asthma is routinely classified based on patient's immune status, with high serum levels of immunoglobulin E (IgE) or skin reactivity to common allergens in atopic asthmatics, and the absence of these in non-atopic patients (Pekkanen et al., 2012). Besides atopic/non-atopic classification, there are additional factors underlying asthma pathophysiology, resulting in distinct profiles of cellular infiltration in the airways, clinical symptoms, and treatments responses (Lotvall et al., 2011).

The immunology of asthma further highlights the complexity of this group of conditions. Asthma is classically considered an IgE-mediated, lymphocyte T helper 2 (Th2)-associated pathology, with an allergic inflammatory infiltrate characterized by eosinophils, mast cells, and $CD4^+$ T cells producing interleukin-4 (IL-4), IL-5, and IL-13 in the airways (Martinez and Vercelli, 2013). However, increased immune profiling in asthmatics has revealed diverse disease immune patterns of Th1, Th2, Th9, Th17 T cell subsets, and mixed immune responses (Lambrecht and Hammad, 2015).

The factors that drive the development of asthma and the heterogeneity of its underlying immune responses are likely a combination of genetic and environmental influences. However, only environmental factors are likely able to explain the rapid and increasing societal burden imposed

by asthma (van Tilburg Bernardes and Arrieta, 2017). Among these are factors directly and indirectly related to microbial exposures and perturbations during early life, such as respiratory infections (Stein et al., 1999; Busse et al., 2010; Olenec et al., 2010), antibiotic use (Marra et al., 2009; Russell et al., 2012; Patrick et al., 2020), birth by Caesarean section (Thavagnanam et al., 2008; Roduit et al., 2009; Darabi et al., 2019), reduced breastfeeding (Nagel et al., 2009; Kull et al., 2010), urban (vs. farm) upbringing (Wong and Chow, 2008; Lawson et al., 2011; Lawson et al., 2017), and pet exposures (Hugg et al., 2008; Fall et al., 2015). Human studies have linked these factors to distinct patterns of early-life microbial colonization that precede asthma and similar atopic disorders (Bisgaard et al., 2007; Arrieta et al., 2015; Fujimura et al., 2016; Arrieta et al., 2018), suggesting that the large community of microbes that colonize the intestinal and respiratory mucosae is an influential element in asthma pathogenesis.

While initial methods applied in microbiome studies mainly supported the survey of bacterial communities, advances in methodologies and extended curation of taxonomic reference databases to amplify, sequence, and classify the small subunit ribosomal RNA gene (18S) and internal transcribed spacer (ITS) marker have also allowed for the characterization of fungi within the microbiome (Huseyin et al., 2017; Hoggard et al., 2018). These have confirmed that, just like bacteria, fungi are also linked to asthma and atopy (Crameri et al., 2014; Fujimura et al., 2016; Arrieta et al., 2018; Goldman et al., 2018).

As ubiquitous members of terrestrial and aquatic ecosystems, fungi are part of the complex community of microorganisms that colonize mammalian epithelial and mucosal surfaces exposed to the environment (Nash et al., 2017; van Tilburg Bernardes et al., 2020). Current microbiome research has attributed fundamental roles to the bacterial microbiome in colonization resistance, nutrition, and providing neurological and immunoregulatory signals for normal host development [reviewed in (Dominguez-Bello et al., 2019) and (Cryan et al., 2019)]. However, the fungal microbiome, known as the mycobiome, has recently started to gain attention due to its important role in host health and disease (Huseyin et al., 2017).

Throughout infant development, and in parallel with the establishment of the bacterial microbiome, the mycobiome encounters ecological pressures and undergoes substantial compositional changes (**Figure 1**) (Fujimura et al., 2016; Laforest-Lapointe and Arrieta, 2017; Ward et al., 2018). Despite being outnumbered by orders of magnitude by the bacterial microbiome, the mycobiome elicits important immunomodulatory functions throughout early-life development (Kumamoto, 2016; Michalski et al., 2017; van Tilburg Bernardes et al., 2020). For example, our recent work showed that early-life fungal colonization distinctly altered innate and adaptive immune features, and impacted colitis onset and asthma development in gnotobiotic mice (van Tilburg Bernardes et al., 2020), supporting that fungal-derived microbial signals are important in host immune development.

Gut mycobiome studies in infant populations have found significant associations between mycobiome alterations and subsequent asthma and atopy susceptibility (Fujimura et al., 2016; Arrieta et al., 2018). Like bacteria, gut fungi also respond to environmental perturbations, such as antibiotic treatment (Samonis et al., 1993; Azevedo et al., 2015), which is a strong risk factor for asthma development in children (Marra et al., 2009; Martel et al., 2009; Murk et al., 2011; Arrieta et al., 2018). Further, several species of fungi are triggers of asthma and other atopic disorders (Denning et al., 2006; Agarwal and Gupta, 2011; Crameri et al., 2014), suggesting a role for fungi as part of the

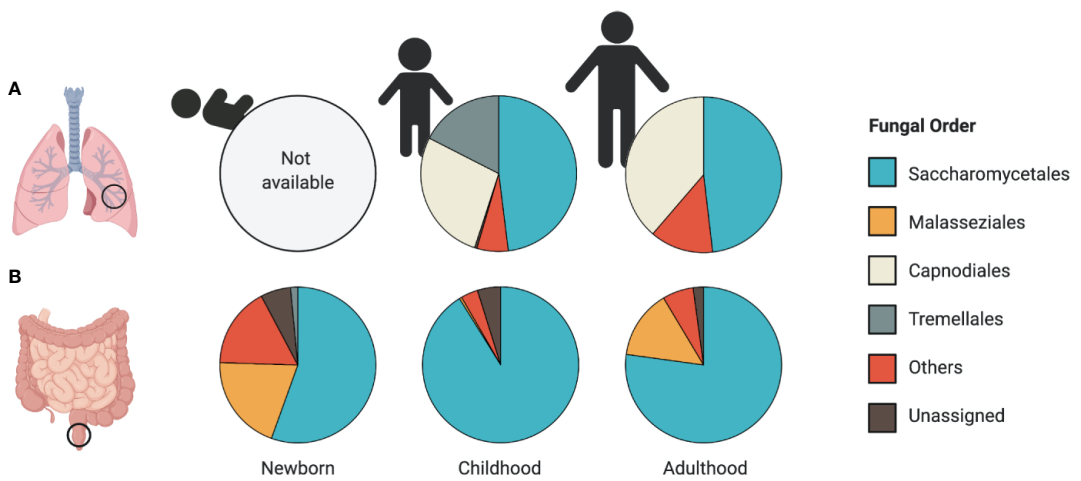

FIGURE 1 | Patterns of airway and intestinal mycobiome development. Relative abundance plots of the most abundant fungal taxa at the Order level reported in **(A)** airway and **(B)** stool samples. **(A)** A lack of human studies assessing the mycobiome composition in the airways of newborns limits our understanding of early-life patterns of human airway colonization. Airway mycobiome studies in children (average age, 5.2 years old) and adults (average age, 35.7 years) revealed dominance by Saccharomycetales, along with a large proportion of environmental fungi from the Capnodiales order. **(B)** Early patterns of fungal colonization in neonatal stool reveal a high representation of Malasseziales and Saccharomycetales orders (average age 1 month). The stool mycobiome of children (average age 11 months) and adults (average age 27 years) is dominated by Saccharomycetales. Data presented from studies: **(A)** (van Woerden et al., 2013; Goldman et al., 2018) **(B)** (Fujimura et al., 2016; Nash et al., 2017; Ward et al., 2018).

microbial exposures relevant in both asthma development and exacerbations. In the following sections we will review the current literature on gut, lung, and environmental fungi, their implications on asthma susceptibility and manifestations, the mechanisms by which fungi can mediate the development and persistence of this disease, as well as potential treatment options for asthma that target the mycobiome and mycobiome-induced immunity.

THE INTESTINAL MYCOBIOME

Sequence-based studies have allowed for the characterization of the intestinal mycobiome composition, defining its trajectory throughout life stages, and identifying associations with disease susceptibility. The first culture-independent study of the mycobiome in mammals revealed broad fungal diversity in the murine gut. Scupham et al. (2006), using oligonucleotide fingerprinting of ribosomal RNA (rRNA) genes, identified all major fungal phyla: *Ascomycota*, *Basidiomycota*, *Chytridiomycota*, and *Zygomycota* in the luminal content of laboratory mice (Scupham et al., 2006).

Further efforts to characterize these fungal communities led to a longitudinal study in 15 healthy children from Luxembourg that evaluated the intestinal mycobiome throughout the first year of life, using the 18S rRNA marker gene (Wampach et al., 2017). Stool from 1-day old babies revealed markable fungal diversity detected in meconium samples, suggesting that fungal colonization starts as early as bacterial colonization. From all microeukaryote operational taxonomic units (OTUs) identified in meconium samples, *Saccharomyces* spp. and *Exobasidiomycetes* spp. represented the most abundant and most frequently detected across samples, respectively (Wampach et al., 2017). Their work also demonstrated that, similar to bacteria, mode of birth influences fungal communities, with a higher abundance of *Saccharomyces* spp. and *Exobasidiomycetes* spp. in Caesarean-delivered infants, and higher *Dothideomycetes* spp. and *Pezizomycotina* in vaginally-delivered infants (Wampach et al., 2017). Although, in contrast with what has been described for bacterial succession patterns in the infant microbiome, fungi followed more aleatory temporal shifts in community composition, as evidenced by higher interindividual variation in fungal richness (number of OTUs), diversity (Shannon index), and evenness (Pielou's evenness index) (Wampach et al., 2017). It is important to mention that most published microbiome results are based on comparisons of taxa relative abundance, which are notoriously biased, especially in samples with low microbial biomass. Wampach et al. (2017) demonstrated that samples with very low DNA yields, such as meconium, underestimated richness and altered relative abundance measurements in a 16S dataset. It is to be expected that similar deviations also occur in the mycobiome, especially considering their even lower biomass. Thus, additional methods to quantify total fungal DNA or taxa-specific DNA *via* quantitative PCR (qPCR) can provide necessary technical benchmarks to better interpret amplicon-based sequencing results.

In another study that included 17 healthy term Puerto Rican infants, the fecal mycobiome was dominated by only five fungal species: *Candida albicans*, *C. parapsilosis*, *C. tropicalis*, *Saccharomyces cerevisiae*, and *Cryptococcus pseudolongus*, with the first four species encompassing more than 10% relative abundance each (Ward et al., 2018). This study also showed high intraindividual diversity and no clear common trajectory toward a mature/differentiated community within 30 days of sampling (Ward et al., 2018), suggesting that there is a higher degree of stochasticity influencing the mycobiome composition during the initial colonization process of the human gut compared to bacteria.

A larger prospective study evaluated the mycobiome of 308 US infants using ITS2 sequencing (Fujimura et al., 2016). Participant age significantly impacted the fungal α- and β-diversity, with fungal α-diversity decreasing with age up to one-year. The neonatal mycobiome (~1 month of age) was dominated by *Malassezia* and *Saccharomyces*, and later shifted toward dominance by *Saccharomyces* and *Candida* at ~11 months of age (**Figure 1B**) (Fujimura et al., 2016). In contrast to the bacterial microbiome, which reaches full maturity after month 31 of life (Stewart et al., 2018), the fungal community composition is likely more stable after one year of age, as it is similar to the healthy mycobiome compositions reported in adults (Nash et al., 2017). However, this remains to be confirmed in longer longitudinal studies.

To characterize the composition of the adult intestinal mycobiome, Nash et al. (2017) sequenced the ITS2 and 18S genes in the first large mycobiome study in healthy adults, with a total of 317 participants. This study also highlighted the dominance of yeasts *Saccharomyces*, *Malassezia*, *Candida*, *Cyberlindnera*, *Pichia*, *Debaryomyces*, *Galactomyces*, and *Clavispora*, as well as the common presence of filamentous fungi, *Penicillium*, *Cladosporium*, *Aspergillus*, *Fusarium*, and *Alternaria* in the adult intestinal mycobiome (Nash et al., 2017). The high intra- and interindividual variation also reported in this study suggests that while fungi are common colonizers of the human gut, the specificity of the host-fungal species relationships may be less conserved or may involve less species compared to bacteria. This characteristic of the mycobiome introduces challenges to identify specific fungal taxa that may be associated with human diseases.

THE AIRWAY MYCOBIOME

No longer considered sterile organs, the lungs harbor a diverse community of microorganisms, including fungi (Nguyen et al., 2015). There are very few studies looking into the fungal communities present in the lungs and airways of healthy individuals, and to our knowledge no studies have looked into these communities early in life to assess mycobiome establishment or associations with disease development **(Figure 1A)**. Work by Charlson et al. (2012) reported the presence of fungal communities in bronchoalveolar lavage (BAL) and oropharyngeal wash (OW) samples of six healthy individuals. Fungal communities in OW samples from these healthy volunteers were dominated by fungal species previously characterized in the oral cavity, including *Candida* and

Aspergillus (Ghannoum et al., 2010). Fungi detected in BAL samples of these individuals revealed lower fungal amounts compared to OW, with several reads belonging to the genera *Davidiellaceae*, *Aspergillus*, *Penicillium*, and *Polyporales*, suggesting that fungal colonizers are present at lower concentration in the alveolar regions of the lungs compared to the upper airways (Charlson et al., 2012).

A study by Mac Aogain et al. (2018) further described the airway mycobiome composition in sputum samples of 238 bronchiectasis patients and 10 healthy controls from Asia and Europe. Fungal communities in the sputum of healthy controls were dominated by the *Ascomycota* phylum, with *Candida*, *Saccharomyces*, and *Meyerozyma* as the most commonly detected taxa (Mac Aogain et al., 2018). However, it should be noted that this study did not control for possible contamination of sputum samples with members of the oral mycobiome community, which frequently contains *Candida*, *Saccharomycetales*, *Cladosporium*, among others (Ghannoum et al., 2010). This important consideration is necessary for a reliable characterization of the respiratory mycobiome in infants and adults.

Several more studies have described fungal alterations in the context of chronic respiratory diseases, including asthma. Goldman et al. (2018) analyzed the mycobiome of BAL samples obtained from 15 severe asthmatic children and 11 non-asthmatic controls. Taxonomic analysis revealed 7 fungal genera differentially abundant between groups. Non-asthmatic children had increased abundance of *Davidiella*, *Cryptococcus*, and *Sterigmatomyces*, while children with severe asthma had increased abundance of *Rhodosporidium*, *Pneumocystis*, *Leucosporidium*, and *Rhodotorula* (Goldman et al., 2018). While informative and descriptive of microbial signatures in this asthmatic population, this study remains unable to determine if these specific airway mycobiome signatures are causally implicated in asthma development.

Mycobiome alterations have also been reported in asthmatic adults. A study by van Woerden et al. (2013) reported significant mycobiome compositional changes in induced sputum from 30 asthmatic adults and 13 healthy controls. A more recent study on endobronchial brush (EB) and BAL samples from 39 asthmatic adults and 19 healthy controls further associated mycobiota signatures with specific asthma phenotypes and clinical parameters (Sharma et al., 2019). This study found a decrease in fungal α-diversity (Shannon and Inverse Simpson indices), as well as an over-representation of *Trichoderma*, *Alternaria*, *Cladosporium*, *Penicillium*, and *Fusarium* in asthmatics, while health controls harboured increased abundances of *Blumeria*, *Mycosphaerella*, and different species from the *Fusarium* genera (Sharma et al., 2019). Interestingly, generalized linear regression models also found significant correlations between the abundance of exact sequence variants (ESV) of *Fusarium*, *Aspergillus*, *Cladosporium*, and *Alternaria* with Th2-high asthma (defined by blood eosinophil count >300/μL), *Cladosporium* and *Fusarium* with atopic-asthma (atopic status defined by allergic sensitization tests, skin prick test, or immunosorbent assay), and ESVs from Aspergillaceae, *Mycosphaerella*, and *Cladosporium* with non-atopic-asthma (Sharma et al., 2019). This important finding links distinctive airway mycobiome patterns with the pathophysiological mechanism of asthma. However, this and other microbiome studies in asthmatics (Chatterjee et al., 2008; van Woerden et al., 2013; Goldman et al., 2018; Sharma et al., 2019) are likely confounded by the inflammatory process of the disease itself, as well as its treatments, which can also differ according to asthma immune endotypes. Determining causality and directionality in these associations is important and requires prospective studies of children preceding and following asthma development, as well as longitudinal sampling of asthmatics during exacerbation and remission of asthma manifestations.

EARLY-LIFE FUNGAL EXPOSURES AND ASTHMA SUSCEPTIBILITY

Observations from population-based and animal studies suggest that there is a critical window of opportunity, in which bacterial alterations during early life are important determinants of subsequent asthma susceptibility (Russell et al., 2012; Stiemsma and Turvey, 2017; Sokolowska et al., 2018). Unsurprisingly, the same applies to the mycobiome. Data from animal studies has demonstrated that common gut fungal colonizers can modulate the immune system and predispose the host to allergic airway inflammation. Antimicrobial-induced mycobiome alterations and intestinal expansion of *C. albicans* (Noverr et al., 2004; Noverr et al., 2005), *C. parapsilosis* (Kim et al., 2014), or *Wallemia mellicola* (Skalski et al., 2018) increased the severity of allergic airway inflammation in mice. Expansion of filamentous fungi (*A. amstelodami*, *Epicoccum nigrum*, and *W. sebi*) following antifungal treatment also exacerbated allergic airway responses in experimental mouse models (Wheeler et al., 2016; Li X. et al., 2018). Immune characterizations in these studies revealed that fungal-derived signals modulate airway inflammation by inducing alternative macrophage polarization to an M2 phenotype in the murine lungs (Kim et al., 2014), elevating RORγt$^+$ and GATA3$^+$ CD4$^+$ T cells (Li X. et al., 2018), and increasing Th2 immunity in the airways (Noverr et al., 2004; Noverr et al., 2005; Wheeler et al., 2016; Li X. et al., 2018; Skalski et al., 2018). These studies suggest that alterations to gut fungal communities can increase host predisposition to airway allergic inflammation.

Prospective human cohort studies have investigated early life sensitization to fungal antigens on asthma development later in life. A longitudinal cohort study of 849 children by Stern et al. (2008) found that sensitization to *A. alternata* prior to six years of age was independently associated with chronic asthma by 22 years of age. Harley et al. (2009) reported that air levels of *Ascomycota* and *Basidiomycota* spores within the first 3 months of life are positively correlated with increased wheeze development, pointing to a possible role of airborne fungal spores in early-life immune sensitization events that lead to asthma.

Observations from prospective infant cohort studies that have investigated the gut mycobiome suggest similar implications for

asthma susceptibility. Following observations from a Canadian cohort study which associated early-life microbial alterations with later susceptibility to asthma development (Arrieta et al., 2015), Arrieta et al. (2018) surveyed the bacterial and fungal microbiome in infants from a rural district in Ecuador. This study analyzed stool samples collected at 3 months of age, from 27 children with atopic/wheeze phenotype at 5 years of age and 70 healthy controls. Fecal samples from the infants that later developed atopic/wheeze revealed a higher proportion of total sequenced fungal reads, significantly increased fungal 18S recovered DNA, and overrepresentation of *Pichia kudriavzevii* at 3 months of age (Arrieta et al., 2018), suggesting a link between gut fungal overgrowth preceding asthma and revealing fungal alterations associated with increased child susceptibility to asthma development by school age.

Similarly, Fujimura et al. (2016) identified specific fungal genera correlated to an increased susceptibility to allergic asthma. Using a Dirichlet Multinomial Mixture model to separate participants into defined microbial community types, the study reported that a microbial profile depleted of *Malassezia* and enriched with Saccharomycetales, *Rhodotorula*, Pleosporales, and *Candida* had an increased relative risk of atopy diagnosis by two years of age, and parental reported doctor–diagnosed asthma at four years (Fujimura et al., 2016). This microbial composition was also associated with the pro-inflammatory metabolite 12,13-dihydroxy-9Z-octadecenoic acid (12,13-DiHOME). Sterile fecal water from this high-risk group and 12,13-DiHOME increased $CD4^+IL4^+$ T cells and decreased $CD4^+CD25^+FOXP3^+$ T cells in *ex vivo* culture of human peripheral T cells (Fujimura et al., 2016). This strongly suggests that dysregulation in immune tolerance mechanisms that occur very early in life originate from what Fujimura et al. (2016) referred to as "interkingdom microbiota dysbiosis."

Both of these infant cohort studies (Fujimura et al., 2016; Arrieta et al., 2018) support that fungal alterations are an important part of the dysbiotic patterns predicting subsequent susceptibility to allergic diseases in children. Although majorly outnumbered by bacteria in the microbiome, this may imply that fungi provide important immune signals that, when imbalanced, can lead to immune dysregulation and pediatric asthma development. It remains to be determined how mycobiome alterations originate but it is possible that similar environmental factors known to induce bacterial perturbations are at play. For example, these imbalances may arise from antibiotic exposure, which are known to induce fungal dysbiosis and increase airway inflammation in animal studies (Noverr et al., 2004; Noverr et al., 2005; Kim et al., 2014; Skalski et al., 2018). Antibiotic use during early life has been repeatedly identified as a risk factor to atopy and asthma (Marra et al., 2009; Martel et al., 2009; Murk et al., 2011; Arrieta et al., 2015), suggesting that fungal overgrowth and/or dysbiosis may be part of the collateral microbiome damage caused by antibiotic use during infancy **(Figure 2).** This is further supported in humans by observations that antimicrobial induced fungal overgrowth was associated with an increased risk of allergic asthma development in infants (Arrieta et al., 2018). These early-life mycobiome alterations and fungal overgrowth following environmental perturbations might augment fungal immune recognition or allow for increased secretion of fungal-derived virulence factors. Recognition of these factors by immune cells

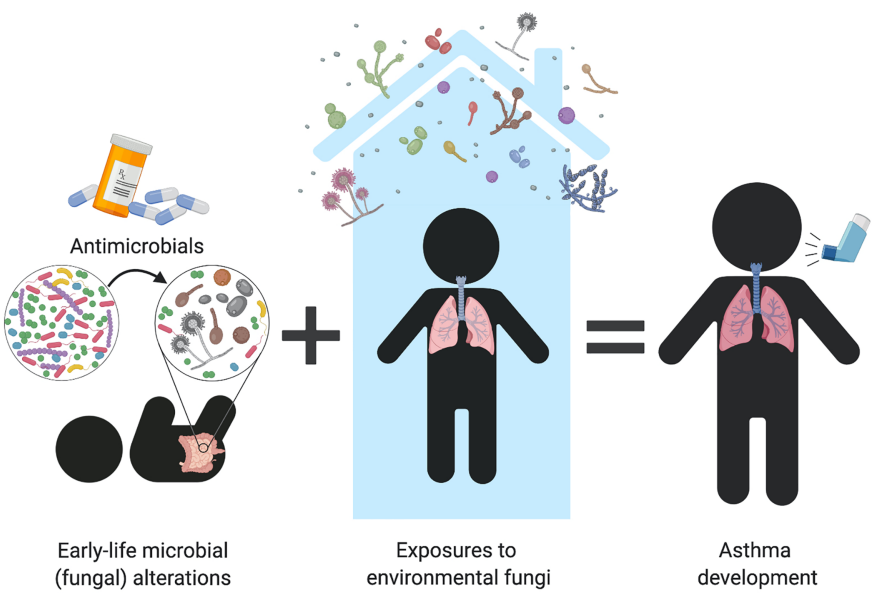

FIGURE 2 | Can early-life fungal dysbiosis contribute to increased pediatric asthma risk? Early-life gut fungal alterations provide immunomodulatory signals that increase infant's susceptibility to asthma. Infant antimicrobial use disrupts the intestinal microbiome and favors fungal overgrowth, which has been associated with allergic airway inflammation in both human and animal studies. Early-life mycobiome dysbiosis may contribute to dysregulated immune mechanisms that lead to immune sensitization to environmental fungi, resulting in fungi-triggered asthma in children and adults.

may induce immunological imbalances that predispose infants to asthma development (further discussed in "Fungal-mediated immune mechanisms in asthma" section).

The increase in prospective and longitudinal infant gut microbiome studies, together with the inclusion of fungi in these surveys is consistently revealing gut bacterial and fungal alterations that may be involved in asthma pathogenesis. However, it is also likely that the lung mycobiome plays a role in altering lung immune responses. Because of the lack of animal or human studies examining the lung mycobiome and its relation to immune development, it remains unknown if succession patterns of lung fungal colonization during infancy, and alterations to these, may also contribute to asthma pathogenesis.

ENVIRONMENTAL FUNGAL EXPOSURES AND ASTHMA DEVELOPMENT

Understanding the effect of diverse fungal exposures early in life is important because we are continuously in contact with environmental fungi which are capable of influencing human immune responses. Fungal spores are dispersed through indoor (Qian et al., 2012; Adams et al., 2013; Barberan et al., 2015) and outdoor air (Wyatt et al., 2013). Additionally, fungi have been detected in high levels on indoor surfaces, by both culture-dependent [25-130 CFU/mg of dust samples (Behbod et al., 2015)] and culture-independent [17-271 OTU detected in dust samples (Adams et al., 2013)] approaches. These environmental exposures likely shape the composition of the lung and gut mycobiome, as evidenced by a high representation of environmental fungi in the airways of adults (van Woerden et al., 2013), as well as the compositional changes in the intestinal mycobiome that parallels that of the surrounding environment (Dollive et al., 2013).

While several studies generalize fungal airway exposures as conducive to atopy and asthma development, others have shown that fungi may play a role in both reducing or increasing the risk of atopy and asthma in early life. For example, findings from Behbod et al. (2015) suggest that compartmental differences in exposure to fungi in early life may influence development of allergic asthma. In this study, increased overall yeast concentration in house dust from the homes of 408 infants of 2-3 months of age, was negatively associated with the development of wheeze and asthma by 13 years of age [hazard ratio (HR) = 0.88 and 0.86, respectively]. In contrast, indoor airborne *Alternaria* increased asthma risk (HR=1.48) (Behbod et al., 2015). The authors propose that this may result from the development of immune tolerance toward yeasts from gut exposures via hand-to-mouth behaviors during early life (Behbod et al., 2015), which may not occur to the same extent with airborne fungi. This interesting possibility remains to be tested experimentally.

In a systematic review of 61 studies conducted by Tischer et al. (2011), visible mould exposure was consistently associated with different reports of asthma, wheeze, and allergic rhinitis [odds ratio (OR) = 1.49, 1.68, and 1.39, respectively]. However, when fungal exposure was further stratified to evaluate specific fungal components, (1,3)-β-D-glucan and extracellular polysaccharides, ubiquitously secreted by most fungal species, were inversely associated with wheeze and asthma in children (Tischer et al., 2011), highlighting that fungal exposure should not be aggregated as a single study variable. Altogether, these findings prompt for more robust methods to investigate the epidemiology and mechanisms by which environmental fungal exposures in early life may influence asthma development or protection.

In addition to asthma development, fungal environmental exposures have also been consistently linked to specific asthma phenotypes. A study by Dannemiller et al. (2016a) found asthma severity and atopic status linked to higher fungal detection in house dust. This cohort of 587 asthmatic children in Connecticut and Massachusetts, revealed a positive association between asthma severity and increased summed concentration of fungal species, including *A. alternata*, *C. albicans*, *C. cladosporioides*, *P. brevicompactum*, *M. sympodialis*, and *R. mucilaginosa* (Dannemiller et al., 2016a; Dannemiller et al., 2016b). Notably, while fungal community composition was not different among the houses of children with mild or severe non-atopic asthma, fungal communities from houses of children with mild atopic asthma had higher abundance of fungi from genus *Vellutella* (Dannemiller et al., 2016a). These observations provide support for the role of environmental fungi as environmental cues capable of modulating the tone and immune phenotype of asthma in children (**Figure 2**). While experimental evidence in animal models is still needed to confirm causality in these observations, the environmental nature of these exposures renders them less susceptible to biological confounding effects, and strongly suggest that these may be involved in the initial allergic sensitizations that lead to asthma development.

FUNGI IN ASTHMA EXACERBATIONS

Not only does fungal exposure during early life play a role in asthma development, but fungal exposures are also well known to induce or exacerbate episodes in asthmatic patients. A large study that included 831 US homes found *A. alternata* in house dust to be correlated with active asthma symptoms (Salo et al., 2006). Sharpe et al. (2015) also identified widespread associations between indoor presence of *Cladosporium*, *Alternaria*, *Aspergillus*, and *Penicillium* and increased asthma exacerbation in adults and children through random-effect estimates in a meta-analysis of 7 studies, suggesting that fungal exposures are conducive to asthma exacerbations, and have implications for disease severity and management.

Sensitization due to previous exposure to specific fungal species is likely to play a role in subsequent exacerbations. In a study on adults hospitalized for asthma, Niedoszytko et al. (2007) found associations between skin prick test sensitization to *Helminthosporium* and *A. pullulans* with increased asthma exacerbations and severity, respectively. Another study in adult asthmatics that harbored *A. fumigatus* in sputum reported an association between *A. fumigatus*-IgE sensitization and asthma severity, neutrophilia, and reduced lung function (Fairs et al., 2010).

A number of studies have also investigated the relationship between exposure and sensitization to fungi and asthma

exacerbation during childhood. A study of 280 children from 37 inner-city schools in Boston, U.S.A. found that exposure to *Alternaria* in classrooms was associated with increased duration of asthma symptoms in children already sensitized to *Alternaria*, compared to sensitized children with a lower classroom exposure level over a 2-week period (Baxi et al., 2019). Welsh et al. (2016) cultured the sputum from children with either acute exacerbation or stable asthma, and found increased concentrations of *A. fumigatus* in the sputum from children experiencing exacerbation, suggesting a role of this fungal species in asthma manifestations. Similarly, the Melbourne Air Pollen Children and Adolescent study found associations between asthma hospitalizations, outdoor total fungal spores, and levels of *Alternaria*, *Leptophaeria*, *Coprinus*, and *Drechslera*, in 644 asthmatics between the ages of 2 and 17 (Tham et al., 2017).

From these studies, it is clear that fungi play an important role in the exacerbation of asthma in children and adults, and that these often emerge from immune sensitization during infancy or childhood. Nonetheless, not all exposures to fungi result in asthma-inducing sensitizations, indicating that, just like with bacteria, many may indeed be protective, and that the underlying mechanisms of host-fungal immune crosstalk stem from the immunogenicity of specific fungal species and/or host immune susceptibilities. While it is evident that not all fungal exposures are detrimental to immune development, certain species, such as those belonging to the genera *Alternaria* and *Aspergillus*, are consistently associated with sensitization in asthmatics and asthma severity. As such, further research on the microbial and host immune mechanisms relevant to asthma pathogenesis should include fungi, both protective and harmful species, from the human microbiome and the environment.

FUNGI AS UNIQUE ALLERGENS

Why are certain fungi and their structures so frequently associated with asthma and other allergic diseases? While this remains unknown, fungi have unique properties that may provide them with the ability to increase asthma susceptibility and induce exacerbations in the host (**Figure 3**). Whether this

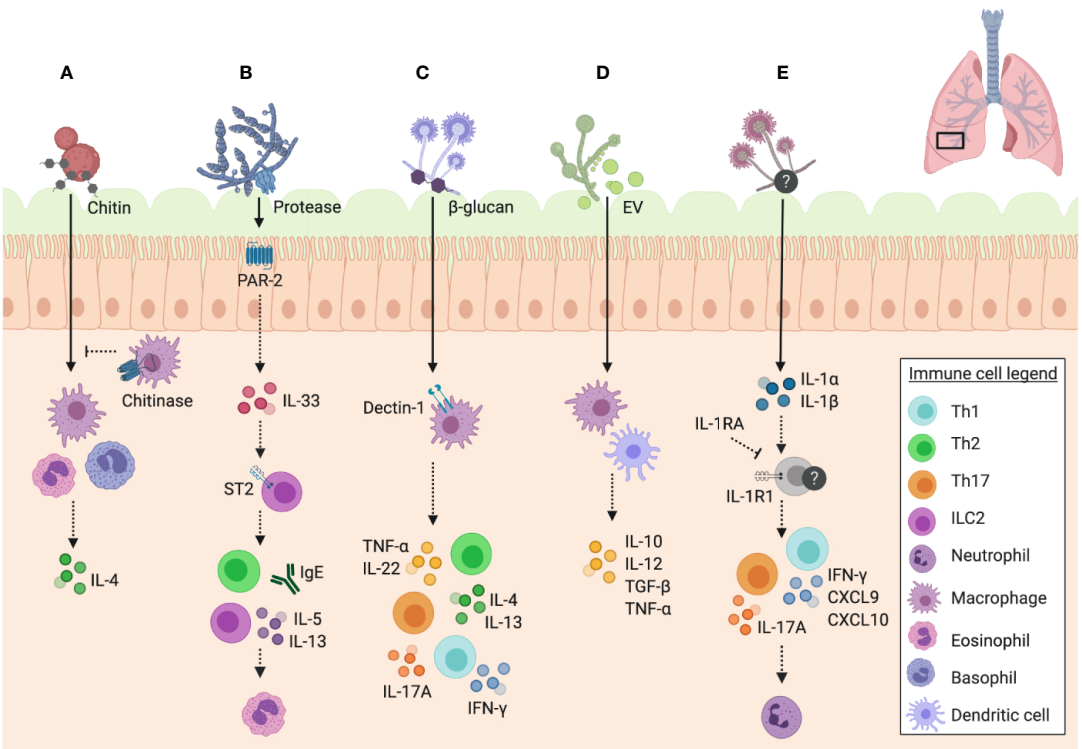

FIGURE 3 | Unique features of fungal immune responses in the airway. Schematic of the unique features of fungi and their interactions with immune mechanisms in the murine airway. **(A)** Chitin in fungal cell walls triggers alternative activation of macrophages (M2 phenotype) and IL-4 expressing eosinophil and basophil responses, which can be inhibited by mammalian chitinases. **(B)** Fungal proteases signal through PAR-2 in the airway epithelium resulting in the release of IL-33, which consequently signals through ST2 to trigger IgE and ILC2 release of IL-5 and IL-13, promoting eosinophil recruitment to the airway. **(C)** β-glucan recognition through dectin-1 on macrophages results in the release of TNF-α, as well as a mixed Th1/Th2/Th17 response with the release of IL-4 and IL-13 by Th2 cells, IFN-γ by Th1 cells, IL-17A by Th17 cells, and IL-22 detected in unfractionated lung cells. **(D)** Extracellular vesicles (EV) trigger the release of cytokines IL-10, IL-12, TGF-β, and TNF-α by macrophages and dendritic cells. **(E)** *A. fumigatus*-induced allergic airway inflammation in mice induces IL-1R1 signalling and Th1 (IFN-γ, CXCL9, and CXCL10) and Th17 responses, with IL-17A promoting neutrophil infiltration. IL-1RA inhibits these pathways downstream of IL-1R1. Data presented from studies: **(A)** Reese et al., 2007; Van Dyken et al., 2011; **(B)** Bartemes et al., 2012; Snelgrove et al., 2014; Castanhinha et al., 2015; Hiraishi et al., 2018 **(C)** Gersuk et al., 2006; Lilly et al., 2012; **(D)** Vargas et al., 2015; and **(E)** Godwin et al., 2019.

comes from earlier sensitization followed by subsequent hypersensitivity, or through direct immunomodulatory properties of fungi remains under debate. A study by Zhang et al. (2017) suggests that the ability of certain fungi to exacerbate asthma symptoms is independent of their capacity to act as initial sensitization allergens, and is reliant on the immunomodulatory abilities of certain fungal components. Specifically, the authors found that children in the Cincinnati Childhood Allergy and Air Pollution Study showed an association between fungal exposure and asthma prevalence in the absence of fungal sensitization (Zhang et al., 2017). These findings were further validated in mice, in which direct exposure to *A. versicolor*, without previous sensitization, resulted in enhanced airway inflammation in a house dust mite (HDM) model (Zhang et al., 2017).

Chitin, the second most common polysaccharide in nature (after cellulose), plays an important role in the development of asthmatic disease following airway exposure to fungi. Chitin is a major component of fungal cell walls, helminths, insects, and crustaceans, but it is not present in mammals (Lee et al., 2008). While mammals express chitinases to enzymatically break down chitin, the biological role of these enzymes in host biology remains incompletely understood. Mammalian chitinases are expressed at inflammation sites, and thus are hypothesized to play roles in host anti-microbial and anti-parasite responses (Lee et al., 2008). Interestingly, both chitin and chitinases are implicated in the pathophysiology of asthma, including fungal asthma (Lee et al., 2008; Shuhui et al., 2009).

A study by Van Dyken et al. (2011) found that while chitin induces an eosinophilic response, mice constitutively expressing a mammalian chitinase are able to limit eosinophilic infiltration following challenge with a fungal preparation derived from house dust (**Figure 3A**). Another study investigated the role of acidic mammalian chitinase (CHIA) in atopic asthma, through detection of polymorphisms of this gene in asthmatic patients in Northern India. The authors identified three specific promoter polymorphisms associated with atopic asthma, total serum IgE, or both, confirming the role of CHIA as an asthma susceptibility gene (Chatterjee et al., 2008). Additionally, Ober et al. (2008) identified *CHI3L1*, the gene encoding a chitinase-like protein (YKL-40) that had been previously associated with asthma severity, as another susceptibility gene for asthma. They specifically identified a single nucleotide polymorphism in the *CHI3L1* promoter region that could be used to predict asthma and serum YKL-40 levels (Ober et al., 2008). Similarly, a study by Wu et al. (2010) was able to identify an association between fungal exposure and specific chitinase single nucleotide polymorphisms in the context of asthma exacerbation as measured by emergency room visits. The relationship between the role of chitinases in recognizing fungi and the genetic susceptibilities of specific chitinase genes in asthma development hint at the capacity of fungi to elicit allergic airway responses, as well as the crucial role of chitinases in the resolution of this inflammation.

It has also been proposed that asthma occurs as a result of the Th2 reaction to fungi as a means to contain what the immune system recognizes as a fungal infection, and that fungal proteases are crucial to this response. The study by Porter et al. (2009) investigated the role of active proteases in the house dust of asthmatic children, in eliciting an airway response in mice. The study established that it was specifically fungal proteases, particularly from *A. niger*, which were found to be active in the house dust as opposed to proteases from other sources, such as mites (Porter et al., 2009). They also established that these proteases are required in combination with *A. niger* conidia to elicit a complete asthmatic disease phenotype, and that protease mutants are able to thrive based on a deficient ability to elicit an airway immune response characteristic of asthma (Porter et al., 2009). This emphasizes the role of unique fungal proteases in asthmatic disease.

A study by Snelgrove et al. (2014) was able to elucidate the underlying immunomodulatory mechanism of *A. alternata* serine proteases using a mouse model. They found that protease activity was absent in other common aeroallergens, and that the serine protease of *A. alternata* possesses signalling capabilities through protease activated receptor-2 (PAR-2) and adenosine triphosphate that results in the rapid airway release of IL-33 (**Figure 3B**). This was responsible for subsequent Th2 airway inflammation and other hallmarks of asthma exacerbation (Snelgrove et al., 2014). Interestingly, it has been found that PAR-2 is upregulated in the airway epithelium of asthmatics relative to healthy controls (Knight et al., 2001), an important piece of evidence for the role of fungal proteases in asthma exacerbation and the possibility of underlying genetic susceptibilities to fungal asthma. Furthermore, alkaline protease 1 (Alp1) of *A. fumigatus* was shown to directly disrupt interactions between airway smooth muscle cells and the extracellular matrix, resulting in airway hyper responsiveness in mice challenged with *A. fumigatus* extract with active Alp1 (Balenga et al., 2015). To investigate these findings in humans, lung samples were stained for Alp1, which was detected in the airway smooth muscle layer of non-atopic asthmatic patients (Balenga et al., 2015). A negative association was found between Alp1 levels and lung function (Balenga et al., 2015), hinting at the role of fungal proteases in airway disease. The underlying mechanisms of fungal protease ability to elicit airway diseases are slowly being uncovered, and are just one important aspect of fungi that makes them distinct to other aeroallergens.

Fungal immunogenicity in the airways may also depend on the life cycle stage of sporulating fungi at the point of exposure. Environmental fungi are often introduced into the airway as resting spores, and may not elicit an immune response until present in metabolically active germinating form. A study by Gersuk et al. (2006) found that alveolar macrophages are capable of distinguishing between resting and active forms of *A. fumigatus*, and that this process relies on recognition of cell wall β-glucans by the innate host receptor dectin-1 on macrophages (**Figure 3C**), resulting in tumor necrosis factor-α (TNF-α) production in order to limit inflammatory responses to active cells. The authors propose that this may be a protective immunological mechanism in order to prevent tissue damage in the absence of a true infectious threat (Gersuk et al., 2006). The ability to control allergic immune responses depending on their

metabolic state is another distinct feature of fungi, which likely confers an advantage to evade immune surveillance.

Like all existing cell types, fungi also have the capacity to secrete extracellular vesicles (EV), which may contribute to their immunomodulatory capacity for asthma development. EV carry enormous amounts of antigenic molecules, are known to modulate immune responses, and due to their elevated presence in experimental asthma models, are proposed to be involved in asthma pathogenesis (Nazimek et al., 2016). Joffe et al. (2016) refer to fungal EV as "virulence bags" based on their 'cargo', and highlight their potential use in vaccine development. Furthermore, Vargas et al. (2015) investigated the immunomodulatory activity of EV from *C. albicans*, a host-associated species with known links to asthma and allergic airway responses (Noverr et al., 2004; Noverr et al., 2005; Fujimura et al., 2016; van Tilburg Bernardes et al., 2020). The authors found that *C. albicans* EV are internalized by both macrophages and dendritic cells and stimulate the release of nitric oxide by macrophages and cytokines such as IL-10, IL-12, transforming growth factor-β (TGF-β), and TNF-α by both cell types (**Figure 3D**) (Vargas et al., 2015). While different studies show the implications of environmental bacteria-derived and host immune cell-derived EV in asthma pathogenesis (Nazimek et al., 2016), the immunomodulatory role of fungal-derived EV has yet to be investigated in the context of asthma.

A number of studies have looked into cross-reactivity between fungal species and the implication this has on airway disease. An early study by Hemmann et al. (1997) identified cross reactivity between *A. fumigatus* and *C. boidinii*, due to antigenic similarity, as well as *Candida* antigen's capacity to bind to IgE from *A. fumigatus* sensitized individuals. Furthermore, Bacher et al. (2019) established an important link between fungal colonization in the gut with susceptibility to fungal mediated airway inflammation. The authors found that *C. albicans* are the main drivers of the development of anti-fungal Th17 cells and provide protective anti-fungal Th17 responses to *C. albicans* in the gastrointestinal tract (Bacher et al., 2019). While *C. albicans*-induced Th17 response has been shown to protect from intestinal and systemic infection (Shao et al., 2019), a subset of these *C. albicans*-reactive Th17 cells are able to cross-react with *A. fumigatus* due to shared homology between certain antigenic peptides, resulting in a pathogenic Th17 response in the airway (**Figure 4A**) (Bacher et al., 2019). The study demonstrated expansion of cross-reactive Th17 cells in the lungs of patients with acute allergic bronchopulmonary aspergillosis, which contributes to exacerbation of airway hyperreactivity (Bacher et al., 2019). Interestingly, cross reactivity has also been proposed between fungal and human antigens. Denning et al. (2006) highlight the homology between a number of fungal and human proteins that result in a cross reactive response between fungi and self-antigens of the host, resulting in an auto-reactive response, which may further exacerbate asthma. Cross reactivity between different fungal species may be an important feature explaining asthma exacerbations to a wide variety of fungi. Importantly, this feature may also imply that the immunological responses to common fungal intestinal colonizers early in life play a fundamental role in airway hyperreactivity. This is further evidenced by data from our group, demonstrating that intestinal fungal colonization induces early-life immune changes, characterized by altered systemic levels of inflammatory cytokines IL-4, IL-6, IL-10, and IL-12, and regulatory T cells (Tregs), which exacerbates airway responsiveness with elevated macrophagic infiltration in an ovalbumin (OVA) challenge mouse model (**Figure 4B**) (van Tilburg Bernardes et al., 2020). Cross reactivity of immunological responses to fungal antigens with human proteins or environmental molecules also establishes fungal colonization as an important factor in the development and manifestation of asthma.

FUNGAL-MEDIATED IMMUNE MECHANISMS IN ASTHMA

The underlying immunological mechanisms that render fungi elicitive of asthmatic disease are highly complex, and there is likely an interplay among the many features of fungi that may help explain the diverse immunopathology of this disease. Allergic asthma is characterized by a Th2 response (Martinez and Vercelli, 2013), consistent with that seen in fungal asthma models. A study by Hoselton et al. (2010) found elevated serum IgE and pulmonary IL-4 levels along with a dramatic increase in leukocyte infiltration following *A. fumigatus* airway challenge of previously sensitized mice. Mannose-binding lectin (MBL) has also been shown to be crucial for early Th2 responses in an *A. fumigatus* mouse model of airway inflammation, such that mice deficient in MBL-A displayed a dampened Th2 cytokine response as well as pro-allergic chemokine expression (Hogaboam et al., 2004). Similarly, chitin found in fungal cell walls is associated with the induction of type 2 inflammation. Reese et al. (2007) found chitin exposure in the airways to be associated with recruitment of IL-4-expressing innate immune cells, eosinophils, and basophils, along with an M2 macrophage phenotype in mice relative to a saline-challenged control (**Figure 3A**). An increased chitin to β-glucan expression ratio in *A. fumigatus* strains resulted in greater eosinophil recruitment in a mouse model of airway inflammation, dependent on γδ-T cells, indicating the role of this T cell subset in the type 2 response to chitin (Amarsaikhan et al., 2017). Using *Ccr1*$^{-/-}$ mice, Blease et al. (2000) showed that C-C Motif Chemokine Receptor 1 (CCR1) signalling is necessary for Th2 responses and airway remodeling in a *A. fumigatus* model of airway inflammation, another mechanism by which fungi are capable of eliciting such airway response.

While Th2 responses are a hallmark of allergic asthma, they are just one component of the immune response involved in fungi driven asthmatic disease. IL-33 is an innate cytokine commonly found in the airways to be associated with asthma, and has been shown to be involved in group 2 innate lymphoid cell (ILC2) development (Bartemes et al., 2012) and airway remodeling with steroid resistance (Saglani et al., 2013). Mice exposed to *A. alternata* showed an elevation of IL-5 and IL-13 derived from ILC2 along with eosinophilia (**Figure 3B**), which was diminished in the absence of ST2 (IL-33 receptor) signalling,

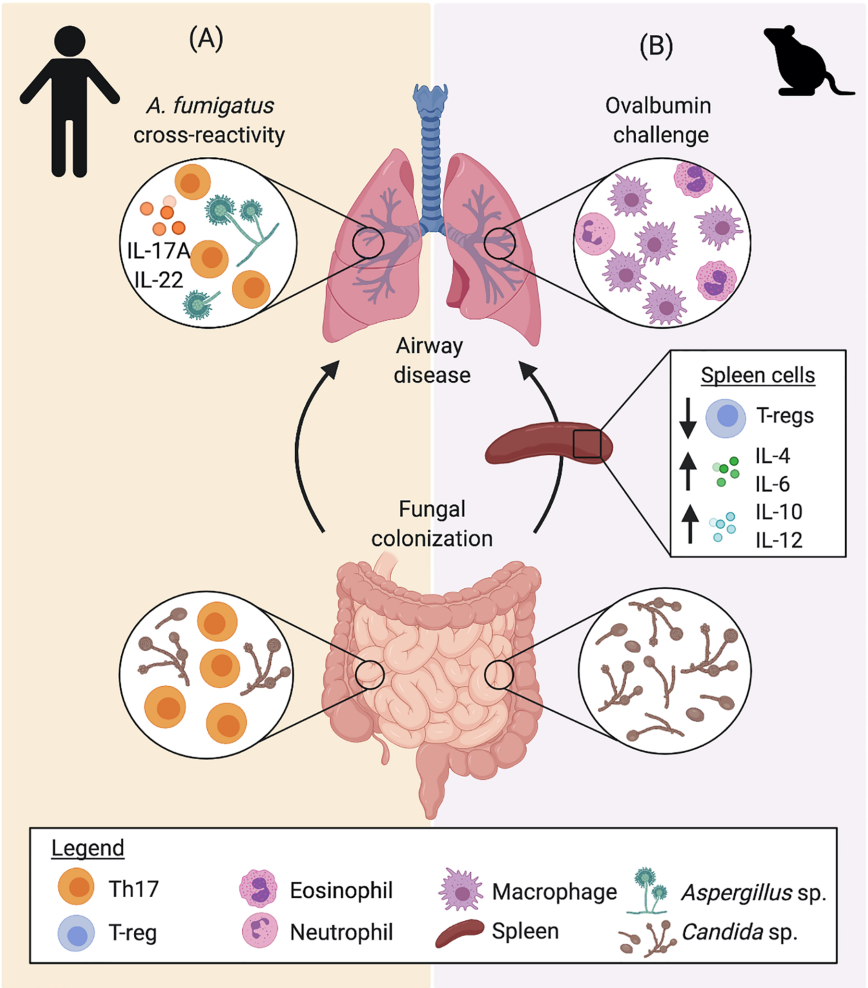

FIGURE 4 | The gut-lung crosstalk in airway inflammation. Gut, systemic, and lung immune responses to *Candida* sp. colonization have been described in **(A)** humans and **(B)** mice, indicating that intestinal fungi impact immune development and that airway immune responses to other fungi and allergens (ovalbumin), respectively. **(A)** Protective $CD4^+$ memory T cells generated from colonization by *C. albicans* secrete elevated levels of IL-17A and IL-22. Upon exposure to *A. fumigatus*, homology between fungal antigens directs the selective expansion of *A. fumigatus*-reactive cells, driving Th17 airway inflammation. **(B)** In mice, intestinal fungi colonization alters early life immune development, inducing increased systemic levels of IL-4, IL-6, IL-10, and IL-12, while reducing the proportion of Tregs. Colonization with fungi also increased airway inflammation in an ovalbumin challenge model, altering the inflammatory phenotype with increased macrophagic infiltration in BAL fluid. Data presented from studies: **(A)** Bacher et al., 2019; and **(B)** van Tilburg Bernardes et al., 2020.

further implicating innate immune mechanisms in fungal asthma (Bartemes et al., 2012). Children with severe asthma with fungal sensitization (SAFS) have greater IgE titers and an association with elevated IL-33 (Castanhinha et al., 2015). When investigated in a neonatal mouse model, *A. alternata* exposure resulted in greater airway IL-33, IL-13-producing ILC, and Th2 cells along with elevated serum IgE independent of corticosteroid treatment, compared to HDM exposure (Castanhinha et al., 2015). These effects were diminished in mice lacking a functional IL-33 receptor (*ST2*$^{-/-}$), suggesting IL-33 as a primary mediator of innate responses in SAFS and an important factor in the resistance to corticosteroid therapy experienced by SAFS patients (Castanhinha et al., 2015). These findings provide evidence for the involvement of innate immunity in fungi-associated asthma development and severity, alongside the well-established role of adaptive immunity.

As previously mentioned, proteases are a unique feature of fungi that contribute to the pathology of fungi-associated asthma, and these enzymes in turn contribute to the specific immunological mechanisms induced in response to fungal airway exposure. Inhaled *Aspergillus*-derived fungal associated proteases (FAP) induced airway eosinophilia in naive mice through protease activated receptor-2 (PAR-2), indicating that this is directly associated with protease activity rather than sensitization (Hiraishi et al., 2018). IL-33 induced by PAR-2 signaling played a crucial role in this response through activation of ILC2 (independent of adaptive immunity) to drive the eosinophilic inflammation seen (**Figure 3B**) (Hiraishi et al.,

2018). This research highlights key innate immune mechanisms by which fungal airway exposure without sensitization can be conducive of steroid resistant asthma.

Th1 responses may also play an important role in fungi-associated asthma, despite the classic predominance of type 2 responses associated with this disease. In an *A. fumigatus* allergic airway model, along with elevated Th2 responses, mice displayed an increase in interferon-γ (IFN-γ), a well characterized Th1 cytokine, upon airway challenge (Hoselton et al., 2010). Godwin et al. (2019) found that the BAL fluid of asthmatic patients with fungal sensitization displayed an elevation in IL-1α and IL-1β, and with an *A. fumigatus* model of airway inflammation, they established that IL-1R1 signaling is associated with Th1 and Th17 responses, which contributes to the severity of fungal asthma (**Figure 3E**). Using *Il1r1*$^{-/-}$ mice, the authors showed that IL-1 plays an important role in neutrophil and eosinophil recruitment to the airway and thus underlies the severity of the inflammatory response (Godwin et al., 2019). They also reported that interleukin-1 receptor antagonist (IL-1RA) treatment reduced Th1 associated IFN-γ, C-X-C Motif Chemokine Ligand-9 (CXCL9), and CXCL10 along with Th17 associated IL-17A, which were directly associated with neutrophil recruitment (Godwin et al., 2019).

Beyond Th1 and Th2 responses, Th17 responses have been shown to play a role in fungi-associated asthmatic disease in response to fungal airway exposure. As previously mentioned, Bacher et al. (2019) displayed a model in which *C. albicans*-reactive T cells drive Th17 responses in the lung against *A. fumigatus* (**Figure 4A**). Recognition of *A. fumigatus via* the dectin-1 receptor in the airway has also been shown to be associated with IL-17A and IL-22 production by CD4$^+$ T cells and unfractionated lung cells, respectively, which results in worsened allergic airway response in a murine model (Lilly et al., 2012). However, dectin-1 signaling was also shown to be associated with CD4$^+$ T cell production of IL-4, IL-13, and IFN-γ to a lesser extent (**Figure 3C**), suggesting an interplay between Th2 and Th17 responses in fungi induced asthma (Lilly et al., 2012). Similarly, Zhang et al. (2017) reported that severe steroid resistant fungal asthma in mice displays a mixed Th2 and Th17 response in a HDM/*A. versicolor* combination model, which is not seen with HDM alone. Co-exposure was associated with both neutrophilia and eosinophilia, highlighting the basis for the steroid resistant phenotype of this model (Zhang et al., 2017).

IL-17A is associated with neutrophil recruitment (Newcomb and Peebles, 2013), which is a hallmark of severe asthma (Fahy, 2009), and may play a direct role in the enhanced severity experienced by patients with fungi associated asthma. This phenomenon was shown in an *A. fumigatus* mouse model of fungal allergic airway disease, whereby decreased recruitment of neutrophils ameliorated airway hyper responsiveness (Park et al., 2006). In order to understand the underlying mechanisms by which fungal exposure results in severe asthmatic disease, it is crucial that other arms of the immune system beyond a classic type 2 allergic response be taken into consideration.

While environmental exposures may explain differences in allergic airways responses, a genetic component has been implicated in fungal-associated immune responses conducive of asthma in children. Knutsen et al. (2010) investigated T cell responses in children with *Alternaria*-sensitive mild and moderate-to-severe asthma and found that the moderate-to-severe group showed increased expression of IL-5 and IL-13 by T cells stimulated with *Alternaria ex-vivo*. Notably, the moderate-to-severe group had a significantly greater frequency of the IL-4 receptor alpha chain (IL-4RA) ile75val polymorphism, which was associated with greater CD23 expression by both CD19$^+$ and CD19$^+$CD86$^+$ B cells stimulated with IL-4 (Knutsen et al., 2010). As well, the moderate-to-severe group showed a reduced allele frequency of HLA-DQB1*03, suggesting its potential role in asthma severity where fungal sensitization is involved (Knutsen et al., 2010). Altogether, these studies highlight the multifactorial association between fungi and asthma, with environmental fungal exposures, innate and adaptive immune mechanisms, genetic susceptibilities, and microbiome features at play.

FUNGI AS TARGETS FOR ASTHMA TREATMENT AND CONTROL

Given the important role of fungi in mediating allergic airway disease, it is imperative to consider them as potential components in strategies to improve symptoms and disease severity. Studies have shown that antibiotic treatment in mice, resulting in a dysbiotic bacterial and fungal gut microbiome, increased susceptibility to fungi driven airway disease (Noverr et al., 2004; Noverr et al., 2005; Kim et al., 2014; Skalski et al., 2018). These findings suggest that the amelioration of fungal dysbiosis may be valuable in the prevention or treatment of fungi-associated asthma.

Due to the severity of fungi-associated asthma and its unique underlying immunopathology, specialized therapeutics must be developed aimed at targeting fungal colonizers and improve disease status and management. While the use of broad-spectrum antifungals may seem helpful, some studies have described deleterious effects to the mycobiome, resulting in host immune dysregulation. Treatment of mice with fluconazole resulted in fungal dysbiosis in the gut and enhanced allergic airway responses when mice were challenged in an HDM model of airway inflammation (Wheeler et al., 2016). Fluconazole selectively depleted *Candida* spp. and allowed for the expansion of *Aspergillus*, *Wallemia*, and *Epicoccum* taxa. A similar induction of fungal dysbiosis was seen with amphotericin-B treatment (Wheeler et al., 2016). Further, these three expanded fungal taxa were verified as causative agents for enhanced airway responses to HDM, as mice that received supplementation with these taxa displayed similar results to those treated with antifungal drugs (Wheeler et al., 2016). Results from our lab also demonstrated that a one-week-long treatment with fluconazole to mouse dams during the pre-weaning period was sufficient to persistently alter the gut fungal ecosystem of mouse pups colonized with defined communities of yeasts and bacteria (van Tilburg Bernardes et al., 2020). Similarly to early life antibiotic treatment,

antifungal-induced microbiome perturbations led to broad systemic immune alterations and increased susceptibility to OVA-induced airway inflammation, characterized by elevated BAL eosinophilia (van Tilburg Bernardes et al., 2020). These results strongly suggest that fungal-derived signals are important during immune development, and that the effects of antifungals are akin to those of antibiotics on the bacterial microbiome, inducing widespread microbiome perturbations that can trigger immune dysregulation and increase susceptibility to asthma.

Nonetheless, targeting of specific fungal colonizers may be a therapeutic avenue to be explored for fungal asthma or SAFS. A randomized clinical trial to investigate the use of oral antifungal, itraconazole, in patients with SAFS was first carried out in 2009 by Denning et al. (2009). In this trial, 60% of patients reported an improved quality of life relative to the placebo group, indicating that this may be a viable therapeutic option for patients suffering from fungal asthma (Denning et al., 2009). Though, it remained unclear whether this effect was due to the depletion of fungi or immunological effect of itraconazole in dampening of Th2 responses. Despite these findings, the use of antifungal drugs for treatment of fungal asthma has not been widely accepted due to the difficulty in identifying the specific subgroup of SAFS patients that would truly benefit from the treatment (Parulekar et al., 2015). The European Respiratory Society/American Thoracic Society Task Force only recommends antifungal therapy for allergic bronchopulmonary aspergillosis, and advises against the treatment for SAFS due to limited evidence of treatment efficacy within this group (Chung et al., 2014). Research into the use of antifungal therapy for fungal-associated asthma is ongoing and a recent retrospective cohort study of 41 patients with culture-proven airway mycosis by Li E. et al. (2018) reported improved asthma control, reduced eosinophilia, and lowered serum IgE associated with antifungal treatment. Larger scale clinical trials are needed to truly establish the benefit and underlying mechanisms by which beneficial results are conferred, along with the safety of antifungals in patients suffering from fungi-associated asthma, as viable treatment options are greatly needed.

An alternative approach to develop fungi-associated asthma therapeutics is to target specific immune responses elicited by fungi in order to improve symptoms and disease severity. One example is inhibitors of fungal proteases, which have been shown to reduce the airway damage associated with fungal proteases (Balenga et al., 2015). Additionally, the improvement in Th1 and Th17 responses following IL-1RA treatment seen by Godwin et al. (2019) suggests that drugs such as Anakinra (recombinant human IL-1RA), which has been recommended for treatment of other inflammatory diseases, including rheumatoid arthritis, may be a treatment option in patients suffering from fungi-associated asthma. A phase I clinical study found that Anakinra significantly reduced inhaled endotoxin-induced airway neutrophilia, along with IL-1β, IL-6, and IL-8, in healthy volunteers relative to the control (Hernandez et al., 2015). As neutrophils have been linked to fungi-associated asthma severity (Park et al., 2006), the findings from this phase I trial are a promising area for future research. Furthermore, the same investigators from this phase I trial (Park et al., 2006) also have two ongoing randomized clinical trials exploring the efficacy of Anakinra as a therapeutic option for allergic manifestation in asthmatic patients (NCT03513471 and NCT03513458). These ongoing trials have great potential to uncover Anakinra's ability to safely control early and/or late phases of asthma exacerbation episodes. Specific targeting of these immunological mechanisms, among others, may be a viable therapeutic option though more research must be carried out to determine safety and viability in treatment of asthmatic patients.

CONCLUSIONS AND FUTURE DIRECTIONS

Fungi, viruses, archaea, and bacteria coinhabit all terrestrial and aquatic environmental niches, including the mammalian mucosae, engaging in diverse ecological interkingdom relationships that shape the overall composition of microbiomes, and their relationship with the host (Frey-Klett et al., 2011; Sharma et al., 2019; van Tilburg Bernardes et al., 2020). Non-bacterial members of the microbiome, are increasingly being recognized as important players in asthma development and manifestation (Barcik et al., 2020), highlighting the importance of multi-kingdom microbial interactions in the pathophysiology of this disease. Nevertheless, the characterization of the direct implications of fungi, and other members of the microbiome in disease manifestation is still nascent. Microbiome studies should move beyond surveying only bacteria, and consider the multi-kingdom nature of these important ecosystems.

Despite continuous advancements in sequencing technologies, there are still important challenges to attain a sensitive and precise assessment of the mycobiome within complex communities (Tiew et al., 2020). Improvements remain necessary in fungal taxonomic databases and in bioinformatic algorithms that can efficiently account for the higher variability in read length and higher rate of genetic insertions and deletions in the regions used in most mycobiome sequencing approaches (i.e., ITS1 and ITS2 regions). Further, there is very little knowledge on the functional role of fungi in the microbiome, how this impacts overall metabolic output, and the community's response to perturbation (e.g., antimicrobials), which are crucial to further understand the role of the microbiome in asthma.

While strong evidence suggests that both the lung and gut mycobiome are important players in asthma, the specific fungal-driven cellular and molecular mechanisms of disease are poorly understood. Despite this, our current state of knowledge renders great potential for microbiome-derived approaches aimed at preventing and treating this disease. To this aim, research must seek to further elucidate the role of fungi in early immune education events and characterize the specific cellular and molecular mechanisms by which early-life fungal dysbiosis promotes or protects from immune responses conducive of asthma. This is especially evident in lung mycobiome studies,

as no prospective study has investigated early life airway alterations that may be associated with asthma development in children, further limiting mechanistic studies aimed at determining the causal role of airway colonizing fungi in disease pathogenesis.

Evidence to date is sufficient to disprove the assumption that all fungal exposures, whether from the environment or the microbiome, are detrimental to health (Tischer et al., 2011; Behbod et al., 2015). Defining which species of fungi are protective or harmful for asthma development and/or exacerbations is an attainable goal if more prospective longitudinal studies survey fungal organisms within the microbiome and the environment of the human population studied.

Moreover, it will be crucial to consider that environmental exposures to allergenic moulds (e.g., *Alternaria*, *Aspergillus*, and *Penicillium*) may become even more prevalent in the face of ongoing climate change. Moulds thrive in moist and warm environments (Weinhold, 2007), thus worldwide rising temperatures may favor the growth of known allergenic fungi, and the emergence of new ones. A recent meta-analysis of 341 publications highlighted how soil microbial communities are sensitive to global change factors (Zhou et al., 2020). Based on a mixed-effect model, the investigators reported that diversity of fungal communities are impacted by changing environmental conditions (Zhou et al., 2020). Hence, aspects of climate change have the potential to alter the dynamics of environmental fungi, which may in turn impact development and/or exacerbation rates of fungi-associated asthma, including changes in precipitation and nutrient availability (Zhou et al., 2020), atmospheric CO_2 levels (Klironomos et al., 1997), and shifts in the duration of seasons (Cecchi et al., 2010), overall contributing to increased levels of fungal aeroallergens.

Finally, we need a more comprehensive understanding on how antimicrobial drugs and other early-life microbiome alterations (e.g., Caesarean sections and formula feeding) impact the infant mycobiome, and which of these alterations may be conducive of asthma. Including fungi in these studies will provide a more ecologically sound framework to design effective probiotic consortia capable of remediating the microbiome perturbations and host immune dysregulation that continue to increase asthma risk around the world.

AUTHOR CONTRIBUTIONS

EvTB, MWG, and M-CA formulated the concept for this review. EvTB and MWG wrote the first draft. All authors contributed to the article and approved the submitted version.

FUNDING

EvTB is funded by the Eyes High Doctoral Recruitment Scholarship. MWG is funded by the Alberta Children's Hospital Research Institute Graduate Scholarship. M-CA is funded by the Cumming School of Medicine, the Alberta Children Hospital Research Institute, the Snyder Institute of Chronic Diseases, the Canadian Institutes for Health Research, the Sick Kids Foundation, the W. Garfield Weston Foundation, The Koopmans Research Fund, and the Canadian Lung Association.

ACKNOWLEDGMENTS

The figures in this review were created with BioRender.com (https://biorender.com/).

REFERENCES

Adams, R.II, Miletto, M., Taylor, J. W., and Bruns, T. D. (2013). The diversity and distribution of fungi on residential surfaces. *PloS One* 8 (11), e78866. doi: 10.1371/journal.pone.0078866

Agarwal, R., and Gupta, D. (2011). Severe asthma and fungi: current evidence. *Med. Mycol.* 49 Suppl 1, S150–S157. doi: 10.3109/13693786.2010.504752

Amarsaikhan, N., O'Dea, E. M., Tsoggerel, A., and Templeton, S. P. (2017). Lung eosinophil recruitment in response to Aspergillus fumigatus is correlated with fungal cell wall composition and requires gammadelta T cells. *Microbes Infect.* 19 (7-8), 422–431. doi: 10.1016/j.micinf.2017.05.001

Arrieta, M. C., Stiemsma, L. T., Dimitriu, P. A., Thorson, L., Russell, S., Yurist-Doutsch, S., et al. (2015). Early infancy microbial and metabolic alterations affect risk of childhood asthma. *Sci. Transl. Med.* 7 (307), 307ra152. doi: 10.1126/scitranslmed.aab2271

Arrieta, M. C., Arevalo, A., Stiemsma, L., Dimitriu, P., Chico, M. E., Loor, S., et al. (2018). Associations between infant fungal and bacterial dysbiosis and childhood atopic wheeze in a nonindustrialized setting. *J. Allergy Clin. Immunol.* 142 (2), 424–434 e410. doi: 10.1016/j.jaci.2017.08.041

Azevedo, M. M., Teixeira-Santos, R., Silva, A. P., Cruz, L., Ricardo, E., Pina-Vaz, C., et al. (2015). The effect of antibacterial and non-antibacterial compounds alone or associated with antifugals upon fungi. *Front. Microbiol.* 6:669. doi: 10.3389/fmicb.2015.00669

Bacher, P., Hohnstein, T., Beerbaum, E., Rocker, M., Blango, M. G., Kaufmann, S., et al. (2019). Human Anti-fungal Th17 Immunity and Pathology Rely on Cross-Reactivity against Candida albicans. *Cell* 176 (6), 1340–1355 e1315. doi: 10.1016/j.cell.2019.01.041

Balenga, N. A., Klichinsky, M., Xie, Z., Chan, E. C., Zhao, M., Jude, J., et al. (2015). A fungal protease allergen provokes airway hyper-responsiveness in asthma. *Nat. Commun.* 6, 6763. doi: 10.1038/ncomms7763

Barberan, A., Dunn, R. R., Reich, B. J., Pacifici, K., Laber, E. B., Menninger, H. L., et al. (2015). The ecology of microscopic life in household dust. *Proc. Biol. Sci.* 282 (1814), 20151139. doi: 10.1098/rspb.2015.1139

Barcik, W., Boutin, R. C. T., Sokolowska, M., and Finlay, B. B. (2020). The Role of Lung and Gut Microbiota in the Pathology of Asthma. *Immunity* 52 (2), 241–255. doi: 10.1016/j.immuni.2020.01.007

Bartemes, K. R., Iijima, K., Kobayashi, T., Kephart, G. M., McKenzie, A. N., and Kita, H. (2012). IL-33-responsive lineage- CD25+ CD44(hi) lymphoid cells mediate innate type 2 immunity and allergic inflammation in the lungs. *J. Immunol.* 188 (3), 1503–1513. doi: 10.4049/jimmunol.1102832

Baxi, S. N., Sheehan, W. J., Sordillo, J. E., Muilenberg, M. L., Rogers, C. A., Gaffin, J. M., et al. (2019). Association between fungal spore exposure in inner-city schools and asthma morbidity. *Ann. Allergy Asthma Immunol.* 122 (6), 610–615 e611. doi: 10.1016/j.anai.2019.03.011

Behbod, B., Sordillo, J. E., Hoffman, E. B., Datta, S., Webb, T. E., Kwan, D. L., et al. (2015). Asthma and allergy development: contrasting influences of yeasts and other fungal exposures. *Clin. Exp. Allergy* 45 (1), 154–163. doi: 10.1111/cea.12401

Bisgaard, H., Hermansen, M. N., Buchvald, F., Loland, L., Halkjaer, L. B., Bonnelykke, K., et al. (2007). Childhood asthma after bacterial colonization

of the airway in neonates. *N. Engl. J. Med.* 357 (15), 1487–1495. doi: 10.1056/NEJMoa052632

Blease, K., Mehrad, B., Standiford, T. J., Lukacs, N. W., Kunkel, S. L., Chensue, S. W., et al. (2000). Airway remodeling is absent in CCR1-/- mice during chronic fungal allergic airway disease. *J. Immunol.* 165 (3), 1564–1572. doi: 10.4049/jimmunol.165.3.1564

Busse, W. W., Lemanske, R. F.Jr., and Gern, J. E. (2010). Role of viral respiratory infections in asthma and asthma exacerbations. *Lancet* 376 (9743), 826–834. doi: 10.1016/S0140-6736(10)61380-3

Castanhinha, S., Sherburn, R., Walker, S., Gupta, A., Bossley, C. J., Buckley, J., et al. (2015). Pediatric severe asthma with fungal sensitization is mediated by steroid-resistant IL-33. *J. Allergy Clin. Immunol.* 136 (2), 312–322 e317. doi: 10.1016/j.jaci.2015.01.016

Cecchi, L., D'Amato, G., Ayres, J. G., Galan, C., Forastiere, F., Forsberg, B., et al. (2010). Projections of the effects of climate change on allergic asthma: the contribution of aerobiology. *Allergy* 65 (9), 1073–1081. doi: 10.1111/j.1398-9995.2010.02423.x

Charlson, E. S., Diamond, J. M., Bittinger, K., Fitzgerald, A. S., Yadav, A., Haas, A. R., et al. (2012). Lung-enriched organisms and aberrant bacterial and fungal respiratory microbiota after lung transplant. *Am. J. Respir. Crit. Care Med.* 186 (6), 536–545. doi: 10.1164/rccm.201204-0693OC

Chatterjee, R., Batra, J., Das, S., Sharma, S. K., and Ghosh, B. (2008). Genetic association of acidic mammalian chitinase with atopic asthma and serum total IgE levels. *J. Allergy Clin. Immunol.* 122 (1), 202–208, 208 e201-207. doi: 10.1016/j.jaci.2008.04.030

Chung, K. F., Wenzel, S. E., Brozek, J. L., Bush, A., Castro, M., Sterk, P. J., et al. (2014). International ERS/ATS guidelines on definition, evaluation and treatment of severe asthma. *Eur. Respir. J.* 43 (2), 343–373. doi: 10.1183/09031936.00202013

Crameri, R., Garbani, M., Rhyner, C., and Huitema, C. (2014). Fungi: the neglected allergenic sources. *Allergy* 69 (2), 176–185. doi: 10.1111/all.12325

Cryan, J. F., O'Riordan, K. J., Cowan, C. S. M., Sandhu, K. V., Bastiaanssen, T. F. S., Boehme, M., et al. (2019). The Microbiota-Gut-Brain Axis. *Physiol. Rev.* 99 (4), 1877–2013. doi: 10.1152/physrev.00018.2018

Dannemiller, K. C., Gent, J. F., Leaderer, B. P., and Peccia, J. (2016a). Indoor microbial communities: Influence on asthma severity in atopic and nonatopic children. *J. Allergy Clin. Immunol.* 138 (1), 76–83 e71. doi: 10.1016/j.jaci.2015.11.027

Dannemiller, K. C., Gent, J. F., Leaderer, B. P., and Peccia, J. (2016b). Influence of housing characteristics on bacterial and fungal communities in homes of asthmatic children. *Indoor Air* 26 (2), 179–192. doi: 10.1111/ina.12205

Darabi, B., Rahmati, S., HafeziAhmadi, M. R., Badfar, G., and Azami, M. (2019). The association between caesarean section and childhood asthma: an updated systematic review and meta-analysis. *Allergy Asthma Clin. Immunol.* 15, 62. doi: 10.1186/s13223-019-0367-9

Denning, D. W., O'Driscoll, B. R., Hogaboam, C. M., Bowyer, P., and Niven, R. M. (2006). The link between fungi and severe asthma: a summary of the evidence. *Eur. Respir. J.* 27 (3), 615–626. doi: 10.1183/09031936.06.00074705

Denning, D. W., O'Driscoll, B. R., Powell, G., Chew, F., Atherton, G. T., Vyas, A., et al. (2009). Randomized controlled trial of oral antifungal treatment for severe asthma with fungal sensitization: The Fungal Asthma Sensitization Trial (FAST) study. *Am. J. Respir. Crit. Care Med.* 179 (1), 11–18. doi: 10.1164/rccm.200805-737OC

Dollive, S., Chen, Y. Y., Grunberg, S., Bittinger, K., Hoffmann, C., Vandivier, L., et al. (2013). Fungi of the murine gut: episodic variation and proliferation during antibiotic treatment. *PloS One* 8 (8), e71806. doi: 10.1371/journal.pone.0071806

Dominguez-Bello, M. G., Godoy-Vitorino, F., Knight, R., and Blaser, M. J. (2019). Role of the microbiome in human development. *Gut* 68 (6), 1108–1114. doi: 10.1136/gutjnl-2018-317503

Fahy, J. V. (2009). Eosinophilic and neutrophilic inflammation in asthma: insights from clinical studies. *Proc. Am. Thorac. Soc.* 6 (3), 256–259. doi: 10.1513/pats.200808-087RM

Fairs, A., Agbetile, J., Hargadon, B., Bourne, M., Monteiro, W. R., Brightling, C. E., et al. (2010). IgE sensitization to Aspergillus fumigatus is associated with reduced lung function in asthma. *Am. J. Respir. Crit. Care Med.* 182 (11), 1362–1368. doi: 10.1164/rccm.201001-0087OC

Fall, T., Lundholm, C., Ortqvist, A. K., Fall, K., Fang, F., Hedhammar, A., et al. (2015). Early Exposure to Dogs and Farm Animals and the Risk of Childhood Asthma. *JAMA Pediatr.* 169 (11), e153219. doi: 10.1001/jamapediatrics.2015.3219

Frey-Klett, P., Burlinson, P., Deveau, A., Barret, M., Tarkka, M., and Sarniguet, A. (2011). Bacterial-fungal interactions: hyphens between agricultural, clinical, environmental, and food microbiologists. *Microbiol. Mol. Biol. Rev.* 75 (4), 583–609. doi: 10.1128/MMBR.00020-11

Fujimura, K. E., Sitarik, A. R., Havstad, S., Lin, D. L., Levan, S., Fadrosh, D., et al. (2016). Neonatal gut microbiota associates with childhood multisensitized atopy and T cell differentiation. *Nat. Med.* 22 (10), 1187–1191. doi: 10.1038/nm.4176

Gersuk, G. M., Underhill, D. M., Zhu, L., and Marr, K. A. (2006). Dectin-1 and TLRs permit macrophages to distinguish between different Aspergillus fumigatus cellular states. *J. Immunol.* 176 (6), 3717–3724. doi: 10.4049/jimmunol.176.6.3717

Ghannoum, M. A., Jurevic, R. J., Mukherjee, P. K., Cui, F., Sikaroodi, M., Naqvi, A., et al. (2010). Characterization of the oral fungal microbiome (mycobiome) in healthy individuals. *PloS Pathog.* 6 (1), e1000713. doi: 10.1371/journal.ppat.1000713

Godwin, M. S., Reeder, K. M., Garth, J. M., Blackburn, J. P., Jones, M., Yu, Z., et al. (2019). IL-1RA regulates immunopathogenesis during fungal-associated allergic airway inflammation. *JCI Insight* 4 (21), e129055. doi: 10.1172/jci.insight.129055

Goldman, D. L., Chen, Z., Shankar, V., Tyberg, M., Vicencio, A., and Burk, R. (2018). Lower airway microbiota and mycobiota in children with severe asthma. *J. Allergy Clin. Immunol.* 141 (2), 808–811 e807. doi: 10.1016/j.jaci.2017.09.018

Harley, K. G., Macher, J. M., Lipsett, M., Duramad, P., Holland, N. T., Prager, S. S., et al. (2009). Fungi and pollen exposure in the first months of life and risk of early childhood wheezing. *Thorax* 64 (4), 353–358. doi: 10.1136/thx.2007.090241

Hemmann, S., Blaser, K., and Crameri, R. (1997). Allergens of Aspergillus fumigatus and Candida boidinii share IgE-binding epitopes. *Am. J. Respir. Crit. Care Med.* 156 (6), 1956–1962. doi: 10.1164/ajrccm.156.6.9702087

Hernandez, M. L., Mills, K., Almond, M., Todoric, K., Aleman, M. M., Zhang, H., et al. (2015). IL-1 receptor antagonist reduces endotoxin-induced airway inflammation in healthy volunteers. *J. Allergy Clin. Immunol.* 135 (2), 379–385. doi: 10.1016/j.jaci.2014.07.039

Hiraishi, Y., Yamaguchi, S., Yoshizaki, T., Nambu, A., Shimura, E., Takamori, A., et al. (2018). IL-33, IL-25 and TSLP contribute to development of fungal-associated protease-induced innate-type airway inflammation. *Sci. Rep.* 8 (1), 18052. doi: 10.1038/s41598-018-36440-x

Hogaboam, C. M., Takahashi, K., Ezekowitz, R. A., Kunkel, S. L., and Schuh, J. M. (2004). Mannose-binding lectin deficiency alters the development of fungal asthma: effects on airway response, inflammation, and cytokine profile. *J. Leukoc. Biol.* 75 (5), 805–814. doi: 10.1189/jlb.0703325

Hoggard, M., Vesty, A., Wong, G., Montgomery, J. M., Fourie, C., Douglas, R. G., et al. (2018). Characterizing the Human Mycobiota: A Comparison of Small Subunit rRNA, ITS1, ITS2, and Large Subunit rRNA Genomic Targets. *Front. Microbiol.* 9:2208. doi: 10.3389/fmicb.2018.02208

Hoselton, S. A., Samarasinghe, A. E., Seydel, J. M., and Schuh, J. M. (2010). An inhalation model of airway allergic response to inhalation of environmental Aspergillus fumigatus conidia in sensitized BALB/c mice. *Med. Mycol.* 48 (8), 1056–1065. doi: 10.3109/13693786.2010.485582

Hugg, T. T., Jaakkola, M. S., Ruotsalainen, R., Pushkarev, V., and Jaakkola, J. J. (2008). Exposure to animals and the risk of allergic asthma: a population-based cross-sectional study in Finnish and Russian children. *Environ. Health* 7:28. doi: 10.1186/1476-069X-7-28

Huseyin, C. E., O'Toole, P. W., Cotter, P. D., and Scanlan, P. D. (2017). Forgotten fungi-the gut mycobiome in human health and disease. *FEMS Microbiol. Rev.* 41 (4), 479–511. doi: 10.1093/femsre/fuw047

Joffe, L. S., Nimrichter, L., Rodrigues, M. L., and Del Poeta, M. (2016). Potential Roles of Fungal Extracellular Vesicles during Infection. *mSphere* 1 (4), e00099-16. doi: 10.1128/mSphere.00099-16

Kim, Y. G., Udayanga, K. G., Totsuka, N., Weinberg, J. B., Nunez, G., and Shibuya, A. (2014). Gut dysbiosis promotes M2 macrophage polarization and allergic airway

inflammation via fungi-induced PGE(2). *Cell Host Microbe* 15 (1), 95–102. doi: 10.1016/j.chom.2013.12.010

Klironomos, J. N., Rillig, M. C., Allen, M. F., Zak, D. R., Pregitzer, K. S., and Kubiske, M. E. (1997). Increased levels of airborne fungal spores in response to *Populus tremuloides* grown under elevated atmospheric CO2. *Can. J. Bot.* 75 (10), 1670–1673. doi: 10.1139/b97-880

Knight, D. A., Lim, S., Scaffidi, A. K., Roche, N., Chung, K. F., Stewart, G. A., et al. (2001). Protease-activated receptors in human airways: upregulation of PAR-2 in respiratory epithelium from patients with asthma. *J. Allergy Clin. Immunol.* 108 (5), 797–803. doi: 10.1067/mai.2001.119025

Knutsen, A. P., Vijay, H. M., Kariuki, B., Santiago, L. A., Graff, R., Wofford, J. D., et al. (2010). Association of IL-4RA single nucleotide polymorphisms, HLA-DR and HLA-DQ in children with Alternaria-sensitive moderate-severe asthma. *Clin. Mol. Allergy* 8:5. doi: 10.1186/1476-7961-8-5

Kull, I., Melen, E., Alm, J., Hallberg, J., Svartengren, M., van Hage, M., et al. (2010). Breast-feeding in relation to asthma, lung function, and sensitization in young schoolchildren. *J. Allergy Clin. Immunol.* 125 (5), 1013–1019. doi: 10.1016/j.jaci.2010.01.051

Kumamoto, C. A. (2016). The Fungal Mycobiota: Small Numbers, Large Impacts. *Cell Host Microbe* 19 (6), 750–751. doi: 10.1016/j.chom.2016.05.018

Laforest-Lapointe, I., and Arrieta, M. C. (2017). Patterns of Early-Life Gut Microbial Colonization during Human Immune Development: An Ecological Perspective. *Front. Immunol.* 8:788. doi: 10.3389/fimmu.2017.00788

Lai, C. K., Beasley, R., Crane, J., Foliaki, S., Shah, J., Weiland, S., et al. (2009). Global variation in the prevalence and severity of asthma symptoms: phase three of the International Study of Asthma and Allergies in Childhood (ISAAC). *Thorax* 64 (6), 476–483. doi: 10.1136/thx.2008.106609

Lambrecht, B. N., and Hammad, H. (2015). The immunology of asthma. *Nat. Immunol.* 16 (1), 45–56. doi: 10.1038/ni.3049

Lawson, J. A., Janssen, I., Bruner, M. W., Madani, K., and Pickett, W. (2011). Urban-rural differences in asthma prevalence among young people in Canada: the roles of health behaviors and obesity. *Ann. Allergy Asthma Immunol.* 107 (3), 220–228. doi: 10.1016/j.anai.2011.06.014

Lawson, J. A., Rennie, D. C., Cockcroft, D. W., Dyck, R., Afanasieva, A., Oluwole, O., et al. (2017). Childhood asthma, asthma severity indicators, and related conditions along an urban-rural gradient: a cross-sectional study. *BMC Pulm. Med.* 17 (1), 4. doi: 10.1186/s12890-016-0355-5

Lee, C. G., Da Silva, C. A., Lee, J. Y., Hartl, D., and Elias, J. A. (2008). Chitin regulation of immune responses: an old molecule with new roles. *Curr. Opin. Immunol.* 20 (6), 684–689. doi: 10.1016/j.coi.2008.10.002

Li, E., Tsai, C. L., Maskatia, Z. K., Kakkar, E., Porter, P., Rossen, R. D., et al. (2018). Benefits of antifungal therapy in asthma patients with airway mycosis: A retrospective cohort analysis. *Immun. Inflammation Dis.* 6 (2), 264–275. doi: 10.1002/iid3.215

Li, X., Leonardi, I., Semon, A., Doron, I., Gao, I. H., Putzel, G. G., et al. (2018). Response to Fungal Dysbiosis by Gut-Resident CX3CR1(+) Mononuclear Phagocytes Aggravates Allergic Airway Disease. *Cell Host Microbe* 24 (6), 847–856 e844. doi: 10.1016/j.chom.2018.11.003

Lilly, L. M., Gessner, M. A., Dunaway, C. W., Metz, A. E., Schwiebert, L., Weaver, C. T., et al. (2012). The beta-glucan receptor dectin-1 promotes lung immunopathology during fungal allergy via IL-22. *J. Immunol.* 189 (7), 3653–3660. doi: 10.4049/jimmunol.1201797

Lotvall, J., Akdis, C. A., Bacharier, L. B., Bjermer, L., Casale, T. B., Custovic, A., et al. (2011). Asthma endotypes: a new approach to classification of disease entities within the asthma syndrome. *J. Allergy Clin. Immunol.* 127 (2), 355–360. doi: 10.1016/j.jaci.2010.11.037

Mac Aogain, M., Chandrasekaran, R., Lim, A. Y. H., Low, T. B., Tan, G. L., Hassan, T., et al. (2018). Immunological corollary of the pulmonary mycobiome in bronchiectasis: the CAMEB study. *Eur. Respir. J.* 52 (1), 1800766. doi: 10.1183/13993003.00766-2018

Marra, F., Marra, C. A., Richardson, K., Lynd, L. D., Kozyrskyj, A., Patrick, D. M., et al. (2009). Antibiotic use in children is associated with increased risk of asthma. *Pediatrics* 123 (3), 1003–1010. doi: 10.1542/peds.2008-1146

Martel, M. J., Rey, E., Malo, J. L., Perreault, S., Beauchesne, M. F., Forget, A., et al. (2009). Determinants of the incidence of childhood asthma: a two-stage case-control study. *Am. J. Epidemiol.* 169 (2), 195–205. doi: 10.1093/aje/kwn309

Martinez, F. D., and Vercelli, D. (2013). Asthma. *Lancet* 382 (9901), 1360–1372. doi: 10.1016/S0140-6736(13)61536-6

Michalski, C., Kan, B., and Lavoie, P. M. (2017). Antifungal Immunological Defenses in Newborns. *Front. Immunol.* 8:281. doi: 10.3389/fimmu.2017.00281

Murk, W., Risnes, K. R., and Bracken, M. B. (2011). Prenatal or early-life exposure to antibiotics and risk of childhood asthma: a systematic review. *Pediatrics* 127 (6), 1125–1138. doi: 10.1542/peds.2010-2092

Nagel, G., Buchele, G., Weinmayr, G., Bjorksten, B., Chen, Y. Z., Wang, H., et al. (2009). Effect of breastfeeding on asthma, lung function and bronchial hyperreactivity in ISAAC Phase II. *Eur. Respir. J.* 33 (5), 993–1002. doi: 10.1183/09031936.00075708

Nash, A. K., Auchtung, T. A., Wong, M. C., Smith, D. P., Gesell, J. R., Ross, M. C., et al. (2017). The gut mycobiome of the Human Microbiome Project healthy cohort. *Microbiome* 5 (1), 153. doi: 10.1186/s40168-017-0373-4

Nazimek, K., Bryniarski, K., and Askenase, P. W. (2016). Functions of Exosomes and Microbial Extracellular Vesicles in Allergy and Contact and Delayed-Type Hypersensitivity. *Int. Arch. Allergy Immunol.* 171 (1), 1–26. doi: 10.1159/000449249

Newcomb, D. C., and Peebles, R. S.Jr. (2013). Th17-mediated inflammation in asthma. *Curr. Opin. Immunol.* 25 (6), 755–760. doi: 10.1016/j.coi.2013.08.002

Nguyen, L. D., Viscogliosi, E., and Delhaes, L. (2015). The lung mycobiome: an emerging field of the human respiratory microbiome. *Front. Microbiol.* 6:89. doi: 10.3389/fmicb.2015.00089

Niedoszytko, M., Chelminska, M., Jassem, E., and Czestochowska, E. (2007). Association between sensitization to Aureobasidium pullulans (Pullularia sp) and severity of asthma. *Ann. Allergy Asthma Immunol.* 98 (2), 153–156. doi: 10.1016/S1081-1206(10)60688-6

Noverr, M. C., Noggle, R. M., Toews, G. B., and Huffnagle, G. B. (2004). Role of antibiotics and fungal microbiota in driving pulmonary allergic responses. *Infect. Immun.* 72 (9), 4996–5003. doi: 10.1128/IAI.72.9.4996-5003.2004

Noverr, M. C., Falkowski, N. R., McDonald, R. A., McKenzie, A. N., and Huffnagle, G. B. (2005). Development of allergic airway disease in mice following antibiotic therapy and fungal microbiota increase: role of host genetics, antigen, and interleukin-13. *Infect. Immun.* 73 (1), 30–38. doi: 10.1128/IAI.73.1.30-38.2005

Ober, C., Tan, Z., Sun, Y., Possick, J. D., Pan, L., Nicolae, R., et al. (2008). Effect of variation in CHI3L1 on serum YKL-40 level, risk of asthma, and lung function. *N. Engl. J. Med.* 358 (16), 1682–1691. doi: 10.1056/NEJMoa0708801

Olenec, J. P., Kim, W. K., Lee, W. M., Vang, F., Pappas, T. E., Salazar, L. E., et al. (2010). Weekly monitoring of children with asthma for infections and illness during common cold seasons. *J. Allergy Clin. Immunol.* 125 (5), 1001–1006 e1001. doi: 10.1016/j.jaci.2010.01.059

Park, S. J., Wiekowski, M. T., Lira, S. A., and Mehrad, B. (2006). Neutrophils regulate airway responses in a model of fungal allergic airways disease. *J. Immunol.* 176 (4), 2538–2545. doi: 10.4049/jimmunol.176.4.2538

Parulekar, A. D., Diamant, Z., and Hanania, N. A. (2015). Antifungals in severe asthma. *Curr. Opin. Pulm. Med.* 21 (1), 48–54. doi: 10.1097/MCP.0000000000000117

Patrick, D. M., Sbihi, H., Dai, D. L. Y., Al Mamun, A., Rasali, D., Rose, C., et al. (2020). Decreasing antibiotic use, the gut microbiota, and asthma incidence in children: evidence from population-based and prospective cohort studies. *Lancet Respir. Med.* 8 (11), 1094–1105. doi: 10.1016/S2213-2600(20)30052-7

Pekkanen, J., Lampi, J., Genuneit, J., Hartikainen, A. L., and Jarvelin, M. R. (2012). Analyzing atopic and non-atopic asthma. *Eur. J. Epidemiol.* 27 (4), 281–286. doi: 10.1007/s10654-012-9649-y

Porter, P., Susarla, S. C., Polikepahad, S., Qian, Y., Hampton, J., Kiss, A., et al. (2009). Link between allergic asthma and airway mucosal infection suggested by proteinase-secreting household fungi. *Mucosal. Immunol.* 2 (6), 504–517. doi: 10.1038/mi.2009.102

Qian, J., Hospodsky, D., Yamamoto, N., Nazaroff, W. W., and Peccia, J. (2012). Size-resolved emission rates of airborne bacteria and fungi in an occupied classroom. *Indoor Air* 22 (4), 339–351. doi: 10.1111/j.1600-0668.2012.00769.x

Reese, T. A., Liang, H. E., Tager, A. M., Luster, A. D., Van Rooijen, N., Voehringer, D., et al. (2007). Chitin induces accumulation in tissue of innate immune cells associated with allergy. *Nature* 447 (7140), 92–96. doi: 10.1038/nature05746

Roduit, C., Scholtens, S., de Jongste, J. C., Wijga, A. H., Gerritsen, J., Postma, D. S., et al. (2009). Asthma at 8 years of age in children born by caesarean section. *Thorax* 64 (2), 107–113. doi: 10.1136/thx.2008.100875

Russell, S. L., Gold, M. J., Hartmann, M., Willing, B. P., Thorson, L., Wlodarska, M., et al. (2012). Early life antibiotic-driven changes in microbiota enhance

susceptibility to allergic asthma. *EMBO Rep.* 13 (5), 440–447. doi: 10.1038/embor.2012.32

Saglani, S., Lui, S., Ullmann, N., Campbell, G. A., Sherburn, R. T., Mathie, S. A., et al. (2013). IL-33 promotes airway remodeling in pediatric patients with severe steroid-resistant asthma. *J. Allergy Clin. Immunol.* 132 (3), 676–685 e613. doi: 10.1016/j.jaci.2013.04.012

Salo, P. M., Arbes, S. J.Jr., Sever, M., Jaramillo, R., Cohn, R. D., London, S. J., et al. (2006). Exposure to Alternaria alternata in US homes is associated with asthma symptoms. *J. Allergy Clin. Immunol.* 118 (4), 892–898. doi: 10.1016/j.jaci.2006.07.037

Samonis, G., Gikas, A., Anaissie, E. J., Vrenzos, G., Maraki, S., Tselentis, Y., et al. (1993). Prospective evaluation of effects of broad-spectrum antibiotics on gastrointestinal yeast colonization of humans. *Antimicrob. Agents Chemother.* 37 (1), 51–53. doi: 10.1128/aac.37.1.51

Scupham, A. J., Presley, L. L., Wei, B., Bent, E., Griffith, N., McPherson, M., et al. (2006). Abundant and diverse fungal microbiota in the murine intestine. *Appl. Environ. Microbiol.* 72 (1), 793–801. doi: 10.1128/AEM.72.1.793-801.2006

Shao, T. Y., Ang, W. X. G., Jiang, T. T., Huang, F. S., Andersen, H., Kinder, J. M., et al. (2019). Commensal Candida albicans Positively Calibrates Systemic Th17 Immunological Responses. *Cell Host Microbe* 25 (3), 404–417 e406. doi: 10.1016/j.chom.2019.02.004

Sharma, A., Laxman, B., Naureckas, E. T., Hogarth, D. K., Sperling, A.II, Solway, J., et al. (2019). Associations between fungal and bacterial microbiota of airways and asthma endotypes. *J. Allergy Clin. Immunol.* 144 (5), 1214–1227 e1217. doi: 10.1016/j.jaci.2019.06.025

Sharpe, R. A., Bearman, N., Thornton, C. R., Husk, K., and Osborne, N. J. (2015). Indoor fungal diversity and asthma: a meta-analysis and systematic review of risk factors. *J. Allergy Clin. Immunol.* 135 (1), 110–122. doi: 10.1016/j.jaci.2014.07.002

Shuhui, L., Mok, Y. K., and Wong, W. S. (2009). Role of mammalian chitinases in asthma. *Int. Arch. Allergy Immunol.* 149 (4), 369–377. doi: 10.1159/000205583

Skalski, J. H., Limon, J. J., Sharma, P., Gargus, M. D., Nguyen, C., Tang, J., et al. (2018). Expansion of commensal fungus Wallemia mellicola in the gastrointestinal mycobiota enhances the severity of allergic airway disease in mice. *PloS Pathog.* 14 (9), e1007260. doi: 10.1371/journal.ppat.1007260

Snelgrove, R. J., Gregory, L. G., Peiro, T., Akthar, S., Campbell, G. A., Walker, S. A., et al. (2014). Alternaria-derived serine protease activity drives IL-33-mediated asthma exacerbations. *J. Allergy Clin. Immunol.* 134 (3), 583–592 e586. doi: 10.1016/j.jaci.2014.02.002

Sokolowska, M., Frei, R., Lunjani, N., Akdis, C. A., and O'Mahony, L. (2018). Microbiome and asthma. *Asthma Res. Pract.* 4:1. doi: 10.1186/s40733-017-0037-y

Stein, R. T., Sherrill, D., Morgan, W. J., Holberg, C. J., Halonen, M., Taussig, L. M., et al. (1999). Respiratory syncytial virus in early life and risk of wheeze and allergy by age 13 years. *Lancet* 354 (9178), 541–545. doi: 10.1016/S0140-6736(98)10321-5

Stern, D. A., Morgan, W. J., Halonen, M., Wright, A. L., and Martinez, F. D. (2008). Wheezing and bronchial hyper-responsiveness in early childhood as predictors of newly diagnosed asthma in early adulthood: a longitudinal birth-cohort study. *Lancet* 372 (9643), 1058–1064. doi: 10.1016/S0140-6736(08)61447-6

Stewart, C. J., Ajami, N. J., O'Brien, J. L., Hutchinson, D. S., Smith, D. P., Wong, M. C., et al. (2018). Temporal development of the gut microbiome in early childhood from the TEDDY study. *Nature* 562 (7728), 583–588. doi: 10.1038/s41586-018-0617-x

Stiemsma, L. T., and Turvey, S. E. (2017). Asthma and the microbiome: defining the critical window in early life. *Allergy Asthma Clin. Immunol.* 13:3. doi: 10.1186/s13223-016-0173-6

Tham, R., Vicendese, D., Dharmage, S. C., Hyndman, R. J., Newbigin, E., Lewis, E., et al. (2017). Associations between outdoor fungal spores and childhood and adolescent asthma hospitalizations. *J. Allergy Clin. Immunol.* 139 (4), 1140–1147 e1144. doi: 10.1016/j.jaci.2016.06.046

Thavagnanam, S., Fleming, J., Bromley, A., Shields, M. D., and Cardwell, C. R. (2008). A meta-analysis of the association between Caesarean section and childhood asthma. *Clin. Exp. Allergy* 38 (4), 629–633. doi: 10.1111/j.1365-2222.2007.02780.x

Tiew, P. Y., Mac Aogain, M., Ali, N., Thng, K. X., Goh, K., Lau, K. J. X., et al. (2020). The Mycobiome in Health and Disease: Emerging Concepts, Methodologies and Challenges. *Mycopathologia* 185 (2), 207–231. doi: 10.1007/s11046-019-00413-z

Tischer, C., Chen, C. M., and Heinrich, J. (2011). Association between domestic mould and mould components, and asthma and allergy in children: a systematic review. *Eur. Respir. J.* 38 (4), 812–824. doi: 10.1183/09031936.00184010

Van Dyken, S. J., Garcia, D., Porter, P., Huang, X., Quinlan, P. J., Blanc, P. D., et al. (2011). Fungal chitin from asthma-associated home environments induces eosinophilic lung infiltration. *J. Immunol.* 187 (5), 2261–2267. doi: 10.4049/jimmunol.1100972

van Tilburg Bernardes, E., and Arrieta, M. C. (2017). Hygiene Hypothesis in Asthma Development: Is Hygiene to Blame? *Arch. Med. Res.* 48 (8), 717–726. doi: 10.1016/j.arcmed.2017.11.009

van Tilburg Bernardes, E., Pettersen, V. K., Gutierrez, M. W., Laforest-Lapointe, I., Jendzjowsky, N. G., Cavin, J. B., et al. (2020). Intestinal fungi are causally implicated in microbiome assembly and immune development in mice. *Nat. Commun.* 11 (1), 2577. doi: 10.1038/s41467-020-16431-1

van Woerden, H. C., Gregory, C., Brown, R., Marchesi, J. R., Hoogendoorn, B., and Matthews, I. P. (2013). Differences in fungi present in induced sputum samples from asthma patients and non-atopic controls: a community based case control study. *BMC Infect. Dis.* 13:69. doi: 10.1186/1471-2334-13-69

Vargas, G., Rocha, J. D., Oliveira, D. L., Albuquerque, P. C., Frases, S., Santos, S. S., et al. (2015). Compositional and immunobiological analyses of extracellular vesicles released by Candida albicans. *Cell Microbiol.* 17 (3), 389–407. doi: 10.1111/cmi.12374

Wampach, L., Heintz-Buschart, A., Hogan, A., Muller, E. E. L., Narayanasamy, S., Laczny, C. C., et al. (2017). Colonization and Succession within the Human Gut Microbiome by Archaea, Bacteria, and Microeukaryotes during the First Year of Life. *Front. Microbiol.* 8:738. doi: 10.3389/fmicb.2017.00738

Ward, T. L., Dominguez-Bello, M. G., Heisel, T., Al-Ghalith, G., Knights, D., and Gale, C. A. (2018). Development of the Human Mycobiome over the First Month of Life and across Body Sites. *mSystems* 3 (3), e00140-17. doi: 10.1128/mSystems.00140-17

Weinhold, B. (2007). A spreading concern: inhalational health effects of mold. *Environ. Health Perspect.* 115 (6), A300–A305. doi: 10.1289/ehp.115-a300

Welsh, K., Pashley, C. H., Satchwell, J., Wardlaw, A. J., and Gaillard, E. A. (2016). Colonisation with filamentous fungi and acute asthma exacerbations in children. *Eur. Respir. J.* 48:PA3354. doi: 10.1183/13993003.congress-2016.PA3354

Wheeler, M. L., Limon, J. J., Bar, A. S., Leal, C. A., Gargus, M., Tang, J., et al. (2016). Immunological Consequences of Intestinal Fungal Dysbiosis. *Cell Host Microbe* 19 (6), 865–873. doi: 10.1016/j.chom.2016.05.003

Wong, G. W., and Chow, C. M. (2008). Childhood asthma epidemiology: insights from comparative studies of rural and urban populations. *Pediatr. Pulmonol.* 43 (2), 107–116. doi: 10.1002/ppul.20755

Wu, A. C., Lasky-Su, J., Rogers, C. A., Klanderman, B. J., and Litonjua, A. A. (2010). Fungal exposure modulates the effect of polymorphisms of chitinases on emergency department visits and hospitalizations. *Am. J. Respir. Crit. Care Med.* 182 (7), 884–889. doi: 10.1164/rccm.201003-0322OC

Wyatt, T. T., Wosten, H. A., and Dijksterhuis, J. (2013). Fungal spores for dispersion in space and time. *Adv. Appl. Microbiol.* 85, 43–91. doi: 10.1016/B978-0-12-407672-3.00002-2

Zhang, Z., Biagini Myers, J. M., Brandt, E. B., Ryan, P. H., Lindsey, M., Mintz-Cole, R. A., et al. (2017). beta-Glucan exacerbates allergic asthma independent of fungal sensitization and promotes steroid-resistant TH2/TH17 responses. *J. Allergy Clin. Immunol.* 139 (1), 54–65 e58. doi: 10.1016/j.jaci.2016.02.031

Zhou, Z., Wang, C., and Luo, Y. (2020). Meta-analysis of the impacts of global change factors on soil microbial diversity and functionality. *Nat. Commun.* 11, 3072. doi: 10.1038/s41467-020-16881-7

Conflict of Interest: The authors declare that the research was conducted in the absence of any commercial or financial relationships that could be construed as a potential conflict of interest.

frontiers in Cellular and Infection Microbiology

PERSPECTIVE
published: 11 March 2021
doi: 10.3389/fcimb.2021.590874

SARS-CoV-2-Indigenous Microbiota Nexus: Does Gut Microbiota Contribute to Inflammation and Disease Severity in COVID-19?

Indranil Chattopadhyay and Esaki M. Shankar *

Department of Life Sciences, Central University of Tamil Nadu, Thiruvarur, India

Gut microbiome alterations may play a paramount role in determining the clinical outcome of clinical COVID-19 with underlying comorbid conditions like T2D, cardiovascular disorders, obesity, etc. Research is warranted to manipulate the profile of gut microbiota in COVID-19 by employing combinatorial approaches such as the use of prebiotics, probiotics and symbiotics. Prediction of gut microbiome alterations in SARS-CoV-2 infection may likely permit the development of effective therapeutic strategies. Novel and targeted interventions by manipulating gut microbiota indeed represent a promising therapeutic approach against COVID-19 immunopathogenesis and associated co-morbidities. The impact of SARS-CoV-2 on host innate immune responses associated with gut microbiome profiling is likely to contribute to the development of key strategies for application and has seldom been attempted, especially in the context of symptomatic as well as asymptomatic COVID-19 disease.

Keywords: ACE2, COVID-19, Dysbiosis, Microbiota (microorganism), SARS-CoV-2 (2019-nCoV), Inflammation

OPEN ACCESS

Edited by:
Steven D. Pletcher, University of California, San Francisco, United States

Reviewed by:
Karl M. Thompson, Howard University, United States
Angelica Thomaz Vieira, Federal University of Minas Gerais, Brazil

***Correspondence:**
Esaki M. Shankar
shankarem@cutn.ac.in

Specialty section:
This article was submitted to Microbiome in Health and Disease, a section of the journal Frontiers in Cellular and Infection Microbiology

Received: *03 August 2020*
Accepted: *28 January 2021*
Published: *11 March 2021*

Citation:
Chattopadhyay I and Shankar EM (2021) SARS-CoV-2-Indigenous Microbiota Nexus: Does Gut Microbiota Contribute to Inflammation and Disease Severity in COVID-19? Front. Cell. Infect. Microbiol. 11:590874. doi: 10.3389/fcimb.2021.590874

INTRODUCTION

Severe acute respiratory syndrome coronavirus 2 (SARS-CoV-2) is responsible for the development coronavirus disease 2019 (COVID-19) globally, described initially from a wet market in Wuhan, China, back in September 2019 (Chan et al., 2020). The World Health Organization (WHO) has reported 114,751,575 confirmed global cases and 2,549,260 deaths as of 3rd March 2021 due to COVID-19 (He Y et al., 2020; Shankar et al., 2021). The high rates of morbidity and mortality in COVID-19 results from the onset of a severe acute respiratory distress syndrome (ARDS) and systemic inflammatory response syndrome (SIRS), which afflicts the pulmonary compartment initially eventually leading to multi-organ failure (MOF) (Chen et al., 2020). The predominant involvement of the respiratory system in COVID-19 pathogenesis mainly stems from the mode of entry of the virus into the host, i.e., respiratory tract, and also owing to the high expression of angiotensin-converting enzyme 2 (ACE2), the classical receptor to which the viral spike protein ligand can engage with, on the respiratory and the gastrointestinal epithelia. Reports also suggest that SARS-CoV-2 inhibits the absorption of nutrients in the GI tract that drive the onset of gastroenteritis in a sizeable number of affected individuals (Zhou et al., 2020).

The human gut microbiota represents a highly complex and dynamic microbial community that plays a critical role in protecting the host from pathogenic microbial invaders (Vemuri et al., 2018). An extensive and integrated network of gut microbiota works in concert with the host to promote health, and any event that disrupts the homeostasis likely entails disease development (Vemuri et al., 2020). It is widely believed that the diversity of gut microbiota directly impacts the overall health of the host. It is also likely that alterations in gut microbiome could determine the natural history and clinical outcome of COVID-19, together with the described underlying co-morbid conditions like type 2 diabetes (T2D), cardiovascular disorders, and obesity warranting manipulation of the gut microbiota by employing several combinatorial approaches.

OVERVIEW OF ACE2-MICROBIOTA NEXUS IN HOST IMMUNITY

It has been shown that ACE2 expression reportedly alters the lung and gut microbiomes during certain underlying conditions involving the cardiac and pulmonary compartments (Cole-Jeffrey et al., 2015). It has also been known that ACE2 is involved in regulating inflammation and maintaining a healthy microbial community in the host (Hashimoto et al., 2012). Gut microbiome is involved in the regulation of genes involved in immune responses and metabolism in the host (Li et al., 2019). Furthermore, ACE2 has been shown to regulate intestinal metabolism of tryptophan, which drives the release of antimicrobial peptides to maintain and sustain the composition of gut microbiota. It has become clear that down-regulation of ACE2 reduces the intestinal absorption of tryptophan that lowers the secretion of antimicrobial peptides entailing gut dysbiosis (He Y. et al., 2020). Bacterial species such as *Bacteroides dorei* appear to have a significant role in regulating host immune responses by suppressing the expression of colonic ACE2 (Yoshida et al., 2018) supported by the finding that critically ill COVID-19 patients develop gastrointestinal symptoms (Du et al., 2020). Hence, gut microbiota seemingly plays a determining role in SARS-CoV-2 infection through the gut-lung axis (Marsland et al., 2015). Evidence suggests that influenza virus-driven lung injury could be enhanced by alteration in gut microbiota that in turn is believed to be associated with a significant reduction in host antiviral surveillance (Ichinohe et al., 2011). Interestingly, over-expression of fecal calprotectin is suggestive of the role of gut inflammation as a critical baseline finding in clinical COVID-19 (Zuo et al., 2020). Hence, it is imperative to address the role of indigenous microbiota as a key target in the development of anti-SARS-CoV-2 therapeutics and strategies.

GUT-LUNG MICROBIOME AXIS: LESSONS LEARNT FROM CLASSICAL RESPIRATORY VIRAL INFECTIONS

The gut microbiome is reportedly involved in digestion and protection against pathogens in the host (Hall et al., 2017), and often encompasses phyla Actinobacteria, Firmicutes, Proteobacteria, and Bacteroidetes. The healthy human colon has a greater abundance of bacterial families such as Bacteroidaceae, Prevotellaceae, Rikenellaceae, Lachnospiraceae, and Ruminococcaceae. Evidence suggests that the gut has a preponderance of Bacteroidetes and Firmicutes whereas the pulmonary compartment harbors a considerable population of Bacteroidetes, Firmicutes, and Proteobacteria (Zhang et al., 2020). Gut microbiota appears to have a serious impact on lung infection mediated *via* the gut-lung axis (Dumas et al., 2018). Gut microbiota regulates the optimal functioning of the innate and adaptive immune systems, and antimicrobial peptides and secondary metabolites derived from intestinal commensals are involved in cellular homeostasis (Negi et al., 2019a). Microbe-associated molecular patterns (MAMPs) as well as pathogen-associated molecular patterns (PAMPs) are recognized by toll-like receptors (TLRs) of host cells that drive the regulation of pro- and anti-inflammatory signals (Negi et al., 2019b), and hence a depletion in gut microbial diversity could inflict significant damage on host health (Mosca et al., 2016). Gut commensals, bacteroides, lactobacillus, and bifidobacteria reportedly release a plethora of short-chain fatty acids (SCFA) such as butyrate, acetate and propionate, which bind with dendritic cells (DCs) and macrophages that drive immunomodulation (Jia et al., 2018). Recent findings suggest that gut microbiota could play a significant role in the induction of ARDS (Dickson, 2016) setting clues to advance our understanding of the likely possibility of the same in determining the onset of SARS-CoV-2-mediated tissue damage originating from hypercytokinemia (Girija et al., 2020) and SIRS (Dhar and Mohanty, 2020). Respiratory viral infections such as influenza virus and respiratory syncytial virus (RSV) reflect a significant impact of alteration in gut microbiome with disease severity and prognosis (Deriu et al., 2016). Influenza virus infection induces alterations of gut microbiome through a type I interferon-dependent mechanism (Abt et al., 2012). It appears that the normal gut microbiota elicits the activation and assembly of inflammasome and T-cell responses by inducing the migration of DCs and macrophages in influenza virus infection (Steed et al., 2017). Microbe-derived secondary metabolites such as SCFAs, produced commonly by bacteroidetes and/or clostridia enhanced the protection attributes against influenza virus infection largely by inducing CD8+ T-cell functions and type I IFN signaling in macrophages (Abt et al., 2012). Hence, gut microbiome plays a significant role in regulating immune responses in systematic and distant mucosal sites, including the lungs (Gu et al., 2020).

The gut-lung axis is bidirectional which means metabolites that are derived from gut bacteria effect on the lung through blood whereas inflammation of the lung modifies the level of gut microbiota. Dysbiosis of gut microbiota induces lung dysfunction *via* alteration of immune responses of neutrophils, T cells, TLRs, and inflammatory cytokines. SARS-CoV-2 induces infection in the lung to activate an immune response in the gastrointestinal tract and disruption of epithelial cells in the lung (Fanos et al., 2020). SARS-CoV-2 induces alterations of lung microbiota such as a higher abundance of *Klebsiella oxytoca*, and *Rothia mucilaginosa* that drive inflammation in the lung

(Han et al., 2020). Higher level of proinflammatory cytokines in the blood due to viral infections induce dysbiosis of gut bacteria and disruption of the gut barrier. Dysbiosis of gut microbiota breaks the integrity of gut barrier which induces the translocation of SARS-CoV-2 from the lung into the gut through the circulatory and lymphatic systems. Inflammation in the gut induces leaky gut that drives the development of sepsis in COVID-19 patients through translocation of bacterial antigens and toxins into the systemic circulation (**Figure 1**). Dysbiosis of gut microbiota also induces pathogenesis in the lung of respiratory distress syndrome (Aktas and Aslim, 2020). SARS-CoV-2 induces alterations of lung microbiota such as a higher abundance of *Klebsiella oxytoca*, and *Rothia mucilaginosa* that drive inflammation in the lung (Han et al., 2020).

Streptococcus sp., *Escherichia* sp., and *Shigella* sp., showed a higher abundance in COVID-19 and H1N1 patients (Gu et al., 2020). The relative abundance of phyla *Actinobacteria and Firmicutes* was significantly reduced in H1N1 patients as compared to COVID-19 patients and healthy controls. At the family level, the number of Lachnospiraceae and Ruminococcaceae, which includes butyrate-producing bacteria (BPB) was drastically reduced in H1N1 patients. Further, the abundance of *Blautia, Agathobacter, Anaerostipes, Fusicatenibacter, Eubacterium hallii* group was significantly reduced. Recent findings also suggests that the frequency of *Fusicatenibacter, Anaerostipes, Agathobacter*, and *E. hallii* from the Lachnospiraceae family was significantly reduced in COVID-19 patients. On the one hand *Streptococcus, Rothia, Veillonella, Erysipelatoclostridium, and Actinomyces* were highly abundant in COVID-19 patients, and on the other hand, bacterial genera such as *Blautia*, *Romboutsia, Faecalibacterium, Fusicatenibacter*, *Collinsella*, *Bifidobacterium*, *and Eubacterium hallii* were reportedly high among healthy subjects. Patients of H1N1 Influenza have higher abundance of *Enterococcus, Prevotella, Finegoldia*, and *Peptoniphilus. Prevotella, Ezakiella, Murdochiella, and*

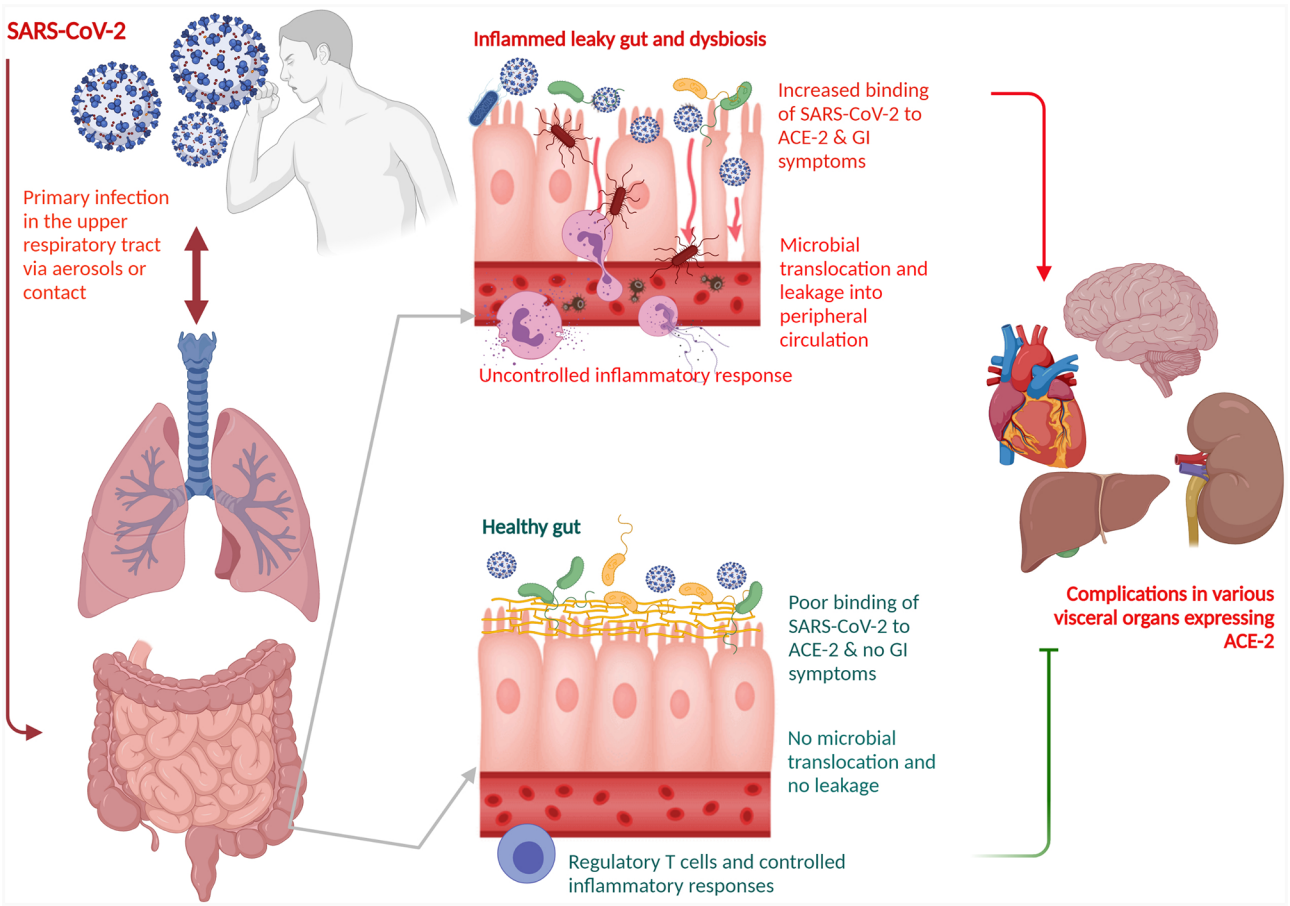

FIGURE 1 | Schematic representation of a role of gut-lung axis with dysbiosis of the gut microbiota for COVID-19 disease management. The gut-lung axis is bidirectional which means metabolites that are derived from gut bacteria effect on the lung through blood whereas inflammation of the lung modifies the level of gut microbiota. SARS-CoV-2 primarily affects the lung. Dysbiosis of gut microbiota breaks the integrity of gut barrier which induces the translocation of SARS-CoV-2 from the lung into the gut through the circulatory and lymphatic systems. The virus binds with the ACE2 on the enterocytes. Inflammation in the gut induces leaky gut that drives the development of sepsis in COVID-19 patients through translocation of bacterial antigens and toxins into the systemic circulation. Dysbiosis of gut microbiota also induces pathogenesis in the lung of respiratory distress syndrome. SARS-CoV-2, severe acute respiratory syndrome coronavirus 2; ACE2, angiotensin-converting enzyme 2.

Porphyromonas showed a higher abundance in H1N1 patients as compared to COVID-19 patients suggesting that respiratory viral pathogenesis seems to be determined also by inflammatory gut microbiome. H1N1-enriched bacteria has shown a positive association with inflammatory cytokines IL-2, IL-4, and IL-6, the later being the predominant culprit behind the onset of cytokine storm in COVID-19 (Gu et al., 2020). Whilst *Rothia* is involved in the development of pneumonia in immunocompromised individuals (Ramanan et al., 2014), both *Streptococcus and Rothia* are associated with disease severity in avian H7N9 virus infection (Lu et al., 2017). Further, H1N1 as well as H7N9 patients showed a higher abundance in opportunistic pathogens such as *Prevotella, Finegoldia, and Peptoniphilus* and elevated levels of IL-2 and IL-4 (Qin et al., 2015). The abundance of *Faecalibacterium prausnitzii, Eubacterium rectale, and Ruminococcus bromii* belong to Firmicutes and *Bifidobacterium adolescentis, Bifidobacterium pseudocatenulatum, and Collinsella aerofaciens* belong to Actinobacteria is reduced in COVID-19 patients. *B. adolescentis* prevents the activation of proinflammatory cytokine by inhibiting the activity of NF- κB (Yeoh et al., 2021). Dysbiosis of the lung microbiome enhances susceptibility to viral infections and also induces the development of secondary bacterial infections to increase mortality rates in COVID-19 patients. *Streptococcus salivarius* K12 showed inhibitory activity against SARS-CoV-2 (Di Pierro, 2020), and the abundance of certain oropharyngeal microbiomes such as haemophilus or streptococcus could likely contribute to severity of SARS-CoV-2 disease (https://doi.org/10.21203/rs.3.rs-127621/v1).

Given the aforementioned observations, it could be assumed that microbial dysbiosis in the lungs of COVID-19 patients likely predict the onset of hyperinflammation-driven ARDS. It has been shown that gut-associated *Enterobacteriaceae* showed a higher abundance in individuals progressing to develop ARDS. A higher abundance of Lachnospiraceae in ARDS patients showed an association with reduced survival. It is also hypothesised that microbiome alterations in gut and lung may predict the development of ARDS in COVID-19 patients (Dickson et al., 2020). Higher abundance of Proteobacteria and Bacteroidetes and a lower abundance of Firmicutes have been reported in influenza virus infection (Groves et al., 2018). Most prevalent bacterial genera such as *Acinetobacter, Chryseobacterium, Burkholderia, Brevundimonas, Sphingobium and Enterobacteriaceae* were reported in necropsy lung tissues of deceased patients with COVID-19. Among Acinetobacter, *Acinetobacter calcoaceticus, Acinetobacter baumannii, Acinetobacter nosocomialis, and Acinetobacter pittii*, with *A.baumannii* (AB) were highly abundant. Of the members belonging to Enterobacteriaceae, *Klebsiella, Escherichia coli, Proteus, and Enterobacte*r were highly abundant (Fan et al., 2020). Further, a higher abundance of *Clostridium hathewayi*, *Actinomyces viscosus*, and *Bacteroides nordii* has also been reported in antibiotic naïve COVID-19 patients. Antibiotic treated COVID-19 patients showed a significant depletion of beneficial symbionts such as *Fecalibacterium prausnitzii, Lachnospiraceae bacterium 5_1_63FAA, Eubacterium rectale, Ruminococcus obeum, and Dorea formicigenerans* in the gut relative to antibiotic naïve COVID-19 patients. Bacterial genus *Coprobacillus, Clostridium ramosum* and *Clostridium hathewayi* belong to phylum Firmicutes showed a positive correlation with COVID-19 severity whereas *Alistipes onderdonkii* and *F. prausnitzii* showed a negative association with disease severity. Furthermore, opportunistic pathogens such as *C.hathewayi, Bacteroides nordii, Actinomyces viscosus* appear to be highly abundant in the gut of COVID-19 patients. Bacteroidetes species such as *Alistipes onderdonkii* and *Bacteroides ovatus* showed a negative correlation with severity of COVID-19. *Bacteroides dorei, Bacteroides thetaiotaomicron, Bacteroides massiliensis*, and *Bacteroides ovatus* belonging to phylum Bacteroidetes showed an inverse negative correlation with SARS-CoV-2 viral loads in fecal samples of COVID-19 patients (Zuo et al., 2020). Interestingly, *B.dorei* has been shown to down-regulate ACE2 expression in the human colon (Yoshida et al., 2018). It also appears that *Alistipes* species are involved in tryptophan metabolism whereas *F. prausnitzii* showed anti-inflammatory properties (Vatanen et al., 2016).

Adding further the likely role of gut microbiota with disease progression, the outer membrane vesicles (OMVs) of *Acinetobacter nosocomialis* have been shown to augment inflammatory responses in epithelial cells (Nho et al., 2015). Enterobacteriaceae such as *E.coli, Klebsiella* sp., and *Proteus* sp. are colonisers of the gut albeit at low levels. It appears that the level of Enterobacteriaceae become elevated during inflammatory conditions engendering from exaggerated release of ROS and nitrogen intermediates by epithelial cells and transmigrating neutrophils in the gut lumen. Enterobactin of *E. coli* prevents the intracellular killing of action of myeloperoxidase of PMNs in the inflamed gut (Zeng et al., 2017). Gut *K. pneumoniae* enhances inflammatory response in human airway epithelial cells through activation of TLR4 and TLR2. Evidence also suggests that MAPKs p38, ERK and JNK regulates the secretion of inflammatory mediators and defensins from epithelial cells during Klebsiella infection. Klebsiella enhances inflammatory response by preventing the action of host proteins such as CYLD and MKP-1 which are involved in immune homeostasis post-inflammation. Klebsiella blocks IL-23/IL-17 and IL-12/IFN-γ signalling (Bengoechea and Sa Pessoa, 2019). Peptidoglycan and teichoic acid of streptococci bind to TLR-2 of epithelial and endothelial cells, monocytes and macrophages, which induce secretion of IL-1β, IL-6, IL-8, and TNF-α (Loughran et al., 2019). Actinomyces induces inflammatory lesions in tissues having PMNs, macrophages, and plasma cells (Engel et al., 1976). Besides, alteration in the gut microbiota has been demonstrated to have an association with several other respiratory infections, inflammatory bowel disease, depression, T2D, cardiovascular disease and hypertension (Schmidt et al., 2018). Studies have revealed that gut microbiota plays an eminent role in the pathogenesis of sepsis and ARDS (Dickson et al., 2016). Similarly, a study from China showed that some patients with COVID-19 presented with gut dysbiosis with decreased levels of *Lactobacillus* and *Bifidobacterium* (Xu et al., 2020).

Higher abundance of *Coprobacillus, Clostridium ramosum*, and *Clostridium hathewayi* led to disease severity in COVID-19 patients. Drugs such as chloroquine phosphate, lopinavir, ritonavir, and remdesivir used for the treatment of COVID-19

are also involved in gut dysbiosis. Application of short-term antibiotics use in COVID-19 treatment may also lead to alterations in gut bacteria. Prolonged use of doxycycline and hydroxychloroquine significantly reduced Bacteroidetes, Firmicutes, and Lactobacillus in the gut of COVID-19 patients. Interestingly, dysbiosis of gut bacteria is noticed even after recovery from COVID-19. FMT may be used to alter the gut microbiota in COVID-19 patients. It is essential to screen the presence of SARS-CoV-2 and gut microbiota profile in stool samples of patients after 35 days from recovery to provide the highest protection for FMT recipients. Stool samples of donors are also needed to screen the presence of SARS-CoV-2 (Kaźmierczak-Siedlecka et al., 2020).

GUT MICROBIOME IN THE ELDERLY COVIDANTS: DOES IT EXPLAIN HIGH MORTALITY RATES?

The increased rates of mortality among the elderly in COVID-19 seem to stem from alterations in gut microbiota. The potential rationale underlying increased rates of mortality among the elderly in COVID-19 due to likely higher abundance of inflammatory bacteria (**Table 1**). The abundance of beneficial bifidobacterial may be depleted in the elderly peoples (Nagpal et al., 2018). Elderly people may be more susceptible to SARS-CoV-2 infection due to less diverse beneficial microorganisms.

It has also been hypothesized that drugs used to treat diabetes mellitus and hypertension might upregulate the expression of ACE2 facilitating SARS-CoV-2 infection (Fang et al., 2020). Taking these factors into consideration, it can be easily speculated that SARS-CoV-2 infection might contribute to gut dysbiosis resulting in generalized inflammation contributing to MODS and other serious clinical worsening, especially in the elderly and patients with underlying clinical conditions.

TABLE 1 | List of elevated bacteria in COVID-19 patients associated with inflammation and immunity.

Bacterial Genus/ Species	Phylum	Mode of action associated with inflammation
Streptococcus	Firmicutes	Induces secretion of pro-inflammatory cytokines such as IL-1β, IL-6, IL-8, and TNF-α from epithelial cells.
Actinomyces viscosus	Actinobacteria	Induces inflammatory lesions in tissues having PMNs, macrophages, and plasma cells.
Burkholderia	Proteobacteria	Type VI effector, TecA of *B. cenocepacia* induces the activation of pyrin inflammasome through the deamidation of Rho GTPases that drive inflammation
Klebsiella		*K. pneumoniae* enhances inflammatory response in human airway epithelial cells through activation of TLR4 and TLR2 and preventing the action of host proteins such as CYLD and MKP-1 which are involved in immune homeostasis post inflammation event
Escherichia coli		Enterobactin of *E. coli* prevents action of bacteriocidal enzyme myeloperoxidase which is secreted from the neutrophil in the inflamed gut
Acinetobacter baumannii		HisF gene of this bacteria is responsible for the reduction of innate immune response.
Acinetobacter nosocomialis		Outer membrane vesicles (OMVs) induce inflammatory responses in epithelial cells

Previous studies showed that dietary supplementation of probiotic formula with *Bifidobacterium lactis* in aged individuals enhanced the tumoricidal functions of natural killer (NK) cells. Probiotics such as *L. johnsonii, L. fermentum, L. reuteri, L. paracasei, L. rhamnosus, L. acidophilus, L. plantarum, belonged to genera Lactobacillus and B. longum, B. breve, B. bifidum, and B. animalis subsp. lactis* were involved in alleviating inflammatory manifestations *via* regulation of innate immune responses (Dhar and Mohanty, 2020). Probiotic bacteria like *L. rhamnosus, B. lactis, and B.breve* are involved in the down-regulation of inflammation through elevation of Treg cells (Feleszko et al., 2007).

Prebiotics such as inulin, fructo-oligosachharides (Fos), galactosachharides (Gos), and polydextrose are involved in the development of host immunity through alterations of gut microbiome. Prebiotics reportedly reduce the levels of the proinflammatory IL-6 that tends to be the prime culprit behind the hitherto described grave prognosis in COVID-19 and enhance the levels of anti-inflammatory IL-10 (West et al., 2017). Protein enriched diet enhances the abundance of gut commensals such as bifidobacteria and lactobacilli simultaneously reduces the pathogenic gut microbiota (Świątecka et al., 2011). Probiotic strains such as bifidobacteria or lactobacilli are not only involved in the clearance of virus from the respiratory tract but also augments the activity of antigen presenting cells, NK cells, T cells to drive the enhanced release of mucosal antibodies in lung fluids (Zelaya et al., 2016). *Lactobacillus casei* induces the phagocytic activity of alveolar macrophages and over expression of IgA, IFN-γ, and TNF-α in the host to protect against flu virus infections. *Bifidobacterium, Lactobacillus paracasei*, and *Lactobacillus rhamnosus* enhanced the efficacy of vaccine response against respiratory infections such as H1N1, H5N1, and H3N2 (He L. H. et al., 2020). Probiotic strains are involved in the regulation of proinflammatory and anti-inflammatory cytokines that likely could ameliorate ARDS complications in COVID-19.

Elderly individuals with hypertension, obesity, and diabetes are more prone to develop severe symptoms due to COVID-19 infections because dysbiosis of the gut microbiome reduces the integrity of the gut barrier, which in turn allows other pathogens to bind the enterocytes. Disruption of the integrity of tight junctions in between enterocytes of the gut called "leaky gut" in COVID-19 patients is responsible for the development of diarrhea, and inflammation due to higher levels of IL-6 in plasma and fecal calprotectin. This also allows SARS-CoV-2 to enter into the blood stream and bind with ACE2 of other body parts. *F. prausnitzii* belonging to class Clostridia and family Ruminococcaceae is responsible for the synthesis of a short-chain fatty acid (SCFA) such as butyric acid in the gut (**Figure 1**). The abundance of this bacteria was reduced in COVID-19 patients. Butyric acid maintains the integrity of gut barrier and

shows anti-inflammatory activity through inhibition of NF-κB activity, activation of G protein-coupled receptors such as GPR41 and GPR43, suppression of histone deacetylase activity, and activation of regulatory T cells (Treg) cells. Fecal microbiota transplantation (FMT), and enhancement of abundance of next-generation probiotics such as butyrate-producing gut bacteria through daily intake of dietary fiber may be used to prevent inflammation and severity in COVID-19 patients (Kim, 2021). Protein extracts of whey and pea enhanced the abundance of Bifidobacterium, and Lactobacillus whereas reduced the abundance of pathogenic bacteria *Bacteroides fragilis* and *Clostridium perfringens* (Świątecka et al., 2011). SCFAs mainly acetate, propionate, and butyrate which are produced by the gut microbiota through the metabolism of resistant starches and dietary fibers provide energy to gut epithelial cells, maintain the integrity of the gut barrier, and suppressed inflammation by blocking the action of LPS and prevention of proinflammatory cytokine productions (Corrêa-Oliveira et al., 2016). Acetate may provide protection against respiratory syncytial virus (RSV) in the lung through the activation of IFN-β *via* GPR43 and IFNAR (Antunes et al., 2019).

Azithromycin which is a commonly used antibiotic for COVID-19 treatment reduced Shannon diversity index of bacterial communities particularly the abundance of Bifidobacterium genus. Other drugs such as metformin, statins, and psychiatric drugs are also involved in the alteration of the gut microbiota as well as enhance the risk of viral infections. Combinatorial approaches of probiotics, prebiotics, and natural products are used to control the balance of gut bacteria. Probiotics suppressed diarrhea by blocking the TLR expression and controlling the humoral and cellular immune responses. Bacterial genera such as Lactobacillus and Bifidobacterium showed strong antiviral action against influenza virus type A. These probiotics suppressed the growth of candida, *E. coli*, pseudomonas, and staphylococci during antibiotic administration in COVID-19 patients. Prebiotics and probiotics inhibit viral replication and infection *via* production of interferon (IFN) by activating plasmacytoid DCs *via* TLR9. LPS of Gram-negative and peptidoglycans (PG) of Gram-positive bacteria interact with viral proteins (Kiousi et al., 2019; Donati Zeppa et al., 2020). Gut microbiota effects on ACE2 at the gut and lung in such a way that probiotics may control the severity of the disease. Following gut colonization, probiotics could contribute to development of immunity against viral infections. Probiotics strains such as *Lactobacillus rhamnosus GG* and *Bifidobacterium longum* are involved in compressing the infection of ICU patients. Bacteriocins which are produced by Lactobacilli and Bifidobacteria are effective against pathogenic bacteria and viruses. Probiotic *Lactobacillus* sp. augments gut immunity through the synthesis of antiviral agents such as mucins and mucus in the intestine. Probiotics control innate and adaptive antiviral immunity through an interaction with dendritic cells, monocytes/macrophages, and lymphocytes. Lactic acid bacteria induces the synthesis of cytokines or chemokines through binding with intestinal epithelial cells *via* toll-like receptors. This also drives the abundance of IgA producing cells of bronchus, mammary glands and intestine which in turn stimulates mucosal immune system. Probiotics stimulate the secretion of IgG and IL-10 from the activated T-cells. It is essential to use probiotics along with prebiotics for the treatment of COVID-19 individuals (Din et al., 2021). Bacteriocin compounds such as staphylococcin 188, enterocin AAR-74, erwiniocin NA4 showed antiviral activity against HIV, HSV, Coliphage, influenza virus, and H1N1 virus (Gohil et al., 2021).

Together, gut microbiome alterations may play a paramount role in determining the clinical outcome of clinical COVID-19 with underlying co-morbid conditions like T2D, cardiovascular disorders, obesity, etc. Research is warranted to manipulate the profile of gut microbiota in COVID-19 by employing combinatorial approaches such as use of prebiotics, probiotics and symbiotics. Prediction of gut microbiome alterations in SARS-CoV-2 infection may likely permit the development of effective therapeutic strategies. Novel and targeted interventions by manipulating gut microbiota indeed represents a promising therapeutic approach against COVID-19 immunopathogenesis and associated co-morbidities. The impact of SARS-CoV-2 on host innate immune responses associated with gut microbiome profiling is likely to contribute to development of key strategies for application and has seldom been attempted, especially in the context of symptomatic as well as asymptomatic COVID-19 disease.

DATA AVAILABILITY STATEMENT

The original contributions presented in the study are included in the article/supplementary material. Further inquiries can be directed to the corresponding author.

AUTHOR CONTRIBUTIONS

IC and ES led the writing of this opinion article. All authors contributed to the article and approved the submitted.

FUNDING

ES is supported by the Department of Science and Technology-Science and Engineering Research Board, Government of India (Grant number CRG/2019/006096), the Indian Council of Medical Research, Government of India (No. 45/2/2020-DDI/BMS) and the Swedish Research Council (VR 2014-02836).

ACKNOWLEDGMENTS

The views, opinions, assumptions, or any other information set out in this article are solely those of the authors and should not be attributed to anyone. The authors salute all the health care workers who are at the front lines of the COVID-19 pandemic, helping patients and their families.

REFERENCES

Abt, M. C., Osborne, L. C., Monticelli, L. A., Doering, T. A., Alenghat, T., Sonnenberg, G. F., et al. (2012). Commensal bacteria calibrate the activation threshold of innate antiviral immunity. *Immunity* 37, 158–170. doi: 10.1016/j.immuni.2012.04.011

Aktas, B., and Aslim, B. (2020). Gut-lung axis and dysbiosis in COVID-19. *Turk J. Biol.* 44 (3), 265–272. doi: 10.3906/biy-2005-102

Antunes, K. H., Fachi, J. L., de Paula, R., da Silva, E. F., Pral, L. P., Dos Santos, AÁ, et al. (2019). Microbiota-derived acetate protects against respiratory syncytial virus infection through a GPR43-type 1 interferon response. *Nat. Commun.* 10 (1), 3273. doi: 10.1038/s41467-019-11152-6

Bengoechea, J. A., and Sa Pessoa, J. (2019). *Klebsiella pneumoniae* infection biology: living to counteract host defences. *FEMS Microbiol. Rev.* 43 (2), 123–144. doi: 10.1093/femsre/fuy043

Chan, J. F., Yuan, S., Kok, K. H., To, K. K., Chu, H., Yang, J., et al. (2020). A familial cluster of pneumonia associated with the 2019 novel coronavirus indicating person-to-person transmission: a study of a family cluster. *Lancet* 395 (10223), 514–523. doi: 10.1016/S0140-6736(20)30154-9

Chen, N., Zhou, M., Dong, X., Qu, J., Gong, F., Han, Y., et al. (2020). Epidemiological and clinical characteristics of 99 cases of 2019 novel coronavirus pneumonia in Wuhan, China: a descriptive study. *Lancet* 395, 507–513. doi: 10.1016/S0140-6736(20)30211-7

Cole-Jeffrey, C. T., Liu, M., Katovich, M. J., Raizada, M. K., and Shenoy, V. (2015). ACE2 and microbiota: Emerging targets for cardiopulmonary disease therapy. *J. Cardiovasc. Pharmacol.* 66 (6), 540–550. doi: 10.1097/FJC.0000000000000307

Corrêa-Oliveira, R., Fachi, J. L., Vieira, A., Sato, F. T., and Vinolo, M. A. (2016). Regulation of immune cell function by short-chain fatty acids. *Clin. Transl. Immunol.* 5, e73. doi: 10.1038/cti.2016.17

Deriu, E., Boxx, G. M., He, X., Pan, C., Benavidez, S. D., Cen, L., et al. (2016). Influenza virus affects intestinal microbiota and secondary salmonella infection in the gut through type I interferons. *PLoS Pathog.* 12, e1005572. doi: 10.1371/journal.ppat.1005572

Dhar, D., and Mohanty, A. (2020). Gut microbiota and Covid-19- possible link and implications. *Virus Res.* 285, 198018. doi: 10.1016/j.virusres.2020.198018

Di Pierro, F. (2020). A possible probiotic (*S. salivarius* K12) approach to improve oral and lung microbiotas and raise defenses against SARS-CoV-2. *Minerva Med.* 111, 281–283. doi: 10.23736/S0026-4806.20.06570-2

Dickson, R. P., Erb-Downward, J. R., Martinez, F. J., and Huffnagle, G. B. (2016). The microbiome and the respiratory tract. *Annu. Rev. Physiol.* 78, 481–504. doi: 10.1146/annurev-physiol-021115-105238

Dickson, R. P., Schultz, M. J., Van Der Poll, T., Schouten, L. R., Falkowski, N. R., Luth, J. E., et al. (2020). Lung microbiota predict clinical outcomes in critically iII patients. *Am. J. Respir. Crit. Care Med.* 01, 555–563. doi: 10.1164/rccm.201907-1487OC

Dickson, R. P. (2016). The microbiome and critical illness. *Lancet Respir. Med.* 4 (1), 59–72. doi: 10.1016/S2213-2600(15)00427-0

Din, A. U., Mazhar, M., Waseem, M., Ahmad, W., Bibi, A., Hassan, A., et al. (2021). SARS-CoV-2 microbiome dysbiosis linked disorders and possible probiotics role. *BioMed. Pharmacother.* 133, 110947. doi: 10.1016/j.biopha.2020.110947. 110947.

Donati Zeppa, S., Agostini, D., Piccoli, G., Stocchi, V., and Sestili, P. (2020). Gut microbiota status in COVID-19: An unrecognized player? *Front. Cell Infect. Microbiol.* 10:576551. doi: 10.3389/fcimb.2020.576551

Du, M., Cai, G., Chen, F., Christiani, D. C., Zhang, Z., and Wang, M. (2020). Multiomics evaluation of gastrointestinal and other clinical characteristics of SARS-CoV-2 and COVID-19. *Gastroenterology* 158 (8), 2298–2301. doi: 10.1053/j.gastro.2020.03.045

Dumas, A., Bernard, L., Poquet, Y., Lugo-Villarino, G., and Neyrolles, O. (2018). The role of the lung microbiota and the gut–lung axis in respiratory infectious diseases. *Cell Microbiol.* 20 (12), e12966. doi: 10.1111/cmi.12966

Engel, D., Epps, D. V., and Clagett, J. (1976). *In vivo* and *in vitro* studies on possible pathogenic mechanisms of *Actinomyces viscosus*. *Infect. Immun.* 14 (2), 548–554. doi: 10.1128/IAI.14.2.548-554.1976

Fan, J., Li, X., Gao, Y., Zhou, J., Wang, S., Huang, B., et al. (2020). The lung tissue microbiota features of 20 deceased patients with COVID-19. *J. Infect.* 81 (3), e64-e67. doi: 10.1016/j.jinf.2020.06.047

Fang, L., Karakiulakis, G., and Roth, M. (2020). Are patients with hypertension and diabetes mellitus at increased risk for COVID-19 infection? *Lancet Respir. Med.* 8 (4), e21. doi: 10.1016/S2213-2600(20)30116-8

Fanos, V., Pintus, M. C., Pintus, R., and Marcialis, M. A. (2020). Lung microbiota in the acute respiratory disease: from coronavirus to metabolomics. *J. Pediatr. Neonat. Individualized Med.* 9 (1), 90139. doi: 10.7363/090139

Feleszko, W., Jaworska, J., Rha, R. D., Steinhausen, S., Avagyan, A., Jaudszus, A., et al. (2007). Probiotic-induced suppression of allergic sensitization and airway inflammation is associated with an increase of T regulatory-dependent mechanisms in a murine model of asthma. *Clin. Exp. Allergy* 37 (4), 498–505. doi: 10.1111/j.1365-2222.2006.02629.x

Girija, A. S. S., Shankar, E. M., and Larsson, M. (2020). Could SARS-CoV-2-induced hyperinflammation magnify the severity of coronavirus disease (CoViD-19) leading to acute respiratory distress syndrome? *Front. Immunol.* 11, 1206. doi: 10.3389/fimmu.2020.01206

Gohil, K., Samson, R., Dastager, S., and Dharne, M. (2021). Probiotics in the prophylaxis of COVID-19: something is better than nothing. *3 Biotech.* 11 (1), 1. doi: 10.1007/s13205-020-02554-1

Groves, H. T., Cuthbertson, L., James, P., Moffatt, M. F., Cox, M. J., and Tregoning, J. S. (2018). Respiratory disease following viral lung infection alters the murine gut microbiota. *Front. Immunol.* 9, 182. doi: 10.3389/fimmu.2018.00182

Gu, S., Chen, Y., Wu, Z., Chen, Y., Gao, H., Lv, L., et al. (2020). Alterations of the gut microbiota in patients with COVID-19 or H1N1 influenza. *Clin. Infect. Dis.* 4, ciaa709. doi: 10.1093/cid/ciaa709

Hall, A. B., Tolonen, A. C., and Xavier, R. J. (2017). Human genetic variation and the gut microbiome in disease. *Nat. Rev. Genet.* 18 (11), 690–699. doi: 10.1038/nrg.2017.63

Han, Y., Jia, Z., Shi, J., Wang, W., and He, K. (2020). The active lung microbiota landscape of COVID-19 patients. *medRxiv* 2008, 2020. doi: 10.1101/2020.08.20.20144014. 20144014.

Hashimoto, T., Perlot, T., Rehman, A., Trichereau, J., Ishiguro, H., Paolino, M., et al. (2012). ACE2 links amino acid malnutrition to microbial ecology and intestinal inflammation. *Nature* 487, 477–481. doi: 10.1038/nature11228

He, L. H., Ren, L. F., Li, J. F., Wu, Y. N., Li, X., and Zhang, L. (2020). Intestinal flora as a potential strategy to fight SARS-CoV-2 infection. *Front. Microbiol.* 11, 1388. doi: 10.3389/fmicb.2020.01388

He, Y., Wang, J., Li, F., and Shi, Y. (2020). Main clinical features of COVID-19 and potential prognostic and therapeutic value of the microbiota in SARS-CoV-2 infections. *Front. Microbiol.* 11, 1302. doi: 10.3389/fmicb.2020.01302

Ichinohe, T., Pang, I. K., Kumamoto, Y., Peaper, D. R., Ho, J. H., Murray, T. S., et al. (2011). Microbiota regulates immune defense against respiratory tract influenza A virus infection. *Proc. Natl. Acad. Sci. U. S. A.* 108 (13), 5354–5359. doi: 10.1073/pnas.101937810

Jia, W., Xie, G., and Jia, W. (2018). Bile acid–microbiota crosstalk in gastrointestinal inflammation and carcinogenesis. *Nat. Rev. Gastroenterol. Hepatol.* 15 (2), 111–128. doi: 10.1038/nrgastro.2017.119

Kaźmierczak-Siedlecka, K., Vitale, E., and Makarewicz, W. (2020). COVID-19 - gastrointestinal and gut microbiota-related aspects. *Eur. Rev. Med. Pharmacol. Sci.* 24 (20), 10853–10859. doi: 10.26355/eurrev_202010_23448

Kim, H. S. (2021). Do an altered gut microbiota and an associated leaky gut affect COVID-19 severity? *mBio* 12 (1), e03022–e03020. doi: 10.1128/mBio.03022-20

Kiousi, D. E., Karapetsas, A., Karolidou, K., and Panayiotidis, M. I. (2019). Probiotics in extraintestinal diseases: Current trends and new directions. *Nutrients* 11, 788. doi: 10.3390/nu11040788

Li, N., Ma, W. T., Pang, M., Fan, Q. L., and Hua, J. L. (2019). The commensal microbiota and viral infection: a comprehensive review. *Front. Immunol.* 10, 1551. doi: 10.3389/fimmu.2019.01551

Loughran, A. J., Orihuela, C. J., and Tuomanen, E. I. (2019). *Streptococcus pneumoniae*: Invasion and inflammation. *Microbiol. Spectr.* 7 (2). doi: 10.1128/microbiolspec.GPP3-0004-2018. 10.1128/microbiolspec.GPP3-0004-2018.

Lu, H. F., Li, A., Zhang, T., Ren, Z. G., He, K. X., Zhang, H., et al. (2017). Disordered oropharyngeal microbial communities in H7N9 patients with or without secondary bacterial lung infection. *Emerg. Microbes Infect.* 6 (12), e112. doi: 10.1038/emi.2017.101

Marsland, B. J., Trompette, A., and Gollwitzer, E. S. (2015). The gut-lung axis in respiratory disease. *Ann. Am. Thorac. Soc.* 12, S150–S156. doi: 10.1513/AnnalsATS.201503-133AW

Mosca, A., Leclerc, M., and Hugot, J. P. (2016). Gut microbiota diversity and human diseases: should we reintroduce key predators in our ecosystem? *Front. Microbiol.* 7, 455. doi: 10.3389/fmicb.2016.00455

Nagpal, R., Mainali, R., Ahmadi, S., Wang, S., Singh, R., Kavanagh, K., et al. (2018). Gut microbiome and aging: physiological and mechanistic insights. *Nutr. Healthy Aging* 4 (4), 267–285. doi: 10.3233/NHA-170030

Negi, S., Das, D. K., Pahari, S., Nadeem, S., and Agrewala, J. N. (2019a). Potential role of gut microbiota in induction and regulation of innate immune memory. *Front. Immunol.* 10, 2441. doi: 10.3389/fimmu.2019.02441

Negi, S., Pahari, S., Bashir, H., and Agrewala, J. N. (2019b). Gut microbiota regulates mincle mediated activation of lung dendritic cells to protect against *Mycobacterium tuberculosis*. *Front. Immunol.* 10, 1142. doi: 10.3389/fimmu.2019.01142

Nho, J. S., Jun, S. H., Oh, M. H., Park, T. I., Choi, C. W., Kim, S. I., et al. (2015). *Acinetobacter nosocomialis* secretes outer membrane vesicles that induce epithelial cell death and host inflammatory responses. *Microb. Pathog.* 81, 39–45. doi: 10.1016/j.micpath.2015.03.012

Qin, N., Zheng, B., Yao, J., Guo, L., Zuo, J., Wu, L., et al. (2015). Influence of H7N9 virus infection and associated treatment on human gut microbiota. *Sci. Rep.* 5:14771. doi: 10.1038/srep14771

Ramanan, P., Barreto, J. N., Osmon, D. R., and Tosh, P. K. (2014). Rothia bacteremia: a 10-year experience at Mayo Clinic, Rochester, Minnesota. *J. Clin. Microbiol.* 52 (9), 3184–3189. doi: 10.1128/JCM.01270-14

Schmidt, T. S. B., Raes, J., and Bork, P. (2018). The human gut microbiome: From association to modulation. *Cell* 172 (6), 1198–1215. doi: 10.1016/j.cell.2018.02.044

Shankar, E. M., Che, K. F., Yong, Y. K., Girija, A. S. S., Velu, V., Ansari, A.W., et al. (2021). Asymptomatic SARS-CoV-2 infection: is it all about being refractile to innate immune sensing of viral spare-parts?-Clues from exotic animal reservoirs. *Pathog Dis 9,* 79 (1), ftaa076. doi: 10.1093/femspd/ftaa076

Steed, A. L., Christophi, G. P., Kaiko, G. E., Sun, L., Goodwin, V. M., Jain, U., et al. (2017). The microbial metabolite desaminotyrosine protects from influenza through type I interferon. *Science* 357, 498–502. doi: 10.1126/science.aam5336

Świątecka, D., Narbad, A., Ridgway, K. P., and Kostyra, H. (2011). The study on the impact of glycated pea proteins on human intestinal bacteria. *Int. J. Food Microbiol.* 145, 267–272. doi: 10.1016/j.ijfoodmicro.2011.01.002

Vatanen, T., Kostic, A. D., d'Hennezel, E., Siljander, H., Franzosa, E. A., Yassour, M., et al. (2016). Variation in microbiome LPS immunogenicity contributes to autoimmunity in humans. *Cell* 165, 842–853. doi: 10.1016/j.cell.2016.05.056

Vemuri, R., Gundamaraju, R., Shastri, M. D., Shukla, S. D., Kalpurath, K., Ball, M., et al. (2018). Gut microbial changes, interactions, and their implications on human lifecycle: An ageing perspective. *BioMed. Res. Int.* 2018, 4178607. doi: 10.1155/2018/4178607

Vemuri, R., Shankar, E. M., Chieppa, M., Eri, R., and Kavanagh, K. (2020). Beyond Just bacteria: Functional biomes in the gut ecosystem including virome, mycobiome, archaeome and helminths. *Microorganisms* 8 (4), 483. doi: 10.3390/microorganisms8040483

West, C. E., Dzidic, M., Prescott, S. L., and Jenmalm, M. C. (2017). Bugging allergy; role of pre-, pro- and synbiotics in allergy prevention. *Allergol. Int.* 66 (4), 529–538. doi: 10.1016/j.alit.2017.08.001

Xu, K., Cai, H., Shen, Y., Ni, Q., Chen, Y., Hu, S., et al. (2020). [Management of corona virus disease-19 (COVID-19): the Zhejiang experience]. *Zhejiang Da Xue Xue Bao Yi Xue Ban* 49, 147–157. doi: 10.3785/j.issn.1008-9292.2020.02.02

Yeoh, Y. K., Zuo, T., Lui, G. C., Zhang, F., Liu, Q., Li, A. Y., et al. (2021). Gut microbiota composition reflects disease severity and dysfunctional immune responses in patients with COVID-19. *Gut* 1. doi: 10.1136/gutjnl-2020-323020.gutjnl-2020-323020.

Yoshida, N., Emoto, T., Yamashita, T., Watanabe, H., Hayashi, T., Tabata, T., et al. (2018). *Bacteroides vulgatus* and *Bacteroides dorei* reduce gut microbial lipopolysaccharide production and inhibit atherosclerosis. *Circulation* 138, 2486–2498. doi: 10.1161/CIRCULATIONAHA.118.033714

Zelaya, H., Alvarez, S., Kitazawa, H., and Villena, J. (2016). Respiratory antiviral immunity and immunobiotics: beneficial effects on inflammation-coagulation interaction during influenza virus infection. *Front. Immunol.* 7, 633. doi: 10.3389/fimmu.2016.00633

Zeng, M. Y., Inohara, N., and Nuñez, G. (2017). Mechanisms of inflammation-driven bacterial dysbiosis in the gut. *Mucosal Immunol.* 10 (1), 18–26. doi: 10.1038/mi.2016.75

Zhang, D., Li, S., Wang, N., Tan, H. Y., Zhang, Z., and Feng, Y. (2020). The cross-talk between gut microbiota and lungs in common lung diseases. *Front. Microbiol.* 11, 301. doi: 10.3389/fmicb.2020.00301

Zhou, P., Yang, X. L., Wang, X. G., Hu, B., Zhang, L., Zhang, W., et al. (2020). A pneumonia outbreak associated with a new coronavirus of probable bat origin. *Nature* 579 (7798), 270–273. doi: 10.1038/s41586-020-2012-7

Zuo, T., Zhang, F., Lui, G. C. Y., Yeoh, Y. K., Li, A. Y. L., Zhan, H., et al. (2020). Alterations in gut microbiota of patients with COVID-19 during time of hospitalization. *Gastroenterology* 159 (3), 944–955.e8. doi: 10.1053/j.gastro.2020.05.048

Conflict of Interest: The authors declare that the research was conducted in the absence of any commercial or financial relationships that could be construed as a potential conflict of interest.

frontiers in Cellular and Infection Microbiology

ORIGINAL RESEARCH
published: 16 March 2021
doi: 10.3389/fcimb.2021.637018

Identification of Microbiome Etiology Associated With Drug Resistance in Pleural Empyema

Zhaoyan Chen[1†], Hang Cheng[2†], Zhao Cai[2], Qingjun Wei[3], Jinlong Li[4], Jinhua Liang[4], Wenshu Zhang[4], Zhijian Yu[5], Dongjing Liu[6], Lei Liu[6], Zhenqiang Zhang[7], Ke Wang[4] and Liang Yang[2*]*

[1] Intensive Care Unit, The First Affiliated Hospital of Guangxi Medical University, Nanning, China, [2] School of Medicine, Southern University of Science and Technology, Shenzhen, China, [3] Department of Orthopedic Trauma and Hand Surgery, The First Affiliated Hospital of Guangxi Medical University, Nanning, China, [4] Pulmonary and Critical Care Medicine, The First Affiliated Hospital of Guangxi Medical University, Nanning, China, [5] Department of Infectious Diseases and Shenzhen Key Laboratory for Endogenous Infection, Shenzhen Nanshan People's Hospital of Shenzhen University, Shenzhen, China, [6] National Clinical Research Center for Infectious Diseases, Shenzhen Third People's Hospital, Southern University of Science and Technology, Shenzhen, China, [7] Department of Respiratory and Critical Care Medicine, Liuzhou People's Hospital, Liuzhou, China

OPEN ACCESS

Edited by:
Kristi Biswas,
The University of Auckland,
New Zealand

Reviewed by:
Aixin Yan,
The University of Hong Kong,
Hong Kong
Hong-Yu Ou,
Shanghai Jiao Tong University, China

***Correspondence:**
Liang Yang
yangl@sustech.edu.cn
Ke Wang
keewang@hotmail.com

[†]These authors have contributed equally to this work

Specialty section:
This article was submitted to Microbiome in Health and Disease, a section of the journal Frontiers in Cellular and Infection Microbiology

Received: 11 December 2020
Accepted: 02 March 2021
Published: 16 March 2021

Citation:
Chen Z, Cheng H, Cai Z, Wei Q, Li J, Liang J, Zhang W, Yu Z, Liu D, Liu L, Zhang Z, Wang K and Yang L (2021) Identification of Microbiome Etiology Associated With Drug Resistance in Pleural Empyema. Front. Cell. Infect. Microbiol. 11:637018. doi: 10.3389/fcimb.2021.637018

Identification of the offending organism and appropriate antimicrobial therapy are crucial for treating empyema. Diagnosis of empyema is largely obscured by the conventional bacterial cultivation and PCR process that has relatively low sensitivity, leading to limited understanding of the etiopathogenesis, microbiology, and role of antibiotics in the pleural cavity. To expand our understanding of its pathophysiology, we have carried out a metagenomic snapshot of the pleural effusion from 45 empyema patients by Illumina sequencing platform to assess its taxonomic, and antibiotic resistome structure. Our results showed that the variation of microbiota in the pleural effusion is generally stratified, not continuous. There are two distinct microbiome clusters observed in the forty-five samples: HA-SA type and LA-SA type. The categorization is mostly driven by species composition: HA-SA type is marked by *Staphylococcus aureus* as the core species, with other enriched 6 bacteria and 3 fungi, forming a low diversity and highly stable microbial community; whereas the LA-SA type has a more diverse microbial community with a distinct set of bacterial species that are assumed to be the oral origin. The microbial community does not shape the dominant antibiotic resistance classes which were common in the two types, while the increase of microbial diversity was correlated with the increase in antibiotic resistance genes. The existence of well-balanced microbial symbiotic states might respond differently to pathogen colonization and drug intake. This study provides a deeper understanding of the pathobiology of pleural empyema and suggests that potential resistance genes may hinder the antimicrobial therapy of empyema.

Keywords: empyema, metagenomic, microbiome, resistome, community structure, *Staphylococcus aureus*

INTRODUCTION

Empyema is defined as the presence of germs and/or macroscopic pus in the pleural cavity, which is a serious infection with high rates of morbidity and mortality (Asai et al., 2017). Previous analysis of pleural effusion microbiome of empyema patients was mainly based on bacterial cultivation (Lasken and McLean, 2014), PCR and Multiplex bacterial PCR (Blaschke et al., 2011; Franchetti et al., 2020). Recently, microbial characterization of empyema was conducted using targeted 16S rRNA metagenomic analysis (Dyrhovden et al., 2019). However, the increase in the complexity of the pathogens and the usage of antibiotic pre-treatment can reduce the sensitivity of the conventional bacterial cultivation (Le Monnier et al., 2006); PCR-based analysis is highly dependent on the design and availability of primers and thus has very low throughput; 16S rRNA amplicon-based metagenomic analysis has a limitation in detecting microbiome at the species level, and may introduce PCR-biases that mask the true community composition (Brooks et al., 2015).

Next-generation sequencing (NGS)-based metagenomic approach has been employed to examine the population structures and functions of the microbiome in human and environmental samples, which provides biomarkers and risk assessment information, such as antibiotic-resistant bacteria and antibiotic-resistance genes (ARGs) (Cote et al., 2016). In this study, we collected pleural effusion (PE) samples from 45 empyema patients and applied NGS metagenomic analysis to characterize the microbial community and antibiotic resistome. We identified two distinct microbial communities in pleural effusion samples, where *Staphylococcus aureus* serves as a biomarker. Furthermore, the abundance of antibiotic resistance genes is correlated with microbial diversity. Our study reveals the potential risks of treatment failure of pleural empyema due to the high abundance of ARGs in the microbial community and provides data for better understanding of the pathophysiological mechanism in empyema.

MATERIALS AND METHODS

Ethics Statement

The research was approved by the Ethical Review Committee of the First Affiliated Hospital of GuangXi Medical University [Approval Number: 2017(KY-E-078)], and filed with the Ethical Committee of Southern University of Science and Technology [Approval Number: 20200090].

Definition of Pleural Empyema and Samples Collection

A pleural empyema is defined as pus (macroscopic purulence) in the pleural space or pleural fluid with organisms present on Gram stain or culture, pleural fluid pH <7.20 or pleural fluid glucose <60 mg/dL with clinical evidence of infection (Light, 2006). 45 empyema patients involved in this study were recruited in the First Affiliated Hospital of GuangXi Medical University from June 2017 to May 2019. The non-repetitive pleural effusion (PE) samples were collected during thoracentesis, transported in a low-temperature transport box, and stored at -80 °C until further processing.

DNA Isolation

DNA of the samples was obtained by mechanical disruption of bacterial cells using the SeptiFast Lysis kit (Roche, Mannheim, Germany) on a MagNALyzer® instrument (Roche Diagnostics GmbH, Mannheim, Germany) followed by DNA extraction and purification on a MagNA Pure compact automated extractor (Roche, Mannheim, Germany). DNA quality and potential contamination were checked on 1% agarose gel. DNA concentration and purity were checked using NanoPhotometer® spectrophotometer (IMPLEN, CA, USA).

DNA-seq Library Construction and Sequencing

Illumina sequencing libraries were prepared with 500ng gDNA template for each sample according to the TruSeq DNA Sample Preparation Guide (Illumina, 15026486 Rev.C). Concentrations of the constructed libraries were measured using Qubit 2.0 and diluted to 1 ng/μL. Agilent 2100 Bioanalyzer and Bio-RAD CFX 96 Real-Time PCR System (use Bio-RAD KIT iQ SYBR GRN) were used to qualify and quantify the sample libraries (library effective concentration >10nM). The qualified libraries were then sequenced on Illumina Hiseq 2500 platform with 150 bp paired-end reads (Anoroad, Beijing, China).

Metagenomic Analysis

The raw reads generated from samples (11.5~21.5 GB) were trimmed and filtered to remove low quality ($Q \leq 20$) and short reads (length < 50 bp) using Trimmomatic (version 0.39) (Bolger et al., 2014). Reads aligned to the human genome (hg38, Genome Reference Consortium Human Reference 38) were removed (identity cutoff ≥ 90%; maximum mismatches, 10 bp) by Bowtie2 (version 2.3.5.1) (Langmead and Salzberg, 2012). Clean Metagenomic sequences were assembled using the MEGAHIT (version 1.2.9) with default parameters (Li et al., 2016) (**Supplemental Table S1**). The open reading frames (ORFs) prediction was then conducted for assembled contigs using Prokka program (version 1.12) (Seemann, 2014). CD-HIT (version 1.12) was used to cluster genes from each sample based on the parameters (BLASTn identities > 95%, coverage > 90%) (Fu et al., 2012). We aligned high-quality reads against the gene catalog using Salmon v1.2.1 (identity cutoff ≥ 95%) and calculated the corresponding relative abundance of each gene (Patro et al., 2017). ARGs were predicted by mapping the metagenomes to the Comprehensive Antibiotic Resistance Database (CARD) database with 80% identities (Alcock et al., 2020). The taxonomic composition was performed using Kraken 2 software (Wood et al., 2019) based on NR databases. To detect the potential biomarkers, the linear discriminant analysis (LDA) effect size (LEfSe) method was used based on a normalized relative abundance matrix (Segata et al., 2011).

Statistical Analysis and Network Analysis

Averages and standard deviations were computed using the base function in R 3.6.2. Venn diagrams were drawn with the Venn Diagram package, while heatmaps were generated using the pheatmap package by R 3.6.2. The α-diversity based on Shannon index on the species and ARGs profile in each sample was calculated to evaluate the species and ARGs diversities by R 3.6.2. Principal Coordinates Analysis (PCoA) was plotted based on Bray-Curtis dissimilarity to compare the species composition and ARGs profiles of the samples on R 3.6.2 in the vegan package. Correlation between microbial composition and resistome was calculated by pairwise Spearman's rank correlation with coefficient > 0.80 and FDR adjusted *P* value <0.01. Co-occurrence network analysis was conducted in R platform with Hmisc and igraph package, and visualized by Gephy 0.9.2.

Availability of Data and Materials

All data generated during this study are available at the Sequence Read Archive (SRA) under BioProject accession number PRJNA657096.

RESULTS

Clinical Characteristics

45 participants were enrolled in the present study. The clinical characteristics and medication history of the individuals who participated in this study are summarized in **Table 1** and **Supplemental Table S2**. The laboratory bacterial culture showed that 12 (26.7%) were positive for culture only. Out of these, nine samples were of monomicrobial infection caused by *Nocardia farcinica* (PE2), *Klebsiella pneumoniae* (PE4), *Mycobacterium* (acid-fast bacilli) (PE8, PE16), *Candida albicans* (PE23), *Klebsiella oxytoca* (PE24), *Streptococcus constellatus* (PE30), *Escherichia coli* (PE41), and *Acinetobacter baumannii* (PE43). Another three samples had a mixed infection caused by *Candida albicans* and *Stenotrophomonas maltophilia* (PE28), *Candida tropical* and *Pseudomonas aeruginosa* (PE31), *Enterococcus faecium* and *P. aeruginosa* (PE40), respectively.

TABLE 1 | Basic characteristics of the study participants with pleural effusion.

	n = 45*
Age, y	50.3 ± 19.4
Male	40 (88.9)
Signs and symptoms	
Pneumonia	26 (57.8)
Diabetes mellitus	10 (12.8)
Hypertension	7 (15.5)
Post-traumatic empyema infection	9 (20)
Tuberculous empyema infection	6 (13.3)
Hospital-acquired empyema infections	7 (15.5)
Anti-infective therapy before sampling	
Performed	41 (91.1)
Antibiotics	41 (91.1)
Anti-tuberculosis	8 (17.8)
Anti-fungal	2 (4.4)
Blood parameters	
Performed	45 (100)
Leucocytes ($\times10^9$/L)	15.3 ± 7.8
Neutrophils ($\times10^9$/L)	12.7 ± 7.5
C-reactive protein (mg/L)	124.6 ± 76.9
Pleural fluid parameters	
Performed	43 (95.6)
Protein (g/L)	42.1 ± 21.5
Glucose (mmol/L)	2.1 ± 3.7
Lactate dehydrogenase (U/L)	2816.9 ± 2300.1
Adenosine deaminase (U/L)	115.6 ± 92.5
Specimen collection time	
2017	12 (26.7)
2018	19 (42.2)
2019	14 (31.1)

*Mean (standard deviation), n (%).

Hierarchical Clustering of the Pleural Empyema Microbia

We characterized the phylogenetic variation across the sequenced samples at the species and phylum levels. The 30 most abundant species (belonged to the six most abundant phyla) in empyema patients are shown in **Figure 1A**. The phylogenetic composition of the sequenced samples confirms that bacteria predominated in all samples and contributed more to phylogenetic diversity than eukaryotes and archaea. The phyla, *Firmicutes*, *Proteobacteria*, *Ascomycota* and *Bacteroidetes*, constitute the vast majority of the dominant pleural effusion microbiota. *Staphylococcus aureus*, *Pasteurella multocida*, *Botrytis cinerea*, *K. pneumoniae*, *Prevotella intermedia*, *Burkholderia pseudomallei* and *Candida dubliniensis* were identified to be the enriched species in empyema patients. Among which, *S. aureus* was the most abundant species across the samples analyzed.

Microbes in the pleural effusion undergo selective pressure from the host as well as from microbial competitors. This typically leads to the homeostasis of the ecosystem in which some species occur in high and many in low abundance (**Figure 1B**). *S. aureus* was the most variable species across samples, agreeing with relative abundance varied dramatically from 0.79% to 61.97%. In 36 samples, *S. aureus* was the most abundant species, with relative abundance ranging from 24.06% to 61.97% (24.06% in PE 30 sample, and more than 40% in other 35 samples). Meanwhile, the dominating species varied extensively across the other 9 samples (the relative abundance of *S. aureus* ranging from 0.79% to 29.04%), which were *Parvimonas micra* (PE3), *K. pneumoniae* (PE4), *Streptococcus intermedius* (PE20), *P. intermedia* (PE23, PE24, PE29), *Bacteroides heparinolyticus* (PE35), *P. aeruginosa* (PE40), and *E. coli* (PE41), respectively.

Comparison of Microbial Community Composition of HA/LA-SA Group

The within-sample (alpha) diversity (Shannon index) and the between-sample (beta) diversity (Principle Coordination Analysis, PCoA) were used to estimate the richness and composition of pleural effusion microbial species. PCoA based on the Bray-Curtis distance revealed that the samples formed two distinct clusters which can be differentiated by the variation in the level of the most

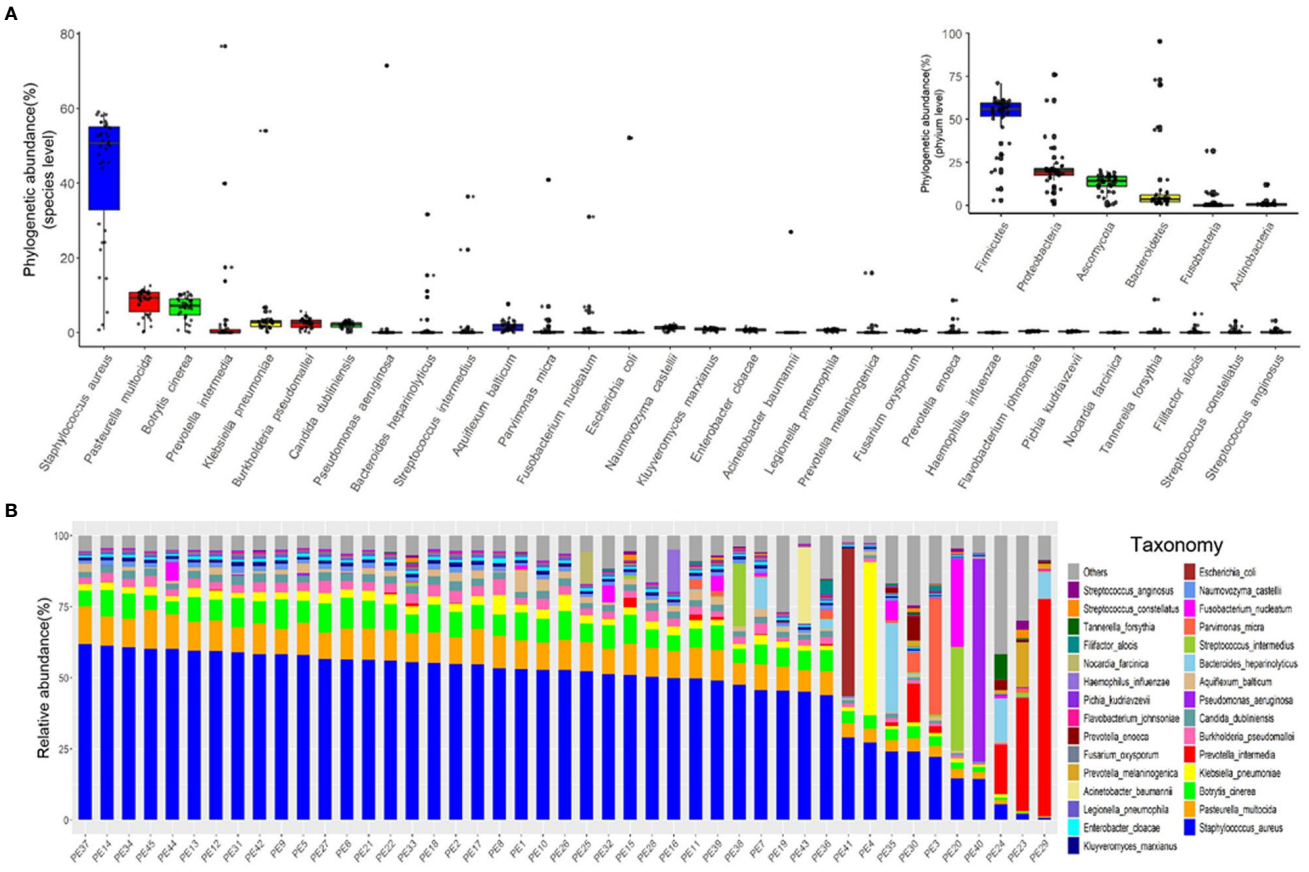

FIGURE 1 | The major microbiome taxa at the phylum and species levels in the pleural effusion samples. **(A)** Box plot of species abundance variation for the 30 most abundant species as determined by read abundance. Species are colored by their respective phylum (see inset for color key). Inset displays the box plot of abundances at the phylum level. **(B)** Stacked bar plot of the 30 most abundant species in the pleural effusion microbiome.

abundant species, *S. aureus* (**Figure 2B**). We designate the two clusters as high abundance *S. aureus* type (HA-SA type, 35/45) and low abundance *S. aureus* type (LA-SA type, 10/45) (**Figure 2A**). As described above, *S. aureus* was the most enriched species with a relative abundance of more than 40% in all 35 samples of the HA-SA type, whereas each sample had distinctive dominating species (except the sample PE) with the relative abundance of *S. aureus* below 30% in the LA-SA type. Meanwhile, the alpha diversity of

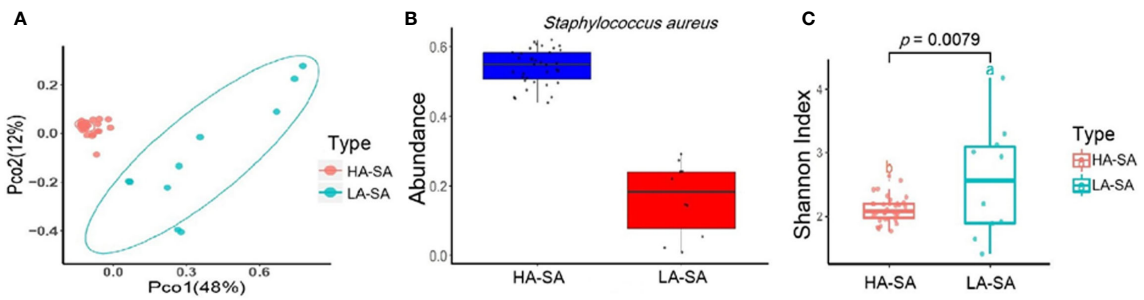

FIGURE 2 | Microbiome composition of the HA-SA and LA-SA type samples. **(A)** Principal Coordinate Analysis. Species among the microbial community for each sample is generated based on the Bray-Curtis similarity matrix in HA- and LA-SA type. The first two components (PCo1 and PCo2) of the PCoA plot explained 48% and 12% variations, respectively, in two groups, with a wider range of within-group distribution in the LA-SA group. **(B)** The abundance levels of the main contributing species of two microbiome types. **(C)** Alpha diversity estimation. Significant differences in Shannon diversity estimates of microbial communities on species level in HA- and LA-SA types.

the LA-SA type was much higher than that of the HA-SA type ($P = 7.91 \times 10^{-3}$, Wilcoxon rank-sum test, **Figure 2C**).

In addition, diversity analysis was also performed to investigate the potential effects of different variables on the composition of the pleural effusion microbiota. Among the 45 samples, pneumonia, diabetes, hypertension, post-traumatic empyema infection, tuberculous empyema infection, hospital-acquired empyema infections, and specimen collection time had no significant effect on the microbiome composition (**Supplemental Figure S1**).

Variation of Microbiome and Biomarkers Between HA/LA-SA Type

To determine the phylogenetic variation of the HA- and LA-SA types, we investigated in detail their differences in composition at the species level. Of the total 2287 detected species, 825 (36.1%) species were identified in HA-SA type while 2194 (95.9%) species were identified in LA-SA type. This was consistent with the results of alpha diversity. There were 732 species shared between the two types, accounting for 22.9% (732/2287) of the total number of species detected. The proportions of the shared species in the two types were 88.7% (732/825) in HA-SA type and 33.4% (732/2287) in LA-SA type, respectively (**Figure 3A**). Structure of the microbial community of the HA-SA type was relatively stable with high inter-sample consistency in the microbial compositions and the enriched species. In contrast, samples in LA-SA type had distinct microbial communities, and the microbiome observed showed no clear clustering (**Figure 3B**).

We screened key biomarkers (*i.e.*, key community members) using the LEfSe method to explore the distinctive microbial species in two types associated with empyema infection. Based on the selection criteria of LDA score of more than 3.5, we identified 18 microbial species as the key discriminants (**Figure 3C**). Ten species including *S. aureus*, *P. multocida*, *B. cinerea*, *Aquiflexum balticum*, *B. pseudomallei*, *C. dubliniensis*, *Naumovozyma castellii*, *Enterobacter cloacae*, *Kluyveromyces marxianus*, and *A. baumannii* were identified as key biomarkers in HA-SA group. Eight species including *Prevotella* spp. (including 4 species), *P. micra*, *K. pneumoniae*, *Tannerella forsythia*, and *Porphyromonas gingivalis* were significantly enriched in the LA-SA group.

Abundant Antibiotic Resistome With Variation Between HA/LA-SA Type

Due to the distinct microbial community profiles of the HA-SA and LA-SA types, we further analyzed the antibiotic resistance genes (ARGs) in the pleural effusion samples. A total of 238 ARGs belonging to 18 ARG classes were detected across the samples. LA-SA type harbored all the 18 ARG classes and HA-SA

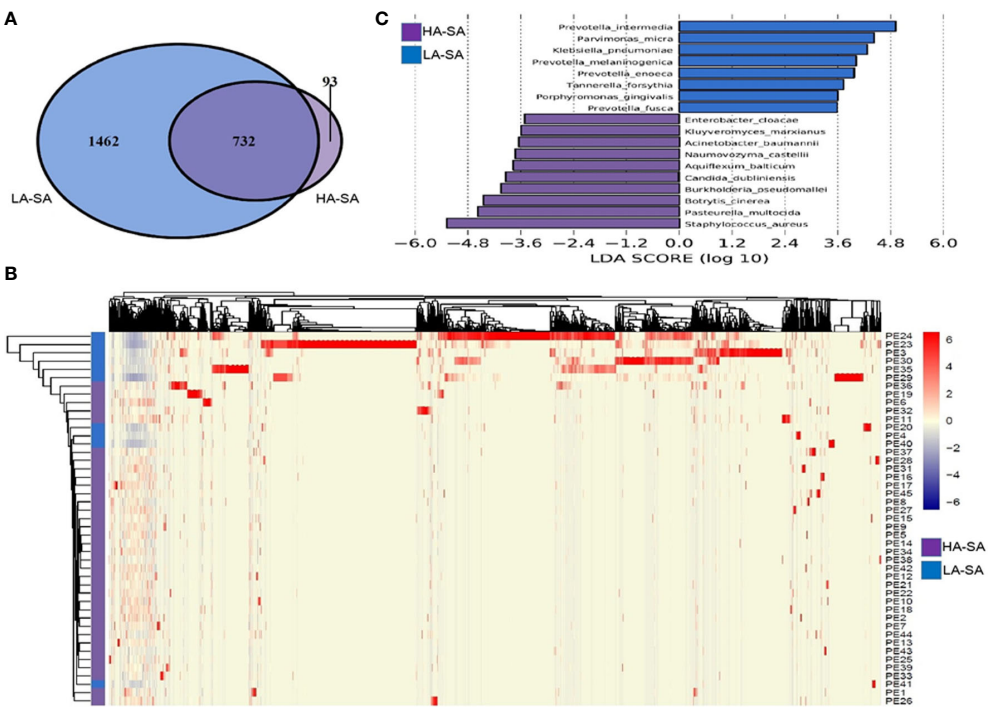

FIGURE 3 | Comparison of pleural effusion microbiome composition among the HA- and LA-SA types. **(A)** Venn diagram showing the number of shared and unique species in the HA- and LA-SA group. **(B)** Heat map of the microbiome species composition for all samples. The abundance of each species was clustered to represent a heatmap. **(C)** Differentially abundant species were identified using linear discriminant analysis (LDA) coupled with effect size measurements (LEfSe). The cutoff value of the linear LDA was ≥3.5.

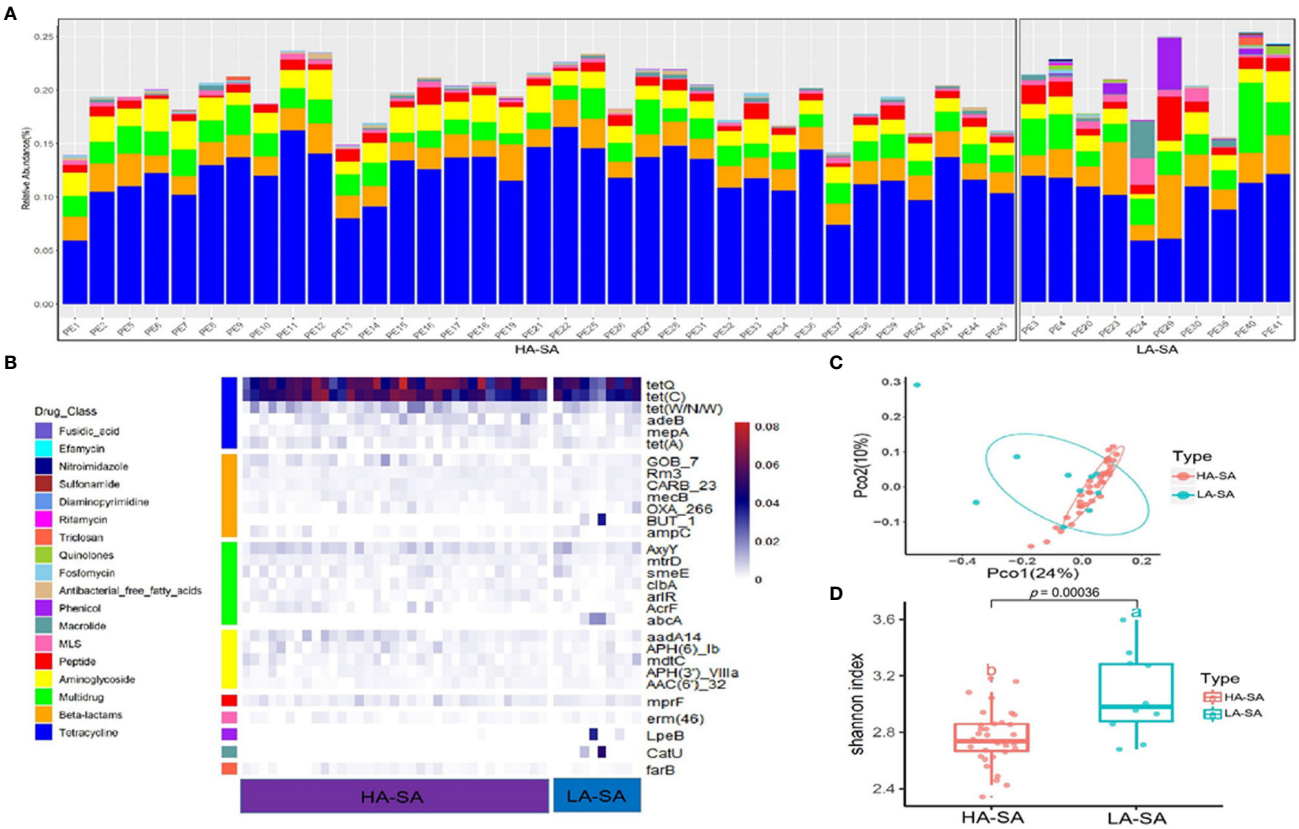

FIGURE 4 | Abundant ARGs in the pleural effusion microbiome. **(A)** Stacked bar plot of antibiotics resistant classes in the pleural effusion metagenome. **(B)** The 30 most abundant ARGs in the HA- and LA-SA type were displayed by heatmap. **(C)** Principal Coordinate Analysis. ARG composition is independent of microbiome community composition. **(D)** Diversity estimates of detected resistance features. Significant differences in Shannon diversity estimates of different resistance features of the CARD database inside the HA- and LA-SA type.

type harbored 16 ARG classes (**Figure 4A**). Nonetheless, the dominant ARG classes in the LA-SA type were in common with that of the HA-SA type's resistome, which is also in agreement with PCoA observations (**Figure 4C**). The abundant ARGs belonging to 6 dominant ARG classes, such as *tetQ* and *tetC* (coding for the tetracycline resistance), Gob-7 beta-lactams resistance gene, *axyY* (multidrug resistance), *aadA14* (aminoglycoside resistance), *mprf* (peptide resistance), *erm46* (MLS resistance) were predominant in both types (**Figure 4B**).

To better understand the influence of HA/LA-SA type on the ARGs in pleural effusion samples, Shannon α-diversity indices for HA/LA-SA type resistome were calculated. These results indicated that higher diversity was observed in the LA-SA type compared to the HA-SA type (**Figure 4D**). Several abundant ARGs detected in the LA-SA type such as *but-1*, *abcA*, *lpeB* and *catU* were undetected in the HA-SA type (**Figure 4B**).

Since the dominant ARG classes were not correlated with microbial composition, we investigated the co-occurrence patterns between ARGs and microbial genera in the HA/LA-SA group using network analysis approach. In this study, if the ARGs and the co-existed microbial taxa possessed the significantly similar abundance trends among the different samples (Spearman's ρ >0.8, *P*-value <0.01), one of the reasonable explanations of the corresponding similar abundance trends was because of some specific microbial taxa carrying some specific ARGs, which has been verified by Forsberg's study (Forsberg et al., 2014). The co-occurrence network in the HA-SA type was comprised of 34 nodes and 22 edges (**Figure 5A**), two bacterial genera were speculated as possible major hosts of ARGs: *Bacteroides* was strongly correlated with macrolide resistance gene (*lpeB*) and beta-lactams resistance genes ($bla_{OXA-266}$ and y56-beta-lactamase gene), whereas *Fusarium* was strongly correlated with aminoglycoside resistance genes (*aac*(6)-IIb and *aadA10*) and tetracycline resistance gene (*adeB*). A more complicated co-occurrence network, comprising of 74 nodes and 66 edges, was observed from the LA-SA type (**Figure 5B**). Six bacterial genera, including *Atopobium*, *Burkholderia*, *Escherichia*, *Clostridium*, *Staphylococcus* and *Tannerella*, were strongly correlated with various ARGs. Especially, *Staphylococcus* in the LA-SA type, was the host of aminoglycoside resistance gene (*armA*), beta-lactams resistance genes (bla_{AIM-1} and bla_{IMP-16}), MLS resistance gene (*erm38*) and tetracycline resistance gene (*tet A*).

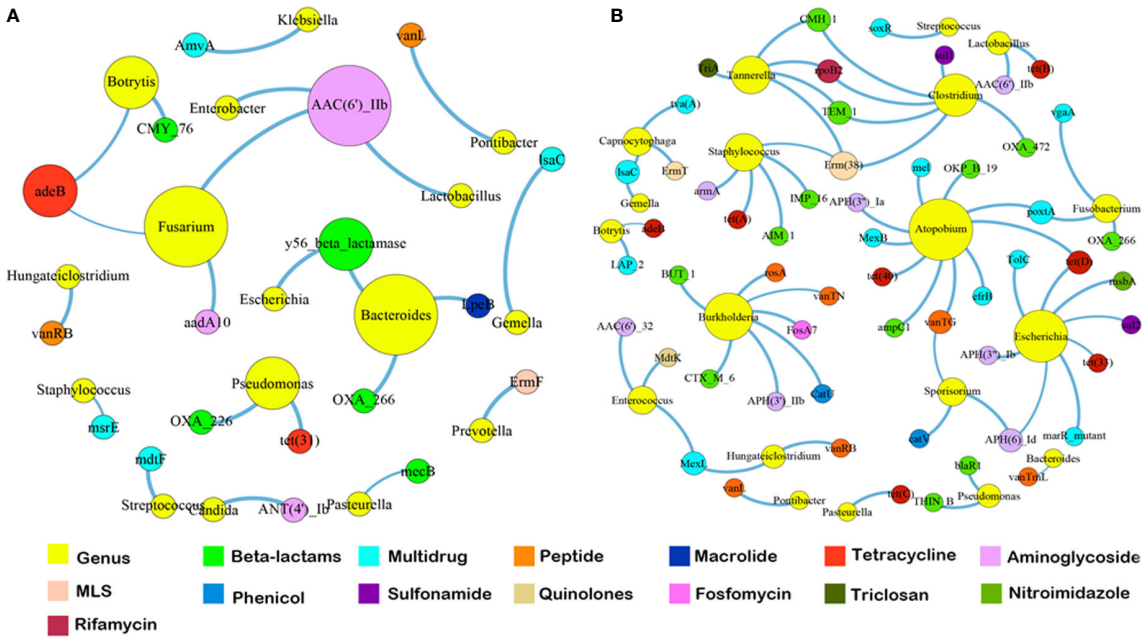

FIGURE 5 | The co-occurrence networks among ARGs and bacterial genera in HA-SA type **(A)** and LA-SA type **(B)**. In the graph, each dot represents a kind of ARG or bacterial genera. The nodes are colored yellow represent bacterial genus; others colored according to ARG types. The size of each node is proportional to the number of its connections (degree). Each line (edge) represents the co-occurrence of two objects. Edge width is proportional to Spearman's ρ value.

DISCUSSION

In this study, the microbiome and resistome of pleural effusion collected from 45 empyema infection patients were explored based on NGS metagenomic analysis.

Previous studies showed that the geographical location of infection is closely related to the expected pathogenic bacteria, and *S. aureus* is the most preponderant species in sub-tropical areas (Hassan et al., 2019). In our study, *S. aureus* was detected in all of the pleural effusion samples and was the most abundant species in the HA-SA type. This suggests that the result of metagenomic analysis follows the geographical pattern and aligns with the findings of previous studies. On the other hand, we also detected other dominant species, which together with *S. aureus* to construct a complex microbiome in pleural effusion. Upon the change in the abundance of *S. aureus* in the microbial communities, we observed two significantly different microbiome compositions among samples, being the HA-SA type and LA-SA type. Virtually, none of the measured host properties, namely pneumonia, diabetes, hypertension, post-traumatic empyema infection, tuberculous empyema infection, hospital-acquired empyema infection and specimen collection time, significantly correlates with the microbiome types.

In the HA-SA type with the relative abundance of *S. aureus* more than 40%, we identified a highly similar and stable core microbial composition with low diversity. Such core microbial community consists of *S. aureus* as core species and 9 other enriched species, including 6 bacteria (*P. multocida*, *A. balticum*, *B. pseudomallei*, *E. cloacae*, *K. marxianus*, and *A. baumannii*) and 3 fungi (*B. cinerea*, *C. dubliniensis*, and *N. castellii*). It was reported that bacteria can thrive in both pleural fluid and pleural tissue (Popowicz et al., 2017). However, the invading mechanisms of microorganisms in the pleural cavity and features of the pathogenesis, such as the role of biofilm formation, have not yet been fully understood (Thomas et al., 2020). A recent study had reported that *P. aeruginosa* can form biofilm in an empyema model (Zhang et al., 2020). Some studies have also pointed out that fungi contribute to biofilm formation while *Candida app.* is the most common fungal flora in biofilm infection (Ramage et al., 2009). *S. aureus* and fungi have synergism in biofilm formation (Boase et al., 2011). In the HA-SA type, the co-existence of *S. aureus* and 3 fungi (including one *Candida* spp.) perhaps contributed to the formation of biofilm which would stabilize the microbiome community and help pathogens to escape from host immune clearance and increase antibiotic resistance (De Rudder et al., 2018).

In comparison, the LA-SA type with the relative abundance of *S. aureus* below 30% had a more diversified microbiome. The microbiome had several significantly enriched biomarkers including *Prevotella* spp. (including 4 species), *P. micra*, *K. pneumoniae*, *T. forsythia*, and *P. gingivalis*, which except for *K. pneumoniae* were anaerobic bacteria. Furthermore, these anaerobic bacteria are involved in various oral infections, especially associated with periodontal infections. Some studies have already found a remarkably high involvement of anaerobic oral bacteria in empyema infection, whereas odontogenic

infections have been identified as a potential risk factor of empyema (Kobashi et al., 2008). The specificity of geographical areas should be emphasized here, the oral microbiome varies across locations and may influence the bacterial composition of pleural empyema (Dyrhovden et al., 2019). The exact mechanisms whereby oral flora gain access to the pleural space are incompletely understood. However, it is speculated that facultative and anaerobic oral bacteria, able to spread *via* deoxygenated venous blood, which is a possible infection route of oral bacterial pleurisy (Dyrhovden et al., 2019).

The positive rate of routine pleural effusion culture of the collected samples was not high, only 26.7%. Standard pleural effusion cultures are usually positive in approximately 20-40% of cases (Menzies et al., 2011). This is likely to be a result of the combination of prior antibiotic treatment, low bacterial concentration in pleural effusion and possibly causal agents that are difficult to be isolated in the laboratory due to stringent requirements. In the HA-SA type, the culture-positive rate was 17.14% (6/35), without any *S. aureus* culture positive results. According to previous reports, the *S. aureus* culture positivity are different depending on whether an empyema is community-acquired or healthcare-acquired. The positive rate is 12% in community-acquired empyema and 20% in Hospital-acquired empyema, respectively (Koma et al., 2017; Brims et al., 2019). We might raise the hypothesis that the *S. aureus* culture negativity in this study may reflect the adaptation of bacteria to a specific host niche, such as *S. aureus* to biofilm, and the niche conditions could not be replicated by the routine *in vitro* culture conditions resulting in negative culturing results (Pommepuy et al., 1996; Lowder et al., 2000; Oliver, 2010). In the LA-SA type, the culture-positive rate was as high as 60% (6/10), and culture-positive pathogens in 3 samples matched with the most abundant species identified by metagenomic analysis. There were not any anaerobic bacteria cultured. The most compelling evidence for "occult" anaerobes in empyema fluid is detection of bacterial DNA or RNA using massive parallel sequencing. This approach identified anaerobic bacteria in 70% patients with empyema and no known etiology (Cobo et al., 2018).

The LA-SA type and HA-SA type possess common ARG classes which the most dominant ARG classes were tetracycline resistance and beta-lactam resistance. On one hand, the microbes growing in pleural effusion and pleural tissue would be selected by antibiotics treatment (91.1%, 41/45), especially beta-lactams antibiotics (39, 86.7%), which is frequently acquired *via* horizontal gene transfer (HGT). Previous research reported that tetracycline resistance genes are often integrated into mobile genetic elements (MGE), and prevalent in a large number of microbial populations colonized in human oral cavity and intestinal tract (Seville et al., 2009). These bacterial populations, functioning as the repository of tetracycline-resistant genes, contribute to the spread of ARGs into pathogenic bacteria through different mechanisms such as HGT, without prior treatment of tetracycline antibiotics. All of the above reasons may lead to the highly similarity in the resistomes of the HA/LA-SA type. Meanwhile, our study showed a higher diversity of ARGs in the samples with increased microbial diversity. It is possible that biofilm formation may contribute to the increase in the antibiotic resistance of the HA-SA type and reduce the dependence on ARGs. The observation that *S. aureus* solely correlating with multidrug resistance gene (*msrE*) in the HA-SA type while a more complex network existing between *S. aureus* and more diverse ARGs in the LA-SA group may support this inference.

In conclusion, the variation of microbiota in the pleural effusion is generally stratified, not continuous. *S. aureus* plays an important role in the shaping the microbial structures. Microbial community does not shape the resistomic profiles of the two types, which possess common ARG classes. The higher the microbial diversity, the more diverse the ARG profiles. These findings highlighted the capacity and advantage of NGS metagenomics for investigating the empyema and pathophysiological mechanisms to provide better understanding of the disease.

DATA AVAILABILITY STATEMENT

The datasets presented in this study can be found in online repositories. The names of the repository/repositories and accession number(s) can be found in the article/ **Supplementary Material**.

ETHICS STATEMENT

The studies involving human participants were reviewed and approved by the ethical review committee of the First Affiliated Hospital of GuangXi Medical University [Approval Number: 2017(KY-E-078)], and the Ethical Committee of Southern University of Science and Technology [Approval Number: 20200090]. The patients/participants provided their written informed consent to participate in this study.

AUTHOR CONTRIBUTIONS

LY and KW conceived the study and participated in data analysis and discussion. ZYC, HC, ZC, QW, JLL, JHL, WZ, ZY, DL, LL, and ZZ carried out the experiments, analyzed the data, and drafted the manuscript. All authors contributed to the article and approved the submitted version.

FUNDING

This work was supported by the National Natural Science Foundation of China under Grant [number 81760024]; Guangdong Natural Science Foundation for Distinguished Young

Scholar under Grant [number 2020B1515020003]; the Southern University of Science and Technology (SUSTech) to LY under Start-up Grants [number Y01416206]; the Medical Excellence Award Funded by the Creative Research Development Grant from the First Affiliated Hospital of Guangxi Medical University.

SUPPLEMENTARY MATERIAL

The Supplementary Material for this article can be found online at: https://www.frontiersin.org/articles/10.3389/fcimb.2021.637018/full#supplementary-material

REFERENCES

Alcock, B. P., Raphenya, A. R., Lau, T. T. Y., Tsang, K. K., Bouchard, M., Edalatmand, A., et al. (2020). CARD 2020: antibiotic resistome surveillance with the comprehensive antibiotic resistance database. *Nucleic Acids Res.* 48 (D1), D517–D525. doi: 10.1093/nar/gkz935

Asai, N., Suematsu, H., Hagihara, M., Nishiyama, N., Kato, H., Sakanashi, D., et al. (2017). The etiology and bacteriology of healthcare-associated empyema are quite different from those of community-acquired empyema. *J. Infect. Chemother.* 23 (10), 661–667. doi: 10.1016/j.jiac.2017.04.011

Blaschke, A. J., Heyrend, C., Byington, C. L., Obando, I., Vazquez-Barba, I., Doby, E. H., et al. (2011). Molecular Analysis Improves Pathogen Identification and Epidemiologic Study of Pediatric Parapneumonic Empyema. *Pediatr. Infect. Dis. J.* 30 (4), 289–294. doi: 10.1097/INF.0b013e3182002d14

Boase, S., Valentine, R., Singhal, D., Tan, L. W., and Wormald, P. J. (2011). A sheep model to investigate the role of fungal biofilms in sinusitis: fungal and bacterial synergy. *Int. Forum Allergy Rhinol.* 1 (5), 340–347. doi: 10.1002/alr.20066

Bolger, A. M., Lohse, M., and Usadel, B. (2014). Trimmomatic: a flexible trimmer for Illumina sequence data. *Bioinformatics* 30 (15), 2114–2120. doi: 10.1093/bioinformatics/btu170

Brims, F., Popowicz, N., Rosenstengel, A., Hart, J., Yogendran, A., Read, C. A., et al. (2019). Bacteriology and clinical outcomes of patients with culture-positive pleural infection in Western Australia: A 6-year analysis. *Respirology* 24 (2), 171–178. doi: 10.1111/resp.13395

Brooks, J. P., Edwards, D. J., Harwich, M. D., Rivera, M. C., Fettweis, J. M., Serrano, M. G., et al. (2015). The truth about metagenomics: quantifying and counteracting bias in 16S rRNA studies. *BMC Microbiol.* 15, 66. doi: 10.1186/s12866-015-0351-6

Cobo, F., Calatrava, E., Rodriguez-Granger, J., Sampedro, A., Aliaga-Martinez, L., and Navarro-Mari, J. M. (2018). A rare case of pleural effusion due to Prevotella dentalis. *Anaerobe* 54, 144–145. doi: 10.1016/j.anaerobe.2018.09.004

Cote, I., Andersen, M. E., Ankley, G. T., Barone, S., Birnbaum, L. S., Boekelheide, K., et al. (2016). The Next Generation of Risk Assessment Multi-Year Study-Highlights of Findings, Applications to Risk Assessment, and Future Directions. *Environ. Health Perspect.* 124 (11), 1671–1682. doi: 10.1289/Ehp233

De Rudder, C., Arroyo, M. C., Lebeer, S., and Van de Wielel, T. V. (2018). Modelling upper respiratory tract diseases: getting grips on host-microbe interactions in chronic rhinosinusitis using in vitro technologies. *Microbiome* 6, 75. doi: 10.1186/s40168-018-0462-z

Dyrhovden, R., Nygaard, R. M., Patel, R., Ulvestad, E., and Kommedal, O. (2019). The bacterial aetiology of pleural empyema. A descriptive and comparative metagenomic study. *Clin. Microbiol. Infect.* 25 (8), 981–986. doi: 10.1016/j.cmi.2018.11.030

Forsberg, K. J., Patel, S., Gibson, M. K., Lauber, C. L., Knight, R., Fierer, N., et al. (2014). Bacterial phylogeny structures soil resistomes across habitats. *Nature* 509 (7502), 612–616. doi: 10.1038/nature13377

Franchetti, L., Schumann, D. M., Tamm, M., Jahn, K., and Stolz, D. (2020). Multiplex bacterial polymerase chain reaction in a cohort of patients with pleural effusion. *BMC Infect. Dis.* 20 (1), 99. doi: 10.1186/s12879-020-4793-6

Fu, L., Niu, B., Zhu, Z., Wu, S., and Li, W. (2012). CD-HIT: accelerated for clustering the next-generation sequencing data. *Bioinformatics* 28 (23), 3150–3152. doi: 10.1093/bioinformatics/bts565

Hassan, M., Cargill, T., Harriss, E., Asciak, R., Mercer, R. M., Bedawi, E. O., et al. (2019). The microbiology of pleural infection in adults: a systematic review. *Eur. Respir. J.* 54 (3), 1900542. doi: 10.1183/13993003.00542-2019

Kobashi, Y., Mouri, K., Yagi, S., Obase, Y., and Oka, M. (2008). Clinical Analysis of Cases of Empyema Due to Streptococcus milleri Group. *Japanese J. Infect. Dis.* 61 (6), 484–486. doi: 10.1097/QAI.0b013e31817c1ed0

Koma, Y., Inoue, S., Oda, N., Yokota, N., Tamai, K., Matsumoto, Y., et al. (2017). Clinical characteristics and outcomes of patients with community-acquired, health-care-associated and hospital-acquired empyema. *Clin. Respir. J.* 11 (6), 781–788. doi: 10.1111/crj.12416

Langmead, B., and Salzberg, S. L. (2012). Fast gapped-read alignment with Bowtie 2. *Nat. Methods* 9 (4), 357–U354. doi: 10.1038/Nmeth.1923

Lasken, R. S., and McLean, J. S. (2014). Recent advances in genomic DNA sequencing of microbial species from single cells. *Nat. Rev. Genet.* 15 (9), 577–584. doi: 10.1038/nrg3785

Le Monnier, A., Carbonnelle, E., Zahar, J. R., Le Bourgeois, M., Abachin, E., Quesne, G., et al. (2006). Microbiological diagnosis of empyema in children: comparative evaluations by culture, polymerase chain reaction, and pneumococcal antigen detection in pleural fluids. *Clin. Infect. Dis.* 42 (8), 1135–1140. doi: 10.1086/502680

Li, D. H., Luo, R. B., Liu, C. M., Leung, C. M., Ting, H. F., Sadakane, K., et al. (2016). MEGAHIT v1.0: A fast and scalable metagenome assembler driven by advanced methodologies and community practices. *Methods* 102, 3–11. doi: 10.1016/j.ymeth.2016.02.020

Light, R. W. (2006). Parapneumonic effusions and empyema. *Proc. Am. Thorac. Soc.* 3 (1), 75–80. doi: 10.1513/pats.200510-113JH

Lowder, M., Unge, A., Maraha, N., Jansson, J. K., Swiggett, J., and Oliver, J. D. (2000). Effect of starvation and the viable-but-nonculturable state on green fluorescent protein (GFP) fluorescence in GFP-tagged Pseudomonas fluorescens A506. *Appl. Environ. Microbiol.* 66 (8), 3160–3165. doi: 10.1128/Aem.66.8.3160-3165.2000

Menzies, S. M., Rahman, N. M., Wrightson, J. M., Davies, H. E., Shorten, R., Gillespie, S. H., et al. (2011). Blood culture bottle culture of pleural fluid in pleural infection. *Thorax* 66 (8), 658–662. doi: 10.1136/thx.2010.157842

Oliver, J. D. (2010). Recent findings on the viable but nonculturable state in pathogenic bacteria. *FEMS Microbiol. Rev.* 34 (4), 415–425. doi: 10.1111/j.1574-6976.2009.00200.x

Patro, R., Duggal, G., Love, M. I., Irizarry, R. A., and Kingsford, C. (2017). Salmon provides fast and bias-aware quantification of transcript expression. *Nat. Methods* 14 (4), 417–419. doi: 10.1038/nmeth.4197

Pommepuy, M., Butin, M., Derrien, A., Gourmelon, M., Colwell, R. R., and Cormier, M. (1996). Retention of enteropathogenicity by viable but nonculturable Escherichia coli exposed to seawater and sunlight. *Appl. Environ. Microbiol.* 62 (12), 4621–4626. doi: 10.1128/Aem.62.12.4621-4626.1996

Popowicz, N. D., Lansley, S. M., Cheah, H. M., Kay, I. D., Carson, C. F., Waterer, G. W., et al. (2017). Human pleural fluid is a potent growth medium for Streptococcus pneumoniae. *PloS One* 12 (11), e0188833. doi: 10.1371/journal.pone.0188833

Ramage, G., Mowat, E., Jones, B., Williams, C., and Lopez-Ribot, J. (2009). Our Current Understanding of Fungal Biofilms. *Crit. Rev. Microbiol.* 35 (4), 340–355. doi: 10.3109/10408410903241436

Seemann, T. (2014). Prokka: rapid prokaryotic genome annotation. *Bioinformatics* 30 (14), 2068–2069. doi: 10.1093/bioinformatics/btu153

Segata, N., Izard, J., Waldron, L., Gevers, D., Miropolsky, L., Garrett, W. S., et al. (2011). Metagenomic biomarker discovery and explanation. *Genome Biol.* 12 (6), R60. doi: 10.1186/gb-2011-12-6-r60

Seville, L. A., Patterson, A. J., Scott, K. P., Mullany, P., Quail, M. A., Parkhill, J., et al. (2009). Distribution of Tetracycline and Erythromycin Resistance Genes Among Human Oral and Fecal Metagenomic DNA. *Microbial Drug Resist.* 15 (3), 159–166. doi: 10.1089/mdr.2009.0916

Thomas, R., Rahman, N. M., Maskell, N. A., and Lee, Y. C. G. (2020). Pleural effusions and pneumothorax: Beyond simple plumbing: Expert opinions on knowledge gaps and essential next steps. *Respirology* 25 (9), 963–971. doi: 10.1111/resp.13881

Wood, D. E., Lu, J., and Langmead, B. (2019). Improved metagenomic analysis with Kraken 2. *Genome Biol.* 20 (1), 257. doi: 10.1186/s13059-019-1891-0

Zhang, L., Li, J., Liang, J., Zhang, Z., Wei, Q., and Wang, K. (2020). The effect of Cyclic-di-GMP on biofilm formation by Pseudomonas aeruginosa in a novel empyema model. *Ann. Trans. Med.* 8 (18), 1146. doi: 10.21037/atm-20-6022

Conflict of Interest: The authors declare that the research was conducted in the absence of any commercial or financial relationships that could be construed as a potential conflict of interest.

frontiers in Cellular and Infection Microbiology

REVIEW
published: 14 May 2021
doi: 10.3389/fcimb.2021.583600

The Airway Pathobiome in Complex Respiratory Diseases: A Perspective in Domestic Animals

Núria Mach[1]*, *Eric Baranowski*[2], *Laurent Xavier Nouvel*[2] and *Christine Citti*[2]

[1] Université Paris-Saclay, Institut National de Recherche Pour l'Agriculture, l'Alimentation et l'Environnement (INRAE), AgroParisTech, Génétique Animale et Biologie Intégrative, Jouy-en-Josas, France, [2] Interactions Hôtes-Agents Pathogènes (IHAP), Université de Toulouse, INRAE, ENVT, Toulouse, France

Respiratory infections in domestic animals are a major issue for veterinary and livestock industry. Pathogens in the respiratory tract share their habitat with a myriad of commensal microorganisms. Increasing evidence points towards a respiratory pathobiome concept, integrating the dysbiotic bacterial communities, the host and the environment in a new understanding of respiratory disease etiology. During the infection, the airway microbiota likely regulates and is regulated by pathogens through diverse mechanisms, thereby acting either as a gatekeeper that provides resistance to pathogen colonization or enhancing their prevalence and bacterial co-infectivity, which often results in disease exacerbation. Insight into the complex interplay taking place in the respiratory tract between the pathogens, microbiota, the host and its environment during infection in domestic animals is a research field in its infancy in which most studies are focused on infections from enteric pathogens and gut microbiota. However, its understanding may improve pathogen control and reduce the severity of microbial-related diseases, including those with zoonotic potential.

Keywords: domestic animals, pathobiome, respiratory infectious diseases, airway microbiota, public health

OPEN ACCESS

Edited by:
Steven D. Pletcher, University of California, San Francisco, United States

Reviewed by:
Kristina Marie Feye, University of Arkansas, United States
Mengfei Peng, University of Maryland, College Park, United States
Amir Ghorbani, The Ohio State University, United States

***Correspondence:**
Núria Mach
nuria.mach@inrae.fr

Specialty section:
This article was submitted to Microbiome in Health and Disease, a section of the journal Frontiers in Cellular and Infection Microbiology

Received: *15 July 2020*
Accepted: *30 April 2021*
Published: *14 May 2021*

Citation:
Mach N, Baranowski E, Nouvel LX and Citti C (2021) The Airway Pathobiome in Complex Respiratory Diseases: A Perspective in Domestic Animals. Front. Cell. Infect. Microbiol. 11:583600. doi: 10.3389/fcimb.2021.583600

INTRODUCTION

Complex respiratory diseases are highly prevalent and can be life threatening in domestic animals in which a prompt diagnosis and targeted treatments are essential (Ericsson et al., 2016; Bond et al., 2017; Oladunni et al., 2019; Ericsson et al., 2020). Besides impacting animal health and welfare, they cause a significant health burden worldwide including high treatment costs, high morbidity, premature mortality, decreased performance and severe consequences to public health and the environment (Kuiken et al., 2005; Holt et al., 2011; Ericsson et al., 2016; Bond et al., 2017; Oladunni et al., 2019; Blakebrough-Hall et al., 2020; Ericsson et al., 2020). For example, the bovine respiratory disease complex (BRDC) is a leading cause of morbidity and economic losses in wealthy countries which ranges from 30% in Belgium (van Leenen et al., 2020) to 49% in Switzerland and up to 80% in the U.S.A. (Hilton, 2014). Similarly, the porcine respiratory disease complex (PRDC) in finishing pigs continues to grow (Qin et al., 2018) with a morbidity rate ranging from 10% in Denmark (Hansen et al., 2010) to 40% in the U.S.A (Harms et al., 2002). As for common livestock animals, the equine respiratory disease complex (ERDC) is an important respiratory infection in horses

(Wasko et al., 2011) that affects up to 66% of the equine population (Wasko et al., 2011) and can quickly disqualify a horse from racing, showing, training or other activities for periods of time ranging from a few days to months. In companion animals, the canine infectious respiratory disease complex (CIRDC) affects 66% of the dogs studied in Europe, including both peat and kenneled dogs (Mitchell et al., 2017). The feline respiratory disease complex has been described as one of the most importance cause of morbidity for cats in U.S.A, with reported incidence as high as 30% (Wagner et al., 2018). Finally, the respiratory disease complex in poultry remains widespread and has become endemic in different countries causing subclinical infections, mild respiratory symptoms and high production losses in birds either raised for meat or eggs (Awad et al., 2014; Guabiraba and Schouler, 2015; Patel et al., 2018; Samy and Naguib, 2018).

Our view on the dynamics of airway diseases has now been broadened to include an additional aspect of the complex system: the microbiota of the host and its environment (Bernardo-Cravo et al., 2020). The properties of the host microbiome have led to the concept of the holobiome in which the host and its microbial communities are merged into a symbiotic superorganism and later, to the concept of pathobiome to further consider microbiome communities in disease state (Vayssier-Taussat et al., 2014). The importance of the pathobiome concept arose from human studies in which disruption of a health-promoting and stable gut microbiome results in dysbiosis– a microbiome community acting as pathogenic entity (Bass et al., 2019). In this concept, the pathogen and host microbiome are assembled, leading to similar issues raised for the holobiome (Bernardo-Cravo et al., 2020).

Much work is required to identify the mechanisms underlying the microorganism relations and perturbations of a balanced and healthy microbiome that lead to a pathobiome (Bass et al., 2019). Commensal microbiome might act as a gatekeeper that provides resistance to infection on the mucosal surface and spreading to the lungs (Man et al., 2017; Li et al., 2019) or enhance disease exacerbation.

The number of studies addressing the role of the respiratory bacterial communities in animal health and disease is limited and almost entirely restricted to animals farmed for foods such as cattle and pigs. Moreover, although microbiota is composed of bacteria, protists, fungi, archaea and viruses, most studies in domestic animals have focused solely on bacterial microbiota.

In cows and feedlot cattle, several studies have reported how a healthy respiratory microbiota is established in the airways and surveyed which host and environmental factors drive it (Timsit et al., 2016; Hall et al., 2017; Holman et al., 2017; Nicola et al., 2017; Zeineldin et al., 2017a; Holman et al., 2018; Stroebel et al., 2018; Amat et al., 2019; McMullen et al., 2020; Zeineldin et al., 2020a). Analogously, predicting when and how respiratory microbiome breaks down is at the heart of several studies in swine (Cortes et al., 2018; Zeineldin et al., 2018; Jakobsen et al., 2019; Megahed et al., 2019; Mou et al., 2019; Wang et al., 2019; Pirolo et al., 2021). For instance, it appears as though that during weaning, several microorganisms act synergistically to mediate the BRDC (Gaeta et al., 2017; Klima et al., 2019; McMullen et al., 2019; Zeineldin et al., 2019) and PRDC (Wang et al., 2018; Li et al., 2021). Aside from ruminants and swine, efforts have focused on characterizing the composition patterns of the upper and lower airways in sheep (Glendinning et al., 2016; Glendinning et al., 2017a), horses (Bond et al., 2017), animals domesticated for companionship (Ericsson et al., 2016; Vientoos-Plotts et al., 2017; Vientós-Plotts et al., 2017; Fastrès et al., 2019; Fastrès et al., 2020b) and commercial birds (Shabbir et al., 2014; Glendinning et al., 2017b; Johnson et al., 2018; Ngunjiri et al., 2019; Abundo et al., 2020; Taylor et al., 2020; Abundo et al., 2021; Kursa et al., 2021).

Determining the underlying causes of respiratory illness is complicated. Species of veterinary interest are subjected to different host variables, environments and pathogens, which could all play a role in disease, either alone or in concert. However, we show evidence supporting the existence of an interplay between respiratory pathogens, commensal microbiota, host and environment in the respiratory apparatus of domestic animals. We untangle whether the airway microbiota act as a gatekeeper that provides resistance to pathogen colonization, thus ensuring resiliency and health in domestic animals. Moreover, we provide an overview of the covariation between airway microbiota, host and environment factors within and between species and we suggest potential applications of this knowledge in veterinary medicine. Lastly, we outline avenues to understand if gut microbiota-derived metabolites could be key molecular mediators of the microbiota-gut-lung axis and affect the onset of the respiratory diseases. Thus, the exploration of the relationships between respiratory pathogens, hosts and respiratory microbiota in domestic animals is timely and novel.

DO DIFFERENCES IN THE RESPIRATORY SYSTEM CONTRIBUTE TO MICROBIOME COMPOSITION? MAMMALS *VERSUS* BIRDS

It is remarkable that mammals and birds, the two great classes of vertebrates capable of sustained high oxygen consumption, present many distinct differences (morphologic, physiologic and mechanic) in the respiratory tract (West et al., 2007) (**Figure 1**). For example, in mammals, the lower respiratory tract (LRT) comprises the trachea, the primary bronchi and the lungs, whereas in birds it involves the syrinx, the air sacs distributed throughout the body, the bronchi, the bronchioles and lungs (Nochi et al., 2018; Abundo et al., 2020; Abundo et al., 2021). Unlike mammals, the avian lungs are essentially rigid and tubular without alveoli (Bernhard et al., 2004) and have a unidirectional airflow in which the lungs are ventilated *via* air sacs (Nochi et al., 2018). By contrast, the mammalian lungs have reciprocating ventilation with large terminal air spaces (alveoli) and reduced airflow in peripheral structures (Bernhard et al., 2004). Additionally, the blood-gas barrier of the avian lung is

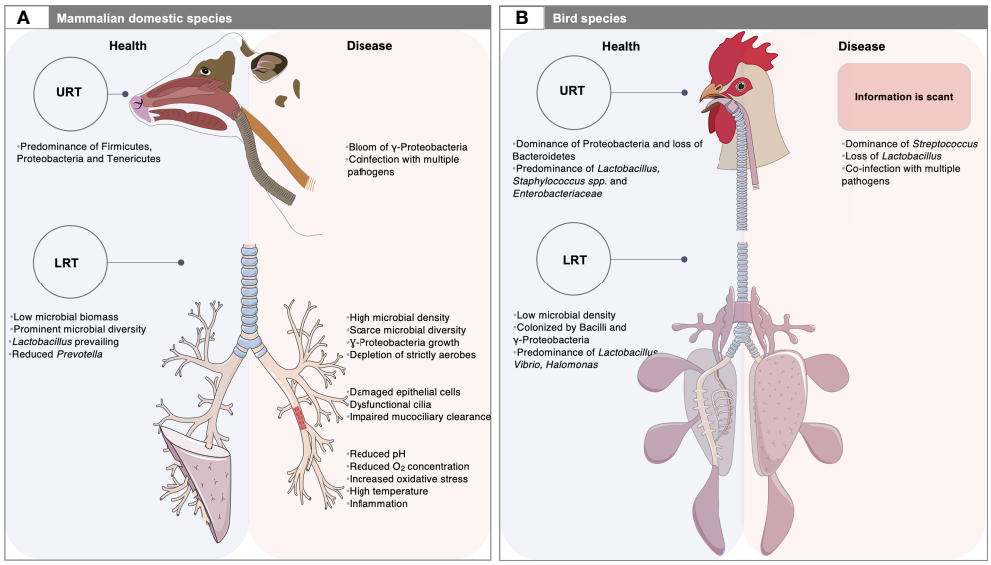

FIGURE 1 | Airway microbiota: a matter of animal species, physiology and diseased settings. **(A)** The respiratory tract of domestic mammals is mainly colonized by Firmicutes, Proteobacteria, Tenericutes and Bacteroidetes. At steady state (left, blue rectangle), the microbial biomass in the low respiratory tract (LRT) is low and likely depends on the balance between migration of bacteria from the upper respiratory tract (URT) and the mucociliary and immune clearance. During respiratory disease (right; red rectangle), the LRT bacterial propagation outpaces the capacity of the airways to clear the microorganisms, which often results in increased microbial density and dysbiosis. Dysfunctional cilia and enhanced mucus production may contribute to reduced clearance and trapping of microorganisms within airways. An outgrowth of γ-Proteobacteria and loss of Firmicutes is observed in mammals, together with a limited microbial diversity, and the exacerbation of respiratory inflammation and loss of mucosal barrier function. In this context, co-infections by other pathogens or pathobionts are frequent. This polymicrobial disease involves microorganisms that act synergistically, or in succession to mediate complex disease processes. Studying such questions is challenging due to the complexity of sample collection. The exploration of LRT microbiota is based on invasive sampling techniques such as bronchoalveolar lavage, bronchus mucosal scraping and tracheal aspirates. Swaps of the deep nasal cavity, nasopharynx, oropharynx, paranasal sinus and tonsil are usually taken to explore the URT site; **(B)** The URT of birds is qualitatively similar to that of mammals. However, the nasal and oral cavities communicate with each other through the choanal cleft region. Their URT is mainly colonized by Firmicutes and Proteobacteria. At the genus level, a healthy ecosystem mainly includes highly dominant taxa, namely *Lactobacillus, Staphylococcus* spp. and members of the *Enterobacteriaceae* family. Unlike mammals, the LRT comprises the syrinx and the air sacs distributed throughout the body. In a stable state, the microbial density in the lung is very low. The LRT is mainly colonized by Bacilli and γ-Proteobacteria. At the genus level, *Lactobacillus* is the dominant bacterial taxon, followed by *Vibrio* and *Halomonas*. Yet, information related to the microbiota composition under respiratory diseases is scant. The assessment of microbiota in the URT is based on choanal swabs, nasal cavity wash and upper and lower tracheal washes, whereas the description of the LRT microbiota depends on lower respiratory lavage. The picture of mammalian LRT was downloaded from smart Servier Medical Art https://smart.servier.com without changes. Servier Medical Art by Servier is licensed under a Creative Commons Attribution 3.0 License. Written permission for publication of the chicken figure and chicken respiratory system drawing has been taken.

approximately 56-67% thinner than that of a mammal of the same body mass while the respiratory surface area is approximately 15% greater (Maina et al., 1989), which altogether have the potential for more efficient gas exchange (West et al., 2007). As a result, the environment of the LRT is very different between mammal and birds (West et al., 2007). The upper respiratory tract (URT) of birds is qualitatively similar to that of mammals. It has a nasal cavity with communicating sinuses, a larynx supported by cartilaginous plates and the trachea, although the nasal and oral cavities communicate with each other through the choanal cleft region, which appears in birds to be related to the incomplete secondary palate (**Figure 1**).

These host factors that themselves change across birds and mammals likely play an important role in structuring the airway microbiomes across species. It is possible that some other aspects of adaptation to flight have a net effect on microbiome composition, diversity and function in birds. For instance, the large mass-specific gas uptake by the avian respiratory system (Brown et al., 1997), as well as the large trachea length, the decreased body mass, the higher metabolic rate, the higher average body temperature (40-41°C) and the higher resting heart rate (~245 beats/min) (Brown et al., 1997) probably influence the airway microbiome. The reduction in genome size compared to all amniotes, coupled with a shrinkage of large numbers of genes involved in the immune function (Lovell et al., 2014) might also consistently impact the microbiome composition and function.

HOST DETERMINANTS IN A MICROBE-DOMINATED WORLD: A MATTER OF SPECIES

The importance of host-related factors to the diversity of respiratory microbiomes is still poorly understood. However, we have observed that more closely related mammals tend to present a similar degree of taxa composition in their

microbiomes, with likely downstream effects on host immunity and metabolic potential (**Table 1**). This may be due to the breathing patterns in mammals and the fact that the anatomy and physiology of both the upper and lower respiratory tract do not differ greatly among mammal species (**Figure 1**). In healthy bovine individuals, the URT microbiota (based on nasal and nasopharyngeal swab samples) is dominated by Proteobacteria, a group of bacteria suggested to have high functional variability (Bradley and Pollard, 2017), followed by Tenericutes, Firmicutes and Bacteroidetes (Gaeta et al., 2017; McMullen et al., 2019). Proteobacteria, Firmicutes, and Bacteroidetes are the three most dominant phyla in the URT bacterial communities in piglets (Slifierz et al., 2015; Correa-Fiz et al., 2016; Wang et al., 2019). Precisely, the composition of the tonsillar and oropharyngeal microbiome of adult pigs resembled that of the nasal microbiota, with Proteobacteria and Firmicutes as the predominant phyla (Lowe et al., 2012; Wang et al., 2018). Similarly, the URT microbiome of healthy horses is mainly dominated by Proteobacteria, Actinobacteria, Firmicutes, and Bacteroidetes (Bond et al., 2017). The most common phyla colonizing the nasal cavity of healthy dogs are Proteobacteria, followed by Firmicutes and Bacteroidetes (Tress et al., 2017). Proteobacteria is also the most abundant phylum in the cat respiratory tract, reaching up to 60% and 62% in the oropharyngeal swabs and BAL, respectively (Vientoos-Plotts et al., 2017).

A noticeable and consistent overlap between URT and LRT profile of microbial communities was observed in mammals (**Table 1**). In ruminants, it is likely the result of regurgitating of feedstuffs during rumination and the formation of aerosols during eructation (Klima et al., 2019). Thus, the oral microbiota in cattle probably acts as secondary reservoirs for the lung (McMullen et al., 2020). No information is available on the relationship between the URT and LRT in pigs, and the existing results of LRT microbiota are divergent at the phyla level (Huang et al., 2019; Jiang et al., 2019; Li et al., 2021). In line with the observation in ruminants, studies in cats and dogs support micro-aspiration of pharyngeal secretions as a primary route of microbial colonization of the LRT (Vientós-Plotts et al., 2017; Vientós-Plotts et al., 2019; Fastrès et al., 2020b). In healthy horses, the similarity between nose and lung microbiomes is expected for biological reasons (Bond et al., 2017), such as the large minute ventilation (60 L/min at rest) of these obligate nasal breathers and the fact that they have complete separation of the nasopharynx and oropharynx owing to their long velum, except when swallowing (Fillion-Bertrand et al., 2019). The end result of this interplay is the microbiome of lungs closely resembles that of the oropharynx in the vast majority of healthy mammals. However, it is not clear to what extent the deep airways are stably colonized by specific taxa or whether the microorganisms are in a dynamic state of flux being permanently cleared and repopulated from the URT.

In poultry, Firmicutes, Proteobacteria, Bacteroides, Actinobacteria and Tenericutes are the main well-documented phyla in the upper respiratory (Sohail et al., 2015; Glendinning et al., 2017b; Ngunjiri et al., 2019; Abundo et al., 2021; Kursa et al., 2021) (**Table 1**). In a stable state, the URT is colonized by Bacilli and Clostridia, whereas the LRT, including air sacs, is populated by Bacilli and γ-Proteobacteria (Abundo et al., 2021). However, birds seem to have lost an association with Bacteroidetes but retained an association with facultative anaerobes species from the Proteobacteria phylum (Taylor et al., 2020). The loss of Bacteroidetes likely increases the proportion of transient environmental microorganisms and decreases the observed degree of host specificity and resilience (Taylor et al., 2020). Indeed, this could also help explain the dominance of Proteobacteria, which make up a large proportion of the airborne microbiome in birds (Cáliz et al., 2018), a source to which flighted animals are constantly exposed. At finer grains, birds present fewer obligate anaerobes and more facultative anaerobes compared to mammals. *Lactobacillus* spp. is the main dominant and stable colonizer of the upper respiratory tract (nasal cavity and choanal cleft), albeit varying relative abundances (Sohail et al., 2015; Glendinning et al., 2017b; Johnson et al., 2018; Abundo et al., 2020; Mulholland et al., 2021). *Lactobacilli* are followed by members of the family *Enterobacteriaceae* and of *Staphylococcus* spp. and *Escherichia-Shigella* (Glendinning et al., 2017b; Ngunjiri et al., 2019; Kursa et al., 2021). In the LRT, *Lactobacillus* are also the dominant bacterial taxa (Johnson et al., 2018; Abundo et al., 2021), outranking *Vibrio* and *Halomonas*, as determined by lower respiratory lavage in turkeys, chicken broilers and chicken layers raised in commercial settings (Abundo et al., 2021).

Collectively, these observations support the emerging idea that the nasal cavity in birds, which has the highest microbiota richness, serves as the mainland from which other respiratory sites are colonized (Abundo et al., 2020). The constant movement of fluid and air in the choana can play a major role in equilibrating the microbiome of URT with that of the gut or environment in birds and secondly, it can be responsible for the vast majority of the constant microbial seeding of the lower airways from both oral and nasal cavity. Bacterial overlap between the respiratory tract and gut has been observed in healthy layers raised in commercial farms (Ngunjiri et al., 2019) and turkeys (Taylor et al., 2020; Kursa et al., 2021), possibly through aerosolization of fecal bacteria and the contact with the litter environment.

Other host-related factors that might affect respiratory microbiota variations among mammals and birds involve mucus secretion, gas concentrations, osmolality, temperature, pH, nutrients such as iron and vitamins, surfactant secretion, blood flow, as well as extracellular DNA (Zhu et al., 2019). Additionally, the IgA secretion and the innate and adaptative immune recognition, including the antimicrobial peptides and the sensing of microbes, are endogenous forces that contribute to regulating the host-microbiota interactions in the respiratory system (Wypych et al., 2019).

ENVIRONMENTAL STRESSORS AS DRIVERS OF THE RESPIRATORY MICROBIOTA COMPOSITION AND DYNAMICS ACROSS SPECIES

In mammalian hosts, the newborn animals are considered sterile *in utero* during a normal pregnancy, but during the first hours of

TABLE 1 | Recent metagenomic studies on the respiratory microbiota of domestic animals.

Specie	*Cohort description*	*Sample type*	*Platform and sequenced region*	*Main phyla*	*Genera*	*α-diversity*	*Reference*
Bovine	Healthy Holstein calves (n=32) *vs* calves with pneumonia (n=16), otitis (n=28) or both diseases (n=5). Time series; d3, d24, d28 and d35 of life. Age: 3 to 35 days of age	NPS	Illumina Miseq (V4)	Proteobacteria (30%-80%), Tenericutes (1%-10%), Firmicutes (1-20%), Bacteroidetes (1-10%)	*Mannheimia* (3-25%), *Mycoplasma* (3-18%), *Moraxella* (2-18%), *Psychrobacter* (3-14%), *Pseudomonas* (1-13%). Abundances of *Mannheimia, Moraxella*, and *Mycoplasma* were significantly higher in diseased *vs* healthy animals	α-diversity indices were not different between healthy and diseased calves	(Lima et al., 2016)
Bovine	Angus-beef cattle from weaning to 40 days after arrival at a feedlot (n=30). Time series: weaning, d0, d40	DNS	Illumina Miseq (V3)	Tenericutes (53.2%), Proteobacteria (34.7%), Firmicutes (4.2%), Bacteroidetes (3.7%), Actinobacteria (3.4%)	*Mycoplasma* (*M. dispar* and *M. bovirhinis*, 52%), *Pasteurella* (11%), *Ralstonia* (10%), *Moraxella* (9%)	No differences in α-diversity over time	(Timsit et al., 2016)
Bovine	Healthy Holstein heifer calves at 14d (n=10) and 28d (n=19) *vs* BRDC at 14d (n=6) and 28d (n=6). Age: 3 to 35 days of age	NPS	Illumina Miseq (Not specified)	Proteobacteria, Firmicutes, Actinobacteria, Bacteroidetes, Tenericutes	Healthy: *Mannheimia haemolytica* (7%), *Psychrobacter* (2-5%), *Actinobacillus* (3-6%), *Mycoplasma* (2-12%), BRDC: *Pseudomonas fluorescens* (0.02 – 13%), *Mycoplasma* (8%), *Mannheimia haemolytica* (6%), *Eubacterium* (6%), *Psychrobacter* (5%). No significant differences were detected between groups	Not specified	(Gaeta et al., 2017)
Bovine	Healthy post-weaned Piedmontese calves (n=11) *vs* calves with respiratory diseases (n=8)	DNS, TA	Illumina Miseq (V4)	DNS: Proteobacteria (36.1%), Tenericutes (27.7%), Firmicutes (18.4%), Bacteroidetes (10.1%), Actinobacteria (6.3%) TA: Tenericutes (78%), Proteobacteria (11%), Fusobacteria (4%), Bacteroidetes (4%), Actinobacteria (3%)	DNS: *Mycoplasma* (27%), *Moraxella* (17%), *Aggregatibacter* (4%), *Sphingomonas* (3%), *Corynebacterium* (1.3%), *Psychrobacter* (1.2%). TA: *Mycoplasma* (77%), *Pasteurella multocida* (7%), *Mannheimia* (1.6%), *Bacteroides* (1.5%), *Ureaplasma* (1.3%). No differences between healthy and the BRDC-affected calves	α-diversity indices were different between TA and DNS samples	(Nicola et al., 2017)
Bovine	Angus weaned beef calves fed with Selenium-biofortified alfalfa hay (Se) for 9 weeks (n=30) *vs* control (n=15). Age: 6.5 to 9 months old	DNS	Illumina Miseq (V4)	Control group: Proteobacteria (44%), Bacteroidetes (24%), Firmicutes (19%); Se group: Bacteroidetes (29%), Proteobacteria (27%), Firmicutes (23%)	Control group: *Moraxellaceae* (19%), *Chitinophagaceae* (13%), *Aggregatibacter* (11%), *Weeksellaceae* (7%) Se group: *Chitinophagaceae* (23%), *Moraxellaceae* (9%) *Ruminococcaceae* (6%)	Se group tended to have an enriched nasal microbiota	(Hall et al., 2017)
Bovine	Angus × Hereford heifers transport to a feedlot (n=14). Time series: d0, d2, d7 and d14. Age: 8 months old	NPS	Illumina Miseq (V4)	Firmicutes (22-42%), Proteobacteria (10-30%), Tenericutes (5-20%), Actinobacteria (5-12%)	*Mycoplasma* (0.003-86%), *Psychrobacter* (0.55-90%), *Clostridium, Flavobacterium, Bacteroides, Rikenellaceae, Mannheimia, Acinetobacter, Corynebacterium, Moraxella, Pasteurella, Streptococcus*	Richness increased following feedlot placement (d2)	(Holman et al., 2017)
Bovine	Healthy Charolais calves (n = 8). Age: 6 to 8-month-old	DNS, BALF	Illumina Miseq (V3-V4)	DNS: Actinobacteria (43.9%), Proteobacteria (15.9%), Tenericutes (12.1%), Bacteroidetes (8.8%), Fusobacteria (0.1%) BALF: Proteobacteria (33.3%), Bacteroidetes (18.2%), Tenericutes (8.8%), Actinobacteria (4.9%), Fusobacteria (3.4%)	DNS: *Rathayibacter* (24.41%), *Mycoplasma* (12.20%), *Corynebacterium* (10.37%), *Clostridium* (2.53%), *Prevotella* (0.28%) BALF: *Mycoplasma* (9.48%), *Bibersteinia* (14.41%), *Prevotella* (11.69%), *Clostridium* (6.85%), *Rathayibacter* (0.07%)	No differences in α-diversity indices between DNS and BALF samples	(Zeineldin et al., 2017b)
Bovine	Healthy weaned feedlot cattle (n=60) *vs* cattle with bronchopneumonia (BP;	NPS, TA	Illumina Miseq (V4)	Tenericutes (47%), Proteobacteria (26%), Firmicutes (21%)	TA healthy group: *Mycoplasma* (46%), *Lactococcus* (18%), *Histophilus* (10%), *Moraxella* (6%), *Mannheimia* (6%)	Lower α-diversity in the NPS and TA of BP *vs* control	(Timsit et al., 2018)

(Continued)

TABLE 1 | Continued

Specie	Cohort description	Sample type	Platform and sequenced region	Main phyla	Genera	α-diversity	Reference
	n=60). Mixed-breed beef steers. Body weight: ~260 kg				Only in NPS healthy group: *Corynebacterium* (0.54%), *Jeotgalicoccus* (0.69%), *Psychrobacter* (0.52%), *Planomicrobium* (0.43%) NPS, TA of BP group: *Mycoplasma bovis* (46%), *Mannheimia haemolytica* (5.6%), *Pasteurella multocida* (2.18%)		
Bovine	Weaned Angus-cross beef heifers transported directly to a feedlot (RANC; n=30) *vs* heifers co-mingled at an auction market for 24 h before being placed in a feedlot (AUCT; n=30). Time series: d0, d2, d7 and d30 after arrival	NPS, TA	Illumina Miseq (V4)	NPS: Tenericutes (41%), Proteobacteria (32%), Firmicutes (5%) TA: Tenericutes (50%), Proteobacteria (14%), Firmicutes (9%), Actinobacteria (4%)	NPS*: Mycoplasma* (40.8%), *Moraxella* (18.7%), *Pasteurella* (6.8%), *Mannheimia* (3.8%) TA: *Mycoplasma* (50.4%), *Pasteurella* (5.7%), *Moraxella* (3.1%)	No differences in α-diversity between RANC and AUCT, but it decreased over time	(Stroebel et al., 2018)
Bovine	Commercial feedlot cattle injected with antimicrobials (n=20) *vs* in-feed antibiotics (n=20). Age: 0 to 12 months	NPS	Illumina Miseq (V3-V4)	Not specified	*Psychrobacter* (20-55%), *Pseudomonas* (1-50%), *Mycoplasma* (1-15%), *Moraxella* (0-10%)	Non specified	(Holman et al., 2018)
Bovine	Healthy feedlot cattle (n=3) *vs* cattle with BRDC (n=15)	BALF	HiSeq 2500 (WMS)	Not specified	Healthy: *Bacillus* (6%), *Enterococcus faecium* (5%), *Brachyspira hampsonii* (4%), *Bacillus obstructivus* (3%), *Streptococcus pneumoniae* (2%) BRDC: *Mannheimia haemolytica* (18.8%), *Mycoplasma bovis* (5%), *Mycoplasma dispar* (3%), *Enterococcus faecalis* (2%), *Bacillus* VT-16-64 (2%)	Not specified	(Klima et al., 2019)
Bovine	Weaned Angus × Herford cross calves transported to feedlot (n=13). Time series: auction market (day 0), and feedlot placement (day 2, 7, 14)	NPS	Illumina Miseq (V4)	Proteobacteria (36.1%), Firmicutes (20.1%), Tenericutes (19.3%), Actinobacteria (12.7%), Bacteroidetes (8.6%)	*Acinetobacter* (1-4%), *Bacteroides* (1-2%), *Bifidobacterium* (0-2%), *Corynebacterium* (0-9%), *Jeotgalicoccus* (1-2%), *Mannheimia* (0-1%), *Methanobrevibacter* (1-5%), *Moraxella* (0-10%)	Increase of richness following transport to an auction market and feedlot	(Amat et al., 2019)
Bovine	Angus × Herford steers transported to a feedlot and injected with antimicrobials (n=12) *vs* in-feed antibiotics (n=12) and untreated (n=12). Time series: d0, d2, d5, d12, d19 and d34. Age: weaned calves	NPS	Illumina Miseq (V4)	Not specified	Untreated: *Acinetobacter* (2-5%), *Corynebacterium* (2-6%), *Jeotgalicoccus* (1-3%), *Moraxella* (1-20%), unclassified *Ruminococcaceae* (2-10%), *Mycoplasma* (1-20%), *Planomicrobium* (2.5-5%), *Psychrobacter* (0-10%)	Richness and α-diversity increased following transport to the feedlot	(Holman et al., 2019)
Bovine	Healthy calves (n=82) *vs* BRDC calves (n=82). Time series: 3-12d, 13-20d, 21-44d. Animals were raised without antimicrobials. Age: newly received feedlot cattle of about ~218 kg	DNS	Illumina Miseq (V4)	Proteobacteria (69%), Tenericutes (23%), Firmicutes (3%), Actinobacteria (2%), Bacteroidetes (2%)	Healthy: *Moraxella* (22%), *Mycoplasma* (17%), *Histophilus* (16.62%) BRDC group: *Mycoplasma* (27%), *Histophilus* (21%), *Moraxella* (18%)	Species richness was lower in BRDC compared to healthy	(McMullen et al., 2019)
Bovine	Healthy pre-weaned calves fed 2 different milk-feeding programs (n=40). Age: 3.5 ± 1.15 days of age. BW: 39.3 ± 4.25 kg	DNS	Illumina Miseq (V1-V3)	Tenericutes (29.5%), Firmicutes (19.3%), Actinobacteria (19%), Proteobacteria (16%), Bacteroidetes (11.5%), Fusobacteria (2.5%)	*Pseudoclavibacter (*13.8%), *Mycoplasma* (29.5%). Differences between feeding regimes were observed for *Streptococcaceae* family and *Histophilus*	No differences in α-diversity between treatments	(Maynou et al., 2019)
Bovine	Healthy calves (n=9) *vs* BRDC affected calves treated with tilmicosin (n=9). Age: 6 to 8 months of age.	NPS	Illumina Miseq (V1-V3)	Firmicutes (27.07%), Actinobacteria (24.51%), *Tenericutes* (16.05%), and Proteobacteria (14.43%).	*Mycoplasma* (18.73%), *Microbacteriaceae* (9.36%), *Acinetobacter* (7.35%), *Corynebacterium* (6.36%)	No differences in α-diversity between groups	(Zeineldin et al., 2020b)

(Continued)

TABLE 1 | Continued

Specie	Cohort description	Sample type	Platform and sequenced region	Main phyla	Genera	α-diversity	Reference
				BRDC-affected and treated calves showed significant decrease in Actinobacteria			
Sheep	Suffolk cross sheep sampled at 3 spatially disparate segmental bronchi (n=6). Time series: day 0, 1 month, and 3 months. Age: 20 months old	SBT	Illumina Miseq (V2-V3)	Not specified	*Staphylococcus* (16%), *Corynebacterium* (9%), *Jeotgalicoccus* (5%), *Streptococcus* (5%)	No difference in richness or α-diversity between different lung sites	(Glendinning et al., 2016)
Sheep	Scottish mule x Suffolk sheep (n=40). Age: 7 weeks old	OPS, BALF	Illumina Miseq (V2-V3)	Not specified	OPS*: Pasteurellaceae (22%), Mannheimia (14%), Fusobacterium (11%), Bibersteinia trehalosi (8%), Neisseriaceae (7%), Moraxella (6%), Bibersteinia (5%)* BALF*: Staphylococcus equorum (13%), Staphylococcus sciuri (6%), Mannheimia (5%), Prevotella (5%)*	No difference in richness or α-diversity	(Glendinning et al., 2017a)
Pig	Healthy commercial pigs (n=30) *vs* pigs with Glässer's disease (n=40). Age: 3-4 weeks old (before weaning)	DNS	Illumina Miseq (V3-V4)	Healthy: Proteobacteria (32.5%), Firmicutes (21.1%), Tenericutes (2.2%), Actinobacteria (1.3%) Glässer: Proteobacteria (44%), Firmicutes (18.5%), Tenericutes (2.2%), Actinobacteria (1.3%)	unclassified *Pasteurellaceae* (27.0%), *Moraxella* (17.2%), *Weeksella* (12.9%), *Haemophilus* (6.1%), Healthy: *Moraxella* (13.6%), *Enhydrobacter* (3.1%), *Haemophilus* (2.8%) Glässer: *Moraxella* (22.2%), *Haemophilus* (9.4%), *Enhydrobacter* (4.3%)	Healthy status was associated to higher species richness and α-diversity	(Correa-Fiz et al., 2016)
Pig	Piglets treated by Ceftiofur Crystalline free acid (CCFA, n=4), Ceftiofur hydrochloride (CHC, n=4), Tulathromycin (TUL, n=4), Oxytetracycline (OTC, n=4), or Procaine Penicillin G (PPG, n=4). Time series: day 0, 1, 3, 7, and 14 after dosing. Age: 8-week-old	DNS	Illumina Miseq (V1-V3)	Firmicutes (46.46%), Proteobacteria (31.87%), Bacteroidetes (9.64%)	*Moraxella* (21.52%), *Clostridium* (19.74%), *Streptococcus* (10.93%), *Calothrix* (5.43%), *Prevotella* (4.49%)	The α-diversity was not affected by treatment	(Zeineldin et al., 2018)
Pig	Cross-bred Yorkshire x Hampshire healthy newborn piglets (n=28). Time series: 8h post-birth, 1, 2, 3 and 4 weeks of age	TS	Illumina Miseq (V4)	Not specified	Post-born piglets were colonized by *Streptococcus, Staphylococcus, Moraxella, Rothia*, and *Pasteurellaceae*. By 1 week of age, members of the *Pasteurellaceae, Moraxellaceae*, and *Streptococcaceae* families were the most dominant	Not specified	(Cortes et al., 2018)
Pig	Healthy cross-bred pigs (n=10) *vs* pigs with Porcine respiratory disease (PRDC) disease (n=23). Age: 2-3 weeks of age (before weaning)	NPS	Illumina Miseq (V3-V4)	Firmicutes (53.11%), Proteobacteria (27.89%), Bacteroidetes (12.17%), Fusobacteria (3.15%), Actinobacteria (2.29%)	Healthy: *Lactobacillus* (30.44-37.28%), *Streptococcus* (23.60-32.26%), *Actinobacillus* (11.48-15.09%), *Bergeyella* (3.10%), *Escherichia-Shigella* (2.24%) PRDC: *Streptococcus* (22.22-26.25%), *Actinobacillus* (9.66-17.63%), *Moraxella* (12.02-15.82%), *Veillonella* (7.16%), *Bergeyella* (4.60-7.46%), *Fusobacterium* (4.64%), *Porphyromonas* (4.31%), *Escherichia-Shigella* (4.19%)	No differences in α-diversity and richness between the healthy and PRDC groups	(Wang et al., 2018)
Pig	Healthy Duroc Landrace Yorkshire cross-breed piglets (n=10) *vs* piglets challenged with Porcine	BALF	Illumina Miseq (V3-V4)	Healthy: Firmicutes (79.8–89.8%), Tenericutes (0.18-2.4%), Proteobacteria (5.3-13.4%)	Healthy: *Anoxybacillus, Caloramator* PRRSV: *Haemophilus parasuis* (35–48%), *Mycoplasma hyorhinis* (27–41%), *Bacteroides* (4–11%), *Chloroplast*	Reduced α-diversity in the PRRSV group	(Jiang et al., 2019)

(Continued)

TABLE 1 | Continued

Specie	Cohort description	Sample type	Platform and sequenced region	Main phyla	Genera	α-diversity	Reference
	reproductive and respiratory syndrome (PRRSV) (n=10). Age: 8 to 10 weeks of age			PRRSV: Proteobacteria (40.8-49%), Firmicutes (2.4–8.8%), Tenericutes (27-40.0%)	(1–3%), unclassified *Chitinophagaceae* (1–7%)		
Pig	Cross-bred pigs with lung-lesion and raised under natural conditions (n=20). Age: 240 days of age	BALF	Illumina Miseq (V3-V4)	Proteobacteria (34.2%), Tenericutes (22.3%), Bacteroidetes (18.8%), Firmicutes (18.1%)	*Mycoplasma* (13.0%), *Methylotenera* (10.9%), *Ureaplasma* (9.2%), *Phyllobacterium* (5.3%), *Prevotella* (4.0%), *Sphingobium* (3.2%), *Lactobacillus* (3.0%), *Thermus* (2.7%), *Streptococcus* (2.4%), *Haemophilus* (1.8%)	Reduced α-diversity in lungs with higher level of lesions	(Huang et al., 2019)
Pig	Commercial healthy pigs at slaughter (n=10)	TS	Illumina Miseq (V3-V4)	Proteobacteria (30–40%), Firmicutes (30%), Fusobacteria (20%), Bacteroidetes (10–20%). No differences between tonsil surface and in deep tonsil tissue	Surface of tonsils: *Actinobacillus* Deep tonsils: *Yersinia, Pasteurella*.	No difference in α-diversity between the surface and the deep tonsil tissue	(Jakobsen et al., 2019)
Pig	Duroc×Landrace×Yorkshire growing pigs exposed to different levels of gaseous ammonia (n=72). Body weight ∼30 kg	DNS, TS	Illumina Miseq (V3-V4)	Proteobacteria (36.4%), Firmicutes (34.8%), Bacteroidetes (19.9%), Actinobacteria (4.1%)	*Moraxella, Pseudomonas, Lactobacillus, Prevotella, Bacteroides, Megasphaera, Streptococcus, Rothia, Allobaculum, Blautia, Oscillospira*	Ammonia concentration decreased the α-diversity	(Wang et al., 2019)
Pig	Commercial weaned pigs housed to simple slatted-floor (S, n=75) *vs* complex straw-based rearing ecosystem (C, n=75). Sampling time: from 164 days post-weaning at the time of slaughter	BMS	Illumina Miseq (V3-V4)	Firmicutes (58.2%), Proteobacteria (30%) Actinobacteria phylum was more abundant in C-raised pigs compared to S-raised pigs	*Bacteroidetes, Clostridium*, *Streptococcus* *Anaerotruncus* (8%) was higher in S-raised pigs whereas *Bacteroidetes* (24.3%) and *Chitinophagaceae* (15.4%) were higher in C-raised pigs	The S ecosystem increased the α-diversity	(Megahed et al., 2019)
Pig	Post-weaned pigs with oxytetracycline parenterally administered (n=21) or in feed (n=22), and the non-medicated feed group (n=22). Time series: days 0 (before start of treatment), 4, 7, 11, and 14	DNS, TS	Illumina Miseq (V4)		DNS untreated: *Streptococcus* (23.61%), *Moraxellaceae* (29.74%), *Actinobacillus* (9.30%), *Moraxella* (3.36%), *Lactobacillus* (2.43%), DNS antibiotic: *Moraxellaceae* (32.84%), *Streptococcus* (12.68%), *Moraxella* (5.01%), *Lactobacillus* (2.15%) Tonsils untreated: *Veillonella* (18.27%), *Streptococcus* (16.31%), *Actinobacillus* (15.46%), *Bacteroides* (13.91%), *Fusobacterium* (6.95%) Tonsils antibiotic: Actinobacillus (22.90%), Bacteroides (17%), *Veillonella* (14.03%), *Streptococcus* (13.60%), *Fusobacterium* (7.09%)	Nasal α-diversity with antibiotic treatment was lower compared to control group. In tonsils, α-diversity was not affected by treatment	(Mou et al., 2019)
Pig	Healthy cross-bred pigs (n=30) *vs* pigs with Glässer's disease, n=51). Age: weaning pigs (3-4 weeks of age)	DNS	Illumina Miseq (V3-V4)	Not specified	Glässer: *Corynebacterium, Clostridium* XI, *Escherichia/Shigella*, Healthy: *Odoribacter, Planobacterium, Phascolarctobacterium.*	Not specified	(Mahmmod et al., 2020)
Pig	Healthy duroc×Landrace×Yorkshire growing pigs (n=8) *vs* diseased pigs with PRDC (n=20). Age: 270 ± 3 days of age	BALF	Illumina Miseq (V3-V4)	Healthy: Proteobacteria (59%), Firmicutes (28.55%), Tenericutes (9.94%), Bacteroidetes (2%) Diseased: Proteobacteria (54%), Firmicutes (34%), Tenericutes (3%), Bacteroidetes (7%)	*Healthy:* Higher abundance of Lactococcus, *Enterococcus*, *Staphylococcus*, *Lactobacillus.* Diseased: Enhanced richness of *Streptococcus*, *Haemophilus*, *Pasteurella*, *Bordetella*	α-diversity was lower in healthy individuals than in diseased group	(Li et al., 2021)

(Continued)

TABLE 1 | Continued

Specie	Cohort description	Sample type	Platform and sequenced region	Main phyla	Genera	α-diversity	Reference
Bird	Birds raised at 3 different farms in Pakistan (n=14)	TA, BALF	454 Roche	Proteobacteria, Firmicutes, Tenericutes, Actinobacteria, Bacteroidetes	Farm A: unclassified ɣ Proteobacteria, Farm B: *Avibacterium* Farm C: unclassified *Enterobacteriaceae, Pseudomonas*	The α-diversity was higher in farms B and C than farm A	(Shabbir et al., 2014)
Bird	Healthy commercial chickens aged 2 days (n = 5), 3 weeks (n = 5) and 30 months (n = 6)	DNS, BALF	Illumina Miseq (V2-V3)		DNS: *Staphylococcus* (8.0%), *Lactobacillus* (6.2%), unclassified *Enterobacteriaceae* (6.0%), *Faecalibacterium prausnitzii* (5.0%), *Staphylococcus equorum* (5.0%), *Lactobacillus reuteri* (4.4%) BALF: *Pseudomonas* (20.7%), *Achromobacter* (4.8%), *Lactobacillus* (4.8%), *Turicibacter* (4.7%), SMB53 (3.6%). The 30-month-old birds showed lower *lactobacilli* but higher *Jeotgalicoccus*, *Staphylococcus* and smb53	The richness and α-diversity were different between DNS and BALF. Richness raised with age	(Glendinning et al., 2017b)
Bird	Commercial Coob 500 broilers from different flocks (n=120). Three grow-out cycles from 0 to 42 d of age. A cross-sectional sampling with different ages (n=90)	TA	Illumina Miseq (V4)	Not specified	*Lactobacillus, Escherichia/Shigella, Staphylococcus, Corynebacterium*, unclassified *Moraxellaceae*, unclassified *Ruminococcaceae*, unclassified *Clostridiales, Ruminococcus, Psychrobacter, Blautia*	Not specified	(Johnson et al., 2018)
Bird	Hy-Line W-36 commercial layers (n=181). Nine grow-out cycles from 5 weeks to > 17 weeks of age	DNS, TA	Illumina Miseq (V3-V4)	Not specified	DNS: *Staphylococcus, Enterobacteriaceae*, unclassified *Lactobacillaceae, Lactobacillus reuteri, Faecalibacterium prausnitzii, Deinococcus*, unclassified *Burkholderiaceae* TA: *Lactobacillus*, *Clostridium, Enterococcus, Escherichia-Shigella, Callibacterium, Irnithobacterium, Staphylococcus, Streptococcus.*	Not specified	(Ngunjiri et al., 2019)
Bird	Healthy commercial turkeys sampled at 3 time points during brooding (1, 3, and 5 weeks) and grow-out (8, 12, and 16 weeks; bn= 104).	DNS, TA	Illumina Miseq (V4)	DNS: Firmicutes and Actinobacteria TA: Proteobacteria	*Deinococcus*, *Corynebacterium*, and *Staphylococcus*	The α-diversity in the nasal cavity or trachea did not change with age	(Taylor et al., 2020)
Bird	Healthy ale Arbor Acres broilers exposed to 4 different levels of ammonia for 21 days (n=228). Age: 22 days of age	TA	Illumina Miseq (V3-V4)	Firmicutes (70%), Proteobacteria (15%)	*Lactobacillus* decreased under different levels of ammonia exposure, whereas *Faecalibacterium, Ruminococcus*, *unclassified Lachnospiraceae, Ruminococcaceae UCG-014, Streptococcus* and *Blautia* increased with ammonia levels	The α-diversity decreased with the ammonia levels	(Zhou et al., 2021)
Horse	Healthy horses (n=3) *vs* healthy horses treated with dexamethasone (n = 3) and *vs* horses with Inflammatory Airway Disease (IAD; n = 7).	DNS, BALF	Illumina Miseq (V3-V4)	Proteobacteria (43.85%), Actinobacteria (21.63%), Firmicutes (16.82%), Bacteroidetes (13.24%)	*Sphingomonas* (15.65%), *Pseudomonas* (14.57%), *Pantoea* (11.68%), *Knoellia* (2.80%), *Agrococcus* (2.61%) Arthrobacter (2.61%). *Streptococcus* was higher in IAD horses. Dexamethasone had no effect	No differences in α-diversity. Decrease in richness in BALF	(Bond et al., 2017)
Horse	Healthy adult horses (n=6) *vs* asthmatic horses (n=6). Animals were at pasture (low antigen exposure), housed indoors and fed good- quality hay ("moderate exposure") or	DNS, BALF	Illumina Miseq (Not specified)	DNS: Proteobacteria, Firmicutes BALF: Proteobacteria, Firmicutes, Bacteroidetes, Actinobacteria, Verrucomicrobia	DNS: *Pasteurella multocida* (39.5%), *Actinobacillus* (23.2%) BALF: *Enterobacteriaceae* (4%), *Pasteurella multocida* (3.0%), *Comamonadaceae* (2%), *Actinobacillus* (1.9%), *Staphylococcus* (1%)	DNS had higher richness and α-diversity than BALF samples	(Fillion-Bertrand et al., 2019)

(Continued)

TABLE 1 | Continued

Specie	Cohort description	Sample type	Platform and sequenced region	Main phyla	Genera	α-diversity	Reference
	poor-quality hay ("high exposure")						
Horse	Healthy horses (n=23) *vs* horses affected with primary (n=14) and secondary sinusitis (n=62). Age: 2 - 30 years old	PS	Illumina Miseq (V4)	Proteobacteria (63%, 23.7–99.0%), Firmicutes (14%, 0.38–64%), Actinobacteria (5.19, 0–62%)	Healthy*: Pseudomonas* (14.6%, 0.2–50.2%), *Delfta* (7.8%, 0–26.2%) *Stenotrophomonas* (6.7%, 0.1–18.2%) *Dokdonella* (5.1%, 0–80.8%) *Aggregatibacter* (4.7%, 0–71.0%) *Acinetobacter* (3.6%, 0–20.3%) *Achromobacter* (2.7%, 0–20.6%). Sinusitis: *Streptococcus equi* subsp. *Zooepidemicus*, *Fusobacterium*	No differences in Simpson diversity index between healthy and sinusitis groups	(Beste et al., 2019)
Horse	Healthy horses (n=4) *vs* horses with naturally occurring mild asthma (n = 16). Body weight ~435-612 kg Horses were treated with nebulized dexamethasone for 14 d.	NPS, BALF	Illumina Miseq (V4)	NPS: Proteobacteria (37.81%), Bacteroidetes (25.71%), Actinobacteria (17.77%), Firmicutes (17.9%)	*Hymenobacter* (16.51%), *Staphylococcus* (13.49%), *Pedobacter* (6.33%), *Moraxella* (4.50%), *Sphingomonas* (3.75%), *Pseudomonas* (3.62%)	Nebulized dexamethasone treatment decreased α-diversity in the nasopharynx	(Bond et al., 2020)
Dog	Healthy female dogs (n=16). Age: 2 - 8 years of age	DNS, NPS, BALF	Illumina Miseq (V4)	DNS: Proteobacteria (55.40%), Actinobacteria (0.73%) NPS: Proteobacteria (60.79%), Tenericutes (7.04%), Actinobacteria (0.41%) BALF: Proteobacteria (88.53%), Actinobacteria (2.61%)	DNS: unclassified *Pasteurellaceae* (7.20%), *Brevundimonas diminuta* (2.69%), Cardiobacteriales (2.11%) NPS: *Porphyromonas* (8.32%), Fusobacterium (2.96%), unclassified *Weeksellaceae* (2.70%), unclassified *Neisseriaceae* (3.36%) BALF: *Brevundimonas diminuta* (22.48%), *Sphingopyxis alaskensis* (2.37%), unclassified *Pasteurellaceae* (2.36%), *Propionibacteriaceae* unclassified (1.9%), unclassified *Bradyrhizobiaceae* (1.23%), unclassified *Methylobacteriaceae* (1.68%)	BALF in healthy dogs had equivalent richness to DNS	(Ericsson et al., 2016)
Dog	Healthy dogs (n = 23), dogs with malignant nasal neoplasia (n = 16), and dogs with chronic rhinitis (n = 8). Age ~6 years old	DNS	Illumina Miseq (V4)	Healthy: Proteobacteria (83.4%, 37.4%— 98.5%), Firmicutes (4.8%, 0.4–20.8%), Bacteroidetes (2.6%, 0.1–12.5%), Cyanobacteria (2.1%, 0.0–11.6%), Actinobacteria (2.1%, 0.1–8.6%).	Healthy group: *Moraxella* (59.2%), *Phyllobacterium* (3.4%), family *Cardiobacteriacea* (2.1%), *Staphylococcus* (1.7%). Diseased group: *Moraxella* (34.5%, 0.7–77.3%), order Streptophyta (6.4%, 0.0–16.6%), *Riemerella* (4.4%, 0.0–25.3%), family *Pasteurellaceae* (2.9%, 0.2–17.1%)	Shannon diversity index was lower for the healthy dogs than for the diseased dogs	(Tress et al., 2017)
Dog	Healthy client-owned dogs (n=5) *vs* client-owned dogs diagnosed with bacterial pneumonia (n=15)	OPS, BALF	Illumina Miseq (V4)	Not specified	OPS healthy: *Escherichia-Shigella* (15.33%), *Prevotella* (15.21%), *Streptococcus* (10.88%), *Bacteroides* (10.96%), *Mycoplasma canis* (7.67%), Acinetobacter (3.90%), BALF healthy: *Streptococcus* (96.4%)	Richness was decreased with pneumonia	(Vientós-Plotts et al., 2019)
Dog	Healthy research dogs (n=16) *vs* client-owned dogs diagnosed with Chronic Bronchitis (n=53). Age: between 8 and 9 years old	BALF	Illumina Miseq (V4)	Not specified	BALF healthy: *Pseudomonas stutzeri* (29.5%), *Acinetobacter* (20.9%), and *Brevundimonas* (20.1%) BALF diseased: *Acinetobacter* (22.3%), *Bradyrhizobium* (9.3%), *Brevundimonas* (8.3%), *Agrobacterium radiobacer* (7.1%)	Diseased dogs had lower richness than healthy research dogs	(Ericsson et al., 2020)
Dog	Healthy west highland white terriers (n=6) *vs* west highland white terriers with idiopathic pulmonary fibrosis (n=11)	BALF	Illumina Miseq (V1–V3)	Proteobacteria, Actinobacteria, Firmicutes, Bacteroidetes	Healthy group: *Cutibacterium, Staphylococcus, Streptococcus, Pseudomonas, Corynebacterium*, unclassified *Pasteurellaceae*, *Acinetobacter, Conchiformibius, Flavobacterium*, *Porphyromonas*.	Lower α–diversity in diseased dogs compared to healthy	(Fastrès et al., 2020a)

(Continued)

TABLE 1 | Continued

Specie	Cohort description	Sample type	Platform and sequenced region	Main phyla	Genera	α-diversity	Reference
					Diseased group: *Brochothrix, Curvibacter, Pseudarcicella*, unclassified *Flavobacteriaceae*		
Dog	Healthy dogs of different breeds (n=45) *vs* dogs diagnosed with idiopathic pulmonary fibrosis (n=11) exposed to different living conditions	BALF	Illumina Miseq (V1–V3)	Healthy: Proteobacteria, Actinobacteria, Firmicutes, Bacteroidetes	BALF healthy: *Cutibacterium, Staphylococcus, Streptococcus, Pseudomonas, Corynebacterium_1, Pasteurellaceae genus, Acinetobacter, Conchiformibius, Flavobacterium and Porphyromonas* (all together ~23% of bacterial population) BALF diseased: predominance of *Rhodoluna, Brochothrix, Curvibacter, Pseudarcicella*, *Flavobacteriaceae* family	No differences between living conditions for the α-diversity and the evenness. No differences between healthy and diseased dogs	(Fastrès et al., 2020b)
Cat	Healthy cats (n=6). Time series: day 0, week 2, and week 10. Age < 1 year old	OPS, BALF	Illumina Miseq (V4)	OPS Proteobacteria (60%, 54.78-74.28) BALF: Proteobacteria (62.36%, 27.26-81.65%)	OPS *Pasteurellaceae* (15.99%), *Moraxellaceae* (14.79%), *Porphyromonadaceae* (12.45%), *Pseudomonadaceae* (10.21%), *Paraprevotellaceae* (5.46%). BALF: *Pseudomonadaceae* (34.24%), *Sphingobacteriaceae* (22.56%), *Bradyrhizobiaceae* (15.86%).	OPS was richer than BALF. No differences in richness between time points	(Vientoos-Plotts et al., 2017)
Cat	Probiotic administration in healthy cats (n=6). Time series: baseline and after probiotic administration. Age < 1 year old	OPS, BALF	Illumina Miseq (V4)	Actinobacteria (59.27%), Firmicutes (40.67%)	*Bifidobacterium* (35.93%), *Bifidobacterium animalis* (23.29%), *Streptococcus* (25.53%), *Lactobacillus zeae* (11.64%), *Lactobacillus* (3.21%)	Probiotic increased the richness in the OPS and BALF	(Vientós-Plotts et al., 2017)
Cat	Healthy cats (n = 28) *vs* cats with nasal neoplasia (n = 16), and cats with feline upper respiratory tract disease (FURTD; n = 15). Age ranged from 6 months to 14.0 years	DNS	Illumina Miseq (V4)	Proteobacteria, Firmicutes, and Bacteroidetes	Healthy: *Moraxella* (33%), unclassified *Bradyrhizobiaceae* (11.3%), *Sediminibacterium* (5.8%), *Staphylococcus* (4.3%), *Pseudomonas* (2.3%) FURTD: *Moraxella* (38.6%), unclassified *Bradyrhizobiaceae* (8.8%), *Staphylococcus* (6.3%), *Chlamydia* (5.7%), *Pasteurella* (5.7%), *Sediminibacterium* (4.6%), *Bibersteinia* (4%) Neoplasia: *Moraxella* (15.8%), unclassified *Bradyrhizobiaceae* (20.6%), unclassified *Chitinophagaceae* (7.3%), *Phyllobacterium* (6.6%), *Pasteurella* (5.1%)	No differences between health and diseased cats	(Dorn et al., 2017)

BALF, Bronchoalveolar lavage fluid; BMS, Bronchus mucosal scraping; DNS, deep nasal swap; NPS, nasopharyngeal swaps; OPS, Oropharyngeal swabs; PS, Paranasal sinus; SBT, Segmental bronchi throat; TA, tracheal aspiration; TS, tonsil swabs; WMS, whole metagenome sequencing.

life, a wide range of microorganisms are acquired after the passage through the birth canal, during suckling and maternal care, and from the immediate environment at delivery, such as pen material, feed and feces. Consequently, the microbiota of the calf URT is highly similar to the maternal vaginal microbiota (Lima et al., 2019). Immediately after birth, the airway microbiota in ruminants evolves and reaches a maximum of diversity within one month of age (Timsit et al., 2017; Lima et al., 2019). The taxa organisms detected in the LRT shift from Proteobacteria and Firmicutes to Bacteroidetes and Tenericutes across age (Lima et al., 2019). Such microbiota changes are thought to be intertwined with immune system maturation that promotes tolerance to environmental allergens (Ramírez-Labrada et al., 2020). If the colonization process is disrupted, the animal may develop a dysbiotic microbiota, causing a predisposition to contracting complex respiratory disease. An elegant review by Zeineldin et al. (2019) about ruminants declared that changes in diet (Hall et al., 2017; Maynou et al., 2019), antimicrobial use (Collie et al., 2015; Timsit et al., 2017; Holman et al., 2018; Holman et al., 2019; McMullen et al., 2019), pathogen exposure (Holman et al., 2015), as well as early life management procedures, including weaning, vaccination, commingling, long-distance transportation and housing (Timsit et al., 2016; Holman et al., 2017; Timsit et al., 2017; Zeineldin et al., 2017a; McMullen et al., 2018; Amat et al., 2019) are major contributing factors to the initial seeding

disruption of the airway microbiota and have been associated with various health outcomes later in life (**Figure 2**).

Along the same lines, the nasal microbiota of piglets following delivery resembles that of the sow and depends on the route by which the pig is delivered and the feeding type (Wang et al., 2013a). The tonsillar microbiota of piglets following birth resembles the sow vaginal and teat skin microbiota, indicating that these two body sites contribute to the colonization of the URT (Pena Cortes et al., 2018). However, no studies have examined the initial seeding and development of the LRT microbiome in swine. Thereafter, the microbiota begins to stabilize and progress toward and adult-like composition 2–3 weeks after the weaning (Slifierz et al., 2015; Cortes et al., 2018). As previously described in the gut (Mach et al., 2015), weaning is the critical period for the establishment of a robust and stable adult-like microbiota composition in piglets (Pirolo et al., 2021). Alongside weaning, other key environmental factors can modify the composition of the URT microbiota early in life, including the addition or removal of feed antibiotics (Zeineldin et al., 2018; Correa-Fiz et al., 2019; Mou et al., 2019; Zeineldin et al., 2019), gaseous ammonia concentration (Michiels et al., 2015; Wang et al., 2019), type of floor (Megahed et al., 2019) or feeding strategies (Weese et al., 2014).

The way in which different bacteria populate the respiratory microbiota is unknown in horses. Yet, it is not demonstrated that mode of birth, type of diet and antibiotic use have profound effects on the respiratory microbiome of newborn up to some months or years of age in horses. The age at which the respiratory microbiota acquires an adult-like configuration is still unclear. Maternal separation at weaning has a pivotal influence on the gut microbiome composition in foals (Mach et al., 2017). This likely holds true for the respiratory microbiota. Our previous findings in the gut (Mach et al., 2020; Mach et al., 2021a; Mach et al., 2021b) also highlight the possibility that the airway microbiota may be particularly sensitive to where a horse lives and what a horse does. In fact, short-term changes in housing and forage type alters the pulmonary microbiota in horses (Fillion-Bertrand et al., 2019), as well as the contact with animals and people who work at horse facilities, veterinary health care and medication (Kauter et al., 2019).

In a similar manner, published literature on the effects of birth mode on the respiratory microbial composition during the first years of life in companion animals is scant. Whether C-section is associated with lower bacterial diversity and linked with allergy is also unclear. Nonetheless, the combined effect of passive (living environment) and active (lifestyle) factors on the airway microbiota in companion animals from developed countries have started to receive attention for its role in complex respiratory diseases, especially asthma (**Figure 2**). At least, dogs living in urban environments (worse air quality/air pollution) and exposed to an urban-type lifestyle (e.g., living closed in apartments for hours and in a single-person family without other pets) may present an altered microbiota and be more susceptible to respiratory diseases compared to those living in a rural environment and farming lifestyle (Lehtimäki et al., 2018). In agreement with the posited hypothesis, climate change that affects air quality has been shown to lead to alterations in microbial communities in the dog airways (Ericsson et al., 2020). Therefore, the living conditions are suspected to play a role in the airway microbiota in dogs, while no differences are found between types of breeds (Fastrès et al., 2020b). This assumed interplay between urban-type lifestyle, microbial exposure, host microbiota and respiratory disease needs to be confirmed in cats. The information of whether the microbiota of urban cats is more alike than rural ones is still lacking.

Concerning the airway microbiota in birds, the initial colonization of commercially hatched chickens is mainly dependent on the hatchery environment and transport to the farm (Brugman et al., 2018; Kubasova et al., 2019). Notably, some microorganisms can be acquired in the pre-hatching phase, directly from the mother in the oviduct of the hen, or from the environment through the pores in the eggshell (Kers et al., 2018). After birth, lower airway microbiota of commercial chickens kept indoors gradually assembles, without clear separation between brooding, growing and laying stages, while nasal microbiota shifts drastically after the birds transitioned to the laying stage (17 weeks onward) (Ngunjiri et al., 2019). Yet, despite the results by Ngunjiri et al. (2019), little is known about what drives the acquisition and development of the respiratory microbiota during early in life in poultry. Information is scant when focusing on chicks that have any form of contact with adult hen microbiota, chicks that live outdoors throughout their whole life or free-range organic chicken. Exposure to chronic heat-stress (Sohail et al., 2015), atmosphere ammonia concentrations (Liu et al., 2020; Zhou et al., 2021), housing and environmental conditions (Kursa et al., 2021), as well as performance stress (Kursa et al., 2021) are known to shape the composition of the respiratory tract microbiota in domestic birds. As for gut, environmental factors such as biosecurity level, disease onset, litter and feed access may each influence the poultry airway microbiota establishment after hatching (Kers et al., 2018) (**Figure 2**). Antibiotic treatments and vaccinations, which are often administrated *via* spray or eye/nose drops, may also affect the development of the microbiota.

FRENEMIES: *LACTOBACILLUS* AND *PROTEOBACTERIA* IN COMPLEX RESPIRATORY DISEASES

Host mechanisms for pathobiome regulation in the respiratory apparatus might be different between mammalian animal hosts and birds, but they have in common the aim of both preventing the invasion by pathogens and managing symbiotic microorganisms to maximize the benefits for the host. Precisely, the commensal microbiota may directly inhibit the persistence, transmission and evolution of pathogens through mechanisms such as competing for nutrients, bactericidal activity, metabolic inhibition, biofilm formation, quorum sensing, disruption of signaling molecules, and spatial occlusion (Man et al., 2017; Zhu et al., 2019). Additionally, host systemic and respiratory immune response (Man et al., 2017; Zaneveld et al., 2017; Amat et al., 2019; Budden et al., 2019; Li et al., 2019) may indirectly affect the interaction between

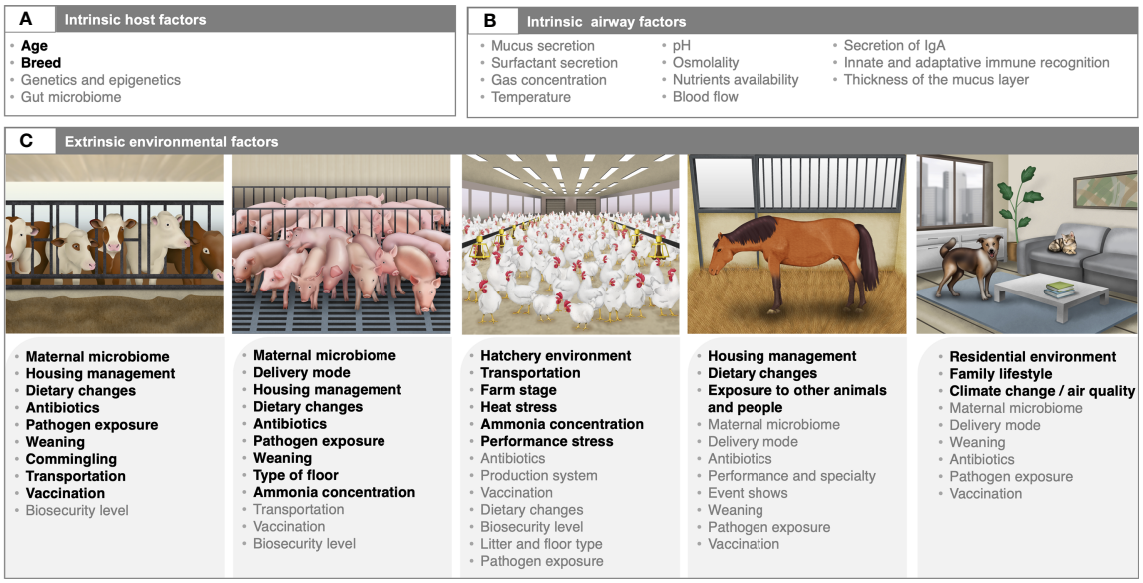

FIGURE 2 | Intrinsic and extrinsic factors affecting the composition and development of the airway microbiota in domestic animals. The respiratory tract microbiota composition and development are dynamic and are shaped by various intrinsic host factors **(A)**, as well as intrinsic airway milieu conditions **(B)**, and environmental variables **(C)**. Factors highlighted in bold are based on published literature. For ruminants and swine, factors are mainly extracted from the review by Zeineldin et al. (2019) and Pirolo et al. (2021), respectively. Variables colored in grey are those that illustrate directional hypothesis made by the authors. Written permission for publication of the domestic animals' drawings in the figure has been taken, except for the horse drawing. Horse drawing has been obtained from Mach et al. (2020).

commensals and pathogens. None of these mechanisms are wholly effective, but they all reflect common actions by commensal microbiota to neutralize threats to their hosts and, by extension, to themselves.

At this time, several examples of possibly actionable mechanisms of competition and cooperation have been reported in ruminants. For instance, microbiota of the alveolar epithelium in adult sheep synthesizes antimicrobial anionic peptides that quickly bind to and inactivate *Mannheimia haemolytica* (Heidari et al., 2002). In cattle, Amat et al. (2019) suggested that the presence of bacteria from the *Lactobacillaceae* family have a competitive exclusion effect on the BRDC-associated *Pasteurellaceae* family. These results were supported by inhibition assays, in which strains within the families of *Lactobacillaceae, Streptococcaceae*, and *Enterococcaceae* displayed *in vitro* antimicrobial activity (Amat et al., 2019). Additionally, *Lactobacillus* were shown to inhibit the growth of *Mannheimia haemolytica in vitro* (Amat et al., 2017). Taken together, commensal species from the *Lactobacillaceae* family may offer resistance to pathogens directly by producing antimicrobials and beneficial metabolites (e.g., lactic acid and SCFA) or indirectly through keeping cells of the innate and adaptive immune system on the tip of their toes, ready to respond rapidly to pathogenic threats when required.

In pigs, the supplementation with the Lactobacillales *Enterococcus faecium* as probiotic carried direct adsorptive trapping of swine influenza viruses (H1N1 and H3N2 subtypes) by direct physical interaction and by reinforcing innate antiviral defense through mediators such as IL-6, TNF-α, IL-10, IFN-α and TLR-3 (Wang et al., 2013b). Evidence that probiotics may be effective in reducing severity, duration, and incidence of respiratory illnesses in herd-based species was stated as being low to very low (Suez et al., 2019).

While an increased prevalence of *Lactobacillus* is a potential diagnostic signature of eubiosis in ruminants and swine, respiratory disorders in those farm animals are often accompanied by an abnormal expansion of Proteobacteria (**Table 1**). More specifically, γ-Proteobacteria, a phylum containing a wide variety of pathobionts, is frequently enriched in the respiratory tract of infected individuals of cattle and pigs, thereby increasing the likelihood of pathogenic responses. In fact, numerous studies in cattle have linked a remarkable loss in α-diversity to a gain in Proteobacteria during disease. For example, the URT of BRDC-affected calves presented higher abundance of *Moraxella, Streptococcus, Haemophilus*, *Neisseria* (Holman et al., 2015), *Pseudomonas* (Gaeta et al., 2017), *Solibacillus* and *Pasteurella* spp. (Zeineldin et al., 2017a). Within the γ-Proteobacteria, *Pasteurella* spp. was also increased by 1.5 in calves with pneumonia, as diagnosed by ultrasonography, compared with calves without pneumonia (Raabis et al., 2021). The lower α-diversity of the nasopharyngeal and tracheal bacterial communities of cattle with bronchopneumonia likely explained why they were colonized by pathogens such as *Mycoplasma bovis, Mannheimia haemolytica* and *Pasteurella multocida* (Timsit et al., 2018). Parallel work by Lima et al. (2016) demonstrated a marked increase in abundance of the *Mannheimia, Moraxella*, and *Mycoplasma* genera in the URT of

three days-old calves coupled to the development of pneumonia and otitis media in calves during the first 60 days of life.

Comparably, a significant gain in the Proteobacteria and loss in Firmicutes, species richness and α-diversity was seen in the nasal microbiota of piglets with Glässer's disease (Correa-Fiz et al., 2016). Interestingly, the *Pasteurellaceae* was one of the main families responsible for the higher abundance in Proteobacteria, with *Haemophilus parasuis*, being clearly increased, as well as the *Mycoplasmataceae* family (Correa-Fiz et al., 2016). The pro-inflammatory bacteria *Moraxella* spp., was significantly increased in the oropharynx of suckling pigs with porcine respiratory disease (Wang et al., 2018), whilst Proteobacteria such as *Sphingobium*, *Haemophilus* and *Phyllobacterium* co-occurred with *Mycoplasma* and *Ureaplasma* in lungs with severe lesions.

Consistent with results observed in pigs and cows, horses infected with equine herpesvirus 1 (EHV-1) had lower nasal bacterial richness, evenness and diversity than healthy horses, conjointly with higher abundance of Proteobacteria (Gomez et al., 2021).

Broadly, a sustained increase in abundance of the phylum Proteobacteria seems a biomarker of dysbiosis in the respiratory tract of cattle, pigs and horses. Whether Proteobacteria are flourishing better when the immune system is stimulated, or whether they actively contribute to the host immune pathology under pathogen infection has still to be explored. As Proteobacteria can tolerate oxidative stress (Million and Raoult, 2018), their expansion is likely linked to the onset of mucosa inflammation following primary infection. Additionally, they encode the metabolic capacity to utilize inflammatory byproducts to survive and prosper under acid and low oxygen conditions (Huffnagle et al., 2017), outcompeting bacteria that lack the metabolic capacity to benefit from inflammation. However, the phylum Proteobacteria, named after the Greek god Proteus, has the largest phylogenetic structure, including 116 validated families of bacteria (Shin et al., 2015). As the name suggests, this phylum presents a large range of morphologies and versatile functions (Shin et al., 2015). Indeed, in cats and dogs, *Pseudomonas* and *Acinetobacter*, microorganisms belonging to the phylum Proteobacteria, probably exert a protective function in the lung of companionship animals **Table 1**). Bacteria in those two genera likely have multiple high-affinity adhesins that mediate binding and biofilm formation preventing the growth of potential pathogens in the lung of cats and dogs (Vientoos-Plotts et al., 2017; Fastrès et al., 2020b). In addition, *Acinetobacter* could play an anti-inflammatory role in the lungs (Fastrès et al., 2020b). Despite arguments regarding beneficial functions of Proteobacteria, a blooming pattern of Proteobacteria following disruption of homeostasis by environmental or host factors can further facilitate inflammation or invasion by exogenous pathogens in mammals.

Yet, the nature of Proteobacteria in the respiratory pathobiome in poultry remains largely unknown. Only Liu et al. (2020), have recently evoked a relationship between the increase of Proteobacteria under seven days of ammonia exposure and respiratory tract diseases in broilers.

COMPLEX RESPIRATORY DISEASE AND COMORBIDITIES: THE MULTIPLE PATHOGEN DISEASE PARADIGM IN A PATHOBIOME CONTEXT

As central finding from respiratory tract microbiota is that most complex airway diseases are caused by pathogens that can be common members of a symbiome in the absence of disease. The well-characterized BRDC is an example of how commensal inhabitants of the respiratory tract (namely *Mannheimia haemolytica, Histophilus somni, Pasteurella multocida, Trueperella pyogenes, Mycoplasma bovis, Arcanobacterium pyogenes, Mycoplasma dispar, Ureaplasma diversum*, and *Mycoplasma bovirhinis)* proliferate in the URT and invade the lung *via* inhalation under specific conditions (Griffin et al., 2010). Likewise, the URT of clinically asymptomatic pigs often harbors pathobionts such *Mycoplasma hyopneumoniae, Haemophilus parasuis, Actinobacillus pleuropneumoniae, Actinobacillus suis, Pasteurella multocida, Bordetella bronchiseptica* and *Streptococcus suis* (Luehrs et al., 2017; Vötsch et al., 2018) that can all prone to disease. In dogs, many potential pathogens involved with CIRDC*, e.g.*, *Mycoplasma cynos*, *Bordetella bronchiseptica* and *Streptococcus* spp. are common members of the respiratory microbiota (Day et al., 2020). Similarly, the URT is also a reservoir of opportunistic pathogens in domestic birds. Potential respiratory pathogens, namely *Avibacterium, Gallibacterium, Mycoplasma*, and *Ornithobacterium*, are found in the URT of turkeys (Kursa et al., 2021).

The next complexity that we can bring in is that the modifications of the airway microbiota resulting from primary virus infections often act as a disturbance for secondary infections (Zeineldin et al., 2019). The one pathogen-one disease paradigm is often insufficient to elucidate many of the respiratory diseases (Vayssier-Taussat et al., 2014; Vayssier-Taussat et al., 2015).

A plethora of examples in swine illustrates the framework in which co-infection occurs. Swine influenza virus enhances the morbidity of *Streptococcus suis* infection by decreasing mucociliary clearance, damaging epithelial cells, and by facilitating its adherence, colonization and invasion in the lungs (Meng et al., 2016). Swine influenza virus also compensates for the lack of suilysin (cytotoxic protein secreted by *Streptococcus suis*) in the adherence and invasion process of suilysin-negative *Streptococcus suis* (Meng et al., 2019). Similarly, a synergism between nasal *Staphylococcus aureus* and pathobionts such as *Pasteurella multocida* and *Klebsiella* spp. have also been reported in pigs (Espinosa-Gongora et al., 2016). Co-occurrence between the porcine reproductive and respiratory syndrome virus (PRRSV), *Haemophilus parasuis* and *Mycoplasma hyorhinis* in pig lungs is repeatedly observed (Jiang et al., 2019). Contrastingly, the virulence of one pathogen may be reduced by co-infection with another, as it has been shown for the bacterium *Escherichia/Shigella* in the respiratory tract of weaning piglets, which inhibited the virulence of *Haemophilus parasuis* or the presence of *Phascolarctobacterium* in the respiratory tract (Mahmmod et al., 2020). On the host side, respiratory pathogens can also modulate

innate and adaptive immune responses (e.g. weakening monocyte activity, suppressing phagocytic capacity of alveolar macrophages, among others) that therefore promote secondary bacterial infection (Zeineldin et al., 2019). For example, PRRSV infection of bone marrow-derived dendric cells regulated the innate immune system by partially acting on the phagocytosis of *S. suis*, but mainly by modulating the development of an exacerbated inflammatory response (Auray et al., 2016). Similarly, *in vitro* co-infection of swine epithelial cells with *S. suis* and swine influenza virus showed an important synergy between the two pathogens regarding the up-regulation of genes coding for inflammatory mediators (Dang et al., 2014). Cells co-infected with PRRSV and porcine circovirus produced more TNF than cells infected with just one of the pathogens (Shi et al., 2010), whereas an exacerbated inflammatory response was described in pigs co-infected with PRRSV and *Mycoplasma hyopneumoniae* (Thanawongnuwech et al., 2004).

Another case in point are the low pathogenic avian influenza viruses (LPAIV) that, during outbreaks, even in the antibiotic era, are coupled to co-infections by pathogens such as *Mycoplasma gallisepticum, Mycoplasma synoviae*, *Ornithobacterium rhinotracheale*, avian pathogenic *Escherichia coli* (APEC) and *Staphylococcus aureus*, which are responsible for a higher mortality rate (Much et al., 2002; Belkasmi et al., 2020) and a marked reduction in egg production of laying hens (Umar et al., 2016). Moreover, it appears as though that concurrent pathogens such as infectious bronchitis virus (IBV), the APEC, the avian pneumovirus and the LPAIV act synergistically or cumulatively to mediate complex infectious processes (Awad et al., 2014; Guabiraba and Schouler, 2015; Patel et al., 2018).

THE GUT-LUNG AXIS DURING RESPIRATORY DISEASES: KEY TO UNDERSTANDING HOLOBIONT FUNCTIONING

The pathophysiology of the complex respiratory diseases in domestic animals seems more complex than previously assumed. It has been recently posited that respiratory comorbidities might be partly modulated by the bidirectional inter-organ communication with the gastrointestinal tract, referred to as the gut-lung axis (Dang and Marsland, 2019). This new field of research is now investigating how gut microbiota modulates the onset of respiratory infections (Niederwerder, 2017) and whether the airway microbiota in turn, influence host epithelial and immune cells to adjust inflammatory responses at distal sites such gut (Budden et al., 2017; Wypych et al., 2019).

The gut of ruminants (Ramayo-Caldas et al., 2019), pigs (Mach et al., 2015; Ramayo-Caldas et al., 2016), horses (Mach et al., 2020; Mach et al., 2021a), companion animals (Alessandri et al., 2020) and chickens (Rychlik, 2020) accommodates a complex community of microorganisms that live in a commensal relationship with their hosts and provide significant contributions to the metabolism and immune responses. It might be hypothesized that in symbiosis, gut microbiota ensures the uptake of microbial metabolites that favorably affects the immune and endocrine pathways involved in respiratory disease and progression, whereas the lungs maintain inflammatory homeostasis in the gut by controlling immune response. Even if the mechanisms bridging gut microbiota with the alterations of respiratory disease outcome are still poorly understood in domestic animals, a growing body of research in swine supports that the crosstalk between the gut and airways microbiome. The gut microbiome composition in growing pigs following an exposure to a non-pathogenic oral microbial inoculum modulated microbial communities and was beneficial upon challenge with *Mycoplasma hyopneumoniae* (Schachtschneider et al., 2013). Similarly, the gut microbiome diversity and composition in piglets determined the respiratory disease progression in pigs after *M. hyopneumoniae* inoculation [Surendran Nair et al. (2019); **Figure 3A**]. Likewise, increased fecal microbiome diversity was associated with improved health outcomes after experimental co-infection with PRRSV and porcine circovirus type 2 (PCV2) (Niederwerder et al., 2016; Ober et al., 2017; Niederwerder et al., 2018).

Several recent studies in domestic birds have also tackled this broader question of the gut-lung axis. Antibiotic treatment in day-old layer chickens resulted in a significant depletion of the gut microbiota, a down-regulation of the type I interferon response and higher shedding of LPAIV of H9N2 subtype in the oropharynx and cloacal section (Yitbarek et al., 2018a). A similar study (Yitbarek et al., 2018b) reported that depletion of the gut microbiota in young chickens using antibiotic treatment increased both oropharyngeal and cloacal levels of the LPAIV of H9N2 subtype and decreased the expression of IFN-α and IFN-β in the gut and respiratory tract (**Figure 3B**). Likewise, depletion of gut microbiota increased the severity of Marek's disease in infected chickens, coupled to an increase in the transcription of IFN-α, IFN-β and IFN-γ in the bursa of *Fabricius* at four days post-infection (Bavananthasivam et al., 2021). In another study developed in chickens, *Lactobacillus salivarius* intake alleviated lung inflammation injury caused by *Mycoplasma gallisepticum* infection and increased host defense against *Escherichia coli* by improved gut microbiota composition (Wang et al., 2021). Antibiotic-treated ducks had increased levels of intestinal highly pathogenic avian influenza virus (HPAIV) of H5N9 subtype associated with a reduced antiviral immune response, but no higher viral titers in the respiratory tract (Figueroa et al., 2020). Finally, the oral administration of *E. coli* O86:B7 expressing high levels of galactose-α-1,3-galactose (α-Gal) in turkeys was found to abrogate anti-α-Gal IgA response in lungs and to protect against experimental *Aspergillus fumigatus* infection (Mateos Hernández et al., 2020). The authors suggested that gut microbiota generates α-Gal-specific antigen-specific regulatory T cells (Tregs) in the gut, which can then migrate to the lungs, promoting disease tolerance which prevents the systemic upregulation of pro-inflammatory cytokines (Mateos Hernández et al., 2020).

As outlined above, knowledge regarding the crosstalk mechanisms by which the airway microbiota affects immune

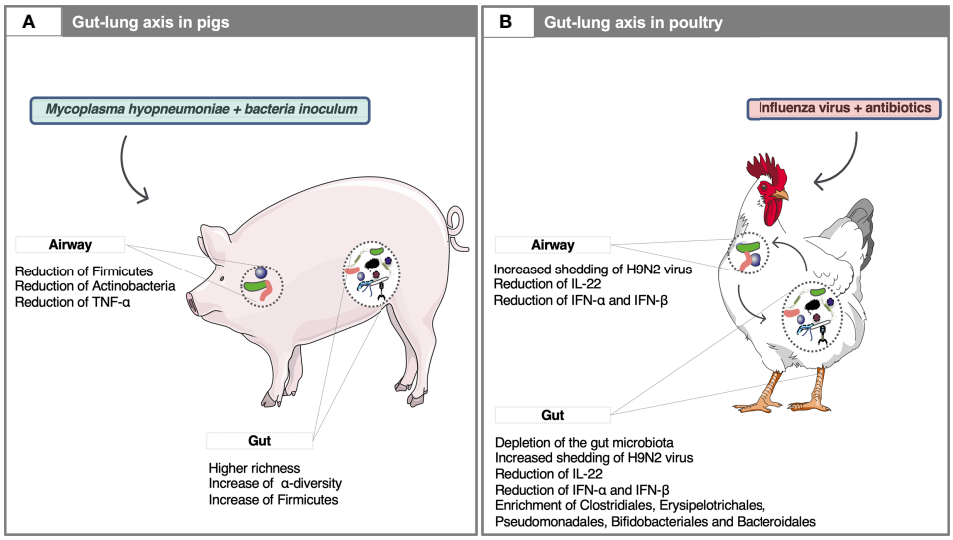

FIGURE 3 | Examples of the gut-lung axis cross-talk in domestic animals. **(A)** The gut microbiota composition affects systemic immune responses and lowers the severity of *M. hyopneumoniae* infection in the respiratory tract of pigs. For example, the administration of oral microbial inoculum increased Firmicutes such as *Roseburia, Barnesiella, Blautia, Dorea* in the gut and reduced the relative abundance of Actinobacteria and Firmicutes phyla in the airways microbiota, as well as the levels of TNF-α in the lungs and their lesions (Schachtschneider et al., 2013). Young pigs with low microbial diversity in the gut showed severe lung lesions on exposure to *M. hyopneumoniae*, whereas the opposite trend was observed in piglets with higher SCFA producing taxa in the gut (*e.g.*, *Ruminococcus*, *Prevotella*, *Ruminiclostridium*, and *Oscillospira*) (Surendran Nair et al., 2019). In addition to having local effects in the gut, SCFAs enter the circulation, modulate bone-marrow hematopoiesis and thereby can promote regulatory or pro-inflammatory responses in the lung (Surendran Nair et al., 2019); **(B)** In H9N2 subtype LPAIV infected chickens, microbiota gut depletion using antibiotics have shown to reduce IFN response, which plays an important role in innate responses to viral infections in the gut and airways and increase the influenza virus shedding from the upper respiratory and gastrointestinal tracts (Yitbarek et al., 2018a). Along with IFNs, treatment of chickens with antibiotics for 12 days resulted in reduced interleukin 22 expression in the respiratory tract after gut microbiota depletion and in enrichment with class Erysipelotrichia, Bacteroidia and with order Clostridiales, Erysipelotrichales, Pseudomonadales, Bifidobacteriales and Bacteroidales (Yitbarek et al., 2018b). Written permission for publication of the chicken drawing in the figure has been taken. The pictures of the pig, bacteria and viruses were downloaded from smart Servier Medical Art https://smart.servier.com without changes. Servier Medical Art by Servier is licensed under a Creative Commons Attribution 3.0 License.

response in the gut is scant (Brown et al., 2017; Mazel-Sanchez et al., 2019). It is postulated that gut microbiota can reach occasionally the lungs through aspiration of vomit or esophageal reflux, therefore exposing pattern-recognition receptors (PRRs) expressed by host cells to peptidoglycans or lipopolysaccharides and stimulating the immune response. Alternatively, these microbe-associated molecular patterns can be transported *via* the circulation together with other gut-derived microbial metabolites known to have immunomodulatory properties such as short-chain fatty acids (SCFA) or indole derivates (Maslowski et al., 2009; Wypych et al., 2019). Avian influenza virus infections have shown to alter the intestinal microbiota in domestic poultry and aquatic birds (Zhao et al., 2018). However, these alterations are likely the outcome of the viral replication in the avian intestinal tract, rather than a cross-talk between respiratory and intestinal mucosal surfaces.

THE ZOONOTIC POTENTIAL OF INFLUENZA A VIRUSES: A CRAWLING THREAT

Because species of veterinary interest are in regular and increasingly close contact with humans, especially in developing countries, understanding the environmental and host determinants that allow pathogens to develop in the respiratory system of livestock and occasionally to be transmitted to and cause diseases in humans is also a relevant research questions today (Peiris et al., 2012). Influenza A viruses, which are commonly found during the onset of complex respiratory diseases in livestock, highlight the problem of devastating zoonotic infections that can arise from veterinary species such as avian and mammalian animal hosts (Kuiken et al., 2005; Mostafa et al., 2018). For instance, in one study involving 125 farrow-to-finish pig hers in France, Influenza A viruses of H1N1 subtype was reportedly found during respiratory disorders (Fablet et al., 2012). Of particular concern is the emergence of the LPAIV of H7Nx subtypes infecting humans, which are frequently reported in commercial poultry, backyards and live bird markets in numerous countries in Europe, Asia and Africa (Abdelwhab et al., 2014; Richard et al., 2014). While H7N2, H7N3 and H7N7 subtypes LPAIV occasionally infect humans causing mild, if any, clinical manifestations (Gao et al., 2013), the emerged H7N9 subtype LPAIV in China causes a high mortality rate in humans (40%) and have pandemic potential (Horman et al., 2018). Additionally, a growing threat to both animal and human health is emerging from the H9N2 subtype LPAIV, endemic in

poultry in many areas of Eurasia and Africa (Peacock et al., 2019).

CONCLUSIONS

The last decade has brought substantial insights into the characterization of the respiratory microbiota in species of veterinary interest. Sterility of the airways has been rejected. The mechanisms behind the colonization of the respiratory system in the different species have started to be explored, as well as the microbial communities occupying the different niches in the airways. Yet nothing is known about the role eukaryotes, archaea and phages play in the respiratory tract in domestic animals.

Collectively, the results obtained in the last years suggest some degree of convergence in the airway respiratory microbiota of mammals. At the phylum level, mammals harbor Firmicutes, Bacteroidetes and Proteobacteria in the upper and lower respiratory system. This is juxtaposed with domestic birds, in which we observed a reduction of Bacteroidetes but increased abundance of Proteobacteria, sustaining the host-specific microbe associations. Although these differences are not yet fully understood, the hypothesis that birds are merely "feathered" mammals with a few specific differences related to flight and production of large yolky eggs is an erroneous assumption. Therefore, not all of the results obtained on one species can be directly translated to the other ones.

The increase in the prevalence of respiratory disorders in farm and companion animals have reached epidemic statistical levels in wealthy countries that generate a greater need to monitor and control their impact on morbidity and mortality. The increasing demands for livestock products coupled to the intensification of marked-oriented systems in many countries, climate change, ecology incursion, as well as movements of people, animals and products increase the risk of complex respiratory disease development worldwide (Kuiken et al., 2005), even if data for regions in South America, Asia, Middle-Est and Africa is scant. The prevention and treatment of respiratory diseases are of paramount importance, not only because they can induce immunosuppression and render animals susceptible to opportunistic infections, but also because it may increase the risk of cross-species transmissions, foodborne and zoonotic diseases.

Disorders in the respiratory tract are compatible with a "ménage à quatre" situation, as they depend on the intricate interactions between the pathogen(s), multiple symbionts of the respiratory tract, the host response and the environmental conditions. There is evidence showing that various environmental factors such as abrupt weaning, antibiotic administration and housing management often disrupt the respiratory microbial ecosystem and increase susceptibility to infections in animal species used for food. Under unfavorable environmental conditions, the symbionts themselves can act as opportunistic pathogens or not provide the same degree of protection. An example hereof is that the respiratory disease complex in bovine, porcine and commercial birds often imply pathobionts. Pigs, ruminants and birds, which frequently switch environments through their intense production lives, are more prone to exhibit respiratory disorders. Modulation of husbandry environment may facilitate the manipulation of the pathobiotic systems. Beyond farm animals, urbanized lifestyle, featuring restricted animal contact and house confinement promotes changes in airway microbiota in both companion animals and horses.

The commensal microbiota composition may affect the pathogen infectivity or the expansion of pathobionts beyond a level of tolerance, either directly *via* the secretion of molecules with antimicrobial activity or indirectly *via* immune-mediated modifications. Of the remaining questions are: which taxa or mixtures of these, if any, make animals more susceptible or resistant to respiratory disorders in each of the domestic species. Thus far, data in mammals have identified members of the *Lactobacillaceae* family as key protective hub taxa in the respiratory tract. Conversely, the expansion in Proteobacteria coupled with a drop in Firmicutes and in diversity has been associated with a pathobiome context in cows, pigs and horses. Proteobacteria seem benign when they are in minor proportion, whereas, under the onset of disease, they trigger inflammatory responses.

The blooming of Proteobacteria could be a potential biomarker for respiratory disease states in mammals and birds, however, trends and nuances are noted. Species within the Proteobacteria phylum have a protective role in immune response against infection or inflammation, as shown in companionship animals. Therefore, one can speculate that bacteria from the phylum Proteobacteria have as yet unidentified functions, and so a better understanding of such functions is key to identifying their symbiotic or their pathological relations with hosts.

To date, re-establishment of respiratory eubiosis after infections and preventive treatment with probiotics has not been demonstrated in domestic animals. Nonetheless, manipulation of gut microbiota in swine and domestic birds has shown to shape their immune response and interfere with the course of respiratory disease. The existence of a gut-lung axis paves the way for new approaches in the management of respiratory disease in domestic animals.

FUTURE PERSPECTIVES

Despite significant efforts towards understanding the link between the pathogen(s), the commensal host-microbiota and the environment, this research field has just started to explore the mechanisms by which pathobiome disrupts respiratory homeostasis in animals. An improved understanding of the spatial distribution and temporal changes from a commensal microbiota to a pathobiome state would provide valuable information (biomarkers) to implement preventive measures or treatments, before observation of clinical signs or symptoms. Both symbiome and pathobiome vary over time and between individuals. Thus, longitudinal studies focusing

on the aforementioned quadrangular interactions are needed to understand the role that the symbiome and pathobiome may have in agent-associated disease outbreaks, as well as the forces at play. These should concentrate on gaining a better understanding of the shifts of the microbiota composition and function in different sections of the respiratory and gastrointestinal systems, and whether the microbiota shifts occur before, and cause a change in respiratory health status, or if they are a consequence of a change in health due to a different host and environmental factors. Expanding shotgun metagenomic sequencing and functional metagenomics (*e.g.*, metatranscriptomics, metaproteomics, metabolomics) of the respiratory tract is required to address this important issue. Advances in sequencing and database annotation are critical for further advances in the field that have the potential to optimize the methods to mitigate diseases, including those related to emerging zoonotic pathogens.

AUTHOR CONTRIBUTIONS

NM designed the structure of this review and wrote the manuscript. EB, LN, and CC have contributed to the reviewing and editing of the manuscript. All authors contributed to the article and approved the submitted version.

FUNDING

This work was supported by financial supports from INRAE.

ACKNOWLEDGMENTS

The authors are very grateful to Estel Blasi, who drew the images.

REFERENCES

Abdelwhab E. M., Veits J., and Mettenleiter T. C. (2014). Prevalence and Control of H7 Avian Influenza Viruses in Birds and Humans. *Epidemiol. Infect.* 142, 896–920. doi: 10.1017/S0950268813003324

Abundo M. E., Ngunjiri J. M., Taylor K. J. M., Ji H., Ghorbani A., Kc M., et al. (2020). Evaluation of Sampling Methods for the Study of Avian Respiratory Microbiota. *Avian Dis.* 64, 277–285. doi: 10.1637/aviandiseases-D-19-00200

Abundo M. E. C., Ngunjiri J. M., Taylor K. J. M., Ji H., Ghorbani A., Mahesh K. C., et al. (2021). Assessment of Two DNA Extraction Kits for Profiling Poultry Respiratory Microbiota From Multiple Sample Types. *PloS One* 16, e0241732. doi: 10.1101/2020.10.21.348508

Alessandri G., Argentini C., Milani C., Turroni F., Cristina Ossiprandi M., van Sinderen D., et al. (2020). Catching a Glimpse of the Bacterial Gut Community of Companion Animals: A Canine and Feline Perspective. *Microb. Biotechnol.* 13, 1708–1732. doi: 10.1111/1751-7915.13656

Amat S., Holman D. B., Timsit E., Schwinghamer T., and Alexander T. W. (2019). Evaluation of the Nasopharyngeal Microbiota in Beef Cattle Transported to a Feedlot, With a Focus on Lactic Acid-Producing Bacteria. *Front. Microbiol.* 10, 1988–2003. doi: 10.3389/fmicb.2019.01988

Amat S., Subramanian S., Timsit E., and Alexander T. W. (2017). Probiotic Bacteria Inhibit the Bovine Respiratory Pathogen Mannheimia Haemolytica Serotype 1 In Vitro. *Lett. Appl. Microbiol.* 64, 343–349. doi: 10.1111/lam.12723

Auray G., Lachance C., Wang Y., Gagnon C. A., Segura M., and Gottschalk M. (2016). Transcriptional Analysis of PRRSV-infected Porcine Dendritic Cell Response to Streptococcus Suis Infection Reveals Up-Regulation of Inflammatory-Related Genes Expression. *PloS One* 11, e0156019. doi: 10.1371/journal.pone.0156019

Awad F., Chhabra R., Baylis M., and Ganapathy K. (2014). An Overview of Infectious Bronchitis Virus in Chickens. *Worlds Poult. Sci. J.* 70, 375–384. doi: 10.1017/S0043933914000385

Bass D., Stentiford G. D., Wang H. C., Koskella B., and Tyler C. R. (2019). The Pathobiome in Animal and Plant Diseases. *Trends Ecol. Evol.* 34, 996–1008. doi: 10.1016/j.tree.2019.07.012

Bavananthasivam J., Astill J., Matsuyama-Kato A., Taha-Abdelaziz K., Shojadoost B., and Sharif S. (2021). Gut Microbiota is Associated With Protection Against Marek's Disease Virus Infection in Chickens. *Virology* 553, 122–130. doi: 10.1016/j.virol.2020.10.011

Belkasmi S. F. Z., Fellahi S., Touzani C. D., Faraji F. Z., Maaroufi I., Delverdier M., et al. (2020). Co-Infections of Chickens With Avian Influenza Virus H9N2 and Moroccan Italy 02 Infectious Bronchitis Virus: Effect on Pathogenesis and Protection Conferred by Different Vaccination Programmes. *Avian Pathol.* 49, 21–28. doi: 10.1080/03079457.2019.1656328

Bernardo-Cravo A. P., Schmeller D. S., Chatzinotas A., Vredenburg V. T., and Loyau A. (2020). Environmental Factors and Host Microbiomes Shape Host–Pathogen Dynamics. *Trends Parasitol.* 36, 616–633. doi: 10.1016/j.pt.2020.04.010

Bernhard W., Haslam P. L., and Floros J. (2004). From Birds to Humans: New Concepts on Airways Relative to Alveolar Surfactant. *Am. J. Respir. Cell Mol. Biol.* 30, 6–11. doi: 10.1165/rcmb.2003-0158TR

Beste K. J., Lawhon S. D., Chamoun-Emanuelli A. M., Duff A. H., Coleman M. C., Griffin C. E., et al. (2019). Culture-Independent and Dependent Evaluation of the Equine Paranasal Sinus Microbiota in Health and Disease. *Equine Vet. J.* 0, 1–9. doi: 10.1111/evj.13168

Blakebrough-Hall C., McMeniman J. P., and González L. A. (2020). An Evaluation of the Economic Effects of Bovine Respiratory Disease on Animal Performance, Carcass Traits, and Economic Outcomes in Feedlot Cattle Defined Using Four BRD Diagnosis Methods. *J. Anim. Sci.* 98, skaa005. doi: 10.1093/jas/skaa005

Bond S. L., Timsit E., Workentine M., Alexander T., and Léguillette R. (2017). Upper and Lower Respiratory Tract Microbiota in Horses: Bacterial Communities Associated With Health and Mild Asthma (Inflammatory Airway Disease) and Effects of Dexamethasone. *BMC Microbiol.* 17, 1–11. doi: 10.1186/s12866-017-1092-5

Bond S. L., Workentine M., Hundt J., Gilkerson J. R., and Léguillette R. (2020). Effects of Nebulized Dexamethasone on the Respiratory Microbiota and Mycobiota and Relative Equine herpesvirus-1, 2, 4, 5 in an Equine Model of Asthma. *J. Vet. Intern. Med.* 34, 307–321. doi: 10.1111/jvim.15671

Bradley P. H., and Pollard K. S. (2017). Proteobacteria Explain Significant Functional Variability in the Human Gut Microbiome. *Microbiome.* 5 (1) 36–59. doi: 10.1186/s40168-017-0244-z

Brown R. E., Brain J. D., and Wang N. (1997). The Avian Respiratory System:A Unique Model for Studies of Respiratory Toxicosis and for Monitoring Air Quality. *Environ. Heal.* 105, 188–200. doi: 10.1289/ehp.97105188

Brown R. L., Sequeira R. P., and Clarke T. B. (2017). The Microbiota Protects Against Respiratory Infection Via GM-CSF Signaling. *Nat. Commun.* 8, 1512–1523. doi: 10.1038/s41467-017-01803-x

Brugman S., Ikeda-Ohtsubo W., Braber S., Folkerts G., Pieterse C. M. J., and Bakker P. A. H. M. (2018). A Comparative Review on Microbiota Manipulation: Lessons From Fish, Plants, Livestock, and Human Research. *Front. Nutr.* 5, 80. doi: 10.3389/fnut.2018.00080

Budden K. F., Gellatly S. L., Wood D. L. A., Cooper M. A., Morrison M., Hugenholtz P., et al. (2017). Emerging Pathogenic Links Between Microbiota and the Gut-Lung Axis. *Nat. Rev. Microbiol.* 15, 55. doi: 10.1038/nrmicro.2016.142

Budden K. F., Shukla S. D., Rehman S. F., Bowerman K. L., Keely S., Hugenholtz P., et al. (2019). Functional Effects of the Microbiota in Chronic Respiratory Disease. *Lancet Respir. Med.* 7, 907–920. doi: 10.1016/S2213-2600(18)30510-1

Cáliz J., Triadó-Margarit X., Camarero L., and Casamayor E. O. (2018). A Long-Term Survey Unveils Strong Seasonal Patterns in the Airborne Microbiome Coupled to General and Regional Atmospheric Circulations. *Proc. Natl. Acad. Sci. U. S. A.* 115, 12229–12234. doi: 10.1073/pnas.1812826115

Collie D., Glendinning L., Govan J., Wright S., Thornton E., Tennant P., et al. (2015). Lung Microbiota Changes Associated With Chronic Pseudomonas Aeruginosa Lung Infection and the Impact of Intravenous Colistimethate Sodium. *PloS One* 82, 3225–3232. doi: 10.1371/journal.pone.0142097

Correa-Fiz F., Fraile L., and Aragon V. (2016). Piglet Nasal Microbiota at Weaning may Influence the Development of Glässer's Disease During the Rearing Period. *BMC Genomics* 17, 404–418. doi: 10.1186/s12864-016-2700-8

Correa-Fiz F., Gonçalves dos Santos J. M., Illas F., and Aragon V. (2019). Antimicrobial Removal on Piglets Promotes Health and Higher Bacterial Diversity in the Nasal Microbiota. *Sci. Rep.* 9, 6545–6554. doi: 10.1038/s41598-019-43022-y

Cortes L. C. P., LeVeque R. M., Funk J. A., Marsh T. L., and Mulks M. H. (2018). Development of the Tonsil Microbiome in Pigs and Effects of Stress on the Microbiome. *Front. Vet. Sci.* 5, 220. doi: 10.3389/fvets.2018.00220

Dang Y., Lachance C., Wang Y., Gagnon C. A., Savard C., Segura M., et al. (2014). Transcriptional Approach to Study Porcine Tracheal Epithelial Cells Individually or Dually Infected With Swine Influenza Virus and Streptococcus Suis. *BMC Vet. Res.* 10, 86. doi: 10.1186/1746-6148-10-86

Dang A. T., and Marsland B. J. (2019). Microbes, Metabolites, and the Gut–Lung Axis. *Mucosal Immunol.* 12, 843–850. doi: 10.1038/s41385-019-0160-6

Day M. J., Carey S., Clercx C., Kohn B., MarsilIo F., Thiry E., et al. (2020). Aetiology of Canine Infectious Respiratory Disease Complex and Prevalence of its Pathogens in Europe. *J. Comp. Pathol.* 176, 86–108. doi: 10.1016/j.jcpa.2020.02.005

Dorn E. S., Tress B., Suchodolski J. S., Nisar T., Ravindran P., Weber K., et al. (2017). Bacterial Microbiome in the Nose of Healthy Cats and in Cats With Nasal Disease. *PloS One* 12, 1–23. doi: 10.1371/journal.pone.0180299

Ericsson A. C., Personett A. R., Grobman M. E., Rindt H., and Reinero C. R. (2016). Composition and Predicted Metabolic Capacity of Upper and Lower Airway Microbiota of Healthy Dogs in Relation to the Fecal Microbiota. *PloS One* 11, e0154646. doi: 10.1371/journal.pone.0154646

Ericsson A. C., Personett A. R., Rindt H., Grobman M. E., and Reinero C. R. (2020). Respiratory Dysbiosis and Population-Wide Temporal Dynamics in Canine Chronic Bronchitis and non-Inflammatory Respiratory Disease. *PloS One* 15, 1–18. doi: 10.1371/journal.pone.0228085

Espinosa-Gongora C., Larsen N., Schønning K., Fredholm M., and Guardabassi L. (2016). Differential Analysis of the Nasal Microbiome of Pig Carriers or non-Carriers of Staphylococcus Aureus. *PloS One* 11, e0160331. doi: 10.1371/journal.pone.0160331

Fablet C., Marois-Créhan C., Simon G., Grasland B., Jestin A., Kobisch M., et al. (2012). Infectious Agents Associated With Respiratory Diseases in 125 Farrow-to-Finish Pig Herds: A Cross-Sectional Study. *Vet. Microbiol.* 157, 152–163. doi: 10.1016/j.vetmic.2011.12.015

Fastrès A., Canonne M. A., Taminiau B., Billen F., Garigliany M. M., Daube G., et al. (2020a). Analysis of the Lung Microbiota in Dogs With Bordetella Bronchiseptica Infection and Correlation With Culture and Quantitative Polymerase Chain Reaction. *Vet. Res.* 51, 46. doi: 10.1186/s13567-020-00769-x

Fastrès A., Taminiau B., Vangrinsven E., Tutunaru A. C., Moyse E., Farnir F., et al. (2019). Effect of an Antimicrobial Drug on Lung Microbiota in Healthy Dogs. *Heliyon* 5, e02802. doi: 10.1016/j.heliyon.2019.e02802

Fastrès A., Vangrinsven E., Taminiau B., Tutunaru A.-C., Jabri H., Daube G., et al. (2020b). Assessment of Lung Microbiota in Healthy Dogs: Influence of the Type of Breed, Living Conditions and Canine Idiopahtic Pulmonary Fibrosis. *BMC Microbiol.* 20, 84. doi: 10.1186/s12866-020-01784-w

Figueroa T., Bessière P., Coggon A., Bouwman K. M., van der Woude R., Delverdier M., et al. (2020). Themicrobiota Contributes to the Control of Highly Pathogenic H5N9 Influenza Virus Replication in Ducks. *J. Virol.* 94, e00289–e00220. doi: 10.1128/jvi.00289-20

Fillion-Bertrand G., Dickson R. P., Boivin R., Lavoie J. P., Huffnagle G. B., and Leclere M. (2019). Lung Microbiome is Influenced by the Environment and Asthmatic Status in an Equine Model of Asthma. *Am. J. Respir. Cell Mol. Biol.* 60, 189–197. doi: 10.1165/rcmb.2017-0228OC

Gaeta N. C., Lima S. F., Teixeira A. G., Ganda E. K., Oikonomou G., Gregory L., et al. (2017). Deciphering Upper Respiratory Tract Microbiota Complexity in Healthy Calves and Calves That Develop Respiratory Disease Using Shotgun Metagenomics. *J. Dairy Sci.* 100, 1445–1458. doi: 10.3168/jds.2016-11522

Gao R., Cao B., Hu Y., Feng Z., Wang D., Hu W., et al. (2013). Human Infection With a Novel Avian-Origin Influenza A (H7n9) Virus. *N. Engl. J. Med.* 368, 1888–1897. doi: 10.1056/nejmoa1304459

Glendinning L., Collie D., Wright S., Rutherford K. M. D., and McLachlan G. (2017a). Comparing Microbiotas in the Upper Aerodigestive and Lower Respiratory Tracts of Lambs. *Microbiome* 5, 145. doi: 10.1186/s40168-017-0364-5

Glendinning L., McLachlan G., and Vervelde L. (2017b). Age-Related Differences in the Respiratory Microbiota of Chickens. *PloS One* 12, e0188455. doi: 10.1371/journal.pone.0188455

Glendinning L., Wright S., Pollock J., Tennant P., Collie D., and McLachlan G. (2016). Variability of the Sheep Lung Microbiota. *Appl. Environ. Microbiol.* 82, 3225–3238. doi: 10.1128/AEM.00540-16

Gomez D. E., Arroyo L. G., Lillie B., and Scott Weese J. (2021). Nasal Bacterial Microbiota During an Outbreak of Equine Herpesvirus 1 at a Farm in Southern Ontario. *Can. J. Vet. Res.* 85, 3–11.

Griffin D., Chengappa M. M., Kuszak J., and McVey D. S. (2010). Bacterial Pathogens of the Bovine Respiratory Disease Complex. *Vet. Clin. North Am. - Food Anim. Pract.* 26, 381–394. doi: 10.1016/j.cvfa.2010.04.004

Guabiraba R., and Schouler C. (2015). Avian Colibacillosis: Still Many Black Holes. *FEMS Microbiol. Lett.* 362, 1–8. doi: 10.1093/femsle/fnv118

Hall J. A., Isaiah A., Estill C. T., Pirelli G. J., and Suchodolski J. S. (2017). Weaned Beef Calves Fed Selenium-Biofortified Alfalfa Hay Have an Enriched Nasal Microbiota Compared With Healthy Controls. *PloS One* 12, e0179217. doi: 10.1371/journal.pone.0179215

Hansen M. S., Pors S. E., Jensen H. E., Bille-Hansen V., Bisgaard M., Flachs E. M., et al. (2010). An Investigation of the Pathology and Pathogens Associated With Porcine Respiratory Disease Complex in Denmark. *J. Comp. Pathol.* 143, 120–131. doi: 10.1016/j.jcpa.2010.01.012

Harms P. A., Halbur P. G., and Sorden S. D. (2002). Three Cases of Porcine Respiratory Disease Complex Associated With Porcine Circovirus Type 2 Infection. *J. Swine Heal. Prod.* 10, 27–30.

Heidari M., Hamir A., Cutlip R. C., and Brogden K. A. (2002). Antimicrobial Anionic Peptide Binds In Vivo to Mannheimia (Pasteurella) Haemolytica Attached to Ovine Alveolar Epithelium. *Int. J. Antimicrob. Agents* 20, 69–72. doi: 10.1016/S0924-8579(02)00048-1

Hilton W. M. (2014). BRD in 2014: Where Have We Been, Where are We Now, and Where do We Want to Go? *Anim. Heal. Res. Rev.* 151, 120–122. doi: 10.1017/S1466252314000115

Holman D. B., McAllister T. A., Topp E., Wright A. D. G., and Alexander T. W. (2015). The Nasopharyngeal Microbiota of Feedlot Cattle That Develop Bovine Respiratory Disease. *Vet. Microbiol.* 180, 90–95. doi: 10.1016/j.vetmic.2015.07.031

Holman D. B., Timsit E., Amat S., Abbott D. W., Buret A. G., and Alexander T. W. (2017). The Nasopharyngeal Microbiota of Beef Cattle Before and After Transport to a Feedlot. *BMC Microbiol.* 17, 1–12. doi: 10.1186/s12866-017-0978-6

Holman D. B., Timsit E., Booker C. W., and Alexander T. W. (2018). Injectable Antimicrobials in Commercial Feedlot Cattle and Their Effect on the Nasopharyngeal Microbiota and Antimicrobial Resistance. *Vet. Microbiol.* 214, 140–147. doi: 10.1016/j.vetmic.2017.12.015

Holman D. B., Yang W., and Alexander T. W. (2019). Antibiotic Treatment in Feedlot Cattle: A Longitudinal Study of the Effect of Oxytetracycline and Tulathromycin on the Fecal and Nasopharyngeal Microbiota. *Microbiome* 7, 1–14. doi: 10.1186/s40168-019-0696-4

Holt H. R., Alarcon P., Velasova M., Pfeiffer D. U., and Wieland B. (2011). Bpex Pig Health Scheme: A Useful Monitoring System for Respiratory Disease Control in Pig Farms? *BMC Vet. Res.* 7, 82. doi: 10.1186/1746-6148-7-82

Horman W. S. J., Nguyen T. H. O., Kedzierska K., Bean A. G. D., and Layton D. S. (2018). The Drivers of Pathology in Zoonotic Avian Influenza: The Interplay Between Host and Pathogen. *Front. Immunol.* 9, 1812. doi: 10.3389/fimmu.2018.01812

Huang T., Zhang M., Tong X., Chen J., Yan G., Fang S., et al. (2019). Microbial Communities in Swine Lungs and Their Association With Lung Lesions. *Microb. Biotechnol.* 12, 289–304. doi: 10.1111/1751-7915.13353

Huffnagle G. B., Dickson R. P., and Lukacs N. W. (2017). The Respiratory Tract Microbiome and Lung Inflammation: A Two-Way Street. *Mucosal Immunol.* 10, 299. doi: 10.1038/mi.2016.108

Jakobsen A. M., Bahl M. I., Buschhardt T., Hansen T. B., Al-Soud W. A., Brejnrod A. D., et al. (2019). Bacterial Community Analysis for Investigating Bacterial Transfer From Tonsils to the Pig Carcass. *Int. J. Food Microbiol.* 295, 8–18. doi: 10.1016/j.ijfoodmicro.2019.02.003

Jiang N., Liu H., Wang P., Huang J., Han H., and Wang Q. (2019). Illumina MiSeq Sequencing Investigation of Microbiota in Bronchoalveolar Lavage Fluid and

Cecum of the Swine Infected With PRRSV. *Curr. Microbiol.* 76, 222–230. doi: 10.1007/s00284-018-1613-y

Johnson T. J., Youmans B. P., Noll S., Cardona C., Evans N. P., Peter Karnezos T., et al. (2018). A Consistent and Predictable Commercial Broiler Chicken Bacterial Microbiota in Antibiotic-Free Production Displays Strong Correlations With Performance. *Appl. Environ. Microbiol.* 84, 1–18. doi: 10.1128/AEM.00362-18

Kauter A., Epping L., Semmler T., Antao E.-M., Kannapin D., Stoeckle S. D., et al. (2019). The Gut Microbiome of Horses: Current Research on Equine Enteral Microbiota and Future Perspectives. *Anim. Microbiome* 1, 1–15. doi: 10.1186/s42523-019-0013-3

Kers J. G., Velkers F. C., Fischer E. A. J., Hermes G. D. A., Stegeman J. A., and Smidt H. (2018). Host and Environmental Factors Affecting the Intestinal Microbiota in Chickens. *Front. Microbiol.* 9, 235. doi: 10.3389/fmicb.2018.00235

Klima C. L., Holman D. B., Ralston B. J., Stanford K., Zaheer R., Alexander T. W., et al. (2019). Lower Respiratory Tract Microbiome and Resistome of Bovine Respiratory Disease Mortalities. *Microb. Ecol.* 78, 446–456. doi: 10.1007/s00248-019-01361-3

Kubasova T., Kollarcikova M., Crhanova M., Karasova D., Cejkova D., Sebkova A., et al. (2019). Contact With Adult Hen Affects Development of Caecal Microbiota in Newly Hatched Chicks. *PloS One* 14, e0212446. doi: 10.1371/journal.pone.0212446

Kuiken T., Leighton F. A., Fouchier R. A. M., LeDuc J. W., Peiris J. S. M., Schudel A., et al. (2005). Pathogen Surveillance in Animals. *Science* 309, 1680–1681. doi: 10.1126/science.1113310

Kursa O., Tomczyk G., Sawicka-Durkalec A., Giza A., and Słomiany-Szwarc M. (2021). Bacterial Communities of the Upper Respiratory Tract of Turkeys. *Sci. Rep.* 11, 1–11. doi: 10.1038/s41598-021-81984-0

Lehtimäki J., Sinkko H., Hielm-Björkman A., Salmela E., Tiira K., Laatikainen T., et al. (2018). Skin Microbiota and Allergic Symptoms Associate With Exposure to Environmental Microbes. *Proc. Natl. Acad. Sci. U. S. A.* 115, 4897–4902. doi: 10.1073/pnas.1719785115

Lima S. F., de Souza Bicalho M. L., and Bicalho R. C. (2019). The Bos Taurus Maternal Microbiome: Role in Determining the Progeny Early-Life Upper Respiratory Tract Microbiome and Health. *PloS One* 14, e0208014. doi: 10.1371/journal.pone.0208014

Li N., Ma W. T., Pang M., Fan Q. L., and Hua J. L. (2019). The Commensal Microbiota and Viral Infection: A Comprehensive Review. *Front. Immunol.* 10, 1551–1567. doi: 10.3389/fimmu.2019.01551

Lima S. F., Teixeira A. G. V., Higgins C. H., Lima F. S., and Bicalho R. C. (2016). The Upper Respiratory Tract Microbiome and its Potential Role in Bovine Respiratory Disease and Otitis Media. *Sci. Rep.* 6, 1–12. doi: 10.1038/srep29050

Liu Q. X., Zhou Y., Li X. M., Ma D. D., Xing S., Feng J. H., et al. (2020). Ammonia Induce Lung Tissue Injury in Broilers by Activating NLRP3 Inflammasome Via Escherichia/Shigella. *Poult. Sci.* 99, 3402–3410. doi: 10.1016/j.psj.2020.03.019

Li Z., Wang X., Di D., Pan R., Gao Y., Xiao C., et al. (2021). Comparative Analysis of the Pulmonary Microbiome in Healthy and Diseased Pigs. *Mol. Genet. Genomics* 296, 21–31. doi: 10.1007/s00438-020-01722-5

Lovell P. V., Wirthlin M., Wilhelm L., Minx P., Lazar N. H., Carbone L., et al. (2014). Conserved Syntenic Clusters of Protein Coding Genes are Missing in Birds. *Genome Biol.* 15, 565. doi: 10.1186/s13059-014-0565-1

Lowe B., Marsh T., Isaacs-Cosgrove N., Kirkwood R., Kiupel M., and Mulks M. (2012). Defining the "Core Microbiome" of the Microbial Communities in the Tonsils of Healthy Pigs. *BMC Microbiol.* 12, 20. doi: 10.1186/1471-2180-12-20

Luehrs A., Siegenthaler S., Grützner N., Kuhnert P., and Nathues H. (2017). Occurrence of Mycoplasma Hyorhinis Infections in Fattening Pigs and Association With Clinical Signs and Pathological Lesions of Enzootic Pneumonia. *Vet. Microbiol.* 203, 1–5. doi: 10.1016/j.vetmic.2017.02.001

Mach N., Berri M., Estellé J., Levenez F., Lemonnier G., Denis C., et al. (2015). Early-Life Establishment of the Swine Gut Microbiome and Impact on Host Phenotypes. *Environ. Microbiol. Rep.* 7, 554–569. doi: 10.1111/1758-2229.12285

Mach N., Foury A., Kittelmann S., Reigner F., Moroldo M., Ballester M., et al. (2017). The Effects of Weaning Methods on Gut Microbiota Composition and Horse Physiology. *Front. Physiol.* 8, 535. doi: 10.3389/fphys.2017.00535

Mach N., Lansade L., Bars-Cortina D., Dhorne-Pollet S., Foury A., Moisan M.-P., et al. (2021a). Gut Microbiota Resilience in Horse Athletes Following Holidays Out to Pasture. *Sci. Rep.* 11, 5007–5023. doi: 10.1038/s41598-021-84497-y

Mach N., Moroldo M., Rau A., Lecardonnel J., Le Moyec L., Robert C., et al. (2021b). Understanding the Holobiont: Crosstalk Between Gut Microbiota and Mitochondria During Long Exercise in Horse. *Front. Mol. Biosci.* 8, 656204–656221 doi: 10.3389/fmolb.2021.656204

Mach N., Ruet A., Clark A., Bars-Cortina D., Ramayo-Caldas Y., Crisci E., et al. (2020). Priming for Welfare: Gut Microbiota is Associated With Equitation Conditions and Behavior in Horse Athletes. *Sci. Rep.* 10, 8311–8330. doi: 10.1038/s41598-020-65444-9

Mahmmod Y. S., Correa-Fiz F., and Aragon V. (2020). Variations in Association of Nasal Microbiota With Virulent and non-Virulent Strains of Glaesserella (Haemophilus) Parasuis in Weaning Piglets. *Vet. Res.* 51, 7. doi: 10.1186/s13567-020-0738-8

Maina J. N., King A. S., and Settle G. (1989). An Allomet- Ric Study of Pulmonary Morphometric Parameters in Birds, With Mammalian Comparisons. *Philos. Trans. R. Soc B Biol. Sci.* 326, 1–57. doi: 10.1098/rstb.1989.0104

Man W. H., De Steenhuijsen Piters W. A. A., and Bogaert D. (2017). The Microbiota of the Respiratory Tract: Gatekeeper to Respiratory Health. *Nat. Rev. Microbiol.* 15, 259–270. doi: 10.1038/nrmicro.2017.14

Maslowski K. M., Vieira A. T., Ng A., Kranich J., Sierro F., Yu D., et al. (2009). Regulation of Inflammatory Responses by Gut Microbiota and Chemoattractant Receptor GPR43. *Nature* 461, 1282–1286. doi: 10.1038/nature08530

Mateos Hernández L., Risco-Castillo V., Torres-Maravilla E., Bermúdez-Humarán L., Rakotobe S., GAlon C., et al. (2020). Gut Microbiota Abrogates Anti-α-Gal IgA Response in Lungs and Protects Against Experimental Aspergillus Infection in Poultry. *Vaccines* 8, 285. doi: 10.3390/vaccines8020285

Maynou G., Chester-Jones H., Bach A., and Terré M. (2019). Feeding Pasteurized Waste Milk to Preweaned Dairy Calves Changes Fecal and Upper Respiratory Tract Microbiota. *Front. Vet. Sci.* 6, 159. doi: 10.3389/fvets.2019.00159

Mazel-Sanchez B., Yildiz S., and Schmolke M. (2019). Ménage À Trois: Virus, Host, and Microbiota in Experimental Infection Models. *Trends Microbiol.* 27, 440–452. doi: 10.1016/j.tim.2018.12.004

McMullen C., Alexander T. W., Léguillette R., Workentine M., and Timsit E. (2020). Topography of the Respiratory Tract Bacterial Microbiota in Cattle. *Microbiome* 8, 91. doi: 10.1186/s40168-020-00869-y

McMullen C., Orsel K., Alexander T. W., van der Meer F., Plastow G., and Timsit E. (2018). Evolution of the Nasopharyngeal Bacterial Microbiota of Beef Calves From Spring Processing to 40 Days After Feedlot Arrival. *Vet. Microbiol.* 225, 139–148. doi: 10.1016/j.vetmic.2018.09.019

McMullen C., Orsel K., Alexander T. W., van der Meer F., Plastow G., and Timsit E. (2019). Comparison of the Nasopharyngeal Bacterial Microbiota of Beef Calves Raised Without the Use of Antimicrobials Between Healthy Calves and Those Diagnosed With Bovine Respiratory Disease. *Vet. Microbiol.* 231, 56–62. doi: 10.1016/j.vetmic.2019.02.030

Megahed A., Zeineldin M., Evans K., Maradiaga N., Blair B., Aldridge B., et al. (2019). Impacts of Environmental Complexity on Respiratory and Gut Microbiome Community Structure and Diversity in Growing Pigs. *Sci. Rep.* 9, 13773. doi: 10.1038/s41598-019-50187-z

Meng F., Tong J., Vötsch D., Peng J. Y., Cai X., Willenborg M., et al. (2019). Viral Coinfection Replaces Effects of Suilysin on Streptococcus Suis Adherence to and Invasion of Respiratory Epithelial Cells Grown Under Air-Liquid Interface Conditions. *Infect. Immun.* 87, 1–12. doi: 10.1128/IAI.00350-19

Meng F., Wu N. H., Seitz M., Herrler G., and Valentin-Weigand P. (2016). Efficient Suilysin-Mediated Invasion and Apoptosis in Porcine Respiratory Epithelial Cells After Streptococcal Infection Under Air-Liquid Interface Conditions. *Sci. Rep.* 6, 26748. doi: 10.1038/srep26748

Michiels A., Piepers S., Ulens T., Van Ransbeeck N., Del Pozo Sacristán R., Sierens A., et al. (2015). Impact of Particulate Matter and Ammonia on Average Daily Weight Gain, Mortality and Lung Lesions in Pigs. *Prev. Vet. Med.* 121, 99–107. doi: 10.1016/j.prevetmed.2015.06.011

Million M., and Raoult D. (2018). Linking Gut Redox to Human Microbiome. *Hum. Microbiome J.* 10, 27–32. doi: 10.1016/j.humic.2018.07.002

Mitchell J. A., Cardwell J. M., Leach H., Walker C. A., Le Poder S., Decaro N., et al. (2017). European Surveillance of Emerging Pathogens Associated With Canine Infectious Respiratory Disease. *Vet. Microbiol.* 212, 31–38. doi: 10.1016/j.vetmic.2017.10.019

Mostafa A., Abdelwhab E. M., Mettenleiter T. C., and Pleschka S. (2018). Zoonotic Potential of Influenza A Viruses: A Comprehensive Overview. *Viruses* 10, 1–38. doi: 10.3390/v10090497

Mou K. T., Allen H. K., Alt D. P., Trachsel J., Hau S. J., Coetzee J. F., et al. (2019). Shifts in the Nasal Microbiota of Swine in Response to Different Dosing Regimens of Oxytetracycline Administration. *Vet. Microbiol.* 237, 108386. doi: 10.1016/j.vetmic.2019.108386

Much P., Winner F., Stipkovits L., Rosengarten R., and Citti C. (2002). Mycoplasma Gallisepticum: Influence of Cell Invasiveness on the Outcome of Experimental Infection in Chickens. *FEMS Immunol. Med. Microbiol.* 34, 181–186. doi: 10.1016/S0928-8244(02)00378-4

Mulholland K. A., Robinson M. G., Keeler S. J., Johnson T. J., Weber B. W., and Keeler C. L. (2021). Metagenomic Analysis of the Respiratory Microbiome of a Broiler Flock From Hatching to Processing. *Microorganisms* 9, 1–18. doi: 10.3390/microorganisms9040721

Ngunjiri J. M., Taylor K. J. M., Abundo M. C., Jang H., Elaish M., Mahesh K. C., et al. (2019). Farm Stage, Bird Age, and Body Site Dominantly Affect the Quantity, Taxonomic Composition, and Dynamics of Respiratory and Gut Microbiota of Commercial Layer Chickens. *Appl. Environ. Microbiol.* 85, 1–17. doi: 10.1128/AEM.03137-18

Nicola I., Cerutti F., Grego E., Bertone I., Gianella P., D'Angelo A., et al. (2017). Characterization of the Upper and Lower Respiratory Tract Microbiota in Piedmontese Calves. *Microbiome* 5, 152. doi: 10.1186/s40168-017-0372-5

Niederwerder M. C. (2017). Role of the Microbiome in Swine Respiratory Disease. *Vet. Microbiol.* 209, 97–106. doi: 10.1016/j.vetmic.2017.02.017

Niederwerder M. C., Constance L. A., Rowland R. R. R., Abbas W., Fernando S. C., Potter M. L., et al. (2018). Fecal Microbiota Transplantation is Associated With Reduced Morbidity and Mortality in Porcine Circovirus Associated Disease. *Front. Microbiol.* 9, 1631–1649. doi: 10.3389/fmicb.2018.01631

Niederwerder M. C., Jaing C. J., Thissen J. B., Cino-Ozuna A. G., McLoughlin K. S., and Rowland R. R. R. (2016). Microbiome Associations in Pigs With the Best and Worst Clinical Outcomes Following Co-Infection With Porcine Reproductive and Respiratory Syndrome Virus (PRRSV) and Porcine Circovirus Type 2 (PCV2). *Vet. Microbiol.* 188, 1–11. doi: 10.1016/j.vetmic.2016.03.008

Nochi T., Jansen C. A., Toyomizu M., and van Eden W. (2018). The Well-Developed Mucosal Immune Systems of Birds and Mammalsallow for Similar Approaches of Mucosal Vaccination in Both Types of Animals. *Front. Nutr.* 5, 60. doi: 10.3389/fnut.2018.00060

Ober R. A., Thissen J. B., Jaing C. J., Cino-Ozuna A. G., Rowland R. R. R., and Niederwerder M. C. (2017). Increased Microbiome Diversity at the Time of Infection is Associated With Improved Growth Rates of Pigs After Co-Infection With Porcine Reproductive and Respiratory Syndrome Virus (PRRSV) and Porcine Circovirus Type 2 (PCV2). *Vet. Microbiol.* 208, 203–211. doi: 10.1016/j.vetmic.2017.06.023

Oladunni F. S., Horohov D. W., and Chambers T. M. (2019). Ehv-1: A Constant Threat to the Horse Industry. *Front. Microbiol.* 10, 2668. doi: 10.3389/fmicb.2019.02668

Patel J. G., Patel B. J., Patel S. S., Raval S. H., Parmar R. S., Joshi D. V., et al. (2018). Metagenomic of Clinically Diseased and Healthy Broiler Affected With Respiratory Disease Complex. *Data Br.* 19, 82–85. doi: 10.1016/j.dib.2018.05.010

Peacock T. P., James J., Sealy J. E., and Iqbal M. (2019). A Global Perspective on h9n2 Avian Influenza Virus. *Viruses* 11, 1–28. doi: 10.3390/v11070620

Peiris J. S. M., Poon L. L. M., and Guan Y. (2012). Surveillance of Animal Influenza for Pandemic Preparedness. *Science* 335, 1173–1174. doi: 10.1126/science.1219936

Pena Cortes L. C., Leveque R. M., Funk J., Marsh T. L., and Mulks M. H. (2018). Development of the Tonsillar Microbiome in Pigs From Newborn Through Weaning. *BMC Microbiol.* 18, 35. doi: 10.1186/s12866-018-1176-x

Pirolo M., Espinosa-Gongora C., Bogaert D., and Guardabassi L. (2021). The Porcine Respiratory Microbiome: Recent Insights and Future Challenges. *Anim. Microbiome* 3, 9. doi: 10.1186/s42523-020-00070-4

Qin S., Ruan W., Yue H., Tang C., Zhou K., and Zhang B. (2018). Viral Communities Associated With Porcine Respiratory Disease Complex in Intensive Commercial Farms in Sichuan Province, China. *Sci. Rep.* 8, 13341. doi: 10.1038/s41598-018-31554-8

Raabis S. M., Quick A. E., Skarlupka J. H., Suen G., and Ollivett T. L. (2021). The Nasopharyngeal Microbiota of Preweaned Dairy Calves With and Without Ultrasonographic Lung Lesions. *J. Dairy Sci.* 21, 27–28. doi: 10.3168/jds.2020-19096

Ramayo-Caldas Y., Mach N., Lepage P., Levenez F., Denis C., Lemonnier G., et al. (2016). Phylogenetic Network Analysis Applied to Pig Gut Microbiota Identifies an Ecosystem Structure Linked With Growth Traits. *ISME J.* 10, 2973–2977. doi: 10.1038/ismej.2016.77

Ramayo-Caldas Y., Zingaretti L., Popova M., Estellé J., Bernard A., Pons N., et al. (2019). Identification of Rumen Microbial Biomarkers Linked to Methane Emission in Holstein Dairy Cows. *J. Anim. Breed. Genet.* 00, 1–11. doi: 10.1111/jbg.12427

Ramírez-Labrada A. G., Isla D., Artal A., Arias M., Rezusta A., Pardo J., et al. (2020). The Influence of Lung Microbiota on Lung Carcinogenesis, Immunity, and Immunotherapy. *Trends Cancer* 6, 86–97. doi: 10.1016/j.trecan.2019.12.007

Richard M., De Graaf M., and Herfst S. (2014). Avian Influenza A Viruses: From Zoonosis to Pandemic. *Future Virol.* 9, 513–524. doi: 10.2217/fvl.14.30

Rychlik I. (2020). Composition and Function of Chicken Gut Microbiota. *Animals (basel)* 10 (1), 103–123. doi: 10.3390/ani10010103

Samy A., and Naguib M. M. (2018). Avian Respiratory Coinfection and Impact on Avian Influenza Pathogenicity in Domestic Poultry: Field and Experimental Findings. *Vet. Sci.* 5, 23. doi: 10.3390/vetsci5010023

Schachtschneider K. M., Yeoman C. J., Isaacson R. E., White B. A., Schook L. B., and Pieters M. (2013). Modulation of Systemic Immune Responses Through Commensal Gastrointestinal Microbiota. *PloS One* 8, e53969. doi: 10.1371/journal.pone.0053969

Shabbir M. Z., Malys T., Ivanov Y. V., Park J., Bakr Shabbir M. A., Rabbani M., et al. (2014). Microbial Communities Present in the Lower Respiratory Tract of Clinically Healthy Birds in Pakistan. *Poult. Sci.* 94, 612–620. doi: 10.3382/ps/pev010

Shi K. C., Guo X., Ge X. N., Liu Q., and Yang H. C. (2010). Cytokine mRNA Expression Profiles in Peripheral Blood Mononuclear Cells From Piglets Experimentally Co-Infected With Porcine Reproductive and Respiratory Syndrome Virus and Porcine Circovirus Type 2. *Vet. Microbiol.* 140, 155. doi: 10.1016/j.vetmic.2009.07.021

Shin N. R., Whon T. W., and Bae J. W. (2015). Proteobacteria: Microbial Signature of Dysbiosis in Gut Microbiota. *Trends Biotechnol.* 33 (9), 496–503. doi: 10.1016/j.tibtech.2015.06.011

Slifierz M. J., Friendship R. M., and Weese J. S. (2015). Longitudinal Study of the Early-Life Fecal and Nasal Microbiotas of the Domestic Pig. *BMC Microbiol.* 15, 184. doi: 10.1186/s12866-015-0512-7

Sohail M. U., Hume M. E., Byrd J. A., Nisbet D. J., Shabbir M. Z., Ijaz A., et al. (2015). Molecular Analysis of the Caecal and Tracheal Microbiome of Heat-Stressed Broilers Supplemented With Prebiotic and Probiotic. *Avian Pathol.* 44, 67–74. doi: 10.1080/03079457.2015.1004622

Stroebel C., Alexander T., Workentine M. L., and Timsit E. (2018). Effects of Transportation to and Co-Mingling at an Auction Market on Nasopharyngeal and Tracheal Bacterial Communities of Recently Weaned Beef Cattle. *Vet. Microbiol.* 223, 126–133. doi: 10.1016/j.vetmic.2018.08.007

Suez J., Zmora N., Segal E., and Elinav E. (2019). The Pros, Cons, and Many Unknowns of Probiotics. *Nat. Med.* 25, 716–729. doi: 10.1038/s41591-019-0439-x

Surendran Nair M., Eucker T., Martinson B., Neubauer A., Victoria J., Nicholson B., et al. (2019). Influence of Pig Gut Microbiota on Mycoplasma Hyopneumoniae Susceptibility. *Vet. Res.* 50, 86. doi: 10.1186/s13567-019-0701-8

Taylor K. J. M., Ngunjiri J. M., Abundo M. C., Jang H., Elaish M., Ghorbani A., et al. (2020). Respiratory and Gut Microbiota in Commercial Turkey Flocks With Disparate Weight Gain Trajectories Display Differential Compositional Dynamics. *Appl. Environ. Microbiol.* 86, e00431–e00420. doi: 10.1128/AEM.00431-20

Thanawongnuwech R., Thacker B., Halbur P., and Thacker E. L. (2004). Increased Production of Proinflammatory Cytokines Following Infection With Porcine Reproductive and Respiratory Syndrome Virus and Mycoplasma Hyopneumoniae. *Clin. Diagn. Lab. Immunol.* 11, 901–908. doi: 10.1128/CDLI.11.5.901-908.2004

Timsit E., Workentine M., Crepieux T., Miller C., Regev-Shoshani G., Schaefer A., et al. (2017). Effects of Nasal Instillation of a Nitric Oxide-Releasing Solution or Parenteral Administration of Tilmicosin on the Nasopharyngeal Microbiota of Beef Feedlot Cattle at High-Risk of Developing Respiratory Tract Disease. *Res. Vet. Sci.* 115, 117–124. doi: 10.1016/j.rvsc.2017.02.001

Timsit E., Workentine M., Schryvers A. B., Holman D. B., van der Meer F., and Alexander T. W. (2016). Evolution of the Nasopharyngeal Microbiota of Beef

Cattle From Weaning to 40 Days After Arrival at a Feedlot. *Vet. Microbiol.* 187, 75–81. doi: 10.1016/j.vetmic.2016.03.020

Timsit E., Workentine M., van der Meer F., and Alexander T. (2018). Distinct Bacterial Metacommunities Inhabit the Upper and Lower Respiratory Tracts of Healthy Feedlot Cattle and Those Diagnosed With Bronchopneumonia. *Vet. Microbiol.* 221, 105–113. doi: 10.1016/j.vetmic.2018.06.007

Tress B., Dorn E. S., Suchodolski J. S., Nisar T., Ravindran P., Weber K., et al. (2017). Bacterial Microbiome of the Nose of Healthy Dogs and Dogs With Nasal Disease. *PloS One* 12, e0176736. doi: 10.1371/journal.pone.0180299

Umar S., Guerin J. L., and Ducatez M. F. (2016). Low Pathogenic Avian Influenza and Coinfecting Pathogens: A Review of Experimental Infections in Avian Models. *Avian Dis.* 61, 3–15. doi: 10.1637/11514-101316-review

van Leenen K., Van Driessche L., De Cremer L., Masmeijer C., Boyen F., Deprez P., et al. (2020). Comparison of Bronchoalveolar Lavage Fluid Bacteriology and Cytology in Calves Classified Based on Combined Clinical Scoring and Lung Ultrasonography. *Prev. Vet. Med.* 176, 104901. doi: 10.1016/j.prevetmed.2020.104901

Vayssier-Taussat M., Albina E., Citti C., Cosson J. F., Jacques M. A., Lebrun M. H., et al. (2014). Shifting the Paradigm From Pathogens to Pathobiome New Concepts in the Light of Meta-Omics. *Front. Cell. Infect. Microbiol.* 4, 29. doi: 10.3389/fcimb.2014.00029

Vayssier-Taussat M., Kazimirova M., Hubalek Z., Hornok S., Farkas R., Cosson J. F., et al. (2015). Emerging Horizons for Tick-Borne Pathogens: From the "One Pathogen-One Disease" Vision to the Pathobiome Paradigm. *Future Microbiol.* 10, 2033–2043. doi: 10.2217/fmb.15.114

Vientoos-Plotts A. I., Ericsson A. C., Rindt H., Grobman M. E., Graham A., Bishop K., et al. (2017). Dynamic Changes of the Respiratory Microbiota and its Relationship to Fecal and Blood Microbiota in Healthy Young Cats. *PloS One* 12, 1–17. doi: 10.1371/journal.pone.0173818

Vientós-Plotts A. I., Ericsson A. C., Rindt H., and Reinero C. R. (2017). Oral Probiotics Alter Healthy Feline Respiratory Microbiota. *Front. Microbiol.* 8, 1287. doi: 10.3389/fmicb.2017.01287

Vientós-Plotts A. I., Ericsson A. C., Rindt H., and Reinero C. R. (2019). Respiratory Dysbiosis in Canine Bacterial Pneumonia: Standard Culture vs. Microbiome Sequencing. *Front. Vet. Sci.* 6, 354. doi: 10.3389/fvets.2019.00354

Vötsch D., Willenborg M., Weldearegay Y. B., and Valentin-Weigand P. (2018). Streptococcus Suis - The "Two Faces" of a Pathobiont in the Porcine Respiratory Tract. *Front. Microbiol.* 9, 480. doi: 10.3389/fmicb.2018.00480

Wagner D. C., Kass P. H., and Hurley K. F. (2018). Cage Size, Movement in and Out of Housing During Daily Care, and Other Environmental and Population Health Risk Factors for Feline Upper Respiratory Disease in Nine North American Animal Shelters. *PloS One* 13 (1), e0190140. doi: 10.1371/journal.pone.0190140

Wang Q., Cai R., Huang A., Wang X., Qu W., Shi L., et al. (2018). Comparison of Oropharyngeal Microbiota in Healthy Piglets and Piglets With Respiratory Disease. *Front. Microbiol.* 3218, 3218–3229. doi: 10.3389/fmicb.2018.03218

Wang Z., Chai W., Burwinkel M., Twardziok S., Wrede P., Palissa C., et al. (2013b). Inhibitory Influence of Enterococcus Faecium on the Propagation of Swine Influenza A Virus In Vitro. *PloS One* 8, e53043. doi: 10.1371/journal.pone.0053043

Wang T., He Q., Yao W., Shao Y., Li J., and Huang F. (2019). The Variation of Nasal Microbiota Caused by Low Levels of Gaseous Ammonia Exposure in Growing Pigs. *Front. Microbiol.* 10, 1083–1097. doi: 10.3389/fmicb.2019.01083

Wang J., Ishfaq M., and Li J. (2021). Lactobacillus Salivarius Ameliorated Mycoplasma Gallisepticum-Induced Inflammatory Injury and Secondary Escherichia Coli Infection in Chickens: Involvement of Intestinal Microbiota. *Vet. Immunol. Immunopathol.* 233, 110192. doi: 10.1016/j.vetimm.2021.110192

Wang M., Radlowski E. C., Monaco M. H., Fahey G. C., Gaskins H. R., and Donovan S. M. (2013a). Mode of Delivery and Early Nutrition Modulate Microbial Colonization and Fermentation Products in Neonatal Piglets. *J. Nutr.* 143, 795–803. doi: 10.3945/jn.112.173096

Wasko A. J., Barkema H. W., Nicol J., Fernandez N., Logie N., and Léguillette R. (2011). Evaluation of a Risk-Screening Questionnaire to Detect Equine Lung Inflammation: Results of a Large Field Study. *Equine Vet. J.* 43 (2), 145–152. doi: 10.1111/j.2042-3306.2010.00150.x

Weese J. S., Slifierz M., Jalali M., and Friendship R. (2014). Evaluation of the Nasal Microbiota in Slaughter-Age Pigs and the Impact on Nasal Methicillin-Resistant Staphylococcus Aureus (MRSA) Carriage. *BMC Vet. Res.* 10, 1–10. doi: 10.1186/1746-6148-10-69

West J. B., Watson R. R., and Fu Z. (2007). Major Differences in the Pulmonary Circulation Between Birds and Mammals. *Respir. Physiol. Neurobiol.* 157, 382–390. doi: 10.1016/j.resp.2006.12.005.Major

Wypych T. P., Wickramasinghe L. C., and Marsland B. J. (2019). The Influence of the Microbiome on Respiratory Health. *Nat. Immunol.* 20, 1279–1290. doi: 10.1038/s41590-019-0451-9

Yitbarek A., Alkie T., Taha-Abdelaziz K., Astill J., Rodriguez-Lecompte J. C., Parkinson J., et al. (2018a). Gut Microbiota Modulates Type I Interferon and Antibody-Mediated Immune Responses in Chickens Infected With Influenza Virus Subtype H9N2. *Benef. Microbes* 9, 417–427. doi: 10.3920/BM2017.0088

Yitbarek A., Taha-Abdelaziz K., Hodgins D. C., Read L., Nagy É., Weese J. S., et al. (2018b). Gut Microbiota-Mediated Protection Against Influenza Virus Subtype H9N2 in Chickens is Associated With Modulation of the Innate Responses. *Sci. Rep.* 8, 13189. doi: 10.1038/s41598-018-31613-0

Zaneveld J. R., McMinds R., and Thurber R. V. (2017). Stress and Stability: Applying the Anna Karenina Principle to Animal Microbiomes. *Nat. Microbiol.* 2, 17121. doi: 10.1038/nmicrobiol.2017.121

Zeineldin M., Aldridge B., Blair B., Kancer K., and Lowe J. (2018). Microbial Shifts in the Swine Nasal Microbiota in Response to Parenteral Antimicrobial Administration. *Microb. Pathog.* 121, 210–217. doi: 10.1016/j.micpath.2018.05.028

Zeineldin M., Elolimy A. A., and Barakat R. (2020a). Meta-Analysis of Bovine Respiratory Microbiota: Link Between Respiratory Microbiota and Bovine Respiratory Health. *FEMS Microbiol. Ecol.* 96, 127. doi: 10.1093/femsec/fiaa127

Zeineldin M., Lowe J., and Aldridge B. (2019). Contribution of the Mucosal Microbiota to Bovine Respiratory Health. *Trends Microbiol.* 27, 753. doi: 10.1016/j.tim.2019.04.005

Zeineldin M., Lowe J., and Aldridge B. (2020b). Effects of Tilmicosin Treatment on the Nasopharyngeal Microbiota of Feedlot Cattle With Respiratory Disease During the First Week of Clinical Recovery. *Front. Vet. Sci.* 7, 115. doi: 10.3389/fvets.2020.00115

Zeineldin M., Lowe J., de Godoy M., Maradiaga N., Ramirez C., Ghanem M., et al. (2017a). Disparity in the Nasopharyngeal Microbiota Between Healthy Cattle on Feed, at Entry Processing and With Respiratory Disease. *Vet. Microbiol.* 208, 30–37. doi: 10.1016/j.vetmic.2017.07.006

Zeineldin M. M., Lowe J. F., Grimmer E. D., De Godoy M. R. C., Ghanem M. M., Abd El-Raof Y. M., et al. (2017b). Relationship Between Nasopharyngeal and Bronchoalveolar Microbial Communities in Clinically Healthy Feedlot Cattle. *BMC Microbiol.* 17, 1–11. doi: 10.1186/s12866-017-1042-2

Zhao N., Wang S., Li H., Liu S., Li M., Luo J., et al. (2018). Influence of Novel Highly Pathogenic Avian Influenza A (H5N1) Virus Infection on Migrating Whooper Swans Fecal Microbiota. *Front. Cell. Infect. Microbiol.* 8, 46. doi: 10.3389/fcimb.2018.00046

Zhou Y., Zhang M., Liu Q., and Feng J. (2021). The Alterations of Tracheal Microbiota and Inflammation Caused by Different Levels of Ammonia Exposure in Broiler Chickens. *Poult. Sci.* 100, 685–696. doi: 10.1016/j.psj.2020.11.026

Zhu X., Dordet-Frisoni E., Gillard L., Ba A., Hygonenq M. C., Sagné E., et al. (2019). Extracellular DNA: A Nutritional Trigger of Mycoplasma Bovis Cytotoxicity. *Front. Microbiol.* 10, 2753–2766. doi: 10.3389/fmicb.2019.02753

Conflict of Interest: The authors declare that the research was conducted in the absence of any commercial or financial relationships that could be construed as a potential conflict of interest.

Advantages of publishing in Frontiers

OPEN ACCESS
Articles are free to read for greatest visibility and readership

FAST PUBLICATION
Around 90 days from submission to decision

HIGH QUALITY PEER-REVIEW
Rigorous, collaborative, and constructive peer-review

TRANSPARENT PEER-REVIEW
Editors and reviewers acknowledged by name on published articles

Frontiers
Avenue du Tribunal-Fédéral 34
1005 Lausanne | Switzerland

Visit us: www.frontiersin.org
Contact us: frontiersin.org/about/contact

REPRODUCIBILITY OF RESEARCH
Support open data and methods to enhance research reproducibility

DIGITAL PUBLISHING
Articles designed for optimal readership across devices

FOLLOW US
@frontiersin

IMPACT METRICS
Advanced article metrics track visibility across digital media

EXTENSIVE PROMOTION
Marketing and promotion of impactful research

LOOP RESEARCH NETWORK
Our network increases your article's readership